

# GEOLOGIJA

2021 | št.: **64/2**



**ZEMLJA POZNA ODGOVORE**

ZNANOST, OKOLJE, ETIKA

ISSN

Tiskana izdaja / Print edition: 0016-7789  
Spletna izdaja / Online edition: 1854-620X

# GEOLOGIJA

64/2 – 2021



GEOLOGIJA	2021	64/2	139-312	Ljubljana
-----------	------	------	---------	-----------



Izdajatelj: Geološki zavod Slovenije, zanj direktor MILOŠ BAVEC  
Publisher: Geological Survey of Slovenia, represented by Director MILOŠ BAVEC  
Financirata Javna agencija za raziskovalno dejavnost Republike Slovenije in Geološki zavod Slovenije  
Financed by the Slovenian Research Agency and the Geological Survey of Slovenia

**Glavna in odgovorna urednica / Editor-in-Chief: MATEJA GOSAR**  
**Tehnična urednica / Technical Editor: BERNARDA BOLE**

**Uredniški odbor / Editorial Board**

DUNJA ALJINOVIC	MARKO KOMAC
Rudarsko-geološki naftni fakultet, Zagreb	Poslovno svetovanje s.p., Ljubljana
MARIA JOÃO BATISTA	HARALD LOBITZER
National Laboratory of Energy and Geology, Lisbona	Geologische Bundesanstalt, Wien
MILOŠ BAVEC	MILOŠ MILER
Geološki zavod Slovenije, Ljubljana	Geološki zavod Slovenije, Ljubljana
MIHAEL BRENČIČ	RINALDO NICOLICH
Naravoslovnotehniška fakulteta, Univerza v Ljubljani	Università di Trieste, Dip. di Ingegneria Civile
GIOVANNI B. CARULLI	SIMON PIRC
Dip. di Sci. Geol., Amb. e Marine, Università di Trieste	Naravoslovnotehniška fakulteta, Univerza v Ljubljani
KATICA DROBNE	MIHAEL RIBIČIČ
Znanstvenoraziskovalni center SAZU, Ljubljana	Naravoslovnotehniška fakulteta, Univerza v Ljubljani
JADRAN FAGANELI	NINA RMAN
Nacionalni inštitut za biologijo, MBP, Piran	Geološki zavod Slovenije, Ljubljana
JANOS HAAS	MILAN SUDAR
Etvös Lorand University, Budapest	Faculty of Mining and Geology, Belgrade
BOGDAN JURKOVŠEK	SAŠO ŠTURM
Geološki zavod Slovenije, Ljubljana	Institut »Jožef Stefan«, Ljubljana
ROMAN KOCH	MIRAN VESELIČ
Institut für Paläontologie, Universität Erlangen-Nürnberg	Fakulteta za gradbeništvo in geodezijo, Univerza v Ljubljani

Naslov uredništva / Editorial Office: GEOLOGIJA Geološki zavod Slovenije / Geological Survey of Slovenia  
Dimičeva ulica 14, SI-1000 Ljubljana, Slovenija  
Tel.: +386 (01) 2809-700, Fax: +386 (01) 2809-753, e-mail: urednik@geologija-revija.si  
URL: <http://www.geologija-revija.si/>



GEOLOGIJA izhaja dvakrat letno. / GEOLOGIJA is published two times a year.  
GEOLOGIJA je na voljo tudi preko medknjižnične izmenjave publikacij. /  
GEOLOGIJA is available also on exchange basis.

**Izjava o etičnosti**

Izdajatelji revije Geologija se zavedamo dejstva, da so se z naglim naraščanjem števila objav v svetovni znanstveni literaturi razmahnili tudi poskusi plagiatorstva, zlorab in prevar. Menimo, da je naša naloga, da se po svojih močeh borimo proti tem pojavom, zato v celoti sledimo etičnim smernicam in standardom, ki jih je razvil odbor COPE (Committee on Publication Ethics).

**Publication Ethics Statement**

As the publisher of Geologija, we are aware of the fact that with growing number of published titles also the problem of plagiarism, fraud and misconduct is becoming more severe in scientific publishing. We have, therefore, committed to support ethical publication and have fully endorsed the guidelines and standards developed by COPE (Committee on Publication Ethics).

Baze, v katerih je Geologija indeksirana / Indexation bases of Geologija: Scopus, Directory of Open Access Journals, GeoRef, Zoological Record, Geoscience e-Journals, EBSCOhost

**Cena / Price**

Posamezni izvod / Single Issue	Letna naročnina / Annual Subscription
Posameznik / Individual: 15 €	Posameznik / Individual: 25 €
Institucija / Institutional: 25 €	Institucija / Institutional: 40 €

Tisk / Printed by: GRAFIKA GRACER d.o.o.

**Slika na naslovni strani:** Konec letošnjega oktobra je sklenil svojo življenjsko pot geolog dr. Bogomir Celarc. Slika je bila posneta med terenskim delom v Julijskih Alpah (foto: Špela Goričan).

**Cover page:** Geologist dr. Bogomir Celarc passed away at the end of October 2021. Photo was taken during his field work in the Julian Alps (photo: Špela Goričan).

VSEBINA – CONTENTS

<i>Spahić, D. &amp; Gaudenyi, T.</i>	
The role of the pre-Alpine polycrystalline basement in the paleogeographic configuration of multiple Neotethyan oceanic basins .....	143
Vloga predalpidske polikristalinske podlage pri paleogeografski razporeditvi oceanskih bazenov Neotetide	
<i>Jemec Auflič, M., Bokal, G., Kumelj, Š., Medved, A., Dolinar, M. &amp; Jež, J.</i>	
Impact of climate change on landslides in Slovenia in the mid-21st century.....	159
Vpliv podnebnih sprememb na pojavljanje zemeljskih plazov v sredini 21. stoletja v Sloveniji	
<i>Gale, L., Kukoč, D., Rožič, B. &amp; Vidervol, A.</i>	
Sedimentological and paleontological analysis of the Lower Jurassic part of the Zatrnik Formation on the Pokljuka plateau, Slovenia.....	173
Sedimentološka in paleontološka analiza spodnjejurskega dela Zatrniške formacije na Pokljuki, Slovenija	
<i>Čar, J., Jež, J. &amp; Milanič, B.</i>	
Strukturne razmere na stiku Južnih Alp in Dinaridov na zahodnem Cerkljanskem .....	189
Structural setting at the contact of the Southern Alps and Dinarides in western Cerkljansko region (western Slovenia)	
<i>Serianz, L., Cerar, S. &amp; Vreča, P.</i>	
Using stable isotopes and major ions to identify recharge characteristics of the Alpine groundwater-flow dominated Triglavsko Bistrica River.....	205
Uporaba stabilnih izotopov in glavnih ionov za oceno napajalnih značilnosti alpskega rečnega toka Triglavsko Bistrice pod vplivom podzemne vode	
<i>Placer, L., Rupnik Jamšek, P. &amp; <sup>†</sup>Celarc, B.</i>	
The Sistiana Fault and the Sistiana Bending Zone (SW Slovenia) .....	221
Sesljanski prelom in sesljanska upogibna cona	
<i>Torkar, A., Zajc, M., Atanackov, J., Gosar, A. &amp; Brenčič, M.</i>	
Geophysical investigations in the Radovna River Spring area (Julian Alps, NW Slovenia).....	253
Geofizikalne raziskave na območju izvira reke Radovne (Julijske Alpe, SV Slovenija)	
<i>Mali, N., Koroša, A. &amp; Urbanc, J.</i>	
Pesticidi v vodonosniku Krško-Brežiškega polja .....	267
Prevalence of pesticides in Krško-Brežice polje aquifer	
Nove knjige - New books	
<i>Bračič Železnik, B.</i>	
Urednici: Branka Bračič Železnik & Petra Žvab Rožič, 2021: Obrazi Geologije v besedi in sliki. Slovensko geološko društvo, Ljubljana: 328 str.....	289
<i>Vidmar, I.</i>	
Mihail Brenčič, 2021: Dinamika podzemne vode, Oddelek za geologijo. Naravoslovnotehniška fakulteta, Univerza v Ljubljani, Ljubljana: 397 str.....	290

## Poročila - Reports

<i>Jamšek Rupnik, P., Novak, A. &amp; Bavec, M.</i> : 6th Regional Scientific Meeting on Quaternary Geology: Seas, Lakes and Rivers, September 2021, Ljubljana.....	292
<i>Rajver, D.</i> : 6. svetovni geotermalni kongres WGC 2020+1, Reykjavik (Islandija) marec – oktober, 2021.....	294
<i>Bračič Železnik, B.</i> : Poročilo o aktivnostih Slovenskega geološkega društva v letu 2020.....	298
Nekrolog - In memoriam	
<i>Goričan, Š.</i> V spomin akad. dr. Dragici Turnšek Akad. dr. Dragica Turnšek: izbrana bibliografija 1962–2019 .....	306
<i>Zupančič, N.</i> V spomin prof. dr. Valeriji Osterc .....	303
<i>Bavec, M., Gale, L. &amp; Novak, M.</i> V spomin dr. Bogomirju Celarcu..... dr. Bogomir Celarc: izbrana bibliografija (2002–2021)	307
Navodila avtorjem .....	310
Instructions for authors .....	311



# The role of the pre-Alpine polycrystalline basement in the paleogeographic configuration of multiple Neotethyan oceanic basins

Vloga predalpidske polikristalinske podlage pri paleogeografski razporeditvi oceanskih bazenov Neotetide

Darko SPAHIĆ<sup>1</sup> & Tivadar GAUDENYI<sup>2</sup>

<sup>1</sup>Geological Survey of Serbia, Rovinjska 12, 11000 Belgrade, Serbia;  
e-mail: darkogeo2002@hotmail.com; darko.spahic@gzs.gov.rs

<sup>2</sup>Serbian Academy of Sciences and Arts - Geographical Institute "Jovan Cvijic", Djure Jaksica 9,  
11000 Belgrade, Serbia

Prejeto / Received 9. 2. 2021; Sprejeto / Accepted 25. 11. 2021; Objavljeno na spletu / Published online 28. 12. 2021

**Key words:** Dinaric-Hellenic orogen, paleocontinental inheritance, “Drina–Pelagonide continental splinter”, Pelagonides, Inner Dinaric-(Mirdita-Pindos) ocean, Drina-Ivanjica block, Neotethyan ophiolites

## Abstract

The study provides a deeper understanding of the early Mesozoic paleogeographic spatial-temporal relationship by studying the two Adria-Europe intervening basement blocks. The Drina-Ivanjica and Pelagonian crustal fragments play important role in the internal early Alpine oceanic constitution further controlling the late Jurassic emplacement of Tethyan Dinaric-Hellenic ophiolites. The proposed paleogeographic reassessment is driven by the new paleocontinental inheritance data associated with the Variscan – pre-Variscan basement terranes. The recently published data suggest an Avalonian-type inheritance of the Pelagonian basement block which indicates a different pre-Variscan plate-tectonic journey, including separate spatial arrangement during Variscan amalgamation. In turn, Cadomian-type basement inheritance has been documented within the sliced Adria microplate. Thus, the Avalonian inheritance place the Pelagonian block away from the Apulia/Adria (Dinarides). In the investigated context of Paleozoic-Mesozoic paleogeographic transition, the Pelagonian block may represent a segment of the Cimmerian ribbon continent or southernmost segment of the Variscan Europe. With regards the nearby Adria microplate, a Triassic-Jurassic oceanic opening led to the decoupling (spreading away from the main Adria microplate) of the Drina-Ivanjica block. The rifting is in line with the simultaneous yet opposite or westward-directed drift of the Pelagonides. The breakup of south European Variscan configuration eventually result in the spatial alignment of the two basement fragments referred to as the “Drina–Pelagonide continental splinter”. By linking the paleogeographic pre-Jurassic–Jurassic relationship between these continental units, the two landlocked Neotethyan Vardar s.l. basins are extrapolated, “Dinaric Tethys” / Inner Dinaric-(Mirdita-Pindos) and the main Vardar Ocean (Western Vardar Zone).

## Izvleček

Študija prinaša globlje razumevanje zgodnjemezozojskih paleogeografskih prostorsko-časovnih odnosov s preučevanjem razlik v podlagi dveh kontinentalnih blokov med Jadransko in Evropsko ploščo. Fragmenta skorje Drina-Ivanjica in Pelagonija sta igrala pomembno vlogo v notranji zgradbi zgodnjealpidskega oceana, kar je vplivalo tudi na narivanje dinarsko-helenskih ofiolitov v zgornji juri. K ponovnemu razmisleku o paleogeografiji so nas spodbudili novi podatki o značilnostih variskične in predvariskične podlage. Nedavno objavljeni podatki kažejo, da ima Pelagonijski blok podlago avalonijskega tipa, pri Jadranski mikroplošči in njenih fragmentih pa je bil dokumentiran kadomijski tip podlage. Razlike kažejo na različno predvariskično potovanje obeh kontinentalnih blokov in tudi ločeno prostorsko razporeditev med variskično amalgamacijo. Avalonijska preteklost uvršča Pelagonijski blok stran od Apulijske ali Jadranske plošče oziroma Dinaridov. Na prehodu iz paleozoika v mezozoik je bil Pelagonijski blok lahko del Kimerijskega kontinentalnega pasu ali najjužnejši del variskične Evrope. Na bližnji Jadranski mikroplošči je triasno-jursko odpiranje oceana privedlo do ločitve bloka Drina-Ivanjica in njegovega odmika na vzhod od glavne Jadranske mikroplošče. Rifting se ujema s hkratnim drsenjem Pelagonidov v nasprotni smeri, proti zahodu. Razpad južnoevropske variskične konfiguracije je lahko privедel do prostorske poravnave obeh blokov s skupnim imenom Drina-Pelagonija. Z upoštevanjem medsebojnega paleogeografskega položaja kontinentalnih enot pred juro in tekom jure lahko sklepamo, da sta v Neotetidi obstajala dva Vardarska bazena – Dinarska Tetida (Notranji Dinaridi–Mirdita–Pindos) in glavni Vardarski ocean (Zahodna Vardarska cona).

## Introduction

The intriguing lithospheric elements of the Jurassic-earliest Cretaceous paleoceanography in the area of Western Balkan countries (Fig. 1a) underwent final suturing and collisional thrust stacking during the late Mesozoic - Paleogene (e.g., Picha, 2002; Csontos & Vörös, 2004; Schmid et al., 2008; Xypolias et al., 2008; Robertson, 2012; Jolivet et al., 2016; Fig. 1b, c). Due to the exceptional exposure of the Jurassic ophiolite belts, a considerably large cluster of papers discusses important aspects of the exhumed Neotethyan oceanic lithosphere and associated depositional environments (e.g., Bernoulli & Jenkyns, 1974; Dilek et al., 2005, 2007; Saccani et al., 2015, 2017, Tremblay et al., 2015; Dilek & Furnes, 2017; Spahić & Gaudenzi, 2020c and many others). The opening pattern of these landlocked oceans indicates the complex Permian-Triassic architecture of the intervening exotic Variscan peri-Gondwana terranes (including Adria as a Paleozoic continuation of the Austrian Alps; Pamić & Jurković, 2002). These poorly understood continental lithosphere fragments (e.g., Vavasisi et al., 2000; Spahić & Gaudenzi, 2020a, 2020b) represent a segment of the remobilized basement of the Alpine orogen.

The Permian-Triassic Pangea southern margin underwent extensional processes followed by the dispersal of this segment of the Supercontinent (Pamić & Jurković, 2002; Spahić et al., 2020 and references therein). During the Ladinian/Carnian, this southern margin (Greece) was further affected by the poorly constrained Eocimmerian or Minoan terrane low-magnitude “docking” (Mountrakis, 1986; Zulauf et al., 2015; see Neubauer et al., 2019, for a discussion). The complicated processes of crustal weakening, dismemberment of the Triassic continental margin (rollback, rifting, and sea - floor spreading) are also documented within the considerably large Permian-Triassic Adria microplate (e.g., Pamić et al., 1998; Goričan et al., 1999; Dimitrijević, 2001; Dimitrijević et al., 2003). The most complex area is the northeastern tip of the Adria leading edge referred to as the Drina-Ivanjica block (Đoković, 1985; Spahić et al., 2018). This block has a striking N-S alignment with the Pelagonian block of the Hellenides (Figs. 1c and 2a). This elongated seemingly amalgamated paleoceanic splinter assembly comprises a dominantly Neoproterozoic – Paleozoic crystalline continental crust that separate the two Mesozoic ophiolite belts of Tethyan relevance. However, the definition of this “Drina-Pelagonian continental splinter” and its importance in the opening of Mesozoic Tethyan

oceans remains poorly constrained (Mountrakis, 1986; Anders et al., 2007; Zlatkin et al., 2014, 2017; Spahić et al., 2019a and references therein; Figs. 1b, c). Although the majority of recent publications advocate a ‘single ocean model’ (e.g., Schmid et al., 2008; see discussion in Robertson et al., 2009; Handy et al., 2015; Jolivet et al., 2016; Maffione & van Hinsbergen, 2018), the past position and the role of the “Drina-Pelagonian continental splinter” during the Triassic oceanization and latest Jurassic – early Cretaceous Vardar oceanic ophiolite obduction remains unanswered (also in Ferrière et al., 2012).

With a goal to go step forward in contributing the still open issue of the number of Tethyan oceans, the following study focuses on the Pelagonian (Fig. 2a) and Drina-Ivanjica role (Fig. 2b) in the Neotethyan evolution. By applying the update on the pre-Mesozoic paleogeographic inferences (detrital zircon analyses of the Pelagonian block) we pinpoint the principal differences between two basement units (see Žák et al., 2020, for the detrital zircon methodology). The two basement entities are traced during theirs Paleozoic paleogeographic journey that provided the input for reconstructing their position during Neotethyan Vardar Ocean opening and closure. The comparison shows that the Cadomian-type Adria terrane (its NE margin, Drina-Ivanjica block; available detrital zircon data from the nearby Austroalpine basement; Siegesmund et al., 2018) and Avalonian- (Zlatkin et al., 2014, 2017) Pelagonian basement are two discrete microplates. We also introduce the scarce Variscan - Eocimmerian Paleotethyan inferences with a goal to separate the two underlying continental crust segments (prior to Late Jurassic-earliest Cretaceous obduction-related oceanic closure events).

## Regional setting

The complex allochthonous configuration of the Dinaric-Hellenic belt (e.g., Dimitrijević, 1997; 2001; Karamata, 2006; Xypolias et al., 2008; Schmid et al., 2008, 2020) underwent a long-term history of oceanic embayment, terrane drifting, accretion and collision since Neoproterozoic (e.g., “Paleo-Adria”; Franke et al., 2017; Spahić et al., 2018). In the Mesozoic framework, the Dinaric- and Vardar Zone ophiolite-bearing N-NW to S-SE-trending parallel crustal segments (Fig. 1b) representing the vestiges composed of highly heterogeneous ophiolitic mélange (Fig. 2). The Dinaric-Hellenic mélange are consisting of magmatic blocks and a variety of associated sedimentary rocks (Dimitrijević & Dimitrijević,

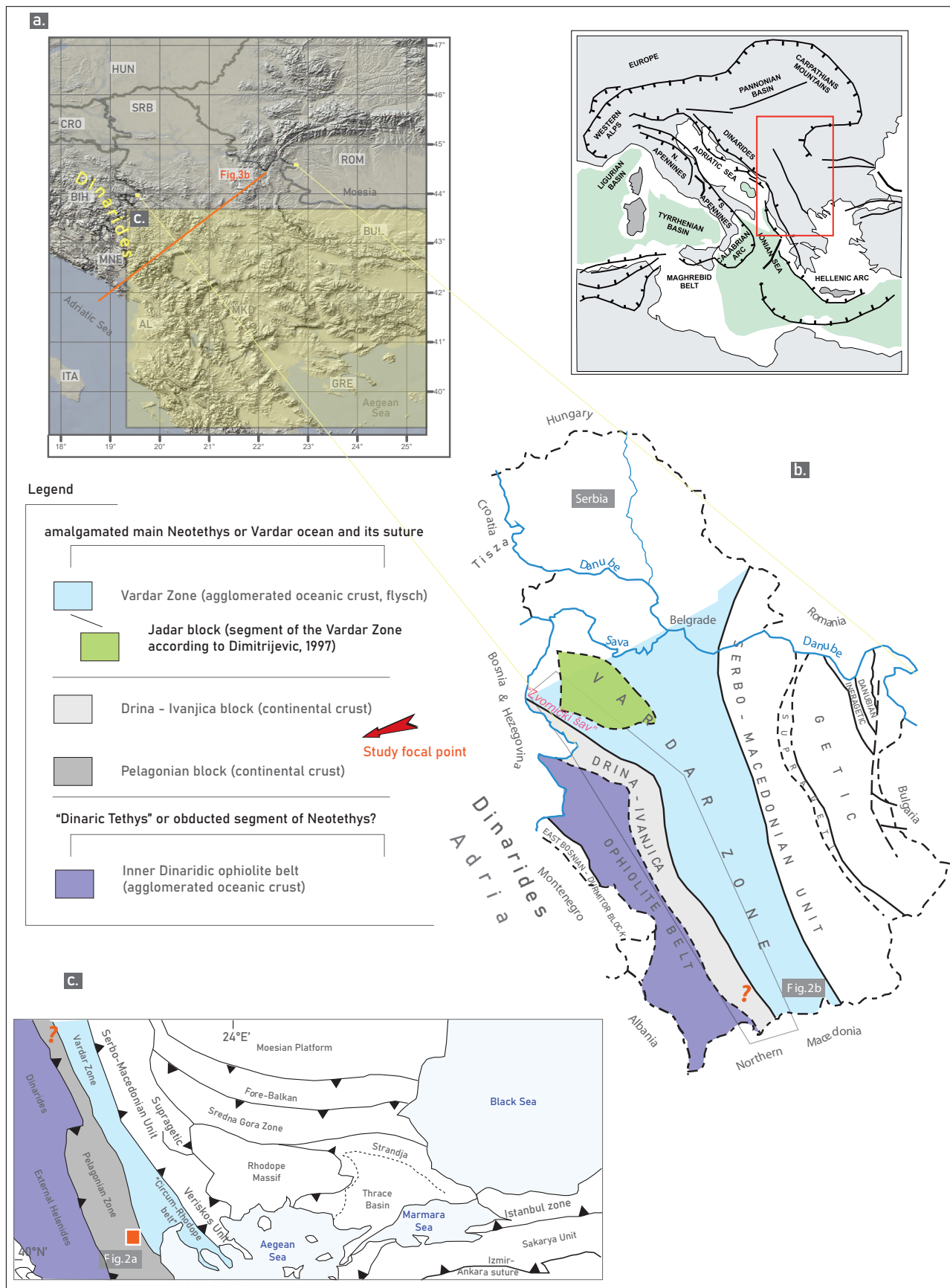


Fig. 1. a. Regional relief map including the countries of former Yugoslavia: SRB-Serbia, MNE-Montenegro, CRO-Croatia, BIH-Bosnia & Herzegovina, MKD-North Macedonia, SLO-Slovenia, HUN-Hungary, ROM-Romania, BUL-Bulgaria, AL-Albania; b. Tectonic sketch map of Serbia (according to concept of Dimitrijević, 1992, map taken from Protić, 1995, also in Dimitrijević, 1997). The main tectonic units are written in the sketch. The Drina-Ivanjica block separating the two-ophiolite belts: to the SW is the Inner Dinaric Ophiolite Belt and to the NE is the Vardar Zone. c. Sketch map of major tectonic elements in the southern Balkan Peninsula and northern Greece (modified after Xypolias et al. 2008 and references therein). The Pelagonian block is thrust over the ophiolite-decorated External Hellenides. Red question mark emphasizes the investigated connection between the Drina-Ivanjica and the Pelagonian block.

1973). The deformation of the mélange belts however varies (Dimitrijević & Dimitrijević, 1975). The prominent ophiolite belt continues to the east-southeast along the Mirdita, Subpelagonian/Pelagonian - Inner Dinaridic Ophiolite Belt zones of the Albanides (*e.g.*, Nance, 1981; Robertson & Karamata, 1994; Dilek et al., 2005, 2007; Saccani et al., 2008; 2011, 2017; Gaggero et al., 2009; Tremblay et al., 2015). Another branch of these ophiolite belts are extending towards to the south in North Macedonia and Greece. Structurally these southern ophiolite belts are belonging to the external section of the Inner Hellenides and most internal segment of the Inner Hellenides (Fig. 1c).

Depending of the chosen paleogeographic model (*sensu* Bernoulli & Laubcher, 1972; adopted by Schmid et al., 2008 among many others or ‘multiple oceans model’, see Spahić & Gaudenyi, 2020, for a discussion; Fig. 3a), ophiolites of similar age are distributed on both sides of the continental splinter: westwards of the intervening the Drina-Ivanjica block and spreading across the Vardar Zone *s.s.* and the Albanides-Hellenides (Fig. 1c; see Fig. 1 of Faul et al., 2014). By applying ‘single ocean model’, the oceanic crust above the Drina-Ivanjica fragment is presumably offscraped after the out-of-sequence Cretaceous – Paleogene thrusting, further affected by the protracted surface exposure (Schmid et al., 2008, 2020; Figs. 3a, b). The compositions of these outcropping oceanic massifs ranges from Jurassic SSZ type-ophiolites formed along the entire length of the Dinarides towards in Albania, and Greece (ranges from 1200 km). The subcontinental Inner Dinarides to depleted mid-ocean ridge/arc compositions have often been documented within the Vardar Zone *s.s.* (to the east of the Drina-Ivanjica block; Fig. 1c).

The Paleozoic configuration of the amalgamated early Alpine Central European terranes (southern Laurussia in the Late Paleozoic framework and slightly postdating Eurasia) was controlled by the recurring Neoproterozoic – Lower to Middle Paleozoic plate-tectonic interplay between the fragmented peri-Gondwanan exotic terrane agglomerations and a fragmented south Euroasian foreland (*e.g.*, Avigad et al., 2016; Zlatkin et al., 2014, 2017; Siegesmund et al., 2018; Spahić & Gaudenyi, 2019a). The early Pan-African to Lower Paleozoic peri-Gondwanan arc interval (Kearey et al., 2009 and references therein) was followed by the late Variscan Paleotethyan closure and assembly of the southern realm of European Pangea (*e.g.*, Stampfli & Kozur, 2006;

Kroner & Romer, 2013; Zulauf et al., 2018; Spahić et al., 2019a). The Middle Paleozoic spreading culminated during Variscan crustal thickening event best recorded along the western Moesian microplate (Iancu et al., 2005; Plissart et al., 2018; Spahić et al., 2019b; Šostek et al., 2020). The Paleotethyan subduction outlived the Variscan event (Pamić & Jurković, 2002; Spahić et al., 2019a), whereas the closure of Paleotethys itself is attributed to the poorly understood Triassic Eocimmerian “docking” (Zulauf et al., 2015). The Eocimmerian “docking” in the region seems to be controlled by the Triassic tectonic interaction among the North African ribbon continent (Stampfli et al., 2001), involving predominantly Cadomian-(Minoan) type crystalline fragments (Zulauf et al., 2015; Spahić et al., 2018; Šostek et al., 2020).

### Geology of Pelagonides and Drina-Ivanjica block

The Pelagonian basement agglomeration is characterized by several magmatic and sedimentary sequences of different age displaced by the Alpine convergence. The Pelagonian nappe-stacked configuration is as follows (Anders et al., 2007; Tremblay et al., 2015; Zlatkin et al., 2014, 2017 and references therein; Fig. 2a): (1) pre-Alpine continental basement, (2) Permo-Triassic metaclastics and Mesozoic marbles, sealed by (3) a Sub-Pelagonian section of Jurassic ophiolites and Upper Cretaceous pelagic and neritic carbonates overlain by the Eocene flysch (Fig. 2a). On the opposite or eastern side (Fig. 1c) is the Vardar / Axios Zone of Inner Hellenides. This ophiolite-bearing zone or eastern side of the Pelagonian block is aligned with the western margin of the Serbo-Macedonian Unit. The Neoproterozoic – Paleozoic framework of Pelagonide basement (proto-Basement) comprises gneiss, granitoides and orthogneiss, schists (metasediments) with early Mesozoic clastics (*e.g.* Zlatkin et al., 2014, 2017; Fig. 2a). The northern gneiss-dominating basement branch of the Pelagonides (North Macedonia; see Spahić et al., 2019a and references therein) and those of Greece are of mixed peri-Amazonian inheritance (*i.e.* Zlatkin et al., 2017). The Variscan-Cimmerian markers likewise Permo-Triassic metaclastics document a Paleotethyan involvement (Mountrakis, 1986; Vavasis et al., 2000; Scherreiks et al., 2014; Zlatkin et al., 2014, 2017).

The Drina-Ivanjica block crops out exposing two considerably large segments: the northwest flank or the Drina block and its southern

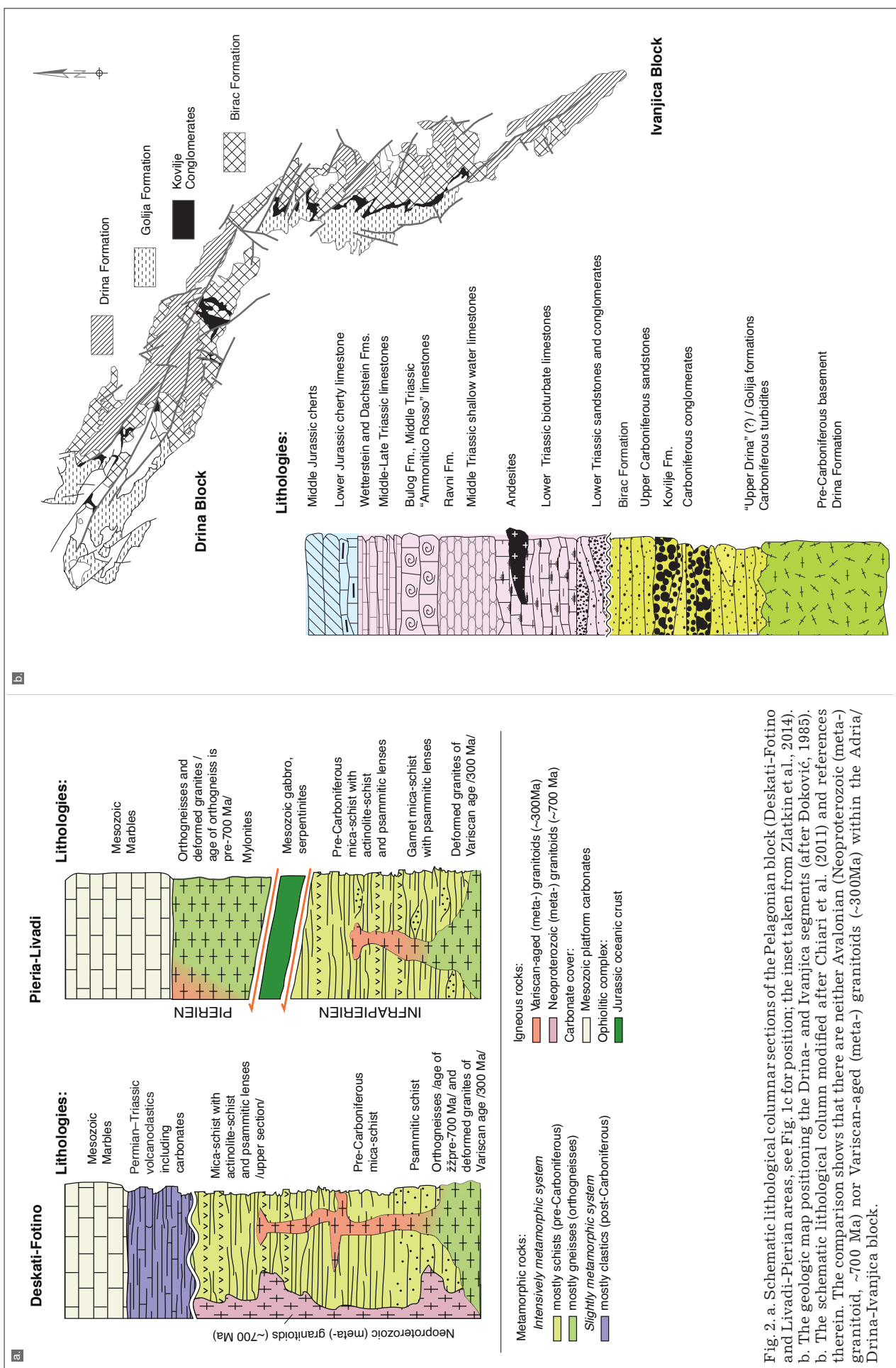


Fig. 2. a. Schematic lithological columnar sections of the Pelagonian block (Deskati-Fotino and Liradi-Pierian areas, see Fig. 1c for position; the inset taken from Zlatkin et al., 2014). b. The geologic map positioning the Draža- and Ivanjica segments (after Đoković, 1985). b. The schematic lithological column modified after Chiari et al. (2011) and references therein. The comparison shows that there are neither Avalonian (Neoproterozoic (meta-) granitoid, ~700 Ma) nor Variscan-aged (meta-) granitoids (~300 Ma) within the Adria/Draža-Ivanjica block.

limb referred to as the Ivanjica block (Figs. 1 and 2b). Stratigraphically, the oldest Neoproterozoic-lower Paleozoic segment is the Drina Formation (Đoković, 1985; Filipović & Sikošek, 1999). The complex depositional environment of the Drina Formation belongs to the ancient north Gondwanan margin (Spahić et al., 2018). The early/late Carboniferous and late Triassic successions (*i.e.* Dimitrijević, 1997; Trivić et al., 2010; Chiari et al., 2011) seal this basement unit. The Drina Formation includes scarce paragneisses, micaschists, amphibolites and minor marble lenses of Neoproterozoic – Lower Paleozoic age. The “Upper Drina Formation” (metasandstones and metapelites and metacarbonates with a Viséan/Namurian conodont fauna) conformably overlies the “Lower Drina Formation”. There is still an open issue of unproven Silurian that is remarkably well developed in eastern Serbia (*e.g.*, Krstić et al., 2005; Spahić et al., 2019b). The Golija Formation, represented by metasandstones, metasiltstone, succeeds the latter formation. The Golija Formation is conformably top-sealed by the Kovilje Formation carrying early/late Carboniferous metaconglomerates and metasandstones. The Kovilje Formation grades into the late Carboniferous Birač Formation consisting of (Bashkirian/Moscovian) metasandstones, metalimestones and metapelites. The Mesozoic sequence is well studied and is represented by the Triassic Kladnica and “Seissian” Formations reaching Middle Jurassic with cherts as the sealing member (Fig. 2b). Neither the magmatic occurrence of the Avalonian stage (ca. 700 Ma) nor the typifying Permian-Triassic imprints of Eocimmerian relevance are recorded within the Drina-Ivanjica block. To make things even more perplexing, the Variscan involvement of the Adria remains poorly constrained (Đoković, 1985; Xypolias et al., 2005; Okay et al., 2006; see Spahić et al., 2019c, for a discussion). On the other hand, the principal differences between the latter two polycrystalline units, the Drina-Ivanjica block

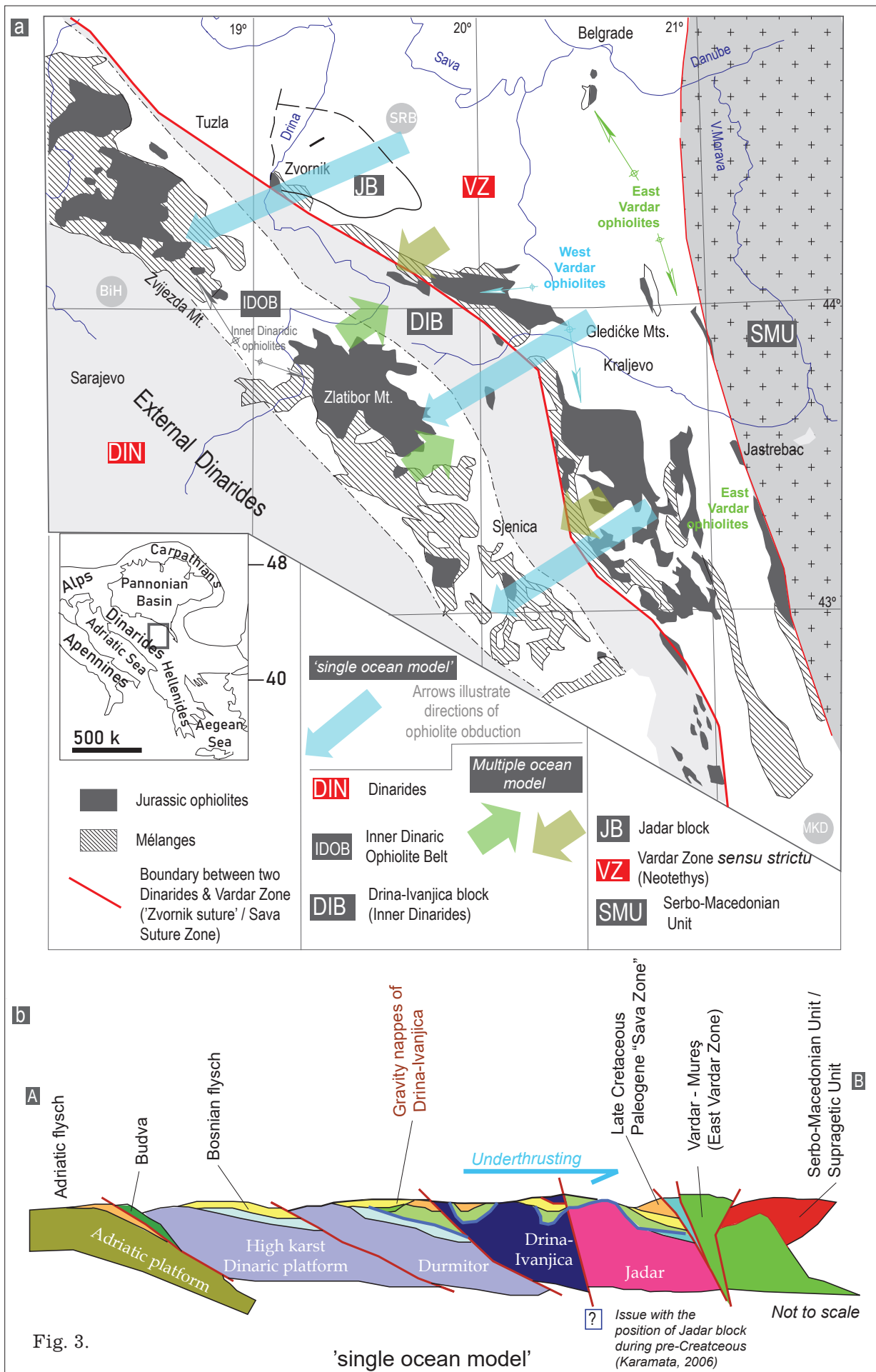
and the Pelagonides (Fig. 1c) were suggested almost a century ago (*e.g.* Cvijić, 1924).

### Early development of the landlocked northwestern PeriNeotethyan oceans

Prominent researchers of former Yugoslavia (Dimitrijević, 1992, also in Protić, 1995 p. 16; Fig. 1b; Dimitrijević, 1997; 2001; Dimitrijević et al., 2003; Karamata, 2006; Fig. 2a) subdivide the Vardar Zone (here referred to as the Vardar Zone *s.s.*) into the Western Vardar Zone, Kopaonik Block, and East Vardar Zone (note that the Inner Dinaric Ophiolite Belt is a separate entity; Fig. 3a). The tectonic concepts of the investigated area of eastern Bosnia and western Serbia, and the proposed first-order units by the aforementioned researchers are almost identical. Dimitrijević (*e.g.*, Dimitrijević, 1997) and Karamata (*e.g.* Karamata & Krstić, 1996; Karamata, 2006) share the same opinion about the position of the main geotectonic units (Fig. 1b). However, with regards to the adjoining Jadar Block (*sensu* Filipović et al., 2003; Kolar-Jurkovsek et al., 2019; Fig. 1b; Fig. 2), this rather isolated entity can be considered either as a (1) footwall entity overridden by the West Vardar ophiolite obduction (Schmid et al., 2008, 2020; Fig. 3b), (2) segment of the Vardar Zone (Dimitrijević, 1997; Fig. 1b) or a Paleozoic entity drifted into the Vardar Zone during the Late Cretaceous (Karamata et al., 1994). Recently, a Paleotethyan involvement for the Jadar Block is suggested (Spahić & Gaudeyti, 2020a). The nearby Tisza Unit is the plate/block is separated by the Vardar Zone *s.s.* from the Jadar (Fig. 1b). The overlying sediments belonging the southern Pannonian Basin (Csontos & Vörös, 2004) hid the contact between the microplates. The southern edge of this underlying Tisza crystalline basement is interfacing both, Inner Dinarides and Vardar Zone. Such complexity between a varieties of the Mesozoic sequences is controlled by the structurally underlying basement entities and their remobilization.

Fig. 3. a. Position of the eastern boundary of the Dinarides, *i.e.* Drina-Ivanjica block at more external positions towards the Vardar Zone (modified after Dimitrijević & Dimitrijević, 1973; Dimitrijević, 2001). The Inner Dinaric Ophiolite belt is a separate Jurassic ophiolite-bearing entity which spreading initially displaced Drina-Ivanjica into a separate ribbon shape crustal fragment. The arrows indicate the ophiolite movements during the Jurassic Neotethyan closure. The blue arrows indicate a ‘single ocean’, green and light brown the ophiolite movements of the two discrete oceans.

b. Regional schematic cross section across the Dinarides and the Vardar Zone, up to the Serbo-Macedonian Unit (redrawn from Csontos et al., 2004; also in Csontos & Vörös, 2004). The interpreted cross section favors ‘single ocean model’, explaining far-travelled ophiolite obduction on top and beyond the Drina-Ivanjica block.



## The Paleozoic input for the early Vardar developments

### *The differences between the NE Adria microplate and the Pelagonian block as input for Variscan – Eocimmerian – Neotethyan inferences*

An Avalonian inheritance of the Pelagonian basement has recently been documented (Zlatkin et al., 2014, 2017). Such Neoproterozoic paleocontinental inferences (ca. 600 Ma old orthogneisses and overstepping late Ediacaran to earliest Cambrian metasedimentary rocks) indicated Avalonian – Amazonian inheritance i.e. a position that is associated with a West African Gondwana proximity, not North African (see Fig. 4 of Spahić et al., 2018 and references therein; Zlatkin et al., 2017). The documented Amazonian paleocontinental inheritance stresses a considerable difference in the early Paleozoic paleoposition with respect to the so-called Cadomian-type ‘Paleo-Adria’ (detrital zircon data by Siegesmund et al., 2018). The ‘Paleo-Adria’ was accommodated in front of the early Paleozoic North Africa (Franke et al., 2017).

The ‘Paleo-Adria’ represents a crustal fragment of the early Paleozoic North African promontory being a predecessor of the Apulia/Adria microplate (Franke et al., 2017). This considerably large microplate was disconnected from the North African margin during the Silurian. Some though earlier studies suggest the Permian or Triassic detaching (*e.g.* Bernoulli, 2001 and references therein; van Hinsbergen et al., 2020). Both concepts nevertheless illustrate the Variscan involvement of the Adria (Pamić & Jurković, 2002) that in turn has not been fully validated across the Dinarides (Okay et al., 2006; Spahić et al., 2020c). The main problem of the eventual Variscan interference revolves around the age of the metamorphic overprint has often been dated as of the dominant Alpine relevance *i.e.* of Jurassic age (*e.g.*, Milovanović, 1984; Porkoláb et al., 2018). Scarce structural evidence of the tentative Variscan involvement of these Neotethyan basement units is identified earlier (*sensu* Đoković, 1985; Borojević-Šoštarić et al., 2012). According to the deformations (*i.e.* Đoković, 1985), it appears that the Drina-Ivanjica block amalgamated with the southwestern Euroasia during the protracted Variscan shortening (Pamić & Jurković, 2002). The late Paleozoic Apulia/Adria occupied westernmost corner of Pangea (see discussion Maffione & van Hinsbergen, 2018; Avigad et al., 2016 and references therein; Spahić & Gaudeyti, 2020a; Fig. 4). Rare rock cooling fission track measurements of the crystalline basement rocks associated with the Apulia/Adria microplate

(External Dinarides, Croatia) occasionally exhibit the Variscan exhumation age (or  $^{40}\text{Ar}/^{39}\text{Ar}$  plateau ages at  $342.9 \pm 3.3$  Ma and  $332.8 \pm 3.1$  Ma in the Sana-Una Unit, Petrova- and Trgovska Gora; Borojević-Šoštarić et al., 2012 and references therein). More frequent is the Alpine exhumation framework having the cooling ages in the range from 159–92 Ma and 50–37 Ma (Mid-Bosnian Schist; Borojević-Šoštarić et al., 2012 and references therein). The issue of the Variscan involvement is rather important as it validates *i.e.*, rules out an eventual Eocimmerian involvement of this microplate (see Stempli et al., 2001, for a discussion). Unlike the Adria microplate, the Pelagonian block has a documented evidence of both Variscan and post-Variscan Paleotethyan involvement (Vavvasis et al., 2000; Zulauf et al., 2015). Earlier studies suggested that the Pelagonian block is a fragment of Cimmerian ribbon continent (Mountrakis, 1986).

### *Reconsidering the Jurassic-early Cretaceous position of the Drina-Ivanjica- and Pelagonian blocks*

The western Pelagonian basement is overridden by the stacked ophiolite-bearing slices of Tethyan relevance referred to as the Mirdita-Pindos-Vourinos (Tremblay et al., 2015 and references therein). Eastern side is characterized by the Early Permian to Early/Middle Triassic rift stage followed by the Middle Triassic Maliac oceanization (De Bono et al., 2001). The majority of the reconstructions illustrate the Drina-Ivanjica block plus Pelagonian basement as a continental segment onto which the Late Jurassic – early Cretaceous Neotethyan or Western Vardar ophiolites were obducted (*e.g.*, Hrvatović & Pamić, 2005; Schmid et al., 2008). However, several new inferences imply a different unaligned position of the two basement units.

The Pelagonian block had two different positions throughout the Paleozoic that unambiguously affected its Jurassic location. The paleo-continental inheritance data indicate the two different locations throughout the late Paleozoic: (i). Pelagonian block may represent a segment of the Euroasian margin directed towards the Sakarya segment positioned to the east of Paleotethyan pivot point (*e.g.*, Vavvasis et al., 2000; Fig. 4). Meaning that the Pelagonian block may represent a crustal fragment or as a crustal fragment separately involved in the Variscan amalgamation of southern Variscan belt (see Zulauf et al., 2015, for a discussion; Spahić et al., 2019b). This marginal crustal fragment underwent

immediate early Permian exhumation (ages are 295–280 Ma; Vavassis et al., 2000), which is not the case for the Adria/Apulia. Consequently, both positions proposed for the Pelagonian fragment have a different early Alpine i.e. pre-rift locations relative to the Apulia/Adria. In other words, the Pelagonian block cannot be aligned with the Drina-Ivanjica block as the northeastern most Adria tip which was more to the west. This paleogeographic situation lasted during the Permian-Triassic (Fig. 4), probably continuing during the Jurassic (Stampfli & Kozur, 2006). The early Alpine extension and interference of the terminal Paleotethyan rollback stage (Vavassis et al., 2000; Stampfli & Borel, 2002; see reconstructions of Moix et al., 2008) induced the embayment of the intervening Maliac Ocean (between Pelagonian block and Serbo-Macedonian Unit; De Bono et al., 2001; Ferrière et al., 2012, 2016; Spahić et al., 2020). The opening of the Maliac produced by the Permian extension (Fig. 4), triggered a rifting off the Pelagonide block, moving it slightly away from the South Euroasian margin or away from the southern Serbo-Macedonian Unit, and its hinterland (also referred to as the "Transdanubian", Moix et al., 2008). Thus, the Pelagonian microplate was sandwiched between the Pindos (to the west) and Maliac Ocean (to the east)

during Late Triassic (see reconstruction of Vavassis et al., 2000; Stampfli & Kozur, 2006; Moix et al., 2008; Zulauf et al., 2015). The modern-day stacked architecture of the pre-Neogene nappes of the External Hellenides is response of the northward Cenozoic subduction (Pindos Ocean) and collision between the Apulia and the Pelagonian microcontinent (Mountrakis 1986; Xypolias et al., 2005).

Considering the separate position of the Drina-Ivanjica block (and entire Apulia/Adria) from the Pelagonian microplate, such a relationship suggests that the early Pindos Ocean could have been in connection with the "Dinaric Tethys". This paleocean was to the west of the Pelagonides and to the southeast of the Drina-Ivanjica block (similar as in Channel & Kozur, 1997; Fig. 5). To the north, the "Dinaric Tethys" as an Upper Triassic – Upper Jurassic segment of a separate Neotethyan mini-ocean was already closed by the early Cretaceous (Pamić, 1998; Faul et al., 2014; Fig. 5). The "Pindos – Mirdita – Dinaric Tethys" oceanic entity (not seaway as there is a documented evidence of separate Jurassic oceanic crust) had no direct link with the more internal Triassic Maliac Ocean (as proposed by Faul et al., 2014). On the other hand, being in the intervening position, the issue of the inheritance of the Adria-derived Kopaonik system (Zelić et al., 2005, 2010; Schefer et al., 2010) remains open for another set of future inferences.

In the early Mesozoic paleogeographic context, during a limited Jurassic interval, several oceans (oceanic lithosphere developed) were identified in the area of the Western Balkan countries (Fig. 5; also, in Dimitrijević, 2001; Karamata, 2006; Stampfli & Kozur, 2006; Spahić & Gaudeyti, 2020c). The developments of the NW Neotethys or Vardar Ocean corresponds to the crustal extension of the Adria microplate and the formation of, at least, two marginal micro-oceans: the "Dinaric Tethys" seems to be a kind of "Red Sea-type" narrow landlocked ocean (Robertson & Karamata, 1994). This rather confined oceanic tract was in the proximity of the advancing Jurassic Vardar Ocean divided by the "Drina – Pelagonide continental splinter", yet in connection with the latter (to the west of Jadar block; Fig. 5). The two oceanic entities can be easily traced by the central-positioned Jurassic continental splinter Drina-Ivanjica continental block (Figs. 1b and 5). The Pelagonian microplate was presumably a segment of the early Alpine south Euroasian margin, a crystalline block which inherited its position after the Variscan amalgamation,

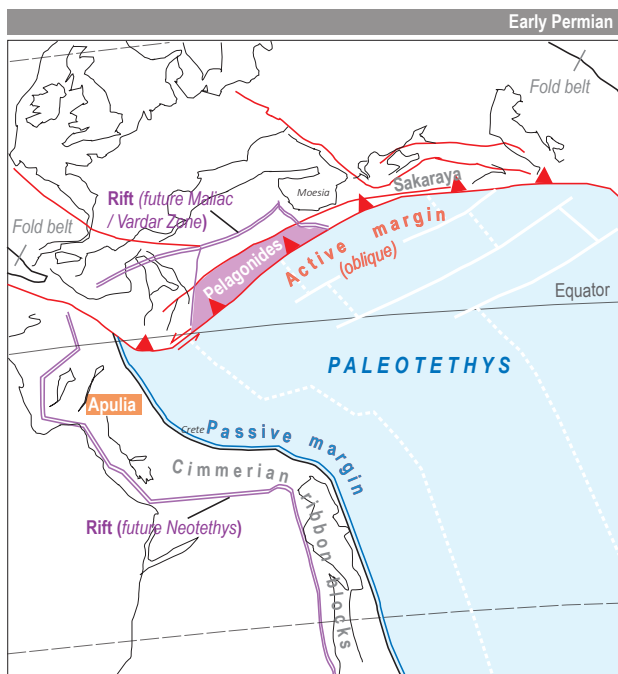


Fig. 4. The position of the Pelagonian block relative to Apulia microplate during Early Permian (inset from Vavassis et al., 2000, slightly modified). The figure pinpoints the position of the Pelagonian block (to the east, adjoining the Sakaraya block), relative to the Apulia, which was more towards the westernmost pivot point of Paleotethys.

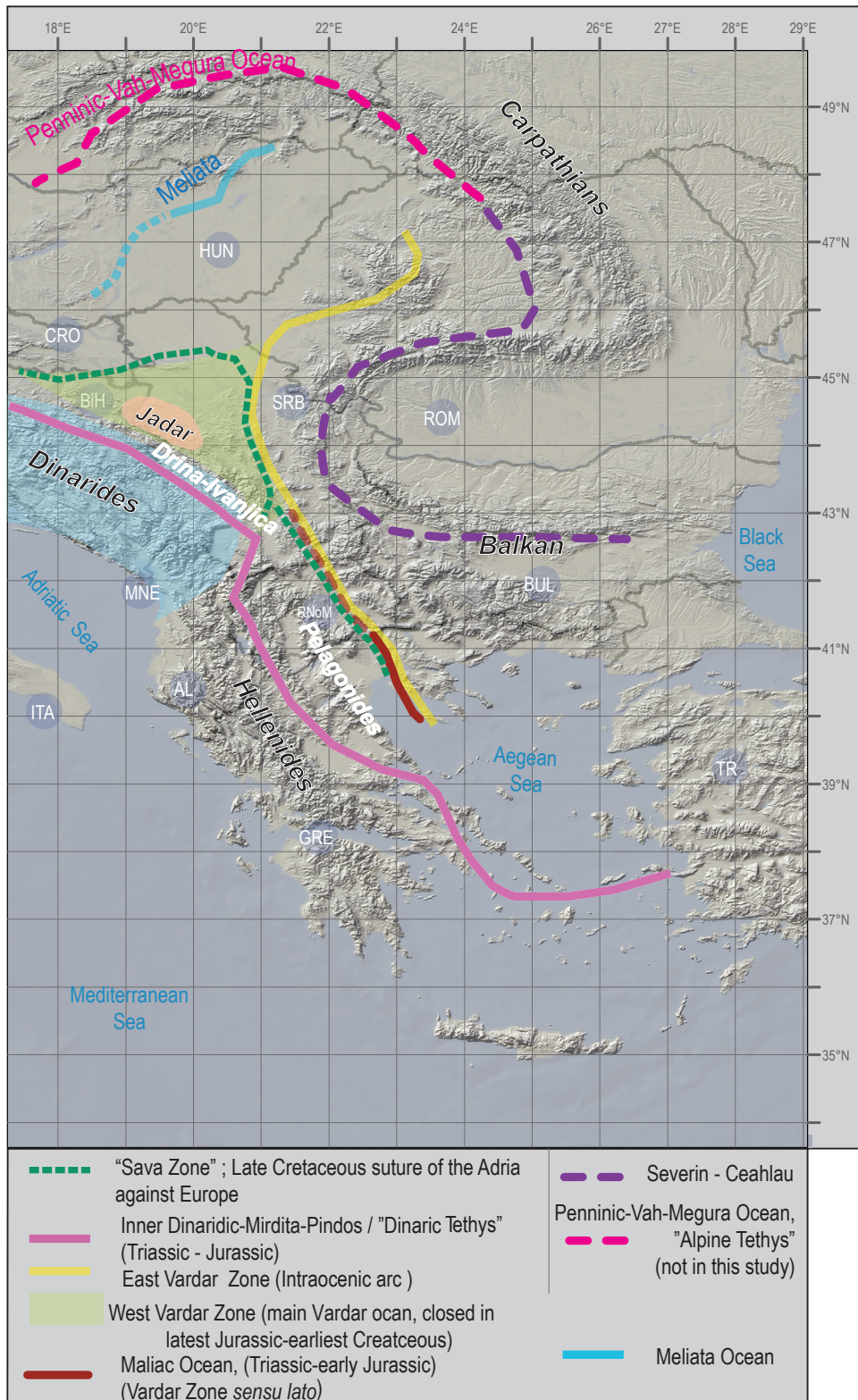


Fig. 5. The remnants of Mesozoic oceanic troughs (ophiolite belts, suture zones) and microcontinents in the wider Carpathian-Balkan-Dinaride-Hellenide areas (some suture traces taken from Csontos and Vörös, 2004, modified and updated). The “Sava Zone” (*sensu* Pamić, 2002) represents a version of the “Late Cretaceous suture” (beyond the scope of this paper). The Drina-Ivanjica block and Pelagonide block are engulfed by several suturing-related troughs: “Dinaric Tethys” to the west, West Vardar Zone to the east, including the “Sava Zone” and the precursory Maliac Ocean.

spatially overridden only after the final emplacement of the Vardar ophiolite during Valanginian time (initiated at latest Bathonian to Early Callovian; Scherreiks et al., 2014), i.e. Early Jurassic consummation of the precursory Maliac Ocean.

During the terminal late Jurassic stage and the closure of the main Neotethys, the Vardar oceanic lithosphere underthrusted the intra-ocean-

ic system (East Vardar Zone) positioned in front of the Serbo-Macedonian Unit (e.g., Boev et al., 2018; Spahić & Gaudenyi, 2019; Figs. 3a and 4). Across the opposite side of the Jurassic ‘Zvornik suture’, in line with the closure of the Neotethys or Vardar Ocean, the West Vardar were ophiolites obducted onto the Adria passive margin (Spahić and Gaudenyi, 2020c). The East Vardar Zone in

North Macedonia was at the back of the Pelagonian basement block, whereas the late Paleocene – Lower Miocene shortening (underthrusting of Apulia beneath Pelagonian block) closed the Pindos Ocean (Xypolias et al., 2008 and references therein). Consequently, there were at least two discrete Triassic–early Jurassic marginal oceanic entities accommodated on both sides of the Pelagonian microplate (Pindos- and Maliac oceans; cf. Ferrière et al., 2012). With regards to the post-dating Late Cretaceous – Paleogene “Sava-(Vardar) Zone” (sensu Pamić, 2002; Schmid et al., 2008) as the principal “oceanic” or Neotethyan suture (Fig. 5), there is no solid evidence of the existence of the post-Jurassic oceanic crust (see Cvetković et al., 2016, for a discussion; Spahić & Gaudenzi, 2021).

## Conclusions

The study emphasizes the Triassic – Jurassic paleogeography of the seemingly interlinked regional microplates: Adria/Apulia with the Drina–Ivanjica block and Inner Dinaric Ophiolite belt, from Pelagonides and Western Vardar oceanic lithosphere. The results show the presence of the two probably subduction-driven distinct Jurassic Tethyan oceans abutting Drina–Ivanjica and Pelagonian block (“Drina–Pelagonide continental splinter”): The Inner Dinaric–(Mirdita–Pindos) Ocean / “Dinaric Tethys” (identified by the Inner Dinaric Ophiolite Belt) and the Vardar Ocean (identified by the West Vardar Zone of Karamata, 2006). The “Dinaric Tethys” / Inner Dinaric–(Mirdita–Pindos) ocean was situated to the southwest of the “Drina–Pelagonian splinter” or Drina–Ivanjica block and to the west of the Pelagonides, whereas the main Neotethys was towards the east.

## Acknowledgement

This research did not receive any specific grant from funding agencies in the public, commercial or not-for-profit sectors. We are grateful anonymous reviewers for constructive and helpful comments on the manuscript. We thank Bernarda Bošković for guidance throughout the manuscript review process.

## References

- Anders, B., Reischmann T. & Kostopoulos, T. 2007: Zircon geochronology of basement rocks from the Pelagonian Zone, Greece: constraints on the pre-Alpine evolution of the westernmost Internal Hellenides. *International Journal of Earth Sciences*, 96: 639–661.
- Avigad, D., Abbo, A. & Gerdes, A. 2016: Origin of the Eastern Mediterranean: Neotethys rifting along a cryptic Cadomian suture with Afro-Arabia. *Geological Society of America Bulletin*, 128/7–8: 1286–1296.
- Bernoulli, D. & Jenkyns, H.C. 1974: Alpine Mediterranean and central Atlantic Mesozoic facies in relation to the early evolution of the Tethys. *Society of Economic Paleontologists and Mineralogists - Special Publication* 18: 129–160.
- Bernoulli, D. & Laubscher, H. 1972: The palinospastic problem of the Hellenides. *Eclogae geologicae Helvetiae*, 65: 107–118.
- Boev, B., Cvetković, V., Prelević, D., Šarić, K. & Boev, I. 2018: East Vardar ophiolites revisited: A brief synthesis of geology and geochemical data. *Contributions, Section of Natural, Mathematical and Biotechnical Sciences. Macedonian Academy of Sciences and Arts*, 39/1: 51–68
- Bortolotti, V., Chairi, M., Marroni, M., Pandolfi, L., Principi, G. & Saccani, E. 2013: Geodynamic evolution of ophiolites from Albania and Greece (Dinaric–Hellenic belt): one, two, or more oceanic basins? *International Journal of Earth Sciences*, 102: 783–811.
- Borojević Šostarić, S., Neubauer, F., Handler, R. & Palinkaš, L. A. 2012: Tectonothermal history of the basement rocks within the NW Dinarides: New  $^{40}\text{Ar}/^{39}\text{Ar}$  ages and synthesis. *Geologica Carpathica*, 63/6: 441–452. <https://doi.org/10.2478/v10096-012-0034-2>
- Channel, J.E.T. & Kozur, H.W. 1997: How many oceans? Meliata, Vardar, and Pindos oceans in Mesozoic Alpine paleogeography. *Geology*, 25/2: 183–186.
- Chiari, M., Djerić, N., Garfagnoli, F., Hrvatović, H., Krstić, M., Levi, N., Malasoma, A., Marroni, M., Menna, F., Nirta, G., Pandolfi, L., Principi, G., Saccani, E., Stojadinović, U. & Trivić, B. 2011: The Geology of the Zlatibor–Maljen Area (Western Serbia): A Geotraverse across the Ophiolites of the Dinaric–Hellenic Collisional Belt. *Ophioliti*, 36/2: 139–166.
- Csontos, L., Gerzina, N., Hrvatović, H., Schmid, S.M. & Tomljenović, B. 2004: Structural evolution of the Internal Dinarides: a preliminary study based on selected regions. *5th International Symposium on Eastern Mediterranean Geology*, Thessaloniki, Greece, 14–20 April 2004, T11-7.
- Csontos, L. & Vörös, A. 2004: Mesozoic plate tectonic reconstruction of the Carpathian region. *Palaeogeography, Palaeoclimatology, Palaeoecology*, 210: 1–56.

- Cvetković, V., Prelević, D. & Schmid, S. 2016: Geology of South-Eastern Europe. In: Papic, P. (eds.): Mineral and Thermal Waters of Southeastern Europe. Environmental Earth Sciences book series. Springer International Publishing, 1–29.
- Cvijić, J. 1924: Geomorfologija – Mophologie Terrestres. Državna štamparija SHS. Belgrade. 1588 p. (in Serbian)
- De Bono, A., Martini, R., Zaninetti, L., Hirsch, F., Stampfli, G.M. & Vavassis, I. 2001: Permo-Triassic stratigraphy of the Pelagonian zone in central Evia island (Greece). *Eclogae Geologicae Helvetiae*, 94: 289–311.
- Dilek, Y. & Furnes, H. 2005: Tethyan ophiolites and Tethyan seaways. *Journal of the Geological Society*, 176: 899–912.
- Dilek, Y., Shallo, M. & Furnes, H. 2005: Rift-drift, seafloor spreading, and subduction tectonics of Albanian ophiolites. *International Geological Review*, 47: 147–176.
- Dilek, Y., Shallo, M. & Furnes, H. 2007: Suprasubduction zone ophiolite formation along the periphery of Mesozoic Gondwana. *Gondwana Research*, 11: 453–475.
- Dimitrijević, M. 1992: Geološka karta Srbije 1: 2,000,000 (Geološki atlas 1) = Geological Map of Serbia, 1: 200,000 (Geological Atlas 1). Faculty of Mining and Geology - University of Belgrade and Geozavod Gemini, Belgrade. (in Serbian)
- Dimitrijević, M.D. 1997: Geology of Yugoslavia. Geoinstitute, Belgrade: 182 p.
- Dimitrijević, M. 1999: Geotectonic map in scale 1: 2,000,000. Ministry for Mining and Energetics of Serbia and Geomagnetic Institute. Belgrade.
- Dimitrijević, M.D. 2001: Dinarides and the Vardar Zone: a short review of the geology. *Acta Vulcanologica*, 13/1–2: 1–8.
- Dimitrijević, M.D. & Dimitrijević, M.N. 1973: Olistostrome Mélange in the Yugoslavian Dinarides and Late Mesozoic Plate Tectonics. *The Journal of Geology*, 81/3: 328–340. <https://www.jstor.org/stable/30084828>
- Dimitrijević, M.D. & Dimitrijević, M.N. 1975: Ofiolitski melanž Dinarida i Vardarske Zone: Geneza i geotektonsko značenje = Ophiolite mélange of the Dinarides and the Vardar Zone: Genesis and its geotectonic importance. II godišnji znanstveni skup, Znanstveni savjet za naftu JAZU, Sekcija za primjenu geologije, geofizike i geokemije, ser. A, 5: Zagreb. 39–46. (in Serbo-Croatian)
- Dimitrijević, M.N., Dimitrijević, M.D., Karamata, S., Sudar, M., Gerzina, N., Kovács, S., Dosztály, L., Gulászi, Z., Less, G. & Pelikán, P. 2003: Olistostome/mélanges – an overview of the problems and preliminary comparison of such formations in Yugoslavia and NE Hungary. *Slovak Geological Magazine*, 9/1: 3–21.
- Doković, I. 1985: Primena strukturne analize na rešavanje građe paleozojskih tvorevina Drinsko-Ivanjičke oblasti = Application of structural analysis in solving the Paleozoic formations of Drina-Ivanjica area – In Serbian. *Geološki anali Balkanskoga poluostrva*, 49: 11–160. (in Serbian, English summary).
- Faul, U.H., Garapić, G. & Lugović, B. 2014: Subcontinental rift initiation and oceancontinent transitional setting of the Dinarides and Vardar zone: Evidence from the Krivaja – Konjuh Massif, Bosnia and Herzegovina. *Lithos*, 202–203: 283–299.
- Ferrière, J., Baumgartner, P.O. & Chanier, F. 2016: The Maliac Ocean: the origin of the Tethyan Hellenic ophiolites. *International Journal of Earth Sciences*, 105/7: 1941–1963.
- Ferrière, J., Chanier, F. & Ditbanjong, F. 2012: The Hellenic ophiolites: eastward or westward obduction of the Maliac Ocean, a discussion. *International Journal of Earth Sciences*, 101/6: 1559–1580.
- Filipović, I. & Sikošek, B. 1999: Pre-Variscan and Variscan successions of the Drina anticlinorium and the Drina-Ivanjica Paleozoic. *Bulletin*, Tome 119 Serbain Academy of Sciences and Arts, Classe Sciences mathématiques et naturelles, Sciences naturelles, 39: 61–71.
- Filipović, I., Jovanović, D., Sudar, M., Pelikán, P., Kovács, S., Less, G. & Hips, K. 2003: Comparison of Variscan–early Alpine evolution of the Jadran Block (NW Serbia) and “Bükkium” (NE Hungary) terranes; some paleogeographic implications. *Slovak Geological Magazine*, 9/1: 23–40.
- Franke, W., Cocks, L.R.M. & Torsvik, T.H. 2017: The Palaeozoic Variscan oceans revisited. *Gondwana Research*, 48: 257–284.
- Gaggero, L., Marroni, M., Pandolfi, L. & Buzzi, L. 2009: Modeling the oceanic lithosphere obduction: Constraints from the metamorphic sole of Mirdita ophiolites (northern Albania). *Ophioliti*, 34/1: 17–42.
- Gerzina, N. 2010: Strukturne karakteristike i tektogeneza Zvorničkog šava = Structural

- Characteristic and Tectogenesis of Zvornik Suture zone. PhD-thesis, Belgrade University, Faculty of Mining and Geology (manuscript), Beograd: 142 p.
- Goričan, S., Karamata, S., Batočanin-Srećković, D. 1999: Upper Triassic (Carnian-Norian) radiolarians in cherts of Sjenica (SW Serbia) and the time span of the oceanic realm ancestor of the Dinaridic Ophiolite Belt. *Bulletin de l'Académie Serbe des Sciences et des Arts* 119 - Classe Sciences Mathématiques et Naturelles, 39: 141–149.
- Handy, M.R., Ustaszewski, K. & Kissling, E. 2015: Reconstructing the Alps-Carpathians-Dinarides as a key to understanding switches in subduction polarity, slab gaps and surface motion. *Int J Earth Sci (Geol Rundsch)*, 104: 1–26.
- van Hinsbergen, D.J.J., Torsvik, T.H., Schmid, S.M., Maťenco, L.C., Maffione, M., Reinoud L.M., Gürer, D. & Spakman, W. 2020: Orogenic architecture of the Mediterranean region and kinematic reconstruction of its tectonic evolution since the Triassic. *Gondwana Research*, 81: 79–229. <https://doi.org/10.1016/j.gr.2019.07.009>
- Hrvatović, H. & Pamić, J. 2005: Principal thrust-nappe structures of the Dinarides. *Acta Geologica Hungarica*, 48/2: 133–151. <https://doi.org/10.1556/ageol.48.2005.2.4>
- Jolivet, L., Faccena, C., Agard, P., de Lamotte, D.F., Menant, A., Sternai, P. & Guillocheau, F. 2016: Neo-Tethys geodynamics and mantle convection: from extension to compression in Africa and a conceptual model for obduction. *Canadian Journal of Earth Sciences*, 53/11: 1190–1204. <https://doi.org/10.1139/cjes-2015-0118>
- Karamata, S. 2006: The geological development of the Balkan Peninsula related to the approach, collision and compression of Gondwanan and Eurasian units. In: Robertson, A.H.F. & Mountrakis, D. (eds.): *Tectonic Development of the Eastern Mediterranean Region*. Geological Society of London, Special Publication, 260: 155–178.
- Karamata, S. & Krstić, B. 1996: Terranes of Serbia and neighbouring areas. In: Knežević-Dorđević, V. & Krstić, B. (eds.): “Terranes of Serbia” - The Formation of the geologic framework of Serbia and Adjacent regions. Department of Petrology; Faculty of Mining and Geology – University of Belgrade, Belgrade: 25–40.
- Karamata, S., Knežević, V., Memović, E. & Popević, A. 1994: The evolution of the northern of the Vardar Zone in Mesozoic. *Bulletin of the Geological Society of Greece*, 32: 479–486.
- Kearey, P., Klepeis, K.A. & Vine, F.J. 2009: *Global Tectonics*. Wiley-Blackwell: 496 p.
- Kolar-Jurkovšek, T., Hrvatović, H., Aljinović, D., Nestell, G.P., Jurkovšek, B. & Skopljak, F. 2019: Konodonti profila Teočak: granična perm-trijas (Conodonts of the Teočak section: Permian-Triassic boundary – in Bosnian). In: *Zbornik radova, 6. knjiga sažetaka. II Kongres geologa Bosne i Hercegovine 2–4.10.2019. Udrženje / Udruga geologa Bosne I Hercegovine, Laktaši: 2–4.*
- Kroner, U. & Romer, R.L. 2013: Two plates – many subduction zones: The Variscan orogeny reconsidered. *Gondwana Research*, 24: 298–329.
- Krstić, N., Maslarević, L.J. & Sudar, M. 2005: On the Graptolite Schists Formation (Silurian-Lower Devonian) in the Carpatho-Balkanides of eastern Serbia. *Geološki anali Balkanskoga poluostrva*, 66: 1–8.
- Maffione, M. & van Hinsbergen, D.J.J. 2018: Reconstructing plate boundaries in the Jurassic Neo-Tethys from the East and West Vardar Ophiolites (Greece and Serbia). *Tectonics*, 37/3: 858–887.
- Milovanović, D. 1984: Petrology of low-metamorphic rocks from the central part of the Drina-Ivanjica Paleozoic. *Glasnik Prirodnjačkog Muzeja ser. A*, 39: 13–139 (in Serbian with English summary).
- Mountrakis, D. 1986: The Pelagonian zone in Greece, a polyphase deformed fragment of the Cimmerian continent and its role in the geotectonic evolution of the Eastern Mediterranean. *Journal of Geology*, 94/3: 335–347. <https://doi.org/10.1086/629033>
- Nance, D. 1981: Tectonic history of a tectonic segment of the Pelagonian zone, north-eastern Greece. *Canadian Journal of Earth Sciences*, 18: 1111–1126.
- Neubauer, F., Yoingjiang, L., Shuyun, C. & Yuan, S. 2019: What is the Austroalpine mega-unit and what are the potential relations to Paleotethyan ocean remnant of southeastern Europe? *Proceedings of the Geologica Carpathica 70 Conference*. Earth Science Institute of the Slovak Academy of Sciences. Bratislava. 16–20.
- Pamić, J. 2002: The Sava-Vardar Zone of the Dinarides and Hellenides versus the Vardar Ocean. *Eclogae geologicae Helvetiae*, 95: 99–113.

- Pamić, J. & Jurković, I. 2002: Paleozoic tectono-stratigraphic units of the northwest and central Dinarides and the adjoining South Tisia. *International Journal of Earth Sciences*, 91/3: 538–554. <https://doi.org/10.1007/s00531-001-0229-8>
- Pamić, J., Gušić, I. & Jelaska, V. 1998: Geodynamic evolution of the Central Dinarides. *Tectonophysics*, 297: 251–268.
- Picha, F.J. 2002: Late orogenic strike-slip faulting and escape tectonics in frontal Dinarides-Hellenides, Croatia, Yugoslavia, Albania, and Greece. *American Association of Petroleum Geologists Bulletin*, 86/9: 1659–1671.
- Porkoláb, K., Kövér, S., Benkó, Z., Héja, G.H., Fialowski, M., Soós, B., Gerzina Spajić, N., Đerić, N. & Fodor, L. 2018: Structural and geochronological constraints from the Drina-Ivanjica thrust sheet (Western Serbia): Implications for the Cretaceous – Paleogene tectonics of the Internal Dinarides. *Swiss Journal of Geosciences*, 112: 1–18. <https://doi.org/10.1007/s00015-018-0327-2>
- Protić, D. 1995: Mineralne i termalne vode Srbije = Mineral and Thermal waters of Serbia. Geoinstitut: 270 p. (in Serbian).
- Robertson, A.H.F. 2012: Late Palaeozoic–Cenozoic tectonic development of Greece and Albania in the context of alternative reconstructions of Tethys in the Eastern Mediterranean region. *International Geology Review*, 54/4: 373–454. <https://doi.org/10.1080/00206814.2010.543791>
- Robertson, A. & Karamata, S. 1994. The role of subduction-accretion processes in the tectonic evolution of the Mesozoic Tethys in Serbia. *Tectonophysics*, 234: 73–94. [https://doi.org/10.1016/0040-1951\(94\)90205-4](https://doi.org/10.1016/0040-1951(94)90205-4)
- Robertson, A., Karamata, S. & Šarić, K. 2009: Overview of ophiolites and related units in the Late Palaeozoic–Early Cenozoic magmatic and tectonic development of Tethys in the northern part of the Balkan region. *Lithos*, 108: 1–36. <https://doi.org/10.1016/j.lithos.2008.09.007>
- Saccani, E., Photiades, A., Sontato, A. & Zeda, O. 2008: New evidence for supra-subduction zone ophiolites in the Vardar Zone of northern Greece: implications for the tectono-magmatic evolution of the Vardar Oceanic basin. *Ophioliti*, 33: 65–85.
- Saccani, E., Beccaluva, L. Photiades, A. & Zeda, O. 2011: Petrogenesis and tectonomagmatic significance of basalts and mantle peridotites from the Albanian-Greek ophiolites and sub-ophiolite mélange. New constraints for the Triassic–Jurassic evolution of the Neo-Tethys in Dinaride sector. *Lithos*, 124/3–4: 227–242. <https://doi.org/10.1016/j.lithos.2010.10.009>
- Saccani, E., Dilek, Y., Marroni, M. & Pandolfi, L. 2015: Continental margin ophiolites of Neotethys: Remnants of Ancient Ocean; Continent Transition Zone (OCTZ) lithosphere and their geochemistry, mantle sources and melt evolution patterns. *Episodes*, 38: 230–249. <https://doi.org/10.18814/epiugs/2015/v38i4/82418>
- Saccani, E., Dilek, Y. & Photiades, A. 2017: Time-progressive mantle-melt evolution and magma production in a Tethyan marginal sea: A case study of the Albanide-Hellenide ophiolites. *Lithosphere*, 10/1: 35–53. <https://doi.org/10.1130/L602.1>
- Schefer, S., Egli, D., Missoni, S., Bernoulli, D., Fügenschuh, B., Gawlick, H.-J., Jovanovic, D., Krystyn, L., Lein, R., Schmid, S. & Sudar, M. 2010: Triassic metasediments in the internal Dinarides (Kopaonik area, southern Serbia): Stratigraphy, paleogeographic and tectonic significance. *Geologica Carpathica*, 61: 89–109.
- Scherreiks, R., Meléndez, G., Boudagher-Fadel, M., Fermeli, G. & Bosence, D. 2014: Stratigraphy and tectonics of a time-transgressive ophiolite obduction onto the eastern margin of the Pelagonian platform from Late Bathonian until Valanginian time, exemplified in northern Evvoia, Greece. *International Journal of Earth Sciences*, 103/8: 2191–2216. <https://doi.org/10.1007/s00531-014-1036-3>
- Schmid, M.S., Bernoulli, D., Fügenschuh, B., Matenco, L., Schefer, S., Schuster, R., Tischler, M. & Ustaszewski, K. 2008: The Alps-Carpathians-Dinarides-connection: a correlation of tectonic units. *Swiss Journal of Geosciences*, 101/1: 139–183. <https://doi.org/10.1007/S00015-008-1247-3>
- Schmid, M.S., Fügenschuh, B., Kounov, A., Matenco, L., Nievergelt, P., Oberhänsli, R., Pleugerg, J., Schefer, S., Schuster, R., Tomljenović, B., Ustaszewski, K. & van Hinsbergend, D.J.J. 2020: Tectonic units of the Alpine collision zone between Eastern Alps and western Turkey. *Gondwana Research*, 78: 308–374. <https://doi.org/10.1016/j.gr.2019.07.005>
- Siegesmund, S., Oriolo, S., Heinrichs, T., Basei, M.A.S., Nolte, N., Hüttenrauch, F. & Schulz, B. 2018: Provenance of Austroalpine basement metasediments: tightening up Early Palaeozoic connections between

- peri-Gondwanan domains of central Europe and Northern Africa. International Journal of Earth Sciences, 107/6: 2293–2315. <https://doi.org/10.1007/s00531-018-1599-5>
- Spahić, D. & Gaudenzi, T. 2018: Primordial geodynamics of Southern Carpathian – Balkan basements (Serbo-Macedonian Mass): Avalonian vs. Cadomian arc segments. Proceedings of the Geologists' Association, 130: 142–156. <https://doi.org/10.1016/j.pgeola.2018.10.006>
- Spahić, D., Glavaš-Trbić, B., Đajić, S. & Gaudenzi, T. 2018: Neoproterozoic – late Variscan geodynamics of the Drina Formation (Drina-Ivanjica metamorphic basement). Geološki anali Balkanskoga poluostrva, 79/2: 57–68. <https://doi.org/10.2298/GABP1802057S>
- Spahić, D., Glavaš-Trbić, B. & Gaudenzi, T. 2019a: A hidden suture within the northern Paleotethyan margin: Paleogeographic/paleo-tectonic constraints on the Paleozoic 'Veles Series' (Vardar Zone, North Macedonia). Proceedings of the Geologists' Association, 130/6: 701–718.
- Spahić, D., Gaudenzi, T. & Glavaš-Trbić, B. 2019b: The Neoproterozoic – Paleozoic basement in the Alpidic Suupragetic/Kučaj units of eastern Serbia: a continuation of the Rheic Ocean? Acta Geologica Polonica, 69/4: 531–548. <https://doi.org/10.24425/agp.2019.126446>
- Spahić, D., Glavaš-Trbić, B., Gaudenzi, T. & Poznanović-Spahić, M. 2019c: Paleozoic paleogeography and tectonic evolution of the Apulia/Adria microplate – is there a Variscan interference or not? In: Zbornik radova, 6. knjiga sažetaka. II Kongres geologa Bosne i Hercegovine 2-4.10.2019. Udruženje / udružuga geologa Bosne i Hercegovine: 42–46.
- Spahić, D. & Gaudenzi, T. 2019: Intraoceanic subduction of the northwestern Neotethys and geodynamic interaction with Serbo-Macedonian foreland: Descending vs. overriding neartrench dynamic constraints (East Vardar Zone, Jastrebac Mts., Serbia). Geološki anali Balkanskoga poluostrva, 80/2: 65–85.
- Spahić, D. & Gaudenzi, T. 2020a: Reconsidering late Paleozoic differences between the Jadran block and the Drina-Ivanjica unit. Geološki anali Balkanskoga poluostrva, 81/1: 1–9.
- Spahić, D. & Gaudenzi, T. 2020b: A few remarks on Triassic paleogeography and the geodynamic link between the Dinarides and the Serbo-Macedonian unit. Geološki anali Balkanskoga poluostrva, 81/1: 79–88.
- Spahić, D. & Gaudenzi, T. 2020c: The role of the 'Zvornik suture' for assessing the number of Neotethyan oceans: Surface – subsurface constraints on the fossil plate margin (Vardar Zone vs. Inner Dinarides). Geoloski anali Balkanskoga poluostrva, 81/2: 63–86.
- Spahić, D., Glavaš-Trbić, B. & Gaudenzi, T. 2020: The inception of the Maliaç Ocean: Regional geological constraints on the western Circum-Rhodope belt (northern Greece). Marine and Petroleum Geology, 113: 104–133. <https://doi.org/10.1016/j.marpetgeo.2019.104133>
- Spahić, D. & Gaudenzi, T. 2021: On the Sava Suture Zone: Post-Neotethyan Oblique Subduction and the Origin of the Late Cretaceous Mini-Magma Pools. Cretaceous Research, 181. <https://doi.org/10.1016/j.cretres.2021.105062>
- Stampfli, G.M. & Borel, G.D. 2002: A plate tectonic model for the Paleozoic and Mesozoic constrained by dynamic plate boundaries and restored synthetic oceanic isochrons. Earth Planetary Science Letters, 196: 17–33.
- Stampfli, G.M., Borel, G.D., Cavazza, W., Mosar, J. & Ziegler, P.A. 2001: Palaeotectonic and palaeogeographic evolution of the western Tethys and PeriTethyan domain (IGCP Project 369). Episodes, 24: 222–228. <https://doi.org/10.18814/epiugs/2001/v24i4/001>
- Stampfli, G.M. & Kozur, H.W. 2006: Europe from the Variscan to the Alpine cycles. In: Gee, D.G. & Stephenson, R.A. (eds.): European Lithosphere Dynamics. Geological Society of London, Memoirs, 32: 57–82.
- Šostek, A., Zavašnik, J., O'Sullivan, P., Herlec, U., Potočnik, B., Krajnc, B., Palinkaš, L., Zupančič, N. & Dolenc, M. 2020: Geochemistry of Bashibos-Bajrambos Metasedimentary Unit, Serbo-Macedonian massif, North Macedonia: Implications for Age, Provenance and Tectonic Setting. Chemie der Erde – Geochemistry, 80/4:125664. <https://doi.org/10.1016/j.chemer.2020.125664>
- Tomljenović, B., Csontos, L., Márton, E. & Márton, P. 2008: Tectonic evolution of the northwestern Inner Dinarides as constrained by structures and rotation of Medvednica Mountains, North Croatia. In: Siegesmund, S., Fügenschuh, B. & Froitzheim N. (eds.): Tectonic Aspects of the Alpine-Dinaride-Carpathian System. Geological Society of London, Special Publications, 298: 145–167.
- Tremblay, A., Meshi, A., Deschamps, T., Goulet, F. & Goulet, N. 2015: The Vardar zone as a suture for the Mirdita ophiolites, Albania: Constraints from the structural analysis of the Korabi-Pelagonia zone. Tectonics, 34/2: 352–375. <https://doi.org/10.1002/2014TC003807>

- Trivić, B., Cvetković, V., Smiljanić, B. & Gajić, R. 2010: Deformation pattern of the palaeozoic units of the Tethyan suture in the central Balkan Peninsula: a new insight from study of the Bukulja-Lazarevac Paleozoic unit Serbia. *Ophioliti*, 35/1: 21–32. <https://doi.org/10.4454/ophioliti.v35i1.384>
- Vavvasis, I., Bono, A. de, Stampfli, G.M., Giorgis, D., Valloton, A. & Amelin, Y. 2000: U-Pb and Ar-Ar geochronological data from the Pelagonian basement in Evia (Greece): geodynamic implications for the evolution of Paleotethys. *Schweizerische mineralogische und petrographische Mitteilungen*, 80: 21–33. <https://doi.org/10.5169/seals-60948>
- Xypolias, P., Koukouvelas, I. & Gernold, Z. 2008: Cenozoic tectonic evolution of northeastern Apulia: insights from a key study area in the Hellenides (Kythira, Greece). *Zeitschrift der Deutschen Gesellschaft für Geowissenschaften*, 159/3: 439–455. <https://doi.org/10.1127/1860-1804/2008/0159-0439>
- Zelić, M., D’Orazio, M., Malasoma, A., Marroni, M. & Pandolfi, L. 2005: The Metabasites from the Kopaonik metamorphic complex, Vardar Zone, southern Serbia: remnants of the rifting-related magmatism of the Mesotethyan domain or evidence for Paleotethys closure in the Dinaric-Hellenic belt? *Ophioliti*, 30/2: 91–101.
- Zelić, M., Marroni, M., Pandolfi, L. & Trivić, B. 2010: Tectonic setting of the Vardar suture zone (Dinaric-Hellenic belt): the example of the Kopaonik area (southern Serbia). *Ophioliti*, 35/1: 33–47.
- Zlatkin, O., Avigad, D. & Gerdes, A. 2014: Peri-Amazonian provenance of the Proto-Pelagonian basement (Greece), from zircon U-Pb geochronology and Lu-Hf isotopic geochemistry. *Lithos*, 184–187: 379–392. <https://doi.org/10.1016/J.LITHOS.2013.11.010>
- Zlatkin, O., Avigad, D. & Gerdes, A. 2017: The Pelagonian terrane of Greece in the peri-Gondwanan mosaic of the Eastern Mediterranean: Implications for the geological evolution of Avalonia. *Precambrian Research*, 290: 163–183. <https://doi.org/10.1016%2Fj.precamres.2017.01.005>
- Zulauf, G., Dörr, W., Fisher-Spurlock, S.C., Gerdes, A., Chatzaras, V. & Xypolias, P. 2015: Closure of the Paleotethys in the External Hellenides: Constraints from U-Pb ages of magmatic and detrital zircons (Crete). *Gondwana Research*, 28/2: 642–667. <https://doi.org/10.1016/j.gr.2014.06.011>
- Zulauf, G., Dörr, W., Marko, L. & Krahl, A. 2018: The late Eo-Cimmerian evolution of the external Hellenides: constraints from microfabrics and U-Pb detrital zircon ages of Upper Triassic (meta)sediments (Crete, Greece). *International Journal of Earth Sciences*, 107: 2859–894. <https://doi.org/10.1007/s00531-018-1632-8>
- Žák, J., Svojtkab, M., Hajnáa, J. & Ackerman, L. 2020: Detrital zircon geochronology and processes in accretionary wedges. *Earth-Science Reviews*, 207: 103–214. <https://doi.org/10.1016/j.earscirev.2020.103214>



# Impact of climate change on landslides in Slovenia in the mid-21st century

## Vpliv podnebnih sprememb na pojavljanje zemeljskih plazov v sredini 21. stoletja v Sloveniji

Mateja JEMEC AUFLIČ<sup>1</sup>, Gašper BOKAL<sup>1</sup>, Špela KUMELJ<sup>1</sup>, Anže MEDVED<sup>2</sup>,  
Mojea DOLINAR<sup>2</sup> & Jernej JEŽ<sup>1</sup>

<sup>1</sup>Geological Survey of Slovenia, Dimičeva ulica 14, SI-1000 Ljubljana, Slovenija; e-mail:  
mateja.jemec@geo-zs.si, gasper.bokal@geo-zs.si, spela.kumelj@geo-zs.si, jernej.jez@geo-zs.si  
<sup>2</sup>Slovenian Environment Agency, Vojkova 1b, SI-1000 Ljubljana, Slovenija; e-mail: anze.medved@gov.si,  
mojea.dolinar@gov.si

Prejeto / Received 3. 8. 2021; Sprejeto / Accepted 13. 10. 2021; Objavljeno na spletu / Published online 28. 12. 2021

*Key words:* climate change, landslides, models, hazard, prediction

*Ključne besede:* podnebne spremembe, zemeljski plazovi, modeli, nevarnost, napoved

### Abstract

Slovenia is affected by extreme and intense rainfall that triggers numerous landslides every year, resulting in significant human impact and damage to infrastructure. Previous studies on landslides have shown how rainfall patterns can influence landslide occurrence, while in this paper, we present one of the first study in Slovenia to examine the impact of climate change on landslides in the mid-21st century. To do this, we used the Representative Concentration Pathway (RCP) 4.5 climate scenario and future climatology simulated by six climate models that differed from each other as much as possible while representing measured values of past climate variables as closely as possible. Based on baseline period (1981–2010) we showed the number of days with exceedance of rainfall thresholds and the area where landslides may occur more frequently in the projection period (2041–2070). We found that extreme rainfall events are likely to occur more frequent in the future, which may lead to a higher frequency of landslides in some areas.

### Izvleček

Vsako leto Slovenijo prizadenejo ekstremne in močne padavine, ki sprožijo številne zemeljske plazove, kar povzroči znaten vpliv na človeka in škodo na infrastrukturi. Prejšnje študije plazov so pokazale, kako padavine vplivajo na pojav plazov, medtem ko v tem prispevku predstavljamo eno izmed prvih študij v Sloveniji, ki proučuje vpliv podnebnih sprememb na zemeljske plazove sredi 21. stoletja. V ta namen smo uporabili scenarij značilnih potekov vsebnosti toplogrednih plinov (RCP4.5) in uporabili simulacije šestih podnebnih modelov, ki so se med seboj čim bolj razlikovali, hkrati pa kar najbolj enako predstavljali izmerjene vrednosti podnebnih spremenljivk v obdobju meritev. Na podlagi referenčnega obdobja (1981–2010) prikazujemo število dni, ko padavine presežejo sprožilne količine padavin in območja, kjer se lahko plazovi v projekcijskem obdobju (2041–2070) pogosteje pojavljajo. Rezultati kažejo, da se bodo ekstremni padavinski dogodki v prihodnosti zelo verjetno pojavljali pogosteje kot danes, kar lahko na nekaterih območjih povzroči pogostejše pojavljanje zemeljskih plazov.

### Introduction

Landslides pose a serious threat to populations worldwide, causing fatalities, property damage, and significant economic losses. The occurrence of landslides is influenced by several factors related to the stability of the slopes. Among the most important triggers is rainfall, which is one of the fundamental climate variables. In a chang-

ing climate, the frequency and intensity of rainfall events are expected to increase, although in some places the average amount of rainfall would not show any significant change.

The first beginnings of research on the effects of climate change on slope instabilities and landslides, as well as model scenario studies, date back to the end of the 20th century, when

the Intergovernmental Panel on Climate Change (IPCC) issued the first climate change assessment report Heerdegen (1991). Recently Gariano et al. (2016) published comprehensive research about landslides in a changing climate where research and methods related to climate change impact on landslides are divided into three groups. The first group combines research focus on climate change impact assessment methods. Dikau & Shrott (1999) analyzed landslide outcomes in Europe in relation to climate change between 1850 and 2000, establishing criteria for (a) landslide identification, (b) past precipitation distribution and relationship to climate variables and landslide phenomena, and (c) development of hydrogeological models to assess climate change impacts. Sidle & Ochiai (2006) analyzed the processes that cause landslides. They also considered the effects of climate change on tree species growth and land use but pointed out the complexity of the variables studied. McInnes et al. (2007) published the Proceedings of the Participants in the Conference on Landslides and Climate Change (Ventnor, UK). Crozier (2010) examined the mechanisms of landslides and the stability of slopes affected by climate change. Coe & Godt (2012) identified 14 different methods for estimating the effects of climate change on landslides. They divided all the methods into three groups: a) long-term monitoring of landslide movement, b) feedback analysis, and c) projection analysis. An important finding of all the considered methods is the high uncertainty as a consequence of the prediction of short-term intensive precipitation. On the contrary, studies that attempted to predict landslide activity through changes in air temperature and annual/seasonal precipitation show less uncertainty. The second group focus on the slope stability assessment with climate projections. Numerous studies have examined the impact of climate change on landslides using the method of empirically upgrading the spatial scale of global circular model simulations (GCM) and using past measurements of meteorological variables as an input for slope stability (Buma & Dehn, 1998; Collison et al., 2000; Tacher & Bonnard, 2007; Bonnard et al., 2008; Jakob & Lambert, 2009; Chang & Chiang, 2011; Coe, 2012; Comegna et al., 2013; Rianna et al., 2014; Gassner et al., 2015; Alvioli et al. 2016). The main findings of the research are that the intensity and duration of precipitation significantly affect the rise of groundwater and pore pressure in the soil. The third group investigate climate change impacts on slope stability

and landslide hazard. The influence of climate and its changes on landslides may be defined in general terms as: (a) local or regional (or global), (b) short-term or long-term impact, (c) direct or indirect. Local influence studies have been investigated using total/cumulative precipitation, precipitation intensity, air temperature, weather system (Collison et al., 2000; Malet et al., 2005; Tommasi et al., 2006; Dixon and Brook, 2007; Rianna et al., 2014; Zollo et al., 2014), regionally for areas ranging from a few 100 m<sup>2</sup> to a few 1000 km<sup>2</sup> (Rebetez et al., 1997; Malet et al., 2007; Gariano et al., 2015; Ciabatta et al., 2016), nationally or supra-regionally (Sidle & Dhakal, 2002; Schmidt & Glade, 2003; Winter et al., 2010; Stoffel et al., 2014; Paranunzio et al., 2016). The short-term impacts of climate change span from a few years to a century or two, while the long-term impacts are measured from several centuries to several millennia (Trauth et al., 2000; Schmidt & Dikau, 2004; Borgatti & Soldati, 2010; Yin et al., 2014). Direct impacts of climate are those that directly affect the occurrence of landslides, such as changes in the precipitation regime that affect the amount of precipitation that can cause landslides (Guzzetti et al., 2007; Jakob & Lambert, 2009; Stoffel et al., 2014). Indirect effects of climate affect environmental and landscape conditions, and these affect landslides, for example, a change in precipitation regime can change the type of land use, leading to a change in slope stability (Glade, 2003; Schmid & Glade, 2003; Sidle & Ochiai, 2006; Wasowski et al., 2010).

In Slovenia, the research of climate change impact on landslide occurrences using climate change projections has not yet been studied. Meanwhile Komac (2005), Jemec Auflič & Komac (2013), Jemec Auflič et al. (2016), Jemec Auflič et al. (2018) research rainfall induced landslides based on evidenced landslide events. The results showed that the main triggering factors for numerous shallow landslides are intensive and prolonged rainfall. These findings contributed to the formation of national rainfall induced landslide warning system (MASPREM) in Slovenia in 2013 (Jemec Auflič et al., 2016, Jemec Auflič et al., 2018) which is continuously being developed and improved. The first rainfall threshold curve for rainfall-induced landslides at the national level was presented by Rosi et al. (2016) using a statistical approach, by Jordanova et al. (2020) using an empirical approach, while Bezak et al. (2016, 2018, 2019) introduced rainfall thresholds for the smaller regions in Slovenia using mainly hydrological data. However, extreme or intense

rainfall events trigger more than a hundred landslides in Slovenia every year (Jemec Auflič et al., 2018).

The main objective of this paper is to study climate change impact on landslides in the mid of 21<sup>st</sup> century in Slovenia. For this purpose, we used the Representative Concentration Pathway climate scenario (RCP4.5), which is considered a moderately optimistic scenario and predict a gradual reduction of emissions and a stabilization of the radiative contribution shortly after 2100 (IPCC, 2018). In detail, we present the number of days with exceedance of rainfall thresholds and the area where landslides may occur more frequently in mid of 21st century period. We considered RCP4.5 data as the baseline period (1981–2010) based on which we made the assessment of the impact of climate change on landslides in the future.

## Data and methods

### Climate models data

Climate change scenarios play an important role in the preparation of a landslide risk assessment and adaptation measures. The course of climate change in the future depends on actual current and future greenhouse gas emissions, which are represented by four Representative Concentration Pathway climate scenarios (RCPs). These scenarios are based on human activities and associated emissions of CO<sub>2</sub>, CH<sub>4</sub> and N<sub>2</sub>O, and other air pollutants. The scenarios can be identified by the value of radiative forcing at the end of the 21<sup>st</sup> century, a measure of enhanced greenhouse effect compared to pre-industrial times in units of watts per metre squared (W/m<sup>2</sup>) (van Vuuren et al., 2011). Greater radiative forcing implies greater changes in the climate system.

To assess the impacts of climate change up to the 21st century, the Slovenian Environment Agency (ARSO) uses the simulations of regional climate models from the EURO-CORDEX project (Benestad et al., 2018; Bertalančič et al., 2019). For the purpose of this study, we utilized the climate variable precipitation. The horizontal resolution of the regional models used in our study is around 12 km. The modeling period is 1961–2070 for all models and 1971–2070 for some. The time step of the model results is one day. Out of 14 combinations of global and regional climate models, six models (Table 1) were selected that are as different from each other as possible while matching the measured values of climate variables in the past as closely as possible. All of the six models are considered equally reliable or unreliable.

Data were prepared for the moderately optimistic scenario RCP4.5, which assumes significant mitigation measures for greenhouse gas emissions for two time periods, the baseline period (1981–2010) and the projection period (2041–2070). Daily precipitation data were downscaled from 12 km resolution to 1 km (Fig. 1). The downscaling of the data was performed on a daily basis for all six climate models.

Precipitation are calculated based on the maximum amount of precipitation that falls on a single cell over a one-year period. The average for the entire projection area is then calculated based on all annual maximum precipitation. The precipitation projections are overlaid with the rainfall trigger values within the algorithm, which determines the areas where the rainfall thresholds are exceeded and the degree of exceedance.

Table 1. Table of climate models (abbreviations provided by ARSO), which are abbreviations of the meteorological centers that prepared the data (e.g DMI- Danish Meteorological Institute, KNMI-Netherlands Meteorological Institute, SMHI- Swedish Meteorological and Hydrological Institute, IPSL- Institute Pierre-Simon Laplace France). With \* we marked the CLMcom centre. The Global Climate Model (GCM) provided boundary conditions, and the Regional Climate Model (RCP) recalculated the data to a smaller scale (about 12 km).

Tabela 1. Seznam podnebnih modelov (okrajšave je pripravil ARSO), ki so kratice meteorološkejih centrov, kjer so podatke pripravili (na primer DMI- Meteorološki inštitut Danske, KNMI- Meteorološki inštitut Nizozemske, SMHI- Meteorološki in hidrološki inštitut Švedske, IPSL- Institut Pierre-Simon Laplace Francija). Z \* je označen center CLMcom. Globalni podnebni model (GCM) je dal robne pogoje, regionalni podnebni model (RCP) pa je preračunal podatke v manjšo skalo (okoli 12 km).

Model	Global climate model (GCM)	Regional climate model (RCM)
CCLM1*	CERFACS-CNRM-CM5	CCLM4-8-17
CCLM2*	MPI-ESM-LR	CCLM4-8-17
DMI	EC-EARTH	HIRHAM5
IPSL	IPSL-CM5A-MR	WRF331F
KNMI	HadGEM2-ES	RACMO22E
SMHI	MPI-ESM-LR	RCA4

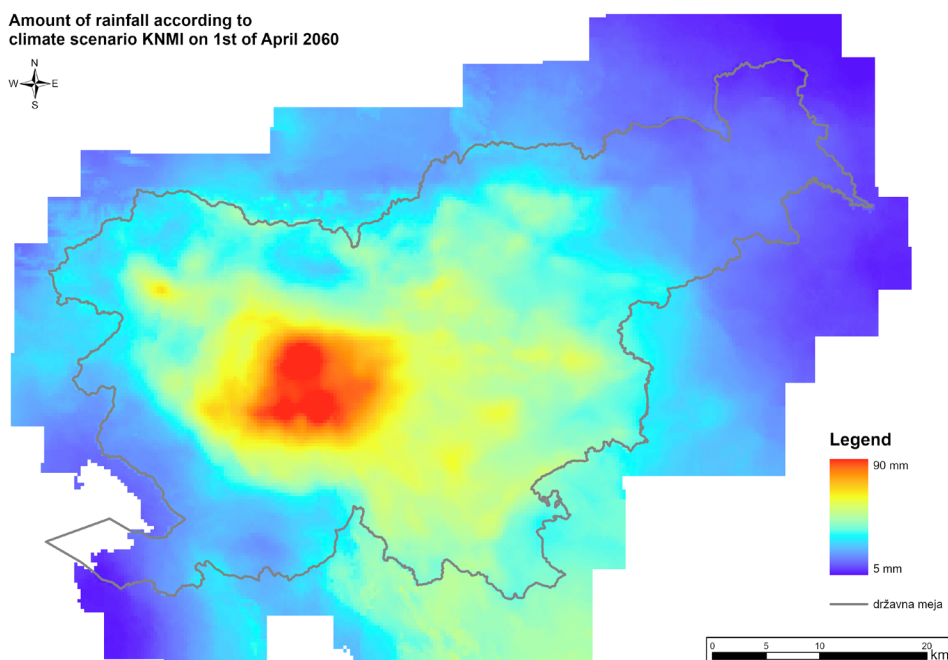


Fig. 1. Example of climate model simulation of daily precipitation downscaled from 12 km resolution to 1 km for Slovenia, produced by ARSO.

Sl. 1. Primer dnevnih padavinskih podatkov simuliranih s podnebnim modelom in z zmanjševanjem skale pretvorjenih iz 12 km ločljivosti v 1 km, ki ga je izdelal ARSO.

### Determination of the rainfall frequency and climate change impact on landslides

Determining the number of days with exceeded rainfall threshold was an important input to the climate change impact assessment. Landslide-triggering rainfall threshold, values determined within the MASPREM system are determined based on engineering-geological map (EG map). EG map was created based on merging the lithology units of Slovenia according to EG characteristics such as soils, soft rocks and rocks; on the basis of their origin and on the basis of the composition, rock strength and particle size ranges (Ribičič et al., 2003). For defining rainfall thresholds, the frequency of spatial occurrence of landslide per spatial unit was correlated with a EG map, and 24-hour maximum rainfall data with the return period of 100 years (Komac et al., 2013; Jemec Auflič et al., 2016). The result of frequency of landslide occurrence and rainfall data provides a good basis for determining the critical rainfall threshold over which landslides occur with high probability. The maximum threshold is defined as the level above which a landslide always occurs (White et al., 1996). In the case of the MASPREM system, the maximum rainfall threshold is 70 mm, especially for the EG units where clayey, slaty clays, marls and scree components predominate.

The number of days with exceeded rainfall threshold for landslide occurrence was determined by an analytical overlap operation following the workflow shown in Figure 2. In the first phase the six time series climate models (RCP4.5)

for baseline and projection periods were separated into individual raster's using ArcGIS set tool "Make NetCDF raster layer" (Fig. 2, A), based on which the extreme yearly precipitation events were defined for the individual raster cell. The cells representing areas with exceeded rainfall threshold have value 1, all other areas were set to 0. In the second step (Fig. 2, B), we created a threshold event model that determined the number of days with exceeded rainfall thresholds based on rainfall thresholds and extreme yearly precipitation events. The main purpose of the analysis was to determine the difference in the number of days with exceeded precipitation triggers in the projection period (2040-2070) compared to the baseline period (1981-2010). This also gave us an overview of the number of extreme events (whether there will be only one extreme event or several) and where they will occur spatially.

To estimate the impact of climate change on landslides by mid-century, extreme yearly precipitation events were combined into 30-year maximum precipitation events using the data grouping model (Fig. 2, C). To assess the impact of climate change on landslides, we used the MASPREM system algorithm (Komac et al., 2013; Jemec Auflič et al., 2016). The system predicts rainfall-induced landslides using fuzzy logic based on the 1:250,000 scale landslide susceptibility map, rainfall thresholds and rainfall forecast model. In this paper 30 years of maximum precipitation events were used as input data to replace the ALADIN forecasts used in the MASPREM system (Fig. 2, D).

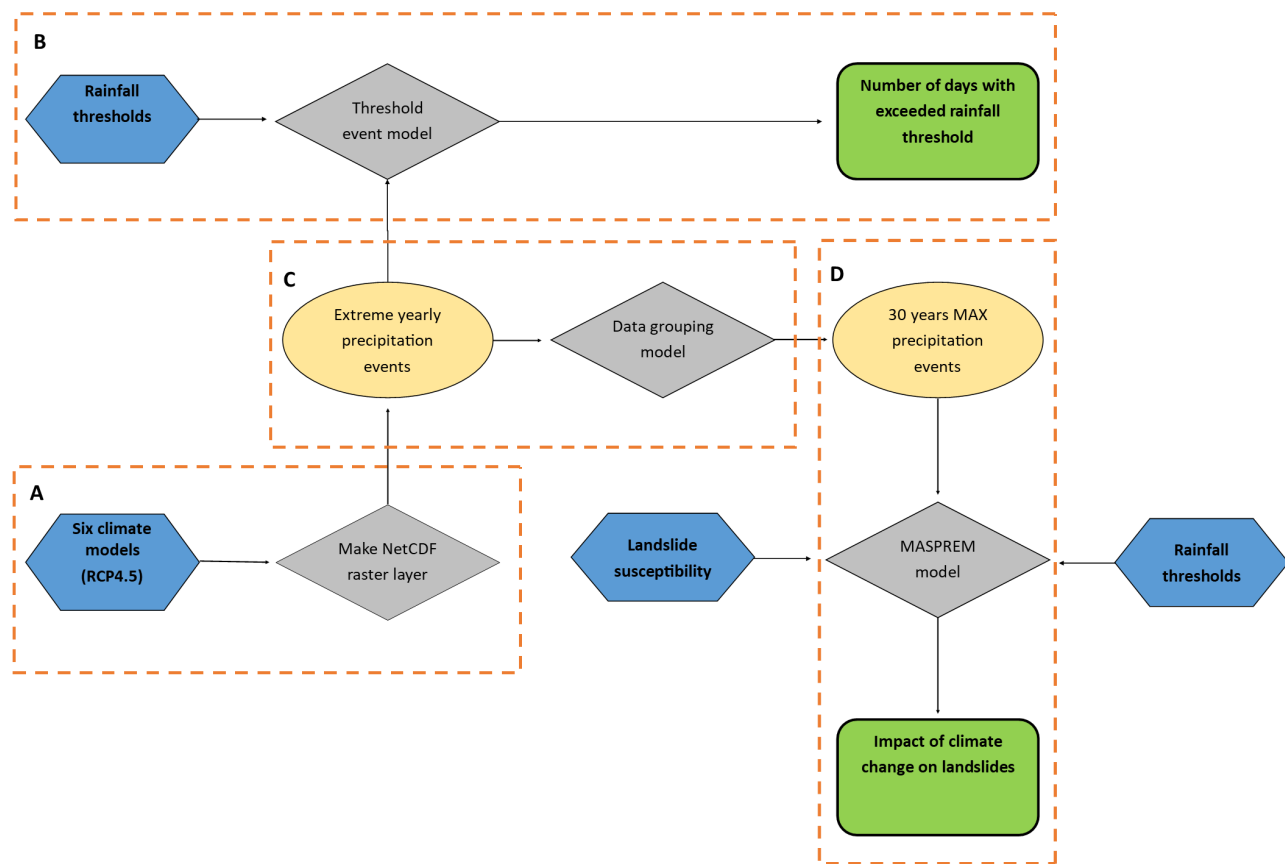


Fig. 2. Workflow to determine the number of days with exceeded rainfall threshold and the impact of climate change on landslides. Letters A, B, C, D indicate different sub-workflows.

Sl. 2. Proces določanja pogostosti padavinskih dogodkov in vpliva podnebnih sprememb na plazove. Označke A, B, C, D označujejo različne procese.

The MASPREM model was then transformed and written into a Python script, allowing the model to run quickly and reliably. This map was overlaid with rainfall thresholds and processed with a 1: 250,000 scale landslide probability model for Slovenia (Komac & Ribičič, 2006). The landslide prediction model was converted from a numerical part to a descriptive part and presented in the form of a 5-point scale: 1 - negligible, 2 - low, 3 - medium, 4 - high, 5 - very high probability. The results in the form of map represent the areas where an increased probability of landslides due to changes in precipitation in the period 2041–2070 can be expected for the entire territory of Slovenia at a scale of 1: 250,000.

The ESRI software environment (ArcGIS Pro 2.5.0, ArcGIS Server 10.8) was used to generate landslide probability in baseline and projection periods, input data, and associated statistics. Scripts were created for each content set using the Python programming language, which automated and streamlined the entire process of creating probability projections. The scripts were created in the ArcPy environment, which allowed the use of ESRI software tools outside of the program itself.

## Results and discussion

The results are presented spatially and in tabular form for the whole Slovenian territory for six climate models (CCLM1, CCLM2, DMI, IPSL, KNMI, SMHI) for the moderately optimistic scenario of greenhouse gas emissions (RCP4.5). The maps of climate change impacts on landslides show only landslide source areas, mainly for the shallow landslides, while deep-seated landslides are more difficult to predict with the applied methodology.

### The frequency of exceedance of rainfall threshold

To estimate the number of days with exceeded rainfall thresholds in the projection period (2041–2070), we compared the number of days when the value of precipitation exceeded 70 mm in baseline and projection periods. Results are tabulated and spatially presented with the percentage of mid-century area which reflect difference in the number of days with trigger precipitation amounts exceeded between the baseline and projection periods for all six models (Figs. 3, 4). Figure 3 shows the percentage of areas with exceeded rainfall thresholds between the baseline and projection periods for six selected climate

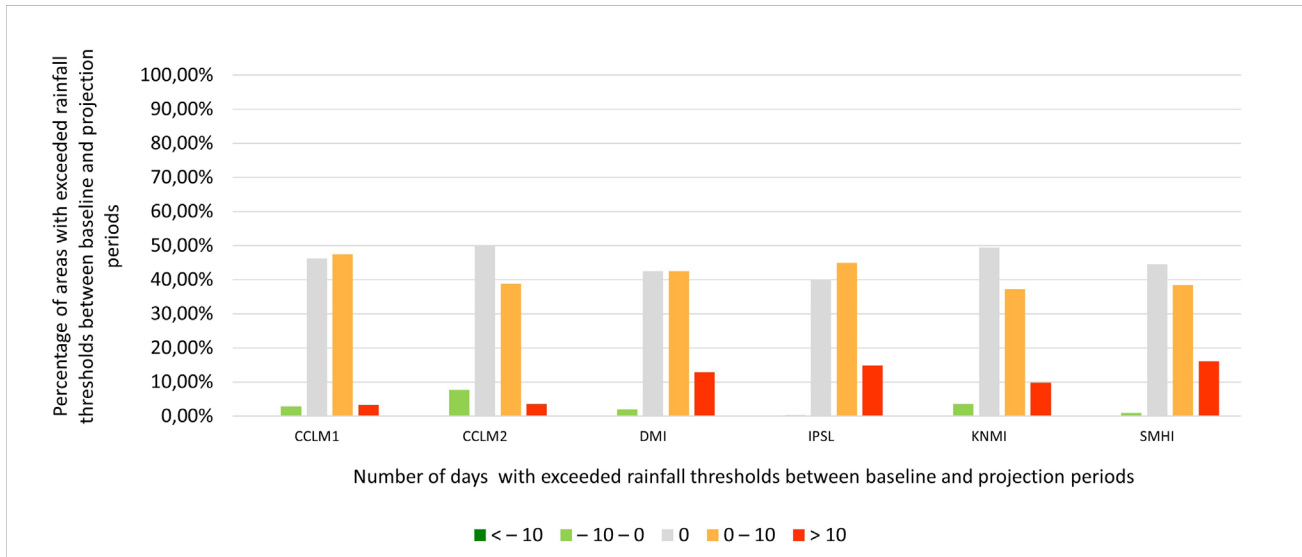


Fig. 3. Percentage of areas with exceeded rainfall thresholds between baseline and projection periods – comparison between six selected climate models simulations.

Sl. 3. Delež površine s preseženimi sprožilnimi količinami, ki ustreza razredu spremembe v številu dni nad sprožilno količino padavin med primerjalnim in projekcijskim obdobjem – primerjava med simulacijami šestih izbranih podnebnih modelov.

models. While the number of days with exceeded rainfall thresholds in 1981–2010 and 2041–2070 periods and the comparison (difference) between them are shown in the Fig. 4. Positive values of the number of days are represented by EG units where more precipitation events are expected in the mid-century (projection period), while negative values indicate EG units where there will be less extreme precipitation events than in the baseline period (1981–2010).

Comparing the number of precipitation days exceeding the exceeded rainfall threshold, i.e. 70 mm of rainfall, between the baseline and projection periods, the area fraction varies within each model (Fig. 3). The frequency of precipitation events in mid-century (2041–2070), when at least 70 mm of precipitation is expected, will be higher in areas in the north-west, north and east of Slovenia than in the baseline period. ARSO indicates a daily precipitation amount of 50 mm or more as very intense rainfall events (Bertalanič et al., 2019). In the case of a moderately optimistic release scenario, the number of days with such intense precipitation will start to increase in the west of the country. Considering the impact of climate change, more than 10 such precipitation events are expected to occur in the middle of the century only in smaller areas of Slovenia, covering 3 to 16 % of the land (Figs. 3, 4, red areas), while up to 10 such events are expected in 37 % to 47 % of the land in the west, north and east of Slovenia according to the annual average (Figs. 3, 4, orange areas). Calculations of the impact of

climate change on the frequency of precipitation events exceeding the rainfall threshold show that in the middle of the century these precipitation events will be lower than in the baseline period only in smaller areas of Slovenia (covering up to 8 %) (Figs. 3, 4, green areas). In recent years, Ujma Journal has reported that, on average, extreme precipitation events (short intense or prolonged rainfall) have caused landslides at least twice a year for the past 20 years (Ujma, 2000–2020). The Ujma Journal, published by the Administration of the Republic of Slovenia for Civil Protection and Disaster Relief, which is responsible for administrative and professional protection, rescue, relief and other tasks related to protection against natural and other disasters in Slovenia, annually collects the most important disaster events in the country, including precipitation-related events that triggered landslides. Although these results are not directly comparable due to uncertainties in climate change prediction models and information sources, as they are on the one hand events that actually occurred and on the other hand, predictions according to climate change prediction RCP4.5, it can be noted that the number of precipitation events that may trigger landslides in the mid-21st century is higher than the exact number of precipitation events that have triggered landslides in recent years. This finding is of particular concern because the prediction models consider all rainfall events with a threshold above 70 mm, above which a landslide always occurs.

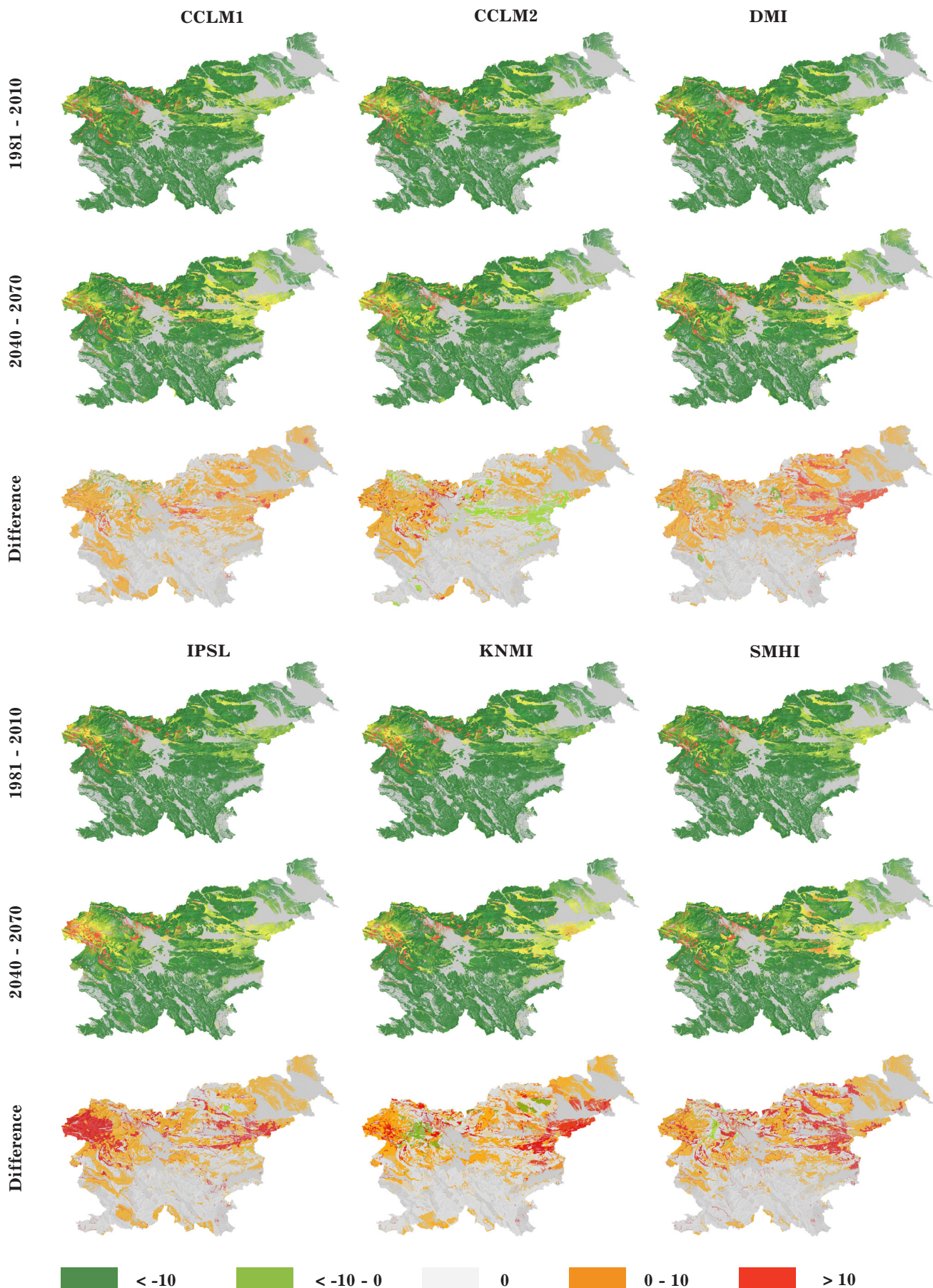


Fig. 4. Number of days with exceeded rainfall thresholds in the periods 1981–2010 and 2041–2070 and comparison (difference) between them.

Sl. 4. Število dni s preseženimi sprožilnimi količinami padavin v obdobjih 1981–2010 in 2041–2070 ter primerjava (razlika) med njimi.

Table 2. Proportion of landslide areas in relation to the moderately optimistic scenario of greenhouse gas emissions between the baseline and projection periods - comparison between six selected climate models simulations.

Tabela 2. Deleži površine plazljivih območij glede na zmerno optimistični scenarij izpustov toplogrednih plinov med primerjalnim in projekcijskim obdobjem – primerjava med simulacijami šestih izbranih podnebnih modelov.

Class	Climate change impact on landslides	CCLM 1 1981- 2010	CCLM 1 2041-2070	CCLM 2 1981-2010	CCLM 2 2041-2070	DMI 1981-2010	DMI 2041-2070
<b>0</b>	Negligible	18,04 %	18,04 %	18,04 %	18,04 %	18,04 %	18,04 %
<b>1</b>	Very low	71,17 %	68,37 %	71,26 %	69,05 %	71,82 %	63,57 %
<b>2</b>	Low	5,33 %	5,04 %	5,93 %	6,39 %	5,87 %	6,38 %
<b>3</b>	Medium	3,54 %	4,60 %	2,89 %	3,02 %	2,51 %	4,16 %
<b>4</b>	High	1,43 %	3,06 %	1,34 %	2,53 %	1,26 %	4,22 %
<b>5</b>	Very high	0,49 %	0,90 %	0,54 %	0,97 %	0,50 %	3,64 %
Class	Climate change impact on landslides	IPSL 1981-2010	IPSL 2041-2070	KNMI 1981-2010	KNMI 2041-2070	SMHI 1981-2010	SMHI 2041- 2070
<b>0</b>	Negligible	18,04 %	18,04 %	18,04 %	18,04 %	18,04 %	18,04 %
<b>1</b>	Very low	74,68 %	63,90 %	71,91 %	65,58 %	72,22 %	65,35 %
<b>2</b>	Low	4,27 %	6,65 %	5,71 %	5,64 %	6,03 %	5,54 %
<b>3</b>	Medium	1,66 %	5,41 %	2,49 %	4,45 %	2,41 %	4,45 %
<b>4</b>	High	0,98 %	4,33 %	1,34 %	4,73 %	0,97 %	4,52 %
<b>5</b>	Very high	0,38 %	1,68 %	0,51 %	1,56 %	0,33 %	2,10 %

### Future patterns

The results of the impact of climate change on the probability of landslides for the territory of Slovenia at a scale of 1: 250,000 are presented in tabular form (Table 2) and spatially with the percentage of the area in the baseline and projection periods for all six models simulations (Fig. 5).

In the moderately optimistic emissions scenario, an increased probability of landslides in classes ranging from low to very high probability is expected in case of all six climate models simulations at mid-century, although the proportions do not differ significantly. Areas with a very high to high probability of landslides will occupy 5% more land in the areas of eastern and northeastern Slovenia and in the area of the Idrijsko Cerkljansko and Škofjeloško hills than in the baseline period (Table 2, Fig. 5, purple areas). By mid-century, the moderate to low probability of landslides will be 7 % higher overall in the areas of eastern, northeastern and northwestern Slovenia and in smaller parts of the Škofjeloško-Cerkljansko area (Table 2, Fig. 5, medium purple areas). In the middle of the century, the percentage of the area with a very low probability of landslides will decrease by up to 10 % (Table 2, Fig. 5, blue areas). As expected,

the proportion of area with a negligible probability of landslides does not change over either time period. These are areas where the natural conditions of the territory (geological structure, morphology) are such that landslides occur very rarely.

Komac and Ribičič (2006) defined 24 % of the area as being at high to very high prone to landslides, considering only the natural geological and geomorphological background of the area. In this study these data were compiled together with rainfall, i.e. climate scenarios, and show that the probability of landslide occurrence in the mid-21st century is almost 8 % higher than in the baseline period according to the susceptibility to landslides given by Komac & Ribičič (2006).

Ciabatta et al. (2016) investigated the impact of climate change on landslide occurrence in Umbria, central Italy, using GCM projections RCP8.5 (the worst scenario) applied to an existing regional landslide early warning system (Ponziani et al., 2012) and assessed increase of landslide occurrence for 30 % in the period 2040-2069. Comparing their results with the similar approach in this paper, except that we used a moderately optimistic climate scenario (RCP4.5), we found an increase in landslide probability of 5

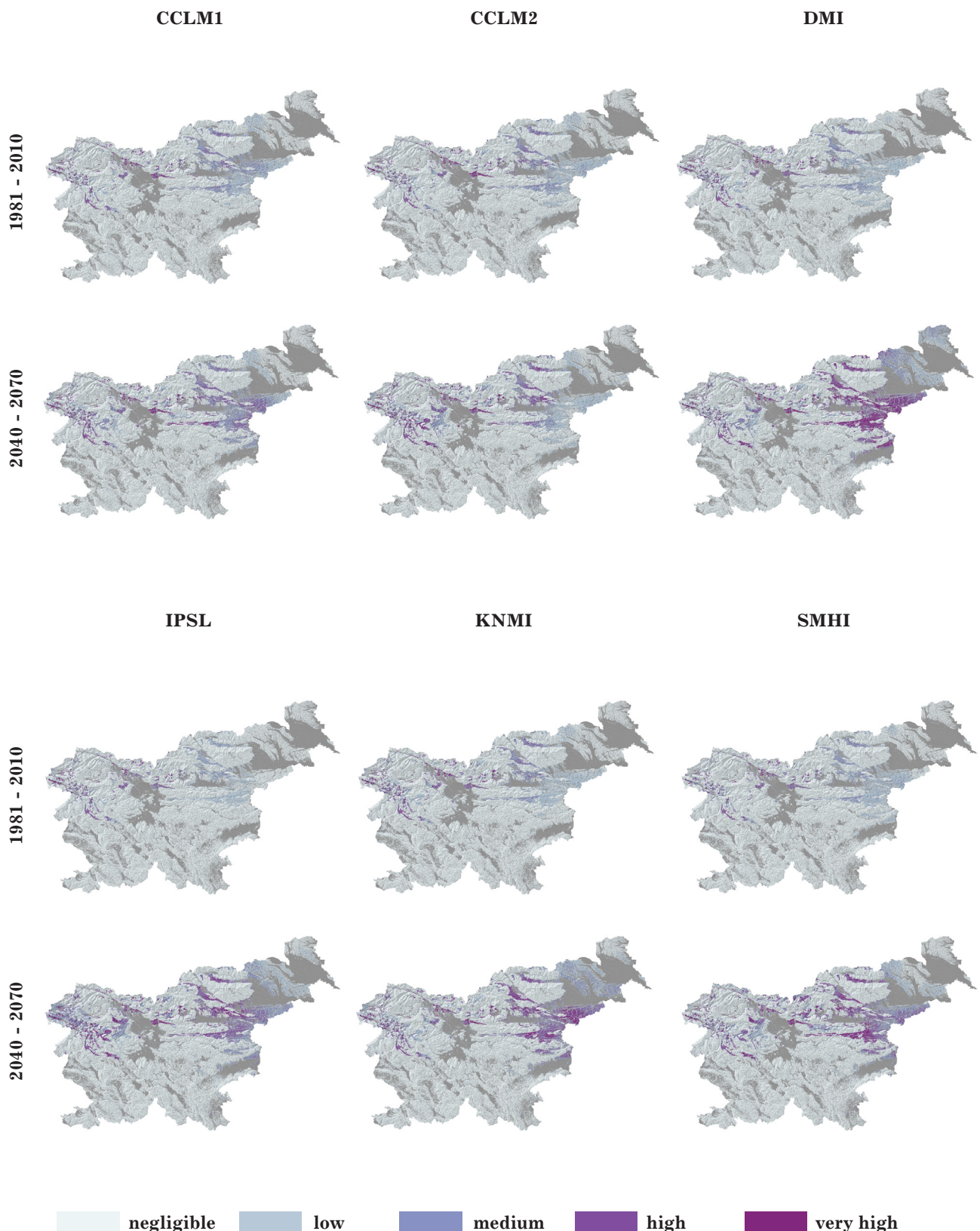


Fig. 5. The impact of climate change on the probability of landslides in the periods 1981-2010 and 2041-2070 for the territory of Slovenia for six models simulations. Landslide susceptibility is divided into 5 classes ranging from negligible to very high using an equal interval algorithm (0,20).

Slovenije za šest modelov. Verjetnost pojavljanja plazov je razdeljena na 5 razredov od zanemarljive do zelo velike z uporabo algoritma enakih intervalov (0,20).

to 7 % for the period from 2040 to 2070. Based on the results of this study, we can assume that the use of RCP8.5 models on the territory of Slovenia would significantly increase the occurrence of landslides in the mid-21st century.

### Conclusions

This paper highlights the impact of changing rainfall patterns in landslide-prone areas in Slovenia by the mid-21st century based on the RCP4.5 moderately optimistic climate scenario. The results indicate that the frequency of rainfall events in the mid-century (2041–2070), when at least 70 mm of rainfall is projected, will be higher in areas in the north-west, north and east of Slovenia. More than 10 such rainfall events are expected in smaller areas of Slovenia covering 3 to 16 % of the area, while up to 10 such events are expected in 37 % to 47 % of areas in the west, north and east of Slovenia. Similarly, the results of the impact of climate change on landslides in Slovenia in the mid-century shows that landslides are more likely to occur in the areas of eastern and northeastern Slovenia and in the area of the Idrijsko-Cerkljansko and Škofjeloško hills. In these areas, about 12 % more landslides are expected with respect to the baseline period.

The authors of the report “Climate change assessment in Slovenia until the end of the 21st century” provided by Bertalanič et al. (2019) clearly indicated that we can expect 20 % more precipitation events in the middle of the century. They also found that a slightly larger increase in precipitation amount is expected in winter in eastern Slovenia. While in the other seasons, the trend and magnitude of precipitation change are strongly dependent on the release scenario and partly on the type of model, and the changes are mostly smaller than the natural variability of precipitation. Moreover, an increase in the intensity and frequency of extreme precipitation is also expected.

Since landslides are closely related to the rainfall distribution, intensity and duration of a rainfall event, the results of the assessment of climate change impacts on landslide occurrence depend strongly on the expected trends in rainfall changes. Predictions of how climate change will impact on landslides depend largely on the climate regime, the geomorphological characteristics of the area, and the geological setting in Slovenia. Gariano et al. (2016) highlighted also the long-standing human interventions in the country, which could speed the occurrence of landslides. The interaction between natural

and human factors is complex and contributes to the uncertainty in assessing the impact of climate change on landslides. Despite potential uncertainties, this study is one of the first in the country to highlight the increasing likelihood of landslides in the mid-21st century as a result of extreme, more intense rainfall. Therefore, these findings should encourage decision makers to develop an adaptation strategy to manage the inevitable impacts and increase the resilience of natural and human systems to the current and future impacts of climate change.

### Acknowledgment

We thank the Slovenian Research Agency (Research Program P1-0011 and research project J1-3024), Administration of the Republic of Slovenia for Civil Protection and Disaster Relief (MASPREM project) and the Ministry of Environment and Spatial Planning for funding this research.

### References

- Alvioli, M. & Baum, R.L. 2016: Parallelization of the TRIGRS model for rainfall-induced landslides using the message passing interface. Environ. Modell. Software 81/C: 122–135. <https://doi.org/10.1016/j.envsoft.2016.04.002>
- Benestad, R., Haensler, A., Hennemuth, B., Illy, T., Jacob, D., Keup-Thiel, E. & Zsebeház, G. 2018: Guidance for EURO-CORDEX climate projections data use (EURO-CORDEX Guidelines Version 1.0 – 2017.08). <https://www.eurocordex.net/imperia/md/content/csc/cordex/euro-cordex-guidelines-version1.0-2017.08.pdf>
- Bertalanič, R., Dolinar, M., Honzak, I., Lokošek, N., Medved, A., Vertačnik, G. & Vlahović, Ž. 2019: Climate change projections for Slovenia over the 21st century: Temperature and precipitation summary. [http://www.meteo.si/uploads/probase/www/climate/text/en/publications/OPS21\\_brosura\\_ENG.pdf](http://www.meteo.si/uploads/probase/www/climate/text/en/publications/OPS21_brosura_ENG.pdf)
- Bezak, N., Šraj, M. & Mikoš, M. 2016: Copula-based IDF curves and empirical rainfall thresholds for flash floods and rainfall-induced landslides. Journal of Hydrology, 541: 272–284. <https://doi.org/10.1016/j.jhydrol.2016.02.058>
- Bezak, N., Brilly, M., Šraj, M. & Mikoš, M. 2018: Intensity-duration-frequency curves for rainfall-induced shallow landslides and debris flows using copula functions: TXT-tool 2.386-1.1. In: Sassa, K., Tiwari, B., Liu, K.-F.,

- McSaveney, M., Strom, A. & Setiawan, H. (eds.): Landslide dynamics: ISDR-ICL landslide interactive teaching tools. Vol. 2, Testing, risk management and country practices. Berlin: Springer, 425–431. [https://link.springer.com/chapter/10.1007/978-3-319-57774-6\\_32](https://link.springer.com/chapter/10.1007/978-3-319-57774-6_32)
- Bezak, N., Jemec Auflič, M. & Mikoš, M. 2019: Application of hydrological modelling for temporal prediction of rainfall-induced shallow landslides. *Landslides*, 16/7: 1273–1283. <https://doi.org/10.1007/s10346-019-01169-9>
- Buma, J. & Dehn, M. 1998: A method for predicting the impact of climate change on slope stability. *Environmental Geology*, 35: 190–96. <https://doi.org/10.1007/s002540050305>
- Bonnard, C., Tacher, L. & Beniston, M. 2008: Prediction of landslide movements caused by climate change: modelling the behaviour of a mean elevation large slide in the Alps and assessing its uncertainties. In: Chen, Z., Zhang, J.M., Li, Z.K., Wu, F.Q. & Ho, K. (eds.): *Landslides and Engineering Slopes. From the Past to the Future*, 217–227. <https://doi.org/10.1201/9780203885284-c13>
- Borgatti, L. & Soldati, M. 2010: Landslides as a geomorphological proxy for climate change: a record from the Dolomites (northern Italy). *Geomorphology*, 120: 56–64. <https://doi.org/10.1016/j.geomorph.2009.09.015>
- Ciabatta, L., Camici, S., Brocca, L., Ponziani, F., Stelluti, F., Berni, N. & Moramarco, T. 2016: Assessing the impact of climate-change scenarios on landslide occurrence in Umbria Region, Italy. *J. Hydrol.* <https://doi.org/10.1016/j.jhydrol.2016.02.007>
- Chang, S.-H. & Chiang, K.-T. 2011: The potential impact of climate change on typhoon triggered landslides in Taiwan, 2010–2099. *Geomorphology*, 133: 143–151. <https://doi.org/10.1016/j.geomorph.2010.12.028>
- Coe, J.A. 2012: Regional moisture balance control of landslide motion: implications for landslide forecasting in a changing climate. *Geology*, 40/4: 323–326. <https://doi.org/10.1130/G32897.1>
- Coe, J.A. & Godt, J.W. 2012: Review of approaches for assessing the impact of climate change on landslide hazards. In: Eberhardt, E., Froese, C., Turner, A.K. & Leroueil, S. (eds.): *Landslides and Engineered Slopes, Protecting Society Through Improved Understanding: Proceedings 11th International and 2nd North American Symposium on Landslides and Engineered Slopes*, Banff, Canada 1. Taylor & Francis Group, 3–8 June London: 371–377.
- Collison, A., Steven W., Griffiths, J. & Dehn, M. 2000: Modelling the impact of predicted climate change on landslide frequency and magnitude in SE England. *Engineering Geology*, 55: 205–18.
- Comegna, L., Picarelli, L., Buccignani, E. & Mercogliano, P. 2013: Potential effects of incoming climate changes on the behaviour of slow active landslides in clay. *Landslides*, 10/4: 373–391. <https://doi.org/10.1007/s10346-012-0339-3>
- Crozier, M. J. 2010: Deciphering the effect of climate change on landslide activity: A review, *Geomorphology*, 124: 260–67.
- Dikau, R. & Schrott, L. 1999: The temporal stability and activity of landslides in Europe with respect to climatic change (TESLEC): main objectives and results, *Geomorphology*, 30: 1.
- Dixon, N. & Brook, E. 2007: Impact of predicted climate change on landslide reactivation: case study of Mam Tor, UK. *Landslides*, 4: 137–147. <https://doi.org/10.1007/s10346-006-0071-y>
- Gariano, S.L. & Guzzetti, F. 2016: Landslides in a changing climate'. *Earth-Science Reviews*, 162: 227–52.
- Gariano, S.L., Brunetti, M.T., Iovine, G., Melillo, M., Peruccacci, S., Terranova, O., Vennari, C. & Guzzetti, F. 2015: Calibration and validation of rainfall thresholds for shallow landslide forecasting in Sicily, Southern Italy. *Geomorphology*, 228: 653–665. <https://doi.org/10.1016/j.geomorph.2014.10.019>
- Gassner, C., Promper, C., Begueria, S. & Glade, T. 2015: Climate change impact for spatial landslide susceptibility. In: Lollino, G., Manconi, A., Clague, J., Shan, W. & Chiarle, M. (eds.): *Engineering Geology for Society and TerritoryClimate Change and Engineering Geology 1*. Springer International Publishing: 429–433.
- Glade, T. 2003: Landslide occurrence as a response to land use change: a review of evidence from New Zealand. *Catena*, 51/3–4: 297–314. [https://doi.org/10.1016/s0341-8162\(02\)00170-4](https://doi.org/10.1016/s0341-8162(02)00170-4)
- Guzzetti, F., Peruccacci, S., Rossi, M. & Stark, C.P. 2007: Rainfall thresholds for the initiation of landslides in central and southern Europe. *Meteorol. Atmos. Phys.*, 98: 239–267. <https://doi.org/10.1007/s00703-007-0262-7>
- Heerdegen, R. 1991: Book reviews: Houghton, J.T., Jenkins, G.J. and Ephraums, J.J. 1990: Climate change - the IPCC scientific assessment. Cambridge: Cambridge University Press for the Intergovernmental Panel on Climate Change (World Meteorological

- Organisation/United Nations Environmental Programme).
- IPCC 2018: Summary for Policymakers. In: Global Warming of 1.5°C. An IPCC Special Report on the impacts of global warming of 1.5°C above pre-industrial levels and related global greenhouse gas emission pathways, in the context of strengthening the global response to the threat of climate change, sustainable development, and efforts to eradicate poverty [Masson-Delmotte, V., P. Zhai, H.-O. Pörtner, D. Roberts, J. Skea, P.R. Shukla, A. Pirani, W. Moufouma-Okia, C. Péan, R. Pidcock, S. Connors, J.B.R. Matthews, Y. Chen, X. Zhou, M.I. Gomis, E. Lonnoy, T. Maycock, M. Tignor, and T. Waterfield (eds.)]. World Meteorological Organization, Geneva, Switzerland, 32 pp.
- Jakob, M. & Lambert, S. 2009: Climate change effects on landslides along the southwest coast of British Columbia. *Geomorphology*, 107/3-4: 275–284. <https://doi.org/10.1016/j.geomorph.2008.12.009>
- Jemec Auflič, M. & Komac, M. 2013: Rainfall patterns for shallow landsliding in perialpine Slovenia. *Natural hazards*, 67/3: 1011–1023. <https://doi.org/10.1007/s11069-011-9882-9>
- Jemec Auflič, M., Šinigoj, J., Krivic, M., Podboj, M., Peternel, T. & Komac, M. 2016: Landslide prediction system for rainfall induced landslides in Slovenia (Masprem) = Sistem opozarjanja na nevarnost proženja zemeljskih plazov v Sloveniji (Masprem). *Geologija*, 59/2: 259–271. <https://doi.org/10.5474/geologija.2016.016>
- Jemec Auflič, M., Šinigoj, J., Krivic, M. & Podboj, M. 2018: Challenges for operational forecasting of rainfall-induced landslides in Slovenia. In: Jemec Auflič, M., Mikoš, M. & Verbovšek, T. (eds.): Advances in landslide research: proceedings of the 3rd Regional Symposium on Landslides in the Adriatic Balkan Region, 11–13 October 2017, Ljubljana, Slovenia. Geological Survey of Slovenia: 71–75.
- Jordanova, G., Gariano, S.L., Melillo, M., Peruccacci, S., Brunetti, M.T. & Jemec Auflič, M. 2020: Determination of Empirical Rainfall Thresholds for Shallow Landslides in Slovenia Using an Automatic Tool. *Water*, 12/5:1449. <https://doi.org/10.3390/w12051449>
- Komac, M. 2005: Rainstorms as a landslide-trigerring factor in Slovenia. *Geologija*, 48/2: 263–279. <https://doi.org/10.5474/geologija.2005.022>
- Komac, M. & Ribičič, M. 2006. Landslide susceptibility map of Slovenia at scale 1:250,000 = Karta verjetnosti pojavljanja plazov v Sloveniji v merilu 1:250.000. *Geologija*, 49/2: 295–309. <https://doi.org/10.5474/geologija.2006.022>
- Komac, M., Šinigoj, J., Jemec Auflič, M., Čarman, M. & Krivic, M. 2013: Landslide hazard forecast in Slovenia - MASPREM. In: Mihalić Arbanas, S. & Arbanas, Ž. (eds.): Landslide and flood hazard assessment, 1st Regional Symposium on Landslides in the AdriaticBalkan Region with the 3rd Workshop of the Croatian-Japanese Project “Risk Identification and Land-Use Planning for Disaster Mitigation of Landslides and Floods in Croatia”, Zagreb, Croatia from March 6th to 9th, 2013: 225–23.
- Malet, J.-P., Remaître, A., Maquaire, O., Durand, Y., Etchevers, P., Guyomarch, G., van Déqué, M. & Beek, L.P.H. 2007: Assessing the influence of climate change on the activity of landslides in the Ubaye Valley. In: McInnes, R., Jakeways, J. & Fairbank, H. (eds.): Landslides and Climate Change: Challenges and Solutions, Proceedings of the International Conference on Landslides and Climate Change. Taylor & Francis, Ventnor, Isle of Wight, 21–24 May 2007, UK: 195–205.
- Malet, J.-P., van Asch, Th.W.J., van Beek, R. & Maquaire, O. 2005: Forecasting the behaviours of complex landslides with a spatially distributed hydrological model. *Nat. Hazards Earth Syst. Sci.*, 5/1: 71–85. <https://doi.org/10.5194/nhess-5-71-2005>
- McInnes, R., Jakeways, J., Fairbank, H. & Mathie, E. 2007: Landslides and Climate Change: Challenges and Solutions, Proceedings of the International Conference on Landslides and Climate Change. Taylor & Francis, Ventnor. <https://doi.org/10.1201/noe0415443180>
- Paranunzio, R., Laio, F., Chiarle, M., Nigrelli, G. & Guzzetti, F. 2016: Climate anomalies associated to the occurrence of rockfalls at high-elevation in the Italian Alps. *Nat. Hazard Earth Sys. Sci. Discuss.* <https://doi.org/10.5194/nhess-2016-100>
- Ponziani, F., Pandolfo, C., Stelluti, M., Berni, N., Brocca, L. & Moramarco, T. 2012: Assessment of rainfall thresholds and soil moisture modeling for operational hydrogeological risk prevention in the Umbria region (central Italy). *Landslides*, 9: 229–237.
- Rebetez, M., Lugon, R. & Baeriswyl, P.-A. 1997: Climatic change and debris flows in high mountain regions: the case study of the Ritigraben torrent (Swiss Alps). *Clim. Chang.* 36: 371–389. <https://doi.org/10.1023/A:1005356130392>

- Rianna, G., Zollo, A.L., Tommasi, P., Paciucci, M., Comegna, L. & Mercogliano, P. 2014: Evaluation of the effects of climate changes on landslide activity of Orvieto clayey slope. *Procedia Earth Plan. Sci.*, 9: 54–63. <https://dx.doi.org/10.1016/j.proeps.2014.06.017>
- Ribičič, M., Šinigoj, J. & Komac, M. 2003: New general engineering geological map of Slovenia. *Geologija*, 46/2: 397–404.
- Rosi, A., Peternel, T., Jemec Auflič, M., Komac, M. & Casagli, N. 2016: Rainfall thresholds for rainfall-induced landslides in Slovenia. *Landslides*, 13: 1571–1577. <https://doi.org/10.1007/s10346-016-0733-3>
- Schmidt, J. & Glade, T. 2003: Linking global circulation model outputs to regional geomorphic models: a case study of landslide activity in New Zealand. *Clim. Res.*, 25: 135–150. <https://doi.org/10.3354/cr025135>
- Schmidt, J. & Dikau, R. 2004: Modeling historical climate variability and slope stability. *Geomorphology*, 60: 433–447. <https://doi.org/10.1016/j.geomorph.2003.11.001>
- Sidle, R.C. & Ochiai, H. 2006: Landslides: Processes, Prediction, and Land Use (American Geophysical Union: United States).
- Sidle, R.C. & Dhakal, A.S. 2002: Potential effects of environmental change on landslide hazards in forest environments. In: Sidle, R.C. (ed.): Environmental Change and Geomorphic Hazards in Forests IUFRO Research Series 9. CABI Publishing, Wallingford, Oxen, UK: 123–165. <https://doi.org/10.1079/9780851995984.0123>
- Stoffel, M., Tiranti, D. & Huggel, C. 2014: Climate change impacts on mass movements – case studies from the European Alps. *Sci. Total Environ.*, 493: 1255–1266. <https://doi.org/10.1016/j.scitotenv.2014.02.102>
- Tacher, L. & Bonnard, C. 2007: Hydromechanical modelling of a large landslide considering climate change conditions. In: McInnes, R., Jakeways, J., Fairbank, H. & Mathie, E. (eds.): *Landslides and Climate Change: Challenges and Solutions* Proceedings of the International Conference on Landslides and Climate Change. Taylor & Francis, Ventnor: 131–141
- Tommasi, P., Pellegrini, P., Boldini, D. & Ribacchi, R. 2006: Influence of rainfall regime on hydraulic conditions and movement rates in the overconsolidated clayey slope of the Orvieto hill (Central Italy). *Can. Geotech. J.* 43: 70–86. <https://doi.org/10.1139/cgj2012-0121>
- Trauth, M.H., Alonso, R.A., Haselton, K.R., Hermanns, R.L. & Strecker, M.R. 2000: Climate change and mass movements in the NW Argentine Andes. *Earth Planet. Sci. Lett.* 179/2: 243–256. [https://doi.org/10.1016/S0012-821X\(00\)00127-8](https://doi.org/10.1016/S0012-821X(00)00127-8)
- Ujma, 2000–2020: Revija za vprašanja varstva pred naravnimi in drugimi nesrečami. Uprava RS za zaščito in reševanje, Ministrstvo za obrambo, ISSN 0353-085X, Ljubljana. <http://www.sos112.si/slo/page.php?src=sv61.htm>
- van Vuuren, D., Edmonds, J., Kainuma, M., Riahi, K., Thomson, A., Hibbard, K., George C. Hurtt, T., Krey, V., Lamarque, J-F., Masui, T., Meinshausen, M., Nakicenovic, N., Steven J. & Smith Rose, S. 2011: The representative concentration pathways: an overview. *Climatic Change*, 109: 5–31
- Wasowski, J., Lamanna, C. & Casarano, D. 2010: Influence of land-use change and precipitation patterns on landslide activity in the Daunia Apennines, Italy. *Q. J. Eng. Geol. Hydrogeol.*, 43: 387–401. <https://doi.org/10.1144/1470-9236/08-101>
- White, I.D., Mottershead, D.N. & Harrison, J.J. 1996: Environmental Systems, 2nd Edition. London: Chapman & Hall London: 616 p.
- Winter, M.G., Dent, J., Macgregor, F., Dempsey, P., Motion, A. & Shackman, L. 2010: Debris flow, rainfall and climate change in Scotland. *Q. J. Eng. Geol. Hydrogeol.*, 43: 429–446. <https://doi.org/10.1144/1470-9236/08-108>
- Zollo, A.L., Rianna, G., Mercogliano, P., Tommasi, P. & Comegna, L. 2014: Validation of a simulation chain to assess climate change impact on precipitation induced landslides. In: K. Sassa, K., Canuti, P., Yin, Y. (eds.), *Landslide Science for a Safer Geoenvironment 1*. Springer International Publishing, 287–292.
- Yin, Z., Qin, X., Yin, Y., Zhao, W. & Wei, G. 2014: Landslide developmental characteristics and response to climate change since the last glacial in the upper reaches of the Yellow river, NE Tibetan plateau. *Acta Geol. Sin. (English edition)*, 88/2: 635–646. <https://doi.org/10.1111/1755-6724.12219>





# Sedimentological and paleontological analysis of the Lower Jurassic part of the Zatrnik Formation on the Pokljuka plateau, Slovenia

## Sedimentološka in paleontološka analiza spodnjejurskega dela Zatrniške formacije na Pokljuki, Slovenija

Luka GALE<sup>1,2</sup>, Duje KUKOČ<sup>3,4</sup>, Boštjan ROŽIČ<sup>1</sup> & Anja VIDERVOL<sup>1,5</sup>

<sup>1</sup>Department of Geology, University of Ljubljana, Aškerčeva c. 12, SI-1000 Ljubljana, Slovenia; luka.gale@ntf.uni-lj.si

<sup>2</sup>Geological Survey of Slovenia, Dimičeva ul. 14, SI-1000 Ljubljana, Slovenia; luka.gale@geo-zs.si

<sup>3</sup>Ivan Rakovec Institute of Palaeontology, Research Centre of the Slovenian Academy of Sciences and Arts, Novi trg 2, 1000 Ljubljana, Slovenia

<sup>4</sup>Croatian Geological Survey, Sachsova 2, HR-1000 Zagreb, Croatia; dkukoc@hgi-cgs.hr

<sup>5</sup>Prijateljev trg 2, SI-1310 Ribnica; anja.vidervol@gmail.com

Prejeto / Received 7. 7. 2021; Sprejeto / Accepted 29. 10. 2021; Objavljeno na spletu / Published online 28. 12. 2021

**Key words:** Lower Jurassic, Bled Basin, Pokljuka Nappe, stratigraphy, foraminifer, Hierlatz facies, Ribnica Breccia, Zajamniki

**Ključne besede:** spodnja jura, Blejski bazen, Pokljuški pokrov, stratigrafija, foraminifera, hierlaški facies, Ribniška breča, Zajamniki

### Abstract

The uppermost Ladinian to Lower Jurassic Zatrnik Formation is the lithostratigraphic unit of the Mesozoic deeper marine Bled Basin. The uppermost part of the Zatrnik Formation and the transition into the overlying Ribnica Breccia was logged at the Zajamniki mountain pasture on the Pokljuka mountain plateau in the Julian Alps. The lowermost part of the section belongs to the “classical” Zatrnik Formation and is dominated by beige micritic limestone and fine-grained calcarenite. Foraminifers *Siphonavulvula*, *?Everticyclammina*, *?Mesoendothyra* and *?Pseudopfenderina* are present, indicating Early Jurassic age. The beige limestone is followed by light pink limestone of the uppermost Zatrnik Formation. Slumps are common in this interval, and crinoids are abundant. Alongside some species already present in beds lower in the succession, *Meandrovoluta asiagoensis* Fugagnoli & Rettori, *Trocholina* sp., Valvulinidae, small Textulariidae, Lagenida, and small *?Ophthalmidium* also occur in this interval. Resedimented limestone predominates through the studied part of the Zatrnik Formation, indicating deposition on the slope or at the foot of the slope of the basin. The switch to crinoid-rich facies within the slumped interval of the Zatrnik Formation may reflect accelerated subsidence of the margins of the Julian Carbonate Platform in the Pliensbachian. The Zatrnik Formation is followed by the formation of the Pliensbachian (?) Ribnica Breccia. Impregnations of ferromanganese oxides, violet colour, and an increase in clay content are characteristic. The foraminiferal assemblage consists of *Lenticulina*, small elongated Lagenida, and epistominids. Individual beds of the Ribnica Breccia were deposited via debris flows. Enrichments in ferromanganese oxides point to slower sedimentation.

### Izvleček

Zgornjeladinijska do spodnjejurska Zatrniška formacija je značilna litostratigrafska enota mezozojskega Blejskega bazena. Zgornji del Zatrniške formacije in prehod v mlajšo Ribniško brečo smo posneli na planini Zajamniki na Pokljuki. Najnižji del posnetega zaporedja pripada “klasičnemu” delu Zatrniške formacije. Najpogosteji litologiji v tem delu sta mikritni apnenec bez barve in drobnozrnat kalkarenit. Določene so bile foraminifere *Siphonavulvula*, *?Everticyclammina*, *?Mesoendothyra* in *?Pseudopfenderina*, ki dokazujejo zgodnjejursko starost. “Klasičnemu” delu Zatrniške formacije sledi svetlo rožnat apnenec, ki še vedno pripada Zatrniški formaciji. Za ta interval so značilne strukture podvodnega plazjenja. Pogosti, v nekaterih plasteh prevladujoči, so delci morskih lilij. Poleg že prej omenjenih rodov foraminifer, so tukaj prisotne še *Meandrovoluta asiagoensis* Fugagnoli & Rettori, *Trocholina* sp., Valvulinidae, drobne Textulariidae, Lagenida, in drobni *?Ophthalmidium*. Resedimenti, ki prevladujejo v obeh posnetih delih Zatrniške formacije, kažejo na sedimentacijo na pobočju ali ob vznožju pobočja. Prehod v rožnat apnenec s pogostimi sledovi plazjenja in obilico ploščic morskih lilij bi lahko odražal pospešeno pogrezanje robov Julijske karbonatne platforme v pliensbachiju. Zatrniški formaciji sledi formacija pliensbachske (?) Ribniške breče. Značilne so impregnacije z železovo-manganovimi oksidi, vijolična barva kamnine in večja količina glinene primes. Foraminiferno združbo sestavljajo *Lenticulina*, drobne razpotegnjene Lagenida in epistominide. Plasti Ribničke breče so bile odložene z drobirskimi tokovi. Obogatitve z železovo-manganovimi oksidi kažejo na počasnejšo sedimentacijo.

## Introduction

The Middle Triassic regional extension of the continental crust at the western margin of the Neotethys Ocean resulted in the formation of numerous intraplatform basins separated by topographic highs and platforms (Buser, 1989, 1996; Bosellini et al., 2003; Kovács et al., 2011). Although by the early Carnian most of the smaller basins were already filled with sediments of prograding platforms and/or clastic deposits (Bosellini et al., 2003; Breda et al., 2009; Breda & Preto, 2011), deeper marine sedimentation continued in the Tolmin (sensu Cousin, 1981; see explanation in Goričan et al., 2012) and Bled basins (Cousin, 1981; Goričan et al., 2012), while another major Triassic basin, the Tarvisio Basin, was additionally established during the Carnian (Gianolla et al., 2010; Gale et al., 2015).

The least known of the three major Triassic basins in the eastern Southern Alps is the Bled Basin, which was established on the basis of the continuous, upper Anisian to Hauterivian deeper marine succession preserved in the Pokljuka Nappe and exposed on the Pokljuka Mountain Plateau and in the surroundings of Bled (Cousin, 1981; Kukoč et al., 2012; Goričan et al., 2012; Kukoč, 2014; Goričan et al., 2018). From the latest Ladinian to the Early Jurassic, a unit consisting largely of thin- to medium-thick beds of limestone with chert nodules several hundreds of meters thick, known as the Zatrnik Formation, was deposited. This lithostratigraphic unit was first mentioned by Diener (1884), and then by Härtel (1920), and Budkovič (1978). The name presently used was introduced by Cousin (1981), but later authors also referred to this unit as Pokljuka Limestone or the Pokljuka Formation (Dozet & Buser, 2009, with references). The latest Ladinian to Norian age of the lower and middle part of the Zatrnik Formation was determined on the basis of bivalves (Buser, 1980), radiolarians (Gale et al., 2019), and conodonts (Kolar-Jurkovšek et al., 1983; Ramovš, 1986, 1998; Gale et al., 2019). The uppermost part of the Zatrnik Formation differs from the rest of the formation in the abundance of echinoderm debris (the “Hierlatz facies” in Budkovič, 1978). The Early Jurassic age of this facies was previously determined on the basis of brachiopods, ammonites, bivalves, fish remains, and foraminifer *Involutina liassica* (Jones) (Härtel, 1920; Budkovič, 1978). However, more detailed sedimentological and biostratigraphic research of the upper part of the Zatrnik Formation was never performed.

The uppermost part of the Zatrnik Formation is located below the Javorski vrh peak, SE of the Zajamniki mountain pasture in what we refer to here as the Zajamniki section. The upper part of this section was previously described by Kukoč (2014) in an unpublished thesis. The section starts with the micritic limestone-dominated “classical” Zatrnik Formation, spans the “Hierlatz facies” of the Zatrnik Formation, and ends with the Ribnica Breccia overlying the Zatrnik Formation. This paper presents the sedimentological and micropaleontological analysis of the logged section, thereby providing some new information on the evolution and sedimentary dynamics of the Bled Basin.

## Geological Setting and Lithostratigraphy

Structurally, the area of the Pokljuka plateau belongs to the Southern Alps (Placer, 2008), more precisely, to the Pokljuka Nappe (Buser, 1986). The Pokljuka Nappe is thought to have formed during Dinaric thrusting and is positioned above the Krn Nappe, which is characterised by a thick succession of Triassic to Lower Jurassic shallow marine carbonates, followed by Middle Jurassic – Cretaceous condensed carbonates (Šmuc, 2005; Šmuc & Rožič, 2010). The primary thrust contacts of the Pokljuka Nappe are completely obliterated by post-thrust faults, and the platform and the basin contacts are along NW-SE and NW-SE-directed steep faults (Goričan et al., 2018). As already mentioned, the Pokljuka Nappe comprises a continuous Anisian to Hauterivian basinal succession (Fig. 2). The succession above the Zatrnik Formation continues with the Ribnica Breccia unit. Its Pliensbachian age was determined on the basis of the foraminifer *Involutina liassica* (Jones) found in clasts and the regional comparison (Kukoč, 2014; Goričan et al., 2012). The succession continues with the uppermost Bajocian- lower Tithonian radiolarite, which is succeeded in turn by upper Tithonian - ? Berriassian Biancone (calpionellid) limestone with chert nodules and marl interlayers. The calpionellid limestone is overlain by the Bohinj Formation (Kukoč et al., 2012), comprising limestone breccia, and calcarenite. Finally, the ?upper Berriassian - Hauterivian flysch-type succession follows (Fig. 2). This succession is informally divided into two parts. The lower part consists of pelagic limestone with marl interlayers and calarenites. The upper part (Studor Formation) is characterized by the presence of sandstone beds increasing in proportion towards the top (Kukoč, 2014; Goričan et al. 2018). Ophiolitic detritus is present

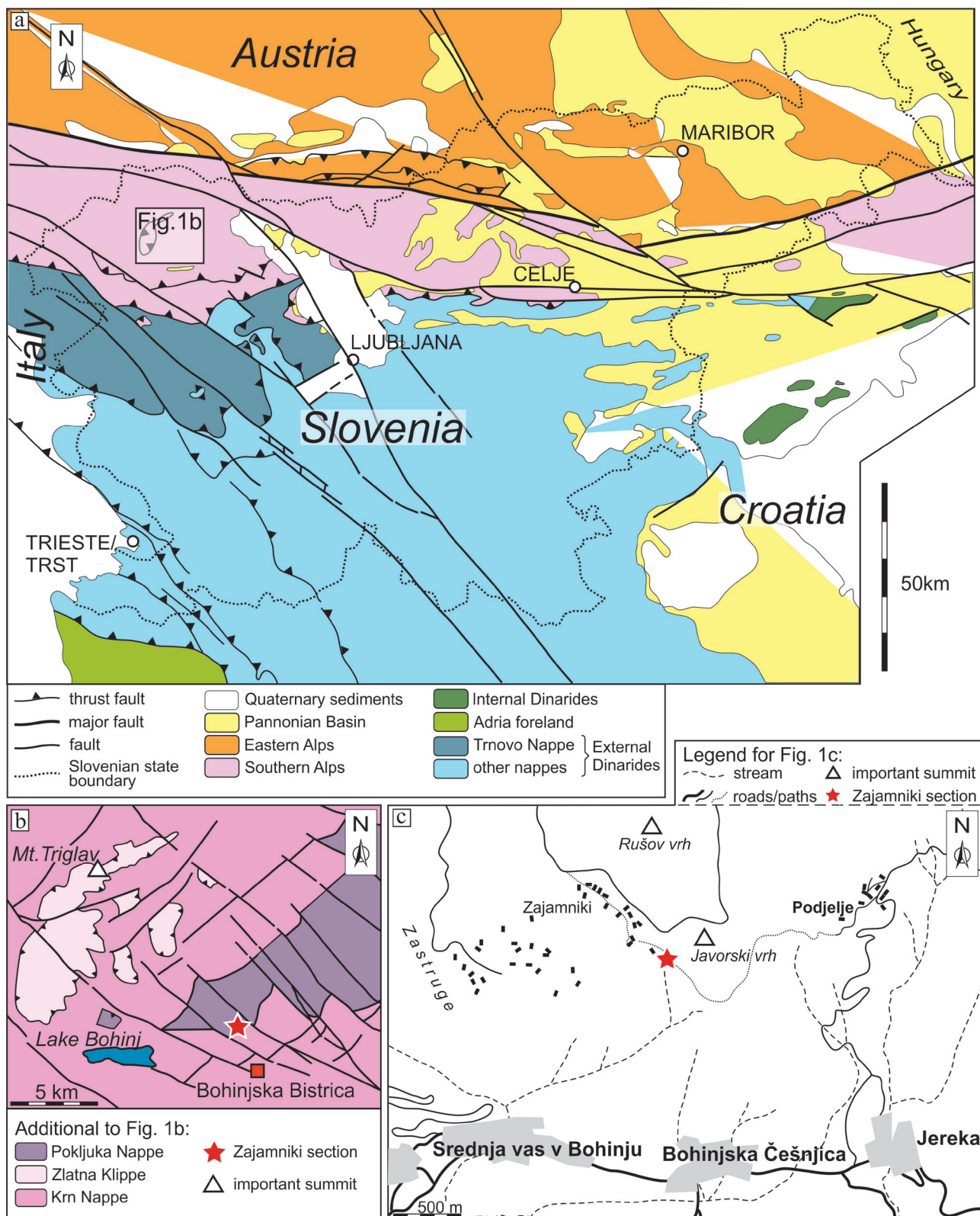


Fig. 1. Geographic and structural position of the studied section. a) Structural subdivision of the Alpine-Dinaric-Pannonian Transition Zone (after Placer, 2008); b) Structure of the central Julian Alps (after Goričan et al., 2018) with the position of the Zajamniki section marked with a star symbol.

from the Bohinj Formation upwards, indicating the ocean-ward position of the Bled Basin (Kučoč et al., 2012; Goričan et al., 2012, 2018).

The studied Zajamniki section is located on the southern slopes of the Pokljuka mountain plateau (1000–1600 m.a.s.l.) in the eastern part of

the Julian Alps in NW Slovenia (Fig. 1). The section starts at  $46^{\circ}18'33.24''$  lat.,  $13^{\circ}56'24.86''$  long., and ends at  $46^{\circ}18'30.33''$  lat.,  $13^{\circ}56'29.21''$  long. On the basis of the geological map, published in Goričan et al. (2018), the succession is in overturned position.

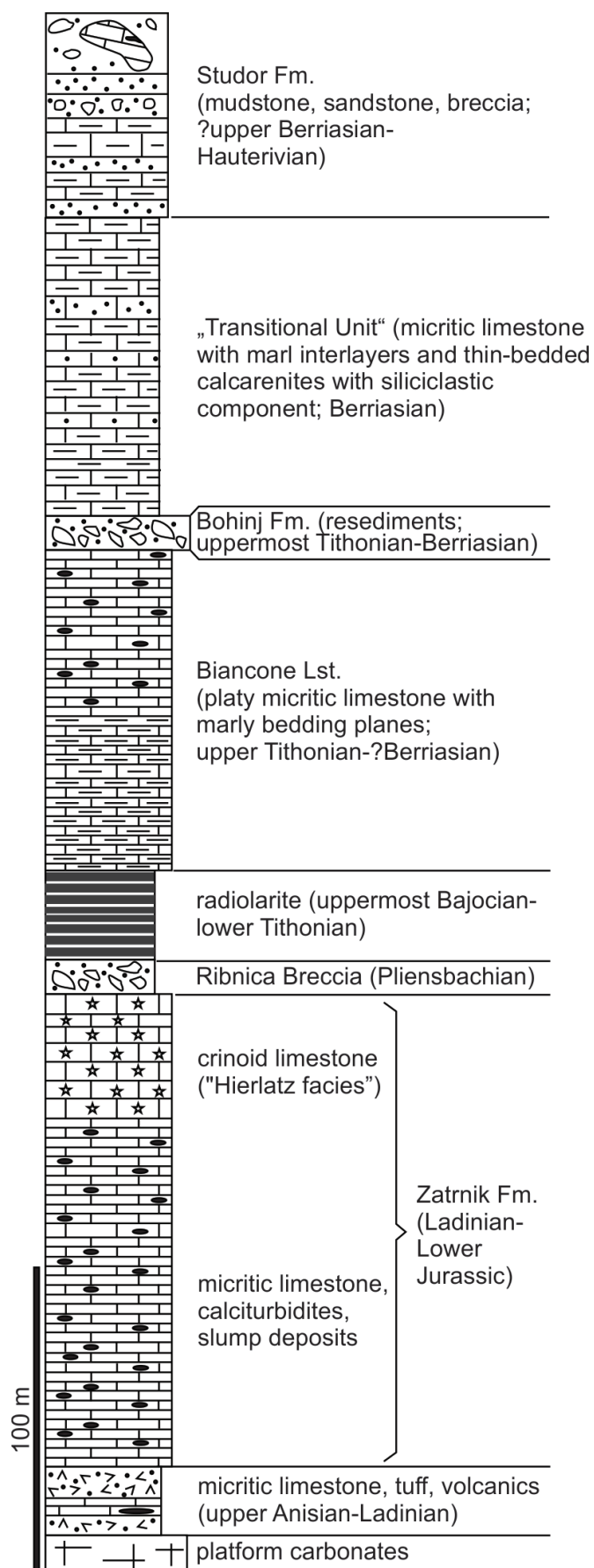


Fig. 2. Lithostratigraphic column of the Bled Basin. Modified after Goričan et al. (2018).

## Materials and methods

The sedimentological investigation of the logged section is based on 57 thin sections  $47 \times 28$  mm in size. Fine-grained calcarenite was sampled rather than mudstone varieties, so there is some bias to the described microfacies assemblage. Carbonates were classified according to classification by Dunham (1962). When adding components to the textural name, we follow suggestion by Wright (1992) and name the predominant grain type first. Point-counting of 300 points in a random grid was performed in JMicroVision v1.2.7 (Copyright 2002–2008 Nicolas Roduit) software. Due to the assumed latest Triassic age for the lower part of the logged succession, five standard-size conodont samples were taken. They were treated in diluted (cca. 8%) acetic acid at the Geological Survey of Slovenia. All conodont samples were negative.

## Lithological description

The total stratigraphic thickness of the Zajamniki section measures approximately 75 m (Figs. 3, 4a). It is divided into three parts: the “classical” Zatrnik Formation (up to 25.8 m), the “Hierlatz facies” of the Zatrnik Formation (from 25.8 to 72.0 m), and the Ribnica Breccia (above 72 m). The “classical” Zatrnik Formation is dominated by beige-coloured, predominantly medium bedded micritic (mudstone to very fine-grained packstone and grainstone) limestone (Fig. 4b). Chert nodules represent up to 30 % of the rock, with the exception of two thinner beds, which are completely silicified. Amalgamation surfaces are common. In addition to micritic limestone, two very thick beds of clast-supported breccia (rudstone?) are present in the lowermost part in beds up to 3.3 m thick. Breccia is normally graded. Clasts are moderately sorted. Clasts are beige, grey, and pale pink in colour, in compositions corresponding to the underlying lithologies. Matrix is subordinate and ochre in colour. Medium-thick beds of fine-grained calcarenite predominate over micritic limestone between the 16<sup>th</sup> and 21<sup>st</sup> metres of the section. Microfacies types from this first part of the section are dense intraclastic-bioclastic wackestone to packstone (MF1), bioclastic-pelletal packstone (MF2), peloid packstone (MF3), intraclastic grainstone (MF4), and poorly sorted intraclastic packstone to floatstone (MF5) (Table 1; Fig. 5).

The “classical” Zatrnik Formation is followed by a thick slumped (Fig. 4c) interval of micritic and crinoid-rich limestone which is strongly silicified in some parts. Such lithology was pre-

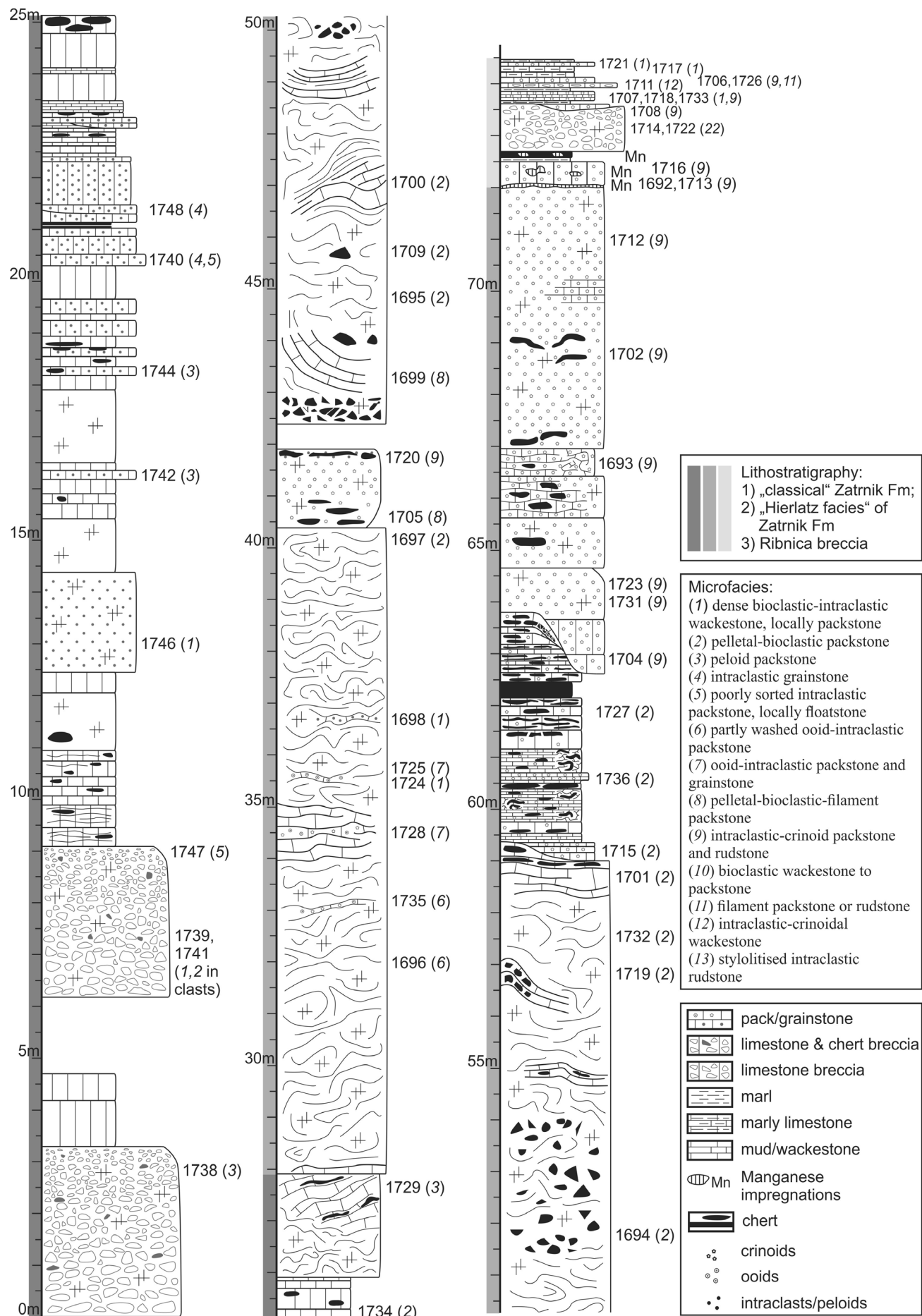


Fig. 3. Sedimentological log of the Zajamniki section. Numbers to the right of the lithology represent thin section numbers. The microfacies type is written in brackets next to the thin section number. For a description of microfacies types see Tables 1–3.

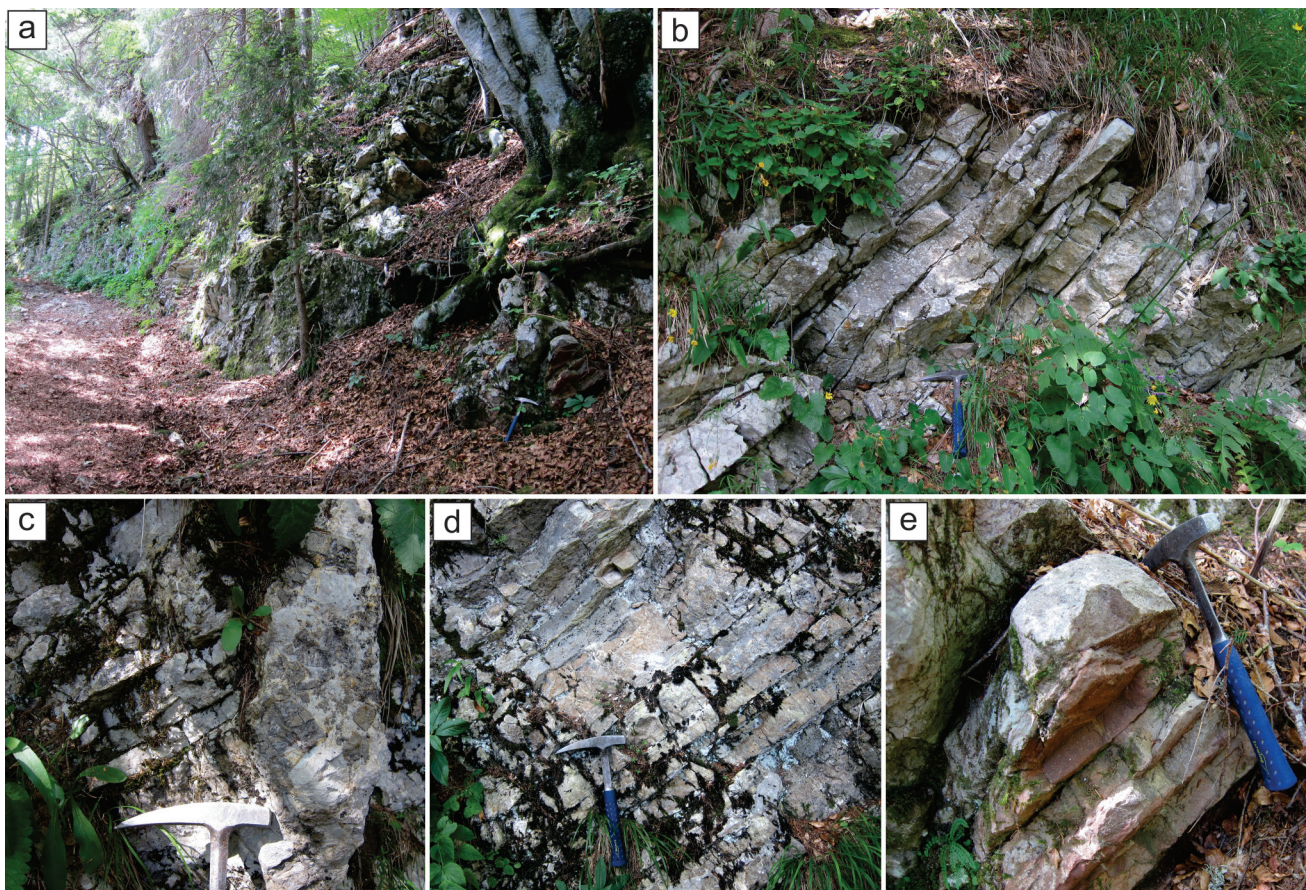


Fig. 4. Field photographs of the section. a: View on the section from the contact with the Ribnica Breccia (hammer). b: Micritic limestones of the Zatrnik Formation. c: Slump scar and slump breccia. d: Silicified limestone of the "Hierlatz facies". e: Contact with the Ribnica Breccia.

Table 1. Descriptions of microfacies (MF) types of the upper Zatrnik Formation from the first 26 m of the Zajamniki section.

MF type	Description	Figures
dense intraclastic-bioclastic wackestone, locally packstone (MF1)	Grains occupy 35 – 40 % of the area of view. They are medium sorted, in some samples poorly sorted due to the presence of larger intraclasts, calcimicrobes and large echinoderm ossicles. Micritic intraclasts (peloids) predominate among grains. They are subangular to subrounded. Only approximately 5 % of the volume is occupied by echinoderm plates, foraminifers, calcimicrobes, fragments of brachiopods, <i>Tubiphytes</i> -like microproblematica. Some echinoderm plates show small borings near their margins. Echinoderm plates are rimmed by syntaxial cement.	4a
bioclastic-pelletal packstone (MF2)	While some samples show vague parallel lamination, others appear bioturbated. Micritic matrix is full of small pellets. Highly notable are particles of calcite monocrystals, which are the largest particles in this MF. They are locally abundant enough to be in point-contacts and forming a great proportion of the rock (in fact, gradually passing into intraclastic-crinoid packstone). They are of various sizes (largest 0.85 mm), randomly oriented, and angular. Brownish inner parts are visible in some, probably representing echinoderm fragments, later overgrown by calcite. Many of them, however, cannot be determined. Ostracods, small foraminifers (nodosariids, <i>Lenticulina</i> , Textulariidae, Ophthalmidiidae) are rare. Sponge spicules are locally present. Fossils are mostly fragmented and/or disarticulated. Thin section 1694 also contains a singular angular clast of chert. Echinoderm plates are rimmed by syntaxial cement.	4b
peloid packstone (MF3)	Some samples show bioturbations, where peloid packstone intermixes with mudstone. Peloids occupy 44 % of area. They are very well sorted and in point contacts. Most are 0.08 – 0.1 mm in size. Echinoderm plates represent 4% of the area, and thalli of <i>Thaumatoporella</i> and foraminifers each 1 %. The latter include <i>Valvulinidae</i> , <i>Siphonvalvulina</i> sp., ? <i>Radoicicina</i> sp., <i>Earlandia</i> sp., glomospiral forms, and "Agerina". Also rare are calcimicrobes and ostracods.	4c
intraclastic grainstone (MF4)	Grains represent 50 % of the area. Sorting is medium to very good. Wide laminae, differing in size grains are visible. Small micritic intraclasts represent most of the grains. They are subangular to subrounded. Foraminifers ( <i>Siphonvalvulina</i> sp., Textulariidae, Valvulinidae, <i>Gaudryina</i> sp., <i>Earlandia</i> sp., <i>Meandrovoluta asiagoensis</i> Fugagnoli & Rettori), spartic particles, echinoderms, ostracods, calcimicrobes, and <i>Thaumatoporella</i> are very rare. Intergranular space is filled with drusy mosaic spar.	4d
poorly sorted intraclastic packstone, locally floatstone (MF5)	Grains are poorly sorted. Large calcimicrobes, micritic intraclasts, and also some echinoderm plates are over 2 mm long, and the largest reach 4.2 mm in size. Grains are chaotically distributed, floating or supporting each other in wackestone and packstone matrix. Besides the clasts mentioned, <i>Thaumatoporella</i> , brachiopod fragments, foraminifers (Pfenderinidae, <i>Reophax</i> sp., <i>Siphonvalvulina gibraltaricensis</i> Boudagher-Fadel, Rose, Bosence & Lord, <i>Everticyclammina</i> ? sp.), sponge fragments, and gastropods are present. Echinoderm plates are rimmed by syntaxial cement.	4e

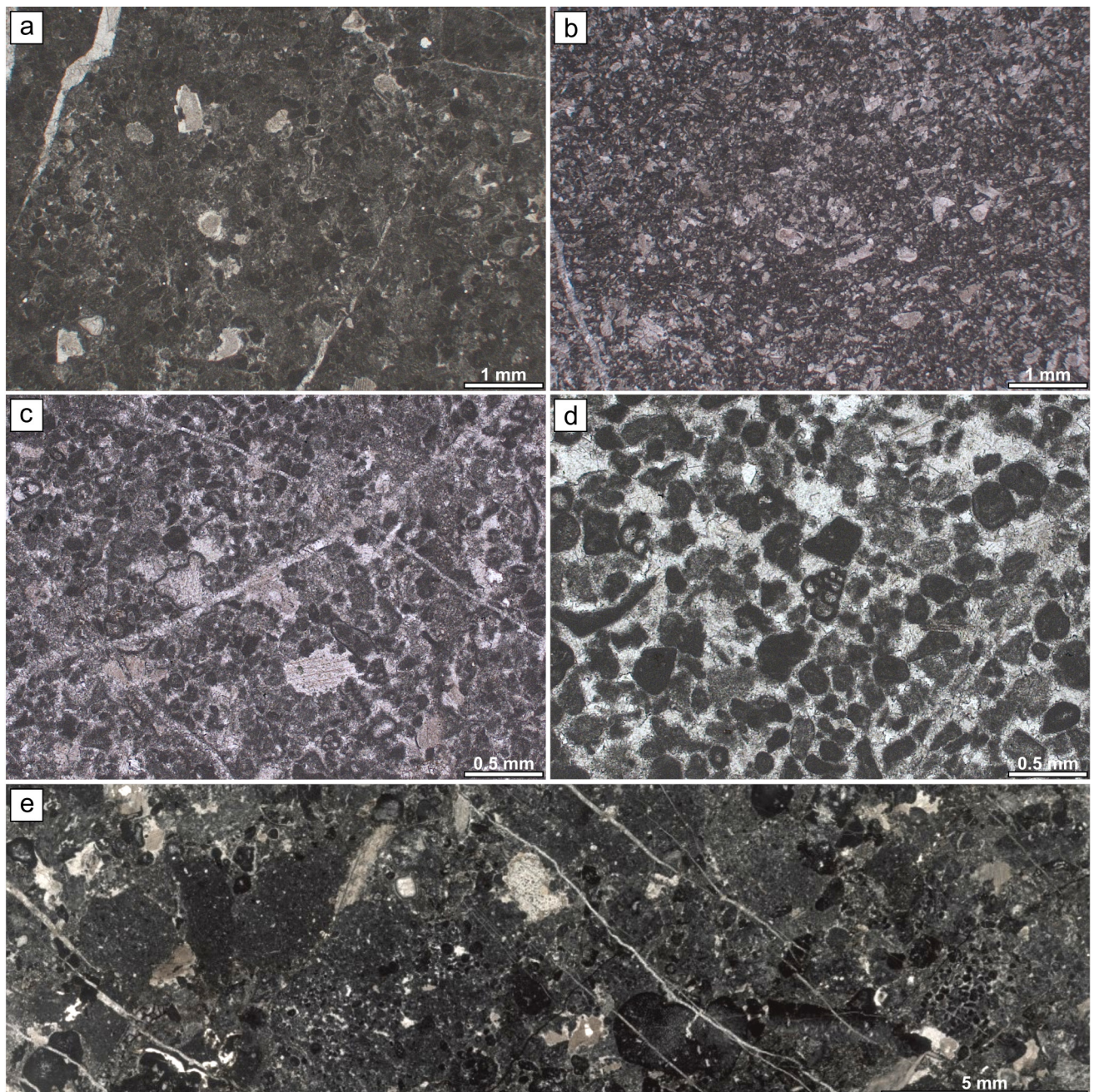


Fig. 5. Microfacies types of the upper Zatrnik Formation from the first 26<sup>th</sup> meters of the Zajamniki section. a: Dense intraclastic-bioclastic wackestone, locally packstone. Thin section 1746. b: Bioclastic-pelletal packstone. Thin section 1715. c: Peloid packstone. Thin section 1744. d: Intraclastic grainstone. Thin section 1740. e: Poorly sorted intraclastic floatstone. Thin section 1747.

viously marked as the “Hierlatz facies” (Goričan et al., 2012), or as the upper part of the Zatrnik Formation, rich in echinoderms (Kukoč, 2014; Goričan et al., 2018). The base of the “Hierlatz facies” is here set at the change in colour (beige colour is substituted by light pink). Thin beds dominate. Parallel lamination is preserved in completely silicified medium thick beds between the 61<sup>st</sup> and 63<sup>rd</sup> meters of the section (Fig. 4d). A sealed paleofault or slump scar outcrops at the 63<sup>rd</sup> meter. Here, the fine-grained limestone beds are downfolded and chert nodules brecciated. The space on the other side of the discontinuity

is filled by bedded coarse calcarenite. In addition to the already described peloid packstone, dense intraclastic-bioclastic wackestone to packstone, and bioclastic-pelletal packstone, the microfacies assemblage in this part of the section also comprises partly washed intraclastic-oolitic packstone (MF6), intraclastic-oolitic packstone and grainstone (MF7), filament-bioclastic-pelletal packstone (MF8), and crinoid-intraclastic packstone and rudstone (MF9) (Table 2; Fig. 6).

The uppermost 2.2 m of the section belong to the Ribnica Breccia. Impregnations with Fe-Mn oxides start at the upper bedding plane of the

Table 2. Description of microfacies (MF) types of the “Hierlatz facies” of the upper Zatrnik Formation between the 26<sup>th</sup> and 72<sup>nd</sup> meters of the Zajamniki section. In addition to these, previously described peloid packstone, dense bioclastic-intraclastic wackestone to packstone, and pelletal-bioclastic packstone are also present (see Table 1).

MF type	Description	Figures
partly washed intraclastic-oolitic packstone (MF6)	Packstone of this type appears more poorly sorted and with much less intergranular cement than in intraclastic-oolitic packstone and grainstone, but the general composition of the two is similar. Grains represent 70 % of the area. They are mostly in point contacts, some in long or concavo-convex contacts. Sorting is poor, with most grains ranging between 0.150 mm and 1.5 mm. The largest grain in thin section measures 3.7 mm. The dominant grains are sub- to well-rounded micritic intraclasts (60 % of area). Some (10 %) of the latter possibly represent micritic ooids. Oolitic envelopes are locally visible, but more common are what appears to be cortices crushed by compaction. Calcimicrobes represent 2 % of the total area, as well as echinoderms and mollusc fragments. Calcimicrobes are abraded, some partly overgrown by oolitic envelopes. Foraminifers ( <i>Siphovalvulina colomi</i> colomi Boudagher-Fadel, Rose, Bosence & Lord, <i>Siphovalvulina</i> sp., ? <i>Everticyclammina</i> sp., Trocholinidae), brachiopods and gastropods are also present. Echinoderm plates have micritic outlines, are bioeroded, or overgrown by syntactical rim cement.	5a
intraclastic-oolitic packstone and grainstone (MF7)	Grains are in point-contacts. In thin section 1725 they are moderately sorted, whereas in thin section 1728 they display a bimodal distribution in size due to the extra presence of small peloids. The grain size is between 0.175 and 0.95 mm. The largest grains are 2.27 mm in diameter. Micritic intraclasts represent 45 % of area. They are surrounded to well-rounded, in thin section 1728 also angular. The well-rounded ones could also be completely micritised ooids. Ooids are the second most common clasts (25 %). Most are of tangential type, but some are recrystallized into radial. They have between 2 and 16 envelopes, which are often partly bioeroded. Their nuclei contain micritic intraclasts, calcimicrobes, bioeroded sparitic particles, gastropods, foraminifers, or dasycladacean algae. Rarely or only sporadically present are sparitic bioclasts, foraminifers, clasts of <i>Pseudolithocodium/Lithocodium</i> , echinoderm plates, and gastropods. Foraminifers within and outside ooids are <i>Siphovalvulina</i> ex gr. <i>gibraltarensis</i> Boudagher-Fadel, Rose, Bosence & Lord, <i>S. ex gr. variabilis/colomi</i> Boudagher-Fadel, Rose, Bosence & Lord, Valvulinidae, ? <i>Everticyclammina</i> sp., “ <i>Nautiloculina</i> ” sp., <i>Meandrovoluta asiagoensis</i> Fugagnoli & Rettori, planispiral porcellaneus forms with porcelaneous walls, Trocholinidae, and Lagenida were recognised. Intergranular space is filled with drusy mosaic cement. Locally, grains are rimmed by granular cement, and the remaining intergranular space filled with micrite. Echinoderms are overgrown by syntactical rim cement.	5b
filament-boioclastic-pelletal packstone... (MF8)	This MF is similar to bioclastic-pelletal packstone (see Table 1), but with a significant amount (20 – 40 % of area) of filaments. These are disarticulated, concordant to bedding plane, and roughly uniform in size. The calcitic particles are here clearly echinoderm plates rimmed by syntactical cement. The two MF types are most like members of the same MF group, differing in different proportions of components.	5c
crinoid-intraclastic packstone and rudstone (MF9)	Concerning the composition, this MF is comparable to bioclastic-pelletal packstone, but with larger intraclasts and crinoids. Within the given level, grains are well sorted. Vertically, however, the grain size varies from 0.25 to over 3 mm. Grading is clearly visible in some samples. Grains represent 85 % of the area. They are in long to stylolitic contacts. Crinoids represent 60 % of the area. Intraclasts represent 25 % of area. They comprise various lithologies: a) mudstone, b) fenestral mudstone, c) bioclastic wackestone with ostracods and sparitic particles, d) bioclastic wackestone with ostracods, sparitic particles, pellets and small foraminifers ( <i>Agerina</i> sp., <i>Planispirillina</i> sp.), e) bioclastic wackestone with sparitic particles, spicules, nodosariids, and juvenile ammonites, f) bioclastic wackestone with sponge spicules, juvenile ammonites and filaments, g) peloid packstone, h) well sorted peloid grainstone, i) peloid-cortoid grainstone, j) calcisiltite. Besides intraclasts, finer-grained varieties of MF 9 contains rare ostracods and foraminifers (nodosariids, <i>Pseudonodosaria</i> , ? <i>Epistominae</i> , <i>Lenticulina</i> sp.). Echinoderm plates are rimmed by syntactical cement. Manganese nodules and impregnations are present in some samples.	5d

slumped limestone at the 72<sup>nd</sup> meter (Fig. 4e). In addition to Fe-Mn impregnations, characteristic features of this interval include violet colour and a higher clay content. The first bed above the slumped interval is marly crinoid limestone. This is followed by 20 cm of marlstone and chert, which includes clasts of limestone, and poorly-sorted polymictic clast-supported breccia one meter thick. Angular clasts range from 4 mm to 10 cm in size, with the bulk of them approximately 2 cm in size. They are in stylolitic contacts. Matrix is subordinate to clasts and red in colour.

The prominent breccia bed is followed by thinner beds of marlstone, marly crinoid limestone, graded calcarenite, and fine-grained breccia. The last three beds in the section are yellowish in colour. The microfacies assemblage of this unit consists of crinoid-intraclastic packstone and rudstone, already described from lower parts of the section, and new microfacies types, which comprise bioclastic wackestone to packstone (MF10), filament packstone or rudstone (MF11), intraclastic-crinoid wackestone (MF12), and stylolitised intraclastic rudstone (MF13) (Table 3; Fig. 7).

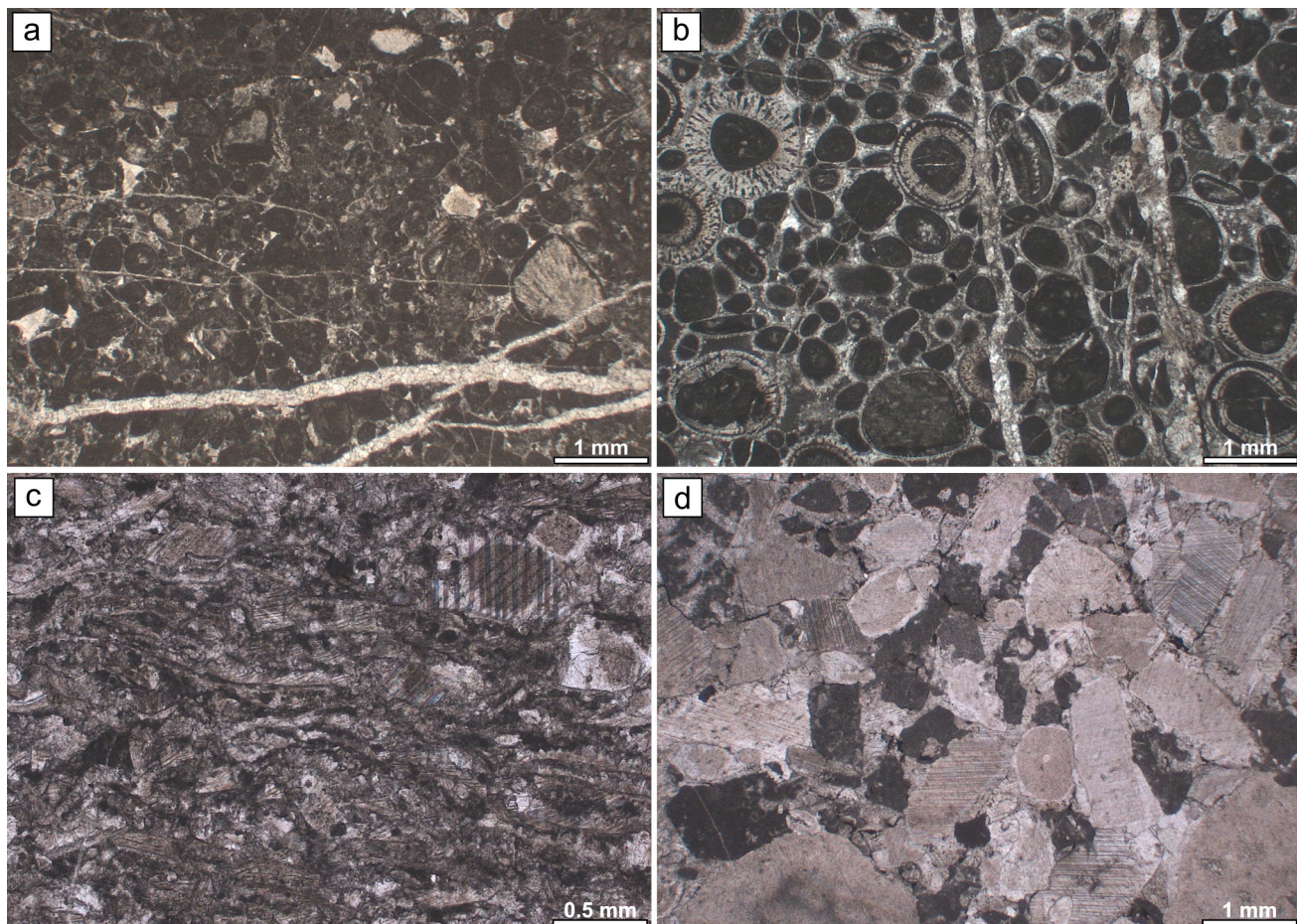


Fig. 6. Microfacies (MF) types of the uppermost Zatrnik Formation. a: Partly washed intraclastic-oolitic packstone. Thin section 1696. b: Intraclastic-oolitic packstone, partly washed. Thin section 1725. c: Filament-bioclastic-pelletal packstone. Thin section 1699. d: Crinoid-intraclastic packstone and rudstone. Thin section 1712.

Table 3. Description of microfacies (MF) types of the Ribnica Breccia from the Zajamniki section. In addition to these, intraclastic-crinoid packstone and rudstone is also present (see descriptions in Table 2).

MF type	Description	Figures
bioclastic wackestone to packstone (MF10)	Grains represent 30 – 50 % of the area. Echinoderm plates predominate (60 – 70 % of grains). Micritic intraclasts form approximately 30 % of grains, foraminifers 1 % of grains, and ostracods 5 % of grains. In packstone variety, peloids occupy additional 10 % of the surface area, and limonitised oncoids locally 5 % of surface. Very rare are apatuchi. Among foraminifers are most common lagenids, including <i>Lenticulina</i> , and less numerous <i>Ophthalmidium</i> and Valvulinidae. Foraminifers are commonly broken, and many bioclasts are bioeroded. Intergranular space is filled with micritic matrix, which is limonitised in some levels.	6a-b
filament packstone and rudstone (MF11)	Filaments are even more abundant and densely packed together than in filament-bioclastic-pelletal packstone. Filaments represent approximately 90 % of the surface, echinoderm plates 5 – 10 %, and peloids only around 2.5 %. The amount of micritic matrix is very small due to grains being in long contacts.	6c
intraclastic-crinoid wackestone (MF12)	Grains represent 60 % of the area. Grains are randomly distributed within the matrix, most are matrix-supported. The most common grains are various intraclasts (21 %): a) mudstone, b) bioclastic wackestone with filaments and juvenile ammonites, c) wackestone with crinoids, and peloid grainstone. Echinoderm plates occupy 13 % of the area. Ferromanganese nodules cover 3.5 % of the area. The rest of the volume is taken by filaments, ostracods, and foraminifers (nodosariids, <i>Lenticulina</i> ). Margins of clasts are often covered by opaque mineral (ferromanganese or limonite crust).	6d
stylolitised intraclastic rudstone (MF13)	Clasts in thin sections are over 3 cm in size. They are in limonitised stylolitic contacts. Intraclasts comprise light pink and beige bioclastic wackestone with sponge spicules, echinoderms, gastropods, nodosariids, and juvenile ammonites. Less common are intraclasts of peloidal-bioclastic wackestone.	6e-f

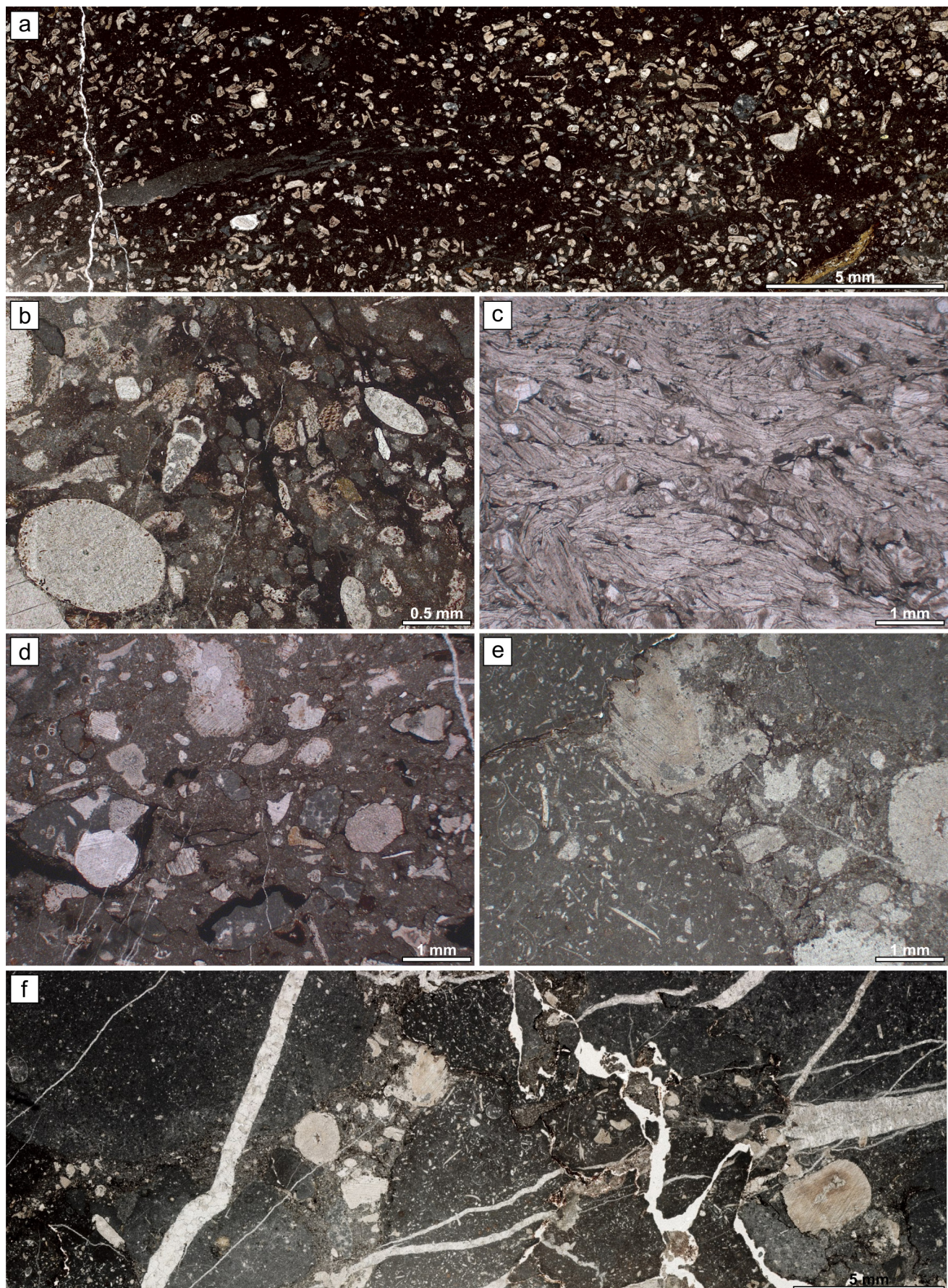


Fig. 7. Microfacies (MF) types of the Ribnica Breccia. a-b: Bioclastic wackestone to packstone. Thin sections 1717 and 1733, respectively. c: Filament packstone or rudstone. Thin section 1726. d: Intraclastic-crinoidal wackestone. Thin section 1711. e-f: Stylolitised intraclastic rudstone. Thin section 1714.

Table 4. Distribution of foraminiferal species in the uppermost Zatrnik Formation and in the Ribnica Breccia in the Zajamniki section.

Sample	Foraminifers																			
	Thaumatoporella	calcimicrobes	Siphovalvulina spp.	?Mesendothyra sp.	?Pseudopfenderina sp.	?Everticyclammina sp.	Miliolida indet.	Earlandia sp.	Valvulinidae	Meandrovoluta sp.	Reophax sp.	Textulariidae	Lagenida (uniserial)	Trocholina sp.	Ophthalmidium sp.	?Nautiloculina sp.	Lenticulina sp.	?Ammobaculites sp.	Spirilina sp.	?Epistominidae
Ribnica Breccia	1721																			
	1717																			
	1706																			
	1711																			
	1737																			
	1733																			
	1718																			
	1707																			
	1708																			
	1722																			
upper part of the Zatrnik Fm. ("Hierlatz facies")	1693																			
	1704																			
	1727																			
	1701																			
	1719																			
	1695																			
	1697																			
	1698																			
	1725	●			●				●	●										
	1724								●											
	1728								●											
	1735	●			●				●											
	1696	●							●											
	1729																			
"classical" Zatrnik Formation	1748	●		●						●	●									
	1740	●	●	●			●			●	●	●	●							
	1744	●		●																
	1742	●		●						●	●									
	1746				●					●										
	1747	●	●	●					●											
	1739																			
	1741	●	●	●	●	●	●													
	1738	●	●																	

### Fossils and age of the uppermost Zatrnik Formation

The age of the investigated interval was determined on the basis of benthic foraminifers. The stratigraphic distribution of foraminifers is shown in Table 4, and some are depicted in Figure 8. Overall, the foraminiferal assemblage consists of small benthic specimens that do not allow

for precise stratigraphic control and are difficult to determine even at the genus or species level. The presence of *Siphovalvulina* spp. in the lower part of the section excludes Triassic age and instead places this part of the section already in the Jurassic (Septfontaine, 1988; Chiocchini et al., 1994). The Triassic-Jurassic boundary thus lies lower in the succession and is not present in the

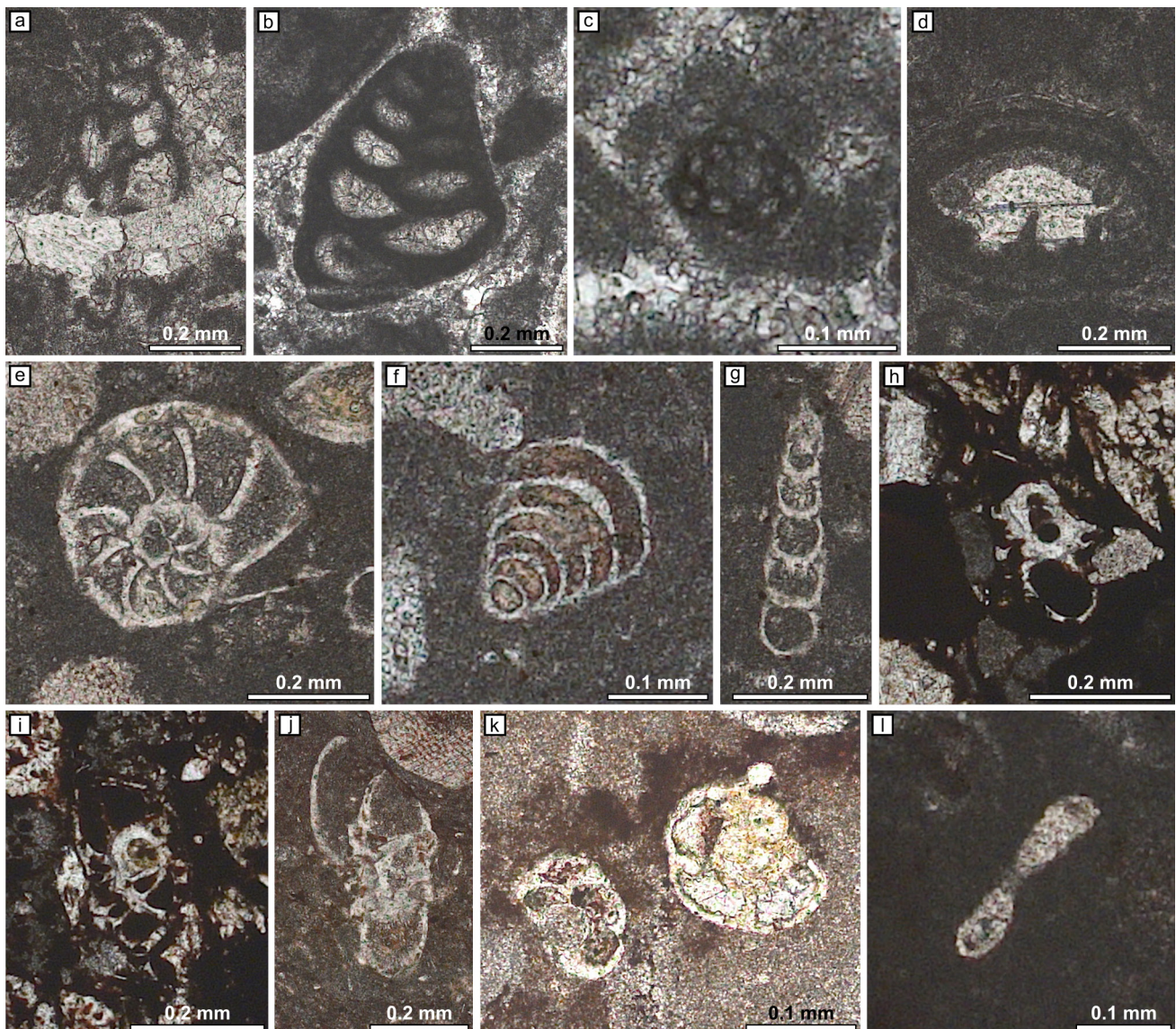


Fig. 8. Some characteristic foraminifers from the uppermost Zatrnik Formation and the Ribnica Breccia. a: *Siphovalvulina* sp. Thin section 1696. b: Valvulinidae. Thin section 1725. c: *Meandrovoluta asiagoensis* Fugagnoli & Rettori. Thin section 1740. d: *Trocholina* sp. Thin section 1735. e: *Lenticulina* sp. Thin section 1721. f: Uniserial Lagenida. Thin section 1722. g: Nodosariid Lagenida. Thin section 1721. h–k: ?Epistominidae. h–i: Thin section 1706. j: Thin section 1717. k: Thin section 1718. l: *Spirillina* sp. Thin section 1708.

logged section. Besides *Siphovalvulina*, which is the most typical genus in the lower part of the section, the assemblage from the first 21 m of the section also consists of a few other species, which, however, are determined with great uncertainty. These are dubious specimens of *?Everticyclammina*, *?Mesoendothyra*, *?Pseudopfenderina*, *Earlandia* sp., and *?Reophax* sp. Calcimicrobes and *?Thaumatoporella* are also commonly present. Similar assemblages characterise the platform tops from the Lower Jurassic of the peri-Mediterranean area (e.g., Chiocchini et al., 1994; Mancinelli et al., 2005; Rožič et al., 2019). *Siphovalvulina* is present also in the lower samples of the "Hierlatz facies" of the Zatrnik Formation. Early Jurassic age is supported by rare occurrences of

*Meandrovoluta asiagoensis* Fugagnoli & Rettori (Fugagnoli et al., 2003). Along with some of the previously present species, *Trocholina* sp., Valvulinidae, small Textulariidae, small elongated and at least partly uniserial Lagenida, and small *?Ophthalmidium* occur. The highest occurrence of *Siphovalvulina*, *Trocholina*, Valvulinidae and *?Everticyclammina* appears in sample 1725, which is 35.6 m from the base of the section. Foraminifers are then scarce until the base of the Ribnica Breccia. The assemblage of the Ribnica Breccia stands in contrast to the assemblages from the Zatrnik Formation. The most common genus is *Lenticulina*, commonly associated with small elongated Lagenida. Several specimens of small epistominids were also determined.

## Sedimentological interpretation

The absence of cross-laminations or other textures related to water depths above the storm weather wave base in the “classical” Zatrnik Formation in the Zajamniki section is consistent with the previous interpretation of the deposition within a deeper marine environment (Gale et al., 2019). Calcimicrobes, *Tubiphytes*-like microproblematica, *Thaumatoporella*, some foraminifers (*Siphovalvulina*, *Meandrovoluta*, *Everticyclammina* – see Gale, 2014) and also small borings on echinoderm plates suggest that at least some of the particles originate from within the photic zone. Due to the presence of parallel lamination in some beds, we suggest that microfacies types 1–4 (see Table 1) deposited as distal turbidites. Bioturbation suggests an oxygenated sea floor. It should be noted, again, that the sampling was biased towards calcarenites, thus possibly omitting hemipelagic microfacies types. The two thicker rudstone beds may represent the base of a turbidite or debris flow deposits (Mullins & Cook, 1986). Slumps in the uppermost part of the Zatrnik Formation could indicate some intensive tectonic-controlled movements of the sea floor. Like the foraminifers *Siphovalvulina*, *Trocholina*, Valvulinidae and ?*Everticyclammina*, which are most numerous here, ooids also originate from the platform top (see Gale, 2014). The facies association of distal turbidites, hemipelagic deposits, clast-supported debris breccias, and slumps points to deposition on a slope of the basin (Mullins & Cook, 1986).

From the 63<sup>rd</sup> meter onwards, virtually only crinoids and intraclasts constitute the resedimented material, while the strictly platform-top elements are missing. Haas and Tardy-Filács (2004) suggested that the large amount of crinoids within the Rhaetian carbonates originated from terrace-like slopes, since crinoids are not a common element of uppermost Triassic carbonate platforms and reefs. Crinoid-dominated sand-sized material was also interpreted to originate from a shallow pelagic environment by Rožič et al. (2017, with references). In light of this study, this could indicate major changes in the topography of the Julian Carbonate Platform and the establishment of a step-like topography along normal faults.

Ferromanganese enrichments at the contact between the Zatrnik Formation and the overlying Ribnica Breccia point to a reduced sedimentation rate (Šmuc & Goričan, 2005). The Ribnica Breccia in the Zajamniki section is thinner and finer grained in the Zajamniki section than in the Rib-

nica Valley, as was noted in Goričan et al. (2012). In the Ribnica Valley, individual beds reach a thickness of up to 5 m, containing up to 40 cm large clasts and chert clasts some 1 m in size. The breccia was interpreted there as debris-flow deposit (Kukoč, 2014; Goričan et al., 2018). Intraclastic-crinoid wackestone and stylolitised intraclastic rudstone, which are part of the microfacies assemblage of the Ribnica Breccia in the Zajamniki section, are also interpreted here as debris-flow deposits (the former due to mud-supported and chaotically distributed clasts, the latter owing to its breccia nature). These mix with possible turbidite deposits (crinoid-intraclastic packstone and rudstone), or gravity-flow deposits of some other type (bioclastic wackestone to packstone). We are unsure how to interpret filament packstone and rudstone – either as autochthonous or allochthonous deposits, but Rožič and Šmuc (2011) recorded identical microfacies types from turbidites within the Perbla Formation of the Slovenian Basin.

## Stratigraphic comparisons

The lack of biostratigraphic data from this and from most of the previously investigated sections mentioned herein does not allow for precise correlations between the sections. However, the successions summarised below follow a similar pattern, suggesting a common cause.

From Mt. Mangart, Šmuc and Goričan (2005) described a stratigraphic succession recording the evolution from the margin of the Julian Carbonate Platform to a deeper basin. The succession starts with Lower Jurassic peloidal and oncoidal limestones, probably deposited in the marginal belt of a shallow-water platform. It then continues with bioclastic limestone rich in echinoderms, ammonites, sponge spicules, and foraminifers *Lenticulina*, *Agerina* (here interpreted as small *Ophthalmidium*), Textulariidae, and Valvulinidae, deposited on a distal shelf, possibly during the Pliensbachian. At the top, this unit contains a few beds of fine-grained breccia and calcarenite, and finally ends with red siliceous limestone impregnated with Fe-Mn. The overlying shale and siliceous limestone contain early Toarcian radiolarian fauna.

Another marginal succession was recorded on Mt. Kobla by Rožič and Šmuc (2009), and Rožič et al. (2014). The lower part of the 150-m-long section is made up of ooidal/peloidal limestone deposited on a carbonate platform. These beds are followed by bioclastic limestone with common sponge spicules and crinoids alternating with

crinoidal limestone. Ammonites suggest Pliensbachian age (Rožič et al., 2014). Neptunian dykes filled with crinoid debris and a breccia bed some meters thick are present at the top. Above follows a bed of marlstone 50 cm thick, impregnated with ferromanganese oxides (Rožič & Šmuc, 2009).

Within the Slovenian Basin, the lowermost Jurassic belongs to the Krikov Formation, followed by the Perbla Formation (Rožič, 2009). The Hettangian–Pliensbachian Krikov Formation in its proximal development in the lower part largely consists of ooidal/peloidal limestone, while its upper part is largely made up of crinoid-rich calciturbidites and is rich in diverse clasts of eroded basinal to slope limestones. The overlying Perbla Formation is Toarcian in age and consists of marlstone and hemipelagic limestone, in the lower part locally impregnated with manganese (Rožič, 2009; Rožič & Šmuc, 2009).

The shift from the micritic Zatrnik limestone to crinoid-dominated Zatrnik limestone thus seems to be in accordance with previous observations and, although precise dating is missing, probably took place during the Pliensbachian, when the accelerated subsidence changed the paleotopography of the Julian Carbonate Platform.

### Conclusions

The following conclusions follow from the present study:

1) The “Hierlatz facies,” as well as the uppermost part of the “classical” Zatrnik Formation, are Early Jurassic in age.

2) The uppermost “classical” Zatrnik Formation consists of distal turbidite deposits, probably hemipelagic deposits, and some debris-flow deposits. Slumping of the sediment is common in the “Hierlatz facies” in the studied section.

3) The shift towards the crinoid-dominated “Hierlatz facies” could be due to changes in the paleotopography of the adjacent platform and its slopes. Comparison to previously recorded successions suggests that the change occurred during the Pliensbachian.

4) The Triassic–Jurassic boundary should be sought a few tens of meters below the “Hierlatz facies” of the Zatrnik Formation. Although sedimentation was largely affected by gravity flows, the facies seems more distal than in the sections of the Slatnik Formation studied so far, thus promising a somewhat more complete record of the Triassic–Jurassic boundary events. Further research will thus be devoted to locating this boundary.

### Acknowledgements

This study was financially supported by the Slovenian Research Agency (Programme No. P1-0011 to L.G.). The technical staff of the Geological Survey of Slovenia is acknowledged for its preparation of thin sections and for processing of the conodont samples.

### References

- Bosellini, A., Gianolla, P. & Stefani, M. 2003: Geology of the Dolomites. *Episodes*, 26: 181–185.
- Breda, A. & Preto, N. 2011: Anatomy of an upper Triassic continental to marginal-marine system: the mixed siliciclastic-carbonate Travenanzes Formation (Dolomites, Northern Italy). *Sedimentology*, 58: 1613–1647.
- Breda, A., Preto, N., Roghi, G., Furin, S., Meneguolo, R., Ragazzi, E., Fedele, P. & Gianolla, P. 2009: The Carnian Pluvial Event in the Tofane area (Cortina d’Ampezzo, Dolomites, Italy). *Geo. Alp.*, 6: 80–115.
- Budkovič, T. 1978: Stratigrafija Bohinjske doline. *Geologija*, 21: 239–244.
- Buser, S. 1980: Explanatory Book to Basic Geological Map SFRY 1: 100.000, Sheet Celovec. Zvezni geološki zavod, Beograd: 62 p.
- Buser, S. 1986: Explanatory Book to Basic Geological Map SFRY 1: 100.000, Sheets Tolmin and Videm (Udine). Zvezni geološki zavod, Beograd: 103 p.
- Buser, S. 1989: Development of the Dinaric and the Julian carbonate platforms and of the intermediate Slovenian Basin (NW Yugoslavia). *Mem. Soc. Geol. It.*, 40: 313–320.
- Buser, S. 1996: Geology of Western Slovenia and its paleogeographic evolution. In: Drobne, K., Goričan, Š. & Kotnik, B. (eds.): International workshop Postojna ‘96: The role of impact processes and biological evolution of planet Earth. Založba ZRC, Ljubljana: 111–123.
- Chiocchini, M., Farinacci, A., Mancinelli, A., Molinari, V. & Potetti, M. 1994: Biostratigrafia a foraminiferi, dasycladali e calpionelle delle successioni carbonatiche Mesozoiche dell’Appennino Centrale (Italia). *Studi Geol. Camerti*, spec. iss. 1994: 9–130.
- Cousin, M. 1981: Les rapports Alpes-Dinarides. Les confins de l’Italie et de la Yougoslavie. *Soc. Géol. Nord*, 5: vol I: 1–521, vol. II Annexe: 1–521.
- Diener, C. 1884: Beitrag zur Geologie des Zentralstockes der julischen Alpen. *Jb. Kais. König. Geol. R.-A.*, 34: 659–706.

- Dozet, S. & Buser, S. 2009: Triassic. In: Pleničar, M., Ogorelec, B. & Novak, M. (eds.): The Geology of Slovenia. Geološki zavod Slovenije, Ljubljana: 161–214.
- Dunham, R.J. 1962: Classification of carbonate rocks according to depositional texture. In: Han, W.E. (ed.): Classification of carbonate rocks, A symposium. American Ass. Petrol. Geol. Mem., Tulsa: 108–121.
- Fugagnoli, A., Giannetti, A. & Rettori, R. 2003: A new foraminiferal genus (*Miliolina*) from the Early Jurassic of the Southern Alps (Calcare Grigi Formation, Northeastern Italy). Rev. Espan. Micropal., 35: 43–50.
- Gale, L. 2014: Lower Jurassic foraminiferal biostratigraphy of Podpeč Limestone (External Dinarides, Slovenia). Geologija, 57/2: 119–146. <https://doi.org/10.5474/geologija.2014.011>
- Gale, L., Celarc, B., Caggiati, M., Kolar-Jurkovšek, T., Jurkovšek, B. & Gianolla, P. 2015: Paleogeographic significance of Upper Triassic basinal succession of the Tamar Valley, northern Julian Alps (Slovenia). Geol. Carpathica, 66: 269–283. <https://doi.org/10.1515/geoca-2015-0025>
- Gale, L., Kolar-Jurkovšek, T., Karničnik, B., Celarc, B., Goričan, Š. & Rožič, B. 2019: Triassic deep-water sedimentation in the Bled Basin, eastern Julian Alps, Slovenia. Geologija, 62/2: 153–173. <https://doi.org/10.5474/geologija.2019.007>
- Gianolla, P., Mietto, P., Rigo, M., Roghi, G. & De Zanche, V. 2010: Carnian-Norian paleogeography in the eastern Southern Alps. Albertiana, 39: 64–65.
- Goričan, Š., Košir, A., Rožič, B., Šmuc, A., Gale, L., Kukoč, D., Celarc, B., Črni, A.E., Kolar-Jurkovšek, T., Placer, L. & Skaberne, D. 2012: Mesozoic deep-water basins of the eastern Southern Alps (NW Slovenia). J. Alp. Geol., 54: 101–143.
- Goričan, Š., Žibret, L., Košir, A., Kukoč, D. & Horvat, A. 2018: Stratigraphic correlation and structural position of Lower Cretaceous flysch-type deposits in the eastern Southern Alps (NW Slovenia). Int. J. Earth Sci., 107: 2933–2953. <https://doi.org/10.1007/s00531-018-1636-4>
- Haas, J. & Tardy-Filácz, E. 2004: Facies changes in the Triassic–Jurassic boundary interval in an intraplatform basin succession at Csővár (Transdanubian Range, Hungary). Sed. Geol., 168/1–2: 19–48. <https://doi.org/10.1016/j.sedgeo.2004.03.002>
- Härtel, F. 1920: Stratigraphische und tektonische Notizen über das Wocheiner Juragebiet. Verh. Geol. Staatsanstalt, 8–9: 134–153.
- Kolar-Jurkovšek, T., Buser, S. & Jurkovšek, B. 1983: Zgornjetriaspne plasti zahodnega dela Pokljuke. RMZ, 30: 151–185.
- Kovács, S., Sudar, M., Grădinaru, E., Gawlick, H.-J., Karamata, S., Haas, J., Péro, C., Gaetani, M., Mello, J., Polák, J., Aljinović, D., Ogorelec, B., Kolar-Jurkovšek, T., Jurkovšek, B. & Buser, S. 2011: Triassic evolution of the tectono-stratigraphic units of the Circum-Pannonian Region. Jb. Geol. B.-A., 151: 199–280.
- Kukoč, D. 2014: Jurassic and Cretaceous radiolarian stratigraphy of the Bled Basin (northwestern Slovenia) and stratigraphic correlations across the Internal Dinarides (PhD thesis). Faculty of Natural Sciences and Engineering, Ljubljana: 257 p.
- Kukoč, D., Goričan, Š. & Košir, A. 2012: Lower Cretaceous carbonate gravity-flow deposits from the Bohinj area (NW Slovenia): evidence of a lost carbonate platform in the Internal Dinarides. Bull. Soc. Géol. France, 183: 383–392.
- Mancinelli, A., Chiocchini, M., Chiocchini, R.A. & Romano, A. 2005: Biostratigraphy of Upper Triassic–Lower Jurassic carbonate platform sediments of the central-southern Apennines (Italy). Riv. Ital. Paleont. Strat., 111/2: 271–283. <https://doi.org/10.13130/2039-4942/6314>
- Mullins, H.T. & Cook, H.E. 1986: Carbonate apron models: Alternatives to the submarine fan model for paleoenvironmental analysis and hydrocarbon exploration. Sed. Geol., 48: 37–79. [https://doi.org/10.1016/0037-0738\(86\)90080-1](https://doi.org/10.1016/0037-0738(86)90080-1)
- Placer, L. 2008: Principles of the tectonic subdivision of Slovenia. Geologija, 51/2, 205–217. <https://doi.org/10.5474/geologija.2008.021>
- Ramovš, A. 1986: Paläontologisch bewiesene Karn/Nor-Grenze in den Julischen Alpen. Newslett. Strat., 16: 133–138.
- Ramovš, A. 1998: Conodonten-Stratigraphie der Obertrias von Slowenien: Ergebnisse eiderer Untersuchungen. Geologija, 40: 223–232. <https://doi.org/10.5474/geologija.1997.009>
- Rožič, B. 2009: Perbla and Tolmin formations: revised Toarcian to Tithonian stratigraphy of the Tolmin Basin (NW Slovenia) and regional correlations. Bull. Soc. Géol. France, 180: 411–430.
- Rožič, B. & Šmuc, A. 2009: Jurska evolucija prehodne cone med Julijsko karbonatno platoformo in Slovenskim bazenom. Geol. Zbornik, 20: 146–151.

- Rožič, B. & Šmuc, A. 2011: Gravity-flow deposits in the Toarcian Perbla Formation (Slovenian basin, NW Slovenia). *Riv. Ital. Paleont. Strat.*, 117/2: 283–294. <https://doi.org/10.13130/2039-4942/5975>
- Rožič, B., Venturi, F. & Šmuc, A. 2014: Ammonites from Mt Kobla (Julian Alps, NW Slovenia) and their significance for precise dating of Pliensbachian tectono-sedimentary event. *RMZ*, 61: 191–201.
- Rožič, B., Kolar-Jurkovšek, T., Žvab Rožič, P. & Gale, L. 2017: Sedimentary record of subsidence pulse at the Triassic/Jurassic boundary interval in the Slovenian Basin (eastern Southern Alps). *Geol. Carpathica*, 68/6: 543–561. <https://doi.org/10.1515/geoca-2017-0036>
- Rožič, B., Popit, T., Gale, L., Verbovšek, T., Vidmar, I., Dolenc, M. & Žvab Rožič, P. 2019: Origin of the Jezero v Ledvicah lake; a depression in a gutter-shaped karstic aquifer (Julian Alps, NW Slovenia). *Acta Carsologica*, 48: 265–282. <https://doi.org/10.3986/ac.v48i3.7446>
- Septfontaine, M. 1988: Towards an evolutionary classification of Jurassic lituolids (foraminifera) in carbonate platform environment. *Rev. Paleobiol.*, spec. vol. 2 (Benthos '86): 229–256.
- Šmuc, A. 2005: Jurassic and Cretaceous stratigraphy and sedimentary evolution of the Julian Alps, NW Slovenia. ZRC Publishing, ZRC SAZU, Ljubljana, 98 p.
- Šmuc, A. & Goričan, Š. 2005: Jurassic sedimentary evolution of a carbonate platform into a deep-water basin, Mt. Mangart (Slovenian-Italian border). *Riv. Ital. Paleont. Strat.*, 111/1: 45–70. <https://doi.org/10.13130/2039-4942/6269>
- Šmuc, A. & Rožič, B. 2010: The Jurassic Prehodavci Formation of the Julian Alps: easternmost outcrops of Rosso Ammonitico in the Southern Alps (NW Slovenia). *Swiss J. Geosci.*, 103/2, 241–255. <https://doi.org/10.1007/s00015-010-0015-3>
- Wright, V.P. 1992: A revised classification of limestones. *Sed. Geology*, 76: 177–185.



# Strukturne razmere na stiku Južnih Alp in Dinaridov na zahodnem Cerkljanskem

## Structural setting at the contact of the Southern Alps and Dinarides in western Cerkljansko region (western Slovenia)

Jože ČAR<sup>1</sup>, Jernej JEŽ<sup>2</sup> & Blaž MILANIČ<sup>2</sup>

<sup>1</sup>Finžgarjeva ulica 18, SI-5280 Idrija, Slovenija; e-mail: joze.car@siol.net

<sup>2</sup>Geološki zavod Slovenije, Dimičeva ul. 14, SI-1000 Ljubljana, Slovenija;  
e-mail: jernej.jez@geo-zs.si, blaz.milanic@geo-zs.si

Prejeto / Received 31. 8. 2021; Sprejeto / Accepted 2. 11. 2021; Objavljeno na spletu / Published online 28. 12. 2021

**Ključne besede:** narivna zgradba, Trnovski pokrov, Tolminski pokrov, stik Južnih Alp in Dinaridov, Slovenski bazen, trias, psevdoziljske plasti

**Key words:** thrust structure, Trnovo nappe, Tolmin nappe, Southern Alps – Dinarides contact, Slovenian basin, Triassic, Pseudozilian beds

### Izvleček

Ozemlje med vasmi Reka v dolini Idrijce, Bukovo pod Kojco in Zakriž pri Cerknem pripada v geografskem in geotektonskem pogledu Dinaridom. Gradijo ga kamnine dveh obsežnih narivnih enot Trnovskega pokrova, ki so bile za več deset kilometrov narinjene od severovzhoda proti jugozahodu v današnjo lego. Preko njih so narinjene kamnine Tolminskega pokrova, ki je na obravnavanem ozemlju najnižja narivna enota Južnih Alp. Pokrov sestavljajo dve notranji narivni grudi in vmesna narivna luska. Narivne enote so bile narinjene od severa proti jugu. V zahodnem delu obravnavanega območja stik med Južnimi Alpami in Dinaridi poteka ob Sovodenjskem prelomu.

Kljub temu, da so kamnine v obravnavanih narivnih enotah približno enake starosti, lahko prepoznamo dva različna stratigrafska razvoja. Posebej izstopa problematika razvoja ladinjsko-spodnjekarnijskih psevdoziljskih plasti, to je zaporedja klastičnih in karbonatnih kamnin, ki se je odložilo v globljemorskem okolju Slovenskega bazena. Tako v Trnovskem kot tudi v Tolminskem pokrovu najdemo psevdoziljske plasti razvite v podobnem, litološko značilnem zaporedju, a so v Tolminskem pokrovu razvite v precej večji debelini kot v Trnovskem pokrovu in navzgor zvezno prehajajo v amfiklinske plasti, medtem ko je debelina psevdoziljskih plasti v Trnovskem pokrovu precej manjša, v normalnem zaporedju pa na njih leži platformni cordevolski dolomit.

### Abstract

The area between the villages of Reka in the Idrijca Valley, Bukovo and Zakriž near Cerkno belongs geographically and geotectonically to the Dinarides. The area consists of two large inner thrust blocks of the Trnovo nappe, which were thrusted for tens of kilometers in the direction of SW to their present position. They are overlain by the Tolmin nappe, the lowest thrust unit of the Southern Alps. The Tolmin nappe was thrusted from N to S and consists of two inner thrust blocks and a smaller intermediate inner sheet. In the western part of the area the contact between Southern Alps and the Dinarides runs along the regional Sovodenj fault.

Although the rocks in the considered thrust units are about the same age, different stratigraphic settings could be recognized. The lithostratigraphic features of the Ladinian-Lower Carnian Pseudozilian beds are particularly striking. Succession of clastic and carbonate rocks was deposited in deep-marine Slovenian basin. In both the Trnovo and Tolmin nappe, Pseudozilian beds occur in the lithologically characteristic sequences but, in the Tolmin nappe, they are developed in a much greater thickness than in the Trnovo nappe and pass continuously upwards into Amphyclina beds, while in the Trnovo nappe, on the other hand, the succession of Pseudozilian beds is much thinner and is overlain by the platform Cordevol dolomite.

## Uvod in problematika

Na ozemlju med vasjo Reka v dolini Idrijce ter vasema Bukovo in Jesenica pod Kojco (1303 m) v zahodni Sloveniji se stikata Trnovski in Tolminski pokrov (Placer, 1981; Placer & Čar, 1997; Placer, 1999; Demšar, 2016). Prvo narivno enoto z značilno smerjo narivanja severovzhod-jugozahod v širšem geografskem pogledu prištevamo k Dinaridom, Tolminski pokrov s smerjo narivanja sever-jug pa Južnim Alpam (Placer & Čar, 1997; Placer et al., 2010). Narivni enoti sta na stiku obeh gorstev zgrajeni iz več narivnih enot nižjega reda v zapletenih medsebojnih odnosih, ki doslej še niso bile natančneje raziskane in interpretirane (Tabela 1). Ker so narivne enote prostorsko obsežne, menimo, da so se ob narivnih kontaktih dogodili dolgi in zapleteni premiki, ki so združili prvotno precej oddaljena zaporedja kamnin. Kljub temu, da so kamnine v narivnih enotah približno enako stare, se v litološki zgradbi med seboj precej razlikujejo. Pri tem preseneča, da se v obeh narivnih enotah, Trnovskem in Tolminskem pokrovu, pojavljajo kamnine psevdoziljskih plasti, ki naj bi nastajale v enotnem globokomorskem Slovenskem bazenu (Buser, 1989). V tem prispevku bomo obravnavali le strukturne lege psevdoziljskih plasti v obeh narivnih enotah, njihovi podrobnejši litološki razvoji pa bodo obravnavani v posebni razpravi.

Pri raziskavah v osemdesetih letih (Skaberne & Čar, 1981–1991) smo se odločili vse vulkanske kamnine, njihove tufe in piroklastične kamnine z vmesnimi vložki drugih kamnin združiti pod imenom '*ladinijske kamnine*'. Prevladajoče črne muljevce z litičnimi peščenjaki, redkejšimi plastnatimi apnenci in značilnimi grebenskimi kopami smo obravnavali kot '*psevdoziljske plasti*'. Horizont nad njimi, kjer se grebanske kope na pojavljajo več, pač pa se močno poveča karbonatna komponenta v obliki plastnatih apnenecov in apnenčevih leč z muljastimi in laporastimi vložki ter redkimi bočnimi prehodi v apnenčev konglomerat, smo poimenovali *amfiklinske plasti*. Amfiklinske plasti postopno, vendar sorazmerno hitro prehajajo v *baški dolomit* (Kossmat, 1910). Takšna razčlenitev je upoštevana tudi v tej razpravi.

Namen prispevka je pojasniti strukturne razmere na stiku Južnih Alp in Dinaridov na zahodnem delu Cerkljanskega in podati razmislek o prostorski legi in razprostranjenosti psevdoziljskih plasti. Problematica geneze kamnin psevdoziljskih plasti ni predmet te razprave.

## Metode

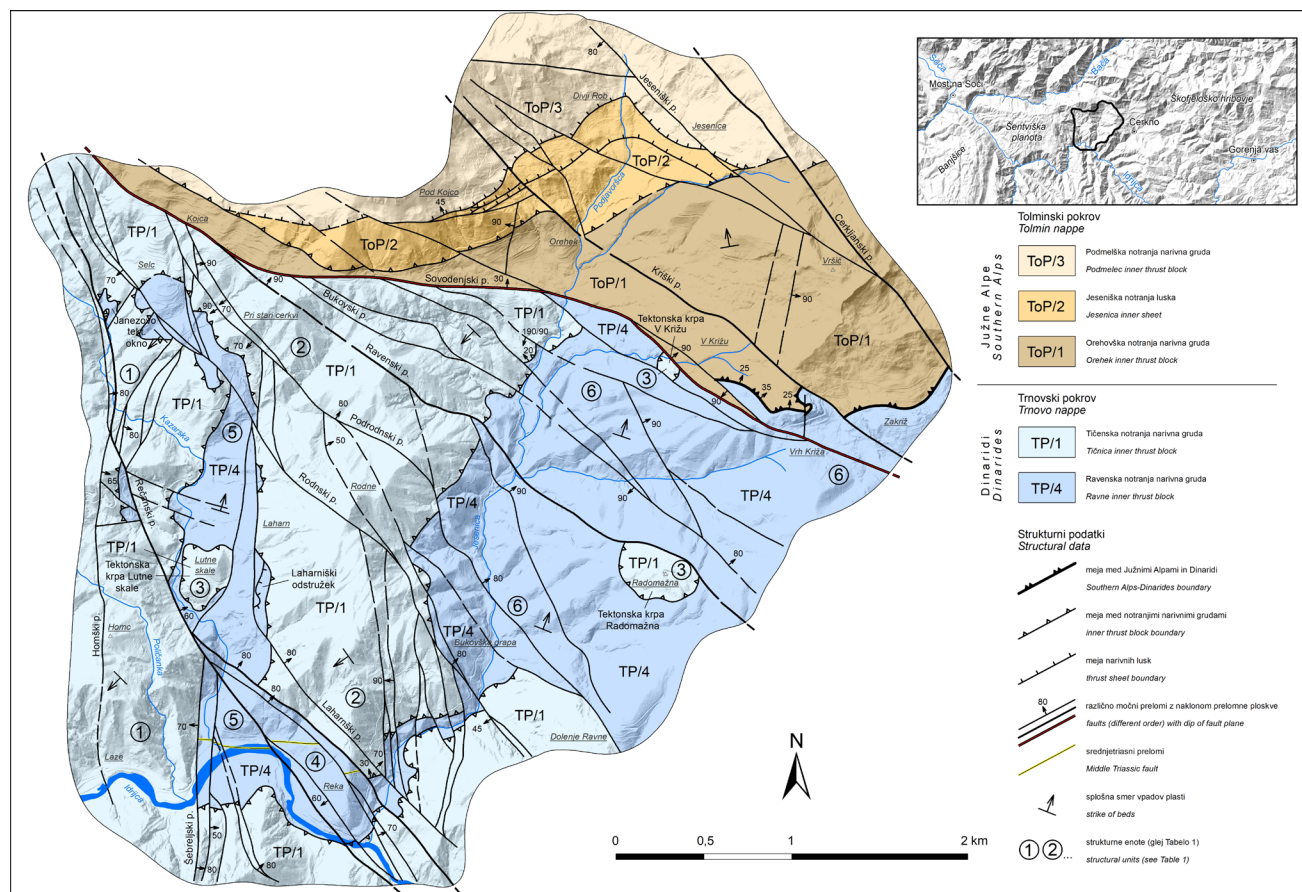
Temeljno raziskovalno delo je bilo strukturno – litološko kartiranje ozemlja v merilu 1: 5 000, ki je potekalo v okviru nalog *Sedimentološke raziskave med Južno karbonatno platformo in Slovenskim bazenom* (Čar, 1998) in *Strukturna zgradba in razvoj triasnih plasti med dolino Idrijce in Kojco* (Čar, 2001). Na kartiranem ozemlju so bili v okviru projekta *Sedimentološke in geokemične raziskave psevdoziljske in ekvivalentnih formacij, 1981–1991* (Skaberne & Čar, 1981–1991) posneti tudi trije podrobni profili psevdoziljskih in amfiklinskih plasti, in sicer Orehek 1 ter Jesenica 1 in 2, ki še niso obdelani in objavljeni. Rezultati kartiranja so bili usklajeni z geološko karto Mlakarja in Čarja (2009) ter Demšarja (2016), še neobjavljenimi rezultati Mlakarjeve geološke karte ozemlja med Cerknim in Žirmi v merilu 1: 25 000 in ugotovitvami raziskav ladinijskih plasti na Stopniku (Čar & Skaberne, 1995; 2003). Od omenjenih geoloških kart se samo prva na južnem robu neposredno stika s karto predstavljeno v tem prispevku. Med ostalima dvema ostaja ožji pas samo pregledanega ozemlja med zaselkom Vrh Križa in vasjo Gorje. Upoštevani so bili tudi neobjavljeni rezultati kartiranj nekaterih delov obravnavanega ozemlja iz 70. let preteklega stoletja na Cerkljanskem v okviru naloge *Širše raziskave na živo srebro* (Placer, Čar, neobjavljena poročila, arhiv RŽS Idrija in GeoZS).

## Rezultati

### Prelomi

Številni prelomi s smerjo severozahod-jugovzhod, ki sekajo ozemlje med Reko, Bukovim in Zakrižem, so najmlajši tektonski elementi obravnavanega ozemlja in sekajo vse starejše strukturne elemente. S severovzhoda omejuje obravnavani teren močan Cerkljanski prelom (po Mlakarju – karta v pripravi za tisk) z Jeseniskim krakom, ki poteka skozi vas Jesenica. Južno od tod seka pobočje Kojce še šibkejši neimenovani prelom. Sledi zelo močan regionalni Sovodenjski prelom. Od njega se pri Zakrižu odcepi Kriški prelom, ki se mimo vasi Orehek nadaljuje v pobočju Kojce (sl. 1).

Proti jugozahodu najdemo več neimenovanih šibkejših prelomov. Sledijo močnejši Bukovski, Ravenski, Podrodniki in Rodnski prelom s širokimi zdrobljenimi conami in v naravi dobro vidnimi premiki. Niz ugotovljenih prelomov se zaključuje z močnim Rečanskim prelomom, ki poteka proti jugovzhodu po dolini Idrije. Med



Sl. 1. Strukturna karta obravnavanega ozemlja.

Fig. 1. Structural map of the studied area.

Podrodnim, Rodnskim in Rečanskim prelomom poteka vrsta vzporednih in veznih prelomov v smeri sever–jug, ki lokalno zapletajo geološke razmere. Na jugozahodni strani Rečanskega preloma potekata še šibkejša, vendar strukturno pomembna Homški in Šebreljski prelom, ki imata prav tako smer sever–jug (sl. 1).

Na kartiranem ozemlju je vsekakor najmočnejši regionalni Sovodenjski prelom (po Mlakarju, v pripravi) (sl. 1), ki se z območja Poljansko-Vrhniškega hribovja vleče čez celotno Cerkljansko in se nadaljuje na Tolminskem. Gleda na zapletene razmere v njegovi široki prelomni coni na kartiranem ozemlju, in predvsem glede na velike razlike v litostratigrafski in strukturni zgradbi med severovzhodnim in jugozahodnim blokom, menimo, da gre za zelo močan prelom z več fazami nastanka. Zelo verjetno je bil, tako kot Idrijski in Zalin prelom na Idrijskem (Čar, 2010), sprva normalni prelom z močnim spustom severovzhodnega bloka, kasneje pa aktiviran kot zmični prelom. Med zaselkoma Nemci ter Kojca in vasjo Bukovo se na Sovodenjski prelom priključijo Bukovski, Ravenski in Podrodniki prelom. Ostali prelomi, ki potekajo jugozahodno od Sovodenjskega preloma, se na območju vasi Bukovo močno približa-

jo (sl. 1) in se nadaljujejo v široki pretrti in zaglinjeni prelomni coni in plazovitem terenu pri vasi Grahovo v Baški grapi.

### Trnovski pokrov (TP)

V podlagi narinve zgradbe idrijskega ozemlja leži Hrušički pokrov (HP), neposredno na njem se nahaja Koševniška vmesna luska (KVL), sledi Čekovniška (ČVL) in nato inverzna Kanomeljska vmesna luska (KaVL). V oklepajih so standarde okrajšave glavnih narinvin enot na geološki karti Idrijsko-Cerkljanskega ozemlja (Mlakar & Čar, 2009). Obravnavano ozemlje do Sovodenjskega preloma prekriva obsežen Trnovski pokrov, ki je najvišja enota v zapleteni narinvi zgradbi Idrijskega ozemlja (Mlakar, 1969; Placer 1973, 1982; Mlakar & Čar, 2009; Čar, 2010). Trnovski pokrov ni enotno zgrajen. V osrednjem delu pri Idriji ločimo Tičensko in Idrijsko notranjo narinvo grudo z oznako TP/1 in TP/2, vzhodno od tod, pri Zaplani, se odpira še Petkovškova notranja narinva gruda z oznako TP/3 (Mlakar & Čar, 2009; Čar, 2010). Tičenska notranja narinva gruda prekriva celotno idrijsko ozemlje, se nadaljuje na Šentviškogorski planoti in na Cerkljanskem. V dolini Idrijce, med Reko

in Stopnikom, se kamnine Tičenske notranje narivne grude nadaljujejo na desnem bregu Idrijce na območju Polic, obsegajo celoten Bukovski vrh in sosednji greben Rodne (sl. 1). Nove raziskave so pokazale, da se na Cerkljanskem pod Tičensko notranjo narivno grudo odpira še ena narivna enota z normalno ležečimi plastmi, ki jo glede na njeno litostratigrafsko sestavo, debelino in obseg lahko opredelimo kot ločeno notranjo narivno grudo Trnovskega pokrova in ni enaka nobeni doslej obravnavani notranji narivni enoti. Poimenovali smo jo Ravenska notranja narivna gruda po Ravnah pri Cerknem. V soglasju s poimenovanjem narivnih enot na Idrijskem (Čar, 2010) ima oznako »TP/4« torej, »četrta notranja narivna gruda Trnovskega pokrova«.

#### *Tičenska notranja narivna gruda (TP/1)*

Tičensko notranjo narivno grudo na obravnavanem ozemlju gradijo Poliška (po vasi Police) in Rodnska (po grebenu Rodne) strukturna podenota ter tri tektonske krpe. Na Reki v dolini Idrijce se kamnine Tičenske notranje narivne grude iz Šebreljskega strukturnega bloka (Čar & Skaberné, 2003) nadaljujejo zvezno v Poliški strukturni podenoti (št. 1 na sl. 1) severno od doline Idrijce proti vasemu Police in Bukovo. Pri zaselku Kojca vzhodno od vasi Bukovo se Poliška strukturna enota v širokem pasu nadaljuje v Rodnski strukturni podenoti (št. 2 na sl. 1), ki obsega obsežen in razvejan greben Rodne. Na južnem obrobju se Rodnska struktura konča ob coni močnega Rečanskega preloma, v Orehovški grapi pa prekriva kamnine Ravenske notranje narivne grude.

#### *Poliška in Rodnska strukturna podenota (št. 1 in 2 na sl. 1 in Tabeli 1)*

Terene obeh strukturnih enot v veliki večini gradi značilen, skoraj bel in neplastnat, kristalast cordevolski dolomit (Schlernski dolomit - Celarc, 2004). Na Rodnah prehaja navzgor zvezno v plastičen, organogen, verjetno julski, dolomit. Na več lokacijah opazujemo zvezne in postopne prehode belega dolomita navzdol v nekaj metrov prehodnega črnega, tanko plastnatega dolomita in dalje v različne ladinjske apnenčeve kamnine z muljasto – laporastimi medplastnimi vložki ali neposredno v piroklastične kamnine. Sedimentoške raziskave profilov ob cesti Laharn–Police in ob cesti Reka–Orehok so pokazale, da so ladinjske kamnine v obeh strukturnih enotah nastajale na obrobju karbonatne platforme, njenem pobočju, najnižji deli dostopnih profilov pa že v globljemorskem bazenskem okolju (Šmuc & Čar, 2002).

Pod vasjo Bukovo na močno tektoniziranem cordevolskem dolomitu Tičenske notranje narivne grude leži diskordantno volčanski apnenec zgornjekredne starosti (Buser, 1986a, 1986b). Kamnine Tičenske notranje narivne grude vpadajo proti jugozahodu, kar je značilen splošen vpad plasti v okviru Trnovskega pokrova tudi na Idrijskem in celotnem Trnovskem gozdu vse do Vipavske in Soške doline.

#### *Tektoniske krpe (št. 3, sl. 1)*

Strukturno pomembno zanimivost obravnavanega ozemlja predstavljajo tri tektonsko-erozijske krpe Tičenske notranje narivne grude na kamninah Ravenske notranje narivne grude (sl. 1). Vse tri krpe so zgrajene iz močno pretrtega cordevolskega dolomita. Najobsežnejša je vzpetina Radomažna v Gorenjih Ravnah, ki leži v celoti na ladinjskih piroklastičnih kamninah Ravenske notranje narivne grude. S severovzhodne strani je tektonska krpa omejena z Ravenskim prelomom. Ob narivu tektonsko popolnoma zdobljen dolomit je viden na več mestih na južnem in zahodnem obrobju krpe. Na levem bregu Kazarske grape pod zaselkom Laharn se nahaja morfološko močno izpostavljena tektonska krpa Lutne skale. Cordevolski dolomit leži na skrilavem muljevcu psevdoziljskih plasti. Na vzhodni strani je tektonska krpa odrezana s prelomom. Prav tako je morfološko izpostavljen tretji, sicer najmanjši erozijski ostanek Tičenske notranje narivne grude, imenovan V Križu, na obsežnem pobočju Križa. Erozijska krpa cordevolskega dolomita leži na psevdoziljskih plasteh in je ukleščena v širši coni Sovodenjskega preloma.

#### *Ravenska notranja narivna gruda (TP/4) (sl. 1)*

Ravensko notranjo narivno grudo delimo na Rečansko, Kazarsko in Zabrezniško strukturno podenoto (št. 4, 5 in 6 na sl. 1 in v Tabeli 1). Podenote gradijo približno enako stare kamnine, ki pa se po litološki sestavi med seboj močno razlikujejo.

#### *Rečanska strukturna podenota (št. 4, sl. 1)*

Kamnine Rečanske strukturne podenote gradijo levi in desni breg doline Idrijce med pritoko ma potokov Jesenica in Kazarska (sl. 1). Domnevamo, da je strukturna enota na območju Reke s severne strani omejena z močnim triasnim normalnim prelomom s smerjo vzhod–zahod. Prelomi neposredno viden, so pa ob njem v stiku različne, tektonsko močno deformirane in spremenjene kamnine. Na južni strani preloma, v Rečanski strukturni podenoti (št. 4), leži v podlagi temnosivi, prekristaljen, porozen in bituminiziran

anizijski dolomit, diskordantno na njem pa nekaj zelenega keratofirskega tufa. Na južni strani so kamnine Rečanske strukturne podenote omejene z narivnico Šebreljskega strukturnega bloka (Čar & Skaberne, 2003) Tičenske notranje narivne grude. Kamnine v Rečanski strukturni podenoti so v normalni stratigrafski legi.

#### *Kazarska strukturna podenota (št. 5, sl. 1)*

Na severni strani zgoraj omenjenega normalnega triasnega preloma pri Reki se pričenja Kazarska strukturna podenota (št. 5), ki se v obliki sorazmerno ozkega tektonskega polokna vleče najprej po Kazarski grapi, nato pa se pod Laharno dvigne v njeno levo pobočje. Pod zaselkom Selc pod Bukovim prekrijejo Kazarsko strukturno podenoto kamnine Tičenske notranje narivne grude (TP/1) (sl. 1 in 3C). Zahodno od Selca, v dnu Kazarske grape, izdanajo kamnine Kazarske strukturno podenote v manjšem Janezovem tektonskem oknu. V tektonskem poloknu, kot tudi v tektonskem oknu, ležijo kamnine v normalnem stratigrafskem zaporedju.

V Kazarski strukturni podenoti, na severni strani srednjetriasnega preloma pri Reki, aniziska podlaga ni vidna. Sledi okrog 170 m debelo pisano zaporedje ladijjskih kamnin. V začetnem delu grape opazujemo črne do temno sive plastnate apnence z medplastnimi tufskimi in apnenčasto-laporastimi vložki. Vmes najdemo tudi vložke biodetritičnega apnanca. Sledi splazela kaotična mešanica omenjenih litoloških členov. Nad njimi leži večja kopa biodetritičnega apnanca. Našte-te litološke člene prekrivajo različki zelenkasto sivega keratofirskega tufa in keratofirja s prehodi v vijolične bazične različke tufov in tufitov z vložki diabazov. Nato se pričenja več sto metrov debela ponavljajoča serija kamnin psevdoziljskih plasti v značilnem razvoju (sl. 1 in 3A). Prevladuje temno siv do črn bituminozni skrilavi muljevec z vložki sivega litičnega peščenjaka in plastmi črnega in piritiziranega apnanca. Vmes ležijo različno velike kope grebenskih apnencov. Pogosti so temno sivi do črni apnenci blatnih kop, redkeje pa skeletni grebenski apnenci s koralami in spužvami. Vložki manjših apnenčevih blatnih kop so pogosteji v spodnjem delu profila, skeletnih grebenskih apnencov je več v zgornjih delih profila pod zaselkom Selc, kjer prekrijejo psevdoziljske plasti kamnine Tičenske notranje narivne grude. Večja še neraziskana apnenčeva kopa leži v Kazarski grapi pod Laharno. V njej je voda izdolbla krajšo sotesko in atraktivne kotle. Na zahodnem pobočju hriba Rodne (698 m), južno od zaselka Laharn, leži na kamninah

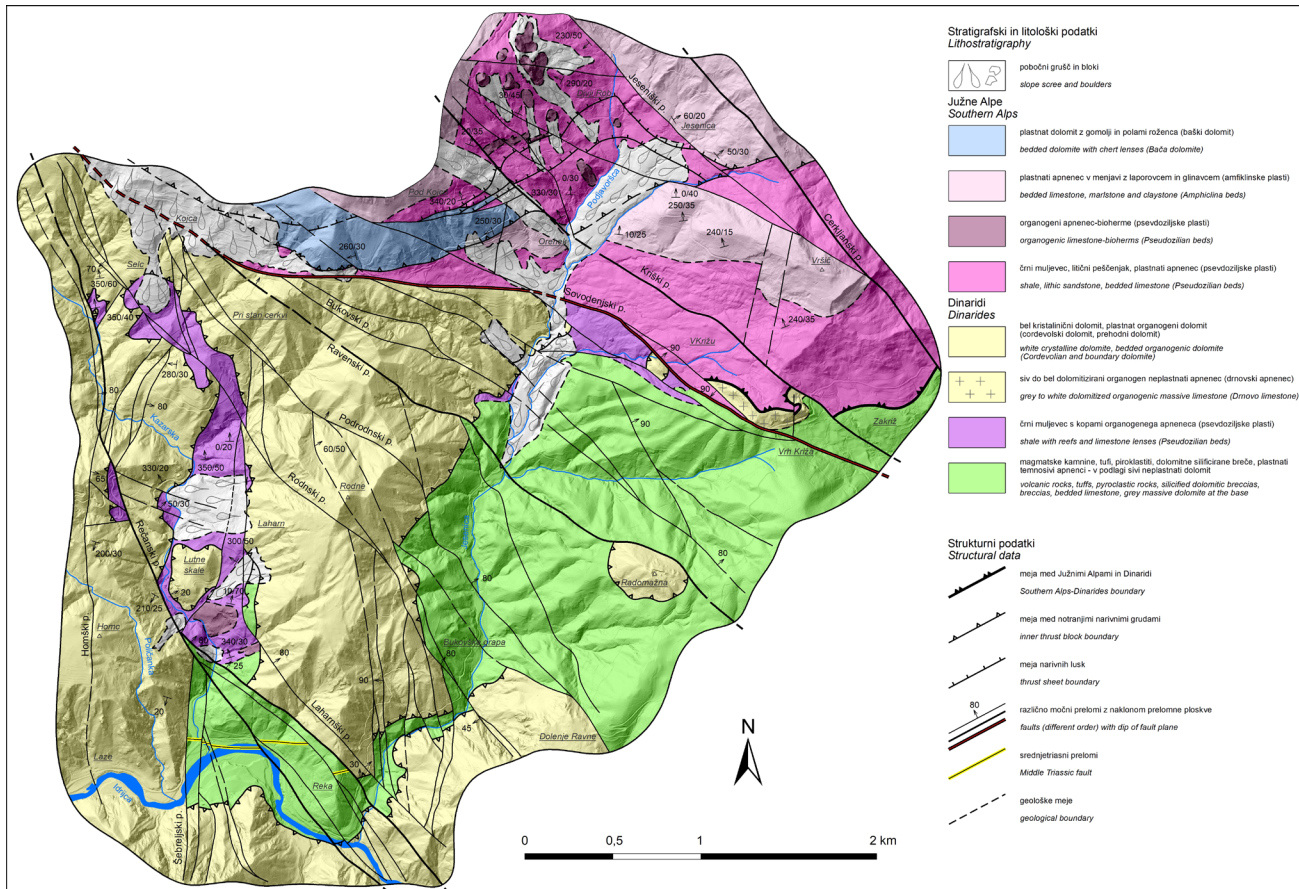
psevdoziljskih plasti neposredno pod narivnico Rodnske strukturne enote obnarivni Laharnski odstružek iz diabaza in diabaznega tufa. Tudi stik s kamninami psevdoziljskih plasti Kazarske strukturne podenote je nariven.

#### *Zabrezniška strukturna podenota (sl. 1, št. 6)*

Zabrezniška strukturna podenota je največja enota Ravenske notranje narivne grude (TP/4). Na Reki v dolini Idrijce je ob potoku Jesenica v ozkem pasu Rečanska strukturna podenota povezana z Zabrezniško strukturno podenoto (imenovana po zaselku Zabreznica). Loči ju Rečanski prelom. Zabrezniška strukturna podenota zajema ves osrednji del Orehovške grape, po kateri se pretaka potok Jesenica (sl. 1). Kamnine podenote gradijo nižje dele vzhodnega obsežnega in močno razbrazdanega pobočja hriba Rodne (698 m) do višine 450 m in celotno levo pobočje Orehovške grape do vrha Velikega Kovka (838 m) in Raven pri Cernem. Od tu se po starejših podatkih Placerja et al. (1977) nadaljuje v dolino Cerknice, kjer zavzema vsaj polovico desnega pobočja doline med Želinom in Cernim. Ta del Zabrezniške strukturne podenote še ni natančneje raziskan. Na območju Vrh Križa se Zabrezniška struktura nadaljuje tudi na drugi strani močnega Sovodenjskega preloma. To potrjujejo litostratigrafski podatki na novi Geološki karti Selške doline (Demšar, 2016), Mlakarjevi karti (v pripravi za tisk) in dodatni pregled terena.

Skoraj celotno dno Orehovške grape in pobočje proti Ravnem nad Cernim do višine okrog 450 m gradi značilen svetlosiv, le tu in tam temnosiv in plastnat ter rahlo laporast aniziski dolomit. V grapi pod zaselkom Zabreznica prehaja dolomit navzdol zvezno v značilen zgornje spodnjetriasni laporasti apnenec z vložki laporovcev (campilske plasti).

Z erozijskim kontaktom na aniziskem dolomitu ležijo litološko zapleteno sestavljeni ladijjske plasti. Na južnem obrobju obravnavane strukturne podenote med kmetijami Andrejna, Urban in Podrodnar najdemo diskordantno na aniziskem dolomitu menjavane različnih keratofirskega in diabaznih tufov in tufitov s prehodi v dolomitni in dolomitno-apnenčev konglomerat s piroklastičnim vezivom in tankimi vložki plastnatih apnencov. Hrib Veliki Kovk (838 m) pri Gorenjih Ravnah gradi okrog 280 m debel kompleks keratofirja z bočnimi prehodi v različne tufe in tufite. Vulkanika kamnina leži lahko neposredno na aniziskem dolomitom ali pa na piroklastičnih kamninah. Severno od tod, na območju obsežnega pobočja Križa, se menjavajo



Sl. 2. Geološka karta obravnavanega ozemlja.

Fig. 2. Geological map of the studied area.

do 50 m debeli pasovi črnega apnenca in temnosive drobnozrnate okremenjene dolomitne breče s keratofirskimi piroklastičnimi kamninami in redkimi vložki rdečkastih do vijoličnih diabaznih tufov. Na pobočju Križa, južno od tektonske krpe V Križu, prehajajo masivne piroklastične kamnine postopno v laminirane piroklastite in skrilave muljevce in dalje v značilno menjavljajo psevdooziljskih kamnin s črnimi skrilavimi muljevci, tankimi vložki litičnega peščenjaka, lečami črnega plastnatega apnenca in apnenčastih grebenskih kop. Psevdooziljske plasti se z območja V Križu vlečejo v ozkem pasu po dolini Jesenice in se izklinjajo med Bukovskim in Ravenskim prelomom ob potoku Jesenica, kjer jih narivno prekriva cordevolski dolomit Rodnske strukture (št. 2 na sl. 1; sl. 3C).

### Tolminski pokrov (ToP)

Južno pobočje hriba Kojca, med vasmi Bukovo, Orehek in Jesenica z vmesnima zaselkoma Kojca in Nemci ter obsežen greben Vršiča nad vaso Zakriž, pripada Tolminskemu pokrovu (ToP) (sl. 1., Tabela 1). V vseh narivnih enotah Tolminskega pokrova na obravnavanem ozemlju so plasti v normalnem stratigraskem zaporedju in vpadajo v splošnem proti severu-severovzhodu.

### Orehovška notranja narivna gruda (ToP/1)

Okolico Orehka, celotno območje Vršiča in terene na drugi strani Cerkljanskega preloma proti vasi Gorje, gradijo kamnine Orehovške notranje narivne grude (ToP/1), ki je v tem delu Cerkljanske najnižja enota Tolminskega pokrova (ToP). Obe enoti se med Bukovim in zaselkom Vrh Križa stikata ob močnem Sovodenjskem prelomu. V preostalem delu terena nad Zakrižem so kamnine Orehovške notranje narivne grude (ToP/1) v narivnem stiku s kamninami Ravenske strukturne enote (TP/4) Trnovskega pokrova v podlagi.

Vzhodni del grebena Vršiča gradi črni skrilavi muljevec in litični peščenjak z vložki črnega apnenca in redkimi grebenskimi kopami psevdooziljskih plasti (sl. 3A). Proti severozahodu postopno prehajajo v značilno zaporedje amfiklinskih plasti. Menjavajo se črni skrilavi muljevec in skrilavi laporovec s temno sivim plastnatim apnencem (sl. 3B). V severnem delu ob potoku Jesenica najdemo le še plastnati apnenec s tankimi skrilavimi laporastimi medplastnimi vložki. Na južnem delu, na območju Križa, so psevdooziljske kamnine Orehovške notranje narivne grude (ToP/1) ob Sovodenjskem prelomu v stiku s psevdooziljskimi plasti Zabrezniške strukturne enote (št. 6), v zahodnem delu, med Orehkom

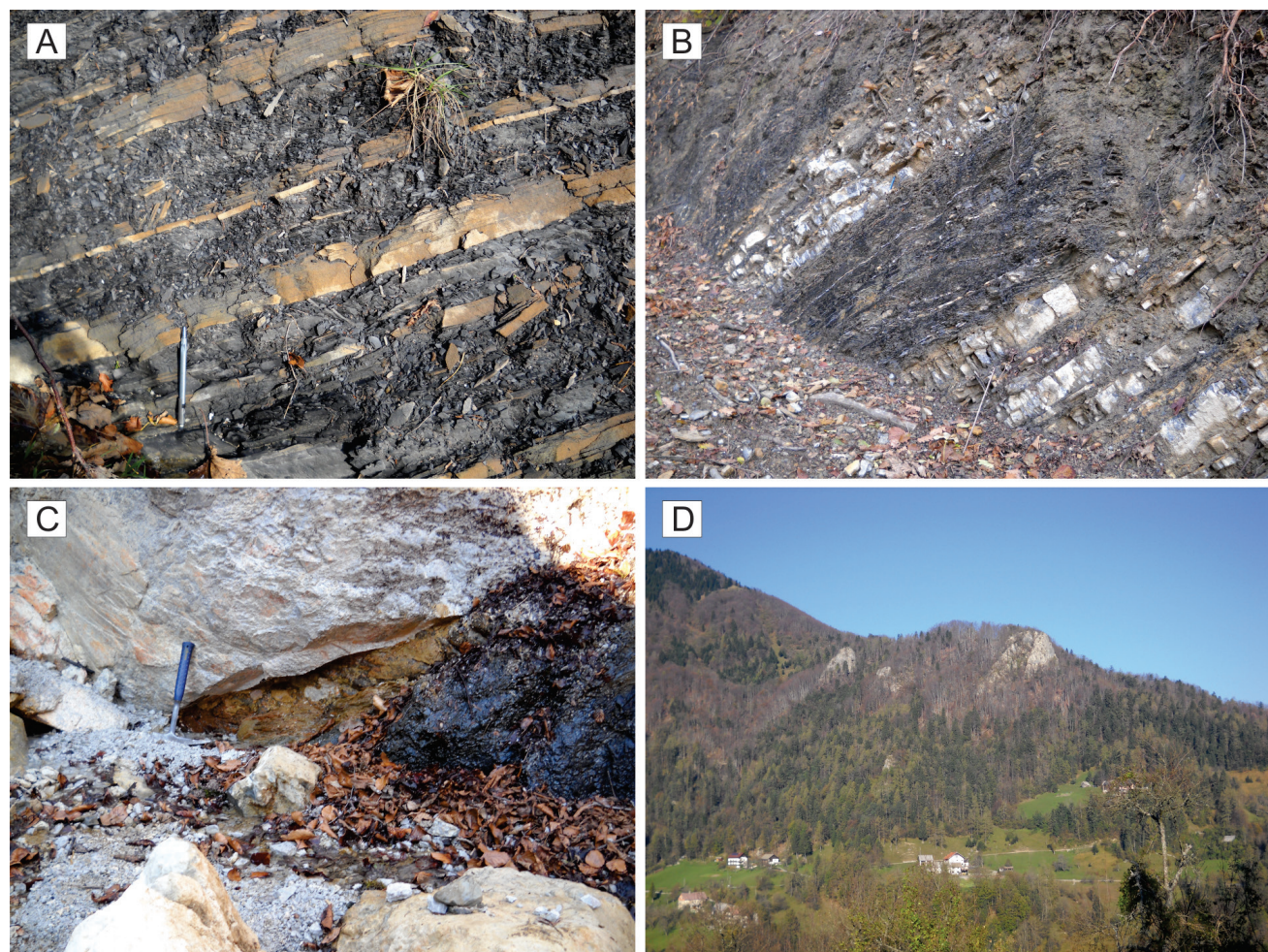
in zaselkom Nemci, pa s cordevolskim dolomitom Tičenske notranje narivine grude (TP/1) (sl. 1). Močno pretrte kamnine Orehovške notranje narivine grude (ToP/1) se vlečejo v ozkem pasu na severovzhodni strani regionalnega Sovodenjskega preloma med zaselkom Nemci in Bukovim.

*Narivni bloki Jeseniške notranje luske (ToP/2) (sl. 1 in 3D)*

Med Orehovško in Podmelško notranjo narivno grudo je na obravnavanem ozemlju Jeseniške notranja luska (ToP/2) zgrajena iz več narivnih blokov (enot). Vzhodni del narivine luske med Cerkljanskim in Kriškim prelomom gradijo psevdoziljske kamnine, zahodni del med Krškim prelomom in območjem nad zaselkom Kojce pa baški dolomit (sl. 2). Zapleten stik obeh kamnin je viden v golici v pobočju nad Orehkom (sl. 1 in 3D). O morebitnem nadalnjem pojavljanju narivnih blokov Jeseniške notranje luske zahodno

od Bukovega in vzhodno od kartiranega ozemlja, na območju vasi Poče in Gorje, nimamo podatkov.

Psevdoziljske plasti vzhodnega dela Jeseniške notranje luske (ToP/2), so v strukturnem pogledu z notranjo 'prerivno' ploskvijo, razdeljene v dva dela. Kamnine spodnje 'etaže' so manj tektonsko pretrte in zato 'trdnejše'. Kamnine zgornjega dela so obnarivno močno pretrte in so na številnih mestih spremenjene v temnosivo do črno tektonsko glico. V pobočju nad Orehkom (pod lokacijo V robuh) se 'prerivna' ploskev naslanja na neimenovani prelom s smerjo skoraj vzhod-zahod. Ob zapletenem izklinjanju zgornje in spodnje etaže Jeseniške notranje luske opazujemo še narivine vložke baškega dolomita in temnosivega tanko plastnatega, verjetno amfiklinskega apnenca (sl. 2). Baški dolomit zahodnega dela luske je močno naguban in pretrt. Osi gub slemenijo v smeri približno severozahod-jugovzhod.



Sl. 3. A – Zaporejje psevdoziljskih plasti pri vasi Jesenica, menjavanje temnega skrilavega muljevca in litičnega peščenjaka; B – Zaporejje amfiklinskih plasti ob potoku Jesenica, menjavanje plasti črnega skrilavega muljevca in apnenca; C – Narivni kontakt med psevdoziljskimi plastmi (spodaj – Zabrežniška strukturna podenota Ravenske notranje narivine grude) in belim cordevolskim dolomitom (zgoraj – Rodnska strukturna podenota Tičenske notranje narivine grude) v Orehovški grapi; D – Kope grebenskega apnenca, imenovane Divji rob, na pobočju Kojce nad vasjo Jesenica. (Foto: J. Čar).

Glede na stratigrafsko sestavo in strukturne razmere so kamninski bloki Jeseniške notranje luske (ToP/2) del Podmelške notranje narivne grude. Pri narivanju grude proti jugu na Ore-hovško narivno grudo (ToP/1) je bil iz njenega vzhodnega spodnjega dela (Jesenica) 'odtrgan' del psevdoziljskih plasti, v zahodnem delu pa večji blok baškega dolomita. Oblikovala sta se dva večja bloka kamnin, ki gradita Jeseniško notranjo lusko (ToP/2). Posamezne bloke kamnin bi glede na nastanek, velikost in lego lahko poimenovali tudi 'odstružki'. Ob narivanju je nastala tudi vmesna šibkejša narivna ploskev, ki deli vzhodni, psevdoziljski, del Jeseniške strukture v dva dela. Zgornja močno pretrta in zaglinjena 'etaža' predstavlja kompenzacijsko narivno cono, ki se kaže kot izravnalna cona med Podmelško in Ore-hovško notranjo narivno grudo.

### Podmelška notranja narivna gruda (ToP/3)

Pobočje Kojce nad Jesenico in Bukovim je del Podmelške notranje narivne grude (ToP/3). Do višine velikih apnenčevih grebenov v okoli ci Divjega roba imajo kamnine značilen psevdoziljski razvoj. Nad grebeni se močno poveča komponenta presedimentiranih piroklastitov, nato pa postopno prehajajo v amfiklinski razvoj plasti in više v pobočju v baški dolomit z roženci (Čar et al., 1981).

### Stik Južnih Alp in Zunanjih Dinaridov

Stik med narivnimi enotami Trnovskega in Tolminskega pokrova je hkrati tudi stik Južnih Alp in Dinaridov. Na zahodnem in osrednjem delu obravnavanega terena je meja med obema gorskima sistemoma ob široki in zapleteni coni regionalnega Sovodenjskega preloma. Prelom se iz doline Bače vleče do vasi Bukovo, poteka čez

Tabela 1. Narivne enote in strukturne podenote ter njihove glavne litostratigrafske značilnosti na obravnavanem ozemlju stika Južnih Alp in Dinaridov.

Table 1. Thrust units and structural subunits and their main lithostratigraphic characteristics of the studied area of Southern Alps and Dinarides.

GEOGRAFSKA ENOTA GEOGRAPHIC UNIT	NARIVNA ENOTA THRUST UNIT	STRUKTURNΑ PODENOTA STRUCTURAL SUBUNIT	OZNAKA SYMBOL	FACIELNE IN LITOSTRATIGRAFSKE ZNAČILNOSTI LITHOSTRATIGRAPHY
Južne Alpe Southern Alps	Tolminski pokrov Tolmin nappe	Podmelška notranja narivna gruda <i>Podmelec inner thrust block</i> ToP/3		Psevdoziljske plasti, amfiklinske plasti in baški dolomit <i>Pseudozilian beds, Amphiclina beds and Bača dolomite</i>
		Jesenška notranja luska <i>Jesenica inner sheet</i> ToP/2		Psevdoziljske plasti in baški dolomit <i>Pseudozilian beds and Bača dolomite</i>
		Orehovška notranja narivna gruda <i>Orehek inner thrust block</i> ToP/1		Psevdoziljske in amfiklinske plasti <i>Pseudozilian beds and Amphiclina beds</i>
Dinaridi Dinarides	Trnovski pokrov Trnovo nappe	Tičenska notranja narivna gruda <i>Tičen inner thrust block</i> TP/1	Poliška strukturna podenota <i>Police structural subunit</i>	1 Karnij - cordevolski dolomit <i>Carnian - Cordevolian dolomite</i>
			Rodnska strukturna podenota <i>Rodne structural subunit</i>	2 Karnij - cordevolski in julski dolomit <i>Carnian - »Cordevolian« and Julian dolomite</i>
			Tektonskie krpe <i>Tectonic klippes</i>	3 Karnij - Cordevolski dolomit <i>Carnian - Cordevolian dolomite</i>
		Ravenska notranja narivna gruda <i>Ravne inner thrust block</i> TP/4	Rečanska strukturna podenota <i>Reka structural subunit</i>	4 Anizijski dolomit in ladiniske piroklastične kamnine <i>Anisian dolomite and Ladinian pyroclastic rocks</i>
			Kazarska strukturna podenota <i>Kazarska structural subunit</i>	5 Vulkanske in piroklastične kamnine z zveznim prehodom v psevdoziljske plasti <i>Volcanic and pyroclastic rocks with normal transition into Pseudozilian beds</i>
			Zabrežniška strukturna podenota <i>Zabrežnica structural subunit</i>	6 Anizijski dolomit, vulkanske in piroklastične kamnine, različne karbonatne in klastične ladiniske kamnine in psevdoziljske plasti <i>Anisian dolomite, volcanic and pyroclastic rocks, Ladinian carbonate and clastic rocks and Pseudozilian beds</i>

zaselke Krtečne, Kojca in Nemci, se nadaljuje pod vasjo Orehek, prečka obsežno pobočje V Križu in se čez Vrh Križa nadaljuje v dolino Cerknice. V tem delu narivni stik med Tolminskim in Trnovskim pokrovom torej ni viden. Narivnica se ponovno pokaže Vrh Križa, kjer poteka na meji med Ravensko (TP/4) in Orehoško notranjo (ToP/1) narivno grudo. Podobne razmere opazujemo tudi dalje proti vzhodu pod vasema Gorje in Poče.

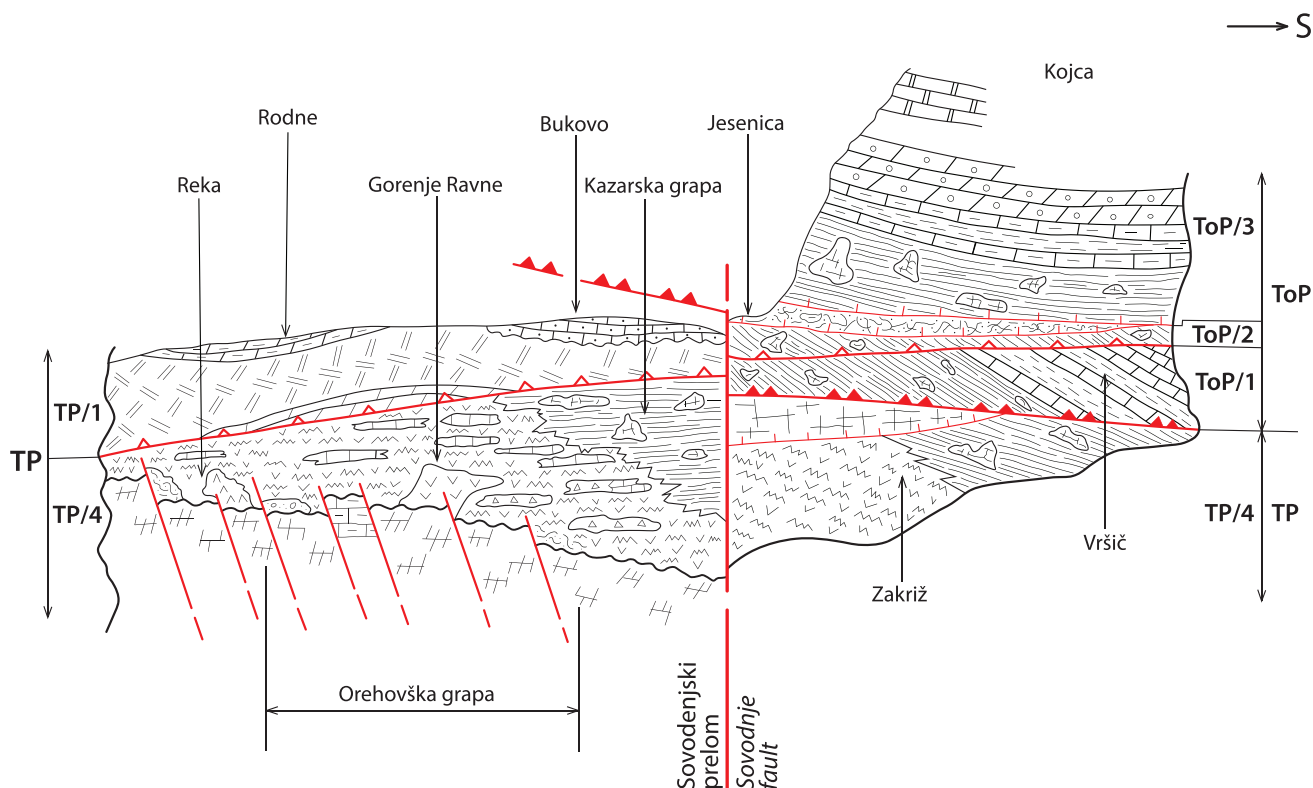
## Diskusija

### Odnosi med narivnimi enotami v Trnovskem pokrovu

Današnja prostorska lega narivnih enot je prikazana v priloženem profilu (sl. 4). Na severni strani regionalnega Sovodenjskega preloma med vasjo Bukovo in zaselkom Vrh Križa se nahaja v podlagi kamnine Trnovskega pokrova (TP). Pripadajo Tičenski in Ravenski notranji narivni grudi (TP/4), ki gradita tudi obsežno ozemlje med Bukovim in Reko v dolini Idrijce jugozahodno od Sovodenjskega preloma in okolico Zakriža. Na celotnem območju med Bukovim in Zakrižem ležijo na Trnovskem pokrovu psevdoziljske in amfiklinske plasti Orehoške notranje narivne grude (ToP/1). Sledijo močno pretrte psevdoziljske plasti in blok baškega dolomita Jeseniške notra-

nje luske (ToP/2), nad njimi pa debel kompleks psevdoziljskih in amfiklinskih plasti, baškega dolomita in jurskih kamnin Podmelške notranje narivna grude (ToP/3), ki gradijo srednji in zgorjni del pobočja Kojce.

Na sliki 5 je izrisan shematski prikaz predvidene prvotne medsebojne lege narivnih enot, ki gradijo obravnavano ozemlje in smeri naranjanja. Idrijsko-Cerkljansko hribovje in celotni Trnovski gozd do Vipavske doline pripada Trnovskemu pokrovu. Sestavljen je iz petih obsežnih notranjih narivnih grud. Peta, ki obsega zgornji del Trnovskega gozda, še ni poimenovana. Njena narivnica poteka po severovzhodnem pobočju Trnovskega gozda nad dolino Belce. Doslej je kartirana med Hudim poljem in Črnin Vrhom nad Idrijo (glej geološko karto – Mlakar & Čar, 2009). Pod Trnovskim pokrovom ležijo na Idrijskem ena vrh druge obsežne Koševniška, Čekovniška in Kanomeljska vmesna luska (Mlakar, 1969; Mlakar & Čar, 2009; Čar, 2010). Vse naštete enote ležijo na kamninah Hrušičkega pokrova, ki tone pod Trnovski pokrov na vzhodnem obrobju Črnovrške planote in ponovno izdanja na območju Poljansko-Vrhniških nizov in Blegoša (Placer & Čar, 1997; Demšar, 2016). Na obravnavanem ozemlju med vasmi Reka, Bukovo in Zakriž ležijo na površini le kamnine Tičenske (TP/1) in Ravenske (TP/4) notranje narivne grude.



Sl. 4. Geološki prikaz stika Južnih Alp in Dinaridov na Cerkljanskem.

Fig. 4. Schematic cross section of a tectonic contact of the Southern Alps and the Dinarides in the Cerkno region.

Dinaridi / Dinarides			Južne Alpe / Southern Alps		
K <sub>2</sub>	volčanski apnenec / Volčé limestone		Tanko plastnati apnenec z rožencem / Thin bedded limestone with chert		
T <sub>3</sub> <sup>2+3</sup>	glavni dolomit / Main dolomite		Plastnati dolomit in stromatolitni dolomit / Bedded dolomite and stromatolitic dolomite		
taval	Klastični razvoj / clastic rock succession		Pisani litično - kremenov konglomerat in peščenjak / Lithic - quartz conglomerate and sandstone		
jul	mejni apnenec / boundary limestone		Plastnati apnenec z laporastimi vložki / Bedded limestone with marlstone intercalations		
	mejni dolomit / boundary dolomite		Plastnati dolomit / Bedded dolomite		
T <sub>3</sub> <sup>1</sup>	apnenčovo - dolomitni razvoj / limestone - dolomite succession		Črni plastnati apnenec z laporastimi vložki / Black bedded limestone with marlstone intercalations		
cordevol			Bel kristalinični dolomit / White crystalline dolomite		
			Bel organogeni apnenec / White organogenic limestone		
			Črni tanko plastnati dolomit / Black thin bedded dolomite		
			Bel dolomitizirani apnenec (Drnovski apnenec) / White dolomitized limestone (Drnovo limestone)		
T <sub>2</sub> <sup>2</sup> - T <sub>3</sub> <sup>1</sup>	psevdolijlske plasti / Pseudolilian beds		Skrilavi glinavec in litični peščenjak z apnenčevimi kopami / Shale and lithic sandstone with reefs and limestone lenses		
T <sub>2</sub>			Različne piroklastične kamnine / Various pyroclastic rocks		
			Piroklastične kamnine z lečami plastnatega apnena / Pyroclastic rocks with bedded limestone lenses		
			Piroklastične kamnine z lečami silif. dolomitnih breč / Pyroclastic rocks with lenses of silicified dolomite breccias		
			Piroklastične kamnine s terigenim materialom in lečami pisanega konglomerata / Pyroclastic rocks with terigenous material and lenses of conglomerate		
			Keratofir in diabaz / Keratophyre and diabase		
			Pisani konglomerat / Conglomerate		
			Keratofirske vložki v diabaznem tufu / Keratophyre and diabase tuff and tuffite		
T <sub>2</sub> <sup>1</sup>			Neplastnat sivi dolomit / Massive gray dolomite		
T <sub>1</sub> <sup>3</sup>	campilske plasti / Campilian beds		Lapornati apnenec in laporovec / Marly limestone and marlstone		

Posebni znaki / Special signs		
od / from C do / to T <sub>3</sub> <sup>1</sup>		Različne karbonatne in klastične kamnine / Various carbonate and clastic sedimentary rocks
		Obnarivno močno pretrte psevdolijlske plasti / Highly tectonically deformed Pseudolilian beds
		Erozionska diskordanca / Erosional unconformity

Tektonika / Tectonics		
		Različni prelomi / Various faults
		Narivna meja med Južnimi Alpami in Dinaridi / Thrust boundary between the Southern Alps and the Dinarides
		Meja med notranjimi grudami / Boundary between the internal thrust blocks
		Meja med narivnimi luskami / Boundary between thrust sheets
		Smer narivanja / Direction of thrusting

Sl. 5. Legenda k sl. 4 in 6.

Fig. 5. Legend to Figs. 4 and 6.

Mnenja o dolžini narivanja v Zunanjih Dinaridih so si dokaj enotna. Mlakar (1969) meni, da znaša premik med Hrušiškim in Trnovskim pokrovom (Mlakar: Žirovsko-trnovski pokrov) 25 km do 30 km. Po ugotovitvah Placerja (1981) je premik med Trnovskim in Hrušiškim pokrovom v profilu čez Idrijo 32 km, po analizi podatkov globoke vrtine Ce-2/95 v Cerknem pa 30,5 km (Placer et al., 2000).

Premru (1980) je opisal narivno zgradbo osrednje Slovenije, ki je rezultat ilirsko-pirenejske in rodanske tektonske faze. Na podlagi palinsplastične karte podaja tudi oceno dolžine horizontalnih premikov posameznih narivov. Povprečna dolžina premikov posameznih narivnih enot v osrednji Sloveniji je po Premrujevem mnenju od 10 km do 20 km. Zapisal je, da alpski narivi segajo daleč na Zunanje Dinaride (Premru, 1980).

Širina prvotnega alpskega prostora in dolžina narivanja alpskih narivnih enot v smeri sever-jug za zdaj še nista ugotovljeni.

### O psevdolijlskih plasteh

Teller (1889) je ob koncu 19. stoletja na podlagi amonita *Trachyceras julium* Mojs. in školjke *Danonna lommeli* Wiss. ugotovil ladijnsko starost glinavca in peščenjaka z vložki tanko plastnatega apnena na Celjskem gradu in jih poimenoval »psevdolijlski skrilavec in peščenjak«. Kot ugotovila Kuščer (1967) s tem imenom Teller ni imel namen poimenovati določen stratigrafski horizont, saj je kasneje litološko in starostno enake kamni ne poimenoval z drugimi lokalnimi imeni.

Pojem »psevdolijlske plasti« sta v stratigrafiskem pomenu začela uporabljati Stache (1899) in nato Kossmat (1906), ki je razširil ime še na lito-

loško podobne sedimentne kamnine v osrednjih in zahodnih Posavskih gubah. Na geološki karti iz leta 1913 se psevdoziljske plasti razprostirajo v bolj ali manj sklenjenih pasovih od Celja do Tolmina (Kossmat, 1913). V tolmaču h geološki karti Škofja Loka – Idrija, ki zajema tudi obravnavano ozemlje, je Kossmat (1910) najrazličnejše piroklastite, tufe in v njih vključene magmatske kamnine obravnaval pod imenom »wengenske plasti in pietra verde«, vse pešcene in skrilave kamnine z vložki konglomeratov, ki se v širokem pasu vlečejo iz Baške grape čez Cerkljansko, pa pod naslovom »peščenoskrilave amfiklinske plasti«. Iz karte je vidno, da je v enoto »amfiklinske plasti« prištel vse kamnine, ki jih danes členimo na »amfiklinske in psevdoziljske plasti«.

V naslednjih sto letih je bilo o psevdoziljskih in amfiklinskih plasteh napisano in objavljenih veliko poročil, preglednih člankov, razprav, opisane so bile v več tolmačih k različnim geološkim kartam, vendar je vsak raziskovalec razlagal stratigrafski obseg »psevdoziljskih plasti« nekoliko drugače, odvisno od razmer na območju, kjer so raziskave potekale. Natančen pregled in analizo ugotovitev starejše literature je pripravil Rakovec (1950). Iz pregleda izhaja različen stratigrafski obseg psevdoziljskih in amfiklinskih plasti z litološkimi bočnimi menjavami. Leta 1980 je Premru (1980) objavil obsežno, širokopotezno zasnovano geološko zgradbo osrednje Slovenije. Po njegovih podatkih se psevdoziljske kamnine nahajajo v Savinskem, Selškem, Trojanskem in Kozjanskem narivu ter kamniški, blegoški in cerkljanski luskasti zgradbi. Mlakar (1980) ugotavlja, da so psevdoziljske plasti na Cerkljanskem bočni ekvivalenti diplopornega dolomita (cordevol) in zato karnijske starosti. Pri tem ni pojasnil lege psevdoziljskih plasti v narivni zgradbi na Cerkljanskem. Turnšek in sod. (1982) uvrščajo klastično-karbonatne kamnine z grebenskimi apnenci na območju med Hudajužno in Zakrižem med amfiklinske plasti. Menijo, da so se odlagale v nekoliko globljem mirnem šelfnem območju in so zgornjeladinijske do srednjekarnijske starosti.

Buser (1986a) je za menjavanje glinaste- ga skrilavca, drob in tufa z vložki keratofirja z obravnavanega ozemlja menil, da »...lahko pripadajo po litološki sestavi psevdoziljskim skladom, ki so nastali v globljem delu Slovenskega jarka«. Med amfiklinske pristeva »glinasti skrilavec in peščenjak, skladovit in grebenski apnenc. V njih ne najdemo plasti tufa in jih s tem ne moremo primerjati z ladijijskimi psevdoziljski- mi skladki«. Ločevanje kamnin psevdoziljskih in

amfiklinskih plasti in ugotavljanje meje med njima pa še vedno ni zadovoljivo rešeno. V tolmaču h geološki karti Selške doline je Demšar (2016) zapisal, da je spodnja meja amfiklinske formacije »...zaradi postopnega litološkega prehoda in podobnosti z nižje ležečimi kamninami psevdoziljske formacije težje določljiva...« in postavil mejo med formacijama sredi menjavanja istih litoloških členov, kar je v stratigrafskem pogledu lahko pravilno, v formacijskem pogledu pa nima pomena. Soglasno z ugotovitvami na Idrijskem, v idrijskem rudišču (Placer, 1982; Čar, 2010) ter na Cerkljanskem (Placer et al., 1977) lahko zaključimo, da naj bi »skrilavo-klastična« sedimentacija potekala od zgornjega anizija do zgornjega tuvala. Iz omenjenih podatkov se vidi, da je pri razčlenitvi ladinijsko – karnijskih piroklastično-magmatskih, psevdoziljskih in amfiklinskih kamnin še veliko nejasnosti. Litostatigrafsko razčlenitev, ki jo uporabljamo v tem prispevku smo pojasnili v uvodu.

### Psevdoziljske plasti v obravnavanih strukturnih enotah

Približno 500 m nad sotočjem Kazarske grape in Idrijce v Kazarski strukturni enoti (št. 5) prehajajo ladinijske piroklastične kamnine zvezno v značilen psevdoziljski razvoj (sl. 3A). V skoraj črnih skrilavih muljevcih se začno pojavljati vložki litičnega peščenjaka in apnenci posameznih organogenih kop. Južno od tektonske krpe Lutne skale se nahaja velika, apnenčeva kopa. V nadaljevanju po dolini Kazarske in njenem levem pobočju najdemo psevdoziljske skrilave muljevce s posameznimi apnenčevimi kopami le v redkih izdankih. Večje golice se nahajajo med Selcem in Žabžami, kjer opazujemo z organizmi bogate kope. Psevdoziljske plasti gradijo tudi Janezovo tektonsko okno visoko v dolini Kazarske grape. Dva manjša tektonsko omejena izdanka psevdoziljskega skrilavega muljevca se nahajata še v desnem pobočju Kazarske grape ob cesti proti Policam (sl. 1) (Šmuc & Čar, 2002).

V Zabrežniški strukturni enoti št. 6 (sl. 1) je v blagem pobočju na jugozahodni strani Sovodenjskega preloma, južno od tektonske krpe V Križu, postopen prehod piroklastičnih kamnin v značilne psevdoziljske plasti (sl. 1). Kamnine se širijo proti zahodu v dolino Jesenice in se tu pokažejo v več izdankih. Okrog 400 m nad zaselkom Mlinar stik piroklastičnih kamnin in psevdoziljskih plasti Ravenske strukturne enote (6) izgine pod narivno ploskvijo Rodnske strukturne enote (sl. 3C).

Obsežne terene gradijo psevdoziljske plasti v okviru vseh treh enot Tolminskega pokrova (ToP). V Orehoški notranji narivni grudi (ToP/1) črni skrilavi muljevci z vložki litičnih peščenjakov in redkimi apnenčastimi kopami gradijo celotno vzhodno območje grebena Vršiča ter obsežno pobočje Križa vse do sotočja Jesenice in Podjavorščice. Spodnji del pobočja pod Jesenicami je pokrit z izpranimi in nasutimi različno veliki- mi bloki apnenčevih grebenskih kop (sl. 1).

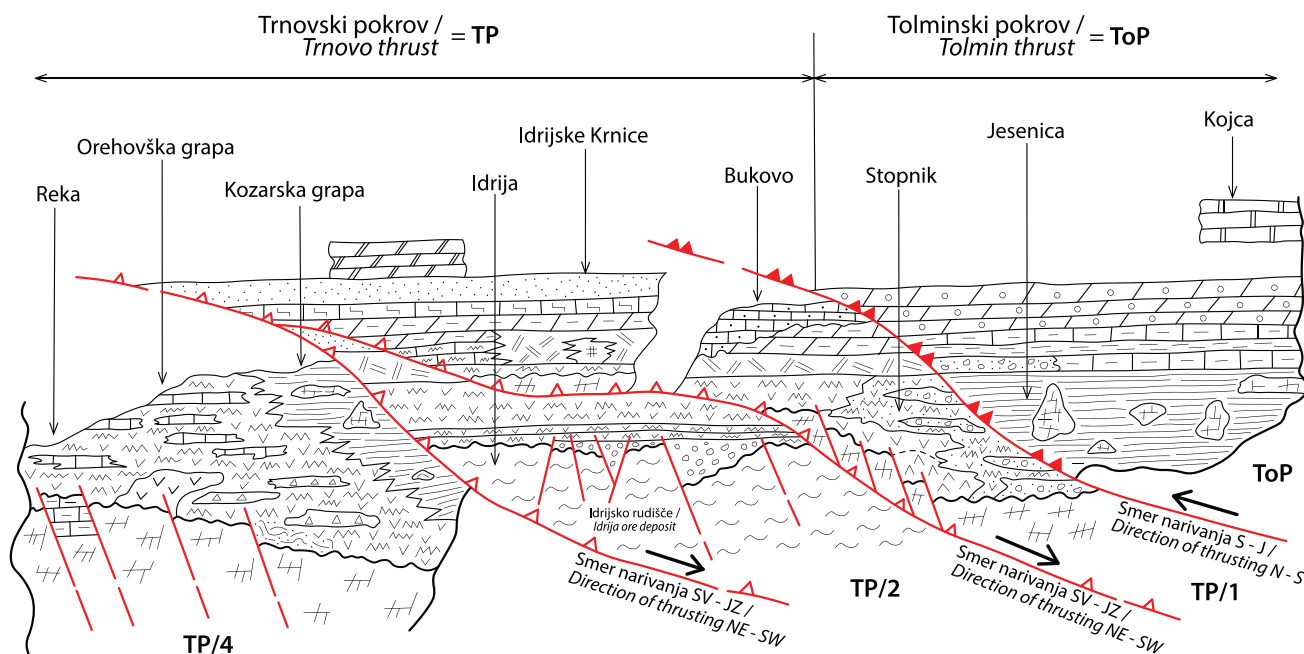
Vzhodno od Oreha najdemo v psevdoziljskih plasteh spodnje strukturne etaže več apnenčevih organogenih kop. Posebno izpostavljena in zanimiva je visoka apnenčeva kopa ob Javorščici, ki se začenja s plastnatim apnencem in se nadaljuje v grebenski apnenec. V okviru zgornje etaže Jeseniške vmesne luske (ToP/2) apnenčaste kope v splošnem ne ležijo v primarni legi, so bolj ali manj premaknjene ali tektonsko uvaljane v močno pretrtih kamninah, ki gradijo močvirnate izravnave in položna pobočja s številnimi manjšimi plazovi in zdrsi v okolini vasi Jesenica (sl. 1).

Nad zgornjo narivnico Jeseniške notranje luske (ToP/2) se nad vasjo Jesenica pričenja mogočen kompleks skrilavih muljevcov v menjavi z litičnimi peščenjaki in v zgornjem delu tudi predsedimentiranimi piroklastičnimi kamninami. Osnovno strukturo gradijo organogeni plastnati apnenci, ki zvezno prehajajo v šest mogočnih grebenskih kop na lokaciji Divji rob, visokih do 110 metrov (sl. 3D). Kossamat (1913) je bil mnenja, da so to verjetno tako imenovani 'cipit bloki', danes bi

jim rekli olistoliti, ki jih je opazoval na območju Dolomitov. Leta 1981 smo jih označili kot 'mirnovodne koralne bioherme' (zatišne plitvomorske grebenske kope) v primarni legi (Čar et al., 1981). Sedimentološke raziskave psevdoziljskih plasti na Malenskem Vrhu v Poljanski dolini kažejo na nastanek v mirnem morskom okolju, zelo verjetno v laguni (Skaberne & Čar, 1986). V novejši razpravi so bili na podlagi raziskanih organskih ostankov, plitvovodnih tekstur, mikrofaciesa plastnatih apnencev in velike debeline klastičnih kamnin mnenja, da so to apnenčevi olistoliti, ki so združnili iz plitvovodnega obroba ali zgornjega dela karbonatne platforme v bazen (Gale et al., 2016). Litološke značilnosti in položaj karbonatnih kamnin kartiranih v okviru naše študije kljub temu kažejo na možnost primarne lege grebenskih apnencev. Različne interpretacije sedimentacijskih pogojev bodo potrjene ali zavrnjene z nadaljnji podrobnejšimi raziskavami.

Nad kompleksom velikih grebenskih bioherm Divji rob prehajajo psevdoziljske plasti postopno v amfiklinske plasti s temnosivimi apnenci ter skrilavimi in laporastimi medplastnimi vložki (slika 3 B). Amfiklinske plasti prehajajo višje v pobočju Kojce zvezno v baški dolomit (Čar et al., 1981; Gale, 2010; Gale et al., 2016).

Zahodni del Jeseniške notranje luske (ToP/2) gradi značilen plastnat baški dolomit, bogat z roženci. Kamnina je nagubana in na številnih mestih močno pretrta.



Sl. 6. Shematski prikaz nastanka narivne zgradbe.

Fig. 6. Schematic cross section of a thrust system original position.

## Zaključki

Na ozemlju med vasjo Reko v dolini Idrijce ter vasema Bukovo in Jesenica pod Kojco (1303 m) v zahodni Sloveniji se stikata dve veliki narivni enoti in sicer Trnovski in Tolminski pokrov (Placer, 1981; Placer & Čar, 1997; Placer, 1999; Demšar, 2016). Prvo narivno enoto z značilno smerjo narivanja severovzhod–jugozahod prištevamo v širšem strukturnem pogledu Zunanjim Dinaridom, Tolminski pokrov s smerjo narivanja sever-jug pa Južnim Alpam (Placer & Čar, 1997; Placer et al., 2010). Narivni enoti sta na stiku obeh gorstev zgrajene iz več narivnih enot nižjega reda v zapletenih medsebojnih odnosih, ki doslej še niso bili natančneje raziskane in interpretirane. Natančnejša razčlenitev narivnih enot v Trnovskem in Tolminskem pokrovu je prikazana v priloženi Tabeli 1.

Raziskano območje seka gost sistem prelomov v smeri severozahod – jugovzhod. Od severovzhoa da proti jugozahodu si sledijo naslednji močnejši prelomi: Cerkljanski, Sovodenjski, Ravenski, Rodnski in Rečanski prelom. Najmočnejši je Sovodenjski prelom, ki je regionalnega pomena. Stik Južnih Alp in Dinaridov poteka v zahodnem in osrednjem delu obravnavanega terena ob Sovodenjskem prelomu, od zaselka Vrh Križa proti vzhodu je stik nariven.

Pomembna ugotovitev naših raziskav je, da se nahajajo tako v Trnovskem kot tudi v Tolminskem pokrovu psevdoziljske plasti, ki so na prvi pogled litološko enake. Podrobne raziskave doslej posnetih profilov bodo pokazale morebitne sedimentološke razlike.

Na obravnavanem ozemlju psevdoziljske plasti niso nikjer ohranjene v neprekinjenem profilu s talnino in krovino. V okviru Trnovskega pokrova sicer opazujemo pri Reki zvezen prehod piroklastičnih kamnin v psevdoziljske plasti, vendar je njihov zgornji del pri zaselku Selc pod Bukovim odrezan z narivom cordevolskega dolomita Tičenske notranje narivne grude (TP/1). Zvezen prehod psevdoziljskih kamnin v mlajši tankoplastnati črn dolomit in nato v bel značilen cordevolski dolomit je ohranjen le v dveh manjših izdankih ob cesti proti vasi Police, ki pa nista neposredno vezana na glavni pas psevdoziljskih plasti, ki poteka po dolini Kazarske grape. Postopen prehod med piroklastičnimi in psevdoziljskimi kamninami je ohranjen tudi na območju Križa južno od tektonske krpe V Križu.

V Orehovški notranji narivni grudi, najnižji enoti alpskih narivov, na pregledanem ozemlju ni ohranjena podlaga psevdoziljskih plasti. Odrezana je z osnovnim narivom Južnih Alp in

Dinaridov. Na območju Vršiča nad vasjo Zakriž opazujemo zvezne prehode v krovinske amfiklinske plasti. Zvezen in postopen prehod je ohranjen tudi na pobočju Kojce nad Divjim robom v okviru Podmelške notranje narivne grude.

Iz terenskih opazovanj in ocene splošnih razmer ugotavljamo, da je debelina psevdoziljskih plasti v okviru alpskih narivnih enot, v Orehovški in Podmelški notranji narivni grudi, precej večja od enakih plasti v dinarski Ravenski notranji narivni grudi. V krovini vseh omenjenih narivnih enot ležijo kamnine najnižjega dela karnija. V Trnovskem pokrovu prehajajo psevdoziljske plasti v značilen cordevolski dolomit, v okviru Tolminskega pokrova pa v amfiklinske plasti (T<sub>3</sub><sup>1</sup> - Demšar, 2016). Kot je ugotovil že Mlakar (1980), je starost cordevolskega dolomita in amfiklinskih plasti enaka, se pa seveda facielno močno razlikujejo, kar kaže na drugačne pogoje sedimentacije.

Iz pomembnih litoloških razlik v stratigrafiskem zaporedju, ki smo jih omenili zgoraj, ob upoštevanju različnih smeri narivanja in predvsem velikih dolžin narivanja, tako v Dinaridih kot Južnih Alpah, domnevamo, da so bila opisana sedimentna zaporedja pred narivanjem zelo oddaljena. Vsekakor velja, da je bilo nekdanje območje sedimentacije bistveno večje in je bilo zaradi narivanja prostorsko močno reducirano.

## Summary

Based on the detailed structural mapping (scale 1: 5,000), we studied the contact between Southern Alps and the Dinarides in the Cerkno region between the villages of Bukovo and Zakriž. The area of the Dinarides is built of the Trnovo nappe (TP). It is divided into two inner thrust blocks and six smaller tectonic subunits (Table 1). Trnovo nappe (TP) was thrust in the direction from NE to SW for about 30 kilometers. In the direction toward south rocks of the Tolmin nappe (ToP) were thrusted onto the Trnovo nappe. Tolmin nappe consists of two inner thrust blocks and inner sheet (Table 1). Length of thrusting is not known.

Trnovo nappe consists of lowest Ravne inner thrust block (TP/4) and the highest Tičen inner thrust block (TP/1). Ravne inner thrust block is divided into Zabreznica, Kozarska and Reka subunit, while Tičen inner thrust block consists of tectonic klippe, Rodne and Police tectonic subunit (Table 1). The oldest rocks within the thrust units of the Trnovo nappe are the Upper Scythian Olenekian (Kampil) marly limestones, which pass continuously into dolomite of Anisian age.

On top of the Anisian dolomite lies unconformably a sequence of variegated Ladinian rocks several hundred meters thick. Near the village of Gorenje Ravne they are represented by extensive outcrops of keratophyre and pyroclastites. In the vicinity of Križ, tuffs and tuffites pass concordantly into Pseudozilian beds. They are exposed in a narrow belt along the valley of the Jesenica stream, where they overlie the rocks of the Tičen inner thrust block. On the other side of the Rodne ridge, in the Kazarska grapa, the Pseudozilian beds reappear below the Tičen inner thrust block in the vicinity of the village of Selc as a tectonic window form. Most of the Tičen inner thrust block is formed by the characteristic Cordevol dolomite (Schlern dolomite - Celarc, 2004), which passes upwards into the Tuvalian layered dolomite.

The Tolmin Nappe (ToP) is subdivided into the lowest Orehovec inner thrust block (ToP/1), the Jesenica inner sheet (ToP/2) and the highest Podmelec inner thrust block (ToP/3) (Table 1). The length of the over-thrust has not yet been determined. The Orehovo and Jesenice overthrust units are dominated by typically developed Ladinian-Cordevolian Pseudozilian beds, which pass continuously into Amphyclina beds. They are represented by dark grey limestone interbedded with mudstone and marlstone. Within the Podmelec inner thrust block, a thick sequence of Bača dolomite lies concordantly above the Amphyclina beds on the Kojca Hill. The western part of Jesenica inner sheet is also built of extensive block of folded and deformed Bača dolomite.

The contact between the main overthrust units of the Trnovo and Tolmin nappe is also the contact of the Southern Alps and the Dinarides. In the western and central part of the studied area, the boundary between the Southern Alps and the Dinarides represents a complex tectonic zone of the regional Sovodenj fault. The fault runs from the Bača valley to the village of Bukovo, across the villages of Kojca and Nemci, continues below the village of Orehek, crosses the slopes of V Križu and continues across Vrh Križa into the Cerknica valley. In the Cerknica valley, the thrust contact between the Tolmin and Trnovo nappe is not visible. It can be seen again in the Vrh Križa area, where it runs along the boundary between the Ravne (TP/4) and the Orehovec (ToP/1) inner thrust block. Similar tectonic conditions are observed eastward, under the villages of Gorje and Poče.

In the Trnovo and Tolmin nappes Ladinian-Carnian Pseudozilian beds are present. It is assumed that they were deposited in the uniform Slovenian trough. Lithologically, the Pseudozilian

beds are represented mainly by black shale with thin intercalations of lithic sandstone and lenses of black layered limestone and massive reef limestone. On the basis of the above-mentioned significant lithological differences in the stratigraphic sequences and taking into account the different thrust directions and particularly long overthrust lengths in both the Dinarides and the Southern Alps, we assume that the sedimentary sequences described were very far apart before tectonic shortening. In any case, the former sedimentation area was clearly larger and was spatially strongly reduced by the nappe structure.

## Literatura

- Buser, S. 1986a: Tolmač lista Tolmin in Videm (Udine), Osnovna geološka karta SFRJ, 1:100.000. Zvezni geološki zavod, Beograd: 103 p.
- Buser, S. 1986b: Osnovna geološka karta SFRJ, list Tolmin in Videm (Udine), 1:100.000. Zvezni geološki zavod, Beograd.
- Buser, S. 1989: Development of the Dinaric and the Julian carbonate platforms and of the intermediate Slovenian basin (NW Yugoslavia). In: Carulli, G. B. Cucchi, F. & Radrizzani, C. P. (eds.): Evolution of the karstic carbonate platform: Relation with other periadriatic carbonate platforms, Trieste, 1987. Mem. Soc. Geol. It., 40: 313-320.
- Celarc, B. 2004: Problematika „cordevolskih“ apnencev in dolomitov v slovenskih Južnih Alpah. Geologija, 47/2: 139-149. <https://doi.org/10.5474/geologija.2004.011>
- Čar, J. 1998: Sedimentološke raziskave prehoda med Dinarsko karbonatno platformo in Slovenskim bazenom. Poročilo o triletnih raziskavah (1985-1998): 1-13, arhiv RŽS Idrija, GZS in MZT Slovenije, Idrija, (neobjavljen).
- Čar, J. 2001: Strukturna zgradba in razvoj triasnih plasti med dolino Idrijce in Kojco. Poročilo o triletnih raziskavah, 1-8, arhiv RŽS Idrija, GZS in MZT Slovenije, Idrija, (neobjavljen).
- Čar, J. 2010: Geološka zgradba idrijsko-cerkljanskega hribovja. Tolmač h geološki karti idrijsko – cerkljanskega hribovja med Stopnikom in Rovtami 1: 25.000 – Geological structure of the Idrija-Cerkno hills. Explanatory Book to the Geological map of the Idrija-Cerkljansko hills. Geološki zavod Slovenije – Geological Survey of Slovenia, Ljubljana: 127 p.
- Čar, J., Skaberne, D., Ogorelec, B., Turnšek, D. & Placer, L. 1981: Sedimentological characteristics of Upper Triassic (Cordevolian) circular quiet water coral bioherms in

- western Slovenia, nortwestern Yugoslavia. SEPM Spec. Publ., 30: 233-240. <https://doi.org/10.2110/pec.81.30.0233>
- Čar, J. & Skaberne, D. 1995: Ladinijske plasti Stopnika. Geološki zbornik, povzetek referatov, 22-26.
- Čar, J. & Skaberne, D. 2003: Stopniški konglomerat = Conglomerates of Stopnik. Geologija, 46/1: 49-64. <https://doi.org/10.5474/geologija.2003.003>
- Demšar, M. 2016: Geološka karta Selške doline 1: 25 000 in Tolmač h geološki karti Selške doline, Geološki zavod Slovenije, Ljubljana: 72 p.
- Gale, L. 2010: Microfacies analysis of the Upper Triassic (Norian) »Bača Dolomite«: early evolution of western Slovenian Basin (eastern Southern Alps, western Slovenia). Geol. Carpathica, 61/4: 293-308. <https://doi.org/10.2478/v10096-010-0017-0>
- Gale, L., Skaberne, D., Peybernes, C., Martini, R., Čar, J. & Rožič, B. 2016: Carnian reefal blocks in the Slovenian Basin, eastern Southern Alps. Facies, 62: 23. <https://doi.org/10.1007/s10347-016-0474-8>
- Kossmat, F. 1910: Eräuterungen zur geologischen Karte Bischofslack und Idria. Wien:101 p.
- Kossmat, F. 1913: Die adriatische Umrandung in der alpinen Faltenregion. Mitt. Geol. Ges., 5: 61-165.
- Kuščer, D. 1967: Tertiary formations of Zagorje. Geologija, 10: 5-85.
- Mlakar, I. 1969: Krovna zgradba idrijsko žirovskega ozemlja = Nappe Structure of the Idrija-Žiri Region. Geologija, 12: 5-72.
- Mlakar, I. 1980: O starosti spodnjega dela psevdooziljskih skladov na Cerkljanskem. Geologija, 23/2: 173-176.
- Mlakar, I. & Čar, J. 2009: Geološka karta idrijsko – cerkljanskega hribovja med Stopnikom in Rovtami 1: 25.000. Geološki zavod Slovenije, Ljubljana, 1 geol. map.
- Placer, L. 1973: Rekonstrukcija krovne zgradbe idrijsko žirovskega ozemlja = Reconstruction of the Nappe Structure of the Idrija-Žiri Region = Rekonstruktion des Deckenbaus des Idrija-Žiri gebietes. Geologija, 16: 317-334.
- Placer, L. 1981: Geološka zgradba jugozahodne Slovenije = Geologic structure of southwestern Slovenia. Geologija, 24/1: 27-60, Ljubljana.
- Placer, L. 1982: Tektonski razvoj idrijskega rušišča = Geologic history of the Idrija mercury deposit. Geologija, 25/1: 7-94.
- Placer, L. 1999: Contribution to the macrotectonic subdivision of the border region between Southern Alps and External Dinarides = Prispevek k makrotektonski rajonizaciji mejnega ozemlja med Južnimi Alpami in Zunanjimi Dinaridi. Geologija, 41: 223-255. <https://doi.org/10.5474/geologija.1998.013>
- Placer, L., Čar, J., Ogorelec, B., Orehek, S., Ramovš, A., Babić, L., Zupanič, J., Čadež, F., Cigale, M. & Hinterlehner, A. 1977: Triadna tektonika okolice Cerknega. MVS, Inštitut za geologijo FNT, Ljubljana: 58 p (neobjavljen).
- Placer, L., Rajver, D., Trajanova, M., Ogorelec, B., Skaberne, D. & Mlakar, I. 2000: Vrtina Ce-2/95 v Cerknem na meji med Južnimi Alpami in Zunanjimi Dinaridi. Geologija, 43/2: 251-266. <https://doi.org/10.5474/geologija.1998.013>
- Placer, L. & Čar, J. 1997: Zgradba Blegoša med Notranjimi in Zunanjimi Dinaridi. Geologija, 40: 305-323. <https://doi.org/10.5474/geologija.1997.016>
- Placer, L., Vrabec, M. & Celarc, B. 2010: The bases for understanding of the NW Dinarides and Istra Peninsula tectonics = Osnove razumevanja tektonske zgradbe NW Dinaridov in polotoka Istre. Geologija, 53/1: 55-86. <https://doi.org/10.5474/geologija.2010.005>
- Premru, U. 1980: Geološka zgradba osrednje Slovenije. Geologija, 23/2: 226-273.
- Rakovec, I. 1950: O nastanku in pomenu psevdooziljskih skladov. Geografski vestnik, 22: 191-214.
- Skaberne, D. & Čar, J. 1981-1991: Sedimentološke in geokemične raziskave psevdooziljske in ekvivalentnih formacij. Neobjavljena fazna poročila 1981 do 1991, arhiv GZL Ljubljana in RŽS Idrija (CUDHg), Idrija.
- Skaberne, D. & Čar, J. 1986: Sedimentološke značilnosti dela »psevdooziljske« formacije na območju Malenskega Vrha, N od Poljan, W Slovenija. 5Th Yugoslav Meeting of Sedimentologists, Brioni.
- Stache, G. 1899: Jahresbericht des Directors. Verh. Geol. Reich., Wien.
- Šmuc, A. & Čar, J. 2002: Upper Ladinian to Lower Carnian Sedimentary Evolution in the Idrija-Cerkno Region, Western Slovenia. Facies, 46/1: 205-216. <https://doi.org/10.1007/BF02668081>
- Teller, F. 1889: Daonella Lommeli in den Pseudo-Gailthalerschichten von Cilli. Verh. Geol. R. A. Wien.
- Turnšek, D., Buser, S. & Ogorelec, B. 1982: Carnian coral-sponge reefs in the Amphicлина beds between Hudajužna and Zakriž (western Slovenia). Razprave IV razreda SAZU, 24: 51-98.





# Using stable isotopes and major ions to identify recharge characteristics of the Alpine groundwater-flow dominated Triglavská Bistrica River

**Uporaba stabilnih izotopov in glavnih ionov za oceno napajalnih značilnosti alpskega rečnega toka Triglavské Bistrice pod vplivom podzemne vode**

Luka SERIANZ<sup>1,2</sup>, Sonja CERAR<sup>1</sup> & Polona VREČA<sup>3</sup>

<sup>1</sup>Geological Survey of Slovenia, Dimičeva ulica 14, SI-Ljubljana, Slovenia; e-mail: luka.serianz@geo-zs.si

<sup>2</sup>Faculty of Civil and Geodetic Engineering, University of Ljubljana, Jamova cesta 2, SI-Ljubljana, Slovenia;

<sup>3</sup>Department of Environmental Sciences, Jožef Stefan Institute, Jamova cesta 39, SI-1000, Ljubljana, Slovenia.

Prejeto / Received 5. 10. 2021; Sprejeto / Accepted 7. 12. 2021; Objavljeno na spletu / Published online 28. 12. 2021

**Key words:** groundwater, oxygen and hydrogen isotopes, hydrogeochemistry, recharge area, Alpine aquifer, Slovenia

**Ključne besede:** podzemna voda, kisikovi in vodikovi izotopi, hidrogeokemija, napajalno območje, alpski vodonosnik, Slovenija

## Abstract

Triglavská Bistrica je typická Alpínská rieka v severozápadnej časti Slovinska. Jej obnovovacia oblasť zahŕňa niektoré najvyššie vrcholy Julianských Alp. Hydrogeologické podmienky a tok rieky závisia hlavne od výmenu medzi karstifikovanou a intergranulárnu akviférou v karbonátových a dolomitových horninách. Preručený priemerný prudkosť rieky je až do niekoľkých m<sup>3</sup>/s. V tomto štúdiu boli z rôznych miest po toku rieky analýzované stabílny izotopy kisika a vodíka, aj koncentrácia tritiumu. Korelácia medzi koncentráciami hlavných ionov naznačuje, že obnovovacia oblasť zahŕňa obidve horniny. Vodné vzorky sú charakterizované negatívnymi hodnotami  $\delta^{18}\text{O}$  a  $\delta^2\text{H}$ . Vzdialosť od pramene rieky je súvisom s rastom nadmorského výšku. Na mieste sčítania V-5, nachádzajúcom sa približne 300 m nad súčiatím s Savo Dolinkou, je predpísaná nadmorská výška obnovy 1,996 m.

## Izvleček

Triglavská Bistrica je tipična alpska reka, ki se nahaja v severozahodnem delu Slovenije. Njeno napajalno zaledje pokriva nekaj najvišjih vrhov v Julijskih Alpah. Hidrogeološke razmere in rečni tok sta v veliki meri odvisna od izmenjave podzemne vode med kraško-razpoklinskim vodonosnikom v karbonatnih kamninah in medzrnskim vodonosnikom v glaciofluvialnih sedimentih. Povprečen pretok reke v spodnjem toku je ocenjen na nekaj m<sup>3</sup>/s. V tej študiji so bila določena razmerja stabilnih izotopov kisika in vodika, koncentracije glavnih ionov in koncentracija aktivnosti tritija v vzorcih vode na različnih lokacijah nizvodno od izvira Triglavské Bistrice. Na osnovi korelacije osnovnih ionov je možno sklepati, da je napajalno zaledje sestavljeno tako iz apnenca kot tudi dolomita. Vrednosti  $\delta^{18}\text{O}$  in  $\delta^2\text{H}$  upadajo dolvodno od izvirnega območja, kar pomeni, da povprečna nadmorska višina napajanja narašča. Na dolvodnom merilnom mestu V-5, ki se nahaja približno 300 m nad sotočjem s Savo Dolinko, znaša izračunana povprečna nadmorska višina napajanja 1.996 m.

## Introduction

Triglavská Bistrica je malá slovenská rieka, ktorá tečie v údolí Vrata a je obklopená najvyššími vrchmi Slovinska. Jej vodný tok je významnou súčasťou karstifikovanej akviféry v karbonatech a dolomitech. Preručený priemerný prudkosť rieky je až do niekoľkých m<sup>3</sup>/s. V tomto štúdiu boli z rôznych miest po toku rieky analýzované stabílny izotopy kisika a vodíka, aj koncentrácia tritiumu. Korelácia medzi koncentráciami hlavných ionov naznačuje, že obnovovacia oblasť zahŕňa obidve horniny. Vodné vzorky sú charakterizované negatívnymi hodnotami  $\delta^{18}\text{O}$  a  $\delta^2\text{H}$ . Vzdialosť od pramene rieky je súvisom s rastom nadmorského výšku. Na mieste sčítania V-5, nachádzajúcom sa približne 300 m nad súčiatím s Savo Dolinkou, je predpísaná nadmorská výška obnovy 1,996 m.

Triglavská Bistrica je typická Alpínská rieka v severozápadnej časti Slovinska. Jej obnovovacia oblasť zahŕňa niektoré najvyššie vrcholy Julianských Alp. Hydrogeologické podmienky a tok rieky závisia hlavne od výmenu medzi karstifikovanou a intergranulárnu akviférou v karbonátových a dolomitových horninách. Preručený priemerný prudkosť rieky je až do niekoľkých m<sup>3</sup>/s. V tomto štúdiu boli z rôznych miest po toku rieky analýzované stabílny izotopy kisika a vodíka, aj koncentrácia tritiumu. Korelácia medzi koncentráciami hlavných ionov naznačuje, že obnovovacia oblasť zahŕňa obidve horniny. Vodné vzorky sú charakterizované negatívnymi hodnotami  $\delta^{18}\text{O}$  a  $\delta^2\text{H}$ . Vzdialosť od pramene rieky je súvisom s rastom nadmorského výšku. Na mieste sčítania V-5, nachádzajúcom sa približne 300 m nad súčiatím s Savo Dolinkou, je predpísaná nadmorská výška obnovy 1,996 m.

Brenčič & Vreča, 2016; Torkar et al., 2016). At the same time, water from the river can infiltrate the banks and surrounding aquifers. These conditions change temporally (seasonally) and spatially (lithology, geomorphological processes, etc.). Hydrogeochemical methods are among the most useful approaches to identify such conditions and determine other physiochemical processes. In carbonate reservoirs, the main chemical parameters describing carbonate equilibrium in groundwater are calcium ( $\text{Ca}^{2+}$ ), magnesium ( $\text{Mg}^{2+}$ ), their molar ratio ( $\text{Ca}^{2+}/\text{Mg}^{2+}$ ), and hydrogen carbonate ( $\text{HCO}_3^-$ ). In addition to chemical parameters, stable isotope ratios of oxygen and hydrogen (expressed as  $\delta^{18}\text{O}$  and  $\delta^2\text{H}$ ) in water can also provide information on recharge areas (Clark and Fritz, 1997), while tritium activity concentration ( ${}^3\text{H}$ ) can provide information on the average residence time of groundwater. A combination of chemical and isotope data has been widely used for hydrogeological research of alpine water streams (Carey & Quinton, 2005; Thiébauda et al., 2010; Shamsi et al., 2019), and the same techniques have been applied also in Slovenia (Kanduč et al., 2012; Torkar et al., 2016).

The Triglavská Bistrica watershed consists of massive limestone and dolomite rocks with fractures and karstic porosity. It is therefore very likely that dissolution of carbonate minerals is the most important hydrogeochemical process affecting the chemical components of natural water flow. There is very little data on the hydrogeochemistry of the groundwater in the monitoring area, but several chemical analyses are available for a spring near the Peričnik waterfall, which was included in the study of the hydrogeochemistry of alpine springs from northern Slovenia (Kanduč et al., 2012). These studies suggest that the water of the alpine springs is dominated by  $\text{HCO}_3^-$ ,  $\text{Ca}^{2+}$  and  $\text{Mg}^{2+}$  ions and that most of the springs were near equilibrium in terms of calcite. These results can be confirmed by recent hydrogeochemical studies in similar environments (Mezga, 2014; Torkar et al., 2016; Serianz et al., 2020b).

It is commonly observed that precipitation gradually becomes depleted in  ${}^{18}\text{O}$  and  ${}^2\text{H}$  isotopes as altitude increases (Dansgaard, 1964). This phenomenon is commonly referred to as the “altitude effect” and results primarily from the cooling of air masses as they ascend a mountain range, accompanied by the dissipation of excess moisture (Gonfiantini et al., 2001; Kern et al., 2020). In the case of  $\delta^{18}\text{O}$ -precipitation, the global average gradient with altitude is  $-2.8 \text{ ‰}/\text{km}$ ,

and ranges from  $-1.7$  to  $-5.0 \text{ ‰}/\text{km}$ ; the European average is  $-2.1 \text{ ‰}/\text{km}$  (Poage and Chamberlain, 2001). On Slovenian territory, for example, the altitude effect on precipitation ranges from  $-0.2 \text{ ‰}$  to  $-0.3 \text{ ‰ } \delta^{18}\text{O}/100 \text{ m}$  (Vreča et al., 2006; Brenčič and Polting, 2008). For Croatia and Slovenia combined, these values range from  $-0.37 \text{ ‰}$  to  $-0.26 \text{ ‰ } \delta^{18}\text{O}/100 \text{ m}$  (Horvatinčić et al., 2005). For other countries, such as Austria, the altitude effect is estimated to be  $-0.21 \text{ ‰ } \delta^{18}\text{O}/100 \text{ m}$  (Kralik et al., 2003) and the value for Italy is estimated at roughly  $0.2 \text{ ‰ } \delta^{18}\text{O}/100 \text{ m}$  (Longinelli and Selmo, 2003). Based on the fact that the isotopic composition in precipitation is reflected in the isotopic composition of groundwater, Mezga et al. (2013) calculated three elevation effects for groundwater following different patterns of precipitation intensity, ranging from  $-0.25 \text{ ‰ } \delta^{18}\text{O}/100 \text{ m}$  for the Alps and the coastal region to  $0.33 \text{ ‰ } \delta^{18}\text{O}/100 \text{ m}$  for the Bela Krajina region (Cerar et al., 2018). Recent studies in the Adriatic-Pannonian region indicate an empirical isotopic altitude effect in modern precipitation for  $\delta^{18}\text{O}$ , which is  $-1.2 \text{ ‰}/\text{km}$  and  $-7.9 \text{ ‰}/\text{km}$  for the  $\delta^2\text{H}$  (Kern et al., 2020).

The objective of this research is to identify the source, type, and amount of the different water components of the Triglavská Bistrica River recharge, to describe their spatial variations using hydrochemical, isotopic, and hydrogeological methods, and to estimate the mean recharge altitude of the Triglavská Bistrica River.

## Study area settings

### General settings

The Triglavská Bistrica River courses through the heart of the Julian Alps in the north-western part of Slovenia and flows on through the Vrata Valley. In Mojstrana, a small settlement at the end of the valley, Triglavská Bistrica flows into the Sava Dolinka River, which joins the Sava Bohinjka River to form the Sava River, the largest tributary of the Danube by water volume. Triglavská Bistrica is a typical Alpine River, which flows in the Vrata glacial valley. It flows under Triglav North, the highest mountain in the country. The largest stream flowing into the river is the Peričnik. The Triglavská Bistrica flows into the Sava Dolinka River about 10 km downstream, with a gradient of about 400 m, and is surrounded by mountains with the greatest number of peaks above 2,500 m a.s.l. in its catchment area. The water percolates out of extensive scree at the foot of the wall (Smolar-Žvanut et al., 2005). On its way to the Sava Dolinka, the Triglavská Bistrica

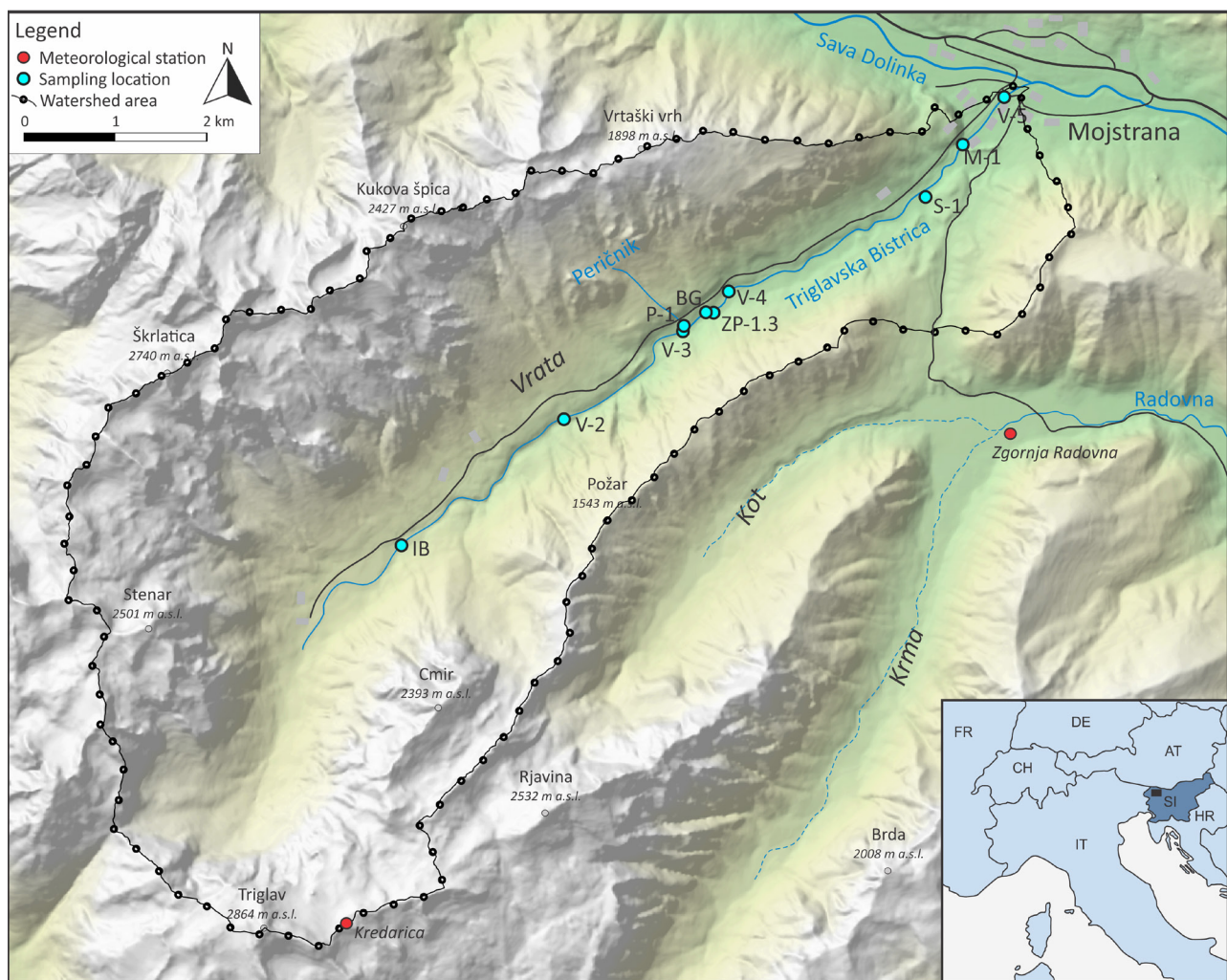


Fig. 1. The observation area and sampling locations (spring MS-1 is not included due to its distance from the Vrata Valley; coordinates of the spring are given in Table 1).

runoff is amplified by lateral inflows. The river discharge is classified as an alpine high mountain snow-rain regime (Hrvatin, 1998), and the effects of snowmelt are still evident in late summer; but in the fall the runoff originates just below the north face of the Triglav Mountain. In shaded kettles and mountain gorges the snow remains all year round.

The wider observation area (Fig. 1) is characterized by a variety of relief forms, fast and expressive altitude changes due to the geological base, and process related to the formation of younger mountains. The landscape is characterized by glacially-formed valleys and rocky highland ridges, peaks with unusual karstic shapes. They climb over the Gate Valley Stenar (2,601 m), Škrlatica (2,740 m), Kukova Špica (2,427 m) and above the junction of the valley's Severna Triglav wall. Some high peaks can be found also in the ridge that divides Vrata and Kot, for example Cmir (2,393 m) and Rjavina (2,532 m). The catchment area of the Triglavská Bistrica is

overgrown with forest in its lower part. At the foot of the valley, glaciers that probably covered the entire Upper Sava Valley (Serianz, 2016) have left behind well consolidated lateral moraines that cause, together with other hydrological parameters, a slower run-off from the valley slopes (Smolar-Žvanut et al., 2005). The diversity of the Alpine valleys influences the climate there, especially temperature (regime of alpine basins and valleys, ridges, and peaks).

### Hydrometeorological data

The climate of the Upper Sava region belongs to the Alpine region, which is characterized by long and snowy winters and short, moderately warm summers, frequent east winds and abundant rainfall. The area along the Vrata Valley is still under the influence of specific climatic conditions, which aggravate the mountainous character of the climate and is a consequence of the altitude. Winter usually lasts four to five months. The average minimum daily temperature in January

is as low as  $-8^{\circ}\text{C}$ , while during the day it can warm above  $0^{\circ}\text{C}$ . In the warmest month, daytime temperatures rise to  $23^{\circ}\text{C}$ . Across the valley upwards, the microclimatic conditions vary even more. An indicator of this is the thickness of the snow cover, which grows with each meter in altitude. There are also large differences between sunny and shady slopes in winter. Thus, sunny slopes in winter are suitable for trips and walks, because they offer the desired sunlight, and shady slopes protect and preserve the snow blanket. At Kredarica meteorological station, which is located at an altitude of 2,514 m, the climate is even more significantly affected by snow. Here, the snow can be as much as an estimated 7 m deep (Nadbath, 2014). Based on the meteorological data available on the web database of the Slovenian Environmental Agency – ARSO (Internet 1), in the period from September 2019 to September 2020, which was representative for the documented hydrogeological investigations, winter temperatures dropped to  $-20^{\circ}\text{C}$ , while during the summer they rise to more than  $20^{\circ}\text{C}$  (Fig. 2). During this period snow was present from November to July, a full 8 months, with snow up to 4 m deep. The specific alpine meteorological conditions also affect the Triglavská Bistrica River hydrograph. Data from past observation at the gauging station in Mojstrana (Internet 2) indicate the presence of a snow-rainy river flow regime, with the largest discharges during the melting period in spring (Fig. 3).

## Hydrogeological settings

The Triglavská Bistrica River recharges from the watershed area extending from the southern side of the Triglav Mountains and the ridges above the Vrata Valley. In this area massive limestones and dolomites and granular dolomites predominate (Jurkovšek, 1987). From a hydrogeological point of view, the carbonate layers, limestones and dolomites form aquifers with fissure, karstic, and karstic-fissure porosity. Faults in the Dinaric and Trans-Dinaric directions run through the catchment area, which influence the geometry of the aquifer. In the lower areas, the carbonate rocks are covered with poorly sorted moraine material and sloping sediments, which are sometimes filled with unsorted clay and sand deposits and are mostly presented by good or medium hydraulic conductivity; however, also low hydraulic conductivity can be observed due to the high heterogeneity of the sediment structure (e.g. clay, silt). Intermediate clay inserts represent hydraulic barriers. The sediments are of glaciofluvial origin (Jurkovšek, 1987). Slope sediments and moraines can be found at the bottom of the Valley, covering the bedrock slopes. These Quaternary deposits are determined by intergranular porosity with good to low hydraulic conductivity. Alluvial deposits of Holocene age up to a few meters thick can also be found along the riverbanks. The alluvial sediments that occur at the bottom of the valley where the Triglavská Bistrica flows represent a highly-permeable and relatively homogeneous intergranular aquifer.

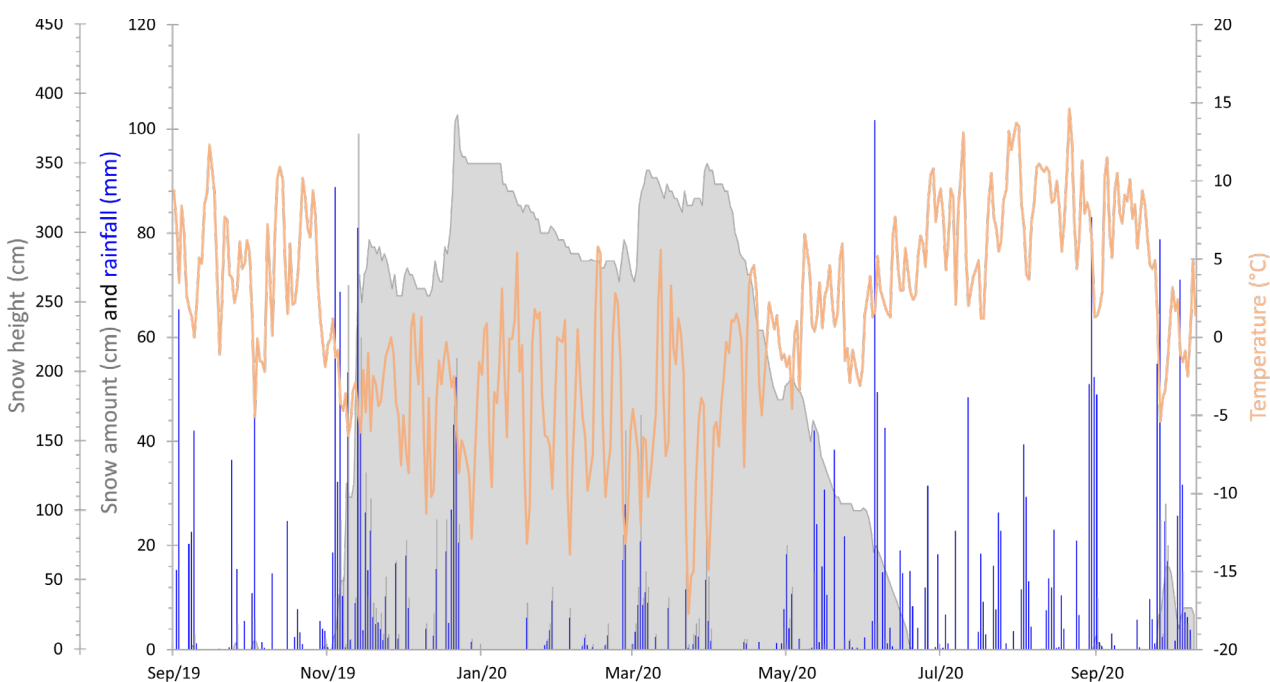


Fig. 2. Meteorological data at the Kredarica station for the period September 2019 to September 2020 (ARSO, 2021).

## Materials and methods

### Gauging station M-1

In the past, regular flow measurements were made at the Triglavská Bistrica River. In the period 1953 to 1990, a water gauging station operated on the Bistrica River in the village of Mojstrana. The surface area of the catchment area of the Bistrica to the gauging station of Mojstrana is 47 km<sup>2</sup>. Since no flow measurements have been made since 1989, a flow tube near the small hydroelectric plant at Mojstrana (M-1) was installed on April 10, 2020, which contains a “diver” that we use to monitor the flow elevation of the Triglavská Bistrica. This monitoring site is located further upstream (~700 m) than the original gauges Mojstrana and Mojstrana I. Discharge measurements were performed along the stretch where monitoring site M-1 is located. The measurements were made using the instant chemical integration method, which is based on the immediate injection of tracers into the river. As a follow-up, common table salt was used, which provides a series of quality measurements due to its physicochemical properties (highly soluble in water, harmless to the environment, etc.) and leads to a strong increase in electrical conductivity. The salt concentration was measured based on electrical conductivity using a “Flo-tracer” measuring device. Based on periodic measurements and a comparison with the measured flow height in the pipe at gauging station M-1 a preliminary stage-discharge rating curve was constructed (power type). Currently, only three representative values are available for adjusting stage-discharge rating curve.

### Water sample collection

Sampling of groundwater and surface water from the Peričnik catchment and springs, as well as from the wider area (Fig. 1), was carried out with the aim of determining the hydrogeological conditions of the recharge area of the Peričnik springs, which are important for the water supply for the western part of the municipality of Jesenice. The joint discharge rate of Peričnik springs ranges from 70 to 120 L/s and supplies some 15,000 users (Internet 3).

Roughly speaking, the monitoring sites were selected based on preliminary cartographic analysis and knowledge of the hydrogeological conditions of the area. The exact location for each monitoring site was determined in the field (Fig. 1, Table 1). At the first sampling, we selected 10 monitoring sites, 6 of which are represented by

Triglavská Bistrica surface water (V-2, V-3, BG, V-4, V-5, M-1), one in the Peričnik stream (P-1), one in the captured Peričnik spring (ZP-1.3), and two surrounding springs (S-1 and MS-1). During the second sampling, we added another monitoring site, Triglavská Bistrica (IB), in addition to the existing ones.

Sampling was conducted in two campaigns, on April 10, 2020 and May 22, 2020. According to the recorded flows at monitoring site M-1 (Fig. 3), the first sampling was conducted at low water level, and the second sampling was conducted at medium water level. Sampling procedures, transport and storage of groundwater samples were carried out in accordance with ISO standards (SIST ISO 5677-11:1996; SIST ISO 5677-03:1996; SIST ISO 5677-6:1996).

In-situ measurements of physico-chemical parameters (i.e. temperature (T), pH, and electrical conductivity (EC)) were carried out using a waterproof HI98194 multimeter from HANNA instruments Inc. (Hanna instruments, 2020). The reported analytical accuracies of the field measurements are ±0.02 for pH, ±0.15 °C for temperature and ±1 % for electrical conductivity.

Water samples were collected to determine the isotopic composition of oxygen ( $\delta^{18}\text{O}$ ) and hydrogen ( $\delta^2\text{H}$ ). Based on the results of the first sampling and in order to get valuable insight into the hydrogeochemical processes and the natural background of the wider area samples for determination additional parameters were collected during the second sampling. Water samples for basic chemical parameters (i.e.  $\text{Na}^+$ ,  $\text{K}^+$ ,  $\text{Ca}^{2+}$ ,  $\text{Mg}^{2+}$ ,  $\text{HCO}_3^-$ ,  $\text{SO}_4^{2-}$ ,  $\text{Cl}^-$ ,  $\text{NO}_3^-$  and total dissolved solids) were collected at 5 locations, and at 3 locations for tritium activity concentration ( ${}^3\text{H}$ ) (Table 1).

Precipitation is sampled according to the most rational approach for monitoring isotopes in precipitation as a monthly composite in the frame of the Slovenian Network of Isotopes in Precipitation (Vreča and Malenšek, 2016, Internet 4) at two meteorological stations (i.e. Kredarica and Zgornja Radovna), which are part of the Slovenian National Meteorological Network maintained by the Slovenian Environmental Agency (ARSO). Precipitation samples were collected by ARSO staff from the classical rain gauge collector three times daily (synoptic station Kredarica) or once per day (precipitation station Zgornja Radovna). The volume of collected precipitation is recorded and the sample is poured into a plastic bottle with a tight-fitting cap. In the laboratory, we removed impurities (e.g. dust, particles) from the composite monthly sample by filtration through

12–25 µm pore-size ashless filter papers before taking aliquots for different isotope analyses. Samples for the analysis of stable isotopes of hydrogen and oxygen were stored in glass bottles (minimum 30 mL).

### Chemical analysis

Chemical analysis of major ions was performed by the Slovenian National Laboratory of Health, Environment and Food, Novo mesto laboratory, in accordance with the lab's methods (accreditation document LP-014, last modification 14 February 2020). For the basic chemical parameters ( $\text{Na}^+$ ,  $\text{K}^+$ ,  $\text{Ca}^{2+}$ ,  $\text{Mg}^{2+}$ ,  $\text{SO}_4^{2-}$ ,  $\text{Cl}^-$ ,  $\text{NO}_3^-$ ) the ion chromatography method (SIST EN ISO 10304-1:2009, SIST EN ISO 17294-2:2005, SIST EN ISO 14911:2000) was used, and for  $\text{HCO}_3^-$  the volumetric method was used (EN ISO 9963-1). The measurement uncertainty for  $\text{NO}_3^-$  is  $\pm 11\%$ , for  $\text{SO}_4^{2-} \pm 8\%$ , for  $\text{Cl}^- \pm 7\%$ , for  $\text{Ca}^{2+} \pm 15\%$ , for  $\text{Mg}^{2+} \pm 12\%$ , for  $\text{Na}^+ \pm 11\%$ , for  $\text{K}^+ \pm 12\%$ , and for  $\text{HCO}_3^- \pm 3\%$ .

The isotopic composition of hydrogen ( $\delta^2\text{H}$ ) and oxygen ( $\delta^{18}\text{O}$ ) was determined at the Jožef Stefan Institute (Ljubljana, Slovenia) using the  $\text{H}_2\text{-H}_2\text{O}$  (Coplen et al., 1991) and  $\text{CO}_2\text{-H}_2\text{O}$  (Epstein and Mayeda, 1953; Avak et al., 1995) equilibration technique. Measurements were performed using a dual inlet isotope ratio mass spectrometer (DI IRMS, Finnigan MAT DELTA plus, Finnigan MAT GmbH, Bremen, Germany) with an automated  $\text{CO}_2\text{-H}_2\text{O}$  and  $\text{H}_2\text{-H}_2\text{O}$  HDOeq 48 Equilibration Unit (custom-made by M. Jaklitsch). All measurements were performed together with laboratory reference materials (LRM) that are regularly calibrated against primary IAEA calibration standards. Water samples were measured as independent duplicates. Results were normalized to the VSMOW/SLAP scale using the Laboratory Information Management System (LIMS) for Light Stable Isotopes (U.S. Geological Survey) and expressed in standard  $\delta$  notation (in ‰). For independent quality control, we used a LRM W-45 with defined isotopic values and an estimated measurement uncertainty of  $\delta^2\text{H} = -60.6 \pm 0.7\%$  and  $\delta^{18}\text{O} = -9.12 \pm 0.04\%$ , and the commercial reference materials USGS 45 ( $\delta^2\text{H} = -10.3 \pm 0.2\%$ ,  $\delta^{18}\text{O} = -2.238 \pm 0.006\%$ ) and USGS 47 ( $\delta^2\text{H} = -150.2 \pm 0.3\%$ ,  $\delta^{18}\text{O} = -19.80 \pm 0.01\%$ ). The average sample repeatability for  $\delta^2\text{H}$  and  $\delta^{18}\text{O}$  was 0.3 and 0.01 ‰, respectively.

Groundwater samples for determination of the tritium activity concentration ( ${}^3\text{H}$ ) were analysed by the Wessling laboratory in Budapest using the IRPA standard (FS-78-15-AKU: 1995) and MSZ 19387:1987 method. This procedure is based on

the principal of selective isotopic enrichment using electrolysis. The volumes of the water samples are reduced from 250 mL or 800 mL to 14–15 mL by electrolytic enrichment, with the factor of tritium enrichment roughly 15–16 or 30–35. The tritium activity of enriched water samples was counted using a liquid scintillation analyser (LD: 0.5 or 0.2 TU, the uncertainty is 5–10 %).

### Data interpretation models

#### *Hydrogeochemistry*

Graphical analysis classification of groundwater type was performed in an AquaChem® 5.1 (Waterloo Hydrogeologic Inc., Waterloo, Canada), where the ion pattern was defined according to the concentration of dominant dissolved species measured in the groundwater. A trilinear Piper diagram (Piper, 1944) was used to determine hydrochemical facies using all major ions for classification. In addition, the molar ratio between  $\text{Ca}^{2+}$  and  $\text{Mg}^{2+}$  in groundwater was used to indicate the relative proportion of rocks in the recharge area. However, values equal to 1 are assumed in the literature to indicate dissolution of dolomite and dolomite prevailing in the recharge area (Mayo and Loucks, 1995). A higher  $\text{Ca}^{2+}/\text{Mg}^{2+}$  molar ratio (>2) is a consequence of the predominant calcite rocks (Katz, 1998). The saturation indices (SI) of dolomite and calcite were calculated to evaluate the chemical equilibrium using an AquaChem® 5.1, based on the following equation:

$$SI = \log (IAP/K_T) \quad (1)$$

where IAP is the ion activity product and  $K_T$  the equilibrium constant at a given temperature. Positive SI values ( $SI > 0$ ) indicate mineral oversaturation and precipitation, while negative SI values ( $SI < 0$ ) indicate unsaturated solutions and mineral dissolution. The assumed tolerance equilibrium range with respect to mineral is  $\pm 0.1$  SI for calcite and  $\pm 0.5$  SI for dolomite.

#### *Stable isotopes*

The stable isotope composition of groundwater ( $\delta^{18}\text{O}$  and  $\delta^2\text{H}$ ) was used to obtain information on the characteristics of the recharge area. The  $\delta^{18}\text{O}$  and  $\delta^2\text{H}$  values were compared with:

- the Global Meteoric Water Line (GMWL) defined as  $\delta^2\text{H} = 8\delta^{18}\text{O} + 10$  (‰) (Craig, 1961), which is very close to the local meteoric water line for the Ljubljana 1981–2010 precipitation isotope record (Vreča et al., 2008 and 2014; Internet 4),

- the Eastern Mediterranean Meteoric Water Line (EMMWL) defined as  $\delta^2\text{H} = 8\delta^{18}\text{O} + 22$  (Gat and Carmi, 1970), and
- the precipitation-weighted local meteoric water lines (reduced major axis regression – RMA) for Kredarica defined as  $\delta^2\text{H} = 8.4\delta^{18}\text{O} + 19$  and for Zgornja Radovna defined as  $\delta^2\text{H} = 8\delta^{18}\text{O} + 11$  (Internet 4).

The  $\delta^{18}\text{O}$  values were also used to determine the mean recharge altitude of the investigated water samples. The calculations used herein were based on:

1.  $\delta^{18}\text{O}$  altitude effect from precipitation in the period 2016–2020 at Kredarica and Zgornja Radovna meteorological stations. Calculations were made separately for snow and total precipitation. The  $\delta^{18}\text{O}$  of snow was determined by a detailed analysis of precipitation data for each monthly sampling campaign at the meteorological station. For  $\delta^{18}\text{O}$  of snow, only those samples where the snow represents 60% or more of total precipitation ( $P_{\text{snow}} \geq 0.6 P_{\text{total}}$ ) were counted. Spring MS-1 average  $\delta^{18}\text{O}$  from both samplings was used as a representative value for applying precipitation mean altitude effect.

2. archive mean altitude effect calculated for Radovna Valley (Torkar et al., 2016) based on linear model  $h_{\text{avg}} = -931.8 \delta^{18}\text{O} - 7650.8$  and Bled area (Serianz et al., 2020b) based on linear model  $h_{\text{avg}} = -939.2 \delta^{18}\text{O} - 7518.6$ .

## Results and discussion

### Triglavská Bistrica hydrograph

The highest measured discharge at the gauging station M-1 for the preliminary stage-discharge rating curve adjustment was  $9 \text{ m}^3/\text{s}$ , while measurements at higher water levels were unsuccessful due to unfavourable measurement conditions. Therefore, the information on some peak discharges above  $9 \text{ m}^3/\text{s}$  (Fig. 3) is relatively poor and will be improved in the future. The Triglavská Bistrica hydrograph shows the measurements (average daily flow, maximum daily flow, and minimum daily flow) from 1973 to 1989 (Internet 2). At the same time, the hydrograph shows the flow for 1980, which was chosen as the reference flow for this period of operation at measuring point Mojstrana I. The archive discharges (Internet 2) are presented for comparison with new measurement at gauging station M-1.

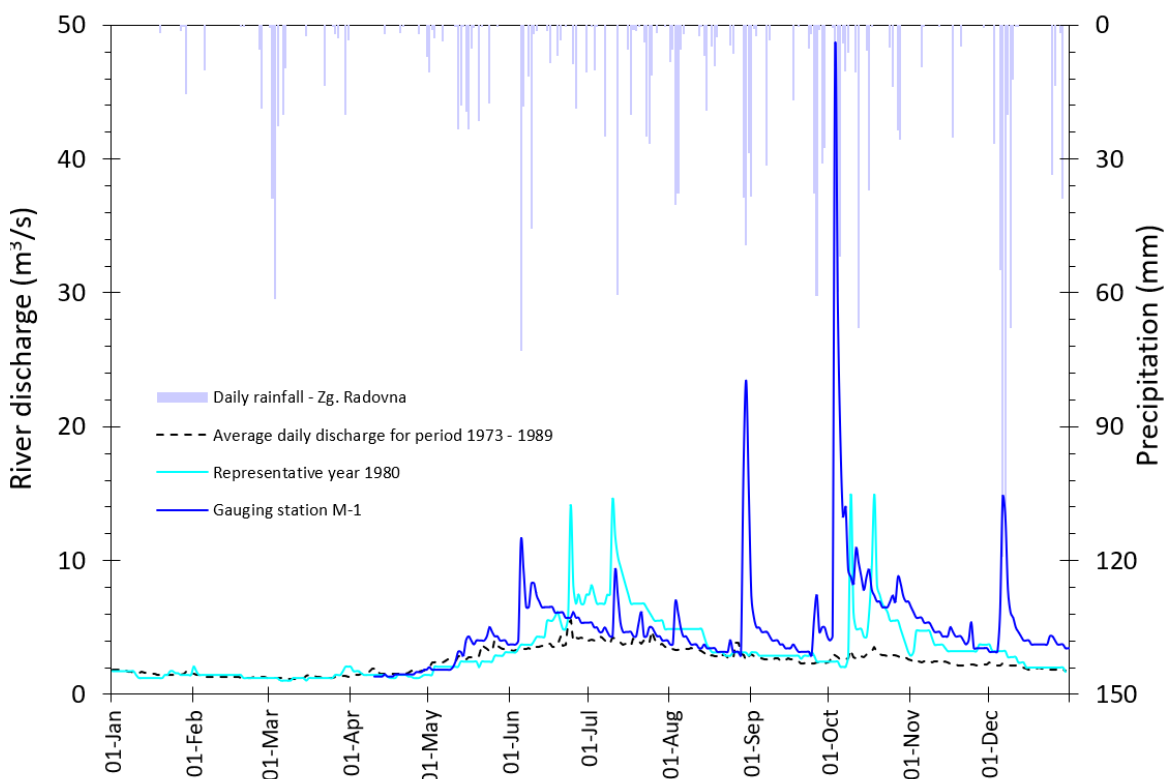


Fig. 3. Triglavská Bistrica River hydrography at gauging station M-1 and archive gauging station Mojstrana, including daily precipitation at the Zgornja Radovna meteorological station.

The Triglavská Bistrica hydrograph illustration has a specific shape, which can be described with snow-rain regime. It can be divided into two parts: (1) period of snow thaw and (2) autumn rainy period (Fig. 3). The start of the snow-melt period can be detected by the small discharges in early spring, which start with the slow rise of discharges, and during the high-thaw period form a specific shape with high discharge values. A few discharge peaks can be observed from the resulting shape as the result of rainy day(s) in the snow-melt period. Once the highest discharge is reached, usually at the beginning of summer, it starts to decline.

### Physio-chemical parameters

The results of the measurements of field parameters, basic chemical analysis, isotopic composition of  $\delta^{18}\text{O}$  and  $\delta^2\text{H}$ , and tritium activity concentrations in groundwater and surface water are summarised in Table 1. Water temperatures in the Peričnik catchment (sampling point ZP-1.3) were 6.0 and 6.1 °C in both sampling campaigns, and slightly higher in surface waters and springs, between 5.7 and 8.3 °C (average 7.0 °C) in the first campaign, and between 7.2 and 9.5 °C (average 8.0 °C) in the second sampling campaign. The pH value of the groundwater in the Peričnik catchments was constant at 8.0 in the first campaign, and 7.9 in the second campaign. The surface water of the Triglavská Bistrica (sampling point BG) has similar values about 100 m upstream from the Peričnik catchments (8.3 and 8.1, respectively). The pH values in the surface water ranged from 8.2 to 8.4 and from 7.2 to 8.3 in the second campaign. The electrical conductivity (EC) of the groundwater in the Peričnik catchment was 192 µS/cm in the first sampling campaign and 187 µS/cm in the second sampling campaign. Similar EC values are also characteristic for the sampling point BG, at 188 µS/cm in the first sampling campaign or slightly lower (173 µS/cm) in the second sampling campaign and at spring S-1 (between 195 and 276 µS/cm). The EC values are lower at the surface water sampling points and range between 110 and 146 µS/cm (average 127.5 µS/cm) in the first sampling campaign. In the second sampling campaign, the values are higher and range between 153 and 201 µS/cm (average 180 µS/cm). In the second sampling campaign, the Bistrica spring (IB) was also sampled, where the measured value from EC was 234 µS/cm.

The basic chemical parameters were only determined in the second campaign, so a compar-

ison of the results between the two sampling campaigns is not possible. The  $\text{Ca}^{2+}$  concentration in the groundwater in the Peričnik catchment is about 26 mg/L. A similar  $\text{Ca}^{2+}$  concentration was also measured at sampling point P-1 (26 mg/L), and slightly higher at sampling point BG (28 mg/L). Upstream of the Peričnik catchment (sampling points V-3 and IB),  $\text{Ca}^{2+}$  concentrations in surface water are slightly higher, reaching 30 and 42 mg/L, respectively.  $\text{Mg}^{2+}$  concentrations indicate the opposite. In the Peričnik catchment, slightly higher concentrations are measured in groundwater (8.4 mg/L), while at upstream sampling points V-3, BG, IB and P-1,  $\text{Mg}^{2+}$  concentrations range between 5.7 and 7.6 mg/L and increase downstream towards the Peričnik catchment. Characteristics similar to those of  $\text{Ca}^{2+}$  in the water are also reflected in the distribution of  $\text{HCO}_3^-$  concentrations in the water. The highest concentrations of  $\text{HCO}_3^-$  in the water were measured at the sampling point IB (160 mg/L). The concentrations decrease downstream and reach 129 mg/L at sampling point BG. Similar concentrations were also measured in the water of the Peričnik catchment (124 mg/L).

The values of carbonate ions ( $\text{Ca}^{2+}$ ,  $\text{Mg}^{2+}$ , and  $\text{HCO}_3^-$ ) in the groundwater indicate the carbonate recharge area. The calculated ratio between calcium and magnesium ions ( $\text{Ca}^{2+} + \text{Mg}^{2+}$ ) and  $\text{HCO}_3^-$  in meq/L is about 1:1. The water samples belong to the Ca-Mg-HCO<sub>3</sub> facies, with low K<sup>+</sup>, Na<sup>+</sup>, Cl<sup>-</sup>, NO<sub>3</sub><sup>-</sup> and SO<sub>4</sub><sup>2-</sup> ion-content, except for the water at the sampling point IB, which belongs to the Ca-HCO<sub>3</sub> facies (Fig. 4). The  $\text{Ca}^{2+}/\text{Mg}^{2+}$  molar ratio for each sampling point shows similar characteristics (Fig. 5a). The  $\text{Ca}^{2+}/\text{Mg}^{2+}$  ratio is 2.0 for the groundwater in the Peričnik catchment, while the ratio for the surface water upstream of the catchment is slightly higher (between 2.39 and 2.61), and is highest for sampling point IB (4.32). The latter shows that the recharge area of the spring is an aquifer dominated by limestone, while other waters are characterized as mainly fed by aquifers dominated by dolomite over limestone.

Figure 5b shows saturation indices (SI) of calcite ( $\text{SI}_{\text{calcite}}$ ) and dolomite ( $\text{SI}_{\text{dolomite}}$ ) in sampled water. Groundwater at sampling point IB is oversaturated with respect to calcite and dolomite, since  $\text{SI}_{\text{calcite}}$  and  $\text{SI}_{\text{dolomite}}$  are both positive ( $\text{SI} > 0$ ), which means that the mineral might precipitate but cannot dissolve (Appelo and Postma, 2005). This groundwater was sampled in the recharge area where limestone prevails.

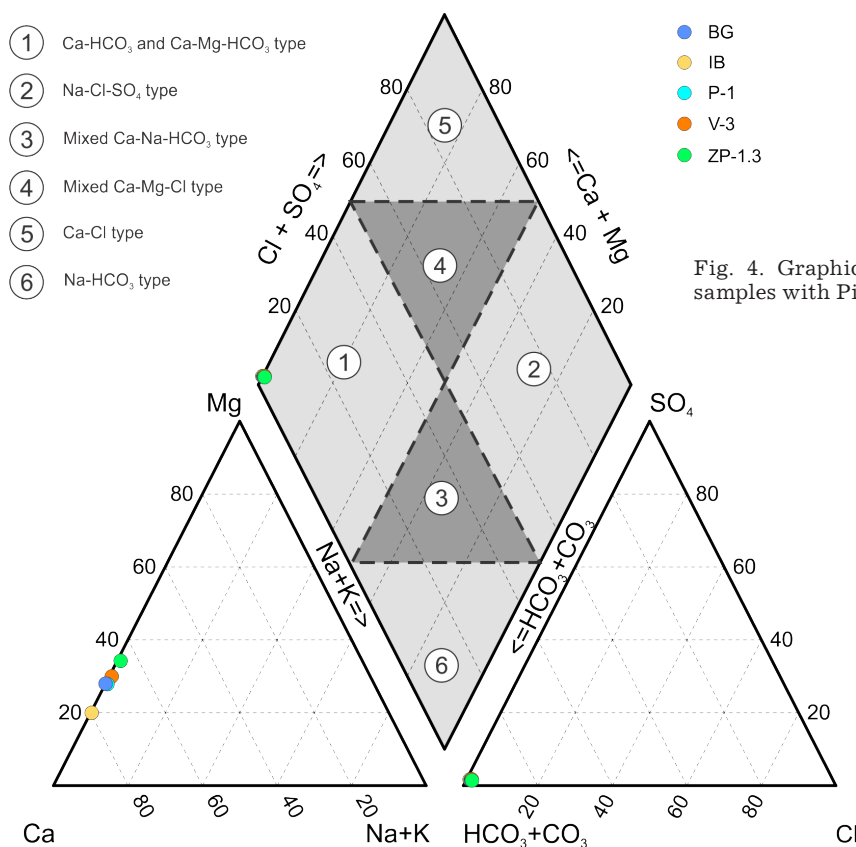


Fig. 4. Graphical analysis of water samples with Piper diagram.

Water at all other sampling points (ZP-1.3, V-3 in P-1) is unsaturated with respect to calcite and dolomite, since  $SI_{\text{calcite}}$  and  $SI_{\text{dolomite}}$  are both negative ( $SI < 0$ ) except BG, where  $SI_{\text{calcite}}$  is approx. zero. The latter shows that minerals may not be reacting at all or may be reacting reversibly, in which case the mineral could be dissolving or precipitating (Appelo and Postma, 2005). The surface water at sampling point V-3 is highly unsaturated with respect to very low  $SI_{\text{dolomite}}$  values, where also the lowest pH value (7.2) is observed. In this case the mineral might dissolve very slowly or not at all, depending on the kinetics of the reaction (Appelo and Postma, 2005).

The measured concentrations of other basic chemical parameters are low and do not indicate significant pollution of groundwater and surface water. Nitrate concentrations ( $\text{NO}_3^-$ ) in groundwater are below 1.95 mg/L, which is below the expected natural background (5 mg/L) (Serianz et al., 2020a). Sulphate concentrations ( $\text{SO}_4^{2-}$ ) range from 0.76 to 1.40 mg/L and chloride concentrations ( $\text{Cl}^-$ ) range from 0.21 to 0.30 mg/L. No major differences between the sampling point of the Peričnik catchment (ZP-1.3) and surface water or springs were detected.

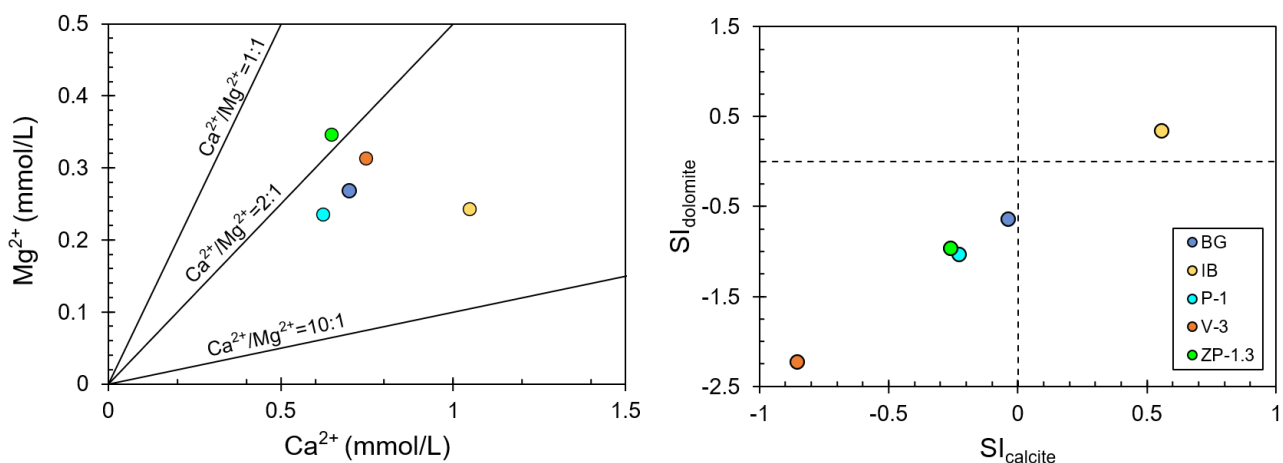


Fig. 5. Scatter plots of a)  $\text{Mg}^{2+}$  (mmol/L) versus  $\text{Ca}^{2+}$  (mmol/L) and b)  $SI_{\text{calcite}}$  versus  $SI_{\text{dolomite}}$ .

Table 1. Sampling locations and results for both sampling campaigns.

Location	Type	Y	X	Z	Sampling date [m a.s.l.]	Q	T	EC	pH	TDS	HCO <sub>3</sub> <sup>-</sup>	Ca <sup>2+</sup>	K <sup>+</sup>	Cl <sup>-</sup>	Mg <sup>2+</sup>	Na <sup>+</sup>	NO <sub>3</sub> <sup>-</sup>	SO <sub>4</sub> <sup>2-</sup>	H <sup>3</sup>	$\delta^{18}\text{O}$	$\delta^2\text{H}$		
					L/s	°C	µS/cm	/	mg/L	mg/L								TU	% <sub>60</sub>	±% <sub>60</sub>	% <sub>60</sub>	±% <sub>60</sub>	
ZP-1.3	Spring	415829	144526	742.8	10.04.2020	6.0	192	8.0										-10.35	0.01	-69.6	0.2		
V-2	River	414188	143357	841.9	10.04.2020	9	5.9	146	8.2									-9.69	0.00	-64.7	0.3		
V-3	River	415512	144356	751.7	10.04.2020	646	6.8	125	8.3									-10.33	0.03	-69.4	0.3		
BG	River	415744	144530	739.0	10.04.2020	762	5.7	188	8.3									-10.40	0.01	-69.8	/		
V-4	River	415971	144767	731.3	10.04.2020	717	7.2	126	8.4									-10.36	0.01	-69.8	0.4		
M-1	River	418536	146392	653.6	10.04.2020	1,400	6.5	125	8.3									-10.47	0.02	-69.8	0.1		
V-5	River	419014	146891	645.8	10.04.2020	1,450	8.3	133	8.4									-10.38	0.01	-70.5	0.1		
P-1	River	415514	144365	752.0	10.04.2020	7.9	110	8.3										-10.69	0.02	-72.5	0.3		
S-1	Spring	418152	145795	678.6	10.04.2020	8.1	195	8.4										-9.93	0.02	-66.8	0.2		
MS-1	Spring	422985	134545	1,216.4	10.04.2020	4.8	167	7.7										-10.07	0.01	-66.6	0.2		
ZP-1.3	Spring	415829	144526	742.8	22.05.2020	6.1	187	7.9	153.5	124	26	0.09	0.23	8.4	0.23	1.95	1.40	3.56	-10.30	0.00	-69.8	0.1	
IB	Spring	412407	141984	945.0	22.05.2020	8.0	234	8.4	211.0	160	42	0.18	0.30	5.9	0.32	1.58	0.76	4.49	-9.69	0.00	-65.7	0.7	
V-2	River	414188	143357	841.9	22.05.2020	200	9.5	201	8.3									-9.97	0.00	-67.2	0.1		
V-3	River	415512	144356	751.7	22.05.2020	1,060	7.7	192	7.2	137.5	129	30	0.10	0.24	7.6	0.29	1.60	1.22		-10.18	0.01	-68.5	0.7
BG	River	415744	144530	739.0	22.05.2020	2,250	7.3	173	8.1	170.1	116	28	0.04	0.23	6.5	0.21	1.49	1.07	5.42	-10.52	0.00	-70.9	0.2
V-4	River	415971	144767	731.3	22.05.2020	2,160	7.2	174	7.8									-10.49	0.02	-70.8	0.0		
M-1	River	418536	146392	653.6	22.05.2020	3,480	8.3	178	7.8									-10.51	0.00	-71.3	0.0		
V-5	River	419014	146891	645.8	22.05.2020	3,500	8.0	181	8.0								-10.49	0.02	-70.8	0.3			
P-1	River	415514	144365	752.0	22.05.2020	7.2	153	8.0	162.3	104	25	0.04	0.21	5.7	0.23	1.41	0.89		-10.93	0.02	-73.3	0.3	
S-1	Spring	418152	145795	678.6	22.05.2020	8.5	276	8.0										-9.96	0.01	-67.4	0.1		
MS-1	Spring	422985	134545	1,216.4	22.05.2020	5.5	170	8.3										-9.55	0.03	-63.1	0.3		

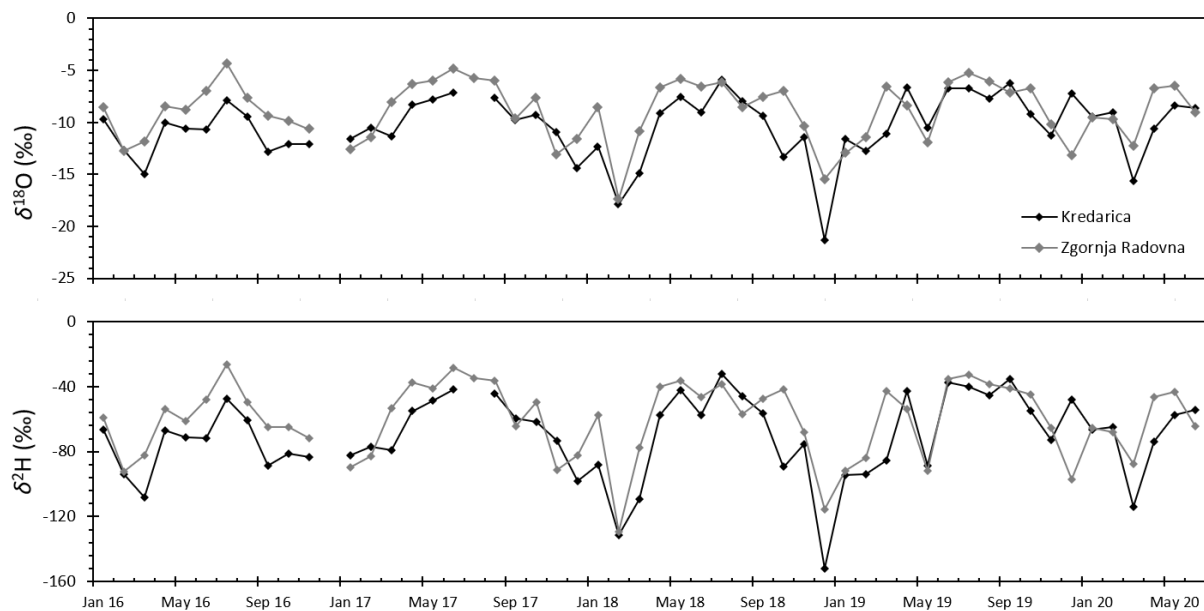


Fig. 6. Isotopic composition of precipitation at the Zgornja Radovna and Kredarica meteorological stations for the period 2016–2020.

## Stable isotopes

### $\delta^{18}\text{O}$ and $\delta^2\text{H}$ in precipitation

The lowest isotopic precipitation values can be observed at the Kredarica meteorological station. The average unweighted values for the observation period 2016–2020 are  $-10.4\text{ ‰}$ , and  $-70.5\text{ ‰}$  for  $\delta^{18}\text{O}$  and  $\delta^2\text{H}$ , respectively. The lowest value was determined in December 2018 and corresponds to the snow precipitation sample. At the Zgornja Radovna meteorological station the average unweighted values for the observation period 2016–2020 are  $-8.9\text{ ‰}$  and  $-60.7\text{ ‰}$  for  $\delta^{18}\text{O}$  and  $\delta^2\text{H}$ , respectively. The average isotopic composition of snow at the Kredarica meteorological station was determined to be  $-13.5\text{ ‰}$  for  $\delta^{18}\text{O}$  and  $-98.1\text{ ‰}$  for  $\delta^2\text{H}$ . Slightly more positive values were observed at Zgornja Radovna:  $-12.1\text{ ‰}$  for  $\delta^{18}\text{O}$ , and  $-87.1\text{ ‰}$  for  $\delta^2\text{H}$ .

The altitude effect was calculated for the two selected meteorological stations – Kredarica and Zgornja Radovna – separately, for total precipitation and for months when snow prevails in the monthly composite sample. These were selected based on a comparison of stable isotope data (Fig. 6) and meteorological parameters (days with snow/rain, amount of precipitation, snow

cover thickness, etc.). It was estimated that the altitude effect in precipitation is  $-0.8\text{ ‰ } \delta^{18}\text{O}/\text{km}$ . This value is in good agreement with the estimated altitude effect based on spring water  $\delta^{18}\text{O}$  values ( $-1.1\text{ ‰ } \delta^{18}\text{O}/\text{km}$ ) in the Radovna River valley in NW Slovenia (Torkar et al., 2016) and ( $-1\text{ ‰ } \delta^{18}\text{O}/\text{km}$ ) in Lake Bled and surroundings (Seriánz et al., 2020b).

### Isotopic composition of water samples

Values for  $\delta^{18}\text{O}$ ,  $\delta^2\text{H}$  and  ${}^3\text{H}$  are presented in Table 1. Values for  $\delta^{18}\text{O}$  in all water samples are between  $-10.9\text{ ‰}$  and  $-9.6\text{ ‰}$ . In general,  $\delta^{18}\text{O}$  values were lower in the second sampling campaign (Fig. 8). Excluding location IB, the differences between both campaigns range from  $0.03\text{ ‰}$  at S-1 up to  $0.5\text{ ‰}$  at MS-1. The first sampling at MS-1 was performed when there was still approx. 50 cm of snowpack in the recharge area, while during the second sampling the snowpack had already melted. The values for  $\delta^2\text{H}$  in all water samples are between  $-73.3\text{ ‰}$  and  $-63.1\text{ ‰}$ .  $\delta^2\text{H}$  values are also lower in the second sampling campaign. Excluding location IB, the differences between both campaigns range from  $0.3\text{ ‰}$  at V-5 up to  $3.5\text{ ‰}$  at MS-1. The results of  $\delta^{18}\text{O}$  and  $\delta^2\text{H}$  measurements in groundwater and surface

Table 2: Altitude effect for snow and total precipitation calculated based on samples from Kredarica and Zgornja Radovna meteorological stations.

Parameter	Equation	Slope ‰/1 km
$\delta^{18}\text{O}_{\text{total}}$	$Y = -0.0008x - 8.272$	-0.8
$\delta^{18}\text{O}_{\text{snow}}$	$Y = -0.0008x - 11.561$	-0.8
$\delta^2\text{H}_{\text{total}}$	$Y = -0.0056x - 56.426$	-5.6
$\delta^2\text{H}_{\text{snow}}$	$Y = -0.0062x - 82.379$	-6.2

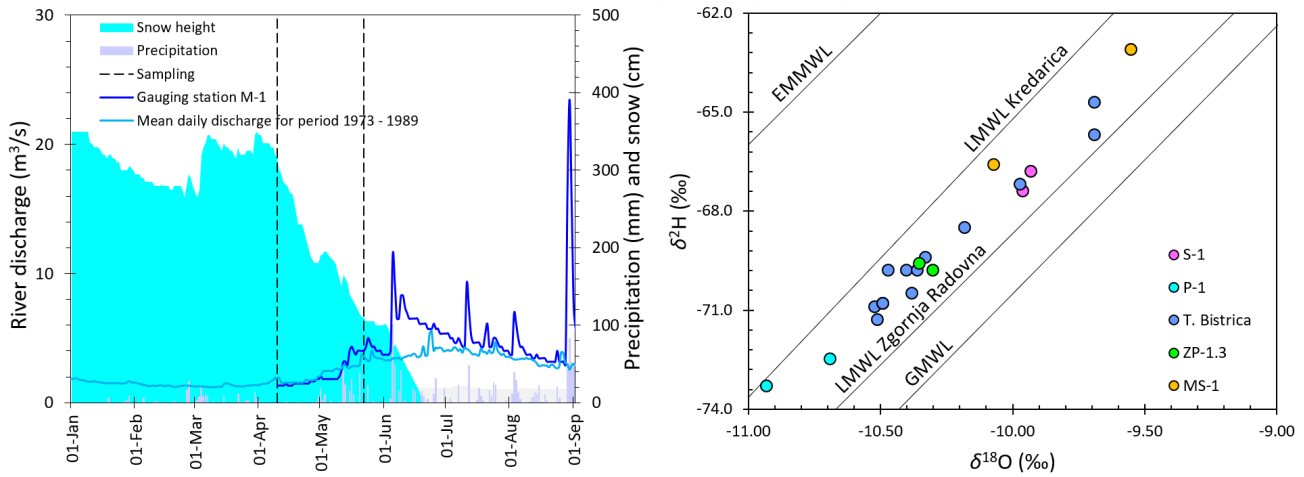


Fig. 7: Meteorological parameters during sampling (left) and the results of stable isotope analysis, together with Global Meteoric Water Line (GMWL) and East Mediterranean Meteoric Water Line (EMMWL)(right).

water are shown in Figure 7b, as compared to the global meteoric line (GMWL) (Craig, 1961). The results show that all water samples are located between LMWLs for Kredarica and Zgornja Radovna.

The isotopic composition also allows us to estimate the mean recharge altitude of the groundwater, namely in conditions where we have reference locations with a known isotopic composition and a correspondingly small recharge area, for which we can estimate the average altitude. As follows from previous research in a wider area (Torkar, 2016; Serianz et al., 2020b),  $\delta^{18}\text{O}$  is particularly suitable for a relevant assessment, and  $\delta^2\text{H}$  yields inapplicable results (indicates higher altitudes than in nature). In the given case, we used the spring Mrzli studenec (MS-1) in Pokljuka (approx. 12 km air distance from the Triglavská Bistrica) and the spring "Na Skedenjcih" (S-1, Fig. 1) as the reference location. Stable isotope analysis has been performed on the MS-1 spring in the past, as this spring, according to the data

available so far from the wider area, represents one of the highest-lying springs with a constant flow and a small drainage area (Serianz et al., 2020b).

Based on the isotopic composition it is also possible to estimate the mean recharge area of a given water sample using the simple linear relationship between the representative water sample with known recharge altitude and isotopic composition. In this case two springs were selected, MS-1 and S-1, based on the assumption that the isotopic signature of spring water is due to the small catchment area equal to the isotopic signature of precipitation at the corresponding altitude. The results, however, suggest only spring MS-1 is appropriate for such hypothesis, while spring S-1 was not appropriate for consideration. Therefore, an alternative approach was used, accounting for average  $\delta^{18}\text{O}$  from both sampling campaigns and a calculated precipitation altitude effect of  $-0.8 \text{ \textperthousand } \delta^{18}\text{O}/\text{km}$ . The results show that the Triglavská Bistrica spring area

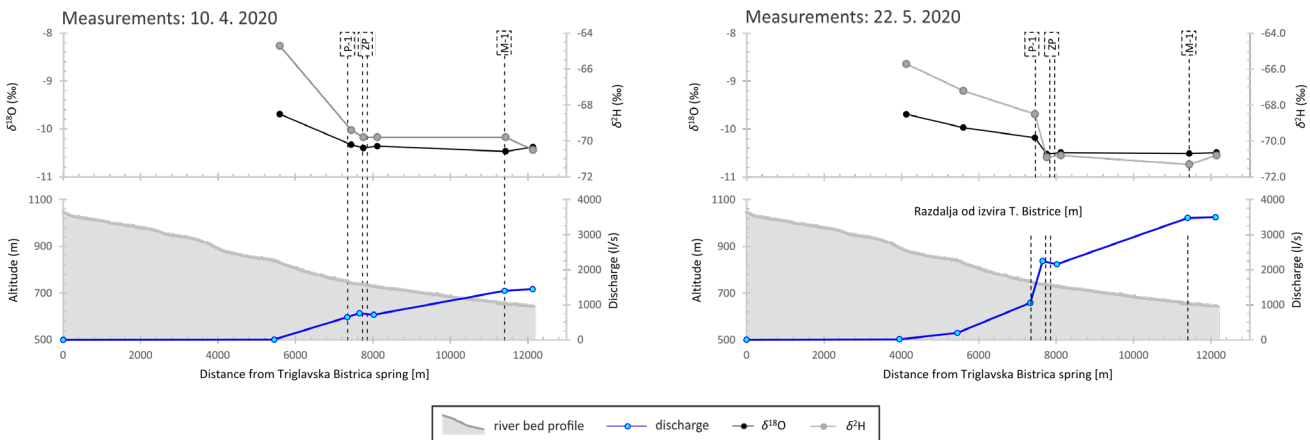


Fig. 8. Graphical analysis of stable isotope analysis.

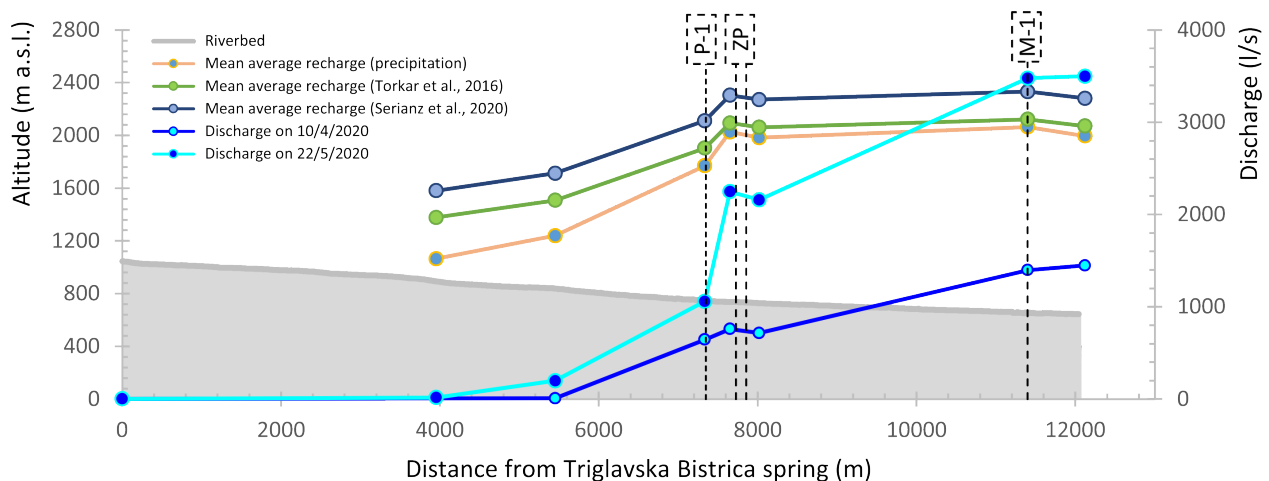


Fig. 9. Hydrogeological parameters of Triglavská Bistrica.

is of local recharge component, while with the distance downstream the regional groundwater recharge component is much more significant (Fig. 9). At the sampling location V-5, which is approx. 300 m upstream from the Sava Dolinka confluence, the average recharge altitude is estimated at 1,996 m a.s.l. (Fig. 9). Mean average recharge is even higher in the case of linear models from literature (Torkar et al., 2016; Serianz et al., 2020b). The calculated mean recharge altitude of the Triglavská Bistrica at its discharge into the Sava Dolinka was evaluated based on a Digital elevation model and was determined as approx. 1,500 m a.s.l.

All water samples analysed for tritium activity concentration can be classified as recent waters (Mezga, 2014). According to the  ${}^3\text{H}$  results in the groundwater in the Peričnik catchment (3.5 TU), it is evident that the lower tritium activity concentration is due to the lower than expected values of tritium, which are characteristic for snow precipitation (Vreča et al., 2013). The recharge area of the Peričnik stream is represented by a high-altitude karstic-fissured aquifer, where dolomite predominates over limestone. As a result, such an aquifer has a higher storage capacity, which is reflected in a longer retention time. Sampling points at Triglavská Bistrica BG and IB, which are located upstream from the Peričnik stream and recharge from both an intermediate flow component in the karstic-fissured aquifer and local flow components in Quaternary aquifers, show slightly higher tritium activities (5.4 TU and 4.5 TU, respectively). For a reliable estimation of retention times, systematic long-term observation of the geochemical and isotope characteristics of all water components (i.e. precipitation, snow, surface- and ground-water) is crucial.

## Conclusions

The hydrogeochemistry of the Triglavská Bistrica is determined by the prevalence of  $\text{Ca}^{2+}$  and  $\text{Mg}^{2+}$  cations and  $\text{HCO}_3^-$  anions. The hydrogeochemical water types are Ca-Mg-HCO<sub>3</sub> and Ca-HCO<sub>3</sub>, suggesting dolomite and limestone in the recharge area. The spatial variations in water carbonate chemistry along the valley are attributed to different lithologies. That means that the recharge area of the Triglavská Bistrica spring is an aquifer or aquifer system dominated by limestone, while other waters downstream are characterized by the fact that they are mainly fed by aquifers dominated by dolomite over limestone. Analysis of the pH and major ions indicate that the water is alkaline and that carbonate weathering as a process dominates in the recharge area. Other major ions are present in low concentrations and within natural background levels.

The  $\delta^{18}\text{O}$  and  $\delta^{2\text{H}}$  values decrease along the Triglavská Bistrica valley, which means that the mean altitude of the recharge area increases downstream. At the spring, where lower altitude recharge prevails, the groundwater is enriched with  ${}^{18}\text{O}$ , while at the downstream locations groundwater becomes increasingly depleted in  ${}^{18}\text{O}$  due to the increasing impact of snow melt water infiltrated at higher altitudes. The mean recharge altitude area of the Triglavská Bistrica River was estimated at approx. 1,996 m a.s.l. at sampling point V-5, located approx. 12 km downstream from the spring. The concentrations of tritium activity in groundwater correspond to natural processes related to precipitation. However, a more precise analysis of the residence time would require a systematic series of measurements over many years.

The results of this study provide important and useful new information about the hydrogeological characteristics of the recharge area of the Triglavská Bistrica, allowing researchers to compare and define groundwater recharge areas in similar hydrogeological systems. We expect the results of this study could also be used as a basis for different hydrological and hydrogeological studies, where water sources need to be investigated. The Triglavská Bistrica catchment is highly important as a source of drinking water, as it also represents the recharge of the Peričnik spring, which itself is an important water resource for part of the municipality of Jesenice. Therefore, it is very important to understand the dynamics of the different flow components in the studied aquifer system. In view of constant climatic changes, especially increasing air temperature, increasingly shorter snow periods of snow cover, and changing water infiltration, this important resource should be carefully monitored now and in the future.

### Acknowledgments

The authors would like to thank the Municipality of Jesenice for financial support. Part of this research was also funded by the Slovenian Research Agency (ARRS) in the frame of the young researcher programme and research programmes "Groundwater and Geochemistry" (No. P1-0020) of the Geological Survey of Slovenia and "Cycling of substances in the environment, mass balances, modelling of environmental processes, and risk assessment" (P1-0143) of the Jožef Stefan Institute.

### References

- Appelo, C A J. & Postma, D. 2005: Geochemistry, groundwater and pollution. 2nd edition. Rotterdam, Balkema.
- Avak, H. & Brand, W.A. 1995: The finning MAT HDO-equilibration-A fully automated  $\text{H}_2\text{O}$ /gas phase equilibration system for hydrogen and oxygen isotope analyses. Thermo Electron. Corp. Appl. News, 11: 1–13.
- Brenčič, M. & Poltnig, W. 2008: Groundwater Karavanke: hidden wealth. Ljubljana and Graz: Geological Survey of Slovenia & Joanneum Research Forschungsgesellschaft, Report.
- Brenčič, M. & Vreča, P. 2016: Hydrogeological and isotope mapping of the karstic River Savica in NW Slovenia. Environ. Earth Sci, 75(65). <https://doi.org/10.1007/s12665-016-5479-7>
- Carey, S. K. & Quinton, W. L. 2005: Evaluating runoff generation during summer using hydrometric, stable isotope and hydrochemical methods in a discontinuous permafrost alpine catchment. *Hydrological Processes: An International Journal*, 19/1: 95–114.
- Cerar, S., Mezga, K., Žibret, G., Urbanc, J. & Komac, M. 2018: Comparison of prediction methods for oxygen-18 isotope composition in shallow groundwater. *Science of the Total Environment*, 631–632: 358–368. <https://doi.org/10.1016/j.scitotenv.2018.03.033>
- Clark, I. & Fritz, P. 1997: Environmental Isotopes in Hydrogeology. CRC Press: New York: 328 p.
- Coplen, T., Wildman, J. & Chen, J. 1991: Improvements in the gaseous hydrogen-water equilibration technique for hydrogen isotope ratio analysis. *Analytical Chemistry*, 63: 910–912.
- Craig, H. 1961: Isotope variations in meteoric waters. *Science*, 133/3465: 1702–1703.
- Dansgaard, W. 1964: Stable isotopes in precipitation. *Tellus*, 16: 436–468.
- Epstein, S. & Mayeda, T. 1953: Variations of  $^{18}\text{O}$  content of waters from natural sources. *Geochimica et Cosmochimica Acta*, 4: 213–224.
- Gat, J.R. & Carmi, I. 1970: Evolution of the isotopic composition of atmospheric waters in the Mediterranean Sea area. *Journal of Geophysical Research*, 75: 3039–3048. <https://doi.org/10.1029/JC075i015p03039>
- Gonfiantini, R., Roche, M.-A., Olivry, J.-C., Fontes, J.-C. & Zuppi, G.M. 2001: The altitude effect on the isotopic composition of tropical rains. *Chemical Geology*, 181: 147–167.
- Hanna instruments. Instruction manual: HI98194, HI98195, HI98196 Multiparameter Meters pH/mV, ORP, EC, TDS, Resistivity, Salinity, Seawater, Dissolved Oxygen, Atmospheric Pressure and Temperature, 2020a. (16. 7. 2020).
- Horvatinčić, N., Krajcar Bronić, I., Barešić, J., Obelić, B. & Vidić, S. 2005: Tritium and stable isotope distribution in the atmosphere at the coastal region of Croatia. In: Final report of a coordinated research project 2000–2004 (IAEA-TECDOC Series No. 1453) – Isotopic Composition of Precipitation in the Mediterranean Basin in Relation to Air Circulation Patterns and Climate). Vienna (AU) IAEA, 37–50.
- Hrvatin, M. 1998: Pretočni režimi v Sloveniji. *Geografski zbornik*, 38: 59–87.

- Nadbath, M. 2014: Meteorološka postaja Kredarica. Naše okolje. Internet: <https://meteo.arso.gov.si/uploads/probase/www/climate/text/sl/stations/kredarica.pdf> (15.9.2021)
- Jurkovšek, B. 1987: Osnovna geološka karta SFRJ, 1:100.000. Tolmač listov Beljak (Villach) in Ponteba: L 33-51, L 33-52. Zvezni geološki zavod. Beograd: 58 p.
- Kanduč, T., Mori, N., Kocman, D., Stibilj, V. & Grassa, F. 2012: Hydrogeochemistry of Alpine springs from North Slovenia: insights from stable isotopes. *Chemical Geology*, 300–301: 40–54.
- Katz, B.G. 1998: Using  $\delta^{18}\text{O}$  and  $\delta\text{D}$  to Quantify Ground-Water/Surface-Water Interactions in Karst Systems of Florida. In: National Water Quality Monitoring Council Conference: Critical Foundations to Protect Our Waters. Reno, Nevada. U.S. Environmental Protection Agency, Washington D.C.
- Kern, Z., Hatvani, I.G., Czuppon, G., Fórizs, I., Erdélyi, D., Kanduč, T., Palcsu, L. & Vreča, P. 2020: Isotopic ‘Altitude’ and ‘Continental’ Effects in Modern Precipitation across the Adriatic–Pannonian Region. *Water*, 12/6:1797. <https://doi.org/10.3390/w12061797>
- Kralik, M., Papesch, W. & Stichler, W. 2003: Austrian Network of Isotopes in Precipitation (ANIP): Quality assurance and climatological phenomenon in one of the oldest and densest networks in the world. In: IAEA. Isotope Hydrology and Integrated Water Resources Management. Proceedings; 2003 May 19–13; Vienna (AU): International Atomic Energy Agency and the International Association of Hydrogeologists in cooperation with the International Association of Hydrological Sciences, 146–149.
- Longinelli, A. & Selmo, E. 2003: Isotopic composition of precipitation in Italy: a first overall map. *Journal of Hydrology*, 270/1-2: 75–88.
- Mayo, L. & Loucks, M.D. 1995: Solute and isotopic geochemistry and ground water flow in the central Wasatch Range, Utah. *Journal of Hydrology*, 172: 31–59.
- Mezga, K., Urbanc, J. & Cerar, S. 2013: The isotope altitude effect reflected in groundwater: a case study from Slovenia. *Isotopes in environmental and health studies*, 50/1: 33–51. <https://doi.org/10.1080/10256016.2013.826213>
- Mezga, K. 2014: Natural hydrochemical background and dynamics of groundwater in Slovenia: doctoral dissertation. Nova Gorica: 226 p.
- Piper, A.M. 1944: A graphic procedure in the geochemical interpretation of water-analyses. *Eos, Transactions American Geophysical Union*, 25/6: 914–928.
- Poage, M.A. & Chamberlain, C.P. 2001: Empirical Relationships Between Elevation and the Stable Isotope Composition of Precipitation and Surface Waters: Considerations for Studies of Paleoelevation Change. *American Journal of Science*, 301: 1–15.
- Serianz, L. 2016: Tri-dimensional Model of the Radovna Glacier from the Last Glacial Period. *Geologija*, 59/2: 193–204. <https://doi.org/10.5474/geologija.2016.011>
- Serianz, L., Cerar & S., Šraj, M. 2020a. Hydrogeochemical characterization and determination of natural background levels (NBL) in groundwater within the main lithological units in Slovenia. *Environmental Earth Sciences*, 79: 373 <https://doi.org/10.1007/s12665-020-09112-1>
- Serianz, L., Rman, N. & Brenčič, M. 2020b: Hydrogeochemical Characterization of a Warm Spring System in a Carbonate Mountain Range of the Eastern Julian Alps, Slovenia. *Water*, 12/7/5: 1427. <https://doi.org/10.3390/w12051427>
- Shamsi, A., Karami, G. H., Hunkeler, D. & Taheri, A. 2019: Isotopic and hydrogeochemical evaluation of springs discharging from high-elevation karst aquifers in Lar National Park, northern Iran. *Hydrogeology Journal*, 27/2: 655–667. <https://doi.org/10.1007/s10040-018-1873-4>
- Smolar-Žvanut, N., Mikoš, M. & Breznik, B. 2005: The impact of the dam in the Bistrica River on the aquatic ecosystem. *Acta Hydrotechnica*, 23/39: 99–115.
- SIST ISO 5667-03:1996. Water quality, sampling – part 3: instructions for storage and handling of samples.
- SIST ISO 5667-11:1996. Water quality, sampling – part 11: guidance on sampling of groundwater, 1–10.
- SIST ISO 5667-6:1996. Water quality, sampling – part 6: guidance on sampling of rivers and water courses.
- Thiébaut, E., Dzikowski, M., Gasquet, D. & Renac, D. 2010: Reconstruction of groundwater flows and chemical water evolution in an amagmatic hydrothermal system (La Léchère, French Alps). *Journal of Hydrology*, 381/3–4, 15, 189–202.
- Torkar, A., Brenčič, M. & Vreča, P. 2016: Chemical and isotopic characteristics of groundwater-dominated Radovna River (NW Slovenia). *Environ. Earth Sci.*, 75: 1296–1314.

- Vreča, P. & Malenšek, N. 2016: Slovenian Network of Isotopes in Precipitation (SLONIP) - a review of activities in the period 1981–2015 = Slovenska mreža opazovanj izotopske sestave padavin (SLONIP) - pregled aktivnosti v obdobju 1981–2015. *Geologija*, 59: 67–83. <https://doi.org/10.5474/geologija.2016.004>
- Vreča, P., Krajcar Bronič, I., Horvatinčić, N. & Barešić, J. 2006: Isotopic characteristics of precipitation in Slovenia and Croatia: comparison of continental and maritime stations. *Journal of Hydrology* 330/3-4: 457–469. <https://doi.org/10.1016/j.jhydrol.2006.04.005>
- Vreča, P., Krajcar Bronič, I., Leis, A. & Brenčić, M. 2008: Isotopic composition of precipitation in Ljubljana (Slovenia). *Geologija*, 51/2:169–180. <https://doi.org/10.5474/geologija.2008.018>
- Vreča, P., Brenčić, M., Sinjur, I., Vertačnik, G., Volk, B. M., Ortar, J., Torkar, A., Stibilj, V. & Pavšek, M. 2013: Izotopska sestava padavin in snega na območju Julijskih Alp in Karavank. *Raziskave s področja geodezije in geofizike* 2012: 17–25.
- Vreča, P., Krajcar Bronič, I., Leis, A. & Demšar, M. 2014: Isotopic composition of precipitation at the station Ljubljana (Reaktor), Slovenia – period 2007–2010. *Geologija*, 57/2: 217–230. <https://doi.org/10.5474/geologija.2014.019>
- Internet sources:
- Internet 1: Archive of weather observations. Slovenian Environment Agency. Internet: <http://meteo.ars.si> (1. 3. 2021).
- Internet 2: Archive of hydrological data. Slovenian Environment Agency. Internet: <http://vode.ars.si/hidarhiv> (5. 2. 2021).
- Internet 3: <https://jeko.si/vodovod-pericnik-2> (1. 9. 2021)
- Internet 4: <https://slonip.ijs.si/> (7. 8. 2021)



# The Sistiana Fault and the Sistiana Bending Zone (SW Slovenia)

## Sesljanski prelom in sesljanska upogibna cona

Ladislav PLACER, Petra JAMŠEK RUPNIK & <sup>†</sup>Bogomir CELARC

Geološki zavod Slovenije, Dimičeva ul. 14, SI-1000 Ljubljana, Slovenija;  
e-mail: ladislav.placer@telemach.net; petra.jamsek-rupnik@geo-zs.si;

Prejeto / Received 27. 9. 2021; Sprejeto / Accepted 24.11. 2021; Objavljeno na spletu / Published online 28. 12. 2021

**Key words:** Sistiana Fault, Sistiana Bending Zone, adjusting fault, Adria Microplate, Gulf of Trieste

**Ključne besede:** Sesljanski prelom, sesljanska upogibna cona, izravnalni prelom, Jadranska mikroplošča, Tržaški zaliv

### Abstract

The Sistiana Fault is an alleged disjunctive deformation of Microadria in the sea bottom of the Gulf of Trieste. Onshore, it is visible only in the Sistiana Bay, but towards the northeast it soon pinches-out, in structural-geometric terms it diminishes soon after the crossing of the thrust boundary of the Dinarides, or the Istrian-Friuli Underthrustig Zone, respectively. Further to the northeast, only the bending zone is developed in the External Dinarides, which stretches all the way from the Sistiana Bay to the Idrija-Žiri area. We named it the Sistiana Bending Zone. Its direction can be determined based on geological maps and is around 60°, so we conclude that the Sistiana Fault should extend approximately in this direction. In the bending zone, the Trieste-Komen Anticlinorium, the Vipava Synclinorium, the Trnovo Nappe opposite to the Hrušica Nappe and the Raša and Idrija Faults are laterally bent. The size of the bend is the largest in the Sistiana Bay, and in the east-northeast direction it decreases linearly. The general geological circumstances suggest that the Sistiana Fault has not been recently active.

### Izvleček

Sesljanski prelom je domnevna disjunktivna deformacija Mikroadrije v podmorju Tržaškega zaliva. Na površju je viden le v Sesljanskem zalivu, vendar se proti severovzhodu kmalu izklini, v strukturno-geometrijskem smislu izzveni kmalu zatem, ko preseka narivno mejo Dinaridov, oziroma istrsko-furlansko podrivo cono. Naprej proti severovzhodu je v Zunanjih Dinaridih razvita le še upogibna cona, ki se vleče vse od Sesljanskega zaliva do idrijsko-žirovskega ozemlja. Imenujemo jo sesljanska upogibna cona. Njena smer je določljiva na podlagi podatkov geoloških kart in znaša okoli 60°, zato sklepamo, da naj bi Sesljanski prelom potekal približno v tej smeri. V upogibni coni so bočno upognjeni Tržaško-Komenski antiklinorij, Vipavski sinklinorij, Trnovski pokrov nasproti Hruščkemu pokrovu ter Raški in Idrijski prelom. Velikost upogiba je največja v Sesljanskem zalivu, proti vzhodu-severovzhodu pa se linearно manjša. Iz splošne geološke slike izhaja domneva, da Sesljanski prelom recentno ni aktiven.

### Introduction

The plicative and disjunctive structures in the northwestern part of the External Dinarides in the hinterland of the Gulf of Trieste and Istra Peninsula are curved in the northwest direction (Fig. 1). This deformation was the result of the movement of the Adria Microplate Structural Block (Microadria) between the left-lateral strike-slip Sistiana Fault and the right-lateral strike-slip Kvarner Fault toward the Dinarides (Placer et al., 2010). This structural block was called the Istra Block, while the vast deformed hinterland area of

### Uvod

V severozahodnem delu Zunanjih Dinaridov so plikativne in disjunktivne strukture v zaledju Tržaškega zaliva in polotoka Istre izbočene proti severovzhodu (sl. 1). Po Placerju in sodelavcih (2010) je deformacijo povzročilo premikanje strukturnega bloka Jadranske mikroplošče (Mikroadrije) med Sesljanskim in Kvarnerskim prelomom proti Dinaridom. Prvi naj bi bil levovzmični, drugi desnozmični. Blok so poimenovali istrski blok, obsežno deformirano območje Dinaridov v zaledju pa istrsko potisno območje.

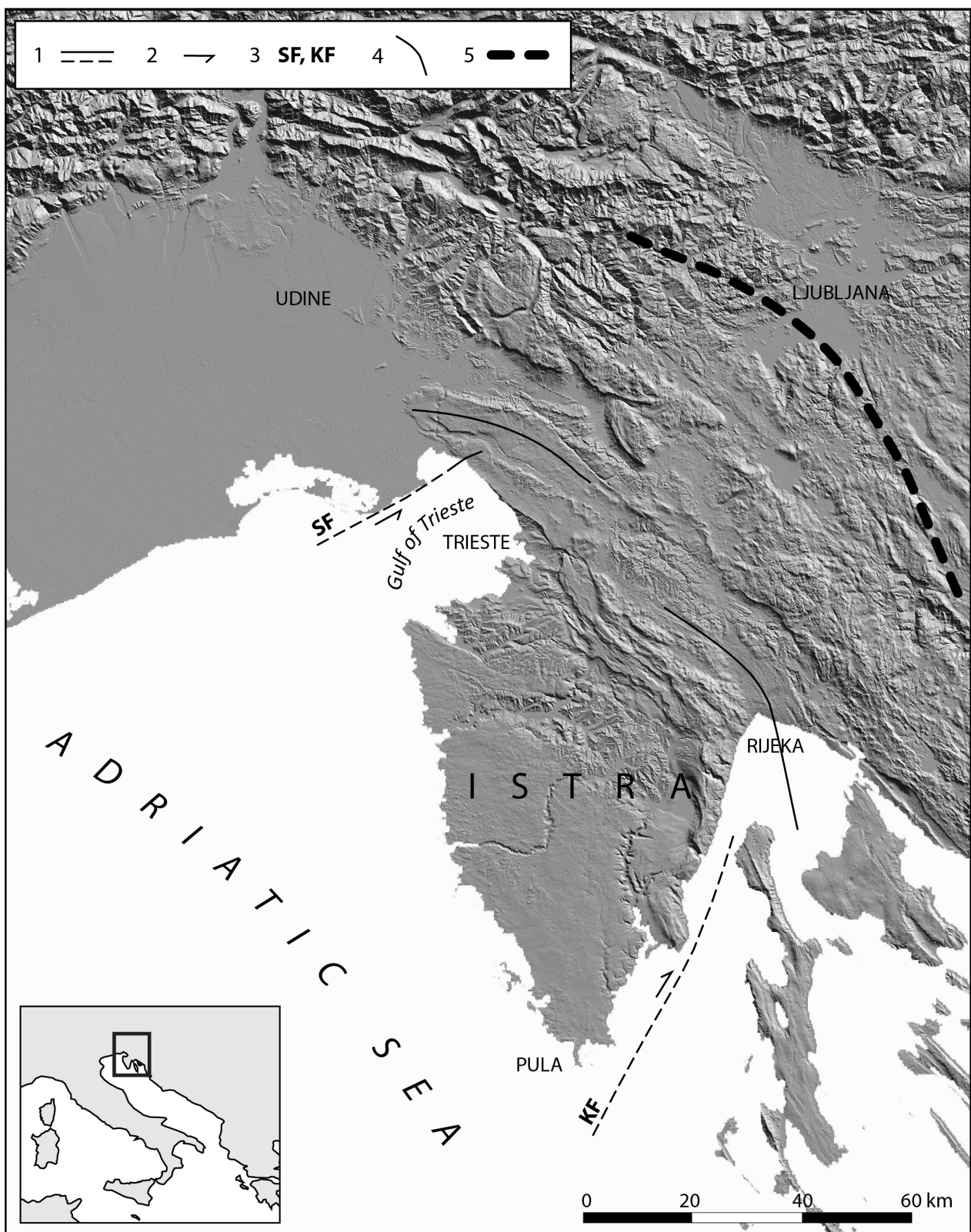


Fig. 1. Istra Pushed Area.

Sl. 1. Istrsko potisno območje.

1 Fault: proven, inferred / prelom: ugotovljen, domneven

2 Relative direction of the fault block displacement / relativna smer premika prelomnega krila

3 SF – Sistiana Fault / Sesljanski prelom, KF – Kvarner Fault / Kvarnerski prelom

4 Laterally bent structures of Dinarides / bočno upognjene strukture Dinaridov

5 Approximate boundaries of the Istra Pushed Area effects / približna meja vidnih učinkov istrskega potisnega območja

the Dinarides was named the Istra Pushed Area. While the exact direction of the block's movement has not yet been established, it could be assumed, in view of the recent orientation of Microadria, that the block traveled in a northeasterly to easterly direction. While this was a multiphase event, details of the exact timing of such have not yet been determined.

Northwest of the Sistiana Fault, along with the Istra Block, also the Friuli Block was displaced toward the Dinarides, but not to such an extent as the Istra Block, owing to the geometry of the displacements. Consequently, the Istra Block was the northeastern-most displaced part of Microadria.

The theory of underthrusting and pushing against the Dinarides (Placer et al., 2010) is based on analysis of existing geological maps and field investigations. The Čičarija and Trieste-Komen Anticlinorioum formed mainly as the result of Dinaric thrusting, while its lateral deformation developed later, definitely during the pushing of the Istra Block against the Dinarides. Underthrusting was the extreme expression and consequence of these movements, while the entire area experienced a multiphase contraction in the form of folding and displacements along secondary reverse faults.

Blašković & Aljinović (1981) and Blašković (1991) already discussed this pushing toward the Dinarides in the Istra and Kvarner areas. Carulli & Cucchi (1991) first described the Sistiana Fault in the Sistiana Bay northwest of Trieste. Later, different aspects of it were investigated by Carulli (2006, 2011), Busetti et al. (2010), Placer et al. (2010), Cucchi & Piano (2013), Placer (2015) and others. It was discovered that it pinches out after a few kilometers from the shore inland, in the NE direction, while in the offshore direction it continues below the sea-bottom towards the southwest. In the northeast, in the direction of the fault's apparent continuation, there are laterally-bent Dinaric structures. Their axis of bending could be approximately determined, therefore Placer et al. (2010, Fig. 27) introduced the term Sistiana Zone and established its direction. Displacements along the Sistiana Fault were determined as a left-lateral strike-slip based on the position of the bent structures.

In eastern Istria, opposite the Sistiana Zone, we find bent structures in a mirrored configuration that are probably connected with the supposed Kvarner Fault in the SSW-NNE direction. The direction and position of the bent structures can be determined in the same way as they can for the Sistiana Zone, although the axis of bending is

Natančnejša smer premika bloka še ni določena, vsekakor pa se je, glede na današnjo orientacijo Mikroadrije, pomaknil proti severovzhodu do vzhodu. Dogajanje je bilo večfazno, pričetek še ni natančneje ugotovljen.

Poleg istrskega bloka naj bi bil proti Dinaridom pomaknjen tudi furlanski blok severozahodno od Sesljanskega preloma, vendar je zaradi geometrije premikov istrski blok najbolj proti severovzhodu potisnjeni del tega dela Mikroadrije.

Ideja o podrivanju in potiskanju proti Dinaridom (Placer et al., 2010) je utemeljena na analizi podatkov geoloških kart in terenskega opazovanja. Čičarijski in Tržaško-Komenski antiklinorij sta v glavnem nastala pri narivanju Dinaridov, njuna bočna deformacija pa je nastala pozneje, vsekakor pri potiskanju istrskega bloka proti Dinaridom. Pri tem se je v najbolj ekstremnih primerih uveljavilo podrivanje, na celotnem območju pa stiskanje prostora v obliki gubanja in premikov ob sekundarnih reverznih prelomih. Dogajanje je bilo večfazno.

O strukturah potiskanja proti Dinaridom na območju Istre in Kvarnerja sta pisala že Blašković in Aljinović (1981) in Blašković (1991). Sesljanski prelom sta v Sesljanskem zalivu, severozahodno od Trsta, odkrila Carulli in Cucchi (1991), pozneje so ga iz različnih vidikov obravnavali Carulli (2006, 2011), Busetti in sodelavci (2010), Placer in sodelavci (2010), Cucchi in Piano (2013), Placer (2015) idr. Pri teh raziskavah je bilo ugotovljeno, da se od obale proti severovzhodu že po nekaj kilometrih izklini, proti jugozahodu pa naj bi se domnevno nadaljeval v podmorju Tržaškega zaliva. Na severovzhodu, kjer ni več preloma, se v njegovi smeri nahajajo bočno upognjene dinarske strukture, katerih os upogiba je mogoče približno določiti, zato so Placer in sodelavci (2010, sl. 27) uporabili izraz sesljanska cona in ji določili smer. Glede na lego upognjenih struktur, so vsi raziskovalci opredelili Sesljanski prelom kot levi zmk.

Nasproti sesljanske cone ležijo v vzhodni Istri v zrcalni legi upognjene strukture, ki naj bi bile povezane z domnevnim Kvarnerskim prelomom v smeri SSW-NNE. Enako kot sesljanski coni je mogoče tudi tu upognjenim strukturam določiti smer in lego, vendar os upogiba tu ne leži neposredno v podaljšku domnevnega Kvarnerskega preloma. Govorimo o kvarnerski coni, ki pa je bistveno večja in kompleksnejša od sesljanske. Kvarnerski prelom ne izdanja nikjer, kot hipotetičnega sta ga zaradi neskladja med zgradbo Istre in otoka Cresa uvedla Šikić in Polšak (1973). Pojem Kvarnerskega preloma je potrebno razumeti

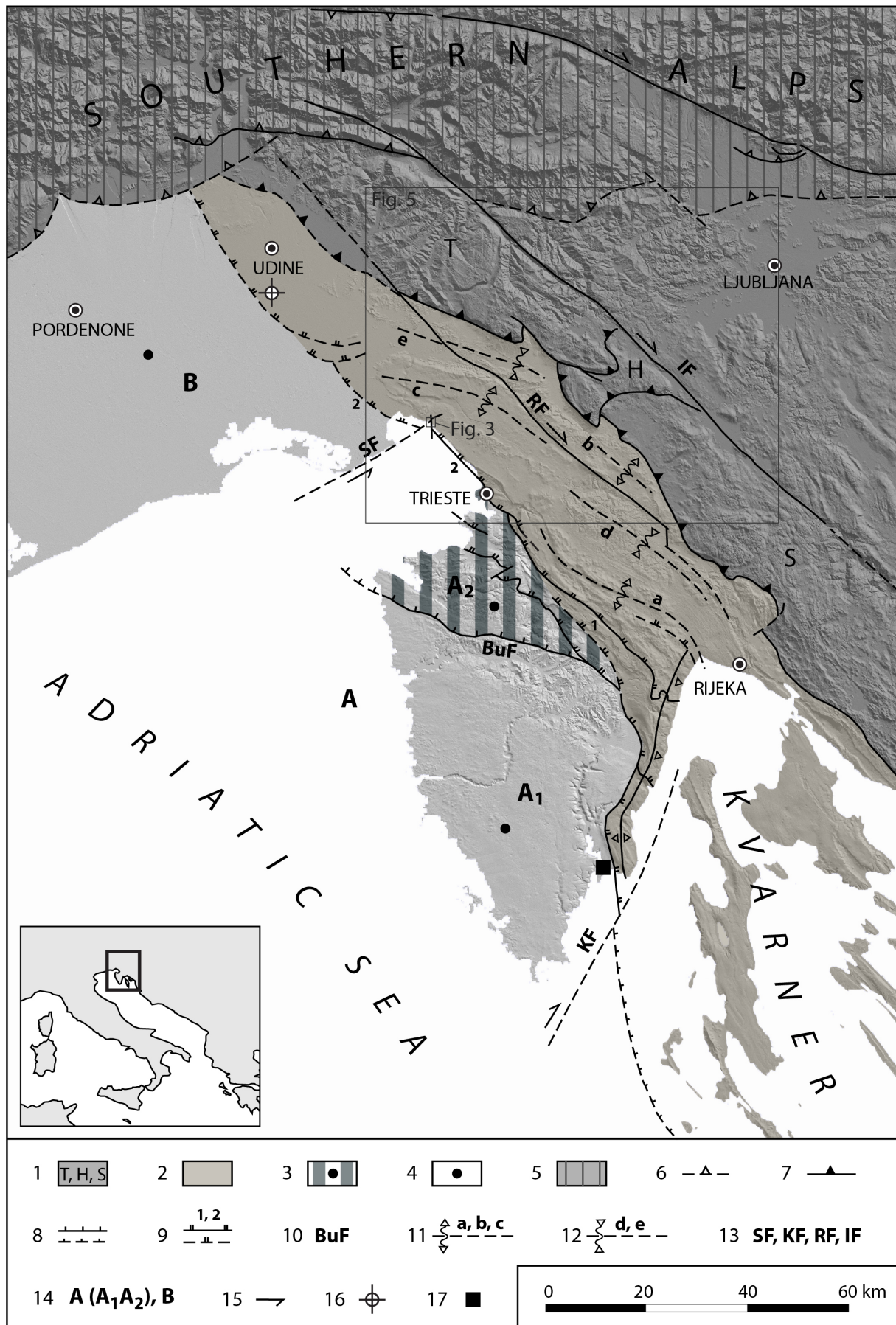


Fig. 2. Structural sketch of the Istra Pushed Area. Amended after Placer et al. (2010, Fig. 4). Basic data according to Basic geological map of Yugoslavia (OGK) and Carulli (2006).

Sl. 2. Strukturna skica istrskega potisnega območja. Dopolnjeno po Placer et al. (2010, sl. 4). Osnovni podatki Osnovna geološka karta Jugoslavije (OGK) in Carulli (2006).

not positioned in the continuation of the supposed Kvarner Fault. This is the Kvarner Zone, and it is significantly larger and more complex compared to the Sistiana Zone. There are no known outcrops of the Kvarner Fault. Due to the disparity between the structures of Istra and the island of Cres, it was introduced by Šikić & Polšak (1973). The term Kvarner Fault needs to be understood in the wider sense, as it could represent a fault or a wider and more complex tectonic zone of uncertain origin.

In the coastal area, structures in the northwestern block of the Sistiana Zone strike in the W-E direction (the northwest part of the Trieste-Komen Anticlinorium), while in the southeastern block of the Kvarner Zone (southeastern part of the Čičarija Anticlinorium, Cres Island), structures strike in the N-S direction. The Istra Pushed Area therefore took on a semicircular shape, which covers the frontal part of the Dinarides between the Southern Alps and the central Kvarner area, while in the interior its effects are visible up to the Ljubljana Basin (Placer, 2008; Placer et al., 2010, Fig. 27; Placer et al., 2921).

The flexural structures associated with the Kvarner Fault occupy a far larger area than those in the extension of the Sistiana Fault. They also have a significantly more complex structure, with overprinting deformations from different evolutionary stages, which makes their study more difficult. Therefore, the Sistiana Zone is more suita-

širše, lahko da gre resnično za prelom, lahko pa za široko in kompleksno tektonsko cono nejasne geneze.

Strukture v severozahodnem krilu sesljanske cone imajo v priobalnem pasu smer W-E (severozahodni del Tržaško-Komenskega antiklinorija), v jugovzhodnem krilu kvarnerske cone pa imajo smer N-S (jugovzhodni del Čičarijskega antiklinorija, otok Cres). Istrsko potisno območje ima zaradi tega polkrožno obliko, ki zajema čelni del Dinaridov med Južnimi Alpami in osrednjim Kvarnerjem, v notranjost pa sega njen vidni učinek nekako do Ljubljanske kotline (Placer, 2008; Placer et al., 2010, sl. 27; Placer et al., 2021).

Upognjene strukture povezane s Kvarnerskim prelomom zavzemajo mnogo večji prostor kot tiste v podaljšku Sesljanskega preloma. Imajo tudi kompleksnejšo zgradbo, kar pomeni, da se v njih prekrivajo deformacije različnih stopenj razvoja, zaradi česar je njihovo proučevanje težavnejše. Zato je sesljanska cona primernejša za pilotsko raziskavo geneze prečno upognjenih struktur Zunanjih Dinaridov.

Zaradi terminološke korektnosti je izraz sesljanska cona dopolnjen z opisom tipa in smeri deformiranja, zato smo uporabili izraz sesljanska bočno upogibna cona, skrajšano sesljanska upogibna cona. Enako velja za kvarnersko cono, oziroma kvarnersko bočno upogibno cono, skrajšano kvarnersko upogibno cono.

Fig. 2. / Sl. 2.

1 Dinarides: External Dinaric Thrust Belt: T – Trnovo Nappe, H – Hrušica Nappe, S – Snežnik Nappe / Dinaridi: Zunanjedinarski narivni pas: T – Trnovski pokrov, H – Hruški pokrov, S – Snežniški pokrov

2 Dinarides: External Dinaric Imbricate Belt / Dinaridi: Zunanjedinarski narivni pas

3 Microadria: Parautochton *sensu stricto* / Mikroadrija: paravtohton *sensu stricto*

4 Microadria: Stabile core / Mikroadrija: stabilno jedro

5 Southern Alps / Južne Alpe

6 Southern Alps Thrust boundary / meja narivne cone Južnih Alp

7 External Dinaric Thrust Belt boundary / meja Zunanjedinarskega narivnega pasu

8 Boundary of the Dinarides / meja Dinaridov

9 Istra-Friuli Underthrust Zone: 1 – Črni Kal Thrust Fault, 2 – Palmanova Thrust Fault / istrsko-furlanska podrivna cona: 1 – Crnokalski narivni prelom, 2 – Palmanovski narivni prelom

10 BuF – Buje reverse Fault / Bujski reverzni prelom

11 Anticlinorium: a – axis of the Čičarija Anticlinorium, b – axis of the Ravnik Anticlinorium, c – axis of the Trieste-Komen Anticlinorium / antiklinorij: a – os Čičarijskega antiklinorija, b – os Ravenskega antiklinorija, c – os Tržaško-Komenskega antiklinorija

12 Synclinorium: d – axis of the Brkini Synclinorium, e – axis of the Vipava Synclinorium / sinklinorij, d – os Brkinskega sinklinorija, e – os Vipavskega sinklinorija

13 Important sub-vertical faults: SF – Sistiana Fault, KF – Kvarner Fault, RF – Raša Fault, IF – Idrija Fault / pomembnejši subvertikalni prelomi: SF – Sesljanski prelom, KF – Kvarnerski prelom, RF – Raški prelom, IF – Idrijski prelom

14 Microadria structural block: A – Istra Block (A<sub>1</sub> – South Istra Structural Wedge, A<sub>2</sub> – North Istra Structural Wedge), B – Friuli Block / strukturni blok Mikroadrije: A – istrski blok (A<sub>1</sub> – južnoistrski strukturni klin, A<sub>2</sub> – severnoistrski strukturni klin), B – furlanski blok

15 Relative displacement direction / relativna smer premika

16 Cargnacco 1 borehole / vrtina Cargnacco 1

17 Koromačno Bay / zaliv Koromačno

ble for the pilot investigations of the transversely bent structures of the External Dinarides.

In order to apply a correct and common terminology, the term Sistiana Zone is supplemented with a description of the type and direction of deformation, which is why we have used the term Sistiana Lateral Bending Zone, abbreviated as Sistiana Bending Zone. The same applies for the Kvarner Zone, or the Kvarner Lateral Bending Zone, abbreviated as Kvarner Bending Zone.

The tectonic push also resulted in the under-thrusting of the Istra-Friuli Underthrust Zone, which is strongly emphasized on the northeastern boundary of the Istrian Block, but is significantly weaker in the Friuli Block.

The structural sketch of the Istra Pushed Area (Fig. 2) is simplified and amended after Placer et al. (2010, Fig. 4). The Southern Alps are separated, but internally remain undivided. The Dinarides are divided in the context of the thrust structure into the External Dinaric Thrust Belt and the External Dinaric Imbricate Belt. Microadria is divided into the imbricated edge of the autochthonous or paraautochthonous *sensu stricto* and autochthonous. The boundary between both units is the Buje Reverse Fault (BuF). The Istra Block is denominated with A, and the Friuli Block with B. The Istra Block is further subdivided into two structural wedges, namely the South Istrian ( $A_1$ ) and the North Istrian ( $A_2$ ) Structural Wedge.

The Istra-Friuli Underthrust Zone is segmented: the central fault structures in the zone are the Črni Kal and Palmanova thrust faults. The first can be ascribed to the Učka Thrust, while the second can be traced also northwest from the Sistiana Fault based on deep borehole data and geophysical sounding (Nicolich et al., 2004, Tavola 1, Tavola 2; Carulli, 2006). The Istra-Friuli Underthrust Zone stretches to the Kvarner Fault in the southeastern direction. According to the field investigations, the Istra-Friuli Underthrust Zone is the most tectonically deformed at the tip of the South Istra Structural Wedge. Available data from the Cagnacco 1 borehole well south of Udine (Venturini, 2002) and from the last visible outcrop of the Dinarides thrust boundary in Koromačno on the eastern coast of Istra point (Fig. 2) to the proportionally lesser tectonic deformation.

It is clear from the general structural sketch of the Istra Pushed Area that the deformations of underthrusting and pushing due to the activity of the Microadria are most pronounced in the extension of the axis of the South Istrian Structural Wedge, where the Čičarija Anticlinorium and the Brkini Synclinorium are bent due to lateral push

Posledica potiskanja v istrsko-furlanski podrivni coni je bilo tudi podrivanje, ki je močno poudarjeno na severovzhodni meji istrskega bloka, bistveno šibkeje pa v furlanskem bloku.

Strukturna skica istrskega potisnega območja na sliki 2 je povzeta po Placerju in sodelavcih (2010, sl. 4) ter poenostavljena in dopolnjena. Južne Alpe so ločene toda nerazčlenjene, Dinaridi so razčlenjeni v smislu narivne zgradbe na Zunanjedinarski narivni pas in Zunanjedinarski naluskani pas, Mikroadria je razdeljena na naluskani rob avtohton ali paravtohton *sensu stricto* in avtohton. Meja med obema enotama je Bujski reverzni prelom (BuF). Istrski blok je označen z A, furlanski blok z B. Istrski blok je nadalje razdeljen na dva strukturna klina, južnoistrski ( $A_1$ ) in severnoistrski strukturni klin ( $A_2$ ).

Istrsko-furlanska podrivna cona je segmentirana; osrednji prelomni strukturi v njej sta Črnokalski in Palmanovski narivni prelom. Prvega je mogoče povezati z narivom Učke, drugega pa je mogoče na podlagi podatkov globokih vrtin in geofizikalnega sondiranja (Nicolich et al., 2004, tavola 1, tavola 2; Carulli, 2006) slediti tudi severozahodno od Sesljanskega preloma. Proti jugovzhodu sega istrsko-furlanska podrivna cona formalno do Kvarnerskega preloma. Po podatkih terenskega profiliranja je istrsko-furlanska podrivna cona najbolj tektonizirana v konici južnoistrskega strukturnega klina. Dostopni podatki vrtine Cagnacco 1 južno od Vidma/Udin (Venturini, 2002) in na skrajnem vidnem izdanku narivne meje Dinaridov v Koromačnem na vzhodni obali Istre (sl. 2) kažejo na sorazmerno manjšo stopnjo porušenosti.

Iz splošne strukturne skice istrskega potisnega območja izhaja, da so deformacije podrivanja in potiskanja zaradi aktivnosti Mikroadrije najbolj izražene v podaljšku osi južnoistrskega strukturnega klina, kjer sta zaradi bočnega potiska usločena Čičarijski antiklinorij in Brkinski sinklinorij (a in d na sl. 2). Potisk je kombiniran s podrivanjem; pod istrsko-furlansko podrivno cono je proti VSV potisnjen jugovzhodni del Bujskega preloma (BuF) in skupaj z njim ustrezeni del paravtohton ali *sensu stricto*, pod Snežniški pokrov pa del severovzhodnega krila Brkinskega sinklinorija in jugovzhodni del Ravniškega antiklinorija.

Sesljanski prelom je del vertikalne segmentacije Mikroadrije, sesljanska bočno upogibna cona pa je prizadela Zunanjedinarski naluskani in Zunanjedinarski narivni pas. Zaradi tako jasnih razmerij med Mikroadrijo in Dinaridi nudi to območje možnosti za posredno ugotavljanje

(a and d on Fig. 2). The pushing is combined with underthrusting; beneath the Istrian-Friuli Underthrusting Zone, the southeastern part of the Buje Fault (BuF) and its corresponding part of the autochthonous *sensu stricto* are pushed, while part of the northeastern limb of the Brkini Synclinorium and the southeastern part of the Ravnik Anticlinorium is pushed under the Snežnik Nappe.

The Sistiana Fault is part of the vertical segmentation of the Microadria, and the Sistiana Lateral Bending Zone affected the External Dinaric Imbricate Belt and Thrust Belt. Due to such clear relationships between the Microadria and the Dinarides, this area offers the opportunity to indirectly determine in depth the geometric relationship between these two units and provide the necessary data for structural modeling.

### Sistiana Fault

The Sistiana Fault is visible on the surface only along the coast of the Sistiana Bay. A structural sketch of the vicinity of the bay is represented in Fig. 3A and is based on data from the Carta Geologica del Carso Classico Italiano (Cucchi & Piano, 2013) and our own investigations. All main components of the composition were confirmed: the Sistiana Fault (I), the N-S directed fault (II), and the Trieste reverse fault (III), which is part of the thrust system of the wider area. There are flysch and marlstone outcroppings between faults no. I and II, while the neighboring units are composed of Cretaceous, Paleocene, and Eocene limestones. Flysch beds appear in the inverse position.

The Sistiana Fault outcrops only on the northern slopes of the Sistiana Bay in the northeastern block of fault no. IV (30/80) (Fig. 4); however, its fault plane is visible only in the rock-face under the starting point of the Rilke Path (point no. 1). Only the dip direction, and not the dip angle, could be measured (310/?). Further to the east-northeast, the fault plane is identifiable only up to fault no. III. From here and up to fault no. II, the situation is unclear, because the area is covered. On the other side of fault no. II there is a surface 350/80, which is visible in the highway cut and probably belongs to the Sistiana Fault. In the southwestern block of fault no. IV, the Sistiana Fault is displaced in the southeastern direction, but it is covered with tailings of the abandoned quarry. Its extension can be reconstructed after the limestone outcrop on the coast. Fault no. IV and some faults further north, of which two are represented on the map, prove that the Sistiana Fault is segmented. Some faults are positioned transversely and obliquely on the Sistiana Fault. They are visible in the rock-face

geometrijskega razmerja med temo dvema enotama v globini in potrebne podatke za izvajanje modelnih raziskav.

### Sesljanski prelom

Seljanski prelom je na površju viden edino v Sesljanskem zalivu, zato si oglejmo strukturno skico okolice zaliva, ki je prikazana na sl. 3A, njena izdelava temelji na podatkih s Carta geologica del Carso classico italiano (Cucchi & Piano, 2013) in lastnem orientacijskem ogledu. V območju zaliva so bile potrjene vse bistvene komponente zgradbe: Sesljanski prelom (I), prelom N-S (II) in Tržaški reverzni prelom (III), ki je del narične zgradbe širšega ozemlja. Med prelomoma št. I in II izdanjata fliš in lapor, bližnje kamnine so kredni, paleocensi in eocensi apnenci. Flišne plasti so prevrnjene.

Sesljanski prelom izdanja le v severnem počaju Sesljanskega zaliva v severovzhodnem krilu preloma IV (30/80) (sl. 4); vendar je njeovo prelomno ploskev mogoče videti le v steni pod začetnim delom Rilkejeve poti (točka št. 1), kjer pa se da določiti le njeno smer ne pa tudi vpadnega kota (310/?). Naprej proti vzhodu-severovzhodu je trasa določljiva le do preloma št. III. Od tu do preloma št. II so zaradi prekritosti razmere nejasne. Na drugi strani preloma št. II pripada Sesljanskemu prelomu verjetno ploskev 350/80, ki je vidna v useku avtoceste. V jugozahodnem krilu preloma IV je Sesljanski prelom zamaknjen proti jugovzhodu, vendar na površju ni več viden, saj je zasut z jalovinskim materialom opuščenega kamnoloma. Njegov potek je mogoče rekonstruirati po izdanku apnenca na obali. Prelom IV in nekaj prelomov severno od tega, od katerih sta na sliki 3 vrisana dva, dokazujo, da je Sesljanski prelom segmentiran. Prelomov, ki ležijo prečno ali poševno na Sesljanskega, je v jugozahodnem krilu preloma IV več; vidni so v steni opuščenega kamnoloma, vendar je njihov odnos do Sesljanskega preloma neznan. Po analogiji bi ga lahko tudi ti sekali, kot je hipotetično prikazano na sliki 3A. Interpretacija smeri Sesljanskega preloma na tem odseku je povzeta po prvotni morfologiji severozahodnega dela Sesljanskega zaliva, ki je vidna na karti druge izmere Vojaškega zemljevida Habsburške monarhije 1806-1869 na sliki 2B - levo (Historical Maps of the Habsburg Empire. The Second Military Survey 1806-1869). Tu je izrisana prvotna obala zaliva, ki so jo sestavliali kredni, paleocensi in eocensi apnenci pred pričetkom izkoriščanja kamnoloma. Zgradbo in potek obale potrjuje tudi Geološka karta 1:75.000 (Stache,

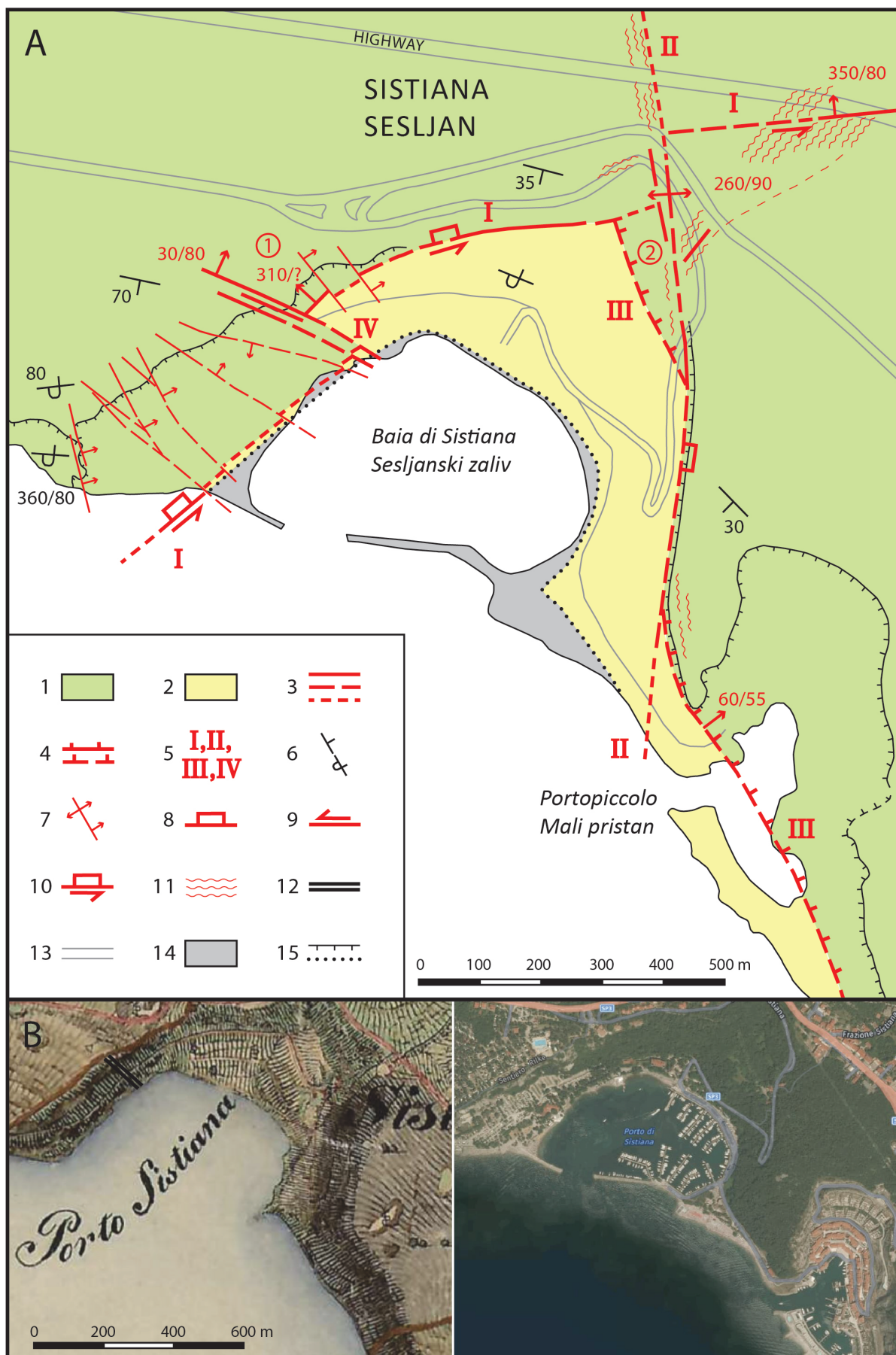


Fig. 3. Sistiana Bay. A. Structural sketch. Amended after Cucchi & Piano (2013); B. Sistiana Bay: left – Historical Maps of the Habsburg Empire 1806–1869, The Second Military Survey; right – satellite picture, Mapaire.

Sl. 3. Sesljanski zaliv. A. Strukturna skica. Dopolnjeno po Cucchi in Piano (2013); B. Sesljanski zaliv: levo – Vojaški zemljevid Habsburške monarhije 1806-1869, druga izmera; desno – satelitski posnetek, Mapaire.

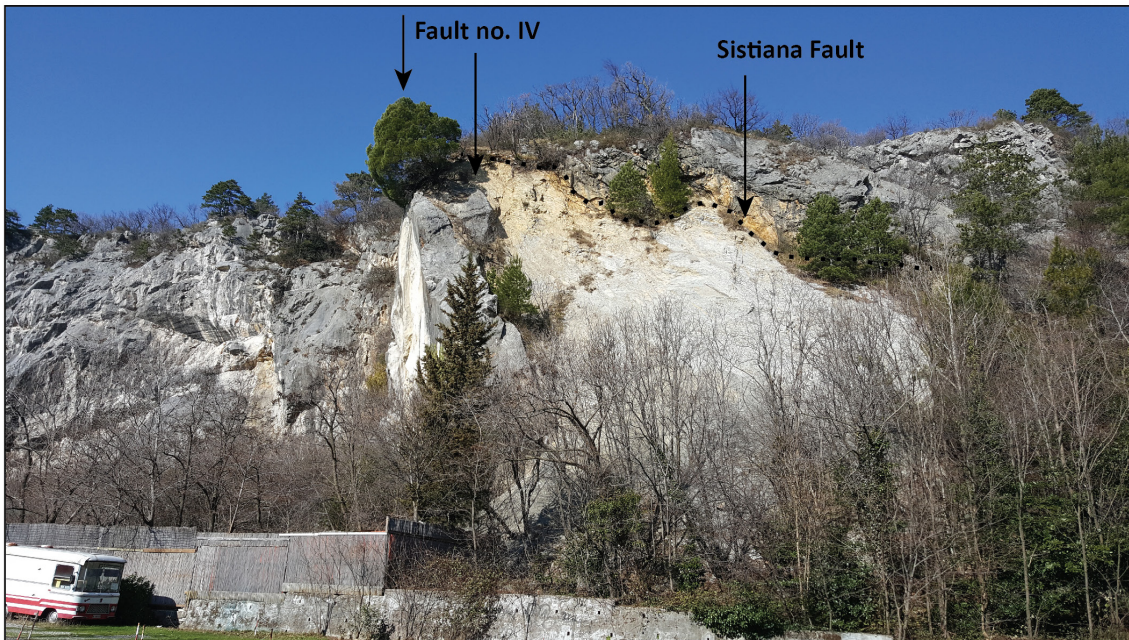


Fig. 4. Sistiana Bay. In the middle of the photo is fault no. IV (30/80), cutting the Sistiana Fault. Left: Cretaceous limestone. Right: Eocene Transitional marlstone, above is a rock face as a fault plane of the Sistiana Fault, behind it is Cretaceous limestone.

Sl. 4. Sesljanski zaliv. Sredi slike je prelom IV (30/80), ki sekajo Sesljanski prelom. Levo: Kredni apnenec. Desno: eocenski prehodni lapor, nad njim stena kot prelomna ploskev Sesljanskega preloma, zadaj kredni apnenec.

of the abandoned quarry, but their relationship to the Sistiana Fault is unknown. By analogy, they could also cut it, as is hypothetically represented in Fig. 3A. An interpretation of the direction of the Sistiana Fault in this stretch is summarized after the morphology of the northwestern part of Sistiana Bay, as represented in the Historical Maps of the Habsburg Empire. The Second Military Survey 1806–1869 (Fig. 2B – left). The original coast is presented, with Cretaceous, Paleocene, and Eocene limestones before quarrying. The composition and shape of the coast before quarrying is also confirmed in the Geological map 1:75.000

1920), ki je bila izdelana v drugi polovici 19. stoletja, ko tam še ni bilo kamnoloma. Na karti se vidi tudi geološka meja, ki jo danes interpretiramo kot prelom št. IV (30/80).

Na območju točke št. 1 (sl. 3A) so v jugovzhodnem krilu Sesljanskega preloma vidne prehodne plasti, ki pa so priključene flišnim kamninam. Razmere so poenostavljene.

Prelom št. II v smeri N-S je bil določen po morfološkem kriteriju in po izdanku v useku ceste v zaliv (260/90). Prelom št. III je viden v vhodnem delu Malega pristana (Portopiccolo), kjer ima smer 60/55; tu ga spremeljajo razpoke v

Fig. 3. / Sl. 3.

- 1 Cretaceous and Paleogene limestones / kredni in paleogenski apnenci
- 2 Eocene Transitional marlstone and Flysch / eocenski prehodni lapor in fliš
- 3 Important fault: visible, covered or interpolated or extrapolated, uncertain / pomembnejši prelom: viden, prekrit ali interpoliran ali ekstrapoliran, negotovo določen
- 4 Important reverse fault: visible, covered / pomembnejši reverzni prelom: viden, prekrit
- 5 Faults: no. I – Sistiana Fault, no. II – N-S fault (260/90), no. III – Trieste reverse fault (60/55), no. IV – sub-vertical fault (30/80) / prelomi: št. I – Sesljanski prelom, št. II – prelom N-S (260/90), št. III – Tržaški reverzni prelom (60/55), št. IV – subvertikalni prelom (30/80)
- 6 Dip of strata: normal, inverse / plasti: normalne, inverzne
- 7 Fault planes: vertical, inclined / prelomne ploskve: navpične, poševne
- 8 Subsided fault block / ugreznjeno krilo preloma
- 9 Direction of the horizontal component of the displacement along fault / smer horizontalne komponente premika prelomnega krila
- 10 Combined or oblique displacement of the fault block / kombiniran ali poševen premik prelomnega krila
- 11 Significant joint zone / pomembnejša razpoklinska cona
- 12 Fig. B left – location of the contact between Upper Cretaceous and Paleocene limestone after Stache (1920). At this location it is fault no. IV (30/80) in fig. A / sl. B levo, mesto stika zgornjekrednega in paleocenskega apnanca po Stache (1920). Na sl. A je na tem mestu prelom št IV (30/80)
- 13 Road / cesta
- 14 Embankment / nasip
- 15 Edge of the vertical face; position of the coast between 1806–1869 / rob prepadne stene; obala med letoma 1806–1869

(Stache, 1920), elaborated in the second half of the 19<sup>th</sup> century. The geological boundary, now interpreted as fault no. IV (30/80), is well represented.

In the southeastern block of the Sistiana Fault (area of point no. 1 in Fig. 3A) transitional beds incorporated into the flysch are visible. The situation has been simplified.

Fault no. II in the N-S direction was determined according to the morphological criteria and after the outcrop in the roadcut (260/90). Fault no. III is visible in the eastern part of Portopiccolo, with a 60/55 dip, accompanied by joints in the limestone (75/55). Toward the north, up to fault no. II, the fault is determined according to the morphologic step between flysch marlstone and limestone. On the western part of fault no. II, fault no. III is determined after the direction of the western slopes of the valley of the same direction (point no. 2), which we believe is formed in the jointed limestone. Fault no. II is part of the joint-fault zone, as reflected in the series of dolines north of the highway. If we compare the displacements of the Sistiana Fault and fault no. III along fault no. II, it is clear that we are looking at two different phases of displacements.

The carbonate strata along Sistiana Bay are positioned in an easterly, Dinaric direction NW-SE; in the northern and northwestern part they divert to the west-east direction, and from their normal position in the north they divert to the overturned position (360/80). In the direction of Duino, they gradually divert again into the normal position. In the hinterland of the Bay, flysch beds appear in an overturned position and dip to the north.

Cucchi & Piano (2013) considered the Sistiana Fault and fault no. II strike-slip faults, the former with a left-lateral and the latter with a right-lateral displacement. The Sistiana Fault is considered unsegmented, as fault no. II does not cut the first one. Such an interpretation requires at least two strike-slip phases. Our interpretation is slightly different. From the structural sketch (Fig. 3A) it is obvious that a vertical component of the displacement of the block between faults no. I and II larger than the horizontal component. The displacement consisted of a number of components. The displacement of the Sistiana Fault along fault no. II is of secondary origin along the joint-fault zone directed north-south, which part is also fault no. II. Joint-fault zones in this direction are usual in several parts of the Trieste-Komen Anticlinorium. Multiphase displacements are also evidenced by the segmentation of the Sistiana Fault.

From the description above it follows that the origin of the flysch block between the Sistiana

apnencu (75/75), proti severu do preloma št. II, pa je določljiv po morfološki stopnji med flišnim laporjem in apnencem. Na zahodni strani preloma št. II je prelom št. III določen po smeri zahodnega pobočja doline enake smeri (sl. 3A, točka št. 2), za katero smatramo, da se je razvila v razpokanem apnencu. Prelom št. II je del razpoklinsko-prelomnega snopa, kar se odraža v nizu kolinearnih vrtač severno od avtoceste. Če vzposejamo premika Sesljanskega preloma in preloma št. III ob prelomu št. II, je jasno, da gre za dve različni fazi premikov.

Plasti karbonatnih kamnin okoli Sesljanskega zaliva slemenijo vzhodno od tod pretežno v meri Dinaridov NW-SE, na severni in severozahodni strani pa se iz dinarske obrnejo v smer zahod – vzhod in se iz normalne lege proti obali prevrnejo v inverzno lego (360/80). Severno, proti Devinu se plasti polagoma spet obrnejo v normalno lego. Fliš ima v zaledju zaliva inverzno lego ter vpada proti severovzhodu.

Cucchi in Piano (2013) sta Sesljanski prelom in prelom št. II obravnavala kot zmična preloma, prvega kot levi in drugega kot desni zmik. Sesljanski prelom naj bi bil nesegmentiran, prelom št. II pa naj ga ne bi sekal, za kar pa bi bili potrebeni vsaj dve fazi premikov. Sedaj predložena interpretacija je nekoliko drugačna. Iz strukturne skice na sliki 3A izhaja, da je imela navpična komponenta premika bloka med prelomoma št. I in št. II večji obseg od vodoravne in da je bilo premikanje večkomponentno. Premik Sesljanskega preloma ob prelому št. II je sekundarnega izvora, dogodil se je vzdolž razpoklinsko prelomne cone sever-jug, katere del je prelom št. II. Razpoklinsko-prelomne cone te smeri so na območju Tržaško-Komenskega antiklinorija dejavne na več mestih. Večfaznost premikov dokazuje tudi segmentacija Sesljanskega preloma.

Iz napisanega sledi, da je blok flišnih kamnin med Sesljanskim prelomom in prelomom št. II najlažje razložiti z dvigom. To potrjuje tudi pojemanje intenzivnosti Sesljanskega preloma proti vzhodu. Da bi morali ob Sesljanskem prelomu obstajati levozmični premiki izhaja iz njegove regionalne vloge, vendar ima ta komponenta premika v Sesljanskem zalivu sekundarni pomen. Zaradi lažje komunikacije imenujemo blok dvignjenega oziroma vertikalno izrinjenega fliša v zalivu sesljanski izrivni blok.

V zahodni steni opuščenega kamnoloma v Sesljanskem zalivu, imajo tektonske drse različne smeri, zdi pa se, da prevladujejo subhorizontalne in subvertikalne. Podobno je v severnem

Fault and fault no. 2 is best described with the uplift. This also confirms the pinching-out of the Sistiana Fault in the easterly direction. The regional role of the Sistiana Fault infers left lateral strike-slip displacement, although this component of displacement in the Sistiana Bay is of secondary importance. For the sake the simpler communication, we named this uplifted or vertically erected block the Sistiana Pushout Block.

In the western rock face of the abandoned quarry in the Sistiana Bay, slickensides take different directions, but it appears that sub-horizontal and sub-vertical ones prevail. A similar situation is visible on the northern slopes of the bay and in other areas, which makes the Sistiana Bay a first-class structural-geological object for detailed mapping and structural analysis.

For purposes of this paper, we conclude that the Sistiana Block between the Sistiana Fault and fault no. II is vertically erected and that overturned flysch strata at the bottom of the bay most likely belongs to the footwall block of the reverse fault no. III, which represents the deformed position of the Trieste Thrust.

## Sistiana Bending Zone

### General findings

The more pronounced laterally bent Trieste-Komen Anticlinorium and the less pronounced Vipava Sinclinorium are observable in the Sistiana Bending Zone. The bending axis can be precisely determined only in the Sistiana Bay, while on the northeastern side of the Trieste-Komen Anticlinorium such determinative precision is not possible. We can, with a certain degree of probability, assign its location near Spodnja Branica (Fig. 12). The Vipava Sinclinorium is bent, but there are no adequate structures available to help determine the bending axis. However, what is interesting is the fact that the Idrija Fault is also laterally bent in the continuation of the Sistiana Bay – Spodnja Branica direction. With the position of the boundary between the Trnovo and Hrušica Nappes, we can suggest a modification of the original relationship between thrust-units. Based on the Sistiana Bay – Spodnja Branica line, the approximate axis direction of the Sistiana Bending Zone is  $60^\circ$ – $65^\circ$ . The bending axis is not represented as a line, but rather as an area of tolerance seen as a circular section with an angle of about  $5^\circ$  (Fig. 5).

The size of the angle of the lateral bending of individual structural units in the Sistiana Bending Zone can be determined only approximately,

pobočju zaliva in drugod, zato je Sesljanski zaliv prvovrstni strukturno-geološki objekt za detaljno kartiranje in strukturno analizo.

Za potrebe tega članka zadostuje ugotovitev, da je sesljanski blok med Sesljanskim prelomom in prelomom št. II izrinjen navzgor in da inverzija flišnih plasti v dnu zaliva najverjetneje kaže na to, da pripada talinski grudi reverznega preloma št III, ki predstavlja deformirano lego Tržaškega nariva.

## Sesljanska upogibna cona

### Splošne ugotovitve

V sesljanski upogibni coni sta vidno bočno upognjena Tržaško-komenski antiklinorij in Vipavski sinklinorij; prvi bolj, drugi nekoliko manj. Os upogiba je mogoče natančno določiti le v Sesljanskem zalivu, kjer se sprememb smeri plasti dogodi vzdolž prelomne ploskve Sesljanskega preloma, na severovzhodni strani Tržaško-Komenskega antiklinorija pa tako natančnost ni mogoča, lahko pa s precejšnjo mero gotovosti ugotovimo, da se nahaja blizu Spodnje Branice (sl. 12). Vipavski sinklinorij je upognjen, toda za določanje osi upogiba ni na voljo ustreznih struktur, preseneča pa dejstvo, da je v podaljšku smeri Sesljanski zaliv – Spodnja Branica bočno usločen tudi Idrijski prelom. Po legi meje med Trnovskim in Hrušičkim pokrovom je mogoče domnevati, da je spremenjen tudi prvotni odnos med omenjenima krovnima enotama. Glede na črto Sesljanski zaliv – Spodnja Branica, znaša približna smer osi sesljanske upogibne cone  $60^\circ$  do  $65^\circ$ . Na sliki 5 ni izrisana os upogiba temveč območje njene tolerančne lege, zato je sesljanska upogibna cona prikazana kot krožni izsek s kotom okoli  $5^\circ$ .

Velikost kota bočnega upogiba posameznih strukturnih enot v sesljanski upogibni coni je mogoče določiti le približno, kar pa ne moti, saj stopnja natančnosti podatka ne vpliva na končno interpretacijo (sl. 5). V Sesljanskem zalivu ga je mogoče določiti po legi plasti, kjer znaša okoli  $20^\circ$ . Za Tržaško-Komenski antiklinorij je kot upogiba najlaže določiti iz slemenitve Kraške grupe formacij (Jurkovšek et al., 2013) plasti v severovzhodnem krilu antiklinorija ( $a_1, a_2$ ) in izven vpliva Raškega preloma. Ta znaša približno  $18^\circ$ . Iz slike 5 izhaja, da ima velikost kota v Sesljanskem zalivu le ožji pomen, zato je za izhodiščno vrednost najbolje vzeti podatek o upogibu celotnega antiklinorija, torej  $18^\circ$ . Velikost upogiba osi Vipavskega sinklinorija je težko določiti, ker je deformirana zaradi izpostavljenje

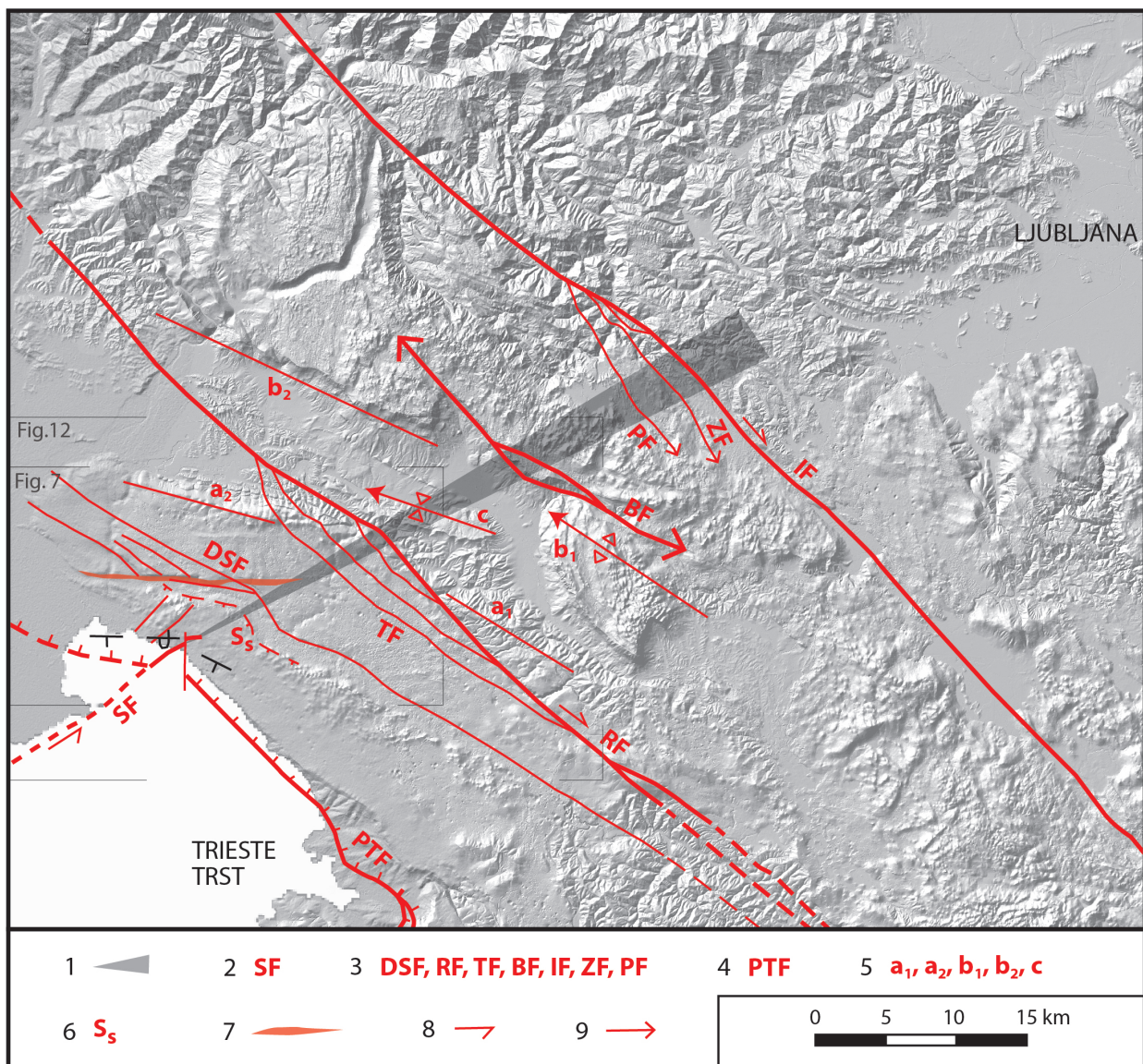


Fig. 5. Sistiana Bending Zone.

Sl. 5. Sesljanska upogibna cona.

1 Sistiana Bending Zone / sesljanska upogibna cona

2 SF – Sistiana Fault / Sesljanski prelom

3 Faults in direction of Dinarides / dinarsko usmerjeni prelomi: DSF – Divača splay of faults / Divaški snop prelomov, RF – Raša Fault / Raški prelom, TF – Tomačevica Fault / Tomačevski prelom, BF – Bela Fault / Belski prelom, IF – Idrija Fault / Idrijski prelom / ZF – Zala Fault / Zalin prelom, PF – Predgriže Fault / Predgriški prelom

4 PTF – Palmanova Thrust Fault / Palmanovski narivni prelom

5 Rotating structures / zasukane strukture: a<sub>1</sub>, a<sub>2</sub> – Direction of the Trieste-Komen Anticlinorium / smer Tržaško-Komenskega antiklinorija, b<sub>1</sub> – Nanos Anticline in the Hrušica Nappe thrust-front / smer Nanoške antiklinale v čelu Hrušiškega pokrova, b<sub>2</sub> – Direction of the Trnovo Nappe thrust-front / smer čela Trnovskega pokrova, c – Planina Syncline in the Vipava Synclinorium / smer Planinske sinklinale v Vipavskem sinklinoriju

6 S<sub>s</sub> – Sistiana Sigmoid, dip of strata / sesljanska sigmoida, vpad plasti

7 Komen Wedge Structural Step / komenski klinasti strukturni prag

8 Relative direction of displacement / relativna smer premika

9 Continuation of the fault, no detailed geological mapping performed / prelom se nadaljuje, ni podrobno geološko kartirano

but this is not of particular importance, because the degree of accuracy of the data does not affect the final interpretation (Fig. 5). In Sistiana Bay, it can be determined after the position of the strata, which amounts to approximately 20°. In the Trieste-Komen Anticlinorium, a bending axis of approx. 18° can be determined from the strike

lege Nanosa v čelnem delu Hrušiškega pokrova, je pa gotovo manjša od upogiba Tržaško-Komenskega antiklinorija. Narej proti severovzhodu sprememba smeri v nakazani smeri ni več tako očitna, vendar obstajajo, saj je bilo že rečeno, da je v širokem loku ukrivljena tudi trasa Idrijskega preloma. Če je tako, bi morala biti eden nasproti

direction of the Kras Group Formation (Jurkovšek et. al., 2013) in the northeastern limb of the anticlinorium ( $a_1$ ,  $a_2$ ), and outside the influence of the Raša Fault. Based on the Fig. 5, the amount of the angle in Sistiana Bay has only minor influence, consequently we took  $18^\circ$  as a base value. The size of the bending of the axis of the Vipava Synclinorium is difficult to determine because of the exposed position of Nanos in the thrust-front of the Hrušica Nappe. It is certainly smaller, compared to the bending of the Trieste-Komen Anticlinorium. Further to the northeast, the change in direction in the indicated continuation is not so obvious, but does exist, since it has already been said that the line of the Idrija Fault is also curved in a wide arc. If this assumption is correct, the Trnovo and Hrušica Nappes also need to be rotated against each other. The amount of the angle of eventual rotation between the two thrust units is difficult to determine, but some general information can be determined. The direction of the thrust-unit is generally determinable by the direction of the dominant slickensides in the principal thrust plane, which are perpendicular to the strike direction of the thrust unit, and by the position of the folds axis formed during the thrusting. In both cases, owing to the inhomogeneity of the thrust units and consequent oscillations in displacement directions the data is only statistical. Under the given conditions, the direction of the Nanos Anticline axis ( $b_1$ ) in the Hrušica Nappe can be determined, while no such information is available for the Trnovo Nappe, but it is possible to approximate the direction of the thrust front ( $b_2$ ), which is not possible at Nanos, because the thrust front is not reliably fixed. Therefore, both figures were used for orientation. The axis of the frontal anticline of the Hrušica Nappe dip in the northwestern direction (304/23) (Placer, 1981, Fig. 1). The thrust-front of the Trnovo Nappe strikes approx. in the  $295^\circ$  direction. Although the data does not represent a reliable starting point, it is nevertheless interesting that the  $9^\circ$  direction obtained is consistent with the decreasing angle of arch of the Sistiana Bending Zone to the northeast. The Trnovo Nappe should therefore be rotated counterclockwise, just like the rest of the blocks northwest of the Sistiana Bending Zone. The direction of the dominant slickensides in the Planina Quarry (Placer, 1994/95, Fig. 6) was not considered, since it is too far from the thrust front of the Hrušica Nappe and does not represent the statistical average.

Clear evidence of a decrease in lateral bending from the southwest to the northeast is seen in

drugemu zasukana tudi Trnovski in Hrušički pokrov. Velikost kota morebitnega zasuka med omenjenima krovnima enotama je težko določljiva, mogoče pa je dati splošno informacijo. Smer krovne enote je na splošno določljiva po smeri dominantnih tektonskih drs v glavni narivni ploskvi, ki ležijo pravokotno na smer narivne enote in po legi osi gub, ki so nastale med narivanjem. V obeh primerih je podatek lahko le statističen, saj so narivne enote nehomogene, zaradi česar do določene mere niha tudi smer premikov. V danih razmerah je pri Hrušičkem pokrovu mogoče določiti smer osi Nanoške antiklinale ( $b_1$ ), medtem ko pri Trnovskem pokrovu takega podatka ni, vendar je mogoče približno izmeriti smer čela krovnega nariva ( $b_2$ ), česar pri Nanosu ni mogoče, ker čelo nariva ni zanesljivo določeno. Zato sta bila za orientacijo uporabljeni omenjeni podatki. Os čelne antiklinale Hrušičkega pokrova vpada proti severozahodu 304/23 (Placer, 1981, sl. 1), čelo Trnovskega pokrova poteka približno v smeri  $295^\circ$ . Čeprav podatka ne predstavlja zanesljivega izhodišča, je vseeno zanimivo, da je dobljena razlika v smereh,  $9^\circ$  skladna z manjšanjem kota usločitve sesljanske upogibne cone proti severovzhodu. Trnovski pokrov naj bi torej bil zasukan v nasprotni smeri urinega kazalca tako kot ostali bloki severozahodno od sesljanske upogibne cone. Smer dominantnih drs v kamnolomu pri Planini (Placer, 1994/95, sl. 6) ni bila upoštevana, ker je kraj preveč oddaljen od čela Hrušičkega pokrova in ne predstavlja statističnega povprečja.

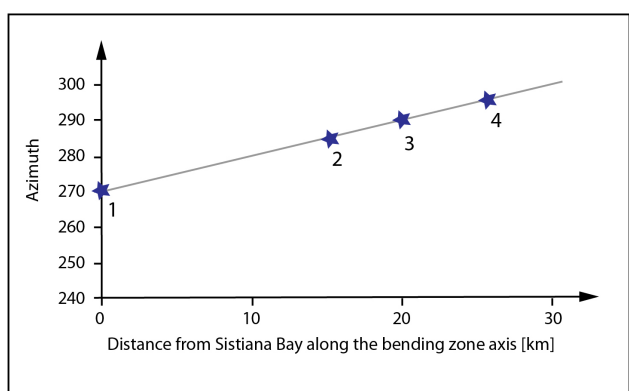


Fig. 6. Diagram of external rotation of the structural units of the northeastern wing of the Sistiana Bending Zone.

Sl. 6. Diagram eksterne rotacije strukturnih enot severozahodnega krila sesljanske upogibne cone.

1 Sistiana Bay (bedding strike) / Sesljanski zaliv (smer plasti)

2  $a_2$  – Northern edge of the Trieste-Komen Anticlinorium / severni rob Tržaško-Komenskega antiklinorija

3 c – Axis of the Planina Syncline is identical with the direction of the Vipava Synclinorium / os Planinske sinklinale je identična s smerjo Vipavskega sinklinorija

4  $b_2$  – Trnovo Nappe thrust-front / čelo Trnovskega pokrova

the change in the azimuth of those structures in the northwestern wing of the Sistiana Bending Zone, which was originally oriented in the Dinaric direction (Fig. 6). The strike of bedding in the Sistiana Bay is approx.  $270^\circ$  (point 1), and in the Liburnian Formation in the northeastern limb of the Trieste-Komen Anticlinorium approx.  $285^\circ$  ( $a_2$ , point 2), while the azimuth of the axis of the northwestern and central part of the Vipava Synclinorium, as determined by the axis of the syncline from the flysch calcarenites, and breccias in the Planina area, is approximately  $290^\circ$  (c, point 3), and the strike of the front of the Trnovo Nappe is  $295^\circ$  ( $b_2$ , point 4). The linear relationship between the points indicates the corresponding order.

The syncline with flysch calcarenites, and breccias in the Planina area on the axis of the Vipava Synclinorium (Planina Syncline) is purely horizontally rotated, together with the northwestern limb of the synclinorium, although it does extend beyond the axis of the Sistiana Bending Zone. The horizon of calcarenites, and breccias is over 100 m thick and represents a weakly ductile unit in flysch rocks of high ductility. It did not bend in the flexural zone, but twisted rigidly. This was possible because the axis of the Planina syncline dips in the west-northwest direction and the bulk of its mass is positioned in the rotating wing of the bending zone. As this paper is dedicated to the regional importance of the Sistiana Bending Zone we have only raised the issue of the “anomalous position” of the clastites in the Planina Syncline. Differences in rock ductility play an important role in the structural and geomorphological analysis of the Istra Pushed Area.

### **Deformation of the faults in the Dinaric direction**

In addition to the units described during the period of thrusting (the Trieste-Komen Anticlinorium, the Vipava Synclinorium, and the Trnovo and Hrušica Nappe), the Dinaric-directed faults are also important: the Paleodivača, Raša, Belsko (Placer et al., 2021) and Idrija faults. The Paleodivača Fault represents the primary structure of the Divača Splay Faults (Fig. 7). Both terms in this article are mentioned in the geological literature for the first time, but we address them only to the extent that it is necessary for a complete presentation of the Sistiana Bending Zone.

All faults are bent in the Sistiana Bending Zone, except that their bending angles are different. The Paleodivača and Idrija faults are bent as much as their bearing units, in the first case the Trieste-Komen Anticlinorium, and in the second, the Trnovo Nappe opposite the Hrušica

Nazoren dokaz manjšanja bočnega upogiba od jugozahoda proti severovzhodu daje spremembu azimuta tistih struktur v severozahodnem krilu sesljanske upogibne cone, ki so prvotno imele dinarsko smer (sl. 6). Azimut slemenitve plasti v Sesljanskem zalivu znaša okoli  $270^\circ$  (točka 1), liburnijskih plasti v severovzhodnem krilu tržaško-komenske antiforme znaša okoli  $285^\circ$  ( $a_2$ , točka 2), azimut osi severozahodnega in osrednjega dela Vipavskega sinklinorija, ki ga določa os sinklinale iz flišnih apnenih peščenjakov in breč na območju Planine, znaša približno  $290^\circ$  (c, točka 3), azimut smeri čela Trnovskega pokrova znaša  $295^\circ$  ( $b_2$ , točka 4). Linearen odnos med točkami kaže na ustrezno zakonitost.

Sinklinala flišnih apnenih peščenjakov in breč na območju Planine v osi Vipavskega sinklinorija (Planinska sinklinala) je v celoti horizontalno zasukana skupaj s severozahodnim krilom sinklinorija, čeprav sega preko osi sesljanske upogibne cone. Paket apnenčevih peščenjakov in breč je v najmočnejšem delu debel več 100 m in predstavlja vložek slabo duktilne kamninske mase v flišnih plasteh visoke duktilnosti. V upogibni coni se ni usločil temveč togo zasukal. To je bilo mogoče zato, ker vpada os Planinske sinklinale proti zahodu-severozahodu in leži pretežni del njegove mase v zasukanem krilu upogibne cone. Ta prispevek je posvečen regionalnemu pomenu sesljanske upogibne cone, zato smo na vprašanje »anomalne lege« paketa debelezrnatih flišnih klastitov v Planinski sinklinali le opozorili. Razlike v duktilnosti kamnin imajo pomembno vlogo v strukturni in geomorfološki analizi istrskega potisnega območja.

### **Deformacije prelomov dinarske smeri**

Poleg opisanih enot, ki so nastale v obdobju narivanja (Tržaško-Komenski antiklinorij in Vipavski sinklinorij ter Trnovski in Hrušički pokrov), so pomemben označevalec upogiba tudi dinarsko usmerjeni prelomi: Paleodivaški, Raški, Belski (Placer in sodelavci, 2021) in Idrijski prelom. Paleodivaški prelom predstavlja primarno strukturo divaškega snopa prelomov (sl. 7). Oba pojma sta v tem članku prvič omenjena v geološki literaturi, vendar ju obravnavamo le toliko, kolikor je potrebno za celovito predstavitev sesljanske upogibne cone.

Vsi omenjeni prelomi so v sesljanski upogibni coni upognjeni, le da je njihov kot upogiba različen. Paleodivaški in Idrijski prelom sta upognjena toliko kot njuni nosilni enoti, v prvem primeru Tržaško-Komenski antiklinorij, v drugem Trnovski pokrov nasproti Hrušičkemu. Raški

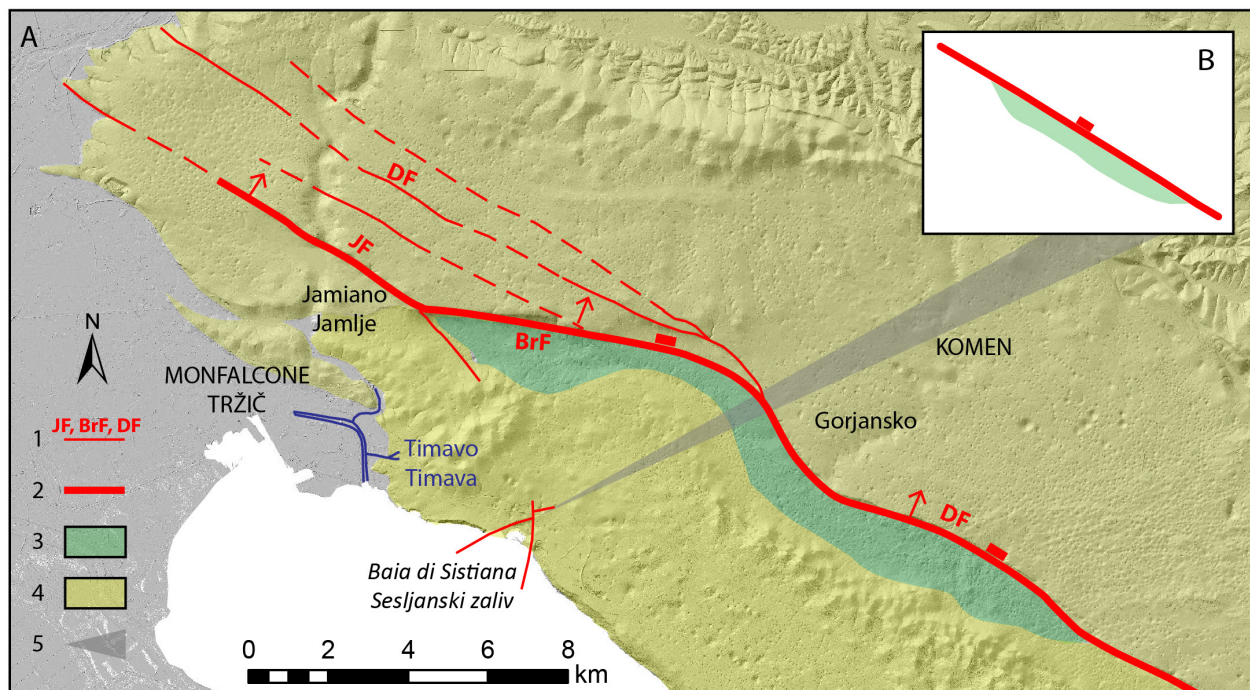


Fig. 7. Paleodivača Fault. Geological bases after Jurkovšek (2010). A. Recent structure. Divača splay of faults; B. Undeformed primary position of the Paleodivača Fault.

Sl. 7. Paleodivački prelom. Geološka osnova po Jurkovšek (2010). A. Sedanja zgradba. Divački snop prelomov; B. Nediformirana prvotna lega Paleodivačkega preloma.

1 Divača splay of faults / divački snop prelomov: JF – Jamiano Fault / Jameljski prelom, BrF – Brestovica Fault / Brestoviški prelom, DF – Divača Fault / Divački prelom

2 Paleodivača Fault, recent structure / Paleodivački prelom, sedanja lega

3 Brje Formation (Early Cretaceous), the oldest unit of the Trieste-Komen Anticlinorium / Brska formacija spodnjekredne starosti. Najstarejše plasti Tržaško-Komenskega antiklinorija

4 Povir Formation and younger units (Late Cretaceous, Paleocene and Eocene) / Povirska formacija in mlajše plasti zgornjekredne, paleocenske in eocenske starosti

5 Sistiana Bending Zone / sesljanska upogibna cona

Nappe. The Raša Fault is less bent than the Trieste-Komen Anticlinorium and the Vipava Synclinorium. The relationship in the Belsko Fault is different because it is related to the deformation of Nanos, but an interpretation of this case would require special discussion, so it is not discussed further here.

The term Divača Fault Splay is based on the data of the Geological map of the Northern part of the Trieste-Komen Plateau 1: 25,000 (Jurkovšek, 2010; Jurkovšek et al., 2013), where a group of dislocations accompany the Divača Fault. Their genesis has been linked to several kinematic phases, which are not the subject of this article. Only the initial formation of the splay, whose central element was the Paleodivača Fault, is relevant. Figure 7A depicts the current shape of the splay, consisting of the Divača Fault, the Brestovica Fault, the Jamiano Fault, the faults between the Divača and Jamiano faults that lean on the Brestovica Fault, and the accompanying faults that extend to the Divača Fault in its northeastern block.

prelom je upognjen manj od Tržaško-Komenskega antiklinorija in Vipavskega sinklinorija. Pri Belskem prelomu je odnos drugačen, ker je povezan z deformacijo Nanosa, vendar bi razlagata tega primera zahtevala posebno razpravo, zato ga puščamo ob strani.

Termin divački snop prelomov je postavljen na podlagi podatkov Geološke karte severnega dela Tržaško-Komenske planote 1: 25.000 (Jurkovšek, 2010; Jurkovšek in sodelavci, 2013), po kateri spremišča Divački prelom skupina dislokacij. Njihova geneza je bila povezana z več kinematskimi fazami, kar pa ni predmet tega članka, pomembna je le izhodiščna oblika snopa, katere središčni element je bil Paleodivački prelom. Na sliki 7A je narisana današnja oblika snopa, ki ga sestavlja Divački prelom, Brestoviški prelom, Jameljski prelom, prelomi med Divačkim in Jameljskim prelomom, ki se naslanjajo na Brestoviški prelom, in prelomi, ki spremiščajo Divačkega v njegovem severovzhodnem krilu. Trase vseh teh so jasno vidne na digitalnem modelu reliefsa iz lidarskih

Traces of all these faults are clearly visible on the digital terrain model based on lidar data. The Paleodivača Fault is now deformed in the splay and connects the Divača Fault branch southeast of Gorjansko, the Brešovica Fault, and the Jamiano Fault branch northwest of Jamlje. During the formation, the fault plane was straight (Fig. 7B) and its north block was subsided, so that the units of the Brje Formation in the southern block met the units of the Sežana Formation in the northern block. The originally straight surface of the Paleodivača Fault is today bent in the Sistiana Bending Zone, together with the Trieste-Komen Anticlinorium.

The bending of the Paleodivača Fault is equal to the bending of the Trieste-Komen Anticlinorium. The Raša Fault cuts the northeastern part of the Trieste-Komen Anticlinorium and the western part of the Vipava Synclinorium (Figs. 2 and 5). If we ignore its genesis and look only at its relation to the Sistiana Bending Zone, three peculiarities are important:

1. In the Sistiana Bending Zone, the fault line is curved, but not as pronounced as the Trieste-Komen Anticlinorium.
2. Shear lenses, which are bounded by the Tomačevica, Kobjeglava, and Lukovica faults, along with some minor ones (Figs. 5 and 8A), are present in the bending zone. We can conclude that the three faults were formed due to the tendency to straighten the curved shear plane of the Raša Fault.
3. The Tomačevica, Kobjeglava, and Lukovica faults are also bent in the Sistiana Bending Zone, but the bending is not so pronounced, so it can only be considered an assumption.

The Tomačevica, Kobjeglava, and Lukovica faults represent secondary faults that are arranged in a series of strike-slip duplexes. Their peculiarity is that they were not formed according to the standard models of the development of the fault zone, but after lateral bending of the strike-slip fault plane. During the subsequent strike-slip, the resistance due to the bulge of the bent surface is counterbalanced by the formation of one or more faults forming one or more fault lenses with the principal fault plane. The resulting faults reflect the tendency to flatten the shear plane or zone, so it is more appropriate to name them in more detail. The terms fault splay, shear lenses, bend, strike-slip duplex, linkage duplex, flower structure, sidewall ripout, and ripout structure are used in the literature for the sake of similar fault geometry terminology (Swanson, 2005; Cunningham & Mann, 2007), but none of the

podatkov. Paleodivački prelom je v snopu danes deformiran in povezuje krak Divačkega preloma jugovzhodno od Gorjanskega, Brešovškega preloma in krak Jameljskega preloma severozahodno od Jamelj. Ob nastanku je bila obravnavana prelomska ploskev ravna (sl. 7B), njeno severno krilo je bilo ugrezljeno, tako da so prišle v stik kamnine Brške formacije v južnem krilu s kamninami Sežanske formacije v severnem krilu. Prvotno ravna ploskev Paleodivačkega preloma je danes upognjena v sesljanski upogibni coni skupaj s Tržaško-Komenskim antiklinorijem.

Upogib Paleodivačkega preloma je enak upogibu Tržaško-Komenskega antiklinorija.

Raški prelom seka severovzhodni del Tržaško-Komenskega antiklinorija in zahodni del Vipavskega sinklinorija (sl. 2 in 5). Če zanemarimo njegovo genezo in si ogledamo le njegov odnos do sesljanske upogibne cone, izstopajo tri posebnosti:

1. V sesljanski upogibni coni je trasa preloma ukrivljena, vendar ne tako močno kot Tržaško-Komenski antiklinorij.
2. V območju upogiba nastopajo prelomne leče, ki jih omejujejo Tomačevski, Kobjeglavski in Lukovški prelom ter nekaj manjših (sl. 5 in 8A). Iz tega izhaja sklep, da so omenjeni trije prelomi nastali zaradi težnje po izravnavi ukrivljene strižne ploskve Raškega preloma.
3. V Sesljanski upogibni coni so enako upognjeni tudi Tomačevski, Kobjeglavski in Lukovški prelom, vendar upognjenost ni izrazita, zato jo je moč obravnavati le kot domnevo.

Tomačevski, Kobjeglavski in Lukovški prelom predstavljajo sekundarne prelome, ki so razporejeni v niz strižnih dupleksov. Izstopajo po tem, da niso nastali po standardnih modelih razvoja prelomne cone, temveč po bočnem upogibu zmične prelomne ploskve. Pri ponovnem zmikanju se upor zaradi grbine upognjene prelomne ploskve uravna z nastankom enega ali več novih prelomov, ki tvorijo z glavno prelomno ploskvijo eno ali več prelomnih leč. Nastali prelomi so odraz težnje po izravnavi strižne ploskve ali cone, zato jih je smiselnoločneje poimenovati. V literaturi se za po videzu podobno geometrijo prelomov uporabljam izrazi snop prelomov (fault splay), strižne leče (shear lenses), prevoj (bend), zmični dupleks (strike-slip duplex), povezovalni dupleks (linkage duplex), pahljačasta struktura (flower structure), stranski izriv (sidewall ripout) in izrivna struktura (ripout structure) (Swanson, 2005; Cunningham in Mann, 2007), vendar nobeden od teh izrazov in pojmov, ki jih opisujejo, ne definira opisanega primera sekundarnih prelomov

terms and the phenomena they describe define the presented example of secondary faults along the Raška Fault. Therefore, we propose a new term, adjusting faults, and for the structure itself, adjusting structure. The relation of the adjusting faults to the principal fault deep in the vertical plane of the axis of the bending zone cannot be discussed without proper laboratory modeling.

The Tomačevica Fault leans asymmetrically toward the Raška Fault trace with respect to the bending zone; in the northwest the leaning angle is larger (splitting side), in the southeast it is smaller (connecting side). We assume that the difference is a result of the geometry of the stress in the bending zone, which is derived from the position of the adjusting fault (Fig. 8B). This characteristic appears in the Tomačevica Fault because it is positioned on the external boundary of the adjusting fault, while the same is not as obvious for the other two faults. This is probably because of the secondary effects, which could be inferred from the complex situation inside the Lukovica strike slip lens and slightly less inside the Kobjeglava strike slip lens. It follows that the Lukovica Fault probably formed first, then the Kobjeglava Fault, and finally the Tomačevica Fault. In contrast to the two lenses between the Tomačevica and Lukovica faults, the splitting part of the lens between the Lukovica and Raška faults is subsided, while the connecting side is uplifted, indicating the effects of dextral strike slip divergence and convergence. This feature is pronouncedly developed only in this case, which again indicates that the Lukovica adjusting fault is the oldest of the three (Fig. 8A). The regional kinematics of the Raška Fault is discussed in another article.

The example in Figure 8B shows the initial phase of the formation of the adjusting fault, with further dextral strike slip activity, dextral strike slip divergence and convergence develop, and in the final phase, the tectonic lens is included in the wider fault zone of the main fault. The development of this process beyond the scope of this article.

In the literature, there is no data to support laboratory modeling for the study of adjusting faults, so we propose a design for a method to conduct an experiment (Fig. 8C).

In the area between Dornberk and Ilirska Bistrica (about 50 km) there is evidence of dextral strike slip and vertical component of movement along the Raška fault; however, the relationship between individual components and lateral bending is not the subject of this article.

ob Raškem prelomu. Zato zanje predlagamo nov termin izravnalni prelomi (adjusting faults), za samo zgradbo pa izravnalna zgradba (adjusting structure). O odnosu izravnalnih prelomov do glavnega preloma v globini v vertikalni ravnini osi upogibne cone, ne moremo razpravljati brez laboratorijskih preizkusov.

Tomačevski prelom se glede na upogibno cono asimetrično naslanja na traso Raškega preloma; na severozahodu je kot priključka večji (odcepilna stran), na jugovzhodu je kot manjši (priključna stran). Domnevamo, da je razlika posledica geometrije napetostnega stanja v območju upogiba, ki je izpeljana iz lege izravnalnega preloma (sl. 8B). Ta značilnost izstopa pri Tomačevskem prelому, ker leži na zunanjji meji izravnalnega snopa, medtem ko pri ostalih dveh ni tako očitna. Verjetno zaradi drugotnih vplivov, na kar bi bilo mogoče sklepati po zapletenih razmerah znotraj lukovške zmične leče in nekoliko manj znotraj kobjeglavske. Iz tega sledi, da je verjetno najprej nastal Lukovški, nato Kobjeglavski in nazadnje Tomačevski prelom. V nasprotju z lečama med Tomačevskim in Kobjeglavskim ter Kobjeglavskim in Lukovškim prelomom je odcepilna stran leče med Lukovškim in Raškim prelomom ugreznjena, priključna pa dvignjena, oboje kaže na učinek desnozmične divergencije in konvergenčije. Pojav je izraziteje razvit le v tem primeru, kar ponovno kaže na to, da je Lukovški izravnalni prelom najstarejši (sl. 8A). O regionalni kinematiki Raškega preloma bo tekla razprava v drugem članku.

Primer na sliki 8B prikazuje inicialno fazo nastanka izravnalnega preloma, pri nadalnjem desnem zmikanju se razvijeta desnozmična divergenca in konvergenca, v končni fazi pa se obprelomna leča vključi v širšo prelomno cono vodilnega preloma. Razvoj tega procesa ne sodi v okvir pričajočega članka.

V literaturi ni podatkov o usmerjenih laboratorijskih preizkusih o nastanku izravnalnih prelomov, zato podajamo predlog izdelave preizkusnega vzorca in način izvedbe eksperimenta (sl. 8C).

Na prostoru med Dornberkom in Ilirsko Bistrico (okoli 50 km) obstajajo dokazi za desnozmično in vertikalno komponento premika ob Raškem prelomu. Razmerje med posameznimi komponentami in bočnim upogibanjem ni predmet tega članka.

Pri interpretaciji izravnalne zgradbe Raškega preloma, se postavlja zanimivo vprašanje nastanka spremljajočih prelomov Idrijskega preloma kot so prikazani na Geološki karti

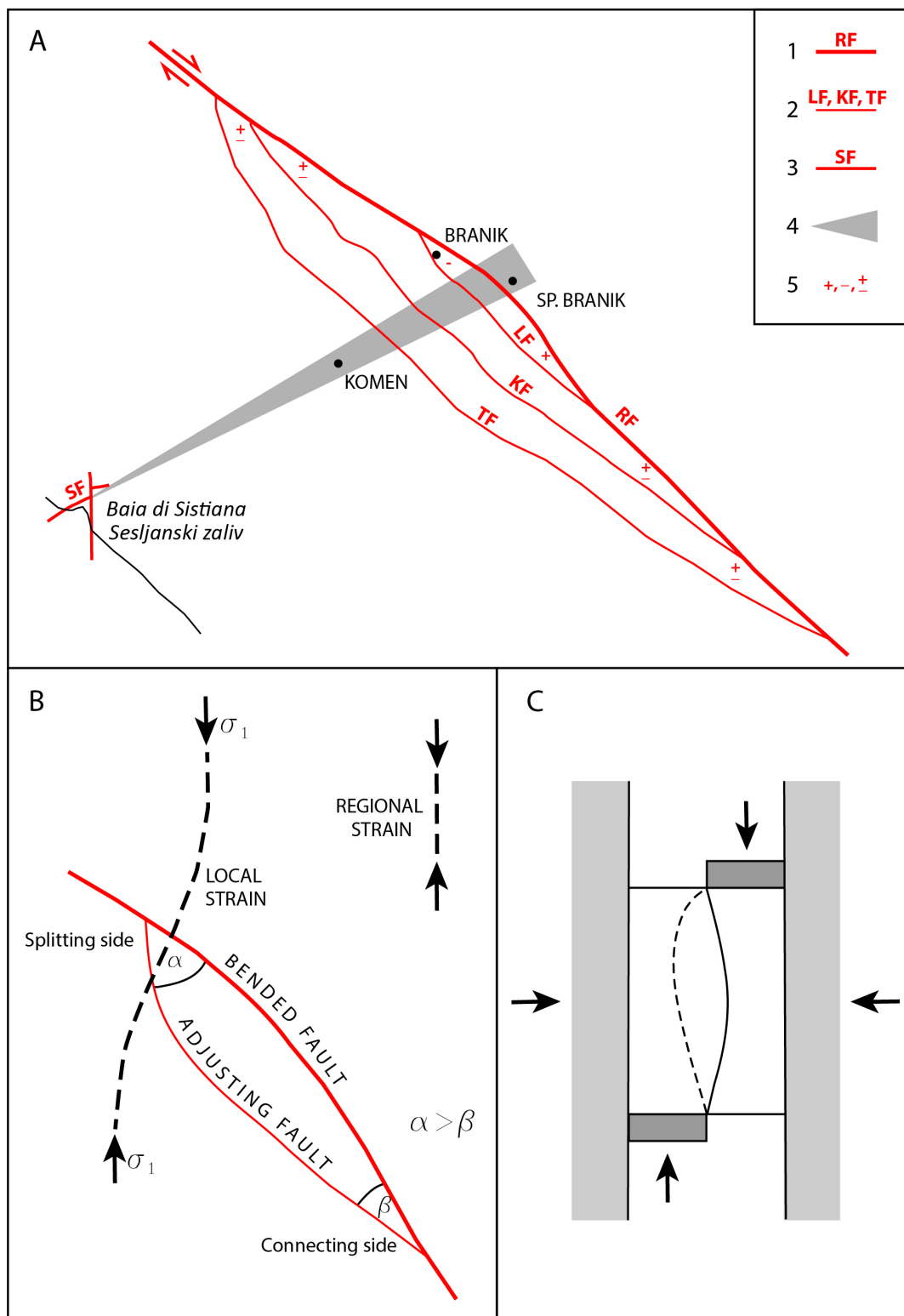


Fig. 8. Origin of the adjusting faults. A. Adjusting structure of the Raša Fault. Geological bases after Jurkovšek (2010) and Placer (2015); B. Dynamic model, initial phase; C. Laboratory modeling proposal.

Sl. 8. Nastanek izravnalnih prelomov. A. Izravnalna zgradba Raškega preloma. Geologija po Jurkovšek (2010), Placer (2015); B. Dinamski model, inicialna faza; C. Predlog laboratorijskega preizkusa.

1 Raša Fault / Raški prelom

2 Adjusting structure of the Raša Fault, adjusting faults / izravnalna zgradba Raškega preloma, izravnalni prelomi: TF – Tomačevica Fault / Tomačevski prelom, KF – Kobeglava Fault / Kobeglavski prelom, LF – Lukovica Fault / Lukovški prelom

3 SF – Sistiana Fault / Sesljanski prelom

4 Sistiana Bending Zone / sesljanska upogibna cona

5 Uplift, subsidence, negligible vertical displacement / dvig, ugrez, neznaten vertikalni premik

In interpreting the adjusting structure of the Raša Fault, an interesting question arises related to the occurrence of the accompanying faults of the Idrija Fault, as represented on the Geological map of the Idrija-Cerkno Hills between Stopnik and Rovte 1: 25.000 (Mlakar & Čar, 2009). Zala and Podgriže Fault are shown in Figure 5. The analogy with the Raša Fault is obvious, as the difference in size and the fact that the adjusting structure of the Idrija Fault indicate a greater degree of development, which would mean that the Idrija Fault is older than the Raša Fault. The latter is also confirmed by the fact that the Idrija Fault is bent as much as its bearing unit (the Trnovo Nappe opposite the Hrušica Nappe), while the Raša Fault is bent less than its bearing unit (northwestern part of the Trieste-Komen Anticlinorium opposite the southeastern part).

### **Deformations of the Trieste-Komen Anticlinorium**

In addition to the bending of the major elements of the structure (Trieste-Komen Anticlinorium, Vipava Synclinorium, Trnovo Nappe opposite the Hrušica Nappe) and the adjusting structures of the bent strike slip faults (Raša Fault, Idrija Fault), there are other deformations which are directly related to the bending. The most important are the Komen Wedge Structural Step (Komen Wedge Step), the Sistiana Sigmoidal Structure (Sistiana Sigmoid), the Ermada Push-out Block, and the Sistiana Push-out Block (Fig. 9).

*Komen Wedge Structural Step.* In the digital terrain model of Spodnji Kras (Fig. 10), a small difference in the average elevation of the Karst Plateau north and south of Komen (profile A) is visible in the Komen area. There is no such difference east of there, but towards the west it gradually increases and reaches about 100 m in the profile of Ivanji Grad (profile B). There is obviously a step there, which is wedge-shaped and runs in a west-east direction between Ivanji Grad and Komen. On the southwest side of the Divača Fault, west of Ivanji Grad, the step maintains its direction and reaches the Monte Cosici Hill (113 m) above Monfalcone. In a later tectonic development, it suffered several transformations west of the Divača Fault and collapsed into several sections but retained its original direction. In this article, we are interested in the Komen Wedge Structural Step as the primary phenomenon, and which originated together with the Sistiana Bending Zone, so we do not consider later deformations. For the purposes of this paper it is enough to conclude, that upon its formation it had a distinct wedge shape

Idrijsko-cerkljanskega hribovja med Stopnikom in Rovtami 1:25.000 (Mlakar & Čar, 2009). Na sliki 5 sta zabeležena Zalin in Predgriški prelom. Analogija z Raškim prelomom je očitna, razlika je v velikosti in v tem, da kaže izravnalna zgradba Idrijskega preloma višjo stopnjo razvoja, kar bi pomenilo, da je Idrijski prelom starejši od Raškega. Slednje potrjuje tudi dejstvo, da je Idrijski prelom upognjen toliko kot njegova nosilna enota (Trnovski pokrov nasproti Hrušiskemu), Raški prelom pa manj od njegove nosilne enote (severozahodni del Tržaško-Komenskega antiklinorija nasproti jugovzhodnemu delu).

### **Deformacije Tržaško - Komenskega antiklinorija**

Poleg upogiba večjih elementov strukture (Tržaško-Komenskega antiklinorija, Vipavskega sinljinorija, Trnovskega pokrova nasproti Hrušiskemu pokrovu) in izravnalnih struktur upognjenih zmičnih prelomov (Raški prelom, Idrijski prelom), obstajajo tudi druge deformacije, ki so neposredno povezane z upogibom. Najpomembnejše so komenski klinasti strukturni prag (komenski klinasti prag), sesljanska sigmoidna zgradba (sesljanska sigmoida), izrivna gruda Grmade in sesljanska izrivna gruda (sl. 9).

*Komenski klinasti strukturni prag.* Na digitalnem modelu reliefa Spodnjega Krasa (sl. 10) je na območju Komna vidna neznatna razlika v povprečni nadmorski višini kraške uravnave severno in južno od Komna (profil A). Te razlike vzhodno od tod ni, proti zahodu pa se postopoma veča in doseže v profilu Ivanji Grad že okoli 100 m (profil B). Obstaja torej prag, ki je klinaste oblike in ima med Ivanjim Gradom in Komnom smer zahod – vzhod. Na jugozahodni strani Divaškega preloma, zahodno od Ivanjega Grada, prag zadrži smer in sega do hriba Košnik / Monte Cosici (113 m) nad Tržičem / Monfalcone. V poznejšem tektonskem razvoju je prag zahodno od Divaškega preloma doživel več transformacij in razpadel na več odsekov, vendar je zadržal prvotno smer. V tem članku nas zanima kot primarni pojav, ki je nastal skupaj s sesljansko upogibno cono, zato kasnejših deformacij ne obravnavamo. Za ta prispevek zadostuje ugotovitev, da je ob svojem nastanku imel vzhodno od Divaškega preloma izrazito klinasto obliko, zahodno od le-tega pa je danes ta spremenjena. Profila Vojščica (profil C) in Sela na Krasu (profil D) kažeta stanje po več transformacijah. Na karti sta narisana Divaški in Selski prelom (Placer, 2015).

Konica klina leži v območju sesljanske upogibne cone. Že na prvi pogled je videti, da sesljanska upogibna cona ni nastala z bočnim

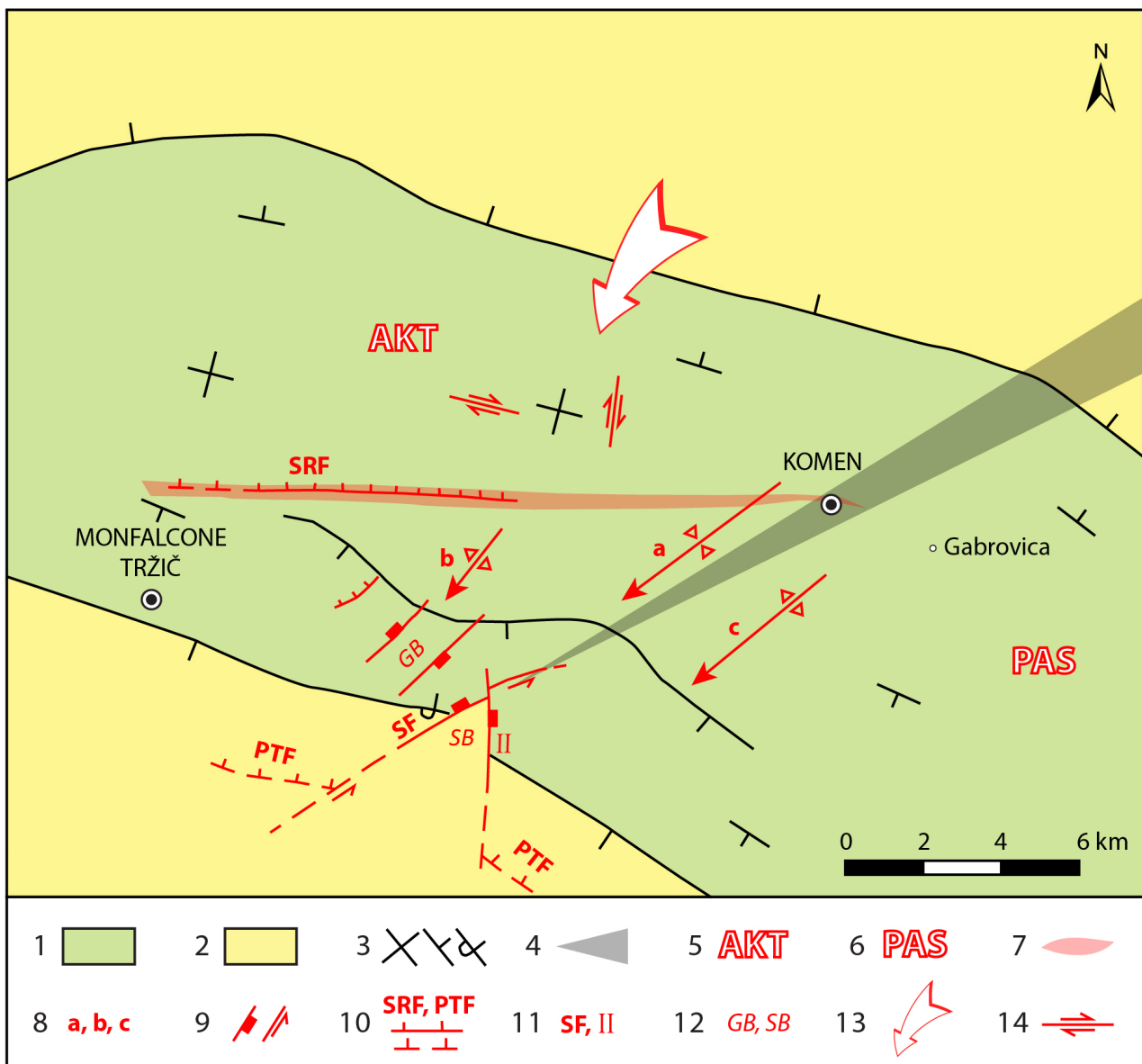


Fig. 9. Structures of the Sistiana Bending Zone in the Trieste-Komen Anticlinorium: Komen Wedge Structural Step, Sistiana Sigmoidal Structure, Monte Ermada Push-out Structure, Sistiana Push-out Block. Geological bases after Jurkovšek (2010) and Cucchi & Piano (2013), structural bases after Placer (2015).

Sl. 9. Strukture sesljanske upogibne cone v Tržaško-Komenskem antiklinoriju: komenski klinasti strukturni prag, sesljanska sigmoidna zgradba, dvignjena gruda Grmade, sesljanska dvignjena gruda. Geološka osnova po Jurkovšek (2010) ter Cucchi in Piano (2013), struktturna osnova po Placer (2015).

1 Cretaceous, Paleocene and Eocene carbonates / kredni, paleocensi in eocensi karbonati

2 Eocene Transitional marlstone and Flysch / eocensi prehodni lapor in fliš

3 Bedding: horizontal, inclined, inverse / plasti: vodoravne, poševne, inverzne

4 Sistiana Bending Zone / sesljanska upogibna cona

5 Active block of bending zone (AKT) / aktivno krilo upogibne cone

6 Passive block of bending zone (PAS) / pasivno krilo upogibne cone (PAS)

7 Komen Wedge Structural Step / komenski klinasti strukturni prag

8 Sistiana Sigmoidal Structure / sesljanska sigmoidna zgradba: a – Gorjansko Syncline / Gorjanska sinklinala, b – Brestovica Anticline / Brestoviška antiklinala, c – Brje Anticline / Brska antiklinala

9 Steep fault: sign for subsided block, relative direction of displacement / strmi prelom: oznaka ugreznjenega krila, relativna smer premika

10 Reverse fault, thrust fault / reverzni prelom, narivni prelom: SRF – Sela Reverse Fault / Selski reverzni prelom, PTF – Palmanova Thrust Fault / Palmanovski narivni prelom

11 SF – Sistiana Fault / Sesljanski prelom, II – fault no. II / prelom št. II

12 GB – Monte Ermada Push-out Block / izrivna gruda Grmade, SB – Sistiana Push-out Block / sesljanska izrivna gruda

13 Direction of external rotation of the active block of bending zone / smer eksterne rotacije aktivnega krila upogibne cone

14 Internal rotation, direction of displacement along the more important planes of the internal discontinuities / interna rotacija, smer premika vzdolž pomembnejših ploskev internih diskontinuitet

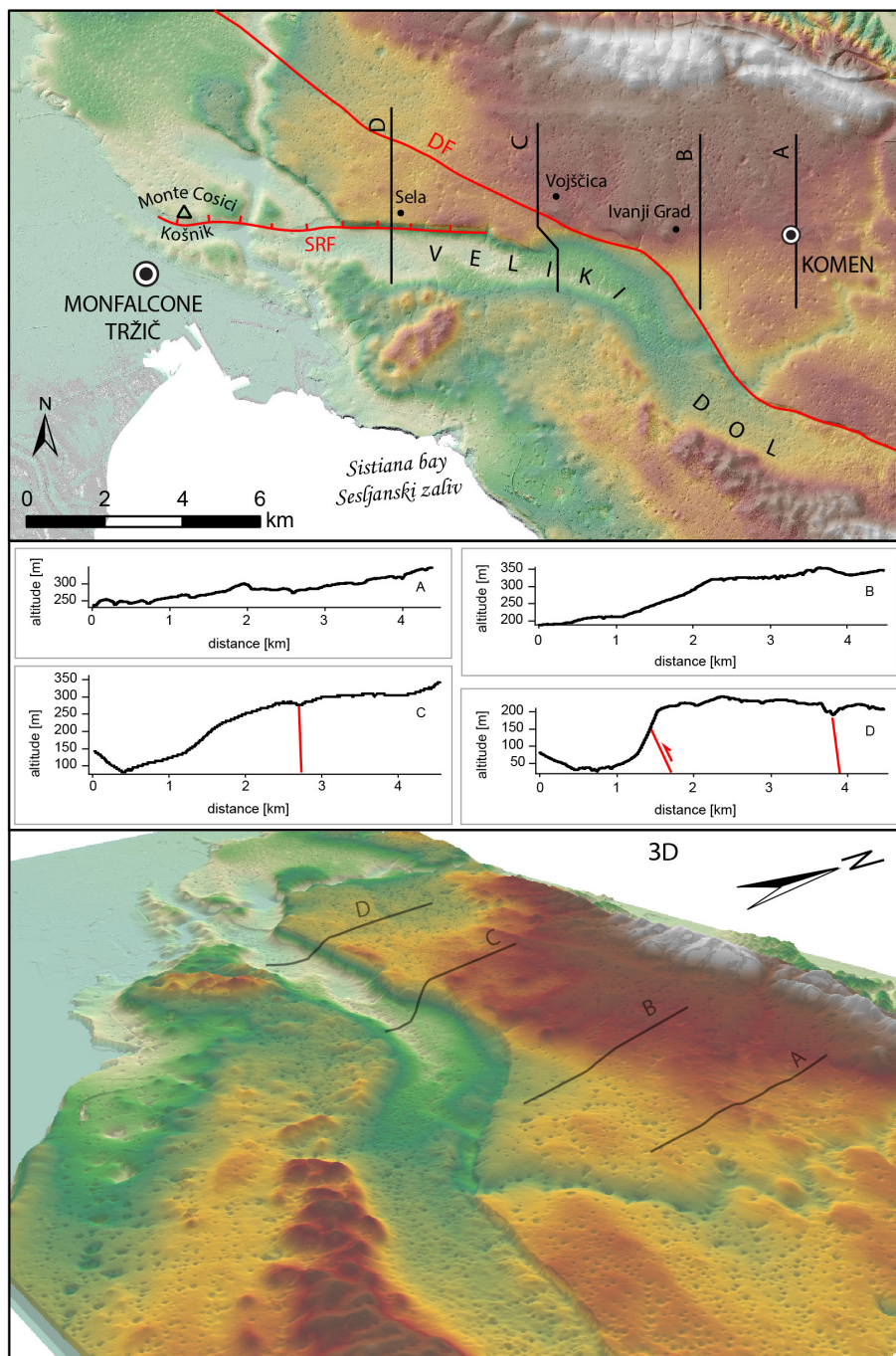


Fig. 10. Komen Wedge Structural Step. Topographic profiles.

Sl. 10. Komenski klinasti strukturi na prag. Topografski profili.

east of the Divača Fault, while west of the fault it is now modified. The profiles Vojščica (profile C) and Sela na Krasu (profile D) show the situation after several transformations. The map shows the Divača and Sela faults (Placer, 2015).

The tip of the wedge is positioned in the area of the Sistiana Bending Zone. It is apparent already upon first glance, that the Sistiana Bending Zone was not formed by a lateral bending characterized by a symmetrical structure, but by a pushing of the southeastern wing of the Sistiana Bending Zone in the northeast to east-northeast direction and a rotation of its northwest wing in a counter-clockwise direction (Fig. 9). Although

upogibom za katerega je značilna simetrična zgradba, temveč pri potisku jugovzhodnega krila sesljanske upogibne cone proti severovzhodu do vzhodu-severovzhodu in rotaciji njenega severozahodnega krila v nasprotni smeri urinega kazalca (sl. 9). Čeprav obravnavamo Tržaško-Komenski antiklinorij, je pri opisovanju dogajanja bolje uporabljali izraz antiforma, ker gre v bistvu za veliko antiklinalo dinarske smeri z blago nagnjenimi krili in subhorizontalnim ter blago nagubanim širokim jedrom. V rotirajočem krilu so se napetosti kompenzirale z internimi zdrssi po obstoječih diskontinuitetah, zato je imelo v kinematskem smislu jugovzhodno krilo

the Trieste-Komen Anticlinorium is examined, use of the term antiform is better, because it is basically a large anticline in the Dinaric direction with slightly inclined limbs and a sub-horizontal, slightly folded and broad hinge zone. In the rotating limb, the stresses were compensated by internal slips along the existing discontinuities, so in a kinematic sense the southeast wing of the bending zone played a passive role (PAS in Figs. 9 and 11) and the northwestern one an active role (AKT in Figs. 9 and 11). The rotational relaxation displacements in the active wing were compensated for by the bedding-planes, joints, and faults. According to the geological map (Jurkovšek, 2010; Cucchi & Piano, 2013), the faults take a largely Dinaric (NW-SE) direction and are sub-vertical, or they dip steeply to the northeast, while the joints are sub-vertical and run in various directions, most often in the Dinaric and N-S direction. In the limbs of the active antiform, internal slips occurred mainly along the bedding-planes and to a minor extent along other discontinuities, so that a large, apparently oblique anticline formed in the northeastern wing; and in the southwestern wing, initially, apparently oblique synclines and later several normal folds formed. We use the qualifier "apparent," because they are actually monoclinic folds. In the central part of the active limb of the antiform, where the bedding was sub-horizontal, the internal rotation could not occur along the bedding-planes but along the joints and faults instead, most easily along the sub-vertical and as perpendicular as possible to the direction of the bending zone.

upogibne cone pasivno vlogo (PAS na sl. 9 in 11), severozahodno pa aktivno (AKT na sl. 9 in 11). Razbremenilne premike rotacije v aktivnem krilu so prevzele lezike, razpoke in prelomi. Slednji so po podatkih geološke karte (Jurkovšek, 2010; Cucchi in Piano, 2013) imeli večinoma dinarsko smer NW-SE in bili subvertikalni ali vpadali strmo proti severovzhodu, razpoke so bile subvertikalne in imele različne smeri, pogoste so zlasti v dinarski smeri in v smeri N-S. V krilih aktivne antiforme so se interni zdrsi dogajali predvsem po lezikah in manj po drugih diskontinuitetah, tako je v severovzhodnem krilu nastala obsežna navidezna poševna antiklinala, v jugozahodnem krilu pa najprej navidezna poševna sinklinala, pozneje pa več normalnih gub. Navidezna zato, ker gre za monoklinalni gubi. V osrednjem delu aktivnega krila antiforme, kjer so bile plasti subhorizontalne, pa se interna rotacija ni mogla dogajati po lezikah temveč po razpokah in prelomih, najlažje po tistih, ki so bile subvertikalne in čim bolj pravokotne na smer upogibne cone.

Poenostavljeni kinematski model komenskega klinastega strukturnega praga je prikazan na sliki 11. Bistven pogoj za njegov nastanek so bile subhorizontalne plasti v jedru Tržaško-Komenskega antiklinorija in razbremenitev ob Selskem reverznem prelomu, ki je nastal v fazi narivanja in ne sega do sesljanske upogibne cone, temveč se izklini že okoli 8 km prej (sl. 9 in 10). Prelom je bil torej inicialna struktura po kateri je prišlo do reaktiviranja reverznega premika. Poleg reverzne je morala, v skladu s pravilom interne

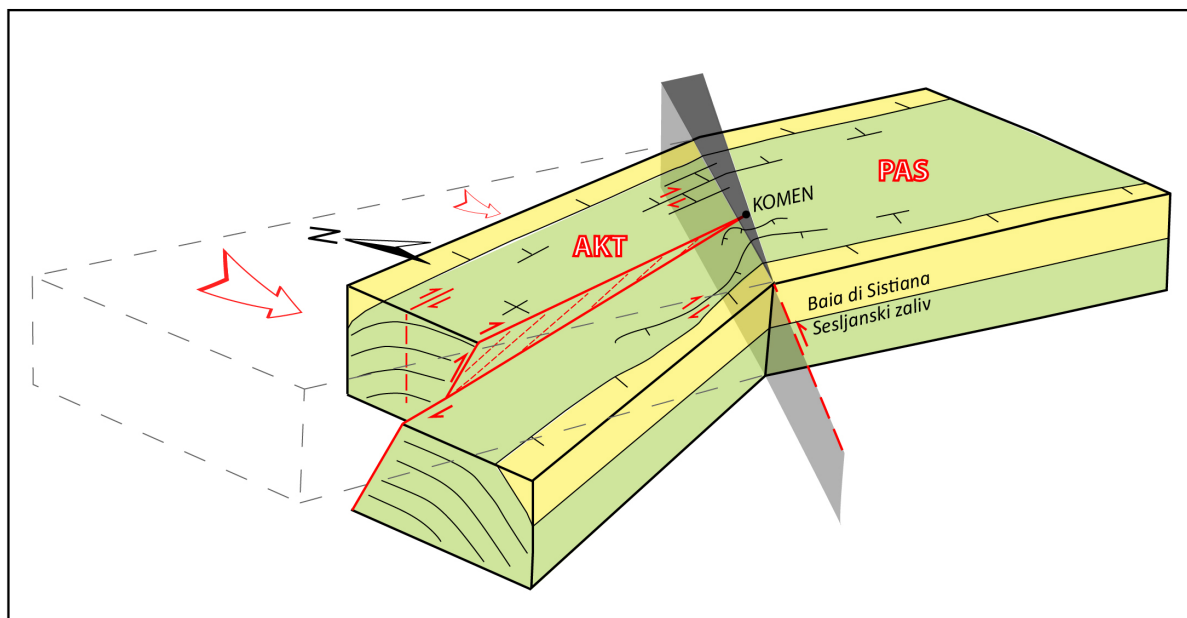


Fig. 11. Kinematic model of the Komen Wedge Structural Step. Legend in Fig. 9.

Sl. 11. Kinematski model komenskega klinastega strukturnega praga. Legenda na sl. 9.

The simplified kinematic model of the Komen Wedge Structural Step is represented in Figure 11. The necessary prerequisite for its formation is the sub-horizontal bedding at the core of the Trieste-Komen Anticlinorium and the relaxation along the Sela Reverse Fault, which formed during the thrusting phase and does not reach as far as the Sistiana Bending Zone, but pinches-out some 8 km before (Figs. 9 and 10). The fault was therefore the initial structure along which the reverse displacement was reactivated. In addition to the reverse component, according to the internal rotation rule there must also be a weak right-lateral displacement component present. Instead of a reverse displacement, a flexure was formed to the east of the area, where the Sela Fault pinches-out, which shallowed in the eastward direction and disappeared at Komen on the axis of the Sistiana Bending Zone (Figs. 10 and 11). The formation of a wedge structural step is therefore the result of the rigidity of the central part of the antiform and the limited folding possibilities. It is clear from the geometry of the wedge structural step that its pronounced shape is developed only in its eastern part near the bending zone, while towards the west it is diminished or subjected to secondary processes.

Before the formation of the Komen Wedge Structural Step there were other existing faults other than the Sela Fault that were not reactivated. This is probably because the Sela Fault formed as a reverse fault and reactivated as such, while others, especially those in the Divača Fault Splay, formed as normal faults. As a result, greater friction was created due to the changed kinematics in their fault planes.

*Sistiana Sigmoidal Structure.* The north and south slopes of the Trieste-Komen antiform are deformed in different ways in the active wing of the bending zone. In the first case the bending was unimpeded, while in the second the area was confined. The Gorjansko Syncline formed here first as an apparent fold, and then from its limbs as the Brestovica Anticline in the northwestern and as the Brje Anticline in the southeastern wing of the bending zone, both of which were normal flexural folds. This is inferred from the fact that all three folds form a characteristic sigmoidal structure (Figs. 9 and 11). The Brje Anticline in the passive wing of the bending zone is less distinct than the Brestovica Anticline in the active wing. The folded area was mapped by Jurkovšek (2010), the folds were spatially determined by Placer (2015), and the names of folds were defined in this article.

The Gorjansko Syncline is integrated into the structure of the wedge structural step, so it must

rotacije, obstajati tudi šibka desna horizontalna komponenta. Vzhodno od območja, kjer se Selski prelom izklini, je namesto reverznega premika nastala fleksura, ki se je proti vzhodu plitvila in pri Komnu izklinila v osi sesljanske upogibne cone (sl. 10). Nastanek klinastega praga je torej posledica togosti osrednjega dela antiforme in omejene možnosti gubanja. Iz geometrije klinastega praga izhaja, da ima izrazito klinasto obliko le njegov vzhodni del v bližini upogibne cone, proti zahodu pa se ta izgubi, oziroma je bila podvržena sekundarnim procesom.

Pred nastankom komenskega klinastega praga, so poleg Selskega preloma obstajali tudi drugi prelomi, ki pa niso bili reaktivirani. Vzrok tiči verjetno v tem, da je Selski prelom nastal kot reverzni in se kot tak reaktiviral, medtem ko so drugi, zlasti tisti v divaškem snopu prelomov, nastali kot normalni prelomi. Zaradi tega je bilo trenje ob spremenjeni kinematiki v njihovih prelomnih ploskvah večje.

*Sesljanska sigmoidna zgradba.* Severno in južno krilo Tržaško-Komenske antiforme je v aktivnem krilu upogibne cone različno deformirano. V prvem primeru je bil upogib neoviran, v drugem je bil prostor utesnjen. V utesnjenem delu je nastala najprej Gorjanska sinklinala, ki je bila zasnovana kot navidezna guba, nato pa iz njenih kril izhajajoči Brestoviška antiklinala v severozahodnem in Brska antiklinala v jugovzhodnem krilu upogibne cone, ki sta bili normalni fleksivni gubi. Na to sklepamo po tem, da tvorijo vse tri gube značilno sigmoidno zgradbo (sl. 9 in 11). Brska antiklinala v pasivnem krilu upogibne cone je manj izrazita od Brestoviške v aktivnem krilu. Območje gub je kartiral Jurkovšek (2010), prostorsko jih je izločil Placer (2015), poimenovane pa so bile v tem članku.

Gorjanska sinklinala je vključena v zgradbo klinastega praga, zato je morala biti zasnovana, ali celo nastati, pred začetkom njegove rasti. Če odnos Gorjanske sinklinale razširimo na celotno sigmoidno zgradbo, je klinasti prag moral nastati v zrelem obdobju razvoja sigmoidne zgradbe.

*Izrivna gruda Grmade.* Pomemben element Brestoviške antiklinale so prelomi v smeri SW-NE severozahodno od Sesljanskega zaliva, ki ležijo v njenem apikalnem delu. Tip gube, prelomi in morfologija tega območja kažejo na dve fazi razvoja, v prvi je nastala guba, ki ima komponente fleksivnega gubanja v drugi fazi pa je prišlo zaradi nezmožnosti nadaljnega gubanja do izrivov posameznih blokov med prelomi vzporednimi osni ravnini gube, za katere domnevamo, da so se regenerirali po conah razpoklinskega

have its roots, or was even formed, before it began to evolve. If we extend the Gorjansko Syncline relation to the entire sigmoidal structure, the wedge structural step must have originated during the mature period of the sigmoidal structure's development.

*Ermada Push-out Block.* The SW-NE directed faults northwest of the Sistiana Bay, which are positioned in its apical part, are important elements of the Brestovica Anticline. The type of fold, faults, and morphology of the area indicate two stages of evolution: the first is the formation of the fold, with components of flexural folding; and in the second stage, due to the impossibility of further folding, the individual blocks between the faults, parallel to the fold axis plane and presumably regenerated along the zones of fissure cleavage, were pushed out. In this way, a ridge of Ermada was formed between Ermada (323 m) and Ter (284 m), as well as some reverse faults (Fig. 9). Without detailed analysis, however, it is not possible to determine whether the two phases of evolution took place consecutively or periodically. The vertical displacement is inferred from the relief itself, while the strike-slip displacement interpreted by Cucchi & Piano (2013) is based on an apparent horizontal movement.

*Sistiana Push-out Block.* Its formation is described in the description of the structure of Sistiana Bay in the chapter on the Sistiana Fault (Figs. 3 and 9).

*Deformation sequence.* Based on the relationship between the four structures of the Sistiana Bending Zone in the Trieste-Komen Anticlinorium, we can conclude the following:

1. The sigmoidal structure began to form before the Komen Wedge Structural Step.
2. The Komen Wedge Structural Step formed due to the limited possibility of contraction of the area in the sigmoidal structure and due to the rigidity of the central part of the anticlinorium.
3. The Komen Wedge Structural Step was formed after the formation of the level surface of the Trieste-Komen Anticlinorium.
4. The Grmada Push-out Block and one or two smaller blocks in the vicinity are the result of extreme contraction in the area of a sigmoidal structure.
5. The Sistiana Push-out Block is positioned along the Sistiana Fault. Its formation is related to the corresponding joint-fault framework and rotation of the active wing of the Sistiana Bending Zone.

klivaža. Tako je nastal greben Grmade med Grmado / Ermada (323 m) in Terom (284 m) ter nekaj reverznih prelomov (sl. 9). Ali sta obe fazi potekali zaporedoma ali s prekinjivo, brez podrobne analize ni mogoče ugotoviti. Da gre za vertikalno izrivanje kaže sam relief, interpretacija Cucchi-ja in Piano-ve (2013) z zmikanjem sloni na navideznem horizontalnem premiku.

*Sesljanska izrivna gruda.* Opis njenega nastanka je podan pri opisu zgradbe Sesljanskega zaliva v poglavju o Sesljanskem prelomu (sl. 3 in 9).

*Zaporedje deformacij.* Na podlagi razmerja med omenjenimi štirimi strukturami sesljanske upogibne cone v Tržaško-Komenskem antiklinoriiju lahko sklenemo naslednje:

1. Sigmoidna zgradba je pričela nastajati pred komenskim klinastim pragom.
2. Komenski klinasti prag je pričel nastajati zaradi omejene možnosti krčenja prostora na območju sigmoidne zgradbe in zaradi togosti osrednjega dela antiklinorija.
3. Komenski klinasti prag je nastal po izoblikovanju uravnave na območju Tržaško-komenskega antiklinorija.
4. Izrivna gruda Grmade in ena ali dve manjši v bližini, so skrajni izraz krčenja prostora v območju sigmoidne zgradbe.
5. Sesljanska izrivna gruda leži ob Sesljanskem prelomu, njen nastanek je povezan z ustreznim razpoklinsko-prelomnim predrišom in rotacijo aktivnega krila sesljanske upogibne cone.

## Deformation sequence

From the characteristics of the Sistiana Bending Zone and its relationships with the fault deformations that cross it, we can establish a deformation sequence for the zone. The criteria for classifying faults preceding the formation of the Sistiana Bending Zone requires that they be as bent as the host tectonic unit. Such, for example, is the Paleodivača Fault, which is bent much like the Trieste-Komen Anticlinorium, and the Idrija Fault, whose bending is approximately the same as the degree of rotation of the Trnovo Nappe opposite the Hrušica Nappe.

The Raša Fault formed during the second half of the growth of the Sistiana Bending Zone, because its bending is smaller than for the Trieste-Komen Anticlinorium. After the bending and subsequent shearing, which may have been a single or multi-stage process, secondary faults of the adjusting structure formed. These, together with the main fault, may have been bent again, but no such research has been undertaken.

The associated faults of the Idrija Fault are included conditionally in the analysis; however, we can reasonably assume that they formed the same way they did at the Raša Fault. This remains an assumption due to the absence of mapping evidence of the trace of the Zala Fault and the Lome Zone towards the southeast (Fig. 5).

The morphology of the Komen Wedge Structural Step indicates that a leveled morphology prevailed before its formation. Since this is a leveled Trieste-Komen Anticlinorium, further research is required in order to open a discussion of the leveled areas inside the External Dinaric Imbricated Belt (parautochton) and their relation to the leveled areas of the External Dinaric Thrust Belt (allochthonous) and Microadria.

The Sistiana Bending Zone is an important indicator of the deformation sequence in a certain time period in a certain space after the formation of the Dinaric thrust structure. Said deformations will need to be related to deformations outside the area. The kinematic phases described in this article were formed in the following order:

1. The formation of the Sistiana Bending Zone evolved gradually in the direction of the pushing of the Istria Block towards the Dinarides. The precise direction of pushing has not yet been determined. At first, the north-western part of the Trieste-Komen Anticlinorium began to rotate, then the process gradually extended to the Vipava Synclinorium and the Trnovo Nappe. Together with these units, disjunctive deformations inside them,

## Zaporedje deformacij

Iz značilnosti sesljanske upogibne cone in njenih odnosov s prelomnimi deformacijami, ki jo prečkajo, je mogoče postaviti zaporedje deformacij tega območja. Merilo za uvrstitev prelomov v čas pred nastankom sesljanske upogibne cone je, da morajo biti enako usločeni kot tektonska enota v kateri ležijo. Tak je Paleodivački prelom, ki je enako usločen kot Tržaško-Komenski antiklinorij, in Idrijski prelom, katerega usločenost je približno tolikšna, kot znaša zasuk Trnovskega pokrova nasproti Hrušičkemu pokrovu.

Raški prelom je nastal v drugi polovici rasti sesljanske upogibne cone, ker je njegova usločenost manjša od usločenosti Tržaško-Komenskega antiklinorija. Po usločitvi in ponovnem strigu, kar je bilo lahko enkratno ali večkratno dejanje, so nastali njegovi sekundarni prelomi izravnalne zgradbe. Ti bi bili skupaj z glavnim prelomom lahko domnevno ponovno usločeni, vendar raziskave v to smer niso bile opravljene.

Pridruženi prelomi Idrijskega preloma so vključeni v analizo pogojno, čeprav upravičeno domnevamo, da so nastali na enak način kot pri Raškem prelому. Vzrok je v odsotnosti dokazov kartiranja o poteku Zalinega preloma in lomske cone proti jugovzhodu (sl. 5).

Morfologija komenskega klinastega strukturnega praga kaže na to, da je pred njegovim nastankom obstajala uravnavna. Ker gre za uravnani Tržaško-komenski antiklinorij, bo pri nadalnjih raziskavah potrebno odpreti razpravo o uravnavah znotraj Zunanjedinarskega naluskane pasu (paravtohtonu) in njihovem odnosu do uravnav Zunanjedinarskega narivnega pasu (alohtonu) in Mikroadrije.

Sesljanska upogibna cona je pomemben kazalec zaporedja deformacij določenega časovnega obdobja in določenega prostora, po nastanku dinarske narivne zgradbe. Nanje bo potrebno vezati deformacije izven tega območja. V tem članku omenjene kinematske faze so nastale po naslednjem zaporedju:

1. Nastanek sesljanske upogibne cone je potekal postopoma v smeri potiskanja istrskega bloka proti Dinaridom. Natančnejsa smer potiskanja še ni določena. Najprej se je pričel upogibati severozahodni del Tržaško-komenskega antiklinorija, na kar se je proces postopoma širil na Vipavski sinklinorij in Trnovski pokrov. Skupaj s temi enotami so se sukale tudi disjunktivne deformacije znotraj le-teh od Istrsko-furianske podprivne cone do Paleodivačkega in Idrijskega preloma. Začetek nastajanja

- from the Istra-Friuli Underthrust Zone to the Paleodivača and Idrija faults, also underwent rotation. Determination of the start of the formation of the Sistiana Bending Zone could be possible with an analysis of the cave sediments in the active wing of the Sistiana Bending Zone in the Trieste-Komen Anticlinorium.
2. In conjunction with the rotation of a part of the Trieste-Komen Anticlinorium the Gorjansko Syncline, the oldest structure of the Sistiana Sigmoidal Structure, began to form.
  3. The Komen Wedge Structural Step began to form after the formation of the Gorjansko Syncline and before the formation of the Sistiana Sigmoidal Structure. The leveling of the Trieste-Komen Anticlinorium predates the Komen Wedge Structural Step.
  4. The Raša Fault formed after a relatively extended period of growth of the Sistiana Bending Zone.
  5. The Raša Fault bent in the further evolution of the bending zone. The reverse component of displacement along the fault with the uplifting NE block is likely to develop or begin to develop at this stage.
  6. An adjusting structure of the Raša Fault is formed in the right-lateral shearing conditions, which gradually includes the Lukovica, Kobjeglava, and Tomačevica faults. It is unclear whether all three adjusting faults represent three stages of bending and displacement or whether this is simply a continuous process.
  7. Assuming that the adjusting structure of the Raša Fault is bent, the bending zone started to grow again. Finally, the Sistiana Sigmoidal Structure and the Ermada Push-out Block have been fully developed. The Sistiana Push-out Block is also formed. The originally uniform Komen Wedge Structural Step assumes its present fragmented appearance, but its formation is also related to other processes.
  8. Recent dynamics is a matter of detailed geodetic surveying and proper interpretation; the position of the geodetic points would have to be based on a sound theoretical framework.

The timing of the inception or formation of the individual phases and dynamics of the events constitutes the fundamental issue of the described deformation sequence. We know only a little about this now, but we can roughly estimate the timing for the inception of the Raša right-lateral strike

sesljanske upogibne cone bi bilo mogoče določiti z analizo jamskih sedimentov aktivnega krila sesljanske upogibne cone v Tržaško-komenskem antiklinoriju.

2. Skupaj s sukanjem dela Tržaško-Komenskega antiklinorija je pričela nastajati Gorjanska sinklinala, ki je najstarejši člen sesljanske sigmoidne zgradbe.
3. Komenski klinasti strukturni prag je pričel rasti po nastanku Gorjanske sinklinale in pred dokončnim izoblikovanjem sesljanske sigmoidne zgradbe. Uravnava Tržaško-Komenskega antiklinorija je starejša od komenskega klinastega praga.
4. Raški prelom je nastal po sorazmerno daljšem obdobju rasti sesljanske upogibne cone.
5. Pri nadaljnji rasti upogibne cone se je Raški prelom usločil. V tej fazi verjetno nastane, ali prične nastajati, reverzna komponenta premika severovzhodnega krila preloma.
6. V desnotrižnih pogojih nastane izravnalna zgradba Raškega preloma, ki postopoma vključuje Lukovški, Kobjeglavski in Tomačevski prelom. Ni jasno ali trije izravnalni prelomi pomenijo tri faze upogibanja in zmikanja, ali gre za kontinuiran proces.
7. Če privzamemo domnevo, da je izravnalna zgradba Raškega preloma usločena, se po njenem nastanku prične ponovna rast upogibne cone. Do sedanjega stanja se dokončno razvije sesljanska sigmoidna zgradba in izrivni blok Grmade. Nastane tudi sesljanska izrivna gruda. Prvotno enoten komenski klinasti strukturni prag dobi sedanjo fragmentirano podobo, vendar je njegov nastanek povezan tudi z drugimi procesi.
8. Sedanje dogajanje je stvar podrobnih geodetskih meritev in ustrezne interpretacije. V ta namen je potrebno postaviti merske točke na podlagi trdnega teoretskega modela.

Temeljni vprašanji opisanega zaporedja sta čas nastanka ali nastajanja posameznih faz in dinamika dogajanja. O tem vemo v tem trenutku malo, vsaj približno pa lahko ocenimo čas nastanka Raškega desnozmičnega preloma. Ob Raškem prelому je v Ilirske Bistrici nastal pull apart-ski bazen (Placer in Jamšek, 2011), v katerem se je sedimentiral premog in nad njim okoli 100 m gline. Ta je po Osnovni geološki karti srednjepliocenske starosti (Šikić in Pleničar, 1975). Podatki so posredni, pridobljeni so bili po primerjavi prikamnin premoga iz rudarskih del v premogovniku in vrtinah, kjer niso našli fo-

slip fault. Along the Raša Fault, a pull-apart basin formed at Ilirska Bistrica (Placer & Jamšek, 2011), in which coal deposited with some 100 m of clay over the top. According to the Basic Geological Map (Šikić & Pleničar, 1975) it is of Middle Pliocene age. However, the related age-data obtained is only indirect, and was determined by comparing the host rock of the coal from mining works and boreholes free of fossils with similar strata in Istria (Petraschek, 1926/26). A *Mastodon arvenensis* was found here, whose age was used to date the basin. The age of the horizon at the lower part of the basin would be about 3.6 myr based on the International Chronostratigraphic Chart (2020/03). The fault formed earlier, probably in the Lower Pliocene or some 5 million years ago. This data is consistent with the results of the modeling of the shear heating connected with heat flow data, which indicates that displacements along the regional right-lateral strike-slip faults in southwestern Slovenia started at the beginning of the Pliocene (Caporali et al., 2013). The Raša Fault originated in the second half of the evolution of the Sistiana Bending Zone, so the onset of such is probably far older.

Moulin et al. (2016) propose activation of the right-lateral strike-slip displacement along the Raša Fault in the Early to Middle Pleistocene, and along the Idrija Fault in the Late Pliocene, based on geomorphological data for western Slovenia. In both cases, the data is valid for a particular segment, which may or may not apply to the entire fault. In addition, calculations assume that a constant average displacement velocity along the faults, which also may or may not be the case. In general, the onset of the regional phase of right-lateral strike-slip activity along the Dinaric faults is set in the beginning of the Pliocene (Vrabec & Fodor, 2006; Čar, 2010; Žibert & Vrabec, 2016).

We have shown that the Paleodivača and Idrija faults originated before the evolution of the Sistiana Bending Zone. The Belsko Fault has not been sufficiently investigated, so it is reasonable to leave it aside; it is mentioned only because it is significantly deformed in the area between the Hrušica and Trnovo Nappes in the Sistiana Bending Zone. Among the faults, only the Raša Fault originated during the growth of the bending zone; as a result, it represents a suitable subject for investigations of the dynamics of bending, right-lateral strike-slip displacements, and formation of the adjusting faults. The initiation and mechanism of the evolution of the Raša Fault is not the subject of this paper. Assuming a constant counter-clockwise rotation of the Adria Microplate (Weber et al., 2010) and the constant growth of the Istra Pushed

silov, s plastmi v Istri (Petraschek, 1926/29). Tu je bil najden *Mastodon arvenensis*, po katerem so sklepali na starost. Po današnji mednarodni časovni lestvici (2020/03) bi bile plasti spodnjega dela bazena potem takem stare okoli 3,6 milijona let. Prelom je moral nastati pred tem, verjetno v spodnjem pliocenu ali na njegovem začetku pred približno 5 milijoni leti. Ta podatek se ujema z rezultati modeliranja stržnega segrevanja prostora v povezavi s podatki toplotnega toka, ki nakazujejo, da so se premiki ob regionalnih desnozmičnih prelomih v jugozahodni Sloveniji pričeli v začetku pliocena (Caporali in sodelavci, 2013). Raški prelom je nastal v drugi polovici razvoja sesljanske upogibne cone, zato je začetek njenega nastajanja precej starejši.

Aktivacijo desnozmičnega premika ob Raškem in Idrijskem prelomu na podlagi geomorfoloških podatkov v zahodni Sloveniji, umeščajo Moulin in sodelavci (2016) za Raški prelom v spodnji do srednji pleistocen, za Idrijski prelom v zgornji pliocen. Seveda gre v obeh primerih za podatke določenega segmenta, ki morda ne velja za celotni prelom. Poleg tega temeljijo izračuni na predpostavki, da je bila povprečna hitrost premika ob prelomih ves čas enaka, kar morda ne drži. Na splošno je začetek regionalne faze desnozmične aktivnosti ob dinarskih prelomih postavljen v začetek pliocena (Vrabec & Fodor, 2006; Čar, 2010; Žibert & Vrabec, 2016).

Videli smo, da sta Paleodivački in Idrijski prelom nastala pred pričetkom rasti sesljanske upogibne cone. Belski prelom še ni dovolj raziskan, zato ga je smiseln pustiti ob strani, omenjen je le zato, ker je na prostoru med Hrušičkim in Trnovskim pokrovom, torej v območju sesljanske upogibne cone, močno deformiran. Od ostalih je med rastjo upogibne cone zanesljivo nastal le Raški prelom, ki je zato primeren za študij dinamike upogibanja, desnega zmikanja in nastajanja izravnalnih prelomov. Vzrok in mehanizem nastanka Raškega preloma ni predmet obravnave tega članka. Pri predpostavljeni konstantni rotaciji Jadranske mikroplošče v nasprotni smeri urinega kazalca (Weber et al., 2010) in konstantni rasti Istrskega potisnega območja, bi po nastanku Raškega preloma proces lahko tekel po treh kinematskih scenarijih: 1. Hkratno ukrivljanje prelomne ploskve v sesljanski upogibni coni in desno zmikanje, ki je lahko vodoravno ali poševno; ko zmikanje po glavni prelomni ploskvi ni več mogoče, nastane izravnalni prelom. 2. Izmenično ukrivljanje in zmikanje; v fazi ukrivljanja so mogoči tudi reverzní premiki. 3. Tektonska zrcala in neravne zglajene

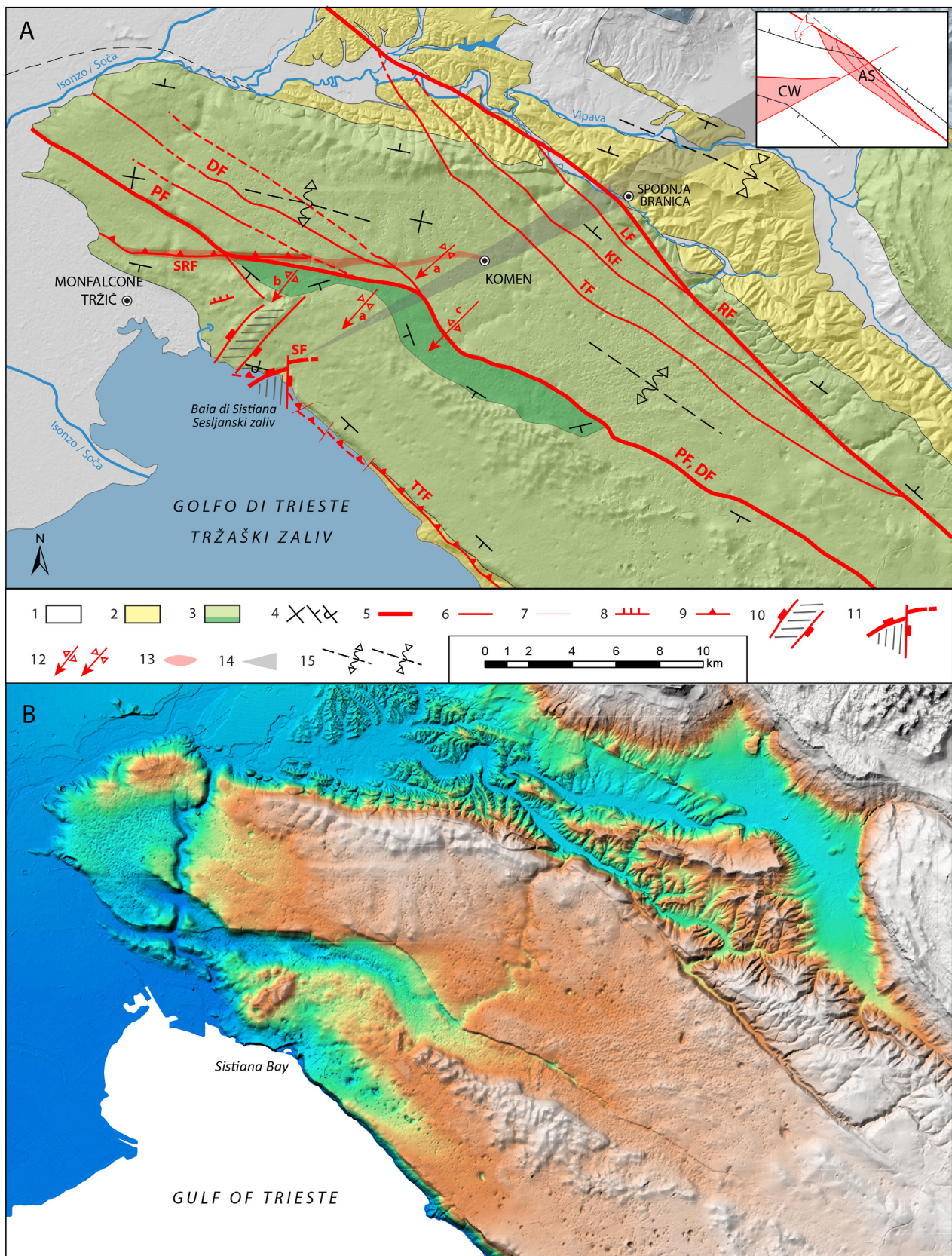


Fig. 12. DTM of the Sistiana Bending Zone. A. Structural basis after Simplified Structural-geological Map of Kras (Placer 2015). CW – Timavo Compressional Wedge; AS – Adjusting structure of the Raša Fault; B. DTM.

Sl. 12. Relief sesljanske upogibne cone. A. Strukturna podlaga po Poenostavljeni strukturno-geološki karti Krasa (Placer 2015). CW – Timavski kompresijski klin; AS – Izravnalna zgradba Raškega preloma; B. Relief.

1 Quaternary sediments / kvartarni sedimenti

2 Transitional Eocene marlstone and Flysch / prehodni eocenski lapor in fliš

Area following the initiation of the Raša Fault, the process could have evolved according to one of three kinematic scenarios: 1. Simultaneous bending of the fault plane in the Sistiana Bending Zone and horizontal or oblique right-lateral strike-slip displacement; when movement along the principal fault plane is no longer possible, the adjusting fault is formed. 2. Alternate bending and strike-slip displacement; during the bending phase, reverse displacements are also possible. 3. Tectonic mirrors and unevenly smoothed planes in the Raša Fault Zone indicate a mixed scenario, in addition to the planes with sub-horizontal and sub-vertical slickensides. This question cannot be definitively answered without a detailed investigation.

### Conclusions

Analysis of the Sistiana Bending Zone provided new insight into a certain section of the Istra Pushed Area deformation sequence and suggests the possibility of future qualitative and quantitative studies of the structure and dynamics of the northeastern part of Microadria.

The Sistiana Push-out Block, the sigmoidal structure with the Ermada Push-out Block, the Komen Wedge Structural Step, and the adjusting structure of the Raša Fault (Fig. 12) are the most prominent structural effects of the evolution of the Sistiana Bending Zone in the Trieste-Komen Anticlinorium.

The Wedge-shaped Structural Step and adjusting faults are new terms in the geological literature.

The sigmoidal structure finally evolved in the area between the Komen Wedge Structural Step and the Sistiana Bending Zone. We propose name Timavo Compressional Wedge for this particular

ploskve v coni Raškega preloma, poleg ploskev z subhorizontalnimi in subvertikalnimi drsami, kažejo na mešani scenarij. Na to vprašanje ne bo mogoče odgovoriti brez detajlnih raziskav.

### Sklepi

Analiza sesljanske upogibne cone je dala vpogled v določeni izsek zaporedja deformacij Istrskega potisnega območja in nakazala možnost nadaljnega kvalitativnega in kvantitativnega študija zgradbe in dinamike severovzhodnega dela Mikroadrije.

Najvidnejše strukturne posledice nastanka sesljanske upogibne cone v Tržaško-komenskem antiklinoriju so sesljanska izrivna gruda, sigmoidna zgradba z izrivno grudo Grmade, komenski klinasti strukturni prag in izravnalna zgradba Raškega preloma (sl. 12).

Klinasti strukturni prag opisanega tipa in izravnalni prelomi predstavljajo novosti v geološki literaturi.

Sigmoidna zgradba se je dokončno izoblikovala na prostoru med komenskim klinastim strukturnim pragom in sesljansko upogibno cono, ki ga zaradi oblike in lažjega sporazumevanja imenujemo timavski kompresijski klin. Ta predstavlja specifični strukturni objekt, ki združuje več vidikov kompresije; narivanje, gubanje, izrivanje in interne razbremenilne zdrse (sl. 12).

Sesljanska upogibna cona je nastajala dolgo obdobje, začetek njenega nastajanja je starejši od 5 milijonov let. Današnje stanje je mogoče oceniti po razmerah v Sesljanskem zalivu, kjer je Sesljanski prelom presekan s prelomom št. IV (30/80) (sl. 4) in nekaj šibkejšimi prelomi severno od tod. Zaradi tega verjetno ni več aktiven, ali pa je njegova aktivnost sekundarnega pomena. Po

Fig. 12. / Sl. 12.

3 Carbonates of Cretaceous, Paleocene, and Eocene age. Darker green Brje Formation of Early Cretaceous age, the oldest outcropping unit in the Trieste-Komen Anticlinorium / karbonati kredne, paleocenske in eocenske starosti, temnejše zeleno Brska formacija spodnjekredne starosti, najstarejše razgaljene plasti Tržaško-Komenskega antiklinorija

4 Dip of bedding / vpad plasti

5 Principal faults / glavni prelomi: RF – Raša Fault / Raški prelom, PF – Paleodivača Fault / Paleodivaški prelom, SF – Sistiana Fault / Sesljanski prelom

6 Secondary faults / drugotni prelomi: LF – Lukovica Fault / Lukovški prelom, KF – Kobjeglava Fault / Kobjeglavski prelom, TF – Tomačevica Fault / Tomačevski prelom, DF – Divača Fault (northwestern part) / Divaški prelom (severozahodni del)

7 Tear fault / raztržni prelom

8 Reverse fault in the Timavo compressional wedge / reverzni prelom v timavskem kompresijskem klinu

9 Reverse and thrust fault of the Istra-Friuli Underthrust Zone / reverzni in narivni prelom istrsko-furlanske podrivne cone: SRF – Sela Reverse Fault / Selski reverzni prelom, TTF – Trieste Thrust Fault / Tržaški narivni prelom

10 Monte Ermada Push-out Block / izrinjena gruda Grmade

11 Sistiana Push-out Block / sesljanska izrivna gruda

12 Sistiana Sigmoidal Structure / sesljanska sigmoidna zgradba: a – Gorjansko Syncline / Gorjanska sinklinala, b – Brestovica Anticline / Brestoviška antiklinala, c – Brje Anticline / Brska antiklinala

13 Komen Wedge Structural Step / komenski klinasti strukturni prag

14 Sistiana Bending Zone / sesljanska upogibna cona

15 Axis of the Trieste-Komen Anticlinorium and Vipava Synclinorium (Planina Syncline) / os Tržaško-Komenskega antiklinorija in Vipavskega sinklinorija (Planinska sinklinala)

area. This is a specific structural object that combines several aspects of compression: thrusting, folding, push-out, and internal relaxation displacements (Fig. 12).

The Sistiana Bending Zone evolved over a long period of time, which began more than 5 million years ago. The current situation in the Zone can be inferred from the situation in the Sistiana Bay, where the Sistiana Fault is cut by fault no. IV (30/80) (Fig. 4) and some less important faults further north. As a result, it is probably no longer active, or its activity is of secondary importance. By analogy, the Sistiana Fault is probably cut by faults, positioned south of fault no. IV (Fig. 3).

The rate of bending decreases gradually towards the northeast in the active wing of the Sistiana Bending Zone. The adjusting structure of the Idrija Fault is also included in the conclusions, although it is only hypothetically related to the Sistiana Bending Zone (Fig. 5). The lateral deformation of the Belsko Fault is different because of factors, which are not addressed in this article.

The direction of the Sistiana Fault offshore in the Trieste Bay is most likely indicated by the direction of the bending zone.

After describing the Sistiana Bending Zone, it is possible to execute an in-depth study of the relationship between the External Dinarides and the active Microadria.

## Reference

- Blašković, I. & Aljinović, B. 1981: Mikrotektonski elementi kao osnova za model tektonske građe šireg područja Kvarnera = Microtectonic elements as a basis for tectonic model of the broader Kvarner area. Simp. Kompleksna naftno-geološka problematika podmorske i priobalnih djelova Jadranskog mora, Split, Zbornik radova = Proceedings, 87-100, Zagreb.
- Blašković, I. 1991: Raspored uzdužnih, reversnih i normalnih rasjeda i konstrukcija oblika i dubina ploha podvlačenja = Disposition of the longitudinal, reverse and normal faults and depths of the underthrusting surfaces. Geol. vjesnik, 44: 247-256.
- Busetti, M., Volpi, V., Nicolich, R., Barison, E., Romeo, R., Baradello, L., Brancatelli, G., Giustiniani, M., Marchi, M., Zanolla, C., Wardell, N., Nieto, D. & Ramella, R. 2010: Dinaric tectonic features in the Gulf of Trieste (northern Adriatic Sea). Bollettino di Geofisica Teorica ed Applicata, 51/2-3:117-128.
- Caporali, A., Neubauer, F., Ostini, L., Stangl, G. & Zulian, D. 2013: Modeling surface GPS velocities in the Southern and Eastern Alps by finite dislocations at crustal depths. Tectonophysics, 590: 136-150.
- Carulli, G. B. & Cucchi, F. 1991: Proposta di interpretazione strutturale del Carso triestino = Proposal of geostructural interpretation of the Karst of Trieste. Atti Ticinesi di Scienze della Terra, 34: 161-166.
- Carulli, G. B. (curated by) 2006: Carta geologica del Friuli Venezia Giulia 1:150.000 = Geological map of the Friuli Venezia Giulia 1:150.000. Ed. Regione Autonoma Friuli Venezia Giulia, Direzione centrale ambiente e lavori pubblici - Servizio geologico.
- Carulli, G. B. 2011: Structural model of the Trieste Gulf: A proposal. Journal of Geodynamics, 51/2-3: 156-165. <https://doi.org/10.1016/J.JOG.2010.05.004>
- Cucchi, F. & Piano, C. (curated by) 2013: Carta geologica del Carso Classico Italiano 1:50.000. Ed. Regione Autonoma Friuli Venezia Giulia,
- analogni verjetno sekajo Sesljanski prelom tudi prelomi južno od preloma št. IV (sl. 3).
- Velikost upogiba aktivnega krila sesljanske upogibne cone se proti severovzhodu polagoma manjša. V zaključku je vključena tudi izravnalna zgradba Idrijskega preloma, čeprav je s sesljansko upogibno cono povezana hipotetično (sl. 5). Bočna deformacija Belskega preloma je drugačna zaradi dejavnikov, ki jih v tem članku nismo obdelali.
- Smer upogibne cone zelo verjetno nakazuje tudi smer Sesljanskega preloma v podmorju Tržaškega zaliva.
- Po opisu sesljanske upogibne cone je mogoče pristopiti k poglobljenemu študiju razmerja med Zunanjimi Dinaridi in aktivno Mikroadrijo.

- Direzione centrale ambiente e lavori pubblici - Servizio geologico.
- Cunningham, W. D. & Man, P. 2007: Tectonics of strike-slip restraining and releasing bends. Geological Society, London, Special Publications 2007, 290: 1-12.
- Čar, J. 2010: Geološka zgradba idrijsko-cerkljanskega hribovja. Tolmač h Geološki karti idrijsko-cerkljanskega hribovja med Stopnikom in Rovtami v merilu 1:25.000 = Geological Structure of the Idrija-Cerkno hills. Explanatory book to the Geological map of the Idrija-Cerkno hills between Stopnik and Rovte 1:25.000. Geological Survey of Slovenia, Ljubljana: 127 p.
- Historical Maps of the Habsburg Empire. The Second Military Survey (1806-1869). <http://mapire.eu/en/>
- International chronostratigraphic chart. International Commission on Stratigraphy 2020/03. [www.stratigraphy.org](http://www.stratigraphy.org)
- Jurkovšek, B. 2010: Geološka karta severnega dela Tržaško - komenske planote 1:25.000 = Geological map of the Northern part of the Trieste-Komen plateau 1:25.000. Geološki zavod Slovenije, Ljubljana.
- Jurkovšek, B., Cvetko Tešović, B., Kolar Jurkovšek, T. 2013: Geologija Krasa = Geology of Kras. Geological Survey of Slovenia, Ljubljana: 205 p.
- Makar, I. & Čar, J. 2009: Geološka karta idrijsko - cerkljanskega hribovja med Stopnikom in Rovtami 1: 25.000 = Geological map of the Idrija - Cerkno hills between Stopnik and Rovte 1:25.000. Geological Survey of Slovenia, Ljubljana.
- Moulin, A., Benedetti, L., Rizza, M., Jamšek Rupnik, P., Gosar, A., Bourles, D., et al. 2016: The Dinaric fault system: large-scale structure, rates of slip, and Plio-Pleistocene evolution of the transpressive northeastern boundary of the Adria microplate. *Tectonics*, 35/10: 2258-2292. <https://doi.org/10.1002/2016TC004188>
- Nicolich, R., Della Vedova, B. & Giustiniani, M. (eds.) 2004: Carta del Sottosuolo della Pianura Friulana = Map of subsurface structures of the Friuli Plain. Regione Autonoma Friuli Venezia Giulia.
- Osnovna geološka karta Jugoslavije (OGK) 1:100.000 = Basic geological map of Yugoslavia 1:100.000. Savezni geološki zavod, Beograd.
- Petráschek, W. 1926/29: Kohlengeologie der Oesterreichischen Teilstaaten. Katowice.
- Placer, L. 1981: Geološka zgradba jugozahodne Slovenije = Geologic structure of southwestern Slovenia. *Geologija*, 24/1: 27-60.
- Placer, L. 1994/95: O zgradbi Soviča nad Postojno = On the structure of Sovič above Postojna. *Geologija*, 37/38: 551-560. <https://doi.org/10.5474/geologija.1995.020>
- Placer, L. 2008: Principles of the tectonic subdivision of Slovenia. *Geologija*, 51/2: 205-217.
- Placer, L., Vrabec, M. & Celarc, B. 2010: The bases for understanding of the NW Dinarides and Istria Peninsula tectonics. *Geologija*, 53/1: 55-86. <https://doi.org/10.5474/geologija.2010.005>
- Placer, L. & Jamšek, P. 2011: Ilirskobistriški fosilni plaz – mesto na plazu = The Ilirska Bistrica fossil landslide – The town on the landslide. *Geologija*, 54/2: 223-228.
- Placer, L. 2015. Simplified structural map of Kras: Kras (Slovene), Carso (Italian) = Geographical unit. *Geologija*, 58/1, 89-93. <https://doi.org/10.5474/geologija.2015.008>
- Placer, L., Mihevc, A. & Rižnar, I. 2021: Tectonics and gravitational phenomena (Nanos, Slovenia) = Tektonika in gravitacijski pojavi (Nanos, Slovenija). *Geologija* 64/1, 35-63, Ljubljana. <https://doi.org/10.5474/geologija.2021.002>
- Stache, G. 1920: Nachtrag zur Geologischen Spezialkarte Görz und Gradisca 1:75.000. Geologischen Staatsanstalt, Wien.
- Swanson, M. T. 2005: Geometry and kinematics of adhesive wear in brittle strike-slip fault zones. *Journal of Structural Geology*, 27/5: 871-887. <https://doi.org/10.1016/j.jsg.2004.11.009>
- Šikić, D. & Pleničar, M. 1975: Osnovna geološka karta Jugoslavije 1:100.000 = Basic geological map of Yugoslavia 1:100.000. Tolmač / Guidebook. List / sheet Ilirska Bistrica. Savezni geološki zavod, Beograd.:44 p.
- Šikić, D. & Polšak, A. 1973: Osnovna geološka karta Jugoslavije 1:100.000 = Basic geological map of Yugoslavia 1:100.000. Tolmač / Guidebook. List Labin / sheet Labin. Savezni geološki zavod, Beograd.
- Venturini, S. 2002: Il pozzo di Cagnacco 1: un punto di taratura stratigrafica nella pianura friulana = The well Cagnacco 1: a stratigraphic reference in the Friuli plain (northeastern Italy. *Mem. Soc. Geol. It. (Roma)*, 57: 11-18.
- Vrabec, M. & Fodor, L. 2006: Late Cenozoic Tectonics of Slovenia: Structural Styles at the Northeastern Corner of the Adriatic Microplate. The Adria Microplate: GPS Geodesy, Tectonics and Hazard. NATO Science Series: IV: Earth and Environmental Sciences, 61. Dordrecht. [https://doi.org/10.1007/1-4020-4235-3\\_10](https://doi.org/10.1007/1-4020-4235-3_10)

Weber, J., Vrabec, M., Pavlovčič Prešeren, P., Dixon, T., Jiang, Y. & Stopar, M. 2010: GPS-derived motion of the Adriatic microplate from Istria Peninsula and Po Plain sites, and geodynamic implications. *Tectonophysics*, 483/3-4: 214-222. <https://doi.org/10.1016/j.tecto.2009.09.001>

Žibret, L. & Vrabec, M. 2016: Paleostress and kinematic evolution of the orogen-parallel NW-SE stricing faults in the NW External Dinarides of Slovenia unraveled by mesoscale fault-slip data analysis. *Geologia Croatica*, 69/3: 295-305. <https://doi.org/10.4154/gc.2016.30>



# Geophysical investigations in the Radovna River Spring area (Julian Alps, NW Slovenia)

## Geofizikalne raziskave na območju izvira reke Radovne (Julijanske Alpe, SV Slovenija)

Anja TORKAR<sup>1</sup>, Marjana ZAJC<sup>2</sup>, Jure ATANACKOV<sup>2</sup>, Andrej GOSAR<sup>1,3</sup> & Mihael BRENCIČ<sup>1,2</sup>

<sup>1</sup>Faculty of Natural Sciences and Engineering, University of Ljubljana, Aškerčeva c. 12, SI-1000 Ljubljana, Slovenia; e-mail: anja.torkar@ntf.uni-lj.si, mihael.bencic@ntf.uni-lj.si

<sup>2</sup>Geological Survey of Slovenia, Dimičeva ulica 14, SI-1000 Ljubljana, Slovenia;  
e-mail: marjana.zajc@geo-zs.si, jure.atanackov@geo-zs.si

<sup>3</sup>Slovenian Environment Agency, Seismology and Geology Office, Vojkova 1b, SI-1000 Ljubljana, Slovenia;  
e-mail: andrej.gosar@gov.si

Prejeto / Received 3. 11. 2021; Sprejeto / Accepted 7. 12. 2021; Objavljeno na spletu / Published online 28. 12. 2021

**Key words:** Ground penetrating radar, Seismic reflection method, Radovna spring, hydrogeology, aquifer geometry, glacial valley, groundwater table

**Ključne besede:** Georadar, refleksijska seizmika, izvir Radovne, hidrogeologija, geometrija vodonosnika, ledeniška dolina, gladina podzemne vode

### Abstract

The Radovna River Valley is located in the north-western part of Slovenia in the Julian Alps, where there is an extensive intergranular aquifer whose depth to pre-Quaternary bedrock is unknown. Therefore, to obtain information about the depth of the valley and the geometry of the aquifer two geophysical methods were used in our study; ground penetrating radar (GPR) and seismic reflection method. The low-frequency GPR method has shown to be useful for determining the depth of the groundwater and the predominant groundwater recharge. Also, the high-resolution seismic method provided an insight about the morphology of the pre-Quaternary basement with the deepest point at 141 meters below surface. Measurements of hydrogeological parameters such as groundwater level and river discharge measurements were carried out in the study area. Both data analyses showed that groundwater level and river discharge are highly fluctuating and rapidly changing, indicating a well-permeable aquifer, implying that such an aquifer is extremely sensitive and vulnerable to extreme climate events. Both the geophysical methods and the hydrogeological information have provided important information about the morphology of the valley and the alluvial aquifer, as well as increasing the knowledge about the Radovna springs system, which will contribute very important information for future hydrogeological studies.

### Izvleček

Dolina reke Radovne leži v severozahodnem delu Slovenije na območju Julijskih Alp, kjer se nahaja obsežen medzrnski vodonosnik, katerega globina do predkvartarne podlage ni znana. Zato smo v naši raziskavi za pridobitev podatkov o globini doline in geometriji vodonosnika uporabili dve geofizikalni metodi; georadar in metodo seizmične refleksije. Metoda nizkofrekvenčnega georadarja se je izkazala za uporabno pri določanju globine podzemne vode in smeri prevladajočega napajanja podzemne vode. Tudi seizmična metoda visoke ločljivosti je omogočila vpogled v morfologijo predkvartarne podlage z najglobljo točko 141 metrov pod površjem. Na območju raziskav so bile opravljene tudi meritve hidrogeoloških parametrov, kot so gladina podzemne vode in pretok v reki. Analiza obeh parametrov je pokazala, da nivo podzemne vode in rečni pretok močno nihata in se hitro spremunjata, kar pomeni, da je tak vodonosnik izjemno občutljiv in ranljiv za ekstremne podnebne dogodke. Tako geofizikalne metode kot hidrogeološki podatki predstavljajo pomembne informacije o morfološki dolini in aluvialnega vodonosnika, prav tako je znanje o sistemu izvirov Radovne večje, kar bo predstavljal pomemben doprinos pri hidrogeoloških raziskavah v prihodnje.

## Introduction

Characterization of the lithology, stratigraphic features and geometry of the aquifer is essential component of modern hydrogeological studies. Quantification of these attributes is difficult in many aquifers, especially where the aquifers consist of alluvial and glacial deposits (Bowling et al., 2007). The sediments in such aquifers consist of different grain sizes and sorting, making it difficult to adequately characterize the hydraulic properties of the aquifer through direct observations. Knowledge of the geometry of the aquifer and definition of the key geometric elements are of great importance for studying hydrogeology and water balance in particular area. The most accurate way to define the depth of the aquifer is with existing or new boreholes. The cost of several boreholes can be a limitation, as was also in our case, in addition to other characteristics of the location. The investigated area, the Radovna spring, is located in the Julian Alps (Fig. 1), inside the Triglav National Park, where traditional hydrogeological methods of investigations are difficult to apply and are restricted. In the Radovna Valley interaction between karstic and intergranular aquifers is present and this is reflected in the water dynamics and also in chemical and isotopic characteristics of the water. The fluvioglacial sediments are composed of a heterogeneous mix of fine-grained and coarse-grained materials and it is difficult to drill enough boreholes for sufficient characterization of the aquifer (McClymont et al., 2012). For these reasons, the definition of the aquifer geometry in this study has been achieved through application of non-invasive geophysical methods.

In the past several independent geological and hydrogeological studies were carried out in the Radovna Valley, but their results are not published and are mainly available in the archive of the Geological Survey of Slovenia and are in details described elsewhere (Torkar & Brenčič, 2015). The investigated area of the Radovna River system is a unique study case for its interaction between karstic and intergranular aquifers and therefore of great interest for hydrogeological studies. The area of the Radovna River is also the most important drinking water source in NW Slovenia supplying 29,700 inhabitants and studies in this area are important for future water management. Between 1960 and 1980 geological mapping was carried out with several shallow boreholes as a part of chalk exploitation in Sr. Radovna. In 1965 in the Krma Valley three boreholes were drilled for planned construction of a tourist cen-

tre with the deepest borehole at 60 m still in the alluvial sediments. Hydrogeological and geomechanical investigations were done in 1977 in the middle part of the valley for a planned but never accomplished high dam water-storage reservoir. Three boreholes were drilled, on both sides of the valley and in the central part with the maximum depth at 103 m. The borehole did not reach the pre-Quaternary basement. Recent studies are directed towards hydrogeological (Torkar & Brenčič, 2015) and hydrogeochemical investigations of water (Kanduč et al., 2012; Torkar et al., 2016) and soil (Ferjan Stanič et al., 2013).

Despite all drilled boreholes, none of the boreholes did reached the pre-Quaternary bedrock. Therefore, there is a lack of information about the depth of the valley and the geometry of the aquifer for future hydrogeological investigations. The aims of this study were to determine the position of the groundwater table and the preferred direction of water recharge using ground penetrating radar (GPR) and to determine the depth of the intergranular aquifer and to reveal the pre-Quaternary bedrock topography with seismic reflection method.

## General Settings

The Radovna spring is located in the north-western part of Slovenia in the Julian Alps in a typically U-shaped narrow glacial valley with very steep slopes. West from the Radovna Valley are glacial valleys Kot and Krma which together with considerable part of eastern Julian Alps represent the recharge area of the Radovna spring (Fig. 1). Both valleys are filled with highly permeable gravel. The altitude of the spring area is around 750 m a.s.l. and the average altitude of surrounding plateaus of Pokljuka and Mežakla are 1228 and 1106 m a.s.l. respectively. The slope of the Pokljuka plateau in the south is steeper than the slope of the Mežakla plateau in the north. The width of the Radovna River Valley varies in the upper part between 300 and 350 meters in the middle part it is around 250 meters and in the lower part it is the narrowest in the Vintgar gorge with only a few meters. The Radovna River flows almost entirely in the Triglav National Park and after its 19.4 km long course discharges into the Sava Dolinka River.

The Radovna spring is positioned in an Alpine region with an average air temperature between -8 °C in January and 23.8 °C in July taken from the meteorological station Rateče (Lat. 46.50, Lon. 13.71, altitude 864 m, 20.7 km distance from the Radovna spring). The standard 30-year

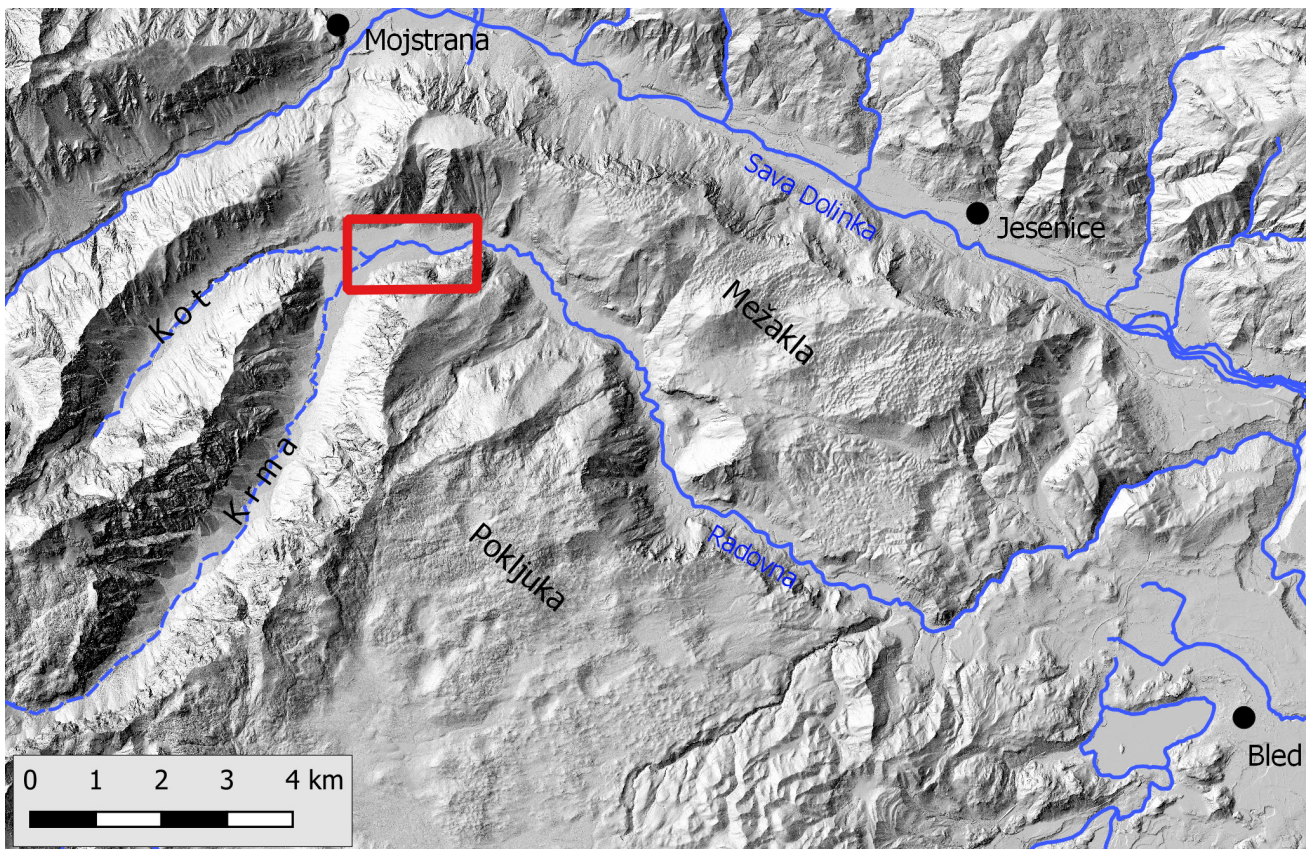


Fig. 1. Position map of the investigated area (red rectangle).

(1981–2010) average annual precipitation from the precipitation station Zg. Radovna is 1701 mm. Highest amount of precipitation falls in the autumn with an average of 584 mm and the lowest in the winter with 346 mm (Nadbath, 2012).

#### Geological and hydrogeological settings

The broader study area, which includes the western part of the Mežakla and Pokljuka plateaus, the Kot and Krma Valleys and the eastern part of the Julian Alps, consists of Triassic limestone, dolomite and dolomitized limestone. In the Radovna Valley Quaternary fluvio-glacial sediments are present and are represented by gravel, sand and partly conglomerate with interbedded lenses of clay (Buser, 1980; Jurkovšek, 1987). In the central part of the valley, chalk deposits were exploited in the past (Iskra, 1982). Chalk mixed with sand occurs also in the north-western part of the valley, where geophysical investigations were conducted. Previous borehole data indicates that the local thickness of the Quaternary sediments in the valley is more than 100 meters (Torkar & Brenčič, 2015).

The recharge area of the Radovna spring is karstified, where nearly all precipitation infiltrates into carbonate rocks and then drains into

the alluvial intergranular aquifer and partly some into the slope deposits. Groundwater in the karst-fractured aquifer and intergranular aquifer occurs in unconfined conditions. Groundwater recharge in the investigated area is very uneven, because snow is predominant form of precipitation in the winter and groundwater has limited recharge during this period. The groundwater table in the study area fluctuates for approximately 20 meters; consequently the Radovna spring changes its locations up and down the valley (up to 2 km) due to different water conditions. The estimated average hydraulic conductivity of limestone and dolomite ranges from  $10^{-5}$  to  $10^{-7}$  m/s and fluvio-glacial sediments with a wide range of average estimated permeability from  $10^{-3}$  to  $10^{-7}$  m/s.

#### Methodology

The geophysical methods used in our investigation were ground penetrating radar (GPR) and seismic reflection method. Both methods were used once on different profiles and time periods due to different purpose of research. For the additional information about the aquifer, instruments for measurements of groundwater level and river discharge were installed in the field.

## Ground penetrating radar

GPR is a non-invasive geophysical method used to investigate the shallow subsurface. Its application and operating principles have been described in various publications (e.g. Annan, 2002; Milsom, 2003; Neal, 2004; Blindow et al., 2007; Jol, 2009). High-frequency electromagnetic signals are emitted into the subsurface where they reflect from different discontinuities or structures back to the surface. The time it takes the signals to propagate from the transmitting antenna to the discontinuity and back to the receiving antenna (the so-called two-way travel time or TWT) is recorded and later converted to depth (Blindow et al., 2007; Jol, 2009). The depth range is mostly determined by the antenna frequency used, although it is also affected by other factors, such as the presence of water and clay (Jol, 2009). For the purpose of defining the depth to the water table, the GPR method has been proven useful in several studies to date (e.g. Doolittle et al., 2006; Mahmoudzadeh et al., 2012; Rejiba et al., 2012; Afshar et al., 2015; Paz et al., 2017).

For the purpose of this study, three GPR profiles were recorded (Figs. 2, 3) in October 2012 using the Malå ProEx GPR recording unit with an unshielded 50 MHz Rough Terrain Antenna (RTA). The flexible tube-like shape of this antenna allows carrying out GPR research even in the most rugged terrain (e.g. Zajc et al., 2014, 2015). It is 9.25 m long, with the distance of 4 m between the transmitter and the receiver (Malå, 2009). The design of the antenna allowed us to manoeuvre through very rough terrain in an overgrown forest, over roots and branches as well as under wires and electric fences.

The longitudinal profile R1 was recorded from the water well at the western end of the profile, which served as a control point due to the known depth of the water table, and along the slope to the location of the Radovna River springs themselves in the east. The purpose of this profile was to determine the position of groundwater table. In addition to the longitudinal profile, two transverse profiles R2 and R3 were recorded to determine whether or not there is a difference in recharge of groundwater from both surrounding plateaus, which could be seen as a slight inclination of the water table to the north or to the south. The transverse profiles also represented additional ways of checking the depth to groundwater levels at the intersections with the profile R1. Table 1 shows the basic data of the recorded GPR profiles.

In order to assure steady signal triggering with the measuring step of 0.2 m, a device containing a measuring thread was used.

In order to apply topographic corrections to GPR profiles, GNSS coordinates were recorded every 50 m along the profile lines, as well as in areas with sudden topographic changes, such as dirt roads and dry riverbeds. The x and y coordinates were used to calibrate the length of the profiles, while the z coordinate was used to determine the elevation of the terrain. During the recording of GPR profiles the locations of these control points were indicated on radargrams using markers.

Table 1. Basic data on recorded GPR profiles.

Profile	R1	R2	R3
Type	longitudinal	transverse	transverse
General direction	W → E	S → N	S → N
Profile length [m]	1070	217	354.5

## Seismic reflection profiling

High-resolution seismic reflection (HRS) method is a shallow, near-surface application of a well-established method regularly used in petroleum industry. It is based on the reflection of artificially generated seismic waves from subsurface structures. Seismic waves reflect on interfaces where the seismic impedance of the sediment or rock changes. Seismic impedance depends on density and seismic wave velocity, so rapid changes in grain size, compaction, lithification and fluid saturation cause reflection of seismic waves (Yilmaz & Doherty, 2001; Yilmaz et al., 2008). The depth range and resolution of the HRS method is not strictly defined, rather the term encompasses seismic reflection surveys down to a depth of several hundred meters. HRS is regularly used in surveys of shallow aquifers and in neotectonic research, targeting recent deformations of young sediments (e.g. Kaiser et al., 2009).

The high-resolution seismic reflection profile HRS Radovna was acquired along a gravel road crossing the Radovna valley in July 2013 (Figs. 2, 4). The active spread used 40 Hz geophones at 2 m spacing and 48 active channels, with the active spread in 'on end' geometry (Tab. 2). A 6-kg sledgehammer was used as a seismic source, stacking 4 to 10 strikes per shot point. Other seismic sources were also considered. The GISCO ESS100 accelerated weight drop, which produces

significantly higher source energy (Atanackov & Gosar, 2013) was not used due to support vehicle mechanical problems. A 12-gauge seismic shotgun was also considered, but was not used due unfavourable dry soil conditions which produces poor signal-to-noise ratio (Atanackov & Gosar, 2013).

Two linked ABEM Terraloc VI 24-channel field seismographs were used for data recording. The full length of the HRS Radovna profile is 416 m with 185 shot gathers recorded in total (Tab. 2). Recording conditions were variable and data acquisition was stopped during periods of increased noise due to traffic. Since wind was almost constantly present, data acquisition could not be limited to intervals with low torque wind.

Table 2. HRS profile Radovna data acquisition parameters.

<b>HRS profile Radovna data acquisition parameters</b>	
Length	416 m
Shot gathers	185
Active channels	48
Geophones	40 Hz
Geophone interval	2 m
Active spread length	94 m
Active spread geometry	,on end'
Offset (shot point – 1st geophone)	2 m
Seismic source	6-kg sledgehammer
Records length	812 ms
Sampling frequency	1000 Hz

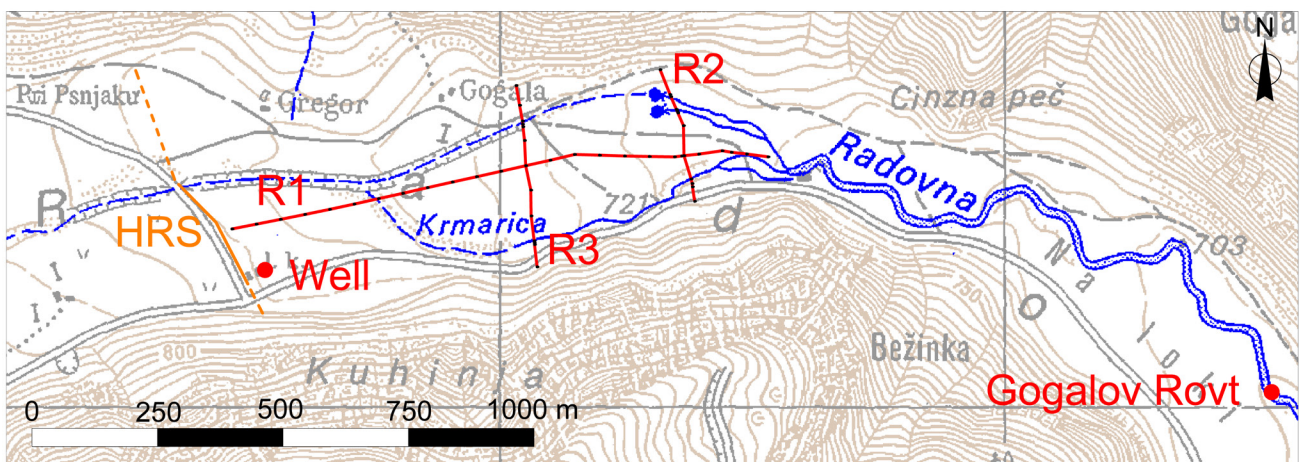


Fig. 2. Position map of seismic reflection profile HRS Radovna, GPR profiles R1, R2 and R3 and location of a well and Gogalov Rovt water level measurement station. Dashed orange line is extrapolation of the HRS profile shown in Fig. 8.



Fig. 3. Part of R1 profile in the field.

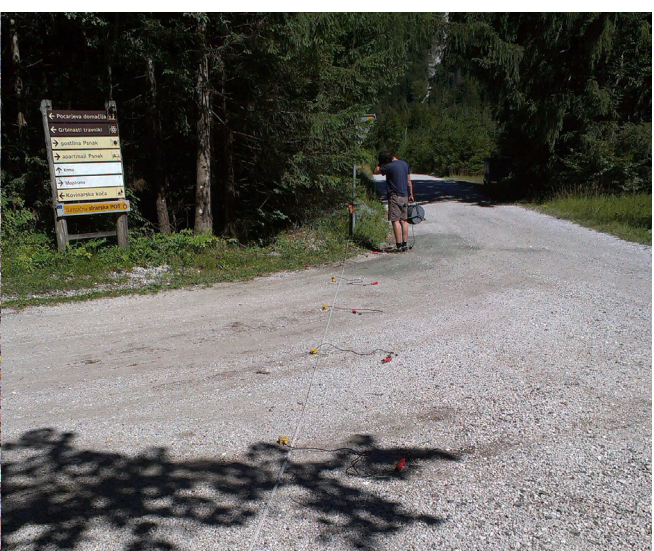


Fig. 4. Part of HRS profile in the field.



Fig. 5. The well location.



Fig. 6. The Gogalov Rovt location for measurements of river water level.

### Measurements of groundwater level and discharge

The groundwater level was measured in a hand-dug well in the hinterland of the Radovna spring (Figs. 2, 5). The depth of the well is 28 meters. The well is dry almost every winter for approximately four months due to low waters and is dry until the snowmelt in the late spring.

The Gogalov Rovt water level station is downstream from the spring, where the discharge in the stream is in one uniform channel (Figs. 2, 6). On this location the discharge is always present, except at the beginning of our investigations, in March 2012, when the climate conditions were very dry, the channel dried up. The water level in the well and at the Gogalov Rovt location was measured every hour with level data logger (Eltratec). The discharge at the Gogalov Rovt was measured with dilution method (Flo-Tracer instrument) and with hydrometric current-meter (A.OTT KEMPTEN Type C2 »10.150«) (Boiten, 2008).

Table 3. GPR processing steps.

Processing Step	Parameter
DC Removal	400 – 700 ns
Time-Zero Adjustment	First negative peak
Background Removal	Normal
Gain	Manual gain
Bandpass Filtering	Low-cut 25 MHz, lower plateau 50 MHz, upper plateau 75 MHz, high-cut 150 MHz
Topographic Correction	GNSS coordinates every 50 m

### Results and discussion

#### GPR

##### Data Processing

For the GPR data processing, the program Reflexw version 6.0.5 from Sandmeier Software was used.

The processing steps were the same for all three radargrams (Tab. 3).

Since the profiles did not contain distinctive diffraction hyperbolas necessary to determine the signal velocity, the latter was calculated based on the depth of the groundwater level measured in the well. At the time of GPR measurements, the depth of groundwater in the well was 21.8 m, which gave the signal velocity of 0.105 m/ns, corresponding to the material dielectric constant  $\epsilon=8$ . These parameters reflect the fluvio-glacial deposits of the investigated area that consist of gravel, sand and partially conglomerate and are influenced by the presence of water. The dielectric constant of dry sand is in the range of  $\epsilon=3-6$ , which is increased in our study by the presence of water (Jol, 2009).

##### GPR results

In Fig. 7 the longitudinal profile R1 is shown together with marked features used to determine the groundwater level. The black frames indicate areas where a well-expressed linear reflector can be seen. This reflector is interrupted between the 500 m and 600 m profile distance (red frame). According to the geology of the area, the reason for this could be the presence of a larger block of rock block above the groundwater. Such isolated rock blocks occur along the entire Radovna Valley and

in the nearby Krma Valley. The presence of such blocks could be the reason for greater signal attenuation, which means that the signal could not reach the groundwater level and this part of the radargram consequently does not contain a linear reflector. Another element, which was also used in the determining of the groundwater level, is the location where water was first seen on the surface. With the help of these features, the level of the water table was depicted, while the measured depth of groundwater in the well and calculated signal velocity made it possible to accurately place it in the subsurface.

In addition to the depth and extent of the water table we also wanted to see, if the potential dip of the groundwater table is visible. The reason for this is that we wanted to check whether it would be possible to determine the groundwater gradient based on the GPR results. The gradient was determined using the depth of the groundwater table in the well, which was projected on the nearest point on the profile R1 (722.06 m a.s.l.), and the depth at the intersection of the profiles R1 and R3 (719.20 m a.s.l.). The difference in the groundwater table of 2.86 m at a distance of 550 m gives the gradient 0.0052. Despite the limited vertical resolution, such a difference should be seen in the radargram; however, the reflector representing the groundwater level appears to be more or less horizontal. This may be

due to the fact that the profile was recorded in a very rugged terrain, causing poor contact between the GPR antenna and the ground. Thus, the groundwater level could not be determined with such accuracy that a gradient or even a concave groundwater table could be seen.

A continuous reflector representing the water table can also be seen on the profile R3 shown in Figure 8, where again it does not have a linear shape. This is due to the skipping of the antenna during recording over branches, roots and fallen trees. However, it is still possible to determine the groundwater table, which runs along the entire profile R3 at the depth of approximately 7.5 m, corresponding to the depth determined at the intersection with the profile R1. Since the reflector is not perfectly smooth, using normal vertical to horizontal scale ratio of radargrams, it is hard to say whether or not the groundwater level is inclined due to an uneven recharge of groundwater from both sides of the valley. In Figure 8, the depth of the radargram is considerably exaggerated compared to its length and the dip of the water table towards N is visible. This means that the water recharge is higher from the S side of the valley, i.e. from the Pokljuka plateau. Along the whole profile R3, which is 354.5 m long, the difference in the depth of the inclined water table is about 1 m.

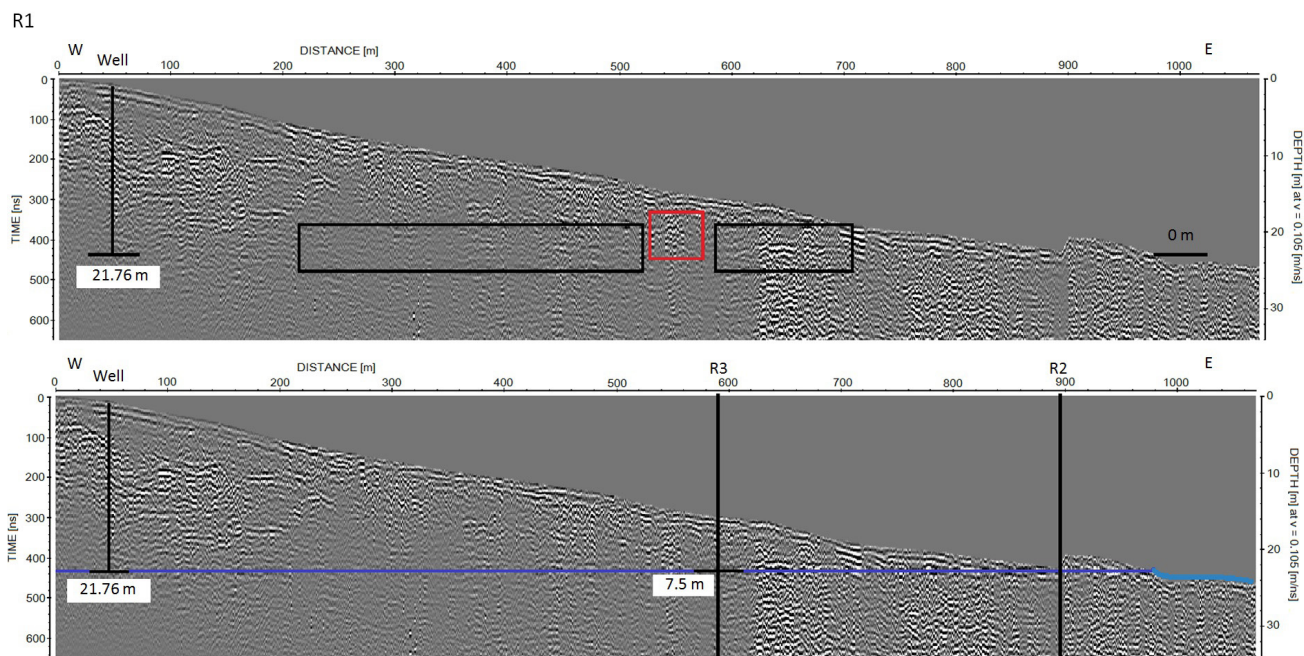


Fig. 7. Interpretation of longitudinal GPR profile R1. Top – features (black frames) used to determine the groundwater level with marked groundwater depth in the well (21.76 m), disrupted part of the reflector (red frame) and point where water was spotted on the surface - spring (dark blue line); bottom – construction of the groundwater level (light blue), water at the surface (dark blue), location of transverse profiles GPR R2 and R3 and groundwater depth at the intersection of profiles R1 and R3 (7.5 m). Vertical exaggeration is approx. 6 ×.

The transverse profile R2 was recorded in the area where the groundwater is just below the surface. Due to the limited vertical resolution of the antenna used, this profile does not contain any linear reflectors, which also applies to the same location on the profile R1. The groundwater depth here is too shallow (probably less than 1 m) to be detected by a low-frequency GPR method, which is optimal for greater depths, therefore this profile is not shown.

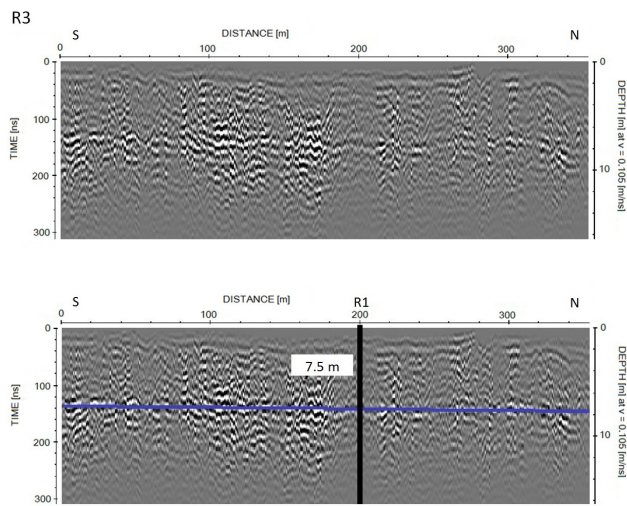


Fig. 8. Interpretation of transverse GPR profiles R3. Top - well pronounced continuous reflector representing groundwater level; bottom - construction of the groundwater level (blue line) and marked location of intersection with longitudinal profile R1 and depth to groundwater (7.5 m). Vertical exaggeration is approx. 7 ×.

### Seismic reflection profile

Obtained data quality for the HRS Radovna profile is highly variable (Fig. 9). The main contributing factors to the variability in data quality are natural noise due to the wind and vegetation and high signal attenuation. High signal attenuation is attributed to the large thickness (20 m) of the unsaturated zone of coarse-grained sediments, which acted as a signal dampener, particularly at high frequencies. On the day of the seismic reflection profiling the groundwater in the nearby well was 22.7 meters below the surface.

### Standard data processing

Data was processed using Parallel Geoscience Seismic Processing Workshop software, first using a fairly standard seismic reflection data processing workflow, including data editing, geometry input, filtering, amplitude corrections, static corrections, velocity analysis and stacking (Tab. 4). In data editing only dead traces were removed. This was followed by early muting direct and refracted waves. Coherent noise was removed with velocity and f-k filters. Velocity analysis was performed using Constant Velocity Stack (CVS) as data quality was too low for useful velocity semblance analysis. Even CVS only produced useful results in the northern part of the profile between Common Mid-Point (CMP) 1120 and 1180. Normal moveout (NMO) stack was done with a constant stacking velocity of 2000 m/s and 50 % stretch mute.

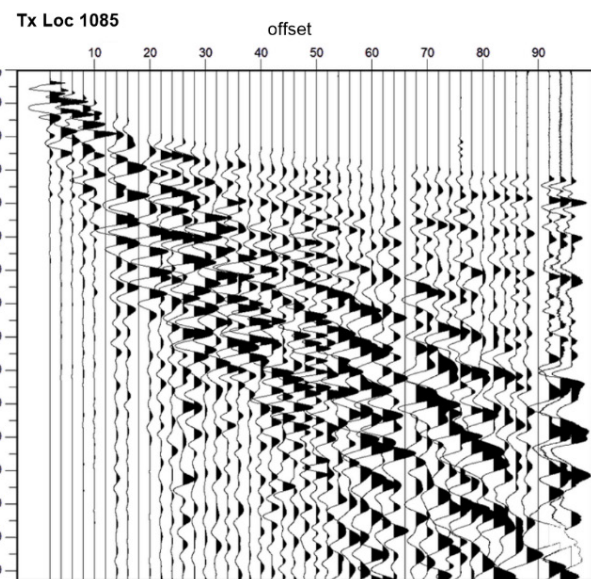
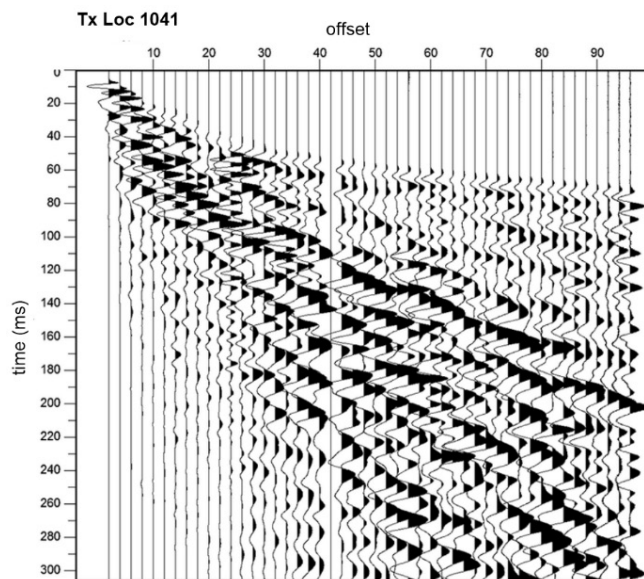


Fig. 9. Two seismic shot gathers displaying the variability in data quality. Left - shot gather at shot point Tx 1041 with almost indiscernible reflectors. Right - shot gather at shot point Tx 1085 with significantly better visibility of reflectors.

Table 4. HRS Radovna profile standard data processing workflow.

Step	Details
<b>Prestack</b>	
Trace editing	
Butterworth filtering	low pass 40 Hz, high pass 200 Hz, low rolloff 18 dB/oct, high rolloff 18 db/oct
Early & tail mute	hand picked
Spherical divergence correction	
AGC	80 ms window, 40 ms overlap
F-k filtering (GR* and GW* attenuation)	velocity filters
Airwave attenuation	f-k filtering
<b>Velocity analysis</b>	
Preliminary analysis	CVS (400-2000 m/s; 50 m/s interval)
Velocity semblance analysis	
<b>NMO correction &amp; stack</b>	
NMO correction	50 % stretch mute velocity from CVS / semblance analysis

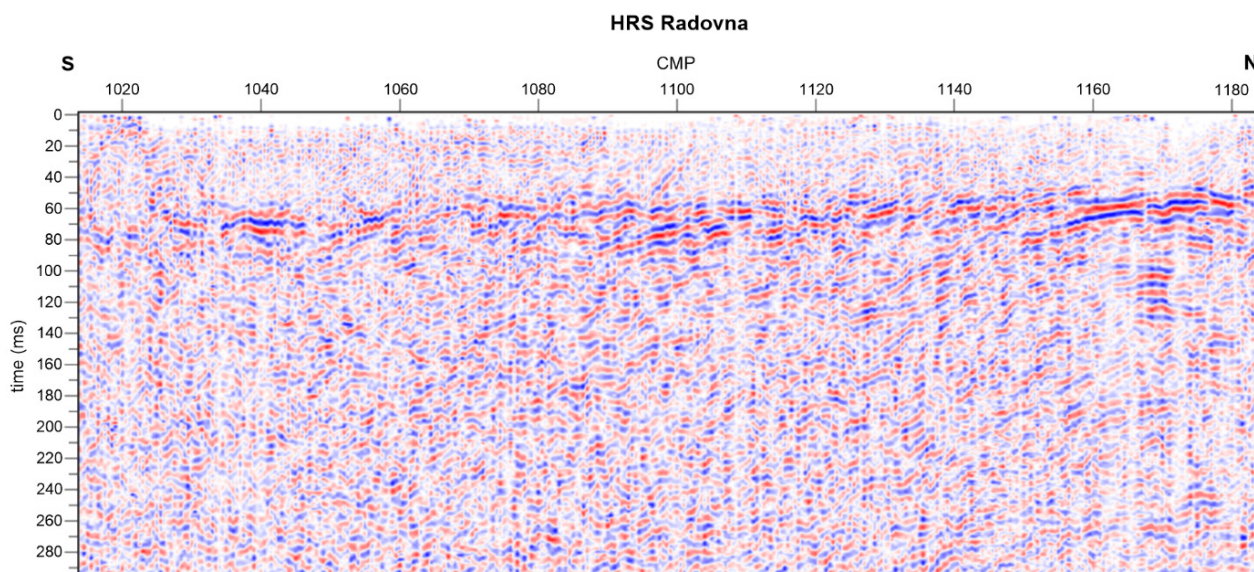


Fig. 10. Stacked section of the high-resolution seismic reflection profile across the Radovna Valley.

Most of the profile is dominated by very poor signal-to-noise ratio, with few reflectors distinguishable from background noise. A stronger southward dipping reflector is evident in the northern part of the profile between CMP 1120 and 1180 and TWT 60 to 130 ms (Fig. 10), which is interpreted as the pre-Quaternary basement. Some fragmented reflectors are visible in the southern part of the profile at between 60 and 100 ms TWT, however, the generally poor data quality precludes any meaningful interpretation.

#### Alternative data processing

Due to the poor general data quality, an alternative approach was attempted in order to obtain some useful data on reflectors and their approximate depths. From the entire dataset, only high-quality shot gathers were selected. Selection criteria included: absence of random noise, low coherent noise and high clarity of seismic reflectors. A total of 9 shot gathers were selected (six of them shown on Fig. 11 and Tab. 5). On each shot gather all distinct reflectors were identified.

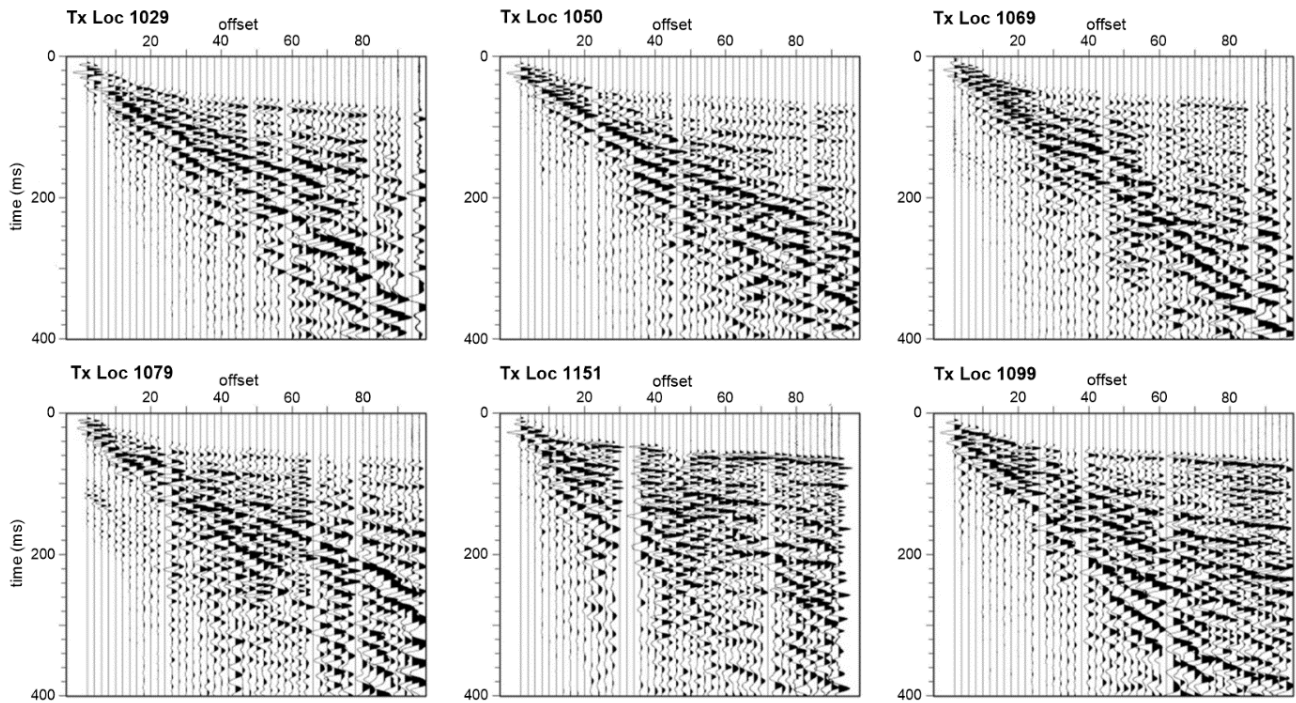


Fig. 11. Six of nine seismic shot gathers used in the alternative processing (shot points 1029, 1050, 1069, 1079, 1099 and 1151).

CMP	h1 (m)	h2 (m)	h3 (m)	h4 (m)	h5 (m)	h6 (m)	h7 (m)	h8 (m)	Bedrock (m)
1029	-37		-63	-81			-125		-125
1050	-37		-57	-70	-95	-109	-125	-141	-141
1062		-40	-59		-87	-100	-122		-122
1079	-34	-43	-55		-83				
1085	-35	-44	-56		-86	-117			-117
1099	-28		-55	-71	-89	-111			-111
1109	-30		-49	-66	-89				
1115		-42		-65	-95				-95
1151	-16		-53						-53

Table 5. Selected seismic shot gathers with depths of interpreted reflectors arranged in nine horizons.

Approximate zero times of the reflectors were determined and then used as a basis for depth conversion.

#### Hydrogeological interpretation

For the purpose of building the model of the Radovna aquifer, data from all nine selected shot gathers was used. At each useful shot gathers individual reflectors were identified and their depth in TWT was estimated. All reflectors were depth converted (Tab. 5) using an average velocity  $v_p$  of 2000 m/s, which is the average seismic wave velocity for glacial sediments (Kearey et al., 2002). It was assumed due to previous investigations that the reflectors within the valley fill sediments are generally horizontal or only slightly dipping, therefore reflections at similar depths were interpreted as the same reflector. From each

selected shot point the deepest reflector was assumed as the depth to the pre-Quaternary basement and on the basis of these data, the shape of the basement was determined. We expect the depths to be accurate to within approximately 30%, accounting for uncertainty in reflector zero times and potential variability in  $v_p$  the valley fill. We expect the depths to be accurate to within approximately 30 %, accounting for uncertainty in reflector zero times and potential variability in  $v_p$  the valley fill.

For the input structural model, the shape of the seismic horizons was linearly interpolated between the data points. Due to the lack of borehole data, it is impossible to characterize the lithological boundaries or sediment transitions that produced the reflectors. It is possible that reflectors are produced by either a major change in grain

sizes in glacial till (different moraine types) or between different types of sediment, such as glacial till, alluvial and glaciofluvial sediments.

From the interpolated data, the schematic cross-section of the valley was plotted (Fig. 12). Since the profile could not be obtained throughout the whole width of the valley, the extrapolated part is represented with dashed line. The line was truncated at the edge of a large pasture, enclosed by an electric fence and occupied by cattle which precluded measurements. Additionally, the very soft grassy surface was inappropriate for data acquisition using impact sources due to high signal attenuation – an effect which has been described elsewhere under similar conditions (Atanackov & Gosar, 2013).

Based on previous research, it is assumed that results represent some sort of stratification of sediments and most likely to reflect the difference between well and poorly granulated sandy gravel layers and layers with glacial dropstones. With the analysis at least seven different layers were determined (Fig. 10). The deepest point of the pre-Quaternary basement is 141 meters deep and was determined with only one shot gather. Though the lack of data, this depth is realistic according to previous investigations in this area, where the depth of the sediments was determined to be at least 100 meters (Torkar & Brenčič, 2015). Similar seismic reflection investigations were done in the area of Sava springs area in a similar parallel valley, where the pre-Quaternary basement was determined to be at the depth of 200 m and is linked to the Sava fault zone (Atanackov et al., 2015). The southern slope of the buried valley is steeper than the northern slope. This corresponds to the shape of valley above the surface. The morphology of the pre-Quaternary basement

is realistic in the whole width of the valley, except between 200 and 300 meters distance, where it is very steep.

### Fluctuation of groundwater level and discharge

Groundwater level in the well (Figs. 2, 5) was measured hourly in the period from 4.10.2011 to 12.4.2016 and contains 37.934 data. Since the well dries up in the winter, the missing data was supplemented with the recession curve, where the data were processed with exponential regression (Posavec et al., 2006; 2010).

During the entire investigation (10/2011–04/2016) we managed to record, both the dry period and floods. From mid-2011 and mid-2012 there was a drought period (ARSO, 2012). In the same year, there was a lot of precipitation, which caused flooding. The fluctuation of the groundwater level in the well is very dynamic. With the instrument we recorded a range of fluctuations up to 19.11 m. With the construction of the curve (dashed line) we recorded a range of fluctuations of up to 28.6 m (Fig. 13), which is much more than previously determined. The groundwater level was the lowest recorded, with the help of a reconstruction, on 11 March 2012 at an altitude of 708.3 m and the highest on 10.11.2012 at an altitude of 736.9 m. The well dried each year, with the exception of 2014, when precipitation in that area was 2394.2 mm, which represents 126 % of the precipitation relative to the reference period 1961–1990.

The groundwater level in the upper part of the Radovna River Valley fluctuates greatly and changes rapidly, indicating well-permeable aquifer, and at the same time such an aquifer is extremely sensitive and vulnerable to extreme climatic events such as drought or lack of snow and

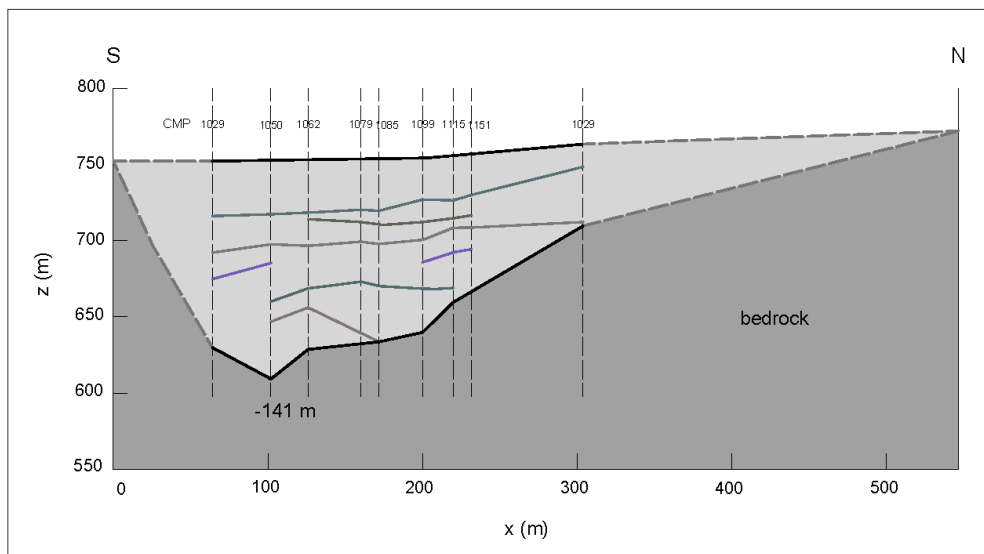


Fig. 12. Schematic N-S cross-section model of the Radovna River Valley derived from HRS profile.

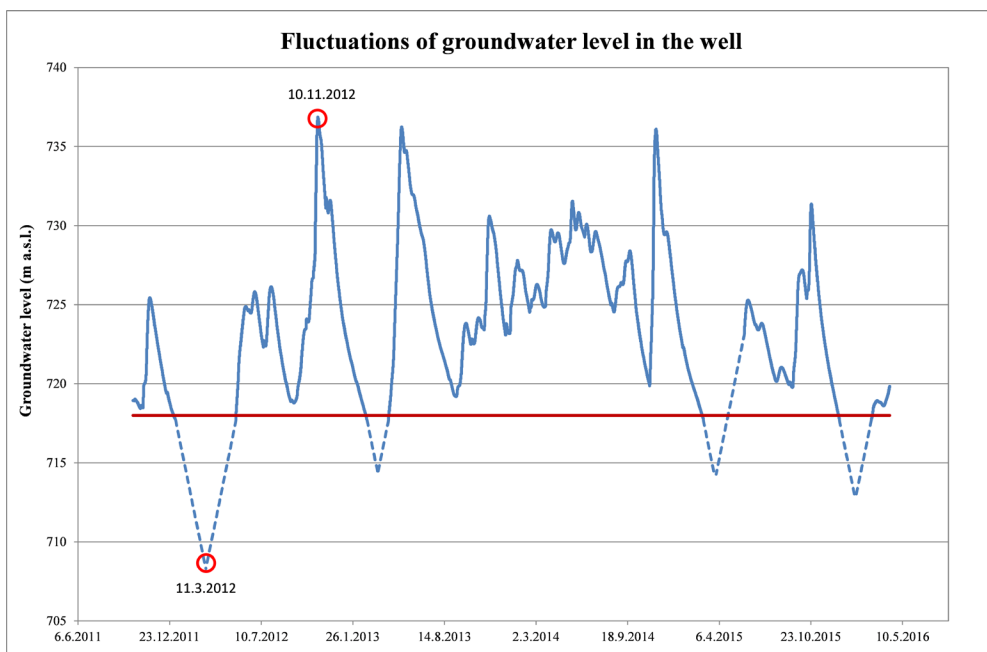


Fig. 13. The fluctuation of the groundwater level in the well in time; dashed line marks the calculated levels by recession curve, the red line indicates the depth of the well.

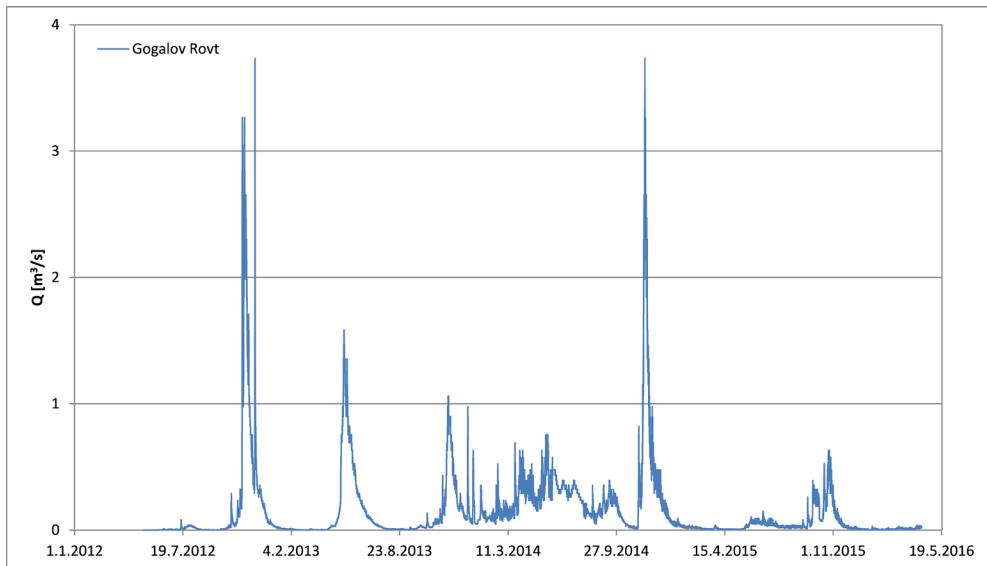


Fig. 14. Discharge of Radovna river as a function of time at location Gogalov Rovt.

floods, or too much water in a short time, which can cause a lot of damage. The fluctuations of the groundwater level are simultaneously reflected at the location of the Radovna Spring, as it moves along the valley up and down according to the amount of water in the aquifer.

At the Gogalov Rovt location (Figs. 2, 6) discharge was measured from 1.3.2012 to 12.4.2016. At the beginning of the measurements the riverbed was dry till the beginning of May, due to extremely low precipitations in 2011 and 2012. The discharge ranged between 0 and  $3.74 \text{ m}^3/\text{s}$ , with an average of  $0.16 \text{ m}^3/\text{s}$  (Fig. 14).

The Gogalov Rovt hydrograph shows a mixed, Alpine snow-rain drainage regime, with minimal discharges in the winter and summer periods and with maximum discharges in spring, during snow melting period, and in autumn during heavy

precipitations. The fluctuations of discharges in the river are a reflection of the fluctuation of the groundwater level in the aquifer and the direct impact of precipitation. In case of heavy precipitation the water in the riverbed increases greatly, but also drains very quickly. The snow melting periods are very different during the observation period on the hydrograph, which is influenced by several factors, such as the thickness of the snow cover, the temperature at the melting time, the amount of rainfall, etc.

## Conclusions

The low-frequency GPR method has shown to be useful for determining the depth of the groundwater table in the hinterland of the Radovna spring. Given the rather unfavourable conditions for GPR measurements that caused

poor antennas ground contact, the results are satisfactory. Although it was impossible to determine the shape of the groundwater table in detail, an insight into the aquifer and calculation of groundwater gradient was obtained with the longitudinal profile R1. A greater recharge from the southern Pokljuka plateau was detected in the transverse profile R3.

The high-resolution seismic reflection profile provided, despite generally poor data quality and necessity to apply alternative interpretation method, highly valuable information on the geometry of the aquifer and the depth of the sediments in the valley. The seismic reflection data gave an insight about the morphology of the pre-Quaternary basement with the deepest point at 141 meters below surface.

Measurements of the groundwater level showed that the fluctuations were very dynamic reaching up to 19.11 meters, and even, 28.6 meters when the curve was extrapolated. Surface water discharges ranged between 0 and 3.74 m<sup>3</sup>/s, with an average of 0.16 m<sup>3</sup>/s, showing a mixed, Alpine snow-rain drainage regime. The fluctuation of groundwater level is directly reflected in the discharges in the river, as the location of the Radovna Spring moves up and down depending on the amount of water in the aquifer.

Both the geophysical and hydrogeological methods provided important information on the morphology of the valley and the alluvial aquifer, adding to the knowledge of the Radovna springs system and providing very important information for future hydrogeological investigations.

### Acknowledgment

The GPR survey was conducted with the support of the Slovenian Research Agency PhD grants 1000-10-310073 and 1000-10-310074. HRS data acquisition was supported by Slovenian Research Agency programme grant P1-0011.

### References

- Afshar, A., Abedi, M., Norouzi, G.-H. & Riahi, M.-A. 2015: Geophysical investigation of underground water content zones using electrical resistivity tomography and ground penetrating radar: A case study in Hesarak-Karaj, Iran. *Engineering Geology*, 196: 183-193. <http://dx.doi.org/10.1016/j.enggeo.2015.07.022>
- Annan, A. P. 2002: GPR—History, Trends, and Future Developments. *Subsurface Sensing Technologies and Applications*, 3: 253-270. <https://doi.org/10.1023/a:1020657129590>
- Atanackov, J., Car, M., Jamšek Rupnik, P., Jež, J., Celarc, B., Novak, M., Milanič, B., Šram, D. & Bavec, Š. 2015: Poročilo o geofizikalnih raziskavah in geološka sinteza raziskav območja Zelencev in Ledin. Geološki zavod Slovenije.
- Atanackov, J. & Gosar, A. 2013: Field comparison of seismic sources for high resolution shallow seismic reflection profiling on the Ljubljana moor. *Acta Geodynamica et Geomaterialia*, 10/1: 19–40. <https://doi.org/10.13168/AGG.2013.0002>
- Blindow, N., Eisenburger, D., Illich, B., Petzold, H. & Richter, T. 2007: Ground Penetrating Radar. *Environmental Geology: Handbook of Field Methods and Case Studies*. Berlin, Heidelberg: Springer Berlin Heidelberg.
- Boiten, W. 2008: *Hydrometry 3rd Edition: A comprehensive introduction to the measurement of flow in open channels*, Leiden, CRC Press Balkema.
- Bowling, J. C., Harry, D. L., Rodriguez, A. B. & Zheng, C. 2007: Integrated geophysical and geological investigation of a heterogeneous fluvial aquifer in Columbus Mississippi. *Journal of Applied Geophysics*, 62: 58-73. <https://doi.org/10.1016/j.jappgeo.2006.08.003>
- Buser, S. 1980: Osnovna geološka karta SFRJ. 1: 100.000, Tolmač lista Celovec (Klagenfurt) L 33-53, Beograd, Zvezni geološki zavod.
- Doolittle, J. A., Jenkinson, B., Hopkins, D., Ulmer, M. & Tuttle, W. 2006: Hydropedological investigations with ground-penetrating radar (GPR): Estimating water-table depths and local ground-water flow pattern in areas of coarse-textured soils. *Geoderma*, 131: 317-329. <https://doi.org/10.1016/j.geoderma.2005.03.027>
- Ferjan Stanič, T., Brenčič, M. & Zupančič, N. 2013: Heavy metal concentrations in soil in the vicinity of former ironworks in Spodnja Radovna, Slovenia. *Geologija*, 56/2: 229-241. <https://doi.org/10.5474/geologija.2013.015>
- Iskra, M. 1982: Elaborat o klasifikaciji, kategorizaciji in izračunu zalog jezerske krede na območju odkopa v Srednji Radovni. [Poročilo v arhivu Geološkega zavoda Slovenije] Geološki zavod Ljubljana.
- Jol, H. M. 2009: *Ground Penetrating Radar Theory and Applications: theory and applications* Amsterdam, Elsevier.
- Jurkovšek, B. 1987: Osnovna geološka karta SFRJ 1:100.000, Tolmač listov Beljak in Ponteba: L 33-51 L 33-52, Beograd, Zvezni geološki zavod.

- Kaiser, A. E., Green, A. G., Campbell, F. M., Horstmeyer, H., Manukyan, E., Langridge, R. M., McClymont, A. F., Mancktelow, N., Finnemore, M. & Nobes, D. C. 2009: Ultrahigh-resolution seismic reflection imaging of the Alpine Fault, New Zealand. *Journal of Geophysical Research: Solid Earth*, 114, B11. <https://doi.org/10.1029/2009jb006338>
- Kanduč, T., Mori, N., Kocman, D., Stibilj, V. & Grassa, F. 2012: Hydrogeochemistry of Alpine springs from North Slovenia: Insights from stable isotopes. *Chemical Geology*, 300/301: 40-54. <https://doi.org/10.1016/j.chemgeo.2012.01.012>
- Kearey, P., Brooks, M. & Hill, I. 2002: An introduction to geophysical exploration, Malden, MA: Blackwell Science, cop. 2002.
- Mahmoudzadeh, M. R., Francés, A. P., Lubczynski, M. & Lambot, S. 2012: Using ground penetrating radar to investigate the water table depth in weathered granites - Sardon case study, Spain. *Journal of Applied Geophysics*, 79: 17-26. <https://doi.org/10.1016/j.jappgeo.2011.12.009>
- Malá 2009: ProEx-Professional explorer control unit. Operating manual v 2.0.
- McClymont, A. F., Hayashi, M., Bentley, L. R. & Liard, J. 2012: Locating and characterising groundwater storage areas within an alpine watershed using time-lapse gravity, GPR and seismic refraction methods. *Hydrological Processes*, 26: 1792-1804. <https://doi.org/10.1002/hyp.9316>
- Milsom, J. 2003. Field Geophysics, West Sussex, John Wiley & Sons Ltd.
- Nadbath, M. 2012: Meteorološka postaja Zgornja Radovna. Naše okolje, Bilten Agencije RS za okolje, XIX, 1-5.
- Neal, A. 2004: Ground-penetrating radar and its use in sedimentology: principles, problems and progress. *Earth-Science Reviews*, 66/3-4: 261-330. <https://doi.org/10.1016/j.earscirev.2004.01.004>
- Paz, C., Alcalá, F. J., Carvalho, J. M., Ribeiro, L. 2017: Current uses of ground penetrating radar in groundwater-dependent ecosystems research. *Sci Total Environ.*, 595: 868-885. <https://doi.org/10.1016/j.scitotenv.2017.03.210>
- Posavec, K., Bačani, A. & Nakić, Z. 2006: A Visual Basic Spreadsheet Macro for Recession Curve Analysis. *Ground Water*, 44: 764-767. <https://doi.org/10.1111/j.1745-6584.2006.00226.x>
- Posavec, K., Parlov, J. & Nakić, Z. 2010. Fully Automated Objective-Based Method for Master Recession Curve Separation. *Ground Water*, 48: 598-603. <https://doi.org/10.1111/j.1745-6584.2009.00669.x>
- Rejiba, F., Bobée, C., Maugis, P. & Camerlynck, C. 2012: GPR imaging of a sand dune aquifer: A case study in the niayes ecoregion of Tanma, Senegal. *Journal of Applied Geophysics*, 81: 16-20. <https://doi.org/10.1016/j.jappgeo.2011.09.015>
- Torkar, A. & Brenčič, M. 2015: Spatio-temporal distribution of discharges in the Radovna River valley at low water conditions. *Geologija*, 58/1: 47-56. <https://doi.org/10.5474/geologija.2015.003>
- Torkar, A., Brenčič, M. & Vreča, P. 2016: Chemical and isotopic characteristics of groundwater-dominated Radovna River (NW Slovenia). *Environmental Earth Sciences*, 75: 1-18. <https://doi.org/10.1007/s12665-016-6104-5>
- Yilmaz, Ö. & Doherty, S. M. 2001: Seismic Data Analysis: Processing, Inversion, and Interpretation of Seismic Data, Society of Exploration Geophysicists.
- Zajc, M., Celarc, B. & Gosar, A. 2015: Structural-geological and karst feature investigations of the limestone-flysch thrust-fault contact using low-frequency ground penetrating radar (Adria-Dinarides thrust zone, SW Slovenia). *Environmental Earth Sciences*, 73: 8237-8249. <https://doi.org/10.1007/S12665-014-3987-X>
- Zajc, M., Pogačnik, Ž. & Gosar, A. 2014: Ground penetrating radar and structural geological mapping investigation of karst and tectonic features in flyschoid rocks as geological hazard for exploitation. *International Journal of Rock Mechanics and Mining Sciences*, 67: 78-87. <https://doi.org/10.1016/j.ijrmms.2014.01.011>



# Pesticidi v vodonosniku Krško-Brežičkega polja

## Prevalence of pesticides in Krško-Brežice polje aquifer

Nina MALI, Anja KOROŠA & Janko URBANC

Geološki zavod Slovenije, Dimičeva ulica 14, SI – 1000 Ljubljana, Slovenija;  
e-mail: nina.mali@geo-zs.si

Prejeto / Received 25. 10. 2021; Sprejeto / Accepted 17. 12. 2021; Objavljeno na spletu / Published online 28. 12. 2021

*Ključne besede:* podzemna voda, vodonosnik Krško-Brežičko polje, pesticidi

*Key words:* groundwater, aquifer Krško-Brežice polje, pesticides

### Izvleček

Onesnaženje podzemne vode s pesticidi je splošno razširjen problem, tako v svetu kot tudi v Sloveniji. Glede na pretekle velike obremenitve podzemne vode s pesticidi, je bil namen predstavljene raziskave ugotoviti razširjenost pesticidov v podzemni vodi Krško-Brežičkega polja v obdobju 2018 – 2019 in pri tem preveriti uporabnost metode vzorčenja vode s pasivnimi vzorčevalniki. Skupno smo odvzeli 21 vzorcev podzemne vode na enajstih lokacijah in po dva vzorca v rekah Sava in Krka. V vodi smo določili 15 različnih pesticidov in njihovih razgradnih produktov. V vzorcih podzemne vode sta bila največkrat določena atrazin in njegov razgradni produkt desetilatrazin. Sledijo pesticidi desetilterbutilazin, terbutilazin, metolaklor ter simazin. V površinski vodi smo zaznali atrazin, desetilatrazin, klortoluron, metolaklor in terbutilazin. S kvalitativno metodo vzorčenja s pasivnimi vzorčevalniki smo v podzemni in površinski vodi odvzeli skupno 24 vzorcev. Izločili smo 8 pesticidov, ki se pojavljajo v dveh serijah. Pogostnost pojavljanja posameznih pesticidov je po obeh metodah primerljiva. Pasivno vzorčenje vode se je izkazalo za primerno metodo identifikacije prisotnosti pesticidov. Največje obremenitve s pesticidi na Krško-Brežičkem polju prihajajo s kmetijskih površin. Podzemna voda je bolj obremenjena s pesticidi v osrednjem delu polja v smeri toka od zahoda proti vzhodu. Atrazin in desetilatrazin sta še vedno, kljub dvajsetletni prepovedi, najpogosteje in v najvišjih koncentracijah zaznana pesticida v podzemni vodi Krško-Brežičkega polja.

### Abstract

Groundwater pollution with pesticides is a problem that occurs all over the world as well as in Slovenia. Considering the past high loads of groundwater with pesticides, the purpose of the presented research was to determine the presence of pesticides in the groundwater of Krško-Brežičko polje in the period 2018–2019 and to check the applicability of the passive sampling method. A total of 21 groundwater samples were taken at 11 locations and 2 samples each in the Sava and Krka rivers. We identified 15 pesticides and their degradation products. Atrazine and its degradation product desethylatrazine were most frequently determined in groundwater samples. They are followed by desethylterbutylazine, terbutylazine, metolachlor and simazine. Atrazine, desethylatrazine, chlortoluron, metolachlor and terbutylazine were detected in surface water. A total of 24 samples were taken in groundwater and surface water using the qualitative passive sampling method. We singled out 8 pesticides that appear in two campaigns. The frequency and occurrence of individual pesticides by both methods are comparable. Passive sampling has proven to be an appropriate method of identifying the presence of pesticides. The highest loads in the Krško-Brežičko field arise from the agricultural land areas. Groundwater is more contaminated with pesticides in the central part of the field in the direction of groundwater flow from west to east. In the groundwater of the Krško-Brežice field, atrazine and desethylatrazine are still the most frequently detected pesticides with higher concentrations, despite a 20 years long ban on the use of atrazine-based plant protection products.

## Uvod

Pesticidi so splošen izraz za kemična sredstva – kemična in biološka, ki se uporabljajo za uničevanje rastlinskih, živalskih škodljivcev in gliv, ki povzročajo različne bolezni. Izraz zajema glede na njihov namen rabe insekticide, herbicide, fungicide, nematicide itd. Onesnaženje podzemnih vod s pesticidi vzbuja skrb po vsem svetu in je posledica predvsem v kmetijstvu razširjene uporabe pesticidov (Fisher, 2021).

Po svojem nastanku so pesticidi lahko naravne snovi izolirane iz rastlin ali snovi pridobljene s sintezo. Pesticidi so biološko aktivne snovi, praviloma škodljive oz. strupene tudi za človeka. Osnovna ali aktivna spojina v posameznih prvinah okolja lahko razpada v razgradne produkte. Slednji so lahko razpadne in konverzijske snovi ter reakcijski in metabolni produkti. Za posamezne razpadne produkte velja, da so lahko toksični kot osnovne oz. matične spojine. Posamezni pesticidni pripravek vsebujejo eno ali več aktivnih snovi, ki lahko z izpiranjem s padavinskimi vodami pridejo v podzemno vodo (Gonzalez-Rodríguez et al., 2011; Heuvelink et al., 2010; van Eerdt et al., 2014).

V podzemni vodi se pojavljajo tako aktivne snovi kot tudi njihovi razgradni produkti. Zaradi procesov razpadanja aktivnih snovi so v podzemni vodi izmerjene višje koncentracije razgradnih produktov (Kolpin et al., 2004; Lapworth & Goody, 2006; Koroša et al., 2016). V svetu proizvodnja in poraba pesticidov močno narašča (Bernhardt et al., 2017). Sproščanje pesticidov v okolje – emisije predstavljajo tveganja za zdravje ljudi in ekosistemov v celoti (Nienstedt et al., 2012; Shelton et al., 2014; Stehle & Schulz, 2015; Kim et al., 2017; Munz et al., 2017;).

Razpoložljivost kakovostnih virov podzemne vode je ogrožena z naravnimi in antropogenimi obremenitvami, vključno s kmetijstvom (Burri et al. 2019). Onesnaženje podzemne vode s pesticidi je med glavnimi razlogi kemijskega onesnaženja podzemne vode. Kmetijske prakse doprinesejo velike količine hranil in pesticidov v vodonosnike (Sasakova et al., 2018; Bartzas et al., 2015), zaradi česar je podzemna voda neprimerna za oskrbo s pitno vodo ali pa celo za kmetijsko uporabo (Shishaye, 2021). Razumevanje njihovih dolgoročnih učinkov je pomembno za zaščito vodonosnikov pred izpostavljenostjo onesnaženju (Shishaye, 2021). Zaradi zapletenosti procesov toka podzemne vode je težko napovedati časovno obdobje pretoka vode in morebitnega onesnaževala.

Na prenos pesticidov v podzemno vodo vpliva več dejavnikov, npr. lastnosti aktivne snovi in tal,

kar vpliva na sorpcijo in razgradne procese. Prenos skozi tla je večinoma dobro preučen (Petersen et al., 2003; de Jonge et al., 2004; Ogura et al., 2021), ostajajo pa slabše raziskani procesi v nezasičeni in zasičeni coni vodonosnika. Transport pesticidov v vodonosniku je izrazito odvisen od hidrogeoloških lastnosti vodonosnika. Hidravlične lastnosti vodonosnika se lahko prostorsko spreminjajo. Za določanje toka podzemne vode ter skladiščenja in transporta onesnaževala moramo celovito razumeti geološke in hidrogeološke lastnosti vodonosnika (Bartzas et al., 2015). To znanje je bistveno za oceno tveganja onesnaženja podzemne vode in odpornosti vodonosnika v smislu takega onesnaženja.

Izpiranje pesticidov v podzemno vodo je problem tudi za oskrbo s pitno vodo, saj voda onesnažena s pesticidi predstavlja tveganja kroničnih pa tudi akutnih zdravstvenih učinkov (Shaw et al., 2012). Pesticidi kot so atrazin in njegovi razgradnji produkti so pogosto prisotni v podzemni vodi kot posledica razširjene pretekle rabe kot herbicid v kmetijstvu ter zaradi odpornosti proti razgradnji in mobilnosti v okolju (Giddings et al., 2005; APVMA, 2008). V podzemni vodi ostaja dlje kot v tleh zaradi upočasnjenje razgradnje v običajnih anerobnih pogojih in odsotnosti fotodegradacije (Schult, 2016).

V mnogih evropskih državah kakor tudi v Sloveniji je podzemna voda glavni vir vode za javno oskrbo s pitno vodo. Zaradi tega se zahteva dobro kakovostno stanje podzemne vode. V tem kontekstu imajo okvirna vodna direktiva (WFD) in njene podnjene direktive (Direktiva o pitni vodi, Direktiva o podzemni vodi) na evropski ravni namen omejiti obremenitve z onesnaževali, zmanjšati negativne trende onesnaževal v vodi in preprečiti nova onesnaženja. Med onesnaževalci antropogenega izvora so pesticidi, poleg nitratov, med glavnimi viri onesnaženja podzemne vode. V Evropi je raba pesticidov opredeljena z Uredbo o fitofarmacevtskih sredstvih 1107/2009. Standard Evropske unije za pitno vodo iz Direktive o pitni vodi (98/83/ES) in standard kakovosti vode za telesa podzemne vode v skladu z Direktivo o podzemni vodi (2006/118/ES) določata najvišjo koncentracijo posameznega pesticida na 0,1 µg/l in vsoto merjenih pesticidov na 0,5 µg/l. Za oceno stanja oz. obremenitev podzemne vode so pomembne tako osnovne spojine, kot tudi njihovi relevantni razgradni produkti. Za opredelitev stopnje in možnosti razvoja onesnaženja ali za določanje ogroženosti uporabljamo predvsem podatke nacionalnega monitoringa kakovosti podzemne vode, ki podajajo realno sliko

stanja podzemne vode. V Sloveniji z nacionalnim monitoringom redno spremljamo pesticide v površinskih vodah, podzemni vodi in tudi v pitni vodi.

Eden od ukrepov za dobro zaščito podzemne vode je, učinkovit monitoring in eden od izvirov je kako z novimi metodami izboljšati monitoring kakovosti podzemne vode (Mali et al., 2017). Kot alternativa točkovnemu vzorčenju, ki določa onesnaženje v določenem času in prostoru, se je razvila metoda pasivnega vzorčenja vode, ki omogoča neprekinjeno spremljanje v daljšem časovnem obdobju in določanje časovno tehtanih povprečnih koncentracij (Alvarez et al., 2004; Vrana et al., 2014). Pasivno vzorčenje vode se je izkazalo za uporabno orodje za določanje različnih onesnaževal v vodnem okolju (Wille et al., 2011; Seethapathy et al., 2008; Vermeirssen et al., 2009; Nyoni et al., 2011; Ahrens et al., 2015; Mali et al., 2017). Pasivno vzorčenje vode temelji na uporabi in situ naprav/sorbenta, ki lahko akumulira onesnaževala raztopljena v vodi (Ahrens et al., 2015) v daljšem obdobju. In nenazadnje, v primerjavi s klasičnimi metodami vzorčenja vode so stroški monitoringa s pasivnim vzorčenjem nižji.

V nadaljevanju ocenujemo stanje prisotnosti pesticidov v podzemni vodi Krško-Brežiškega polja, ki se uporablja tudi kot vir pitne vode. Na območju Krško-Brežiškega polja najdemo urbano, industrijsko, predvsem pa kmetijsko rabo prostora – vpliv slednje se odraža tudi v pojavljanju pesticidov v podzemni vodi. Po podatkih ARSO (2019) so v črpališčih Krške kotline pesticidi prisotni že vrsto let. V obdobju 2005-2013 monitoring kakovosti pitne vode izkazuje slabo kakovostno stanje kot posledico onesnaženosti podzemne vode z nitrati in pesticidi (Mižigoj, 2014). Med pesticidi je najbolj poznan in pereč problem herbicid atrazin oziroma njegov razpadni produkt desetilatrazin. Atrazin je organski herbicid, ki se je uporabljal za zatiranje plevela in trav v kmetijstvu in je vse od leta 2003 prepovedan. Zaradi slabega kakovostnega stanja pitne vode so l. 2010 prenehali uporabljati črpališče Drnovo, ki trenutno služi le kot rezervni vodni vir. Vzrok so bile večletne presežene koncentracije pesticidov in nitratov v podzemni vodi (Leskovar et al., 2019).

Glede na pretekle velike obremenitve podzemne vode s pesticidi je bil namen raziskave preveriti trenutno stanje prisotnosti pesticidov v podzemni vodi največjih aluvialnih vodonosnikov, med njimi tudi Krško-Brežiškega polja. Izbor pesticidov je narejen glede na uporabo, njihovo mobilnost, razgradnjo in glede na analitič-

ne metode. Za določitev prisotnosti pesticidov v vodonosniku smo preverili tudi uporabnost alternativne metode vzorčenja s pasivnimi vzorčevalniki. V članku predstavljamo rezultate raziskave v obdobju 2018-2019. Cilji raziskave so bili (1) ugotoviti stanje prisotnost izbranih pesticidov in njihove koncentracije, (2) določitev prisotnosti pesticidov s pasivnimi vzorčevalniki, (3) oceniti prostorsko razširjenost pesticidov in (4) povezati rabo prostora z njihovo prisotnostjo v podzemni vodi.

## Območje raziskav

Območje Krško-Brežiškega polja se nahaja na jugovzhodu Slovenije (sl. 1), na severu ga obdaja Bizeljsko, na jugu pa Gorjanci. Glavna vodotoka sta reki Sava in Krka. Območje ima značilnosti zmerno celinskega ali subpanonskega podnebja vzhodne Slovenije. Značilen je celinski padavinski režim, povprečna letna količina padavin je 1018 mm (ARSO, 2014). Povprečna zimska temperatura se giblje med -2 do 0 °C. Osrednji del ima visoke povprečne julijske temperature, te se gibljejo med 20 do 22 °C. Območje Krško-Brežiškega polja pripada vodnemu telesu Krška kotlina (oznaka 1003; Pravilnik o določitvi vodnih tel es podzemnih voda (Uradni list RS 2018), in leži na vodnem območju Donave. Površina vodnega telesa znaša 97 km<sup>2</sup>. V sedimentacijskem bazenu prevladujejo aluvialni nanosi karbonatnega in silikatnega proda in peska kvartarne starosti ter pliocenski peski in gline. Pod pliocenskimi plastmi so miocenski sedimenti, predvsem lapor. Podlago terciarnim kamninam tvorijo sedimentne kamnine mezozojske starosti.

Vodno telo, ki ima značilno povezavo s površinskimi vodami, se nahaja v treh tipičnih vodonosnikih (ARSO, 2009). Prvi, aluvialni, medzrnski vodonosnik je kvartarne starosti. Drugi, medzrnski vodonosnik kvartarne in neogenske starosti, se nahaja pod aluvialnimi nanosi rek Save in Krke ter njunih pritokov. Hidravlična povezava med obema vodonosnikoma je možna, prostorsko pa ni podrobnejše opredeljena. Tretji, termalni kraški in razpoklinski, karbonatni vodonosnik v večjem deležu sestavlajo mezozojski, triasni dolomiti. Karbonatne plasti so večinoma le v posredni hidrodinamski povezavi z zgoraj ležečimi vodonosniki.

Pesticide v podzemni vodi smo ugotavljali na območju Krško-Brežiškega polja v prvem, aluvialnem, medzrnskem vodonosniku kvartarne starosti. Vodonosnik sestavljajo peščeno prodni zapisi rek Save in Krke ter njunih pritokov (ARSO, 2009). Je srednje do visoko izdaten (prepustnosti

$10^{-4}$  do  $10^{-2}$  m/s), mestoma nizko izdaten. V njem se nahaja najpomembnejši del vodnega telesa, ki se uporablja za oskrbo prebivalstva s pitno vodo, zato je tudi najbolj raziskan. Reka Sava predstavlja pomembno hidrodinamsko mejo v aluvialnem vodonosniku, saj ga večinoma drenira, delno pa tudi napaja. Reka Krka drenira vodonosnik na širšem območju Krške vasi vse do sotočja s Savo. Vodonosnik medzrnske poroznosti v peščeno prodnatem savskem zasipu predstavlja bogat vir podzemne vode za javno oskrbo s pitno vodo. Na tem območju sta dve črpališči, črpališče Drnovo in črpališče Brege.

Debelina nezasičene cone prvega vodonosnika znaša do 8 m, srednja vrednost je 3 m. Značilna debelina omočenega dela je 7 m. Kvartarni sedimenti so dobro prepustni, koeficient prepustnosti (K) se giblje v razponu reda velikosti med  $10^{-3}$  m/s in  $10^{-4}$  m/s. Vodonosnik je odprtrega tipa. Učinkovita poroznost je ocenjena na 10-20 %. Generalna smer toka podzemne vode je približno enaka smeri toka reke Save, od SZ proti JV, vendar se smer lokalno spreminja, predvsem na območju jezov. Na sliki 1 je prikaz gladin podzemne vode iz aprila 2019. Spremembe v gladini podzemne vode in nihanje gladin so v veliki meri odvisne tudi od hidrodinamskega odnosa med reko Savo in podzemno vodo, torej tudi od oddaljenosti merilnega mesta od reke Save. Vpliv nihanja gladine Save seže do 400 m od reke v notranjost vodonosnika.

Na območju Krško-Brežiškega polja je raba tal raznolika, od kmetijskih površin, poseljenih površin, industrijskih obratov, prometne infrastrukture, raznih gramoznic ter peskokopov, prometnic, itd. Kmetijstvo in urbanizacija vplivata na vnos širokoga nabora onesnaževal v podzemno vodo. Viri onesnaženja so tako razpršeni kot točkovni. Na območju Krško-Brežiškega polja razpršene vire v glavnem predstavljajo kmetijske površine. Glavne lastnosti razpršenih virov so, da pokrivajo večje površine, generalno dosegajo nižje koncentracije kot točkovna onesnaženja, se bolj naravno redčijo v tleh in na površini, so težje določljivi, ker so manj očitno povezani s povzročiteljem onesnaženja (Lapworth et al., 2012). Ogroženost vodonosnika je zaradi antropogene dejavnosti ocenjena kot zelo visoka. V preteklih letih so vsebnosti nitratov in pesticidov (atrazin, desetilatrazin) občasno presegale mejne vrednosti. Posledica stalnega preseganja mejnih vrednosti za pitno vodo je bila prekinitev uporabe črpališča Drnovo v letu 2010.

## Hidrogeološke razmere na Krško-Brežiškem polju v času raziskav

V sklopu opravljenih raziskav na Krške polje v obdobju 2018-2019 smo ob vzorčenju izmerili tudi gladino podzemne vode, T, pH ter električno prevodnost (EC). V tem času so bile določene vrednosti pH podzemne vode Krško-Brežiškega polja od 7,12 do 7,51 ter EC med 421 in 945 µS/cm. Na območju vodonosnika Krško-Brežiškega polja ima podzemna voda dokaj različno električno prevodnost. Glavni dejavnik, ki vpliva na električno prevodnost podzemnih vod na tem območju je vpliv napajanja podzemne vode iz reke Save. V primerjavi s podzemno vodo, katere izvor je infiltracija padavin na območju Krško-Brežiškega polja, ima podzemna voda z večjim deležem reke Save občutno nižjo električno prevodnost. Električna prevodnost podzemne vode nam torej omogoča opredelitev vrtin, v katerih je pomembnejši delež komponente vode reke Save.

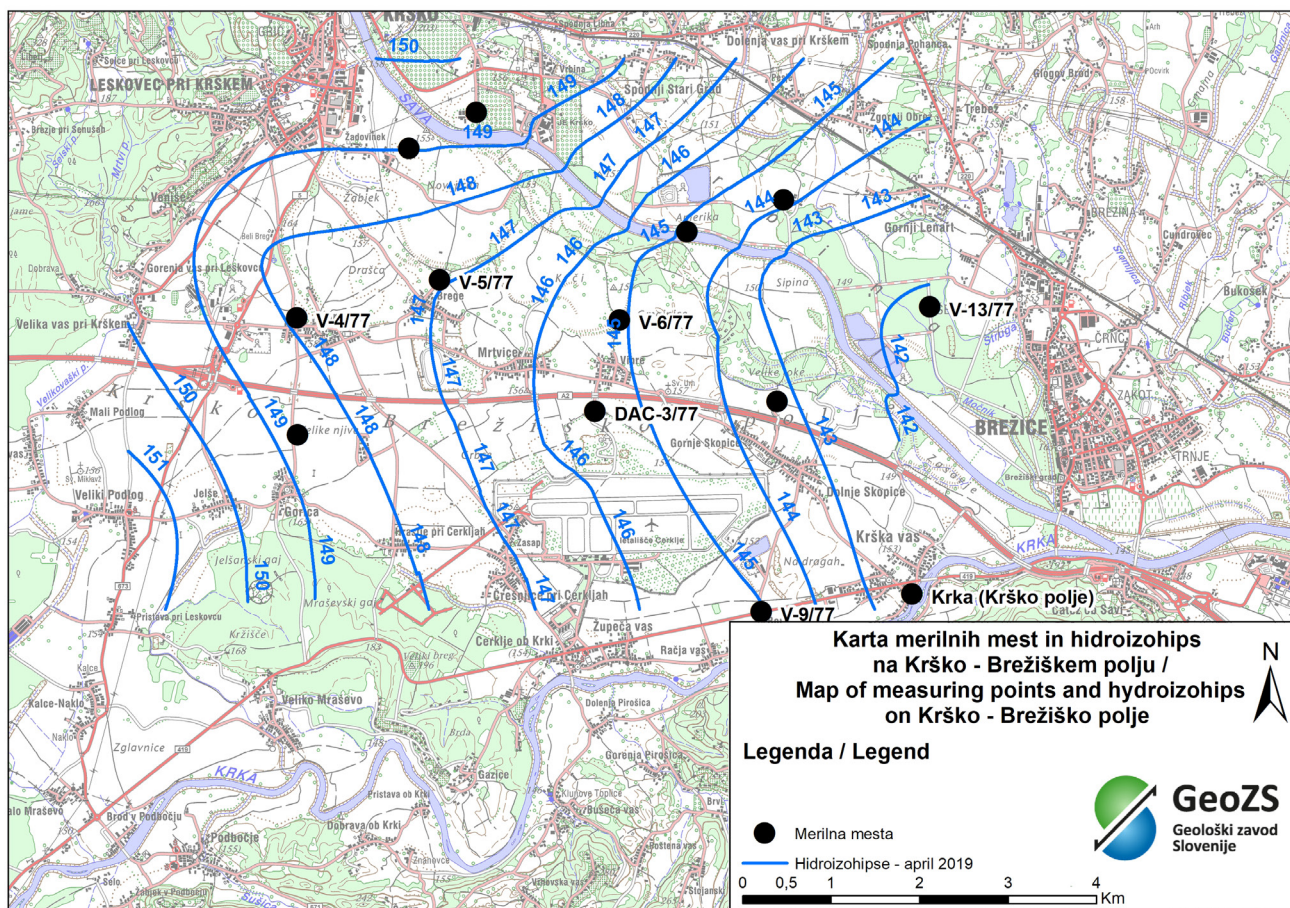
Vrednosti oksidacijsko-reduksijskega potenciala (Eh) nihajo med 5,9 in 193 mV. Vrednosti temperature (T) nihajo med 12,1 in 15,6 °C. Najmanjša debelina nezasičene cone je na območju merilnih mest V-13/77, V-12/77 in V-10/77. Najdebelejša nezasičena cona se nahaja na območju merilnih mest V-4/77, V-9/77 in V-8/77. Meritve smo izvedli v novembру 2018 in aprilu 2019. V novembru 2018 je bila zabeležena nizka gladina podzemne vode, aprila 2019 pa je bila zabeležena visoka gladina podzemne vode glede na dolgotetna povprečja.

## Materiali in metode

### Določitev merilnih mest

Ocena reprezentativnosti merilnih mest je narejena na osnovi navodil ISO standarda »Navodila za vzorčenje podzemne vode« (ISO 5667-11:2010). Izbrana merilna mesta so piezometri s podobnimi lastnostmi, ki lahko vplivajo na ustreznost vzorčenja (globina objekta, vgrajeni materiali, dostopnost, itd.). Glede na to, da je na Krško-Brežiškem polju dobra pokritost z obstoječimi piezometri, smo lahko iz raziskav izključili vaške vodnjake, zajetja ter izvire. Merilna mesta so bila določena na podlagi razpoložljivih podatkov arhiva GeoZS o lokacijah, o litološki zgradbi kamnin, tehnični izvedbi vrtin (globina, premer, lokacija filterov, itd.), meritvah gladin podzemne vode, črpalnih poskusih ter o kemijskih analizah vode.

V merilno mrežo je bilo vključenih 11 merilnih mest podzemne vode in dve merilni mesti površinskih vod. Merilna mesta so razporejena



Sl. 1. Karta merilnih mest, hidroizohips in smeri toka podzemne vode na Krško-Brežiškem polju (aprila 2019).

Fig. 1. Map of the measuring points, hydroisohips and groundwater flow direction in the Krško-Brežice field (April 2019).

po celotnem območju in imajo v svojem zaledju različno pokrovnost in rabe prostora (kmetijska raba, urbana raba ter industrija). Lokacije merilnih mest so prikazane na sliki 1.

### Analiza pokrovnosti in rabe tal

Klasifikacijo rabe prostora smo izvedli z uporabo podatkov CORINE 2012 (Corine land cover – CLC) za rabe zemljišč za Evropo (ARSO, 2016) za celotno območje Krško-Brežiškega polja ter za vsako merilno mesto posebej. Površina območja, ki ga obravnavamo v raziskavi meri  $76 \text{ km}^2$  (sl. 1). Na osnovi baze pokrovnosti tal CLC 2012 in prostorske analize smo določili deleže površine posamezne enote pokrovnosti tal. Razrede pokrovnosti tal smo združili v 4 večje enote: kmetijske površine (71,94 %), gozd (15,51 %), urbana območja (3,96 %) ter industrijska območja (5,65 %), ostalo predstavljajo vodne površine (2,96 %) (reke, jezera, itd.). Urbana območja predstavljajo naselja in zaselki ter vsa infrastruktura, ki služi različnim dejavnostim. V kategorijo »industrijskih površin« smo uvrstili industrijske obrate, cestno in železniško omrežje, letališče, kamnolome in

odlagališča komunalnih odpadkov. V kategorijo kmetijskih zemljišč spadajo njivske površine ter mešane kmetijske površine. Enota gozd združuje vse vrste od listnatega, mešanega in iglastega gozda ter grmičasti gozd. Obdelavo podatkov in izračune smo izvedli z uporabo programske opreme Statistica (Stat Soft Inc., 2012), prostorsko analizo pa z uporabo ArcMap (ESRI Inc., 2004).

Obremenitve, ki vplivajo na kakovost podzemne vode Krško-Brežiškega polja prihajajo iz mešanih virov, tako iz razpršenih kot tudi iz točkovnih virov onesnaženja. Med razpršene vire uvrščamo kmetijske površine, ki so na tem območju v največjem deležu (71,94 %), sledijo gozdne in naravne površine (15,51 %) ter na koncu grajene površine (9,61 %). Delež obremenjenih površin na vodnem telesu Krška kotlina je zelo visok, 82 % (kmetijske in grajene površine skupaj), kar kaže da lahko pričakovane obremenitve povzročajo močne ali prekomerne vplive na podzemno vodo. Med razpršene vire uvrščamo tudi urbanizirana območja.

Na območju Krško-Brežiškega polja je precej gramoznic za izkopavanje proda. Gramoznice

predstavljajo tveganje za podzemno vodo saj je v gramoznih jamah podzemna voda izpostavljena zunanjim vplivom. V kolikor je v bližini gramoznice, ki je lahko potencialni onesnaževalec (zaščitna sredstva, gnojevka, iztok odpadnih vod, itd.), le-ta predstavlja prevodnik za hitro onesnaženje, saj tako onesnaževala hitreje oziroma neposredno preidejo v podzemno vodo. Poleg razpršenih virov na tveganje onesnaženja vplivajo tudi točkovne in linijske obremenitve. Med te spadajo cestni in železniški promet in odlagališča odpadkov. Na tveganje onesnaženja vplivajo tudi razni posegi režima odtoka z umetnimi melioracijskimi kanali, katerih je v vodonosnem sistemu 4,3 km, kar nakazuje na pomembnejše vplive na količinsko stanje podzemne vode. Tudi gradnja hidroelektrarne na tem območju je z različnimi gradbeno-tehničnimi posegi spremenila hidrodinamski odnos med površinskim vodotokom in podzemno vodo in s tem spremenila poti potencialnih onesnaževal.

### Napajalna zaledja meritnih mest

Karakteristike napajalnega zaledja vrtin smo določili glede na hidrogeološke značilnosti vodonosnika, izražene s hitrostjo in smerjo toka podzemne vode (Koroša, 2019). Pretok podzemne vode smo izračunali po Darcy-jevi enačbi. V izračunu smo uporabili povprečni koeficient prepustnosti ( $K$ ) za območje vodonosnika ( $3 \times 10^{-3} \text{ m/s}$ ) (UL RS, št. 63, str. 6537-6538). Gradient je bil določen na podlagi izrisanih hidroizohips. Razdaljo območja napajanja smo določili na podlagi izračuna hitrosti toka podzemne vode gorvodno v obdobju enega leta pravokotno na hidroizohipse. Ker je zajem vode na meritnih mestih le občasen, smo napajalno območje omejili na kot  $30^\circ$ , kot določa metodologija v Pravilniku o kriterijih za določitev vodovarstvenega območja (Uradni list RS, 2016). Za vsako meritno mesto so bili določeni podatki o pokrovnosti in rabi tal ter potencialnih onesnaževalcih.

### Vzorčenje podzemne vode

Za določitev pesticidov v podzemni vodi Krško-Brežiškega polja smo izvedli dve vzorčevalni seriji, in sicer prvo oktobra 2018 in drugo aprila 2019. Vzorčenje na Krško-Brežiškem polju je potekalo na 13 meritnih mestih, od tega se je na 11. mestih vzorčilo podzemno vodo in na dveh površinsko vodo, to sta reki Sava in Krka. Vzorčenje podzemne vode je potekalo s črpalko Grundfos MP-1TM, katere pretok je bil  $0,2 \text{ l/s}$ , 2 m pod gladino podzemne vode na posameznem meritnem mestu. Vzorčenje podzemne vode, transport

vzorcev in njihovo hranjenje ter nadaljnjo obdelavo smo izvedli v skladu s SIST ISO standardi (SIST ISO 5677-11:2010, SIST ISO 5677-3:2012., Reko Savo in reko Krko smo vzorčili v skladu s standardom SIST EN ISO 5667-6:2017. Za kvantitativno kemijsko analizo pesticidov smo odvzeli 1 l vode v rjavu steklenico z zamaški s PTFE folijo. Pri vzorčenju smo uporabili zaščitne rokavice za enkratno uporabo. Vsi vzorci so bili dostavljeni v laboratorij v največ šestih urah, ter nadalje obdelani po postopkih določenih z meritno metodo. Skupno smo odvzeli 25 vzorcev podzemne (21) in površinske (4) vode za kvantitativno kemijsko analizo. V času vzorčenja so bile izvedene tudi terenske meritve parametrov podzemne vode (temperatura vode in zraka, električna prevodnost, pH, redoks potencial, raztopljeni kisik in nasičenost s kisikom).

### Kvantitativne kemijske analize

Za kvantitativno določitev pesticidov v podzemni vodi Krško-Brežiškega polja smo izbrali 15 pesticidov in njihovih razgradnih produktov (2,6-diklorobenzamid, alaklor, atrazin, desetyltrazin, desizopropilatrazin, terbutilazin, desetylterbutilazin, dimetenamid, klortoluron, metazaklor, metolaklor, prometrin, propazin, simazin in terbutrin) (Tabela 1).

Od 15 preiskovanih pesticidov je 6 takšnih, katerih raba je bila v času izvajanja meritev v Sloveniji dovoljena. Med njimi so: terbutilazin, metolaklor, metazaklor, dimetenamid, klortoluron. Ostali pesticidi so prepovedani oziroma so se uporabljali v preteklosti.

Kvantitativne kemijske analize pesticidov v podzemni vodi so bile izvedene v laboratoriju Službe za nadzor kakovosti pitne in odpadne vode JP VOKA SNAGA d.o.o. Uporabljena je bila modificirana metoda EPA 525.2, ki temelji na ekstrakciji na trdno fazo (SPE) in uporabi plinske kromatografije z masno spektrometrijo (GC-MS). Podrobneje so metodo opisali Auersperger in so-delavci (2005). Uporabljena meritna metoda je validirana.

### Pasivno vzorčenje

Prisotnost organskih snovi v podzemni vodi, ki jih s kvantitativnimi analizami ni možno zaznati, smo ugotavljali z metodo vzorčenja s pasivnimi vzorčevalniki. Pasivni vzorčevalniki so inovativna metoda vzorčenja, pri kateri gre za časovno integrirano meritev onesnaževalca v vodi. Gre za enostavno, zanesljivo in stroškovno učinkovito orodje, ki se že uporablja pri izvajanju monitoringov v Evropi in ZDA. Tehnika vzorčenja vode

Tabela 1. Pesticidi, ki so bili vključeni v analizo v podzemni vodi na Krško-Brežiškem polju.

Table 1. Pesticides included in the analysis of groundwater and surfacewater in the Krško-Brežice field.

	CAS št. / CAS no.	Uporaba / Use	Uporaba izvirne aktivne snovi v letih 2018 - 2019 / Use of the active substance in years 2018 - 2019
2,6-diklorobenzamid	2008-58-4	razgradni produkt herbicida diklobenila	Prepovedan
Alaklor	15972-60-8	herbicid	Prepovedan
Atrazin	1912-24-9	herbicid	Prepovedan
Desetilatrazin	6190-65-4	razgradni produkt herbicida atrazina	Prepovedan
Desetilterbutilazin	30125-63-4	razgradni produkt herbicida terbutilazina	Dovoljen
Desizopropilatrazin	1007-28-9	razgradni produkt herbicida atrazina	Prepovedan
Dimetenamid	87674-68-8	herbicid	Dovoljen
Klortoluron	15545-48-9	herbicid	Dovoljen
Metazaklor	67129-08-2	herbicid	Prepovedan
Metolaklor	51218-45-2	herbicid	Dovoljen
Prometrin	7287-19-6	herbicid	Prepovedan
Propazin	139-40-2	herbicid	Prepovedan
Simazin	122-34-9	herbicid	Prepovedan
Terbutilazin	5915-41-3	herbicid	Dovoljen
Terbutrin	886-50-0	herbicid	Prepovedan

\*CAS št. / CAS no. - registrska številka CAS / CAS (Chemical Abstracts Service) Registry Number

s pasivnimi vzorčevalniki je manj občutljiva na ekstremna nihanja koncentracij v vodi (Kot et al., 2000). Metoda vzorčenja s pasivnimi vzorčevalniki pokriva daljše vzorčevalno obdobje in integrira koncentracije onesnaževal skozi čas. Uporablja se tako za kvantitativno kot tudi semi-kvantitativno in kvalitativno določanje različnih onesnaževal. Takšna zasnova monitoringa je bolj ekonomična, saj lahko najprej s kvalitativnimi metodami preliminarno ocenimo stanje vodonosnika in ga kasneje podpremo z natančnimi in točnimi kvantitativnimi analiznimi metodami. Pasivni vzorčevalniki so bili nameščeni v podzemni vodi v dveh obdobjih. Prvo je trajalo od oktobra 2018 do aprila 2019 ter drugo od aprila 2019 do oktobra 2019. Uporabili smo pasivne vzorčevalnike s tkanino iz aktivnega oglja v mrežici iz nerjavečega jekla. Nameščeni so bili v filtrih opazovalne vrtine na sredini omočenega sloja.

Analize pasivnih vzorčevalnikov so bile opravljene v akreditiranem laboratoriju Službe za nadzor kakovosti pitne in odpadne vode JP VOKA SNAGA d.o.o. v Ljubljani. Pripravljeni so bili po standardu ISO 5667- 23:2011 za vzorčenje in internem navodilu TIDD-404-10, izdaja

1.11.2017, ki sta akreditirani po SIST EN ISO/IEC 17025:2005 v skladu s prilogo k akreditacijski listini LP-023 za kemijske analize.

Adsorbiran material na aktivnem oglju je bil po odstranitvi iz vzorčevalnika ekstrahiran, ekstrakt pa analiziran z analitsko metodo plinske kromatografije in masne spektrometrije (GC-MS). Za interpretacijo kromatogramov smo uporabili GC-MS knjižnico z retensijskimi časi za 921 organskih spojin (Agilent USA). Poleg tega se je pri obdelavi rezultatov meritev uporabila NIST 2008 podatkovna baza masnih spektrov. Čeprav je metoda kvalitativna, smo kromatografe GC-MS interpretirali tako, da smo ocenili intenzitete vrhov na lestvici razvrstitev od 1 do 5 in jih ocenili kot „poskusno identifikacijo“ ali „potrjeno identifikacijo“ v skladu s standardom ASTM D 4128 - 01.

Ocenjena maksimalna intenzivnost je povezana z gotovostjo identifikacije in zagotavlja izhodišče za kvantitativno spremeljanje spojin (Magnusson & Örnemark, 2014). Pri rokovanju s pasivnimi vzorčevalniki smo upoštevali in zagojavili skrajne mere oz. kriterije kemijske čistosti.

V seriji pasivnih vzorcev smo uporabili redne slepe in kontrolne vzorce. Pred validacijo so bili optimizirani analitični parametri. Spojine, ki so bile ugotovljene pri slepih vzorcih, so bile izvzete iz poročanja. Tkanina iz aktivnega oglja je bila za postopke nadzora kakovosti shranjena v laboratoriju v ultra čisti vodi v času celotnega trajanja namestitve pasivnih vzorčevalnikov. Analizirana je bila hkrati z odvzetimi pasivnimi vzorčevalniki. Spleti terenski vzorci so se za vsako merilno mesto v skladu s postopkom ISO 5667-23:2011 pripravili v ultra čisti vodi, ki jo je zagotovil laboratorij. Na vsakem merilnem mestu se je tkanina izvlekla in vrnila v ultra čisto vodo.

### Razmerja pesticidov in njihovih razgradnih produktov

Za pojasnilo in analizo prisotnosti razgradnega produkta (desetilatrazin) in primarne spojine (atrazin) smo uporabili razmerje DAR (Adams & Thurman, 1991). DAR je namenjen določitvi »starosti« onesnaženja. Z DAR smo izračunali razmerje med desetilatrazinom in atrazinom, za razdelitev točkovnih in razpršenih virov onesnaženja v podzemni vodi. Majhno razmerje DAR pomeni, da je prisotnega več atrazina v primer-

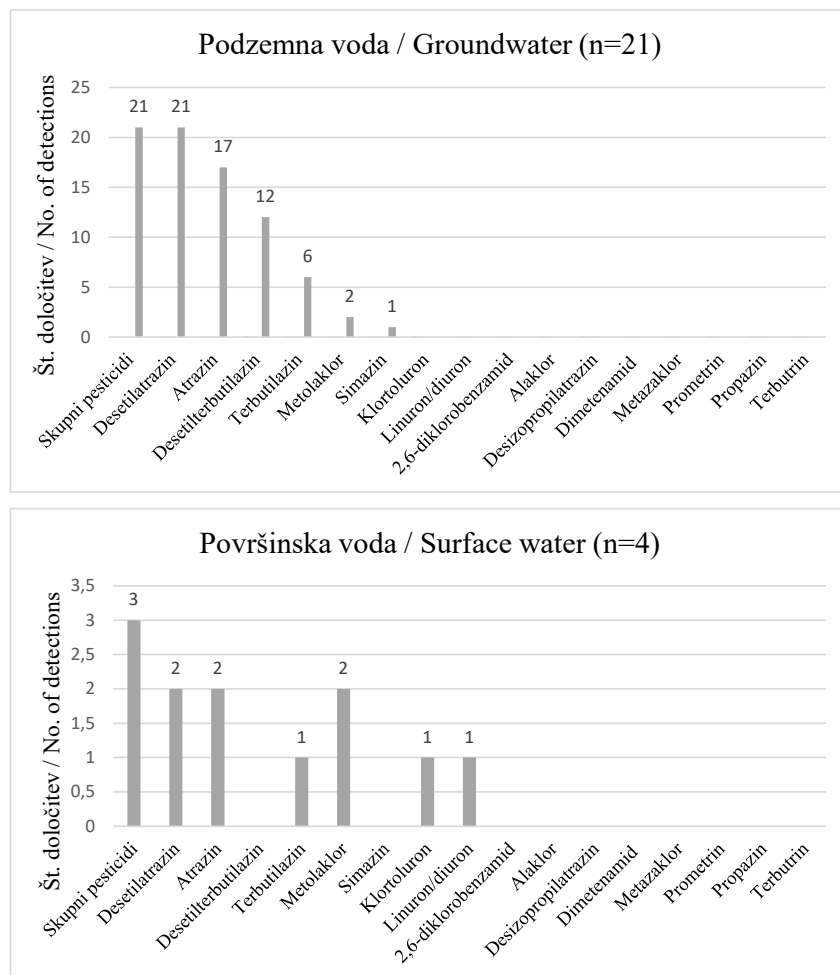
javi z desetilatrazinom, kar nakazuje na »sveže« onesnaženje in je lahko tudi kazalnik točkovnega vira onesnaženja. Podobno kot za razmerje DAR, lahko na osnovi rezultatov vsebnosti terbutilazina in desetilterbutilazina, izračunamo razmerje med desetilterbutilazinom in terbutilazinom (DTA/TBA). Milan in sodelavci (2015) so razmerje DTA/TBA uporabili v podzemni vodi za analizo interakcije med herbicidom in tlemi. Razmerje, manjše od 1, kaže na točkovni vir onesnaženja, saj desetilterbutilazin počasneje izginja v nezasičeni coni kot terbutilazin.

### Rezultati in diskusija

#### Identifikacija pesticidov s kvantitativnimi kemijskimi analizami

##### Prisotnost pesticidov v podzemni vodi

Rezultati identifikacije pesticidov s kvantitativnimi kemijskimi analizami in osnovna statistika meritev zaznanih organskih spojin v podzemni vodi Krško – Brežičkega polja ter reki Savi in Krki so prikazani v tabelah 2a in 2b ter sliki 2. Nad mejo detekcije je bilo določeno 8 pesticidov, od tega smo v podzemni vodi zaznali šest pesticidov. Atrazin in njegov razgradni produkt



Sl. 2. Pogostost pojavljanja pesticidov v podzemni in površinski vodi Krško-Brežičkega polja.

Fig. 2. Frequency of pesticide occurrence in Krško-Brežice polje groundwater.

Tabela 2. Opisna statistika pesticidov v a) podzemni in b) površinski vodi Krško-Brežiškega polja.

Table 2. Descriptive statistics of organic compounds in the a) groundwater and b) surface water of the Krško-Brežiško polje aquifer.

a)

	<b>LOD (µg/l)</b>	<b>LOQ (µg/l)</b>	<b>N</b>	<b>Povp.</b>	<b>Md</b>	<b>Min.</b>	<b>Max.</b>	<b>Std.Dev.</b>
2,6-diklorobenzamid	0,002	0,0067	-					
Alaklor	0,002	0,0067	-					
Atrazin	0,002	0,0067	17	0,013	0,014	0,003	0,025	0,008
Desetilatrazin	0,002	0,0067	21	0,026	0,013	0,004	0,092	0,025
Desetilterbutilazin	0,002	0,0067	12	0,004	0,003	0,002	0,006	0,001
Desizopropilatrazin	0,01	0,0033	-					
Dimetenamid	0,002	0,0067	-					
Klortoluron	0,002	0,0067	-					
Metazaklor	0,005	0,017	-					
Metolaklor	0,002	0,0067	2	0,004		0,003	0,005	0,001
Prometrin	0,002	0,0067	-					
Propazin	0,002	0,0067	-					
Simazin	0,002	0,0067	1	0,003		0,003	0,003	
Terbutilazin	0,001	0,0033	6	0,001	0,001	0,001	0,002	0,000
Terbutrin	0,005	0,017	-					
Skupni pesticidi			21	0,039		0,007	0,120	0,034

b)

	<b>LOD (µg/l)</b>	<b>LOQ (µg/l)</b>	<b>N</b>	<b>Povp.</b>	<b>Md</b>	<b>Min.</b>	<b>Max.</b>
2,6-diklorobenzamid	0,002	0,0067	-				
Alaklor	0,002	0,0067	-				
Atrazin	0,002	0,0067	2	0,005		0,005	0,006
Desetilatrazin	0,002	0,0067	2	0,007		0,006	0,009
Desetilterbutilazin	0,002	0,0067	-				
Desizopropilatrazin	0,01	0,0033	-				
Dimetenamid	0,002	0,0067	-				
Klortoluron	0,002	0,0067	1	0,002		0,002	0,002
Metazaklor	0,005	0,017	-				
Metolaklor	0,002	0,0067	2	0,002		0,002	0,003
Prometrin	0,002	0,0067	-				
Propazin	0,002	0,0067	-				
Simazin	0,002	0,0067	-				
Terbutilazin	0,001	0,0033	1	0,001		0,001	0,001
Terbutrin	0,005	0,017	-				
Skupni pesticidi			3	0,012	0,015	0,002	0,017

\*LOD - meja detekcije / Limit of detection; LOQ - meja določljivosti / Limit of quantification;

N – št. določenih vzorcev nad LOQ / No. of samples above the LOQ; Povp. - povprečna vrednost / Average value;

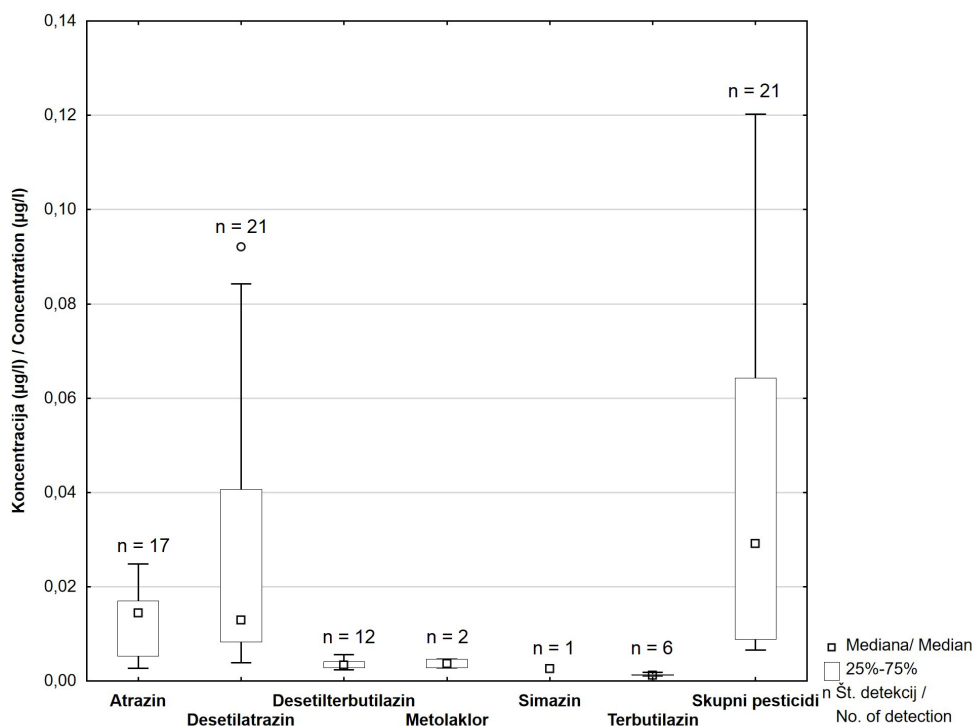
Md – mediana / Median; Min. – najmanjša vrednost / Minimum value; Max. – največja vrednost / Maximum value;

Std.Dev. – standardna deviacija / Standard deviation

desetilatrazin sta bila največkrat določena v vzorcih podzemne vode, desetilatrazin v vseh vzorcih (21) (sl. 2), atrazin pa v 17. S padajočim številom detekcije jima sledijo desetilterbutilazin (12), terbutilazin (6), metolaklor (2) ter simazin (1). Ostali niso bili zaznani niti enkrat. Pesticidi, ki niso bili določeni nad mejo določljivosti (LOQ) ali mejo zaznavanja (LOD) v podzemni vodi so: 2,6-diklorobenzamid, alaklor, desizopropilatrazin, dimetenamid, klortoluron, metazaklor, prometrin, propazin in terbutrin (Tabela 2, sl. 2). V površinski vodi nismo zaznali tudi simazina in

terbutilazina, je pa bil enkrat v istem vzorcu v reki Savi določen klortoluron.

Ker sta reki Sava in Krka pomembni hidravlični dejavnik za podzemno vodo (napajanje/dreniranje) smo prisotnost pesticidov določali tudi v obeh rekah. Atrazin in desetilatrazin sta bila v obeh določena v prvi seriji. Samo enkrat so bili določeni klortoluron in propifenzon v Savi, ter terbutilazin v Krki, vsi v prvi seriji. Nad mejo detekcije je bil določen metolaklor v prvi seriji v Savi in v drugi v Krki.



Sl. 3. Koncentracije izmerjenih pesticidov v podzemni vodi Krško-Brežičkega polja.

Fig. 3. Concentrations of measured pesticides in Krško-Brežice polje groundwater.

Na sliki 3 so predstavljene minimalne, povprečne in maksimalne vrednosti izbranih pesticidov v podzemni vodi Krško-Brežičkega polja. Tisti, ki niso bili niti enkrat določeni nad mejo LOD, niso prikazani.

Koncentracije posameznih pesticidov kot tudi skupne vsote pesticidov ne presegajo dovoljene mejne vrednosti za pitno vodo ( $0,1 \mu\text{g}$ ;  $0,5 \mu\text{g}$ ). Med pesticidi sta največkrat zaznana in to v višjih koncentracijah atrazin (max.  $0,025 \mu\text{g}$ ) in njegov razgradni produkt desetilatrazin (max.  $0,092 \mu\text{g}$ ), čeprav je uporaba atrazina v Sloveniji prepovedana od 1. 2003 (91/414/EGS). Terbutila-

zin, ki je v uporabi nadomestil atrazin, in njegov razgradnji produkt desetilterbutilazin sledita po številu detekcij, vendar so njune koncentracije nižje (terbutilazin max.  $0,001 \mu\text{g}$ , desetilterbutilazin max.  $0,004 \mu\text{g}$ ). V obeh primerih je razgradni produkt zaznan nad mejo detekcije večkrat od matične spojine in po navadi v višjih koncentracijah. Simazin ( $1\times$ ) in metolaklor ( $2\times$ ) se v podzemni vodi pojavljata posamično.

#### Identifikacija pesticidov s pasivnim vzorčenjem

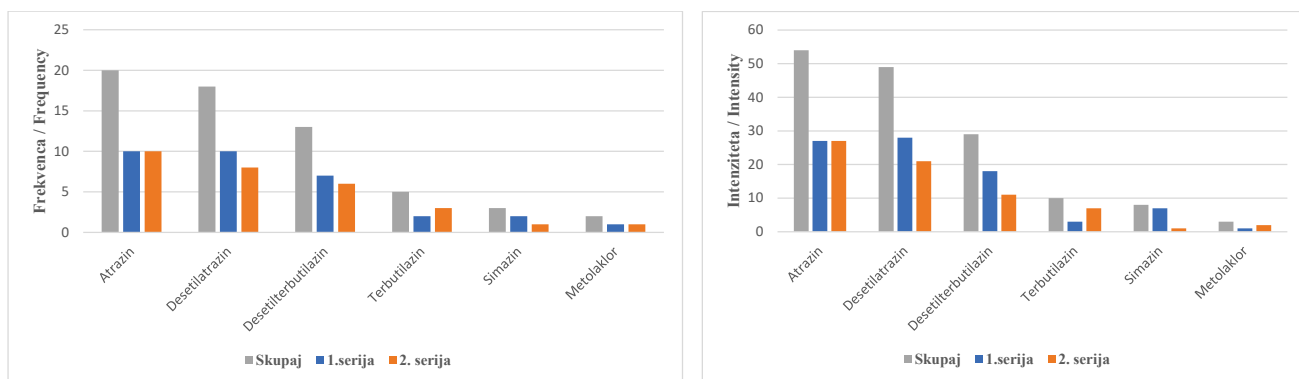
S kvalitativno metodo pasivnih vzorčevalnikov smo na območju Krško-Brežičkega polja skupaj

Tabela 3. Seznam pesticidov določenih v obeh serijah.

Table 3. List of pesticides specified in both series.

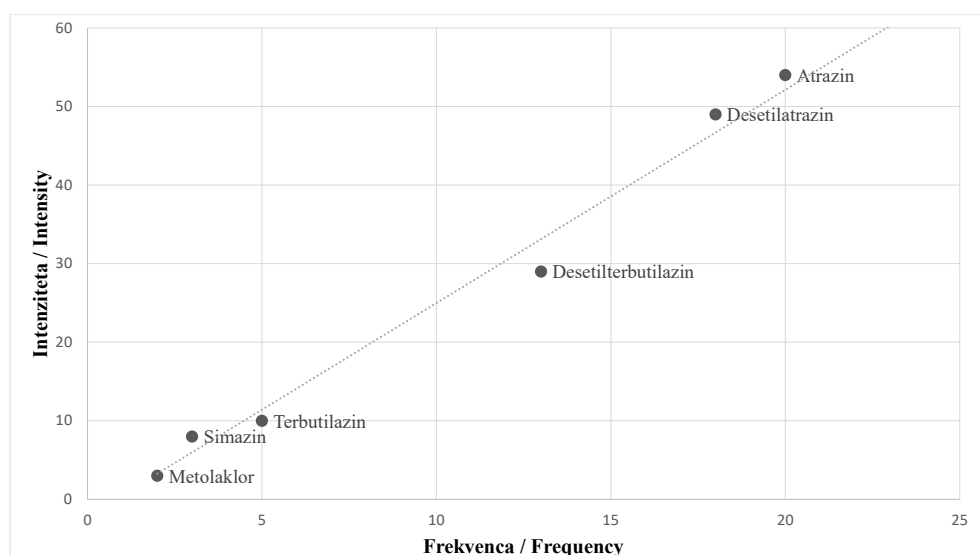
tr	Spojina / Compound	CAS NO.	t.i./c.i.	Razlaga / Explanation	Skupina / Group	Uporaba / Use
11,3	cikluron	2163-69-1	c.i.	herbicid	Pesticidi	K
11,8	dietiltoluamid	134-62-3	t.i.	repelent za mrčes	Pesticidi	K
12,9	desetilterbutilazin	30125-63-4	c.i.	razgradni produkt herbicida terbutilazina	Pesticidi	K
13	desetilatrazin	6190-65-4	c.i.	razgradni produkt herbicida atrazina	Pesticidi	K
13,7	simazin	122-34-9	c.i.	herbicid	Pesticidi	K
13,8	atrazin	1912-24-9	c.i.	herbicid	Pesticidi	K
14,2	terbutilazin	5915-41-3	c.i.	herbicid	Pesticidi	K
17,3	metolaklor	51218-45-2	c.i.	herbicid	Pesticidi	K

CAS št. / CAS no. - registrska številka CAS / CAS (Chemical Abstracts Service) Registry Number



Sl. 4. Prikaz a.) frekvenc in b.) intenzitet določitve izbranih pesticidov s pasivnimi vzorčevalniki.

Fig. 4. Display of a.) Frequencies and b.) Intensity of determination of selected pesticides with passive samplers.



Sl. 5. Razmerja skupnih intenzitet in frekvenc za posamezne pesticide.

Fig. 5. Ratios of total intensities and frequencies for individual pesticides.

v podzemni in površinski vodi (samo v reki Savi) skupno 24 vzorcev. Za namen določitve pesticidov v podzemni vodi smo izločili 8 spojin, ki se pojavljajo v obeh serijah. Seznam pesticidov določenih v obeh serijah (8) je skupaj s CAS (Chemical Abstracts Service) številom podan v tabeli 3. V nadaljnjo analizo smo vključili pesticide, ki smo jih določili tudi s kvantitativnimi kemiskimi analizami in so običajno v uporabi. Izključili smo cirklon in dietiltoluamid.

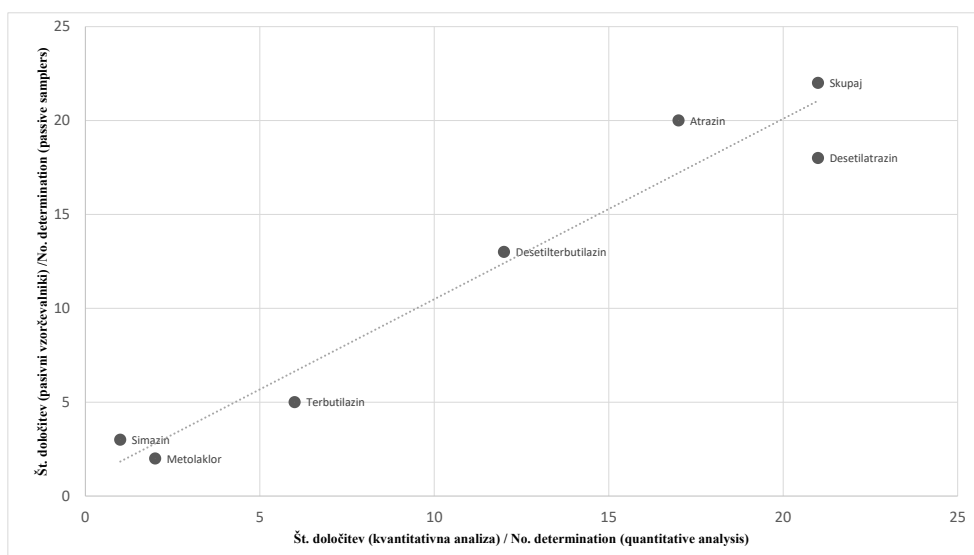
Na sliki 4 so podane frekvence in jakost določitve posameznega pesticida skupaj in po serijah.

Diagrami na slikah 4 in 5 nam kažejo, da sta največkrat in z najmočnejšim signalom tudi po posamičnih serijah zaznana atrazin in desetilatrazin. Sledijo desetilterbutilazin, terbutilazin, simazin in metolaklor. Prisotnost atrazina, njegovega razpadnega produkta desetilatrazina in simazina v podzemni vodi je lahko posledica

starih bremen, počasne razgradnje in hidrogeoloških pogojev ali pa njihove nelegalne uporabe po uveljavitvi prepovedi uporabe.

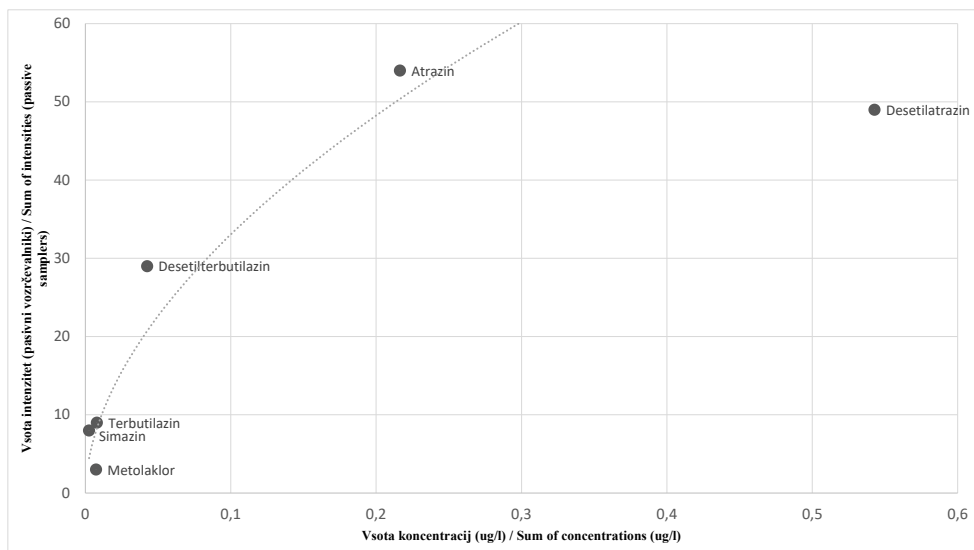
#### Primerjava rezultatov kvantitativnih analiz in analiz pasivnega vzorčenja

Čeprav je pasivno vzorčenje namenjeno identifikaciji prisotnosti spojin in ne kvantitativnem vrednotenju, smo primerjali identifikacijo pesticidov na obo načina. Na sliki 6 je prikazano razmerje skupnega števila pozitivnih določitev (frekvenc) po obeh metodah za posamezno spojino. Vidimo, da je pogostost določitve z metodo pasivnih vzorčevalnikov enaka ali večja. Simazin, desetilterbutilazin in atrazin so bili s pasivnim vzorčenjem detektirani večkrat. Desetilatrazin je bil zaznan v vseh merilnih mestih. Primerjava rezultatov po obeh metodah nam pa lahko da oceno uporabnosti metode pasivnega vzorčenja.



Sl. 6. Število določitev po metodi kvantitativne določitve in pasivnega vzorčenja.

Fig. 6. Number of determinations by the method of quantitative determination and passive sampling.



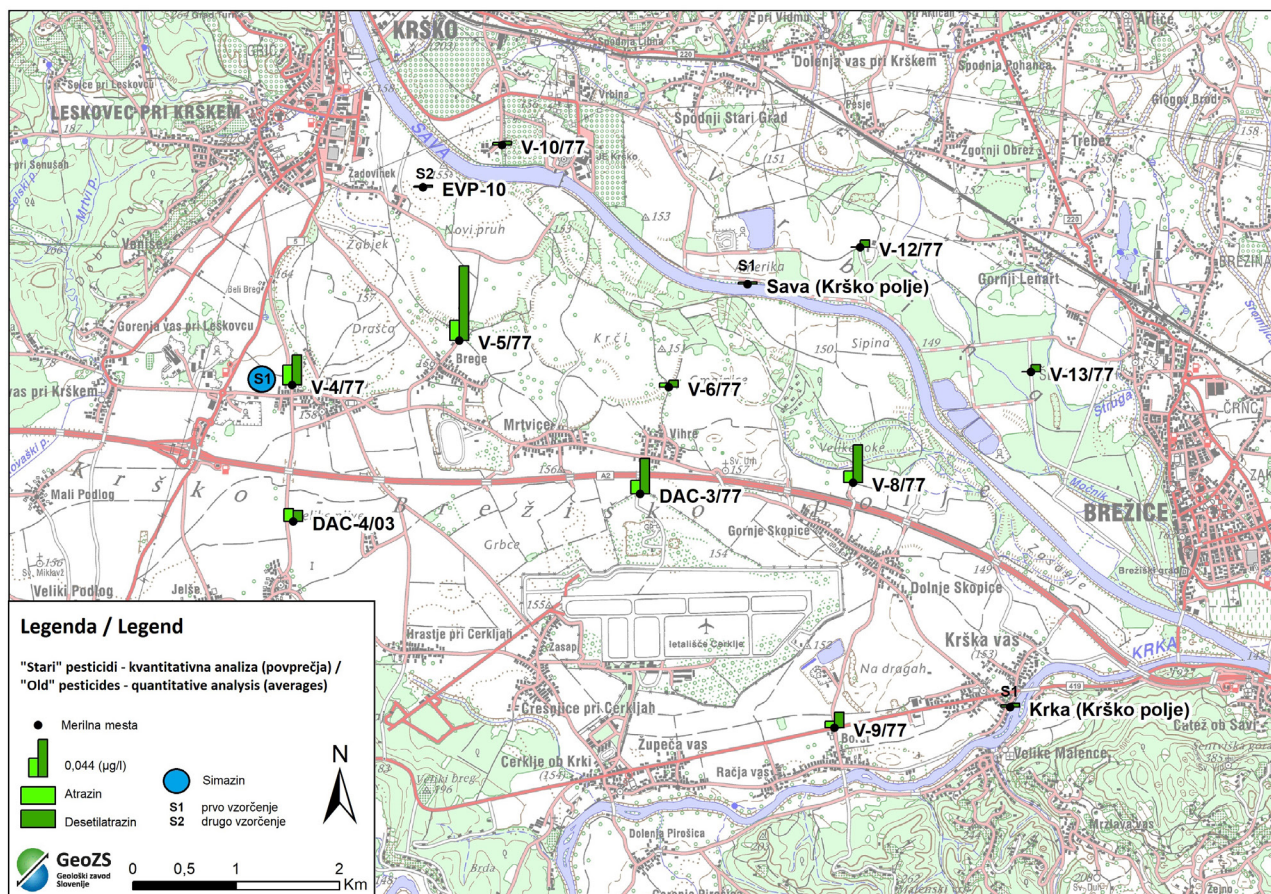
Sl. 7. Primerjava določenih skupnih koncentracij za izbrane pesticide z intenzitetami pasivnega vzorčenja.

Fig. 7. Comparison of certain total concentrations for selected pesticides with passive sampling intensities.

### Prostorska in časovna porazdelitev pesticidov v podzemni vodi

V diagramu (sl. 7) lahko vidimo, da skupne intenzitete izbranih pesticidov v pasivnih vzorčevalnikih naraščajo eksponentno proti skupnim določenim koncentracijam, razen desetilatrazina. Rezultati nakazujejo na omejitve pri pasivnem vzorčenju, ki so posledica izpiranja spojin po daljšem času. Rezultati kažejo, da je metoda vzorčenja s pasivnimi vzorčevalniki primerna za kvalitativno določitev prisotnosti posameznih organskih onesnaževal in da ima metoda po pričakovanjih zaradi daljše izpostavljenosti v vodi večjo verjetnost določitve posameznega onesnaženja.

Vzorčenji smo izvedli v jesenskem (oktober 2018) in pomladnjem (april 2019) obdobju. Iz analize rezultatov je razvidno, da so koncentracije atrazina in desetilatrazina na posameznem mernem mestu dokaj konstantna. Iz karte povprečnih koncentracij obeh pesticidov (sl. 8) je razvidno, da je podzemna voda na desnem bregu reke Save bolj obremenjena z obema pesticidoma in da so največje obremenitve na območju od Drnovega v smeri Brege in Vihre. Koncentracije razgradnega produkta desetilatrazina so višje od koncentracije matične spojine, ki je prepovedana za uporabo od leta 2003. Višje vrednosti atrazina



Sl. 8. Prostorski prikaz povprečnih vrednosti atrazina in desetilatrazina ter določitve simazina na Krško – Brežiškem polju v obdobju okt. 2018 in aprila 2019.

Fig. 8. Spatial representation of atrazine and desethylatrazine average values and determination of simazine in Krško - Brežičko polje in the period Oct. 2018 and April 2019.

od desetilatrazina so zaznane samo na merilnem mestu DAC-4/03 kar lahko kaže na lokalno onesnaženje in možno uporabo v obdobju po preprovedi. Razlog za obstoj desetilatrazina v podzemni vodi so lahko tudi specifične hidrokemijske razmere, ki preprečujejo razpad. Prav tako kot uporaba atrazina, ni dovoljena uporaba simazina. Simazin smo zaznali samo enkrat v prvi seriji na merilnem mestu V-4/77 na Drnovem (sl. 8).

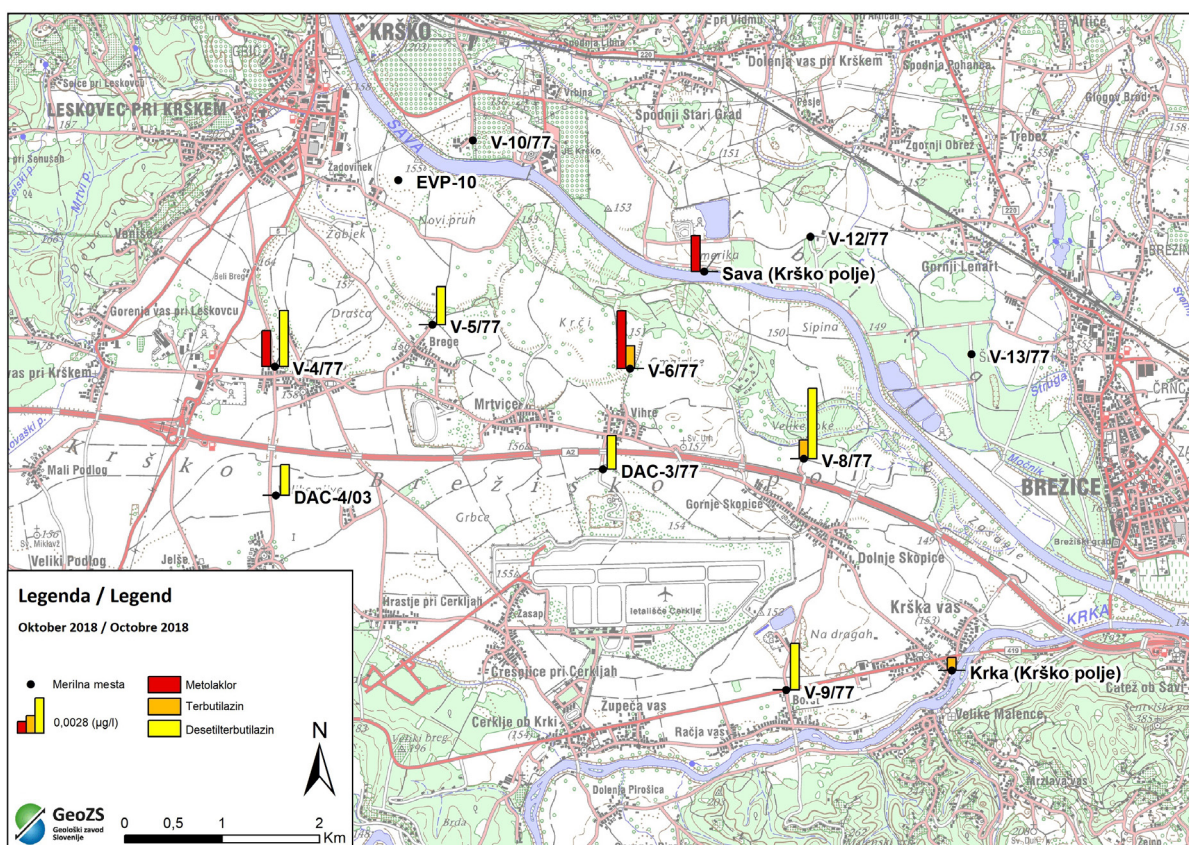
Na sliki 9 so prikazane določene vrednosti terbutilazina, desetilterbutilazina in metolaklora za vsako vzorčevalno obdobje posebej. Iz rezultatov je razvidno, da na območju vodonosnika na levem bregu reke Save nismo zaznali omenjenih treh pesticidov nad LOD. V osrednjem delu vodonosnika so višje vrednosti desetilterbutilazina določene na vseh merilnih mestih podzemne vode razen v V-6/77 konstantno v obeh serijah. Terbutilazin je v prvi seriji okt. 2018 določen na dveh mestih (V-6/77 in V-8/77), v drugi aprila 2019 pa

še v V-4/77 in DAC-3/77. Metolaklor smo določili samo v prvi seriji na merilnih mestih V-4/77 in V-6/77. V površinskih vodah smo v vsaki seriji zaznali po eno detekcijo metolaklora (v reki Savi v prvi seriji in v reki Krki v drugi seriji), drugih dveh pesticidov nismo zaznali.

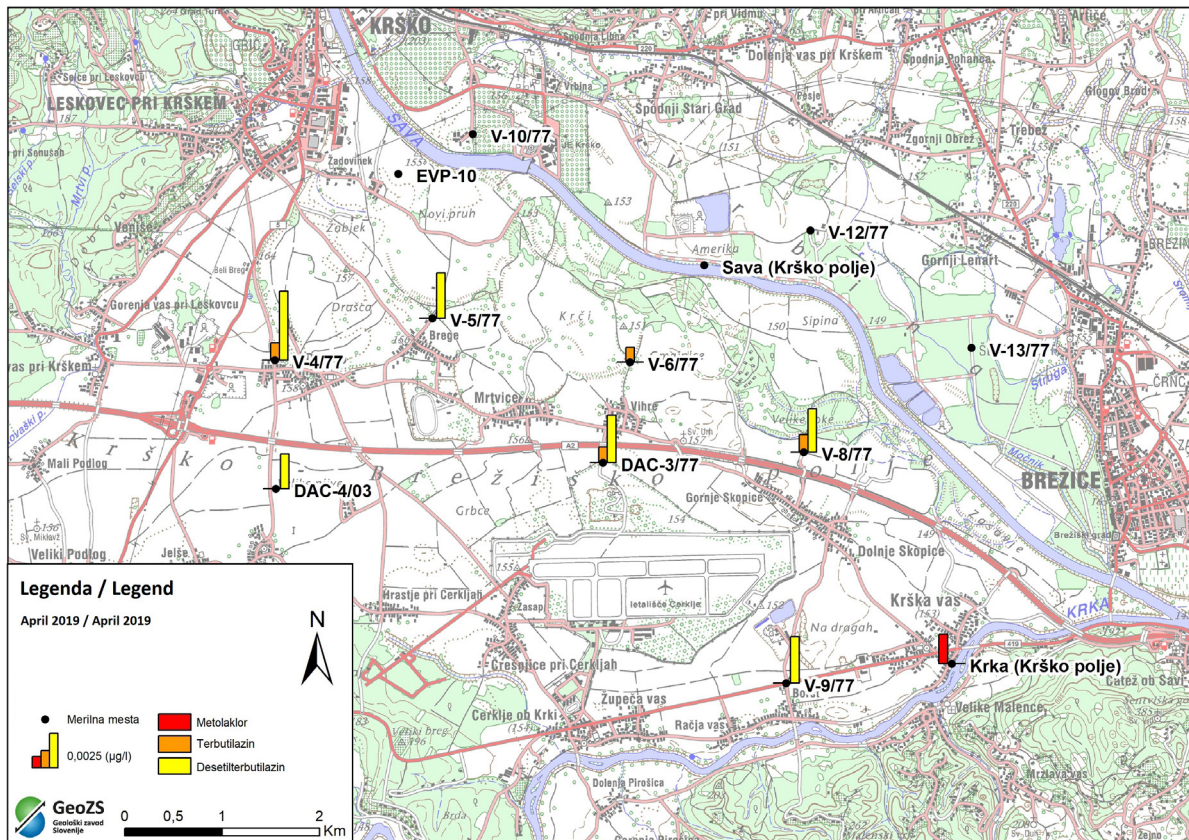
Prav tako smo primerjali intenzitete pesticidov pasivnega vzorčenja v prvi (zimska) in drugi (poletni) seriji po merilnih mestih (sl. 10). Intenziteta signalov v prvi seriji je višja. Izstopajo intenzitete desetilatrazina, desetilterbutilazina in simazina, manjše pa so vrednosti terbutilazina in metolaklora.

Na sliki 11 je prostorski prikaz določitev pasivnega vzorčenja vseh pesticidov v obeh serijah na merilno mesto. Največja obremenjenost s pesticidi je v osrednjem delu Krškega polja (V-4/77, V-5/77 in DAC-3/77). Večje obremenitve se kažejo tudi na merilnem mestu V-9/77.

a)

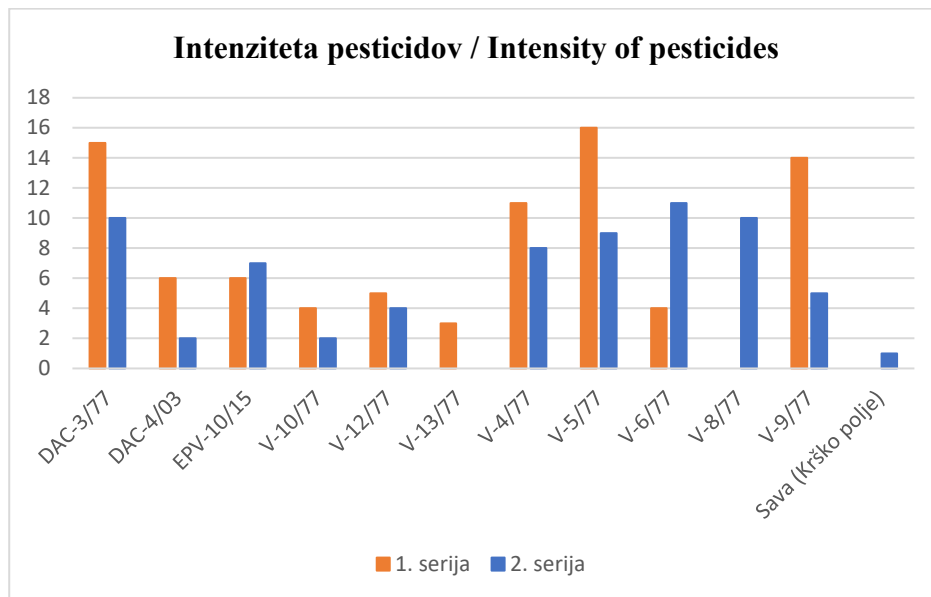


b)



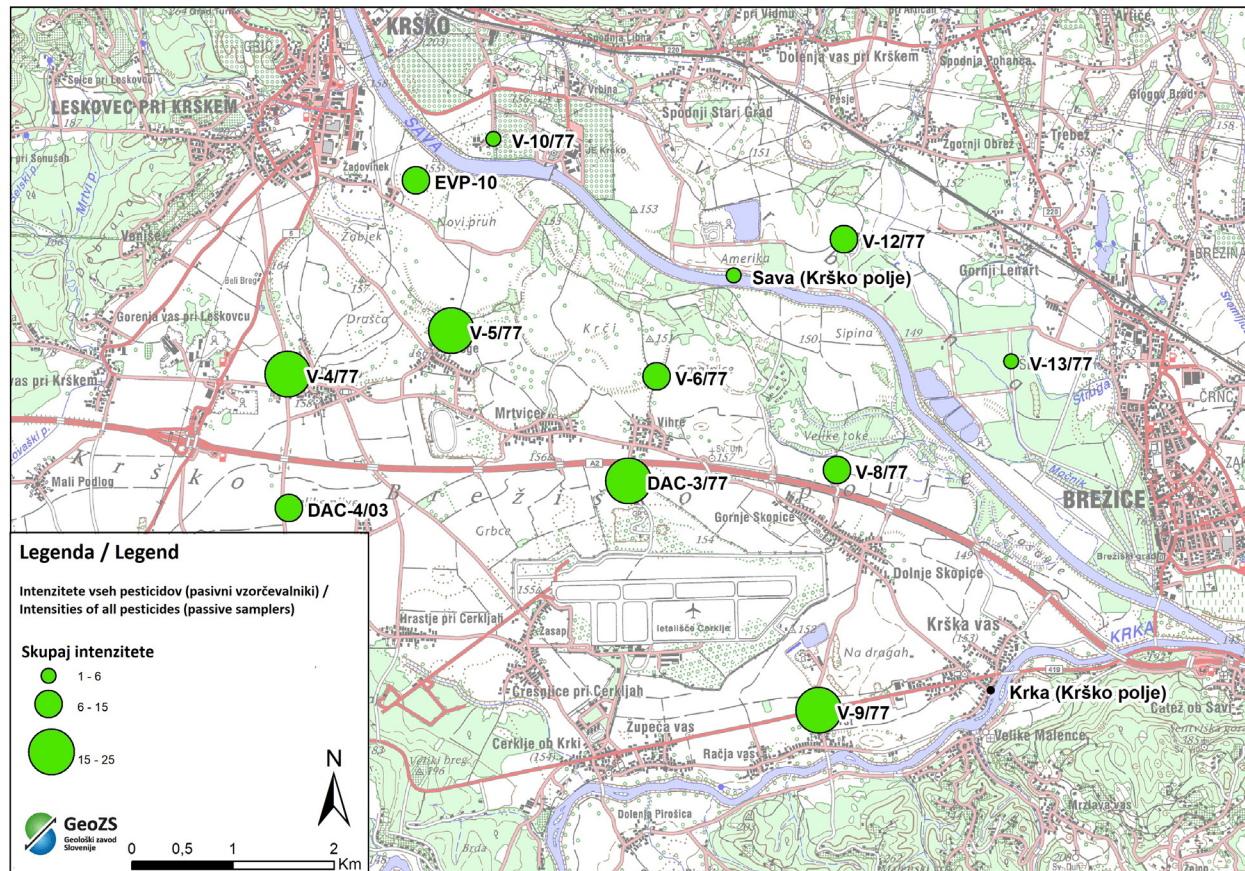
Sl. 9. Prostorski prikaz vrednosti terbutilazina, desetilterbutilazina in matolaklora na Krško - Brežiškem polju v deveh vzorčenjih okt. 2018 (a) in aprila 2019 (b).

Fig. 9. Spatial representation of terbutylazine, desethylerbutylazine and matolachlor values in Krško - Brežice polje in two samplings of oct. 2018 (a) and April 2019 (b).



Sl. 10. Intenziteta določitve pesticidov po merilnih mestih.

Fig. 10. Intensity of pesticide determination by sampling sites.



Sl. 11. Prostorski prikaz intenzitet vseh pesticidov.

Fig. 11. Spatial representation of the intensities of all pesticides at the sampling site.

Podatki za določitev prispevnega oz. napajalnega območja za posamezno merilno mesto so zbrani v tabeli 4. Na podlagi povprečnega koeeficiente prepustnosti ( $3 \cdot 10^{-3}$  m/s) in povprečnega gradienata (0,0014), smo izračunali povprečno površino zaledja za posamezno merilno mesto za obdobje enega leta. Na osnovi baze pokrovnosti tal CLC 2012 in prostorske analize smo določili

deležne posamezne enote pokrovnosti tal za zaledje vsakega merilnega mesta. Merilna mesta z izrazito kmetijskim zaledjem (100 %) so V-5/77, V-6/77, V-9/77, V-10/77, V-12/77, DAC-3/077 in DAC-4/03. Merilno mesto, pri katerem je v zaledju največ gozda je V-13/77. Petdeset odstotkov industrijskega zaledja predstavlja zaledje pri vrtini V-4/77. Pri ostalih vrtinah je zaledje mešano (Tabela 4).

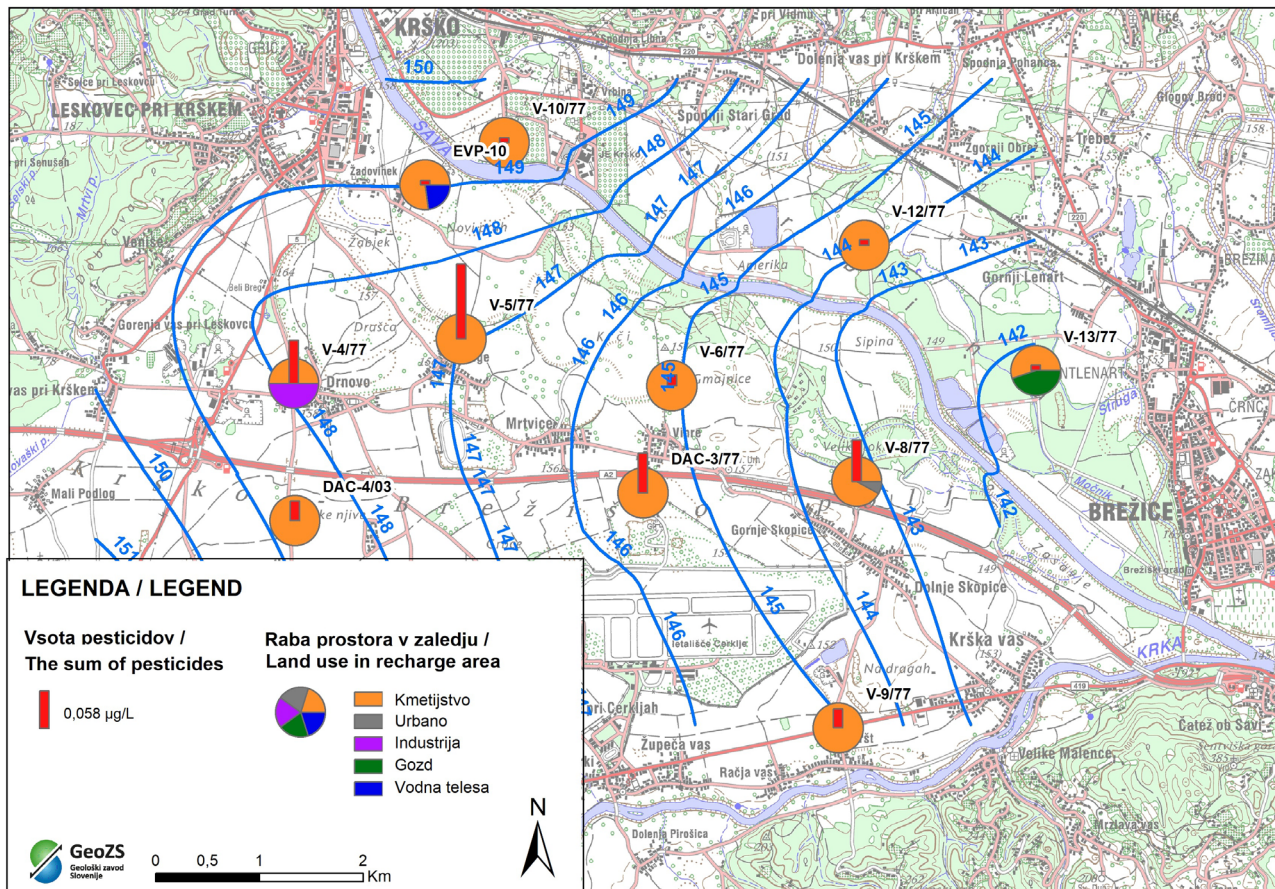
Tabela 4. Podatki o pokrovnosti in rabi tal v zaledju vsakega merilnega mesta na Krško-Brežiškem polju.

Table 4. Background data of each measuring point in the Krško-Brežiškem polju.

Merilno mesto	Kmetijske površine / Agrucultural land	Urbano / Urban	Industrijske površine / Industrial	Gozd / Forest	Vodna telesa / Water bodies
	(%)	(%)	(%)	(%)	(%)
V-13/77	55,04	0	0	44,96	0
V-12/77	100	0	0	0	0
V-10/77	100	0	0	0	0
V-9/77	100	0	0	0	0
V-8/77	91,94	8,06	0	0	0
V-6/77	100	0	0	0	0
V-5/77	100	0	0	0	0
V-4/77	50,02	0	49,98	0	0
EVP-10	77,12	0	0	0	22,88
DAC-4/03	100	0	0	0	0
DAC-3/77	100	0	0	0	0

Za prikaz prisotnosti pesticidov v podzemni vodi na Krško-Brežiškem polju smo uporabili vsote povprečnih vrednosti vseh pesticidov na merilno mesto. Prostorski prikaz povprečne vso-te pesticidov s podatki o pokrovnosti in rabi tal v zaledju merilnih mest je prikazan na sliki 12.

Prostorsko izhajajo največje obremenitve na Krško-Brežiškem polju s kmetijskih površin. Podzemna voda je bolj obremenjena s pesticidi v osrednjem delu polja v smeri toka od merilne-ga mesta V-5/77 proti jugovzhodu proti območju merilnega mesta V-8/77. Merilno mesto V-4/77, ki



Sl. 12. Prostorska porazdelitev povprečne vsote pesticidov v podzemni vodi Krško-Brežiškega polja.

Fig. 12. Spatial distribution of the sum of pesticides in Krško-Brežice polje aquifer.

ima na 50 % zaledja območje urbane in industrijske rabe, ne izstopa s povprečnimi vrednostmi skupnih pesticidov. Samo na tem mestu smo s kvantitativno analizo določili simazin, ki pa je bil določen na tem mestu tudi s pasivnim vzorčenjem.

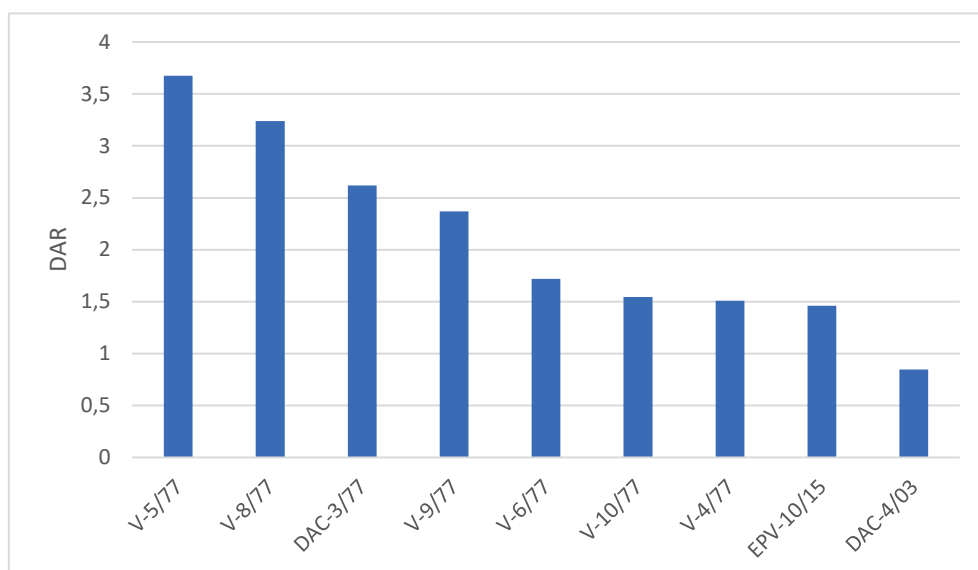
### Razmerje pesticidov in njihovih razgradnih produktov

V podzemni vodi Krško-Brežiškega polja se pojavljata pesticida atrazin in terbutilazin in njuna razgradna produkta desetilatrazin ter desetilterbutilazin, nismo pa zasledili razgradnega produkta atrazina - desizopropilatrazina. Prisotnost atrazina v povečanih koncentracijah v podzemni vodi na nekaterih mestih lahko razložimo kot rezultat njegove uporabe v preteklosti in njegove obstojnosti v okolju. Razmerje DAR smo uporabili pri določitvi »starosti« onesnaženja z atrazinom in njegovim razgradnim produkтом desetilatrazinom. Majhno razmerje DAR kaže na »sveže« onesnaženje in je lahko kazalnik točkovnega vira onesnaženja.

Koefficient DAR smo izračunali iz povprečij za posamezno merilno mesto. Na merilnih mestih V-12/77 in V-13/77 nismo določili atrazina, zato razmerja DAR nismo določili (sl. 13). Najvišje vrednosti DAR so na merilnem mestu V-5/77 (3,7), najnižje pa v V-5/77 (0,8), ki je edina vrednost razmerja pod 1, kar kaže na večjo vsebnost atrazina od razgradnega produkta. Vrednosti DAR nižje od 1 je presenetljiva glede na to, da je prepoved uporabe atrazina v veljavi že dalj časa. Res pa je, da so na tem merilnem

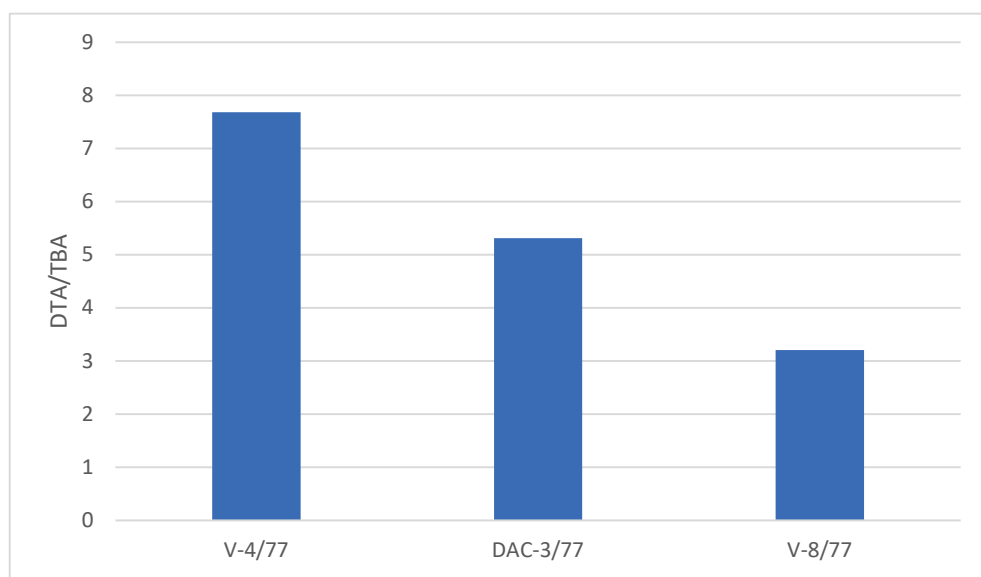
mestu določene vrednosti koncentracij atrazina in desetilatrazina zelo nizke, so pod dovoljeno mejo in zato DAR interpretiramo samo kot indikator možnega izvora atrazina. Visoka pojavnost atrazina je lahko posledica starih bremen zaradi počasne razgradnje in hidrogeoloških pogojev ali pa uporabe po uveljavitvi prepovedi. Čeprav je visok indikator DAR pokazatelj nizke vsebnosti matične spojine, pa je visok DAR v našem primeru na merilnih mestih V-5/77, V-8/77, DAC-3/77 in V-4/77 posledica zelo visokih vrednosti desetilatrazina, ki presegajo celo normativ za pitno vodo (0,1 ug/l). V zadnjem (V-4/77) je tudi povprečna vrednost atrazina relativno visoka, vendar je določena nekoliko pod normativom za pitno vodo (0,09 ug/l).

Na osnovi rezultatov določitve terbutilazina in desetilterbutilazina smo izračunali tudi razmerje med desetilterbutilazinom in terbutilazinom (DTA/TBA) (sl. 14). Razmerje, manjše od 1, kaže na možnost točkovnega (lokalnega) vira onesnaženja. Razmerja DTA/TBA ni bilo mogoče izračunati za vsa merjenja na vseh merilnih mestih, saj so bile koncentracije terbutilazina in/ali desetilterbutilazina na nekaterih mestih pod LOD. V našem primeru smo lahko DTA/TBA izračunali na treh različnih točkah (Slika 14). Najniže izračunano povprečje je na točki V-8/77 (3,2), najviše pa v točki V-4/77 (7,7). Vse vrednosti razmerja so nad 1. Iz osnovnih podatkov je vidno, da so koncentracije terbutilazina zelo nizke okoli 0,01 ug/L, koncentracije desetilterbutilazina so deset krat višje, a so še vedno pod mejo normativa za pitno vodo.



Sl. 13. Povprečno razmerje med koncentracijo desetilatrazina in atrazina (DAR).

Fig. 13. Average ratio of the desethylatrazine to atrazine concentrations (DAR).



Sl. 14. Razmerje DTA/TBA.  
Fig. 14. DTA/TBA ratio.

### Zaključki

Vodonosnik Krško-Brežiškega polja je zaradi rabe prostora in dejavnosti podvržen različnim vplivom urbanega okolja, industrije, infrastrukturnih objektov predvsem pa kmetijskih površin, ki predstavljajo največji delež rabe prostora in so tudi glavni vir pesticidov v okolju in podzemni vodi. V naši raziskavi smo prišli do naslednjih zaključkov:

- Pojav pesticidov v podzemni vodi smo potrdili po celotnem Krško-Brežiškem polju. Koncentracije pesticidov ne presegajo normativov za pitno vodo.
- Atrazin in desetilatrazin sta še vedno, kljub več desetletni prepovedi uporabe fitofarmacevtskih sredstev na osnovi atrazina, najpogosteje in v najvišjih koncentracijah zaznana pesticida v podzemni vodi Krško-Brežiškega polja. Posamezne analize desetilatrazina kažejo na vrednosti višje od normativa za pitno vodo.
- Poleg omenjenih smo iz izbranega nabora 15. pesticidov določili še terbutilazin, desetilterbutilazin, metolaklor in simazin.
- Z metodo vzorčenja s pasivnimi vzorčevalniki smo v dveh serijah vzorčenja poleg imenovanih pesticidov določili tudi cikluron in diethyltoluamid.
- Pasivno vzorčenje je pokazalo, da se z najmočnejšim signalom zaznata atrazin in desetilterbutilazin. Sledijo desetilterbutilazin, terbutilazin, simazin in metolaklor.
- Pasivno vzorčenje je namenjeno identifikaciji prisotnosti spojin in ne kvantitativnem vrednotenju. Kljub temu smo želeli ovrednotiti uporabnost metode. Pogostnost določitve z metodo vzorčenja s pasivnimi vzorčevalniki

se je izkazala za večjo v primerjavi z kvantitativnim določanjem s klasičnim vzorčenjem. Simazin, desetilterbutilazin in atrazin so bili večkrat določeni s pasivnim vzorčenjem. Desetilatrazin je bil zaznan v vseh merilnih mestih.

- Primerjava intenzitet pasivnega vzorčenja in kvantitativne določitve spojin metodološko sicer ni relevantna, vendar primerjava rezultatov kaže, da se z večjo koncentracijo posameznih spojin v vodi veča tudi intenziteta teh spojin v pasivnih vzorčevalnikih.
- Rezultati kažejo, da je metoda vzorčenja s pasivnimi vzorčevalniki primerna za kvalitativno določitev prisotnosti posameznih organskih onesnaževal in da ima metoda po pričakovanjih zaradi daljše izpostavljenosti v vodi večjo verjetnost določitve posameznega onesnaževala.
- Rezultati kažejo, da so koncentracije atrazina in desetilatrazina na posameznem merilnem mestu dokaj konstantne, vendar je podzemna voda na desnem bregu reke Save bolj obremenjena z obema pesticidoma. Največje obremenitve so na območju od Drnovega v smeri Brege in Vihre. Koncentracije razgradnjega produkta desetilatrazina so višje od matične spojine, ki je prepovedana za uporabo od leta 2003, izjema je merilno mesto DAC-4/03. Sklepamo na točkovno onesnaženje in možno uporabo v obdobju po prepovedi.
- Čeprav uporaba simazina ni dovoljena, smo ga zaznali na merilnem mestu V-4/77 na Drnovem, tako s klasično analizo kot pasivnim vzorčenjem.
- Ostali preučevani pesticidi so bili določeni v vodonosniku na desnem bregu Save. Največje

obremenitve podzemne vode na Krško-Brežiškem polju izhajajo iz kmetijskih površin. Največja obremenjenost s pesticidi je v osrednjem delu Krškega polja (V-4/77, V-5/77, V-8/77 in DAC-3/77). Večje obremenitve se kažejo še na merilnem mestu V-9/77. Merilno mesto V-4/77, ki ima na 50 % zaledja območje urbane in industrijske rabe, ne izstopa z povprečnimi vrednostmi skupnih pesticidov.

- Z metodologijo vrednotenja razmerij med razgradnim produkтом in primarnim pesticidom (DAR in DTA/TBA) smo določili »starosti« onesnaženja iz naslova atrazina in terbutilazina. Vrednosti DAR nižje od 1 smo opredelili samo na merilnem mestu V-5/77, kar kaže na večjo vsebnost atrazina od razpadnega produkta. Ker so na tem merilnem mestu koncentracije atrazina in desetilatrazina zelo nizke, je potrebno vrednosti DAR interpretirati z veliko stopnjo previdnosti.
- Razmerja DTA/TBA, ki kaže na točkovno onesnaženje, smo glede na določene, zelo nizke koncentracije terbutilazina in desetilterbutilazina izračunali samo na treh merilnih mestih. Vse vrednosti razmerja so nad 1. Koncentracije desetilterbutilazina so 10 × višje od terbutilazina in so še vedno pod mejo normativa za pitno vodo.

### Zahvala

Raziskava je bila narejena v okviru, raziskovalnega programa »Podzemne vode in geokemija (P1-0025)« in projektov »Učinkovitejša raba vode in hranil v rastlinski pridelavi za varovanje in izboljšanje virov pitne vode - URAVIVO (L4-8221)« ter »Urbana hidrogeologija: Izboljšane metode za določanje pojava, transportnih procesov in izvora ostankov zdravil v virih podzemne vode (Z1-2639)«, ki se izvajata na Geološkem zavodu Slovenije in ju financira Javna agencija za raziskovalno dejavnost RS ter projekta GeoERA (HOVER), ki je prejel sredstva raziskovalnega in inovacijskega programa Evropske unije Obzorje 2020 (v skladu s sporazumom št. 731166).

### Literatura

- Adams, C.D. & Thurman, E.M. 1991: Formation and transport of desethylatrazine in the soil and vadose zone. *Journal of Environmental Quality* 20/3: 540–547. <https://doi.org/10.2134/jeq1991.0047242500200030007x>
- Ahrens, L., Daneshvar, A., Lau, A. E. & Kreuger, J. 2015: Characterization of five passive sampling devices for monitoring of pesticides in water.

*Journal of Chromatography A*, 1405: 1-11. <https://doi.org/10.1016/j.chroma.2015.05.044>

Alvarez, D.A., Petty, J.D., Huckins, J.N., Jones-Lepp, T.L., Getting, D.T., Goddard, J.P. & Manahan, S.E. 2004. Development of a passive, in situ, integrative sampler for hydrophilic organic contaminants in aquatic environments. *Environmental Toxicology and Chemistry*, 23/7: 1640–1648. <https://doi.org/10.1897/03-603>

APVMA 2008: Atrazine Review—Final Review Report & Regulatory Decision Volume Australian Pesticides & Veterinary Medicines Authority, 1-34.

ARSO 2009: Ocena kemisjkega stanja in trendov vodnega telesa podzemne vode 1003 – KRŠKA KOTLINA. Dostopno na: [https://www.google.com/url?sa=t&rct=j&q=&esrc=s&source=web&cd=&ved=2ahUKEwiDptDxlrrzAh-VDy6QKHawgC1YQFnoECAgQAQ&url=https%3A%2F%2Fvode%2Fpodzemne%2520vode%2Fpublikacije%2520in%2520poro%25C4%258Dila%2F1003.pdf&usg=AOvVaw0du23JX\\_rPhJ9DnvOkYsWr](https://www.google.com/url?sa=t&rct=j&q=&esrc=s&source=web&cd=&ved=2ahUKEwiDptDxlrrzAh-VDy6QKHawgC1YQFnoECAgQAQ&url=https%3A%2F%2Fvode%2Fpodzemne%2520vode%2Fpublikacije%2520in%2520poro%25C4%258Dila%2F1003.pdf&usg=AOvVaw0du23JX_rPhJ9DnvOkYsWr) (Pridobljeno 1.9.2021).

ARSO 2014: Klimatološka povprečja 1981–2010. Dostopno na: [https://meteo.arso.gov.si/met/sl/climate/tables/normals\\_81\\_10/](https://meteo.arso.gov.si/met/sl/climate/tables/normals_81_10/) (Pridobljeno 8.10.2021).

ARSO 2016: Karta pokrovnosti tal po CORINE 2012 [digitalno kartografsko gradivo]. Ljubljana: Ministrstvo za kmetijstvo in okolje, Agencija Republike Slovenije za okolje. Dostopno na: <https://gis.arso.gov.si/wfs-web/faces/WFSLayersList.jspx> (Pridobljeno 16.5.2017).

ARSO 2019: Kemijsko stanje podzemnih voda v Sloveniji, Poročilo za leto 2018. Dostopno na: [https://www.arso.gov.si/novice/datoteke/041039-2203\\_kemijsko%20stanje%20voda%202018\\_fin.pdf](https://www.arso.gov.si/novice/datoteke/041039-2203_kemijsko%20stanje%20voda%202018_fin.pdf) (Pridobljeno 16.9.2019).

Auersperger, P., Lah, K., Kus, J. & Marsel, J. 2005: High precision procedure for determination of selected herbicides and their degradation products in drinking water by solid-phase extraction and gas chromatography-mass spectrometry. *Journal of Chromatography A*, 1088: 234–241.

Bartzas, G., Tinivella, F., Medini, L., Zaharaki, D. & Komnitsas, K. 2015: Assessment of groundwater contamination risk in an agricultural area in north Italy. *Information Processing in Agriculture*, 2/2: 109–129.

Bernhardt, E.S., Rosi, E.J. & Gessner, M.O. 2017: Synthetic chemicals as agents of

- global change. *Frontiers in Ecology and the Environment*, 15: 84–90.
- Burri, N.M., Weatherl, R., Moeck, C. & Schirmer, M. 2019: A review of threats to groundwater quality in the Anthropocene. *Sci. Total Environ.*, 684: 136–154. <https://doi.org/10.1016/j.scitotenv.2019.05.236>
- de Jonge, L.W., Kjaergaard, C. & Moldrup, P. 2004: Colloids and colloid-facilitated transport of contaminants in soils: an introduction. *Vadose Zone J.*, 3: 321–325.
- Direktiva 98/83/ES: Direktiva Evropskega Sveta 98/83/ES z dne 3. novembra 1998 o kakovosti vode, namenjene za prehrano ljudi, UL L 330/32.
- Direktiva 2006/118/ES: Direktiva 2006/118/ES Evropskega parlamenta in Sveta z dne 12. decembra 2006 o varstvu podzemne vode pred onesnaževanjem in poslabšanjem. UL L 372/19-31.
- ESRI Inc. 2004: ArcINFO ver 9, Software. Environmental Research Institute. Dopostona: (<http://www.esri.com/>).
- Fisher, I.J., Phillips, P.J., Bayraktar, B.N., Chen, S., McCarthy, B.A. & Sandstrom, M.W. 2021: Pesticides and their degradates in groundwater reflect past use and current management strategies, Long Island, New York, USA. *Science of Total Environment*, 752: 141895. <https://doi.org/10.1016/j.scitotenv.2020.141895>
- Giddings, J.M., Anderson, T.A., Hall, L.W., Kendall, R.J., Richards, R.P., Solomon, K., Williams, W.M. 2005: Atrazine in North American Surface Waters: A Probabilistic Aquatic Ecological Risk Assessment. Society of Environmental Toxicology and Chemistry (SETAC), Pensacola, Florida, USA: 1–30 p.
- González-Rodríguez RM, Rial-Otero R, Cancho-Grande B, Gonzalez-Barreiro, C. & Simal-Gándara, J. 2011: A Review on the Fate of Pesticides during the Processes within the Food-Production Chain. *Critical Reviews in Food Science and Nutrition*, 51: 99–114.
- Heuvelink, G.B.M., Burgers, S.L.G.E., Tiktak, A. & Den Berg, F.V. 2010. Uncertainty and stochastic sensitivity analysis of the GeoPEARL pesticide leaching model. *Geoderma*, 155: 186–192.
- Jarvis, N.J. 2007: A review of non-equilibrium water flow and solute transport in soil macropores: principles, controlling factors and consequences for waterquality. *European Journal of Soil Science*, 58: 523–546.
- Kim, K-H., Kabir, E., Jahan, S.A. 2017: Exposure to pesticides and the associated human health effects. *Science of the Total Environment*, 575: 525–535. <https://doi.org/10.1016/j.scitotenv.2016.09.009>
- Kolpin, D.W., Schnoebelen, D.J. & Thurman, E.M. 2004: Degradates Provide Insight to Spatial and Temporal Trends of Herbicides in Ground Water. *Ground Water*, 42: 601–608. <https://doi.org/10.1111/j.1745-6584.2004.tb02628.x>
- Koroša, A., Auersperger, P. & Mali, N. 2016: Determination of micro-organic contaminants in groundwater (Maribor, Slovenia). *Science of the Total Environment*, 571: 1419–1431. <https://doi.org/10.1016/j.scitotenv.2016.06.103>
- Koroša, A. 2019: Izvor in transport organskih onesnaževal v medzrnskih vodonosnikih. Doktorska disertacija, Univerza v Ljubljani, Naravoslovnotehniška fakulteta, Ljubljana: 207 p.
- Kot, A., Zabiegała, B. & Namieśnik, J. 2000: Passive sampling for long-term monitoring of organic pollutants in water. *TrAC Trends in Analytical Chemistry*, 19/7: 446–459. [https://doi.org/10.1016/S0165-9936\(99\)00223-X](https://doi.org/10.1016/S0165-9936(99)00223-X)
- Lapworth, D.J. & Goody, D.C. 2006: Source and persistence of pesticides in a semi-confined chalk aquifer of southeast England. *Environmental Pollution*, 144/3: 1031–1044. <https://doi.org/10.1016/j.envpol.2005.12.055>
- Lapworth, D.J., Baran, N., Stuart, M.E. & Ward, R.S. 2012: Emerging organic contaminants in groundwater: A review of sources, fate and occurrence. *Environmental Pollution*, 163: 287–303. <https://doi.org/10.1016/j.envpol.2011.12.034>
- Leskovar, J., Arh Marinčič, Š., Resnik, N. & Dokler, T. 2020: Poročilo o kakovosti pitne vode na javnih vodovodih ter odvajajuju in čiščenju odpadnih voda v občinah Krško in Kostanjevica na Krki v letu 2019. Krško, Kostak. Dostopno na: <https://www.google.com/url?sa=t&rct=j&q=&esrc=s&source=web&cd=&ved=2ahUKEwiv4KC-n993zAhUWgP0HHZfwCxQFnoE-CAQQAQ&url=https%3A%2F%2Fwww.kostak.si%2Fimages%2F1-2020%2Fporocilovoda2019.pdf&usg=AOvVaw3bpXM6KIN-1Y9F0v8SupeFD> (Pridobljeno 1.9.2021).
- Magnusson, B. & Örnemark, U. (eds.) 2014: Eurachem Guide: The Fitness for Purpose of Analytical Methods – A Laboratory Guide to Method Validation and Related Topics, 2 edition.
- Mali, N., Cerar, S., Koroša, A. & Auersperger, P. 2017: Passive sampling as a tool for identifying micro-organic compounds in groundwater.

- Science of The Total Environment, 593-594: 722-734. <https://doi.org/10.1016/j.scitotenv.2017.03.166>
- Milan, M., Ferrero, A., Fogliatto, S., Piano, S. & Vidotto, F. 2015: Leaching of S-metolachlor, terbutylazine, desethyl-terbutylazine, mesotrione, flufenacet, isoxaflutole, and diketonitrile in field lysimeters as affected by the time elapsed between spraying and first leaching event. Journal of Environmental Science and Health Part B, 50/12: 851-861. <https://doi.org/10.1080/03601234.2015.1062650>
- Mižigoj, U. 2014: Vpliv onesnaževalcev na vodno okolje v Krškem. Diplomska naloga, Ljubljana, Univerza v Ljubljani, Fakulteta za gradbeništvo in geodezijo: 70 p.
- Munz, N.A., Burdon, F.J., de Zwart, D., Junghans, M., Melo, L., Reyes, M. et al. 2017: Pesticides drive risk of micropollutants in wastewater-impacted streams during low flow conditions. Water Research, 110: 366-377. <https://doi.org/10.1016/j.watres.2016.11.001>
- Nienstedt, K.M., Brock, T.C.M., van Wensem, J., Montforts, M., Hart, A., Aagaard, A., et al. 2012: Development of a framework based on an ecosystem services approach for deriving specific protection goals for environmental risk assessment of pesticides. Science of the Total Environment, 415: 31-38. <https://doi.org/10.1016/j.scitotenv.2011.05.057>
- Nyoni, H., Chimuka, L., Vrana, B. & Cukrowska, E. 2011: Membrane assisted passive sampler for triazine compounds in water bodies - Characterization of environmental conditions and field performance. Analytica Chimica Acta, 694/1-2: 75-82. <https://doi.org/10.1016/j.aca.2011.03.045>
- Ogura, I.P., Zanin Lima, J., Pelinsom Marques, J., Massaro Sousa, L., Guimarães Silvestre Rodrigues, V. & Gaeta Espíndola, EL. 2021: A review of pesticides sorption in biochar from maize, rice, and wheat residues: Current status and challenges for soil application, Journal of Environmental Management, 300, 113753. <https://doi.org/10.1016/j.jenvman.2021.113753>
- Petersen, C.T., Holm, J., Koch, C.B., Jensen, H.E. & Hansen, S. 2002: Movement of pendimethalin, ioxynil and soil particles to field drainage tiles. Pest. Manage. Sci. 59/1: 85-96. <https://doi.org/10.1002/ps.609>
- Sasakova, N., Gregova, G., Takacova, D., Mojzisova, J., Papajova, I., Venglovsky, J. & Kovacova, S. 2018: Pollution of surface and ground water by sources related to agricultural activities. Frontiers in Sustainable Food Systems, 2: 1-11. <https://doi.org/10.3389/fsufs.2018.00042>
- Schult, J. 2016: Herbicides, pesticides and nutrients in the Tindall Aquifer (Katherine Region). Northern Territory Department of Land Resource Management, Report No. 13/2016D, Palmerston: 1-37 p.
- Seethapathy, S., Górecki, T. & Li, X. 2008: Passive sampling in environmental analysis. Journal of Chromatography A, 1184/1-2: 234-253. <https://doi.org/10.1016/j.chroma.2007.07.070>
- Shaw, M.S., Silburn, D.S., Lenahan, M. & Harris, M. 2012: Pesticides in Groundwater in the Lower Burdekin Floodplain Department of Environment and Resource Management, Queensland Government, Brisbane: 1-32 p.
- Shelton, J.F., Geraghty, E.M., Tancredi, D.J., Delwiche, L.D., Schmidt, R.J., Ritz, B. et al. 2014: Neurodevelopmental Disorders and Prenatal Residential Proximity to Agricultural Pesticides: The CHARGE Study. Environmental Health Perspectives, 122: 1103-1109.
- Shishaye, H.A., Tait, D.R., Maher, D.T., Befus, K.M., Erler, D., Jeffreya, L., Reading, M.J., Morgenstern, U., Kaserzon, S., Mueller, J. & Verelle-Hill, W.D. 2021: The legacy and drivers of groundwater nutrients and pesticides in an agriculturally impacted Quaternary aquifer system. Sci. Total Environ., 753/142010. <https://doi.org/10.1016/j.scitotenv.2020.142010>
- SIST ISO 5667-11:2010. Kakovost vode, vzorčenje – 11. del: Navodilo za vzorčenje podzemne vode, 1-10.
- SIST ISO 5667-23:2011. Water quality - Sampling - Part 23: Guidance on passive sampling in surface waters, 1-23.
- SIST EN ISO 5667-03:2012. Kakovost vode, vzorčenje - 3. del: Navodilo za hranjenje in ravnanje z vzorci.
- Sjerps, R.M.A., Kooij, P.J.F. van Loon, A. & van Wezel, A.P. 2019: Occurrence of pesticides in Dutch drinking water sources, Chemosphere, 235: 510-518. <https://doi.org/10.1016/j.chemosphere.2019.06.207>
- Stat Soft Inc. 2012. STATISTICA (Data Analysis Software System), Version 11 - Software. Stat Soft Inc.(www.statsoft.com).
- Stehle, S. & Schulz, R. 2015: Agricultural insecticides threaten surface waters at the global scale. Proceedings of the National Academy of Sciences, 112: 5750-5755.
- Uradni list RS 2016: Pravilnik o kriterijih za dočitev vodovarstvenega območja. Uradni list RS, št. 64/04, 5/06, 58/11 in 15/16.

- Uradni list RS 2018: Pravilnik o določitvi vodnih teles podzemnih voda. Uradni list RS, št. 63/05 in 8/18.
- Van Eerdt, M.M., Spruijt, J., Van der Wal, E., van Zeijts, H. & Tiktak, A. 2014: Costs and effectiveness of on-farm measures to reduce aquatic risks from pesticides in the Netherlands. Pest management science, 70: 1840-1849.
- Vermeirssen, E.L.M., Bramaz, N., Hollender, J., Singer, H. & Escher, B.I. 2009: Passive sampling combined with ecotoxicological and chemical analysis of pharmaceuticals and biocides – evaluation of three Chemcatcher<sup>TM</sup> configurations. Water Research, 43/4: 903-914. <https://doi.org/10.1016/j.watres.2008.11.026>
- Vrana, B., Klucarova, V., Benicka, E., Abou-Mrad, N., Amdany, R., Horakova, S., Draxler, A., Humer, F. & Gans, O. 2014: Passive sampling: an effective method for monitoring seasonal and spatial variability of dissolved hydrophobic organic contaminants and metals in the Danube river. Environmental pollution 184: 101–112. <https://doi.org/10.1016/j.trac.2005.06.006>
- Wille, K., Claessens, M., Rappé, K., Monteyne, E., Janssen, C. R., De Brabander, H. F. & Vanhaecke, L. 2011: Rapid quantification of pharmaceuticals and pesticides in passive samplers using ultra high performance liquid chromatography coupled to high resolution mass spectrometry. Journal of Chromatography A, 1218/51: 9162-9173. <https://doi.org/10.1016/j.chroma.2011.10.039>

## Nove knjige - New books

Urednici: Branka Bračič Železnik & Petra Žvab Rožič, 2021: **Obrazi Geologije v besedi in sliki.**  
Slovensko geološko društvo, Ljubljana: 328 str.

Slovensko geološko društvo že sedemdeset let združuje geoluge in ljubitelje geologije ter promovira geologijo v slovenskem prostoru. To je spoštljiv jubilej, ki ga želimo obeležiti, in knjiga kot dokument s trajnim zapisom časa, v katerem je nastala, se nam je zdela najprimernejša oblika zaznamovanja te visoke obletnice.

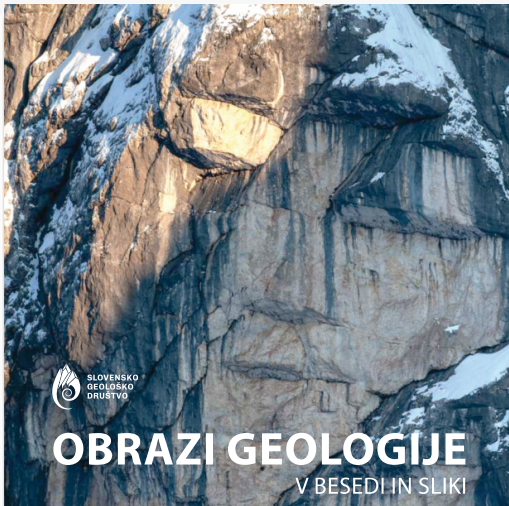
K sodelovanju so bili povabljeni številni geolugi, ki delajo in živijo v Sloveniji ali širnem svetu. Knjiga je rezultat sodelovanja 34 institucij in 102 geologov, ki so v 106 besedah in s številnimi fotografijami predstavili svoje geološko delo. Pestrost geologije se odraža v izboru besed

in načinu opisa ter kaže na raznolikost značajev ljudi, ki jim je skupna geologija tako v poklicnem kot zasebnem življenju.

Ker nam knjiga razkriva marsikateri manj znan obraz oziroma področje delovanja geologov, smo to žeeli poudariti tudi v njenem naslovu: »OBRAZI GEOLOGIJE v besedi in sliki«.

Knjigo je mogoče naročiti po prednaročniški ceni 25 € do 10.1.2022 na spletni strani Slovenskega geološkega društva

<https://www.slovenskogeoloskodrustvo.si/index.php/aktualno>



**Novo**

**OBRAZI GEOLOGIJE**  
V BESEDI IN SLIKI

**NAROČILA:**  
anja.torkar@geo.ntf.uni-lj.si  
branka.bracic.zeleznik@vokasnaga.si

knjiga

**OBRAZI GEOLOGIJE**  
V BESEDI IN SLIKI

Barcode: 978-961-07-0089-1  
cena: 30,00 EUR

Knjigo lahko že naročite v predprodaji!

redna cena: 30 €  
**cena v predprodaji: 25 €**

Mihail BRENČIČ, 2021: **Dinamika podzemne vode.**  
Oddelek za geologijo, Naravoslovnotehniška fakulteta, Univerza v Ljubljani, Ljubljana: 397 str.

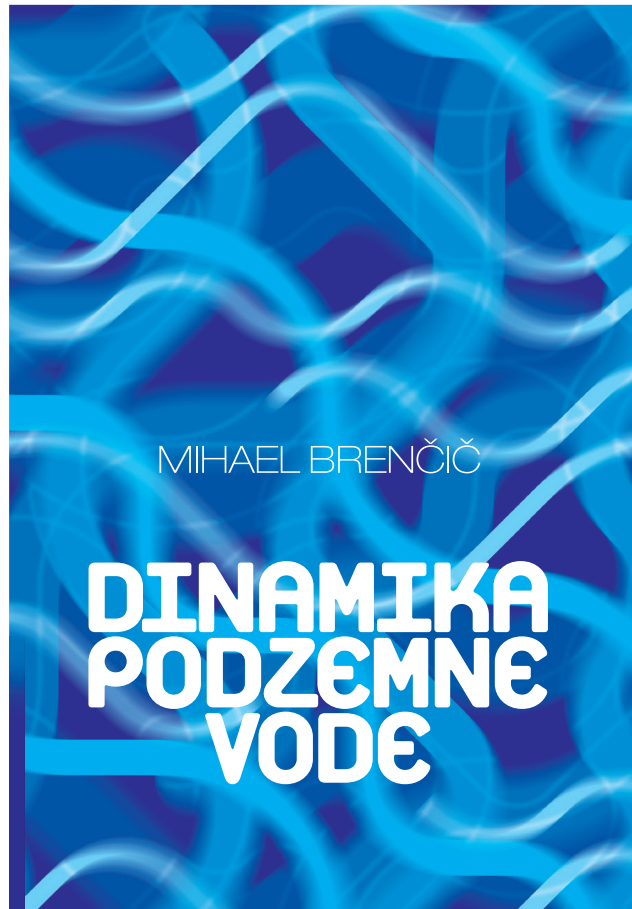
Poznavanje zakonitosti dinamike podzemne vode je ključno za nadgrajevanje obstoječega znanja, pridobljenega s hidrogeološkimi raziskavami, in ostalo strokovno udejstvovanje pri problematikah, ki zadevajo podzemno vodo z vidika njene rabe, zaščite in njene interakcije z ostalimi naravnimi sistemi in antropogenimi dejavnostmi. Velik pomen tega je še posebno izražen v slovenskem prostoru, kot tudi na drugih območjih, ki so s podzemno vodo bogata in kjer vodooskrba prebivalstva iz podzemnih vodnih virov predstavlja pretežni delež celotne oskrbe z vodo.

V letu 2021 je pri Oddelku za geologijo Naravoslovnotehniške fakultete Univerze v Ljubljani izšel učbenik z naslovom Dinamika podzemne vode avtorja prof. dr. Mihaela Brenčiča, ki zapolnjuje vrzel na področju pedagoških besedil o zakonitostih toka podzemne vode v domači literaturi. Strokovni recenzenti knjige so dr. Goran Vižintin, dr. Mitja Janža in dr. Jože Ratej.

Delo obsega 397 strani, je priročnega formata, vsebina je postavljena pregledno in vključuje veliko ilustracij. K preglednosti dela znatno pomore tudi posebno stvarno kazalo na koncu knjige, kot tudi seznam in razlaga posameznih simbolov, uporabljenih v knjigi, z enotami, v katerih se le-ti standardno podajajo.

Z uvodnim in končnim sinteznim poglavjem je učbenik razdeljen v skupno deset poglavij. Uvodnemu poglavju sledijo osnove fizikalnih izhodišč, kjer so opisane glavne fizikalne lastnosti za študij toka podzemne vode v poroznih medijih, to so: definicije in klasifikacije poroznosti, vodonosnikov ter masna in volumska razmerja med posameznimi fazami v poroznih medijih. Obravnavana je viskoznost tekočine, v istem poglavju je definirana tudi hidravlična oz. piezometrična višina, koncept reprezentativnega elementarnega volumna ter komponente vodne bilance.

Tretje poglavje opisuje temeljni zakon dinamike toka podzemne vode v stacionarnih razmerah, Darcyjev zakon. Avtor opiše njegovo izpeljavo, veljavnost ter prikaže laboratorijske preiskave s permeametri, ki slonijo na njegovih zakonitostih. V tem poglavju so prikazane tudi neposredne integracije Darcyjevega zakona v homogenih in heterogenih razmerah različnih hidrodinamskih tipov vodonosnikov.



Četrto poglavje strnjeno opiše parameter uskladiščenja vodonosnikov in njegov pomen za razumevanje osnovne enačbe toka podzemne vode, ki predstavlja vsebino naslednjega, petega poglavja. Osnovna enačba toka je nazorno razložena z izpeljavami v zaprtem, odprttem in pol-zaprtem hidrodinamskem tipu vodonosnika, v primeru toka v ravnini in toka proti vodnjaku, v stacionarnem in nestacionarnem tokovnem režimu. Posebno podpoglavlje obravnavata tudi konsolidacijsko enačbo.

Sesto in sedmo poglavje je namenjeno razlagi osnov dinamike toka podzemne vode v razpoložljivih poroznih medijih ter v medijih z dvojno poroznostjo, ki so v slovenskem prostoru dobro zastopani, zato so te vsebine še posebej dobrodošle. V osmem poglavju avtor opiše pomemben del vodnega kroga, t.j. tok vode v nezasičenem območju.

Kljub temu da avtor na več mestih poudarja predvsem pomen poznavanja osnov in izhodišč

za vse nadaljnje izpeljave in integracije osnovne enačbe toka podzemne vode ter se osredotoča zlasti na analitične modele, deveto poglavje učbenika v celoti posveti numeričnim metodam, ki jih uporabljajo moderna računalniška orodja. Tako se lahko bralec seznaní tudi s postopki, s katerimi se tok podzemne vode računa v ozadju programov za numerično modeliranje, ki dandas poteka preko poenostavljenih uporabniških vmesnikov.

Enačbe za opis hidrogeoloških značilnosti v različnih geoloških okoljih so predstavljene v korakih, skupaj z njihovimi izpeljavami in na podlagi prikazanih skic. Nekatera matematična izhodišča, pomembna za izpeljave in reševanja različnih problemov (npr. osnove reševanja diferencialnih enačb), so posebej natančno predstavljena, preden se jih uporabi na hidrogeoloških primerih. S tem je nakazano osredotočanje avtorja na bralce, ki se teh postopkov šele učijo, seveda pa je dobrodošlo tudi za ostale, ki jih zanimajo osnove končnih izpeljav ali pa jih želijo le ponoviti.

Vsebino učbenika obogatijo slike dvo- ali trodimenzionalnih modelov in ostalih hidrogeolo-

ških konceptov ter diagramov, ki znatno pomagajo pri razlagi vsebin posameznih poglavij in tako postanejo učinkovit vizualni pripomoček za predstavo nekaterih kompleksnejših problemov.

Poseben del učbenika predstavlja njegovo zadnje poglavje z naslovom Razgled po teoriji, kjer je sintezno predstavljen kratek povzetek snovi celotnega dela s ključnimi poudarki za razumevanje dinamike toka podzemne vode v različnih okoljih.

Delo je ena od redkih slovenskih knjig namejena študiju te tematike, saj v slovenskem jeziku do sedaj ni izšlo veliko podobnih besedil, še posebej ne takšnih, ki bi bili primarno pedagoški. Namenjeno je študentom vseh nivojev študija hidrogeoloških vsebin, primarno pa je bilo pripravljeno kot študijsko gradivo pri hidrogeoloških predmetih magistrskega študija. Kljub temu bodo med bralci nedvomno tudi študenti ostalih stopenj študija, hidrogeologi, ki delajo v praksi, kot tudi predstavniki drugih strok, ki z njimi sodelujejo, in ostale zainteresirane javnosti. To je tudi avtorjeva želja, ki jo izrazi v predstavljenem delu, k temu pa bo zagotovo pripomogla tudi dostopna cena publikacije.

*Ines Vidmar*

## Poročila - Report

### 6<sup>th</sup> Regional Scientific Meeting on Quaternary Geology: Seas, Lakes and Rivers, September 2021, Ljubljana

Petra JAMŠEK RUPNIK<sup>1</sup>, Ana NOVAK<sup>1,2</sup> & Miloš BAVEC<sup>1</sup>

<sup>1</sup>Geološki zavod Slovenije, Dimičeva ul. 14, SI-1000 Ljubljana, Slovenia; e-mail: petra.jamsek@geo-zs.si

<sup>2</sup>University of Ljubljana, Faculty of Natural Sciences and Engineering, Department of Geology, Aškerčeva c. 12, 1000 Ljubljana, Slovenia

The 6th Regional Scientific Meeting on Quaternary Geology took place from September 27th through 29th, 2021 in a hybrid form: as a virtual and in-person meeting in Ljubljana, Slovenia. The meeting was primarily intended as an opportunity to bring together researchers working on Quaternary geology, geomorphology, stratigraphy, and related subjects in the Adriatic, Alpine, Dinaric, and Pannonian regions, however, participants more involved in other regions were also welcome. This meeting was the first one hosted by the Slovenian INQUA Committee (SINQUA<sup>1</sup>), while the first 5 meetings were organized by the Croatian INQUA Committee. Together with the Croatian and Italian Quaternary communities, including 19 partner institutions and associations from the region, SINQUA organized this meeting with the main theme "Seas, Lakes and Rivers", which was the focus of the keynote lectures and the virtual excursion. The meeting was attended by about fifty researchers from nine countries.

Full list of organizers: Slovenian INQUA Committee (SINQUA), Croatian INQUA Committee (CRO-INQUA), Geological Survey of Slovenia (GeoZS), Research Centre of the Slovenian Academy of Sciences and Arts (ZRC SAZU), Institute of Archaeology (IzA) & Karst Research Institute (IZRK), Faculty of Natural Sciences and Engineering, University of Ljubljana (UL NTF), CNR - Institute of Geosciences and Earth Resources (IGG), University of Padova (UNIPD), CNR - Institute of Environmental Geology and Geoengineering, Unit of Milano (IGAG), Institute of Quaternary Paleontology and Geology, Croatian Academy of Sciences and Arts (HAZU), Croatian Geological Survey (HGI), Faculty of Science, University of Zagreb (PMF), Faculty of Mining, Geology and Petroleum Engineering, University of Zagreb (RGNF), Archaeological Museum

of Istria (AMI), Flinders University, Adelaide, Australia (FLIN), Slovenian Geological Society (SGD), Geomorphological Society of Slovenia (GMDS), Italian Association for Quaternary Research (AIQUA), Faculty of Arts, University of Ljubljana (UL FF), and Marine Biology Station Piran (NIB-MBP).

Organizing and Scientific Committee: Petra Jamšek Rupnik – chair (GeoZS), Ana Novak – vice-chair (GeoZS, UL NTF), Maja Andrič (ZRC SAZU, IzA), Miloš Bavec (GeoZS), Dea Brunović (HGI), Nina Caf (ZRC SAZU, IzA), Branko Čermelj (NIB-MBP), Goran Durn (RGNF), Igor Felja (PMF), Alessandro Fontana (UNIPD), Andrej Gaspari (UL FF), Ozren Hasan (HGI), Nikolina Ilijanić (HGI), Katarina Jerbić (FLIN), Ida Koncani Uhač (AMI), Ljerka Marjanac (HAZU), Eva Mencin Gale (GeoZS), Slobodan Miko (HGI), Giovanni Monegato (IGG), Andrej Novak (UL NTF), Roberta Pini (IGAG), Tomislav Popit (UL NTF), Mitja Prelovšek (ZRC SAZU, IZRK), Livio Ronchi (UNIPD), Cesare Ravazzi (IGAG), Andrej Šmuc (UL NTF), Astrid Švara (ZRC SAZU, IZRK), Nadja Zupan Hajna (ZRC SAZU, IZRK), Manja Žebre (GeoZS).

The three-day meeting took place in the Atrium of the Research Centre of the Slovenian Academy of Sciences and Arts and through a virtual platform for remote participants. The meeting was opened by Miloš Bavec, representative of SINQUA, Goran Durn, president of CRO-INQUA, and Giovanni Monegato, president of AIQUA. The first two days were devoted to scientific sessions that included 39 presentations on 1) seas & transitional environments, 2) archeology, earthquakes & structural geology, 3) projects, 4) lakes, forelands & mountains, 5) karst, and 6) aeolian sediments. The keynote lectures included presentations by a) Branko Čermelj (NIB-MPB): The

<sup>1</sup> SINQUA formed in 2014 and has been under the auspices of the Slovenian Geological Society, a member of the International Union for Quaternary Research (INQUA), since 2015. Its mission is to connect Quaternary researchers and share the latest research results with both the Slovenian and international Quaternary research community. The main goal is the progress in the field of Quaternary science in Slovenia. You can find more information on the website of the <https://www.slovenskogeologoskodrustvo.si/index.php/mednarodno-sodelovanje/sodelovanje-v-mednarodnih-organizacijah>.

recent sediments of the Gulf of Trieste, the most northern part of the Adriatic – An overview of the last 5 decades of the biogeochemical and sedimentological research, b) Slobodan Miko (HGI): Submerged landscapes of the Eastern Adriatic Sea, c) Andrej Gaspari (UL FF): Underwater archaeological investigations in Slovenia (the Slovenian sea and Ljubljana moor), d) Nadja Zupan Hajna (IZRK): Sediments of a sinking river in karst over time: Škocjan Caves as a case study, e) Nikolina Ilijanić (HGI): Paleolimnology of Holocene karst lakes along the Eastern Adriatic coast. The second day ended with a geological tour of Ljubljana led by Matevž Novak (GeoZS). On the third day, a virtual excursion took us to Quaternary marine, lacustrine and fluvial sites in Slovenia, Italy and Croatia, presented by Alessandro Fontana (UNIPD), Giovanni Monegato (IGG), Petra Jamšek Rupnik (GeoZS), Andrej Šmuc (UL NTF), Maja Andrič (IzA), Nina Caf (IzA), Katarina Jerbić (FLIN), Ana Novak (GeoZS, UL NTF) and Livio Ronchi (UNIPD). More information with the full program is available on the meeting's [website](#).

Despite the hybrid format of the meeting, the presentations stimulated lively discussions in a friendly atmosphere. Many new research results were presented and collected in the Book of abstracts, which is available [online](#). In addition, a special issue of *Quaternary – Seas, Lakes and Rivers in the Adriatic, Alpine, Dinaric and Pannonian Regions during the Quaternary* is in preparation for selected papers.



Fig. 1. The meeting venue was in the center of Ljubljana, in the Atrium of the Research Center of the Slovenian Academy of Sciences and Arts (photo: P. Jamšek Rupnik).

The next meeting, the 7<sup>th</sup> Regional Scientific Meeting on Quaternary Geology, will be organized by the Croatian INQUA Committee in 2024 in Croatia.

### Acknowledgements:

We thank the members of the Organizing and Scientific Committee and our partner institutions and associations who helped us prepare the meeting. We also gratefully acknowledge the financial support provided by the Slovenian Geological Society, the Geomorphological Society of Slovenia and the Geological Survey of Slovenia. We thank the Research Center of the Slovenian Academy of Sciences and Arts for hosting us in their atrium in the beautiful old city center of Ljubljana, and the technical team that took care of the online streaming. A special thanks goes to the keynote speakers, session chairs and virtual excursion leaders. Many thanks also to Matevž Novak for leading the geological tour of Ljubljana, Marko Zakrajšek for preparing the website, Staša Čertalič and Irena Trebušak for their help with the Book of abstracts and promotion of the meeting, Staša Čertalič and Vida Pavlica for designing some of the meeting materials, Metka Leban and Stanka Žibert for taking care of the financial part, Rok Brajkovič for delivery services, and geology students Aleša Uršič Arko and Andrej Bricman for on-site technical support. Many thanks to all participants for coming and sharing their latest research results, hope to see you all again in three years.



Fig. 2. The hybrid form of the meeting attracted more virtual participants. The virtual excursion on the 3rd day of the meeting was mainly followed online (photo: P. Jamšek Rupnik).

<sup>1</sup> <https://www.geo-zs.si/rmqg/>

<sup>2</sup> [https://www.geo-zs.si/PDF/Monografije/6thRMQG\\_BookOfAbstracts.pdf](https://www.geo-zs.si/PDF/Monografije/6thRMQG_BookOfAbstracts.pdf)

<sup>3</sup> [https://www.mdpi.com/journal/quaternary/special\\_issues/6th\\_RMQG](https://www.mdpi.com/journal/quaternary/special_issues/6th_RMQG)



Fig. 3. Geological tour through the city center of Ljubljana led by Matevž Novak (photo: P. Jamšek Rupnik).



Fig. 4. Some of the presentations were pre-recorded. The virtual excursion stop by A. Šmuc, M. Andrič and N. Caf was presented and recorded at the viewpoint above Lake Bohinj (photo: P. Jamšek Rupnik).

## 6. svetovni geotermalni kongres WGC 2020+1, Reykjavik (Islandija) marec – oktober, 2021

Dušan RAJVER

Geološki zavod Slovenije, Dimičeva ul. 14, SI-1000 Ljubljana, Slovenija; e-mail: dusan.rajver@geo-zs.si

Islandija ni bila slučajno izbrana za organizacijo 6. svetovnega geotermalnega kongresa, saj je prvovrstna predstavnica izkoriščanja geotermalne energije. Vendar pa so islandski organizatorji zaradi nastopa pandemije Covid-19 morali njegov potek precej spremeniti. Po prvotnem načrtu bi se kongres moral odvijati v Reykjaviku od 27. apr. do 1. maja 2020. Tako pa ga je moral organizacijski komite (OK) zaradi nastopa pandemije časovno in organizacijsko precej spremeniti. Najprej ga je dne 13. marca 2020 prestavil za dobro leto dni naprej (21. do 26. maja 2021). Vseeno pa so že 27. aprila 2020 izvedli začasni uvodni virtualni dogodek, ki je obsegal nagovore predsednika Islandije, predsednika in izvršne direktorice IGA, predsednika tehničnega komiteja ter dve predavanji o proizvodnji elektrike iz geotermalne energije (G. Hutterer) in neposredni rabi toplote iz geotermalne energije v svetu (J. Lund). Potem pa je OK ugotovil, da tudi ta termin ne bo izvedljiv. Zato so se 4. feb. 2021 odločili, da kongres izvedejo z nekaj mesečnimi virtualnimi dogodki od marca do oktobra 2021 in ga poimenovali »geotermalni semester«. Otvoritveni 2-urni dogodek je bil 30. marca s sedmimi uvodnimi predavanji. Sledili so virtualni celodnevni dogodki (od I do IV), prvi 13. aprila, drugi 11. in 12. maja, tretji 15. junija in četrti 6. julija. Semester se je zaključil s 3-dnevno konferenco v Reykjaviku (glavni dogo-

dek 25.-27. okt. 2021), ki je potekala hibridno (v živo za tiste, ki so prišli na Islandijo in virtualno za ostale registrirane udeležence). Prejšnji svetovni geotermalni kongresi oziroma mednarodni geotermalni simpoziji od leta 1970 dalje so omenjeni v poročilu pred šestimi leti (Rajver, 2015).

V izkoriščanju geotermalne energije je Islandija v svetovnem vrhu glede na prebivalstvo, tako glede neposredne rabe toplote iz geotermalne energije kot tudi proizvodnje elektrike iz nje. Prevladuje neposredna raba, posebej ogrevanje prostorov (44,6 % vse izkoriščene geotermalne energije). Daljinsko ogrevanje Reykjavika z geotermalno energijo (sedaj Reykjavik Energy) je bilo uradno ustanovljeno že leta 1946. Delež geotermalne energije v daljinskem ogrevanju se je zvišal iz 43 % v letu 1970 na sedanjih 90 %. V mestih in vaseh deluje okrog 30 ločenih sistemov geotermalnega daljinskega ogrevanja in dodatno še 200 majhnih sistemov na podeželju. Slednji oskrbujejo z vročo vodo individualne kmetije ali skupine kmetij, kakor tudi poletne koče, rastlinjake in druge uporabnike. Imajo 165 rekreacijskih plavalnih in balneoloških centrov, med nimi jih 140 uporablja geotermalno toploto. Večina plavalnih bazenov je odprta celo leto. Ogrevanje rastlinjakov je za ogrevanjem prostorov druga najvažnejša raba geotermalne energije. Vroč ali delno ohlajeno vodo uporabljajo še za taljenje

snega, industrijske procese (sušilnica morskih alg, dve tovarni soli) in gojenje rib. Islandija je s 755 MW<sub>e</sub> deveta na svetu po nameščeni moči geotermalnih elektrarn in z 21636 TJ (6010 GWh) v letu 2019 na osmem mestu po proizvedeni električni energiji iz teh elektrarn, v neposredni rabi geotermalne energije pa je na petem mestu s 33598 TJ (9333 GWh) izkoriščene energije v istem letu, brez izkoriščanja toplote plitvega podzemlja s topotnimi črpalkami pa celo na tretjem mestu (Ragnarsson et al., 2020; Lund & Toth, 2021).

Kongres je zaradi pandemije težko primerjalni s tistim leta 2015 v Avstraliji. Več kot 5 tisoč prijavljenih, ki so spremljali virtualne dogodke (predstavitev), je precej preseglo število udeležencev na prejšnjem kongresu, le zaključna 3-dnevna konferenca je bila predvsem zaradi pandemije slabše obiskana. Vodja tehničnega programa prof. R. Horne je navedel, da je bilo za letošnji kongres oddanih 2044 prispevkov (referatov), sprejeto jih je bilo 1898 (iz 100 držav oziroma regij), ki so v zborniku kongresa. Med temi je bilo 653 prispevkov sprejeto kot posterji. V

številu prispevkov je ta kongres največji doslej, gre za 42 % porast glede na leto 2015. To je rezultat širitve svetovne dejavnosti v raziskavah in rabi geotermalne energije, kakor tudi vključnosti geotermalne energije v različnih vejah dejavnosti oziroma družbe. Posterske sekcije so bile na spletni strani nepretrgoma odprte od aprila do oktobra 2021 kot video dogodek. Organizatorji so predstavitev ustrezno vsebinsko umestili v virtualne dogodke tako, da so v omenjenih petih dneh potekala štiri vzporedna predvajanja (angl. streams) istočasno, in to po srednjeevropskem času od 10. ure dopoldne pa do 02. ali celo 04. ure zjutraj (pozne ure so bile večinoma namenjene udeležencem iz drugih časovnih pasov).

Navajam sekcije, razdeljene v štiri virtualne dogodke, tematsko porazdelitev sekcij na teh dogodkih, število predstavitev po sekcijah (virtualne predstavitev v petih dneh od aprila do julija in tiste na zaključni konferenci v Reykjaviku) ter porazdelitev prispevkov po sekcijah v zborniku kongresa (v štirih zvezkih):

Dogodek I: Poslovanje & Okolje (Business & Environment)	Število virtualnih predstavitev	Število predstavitev na zaključni konf.	Število vseh prispevkov
Posodobljena poročila držav (Country updates)	46	8*	91**
Izobraževanje v geotermiji	12	5	29
Okoljski in družbeni vidiki	35	5	59
Trajnost in podnebne spremembe	18	5	37
Politika, pravni in regulativni vidiki	17	5	42
Ekonomija in financiranje	18		27
Poslovne strategije	17	5	30
Primeri (Case Histories)	24	5	49
Družbeni in kulturni vidiki	19	5	38
<b>SKUPAJ:</b>	<b>206</b>	<b>43</b>	<b>402</b>

\*od 8 predstavitev je ena predstavitev o izkoriščanju GE na Islandiji, dve predstavitevi pa sta svetovna pregleda izkoriščanja GE (o neposredni rabi oz. proizvodnji električne energije); vse tri so bile plenarne.

\*\*od 91 prispevkov sta dva svetovna pregleda izkoriščanja GE (o neposredni rabi oz. proizvodnji električne energije).

Dogodek II: Geoznanosti (Geosciences)	Število virtualnih predstavitev	Število predstavitev na zaključni konf.	Število vseh prispevkov
Raziskave	71	10	140
Geologija	76	10	151
Geofizika	72	10	155
Geokemija	64	10	132
Ocena virov (Resource Assessment)	39	5	76
Hidrogeologija	18		30
Geomikrobiologija			1
Upravljanje geotermalnega polja	10		20
Veliki podatki in analitika podatkov	11		14
Integrirani energetski sistemi, kaskadna uporaba	12		15
Programska oprema za geotermalne aplikacije	22	5	45
<b>SKUPAJ:</b>	<b>395</b>	<b>50</b>	<b>779</b>

Dogodek III: Inženirstvo (Engineering)	Število virtualnih predstavitev	Število predstavitev na zaključni konf.	Število vseh prispevkov
Vrtanje in dokončanje (ostalih tehnoloških naprav)	60	5	94
Inženiring (geotermalnih) rezervoarjev	54	10	106
Korozija in luščenje (odlaganje kotlovnega fluida)	48	5	77
Tehnologija injektiranja (vračanja izrabljenega fluida)	6		14
Proizvodnja električne energije	36	5	73
Proizvodni inženiring, sistemi za zbiranje pare	18	5	42
<b>SKUPAJ:</b>	<b>222</b>	<b>30</b>	<b>406</b>

Dogodek IV: Najpomembnejši razvoj (Cutting Edge)	Število virtualnih predstavitev	Število predstavitev na zaključni konf.	Število vseh prispevkov
Geotermalne toplotne črpalki (GSHP)	35	5	69
Izboljšani geotermalni sistemi (EGS)	59	5	97
Neposredna raba	29	5	53
Zdravje, turizem in balneologija	5		8
Toplotna iz naftnih/plinskih polj/premoga	5		12
Daljinsko ogrevanje	12		29
Napredna tehnologija (magma, geotlačni sistemi, itd.)	18		25
Agrikultura (kmetijstvo)	5		5
Pridobivanje mineralov in predelava	5		6
Mednarodna sodelava		5	7
<b>SKUPAJ:</b>	<b>173</b>	<b>20</b>	<b>311</b>

Skupno je bilo 996 virtualnih predstavitev v 34 sekcijah in 143 predstavitev na zaključni konferenci (nekatere sicer le preko videa) v 22 sekcijah.

Kam so usmerjeni glavni naporji v raziskavah, razvoju in uveljavljanju geotermalne energije, se vidi iz prevladujočih sekcij z največjim številom prispevkov v kongresnem zborniku: geofizika (155), geologija (151), raziskave (140), geokemijska (132), inženiring geotermalnih rezervoarjev (106), EGS (97), sedanje stanje izkoriščanja po državah (91), problemi s korozijo (77), ocenitev geotermalnih virov (76), proizvodnja električne energije (73), geotermalne toplotne črpalk (69), okoljski in družbeni vidiki (59), neposredna raba (53). Znova se je izkazalo, da so posredne in površinske metode (geofizika, geokemijska in geologija) še naprej zelo pomembne v raziskavah in upravljanju geotermalnih virov. Precejšnje število prispevkov v sekcijah *Poslovanje in okolje* je odraz prizadevanj izraziteje uveljaviti geotermalno energijo med obnovljivimi viri energije. Številni prispevki o raziskavah kažejo na dejavno iskanje novih virov v raznih državah sveta. Velika pestrost prispevkov v še večjem številu sekcij kot na prejšnjem kongresu je postala že težko obvladljiva, vseeno pa lahko najdemo marsikaj poučnega in uporabnega v svojih dejavnostih.

Še nikoli ni bilo na kongresu toliko prispevkov s tematiko o EGS sistemih, kar kaže na zavzetost

močnih raziskovalnih ustanov, vrtalnih podjetij in investitorjev dalje razvijati te sisteme z izboljšanjem poznavanja geofizikalnih in hidrogeokemijskih pogojev kljub poglavitnim težavam glede vrtanja in stimulacije rezervoarja. V sekciji *Geofizika* je bilo poleg seizmičnih metod raziskav veliko prispevkov o uporabi magnetotelurike, seveda predvsem v raziskavah srednje in visoko-temperaturnih sistemov. Izpostavim lahko še nekaj zanimivih prispevkov: (a) prispevek o karakterizaciji geotermalnega rezervoarja (detekcija prelomov, interpretacija seizmičnih faciesov, itd.) z integracijo podatkov več disciplin, gravimetrije, seizmike in VSP, pri tem pa so uporabili umečno inteligenco in še posebej strojno učenje (angl. machine learning) kot obetavni tehniki za asimilacijo velikih podatkov; (b) zanimiv primer kombinacije treh geofizikalnih metod v južnem Čilu; (c) kako pridobiti več geotermalne energije iz globokih razpokanih kamnin podlage v Zgornjoreninskem jarku; (č) prednosti podzemnih mestnih topotnih otokov za plitve geotermične aplikacije (primer mesta Köln); (d) predstavitev obdelav z mehko stimulacijo v geotermalnih rezervoarjih; (e) Prva evropska zbirkica preizkusov topotne odzivnosti (TRT); (f) modeliranje spremembe stopnje topotne izmenjave geosonde v velikem sistemu GSHP. In še bi lahko našteval. Prispevkov o raziskavah v nizko-temperaturnih geotermalnih sistemih ni bilo prav veliko.

Pod okriljem kongresa se je v dneh 23.-24. oktober 2021 odvijalo nekaj kratkih tečajev pred zaključno konferenco. To so bili: (1) *Uncertainty, risk and decision analysis*, (2) *Geothermal drilling: standards, strategies and reduction of risks and costs*, (3) *Utilization of low- to medium- temperature geothermal resources in* (4) *Conceptual modeling of geothermal systems*. Vse to so aktualne téme, kar je dvignilo pomembnost in uspešnost kongresa. V kongresnem centru Harpa je med zaključno konferenco kongresa potekala predstavitev industrije, t.j. nekaterih najbolj znanih razvojnih inštitucij ter proizvajalcev in serviserjev raziskovalne in proizvodne opreme (za vrtine, cevovode, topotne postaje, elektrarne, itd.) v geotermalnih raziskavah in razvoju ter izkoriščanju geotermalne energije. V ponudbi kongresa je bila tudi izvedba petih geotermalnih terenskih izletov med zaključno konferenco in po njej, ter izvedba štirih ekskurzij, vendar mi je ostalo neznano koliko so jih dejansko izvedli.

Kongres v Reykjaviku je pokazal vztrajno rast v geotermalnem razvoju, če primerjamo stanje leta v obdobju treh mejnikov (Tabela 1). Za ta kongres je skupno 89 držav ali regij poročalo o izkoriščanju geotermalne energije za neposredno rabo. Med njimi je 28 držav poročalo o proizvodnji električne energije. Iz dveh državah (Tajvan in Nikaragva) omenjajo namreč le proizvodnjo električne energije, ne pa neposredne rabe njene toplotne. Glede na številke, poročane za WGC 2015, se je v letu 2019 proizvedlo za 29,8 % več električne energije iz geotermalne, porast v neposredni rabi geotermalne toplotne pa je bil še bolj intenziven, kar za 72,3 % več glede na poročano leta 2015 (Tabela 1). Največji delež v porastu prispeva koriščenje toplotne plitvega podzemlja s topotnimi črpalkami (58,8 %), ki se odvija v 58 državah ali regijah. V

zadnjih petih letih so izdelali 2647 vrtin v 42 državah, bodisi za neposredno rabo bodisi za proizvodnjo električne energije.

Glede izkoriščanja geotermalne energije v Sloveniji je ob koncu 2019 znašala nameščena zmogljivost naprav za neposredno rabo 263 MW<sub>t</sub>, letna izkoriščena geotermalna energija pa 1609 TJ ali 447 GWh (Rajver et al., 2020a), ob koncu leta 2020 pa 275 MW<sub>t</sub> in zaradi pandemije nekaj manj izkoriščene energije (1546,5 TJ ali 428,8 GWh), obakrat vključno z geotermalnimi topotnimi črpalkami v koriščenju toplotne plitvega podzemlja (Rajver et al., 2021). Prispevek geotermalnih topotnih črpalk je v letu 2020 znašal 218,2 MW<sub>t</sub> oziroma 1090 TJ (302,7 GWh). Različne vrste uporabe pa zajemajo: individualno ogrevanje prostorov in pripravo sanitarnih voda, daljinsko ogrevanje, klimatizacijo/hlajenje, ogrevanje rastlinjakov, kopanje in plavanje z balneologijo, taljenje snega ter geotermalne topotne črpalki.

Iz Geološkega zavoda Slovenije je kongres (kolikor se je dalo) spremeljal pisec tega prispevka, ki je imel dve virtualni predstavitvi (Rajver et al., 2020a; Rajver et al., 2020b), so pa bile še tri predstavitve (dve virtualni in en poster), v katerih so (so)avtorji sodelavci Geološkega zavoda Slovenije (Diepolder et al., 2020; Klonowski et al., 2020; Goetzl et al., 2020) in pa ena predstavitev, v kateri sta avtorici iz Fakultete za turizem Univerze v Mariboru (Turnšek et al., 2020). Naslednji svetovni geotermalni kongres bo že leta 2023 na Kitajskem, še prej pa bo v oktobra 2022 že naslednji evropski geotermalni kongres v Berlinu. ([www.europeangeothermalcongress.eu](http://www.europeangeothermalcongress.eu)).

Video predstavitev na kongresu bodo na spletni strani dostopne še do konca oktobra 2022 (torej 1 leto od zaključne 3-dnevne konference).

Tabela 1. Stanje izkoriščanja geotermalne energije v svetu; navedena so leta, v katerih je bilo poročano na kongresih (Huttrer, 2020; Lund & Toth, 2021).

Leto	2010	2015	2020
<b>Proizvodnja električne energije</b>			
Instalirana kapaciteta (MWe)	10897	12284	15950
Proizvedena elektrika (GWh/leto)	67246	73549	95098
Koeficient izkoristka	0,72	0,72?	n.p.
Število držav	24	26	30
<b>Neposredna raba</b>			
Instalirana kapaciteta (MW <sub>t</sub> )	48493	70885	107727
Izkoriščena energija (TJ/leto)	423830	592638	1020887
Koeficient izkoristka	0,277	0,265	0,30
Število držav	78	82	88

## Viri

- Diepolder, G.W., Borović, S., Herms, I. & the HotLime Team 2020: HotLime – Mapping and assessment of geothermal plays in deep carbonate rocks. Proceedings, World Geothermal Congress 2020+1, Reykjavik, Iceland, IGA: 9 p.
- Goetzl, G., Dilger, G., Grimm, R., Hofmann, K., Holeček, J., Černak, R., Janža, M., Kozdroj, W., Klonowski, M., Hajto, M., Gabriel, P. & Gregorin, Š. 2020: Strategies for fostering the use of shallow geothermal energy for heating and cooling in Central Europe – Results from the Interreg Central Europe project GEOPLASMA-CE. Proceedings, World Geothermal Congress 2020+1, Reykjavik, Iceland, IGA: 17 p.
- Huttrer, G.W. 2020: Geothermal power generation in the World 2015–2020 Update report. Proceedings, World Geothermal Congress 2020+1, Reykjavik, Iceland, IGA: 17 p.
- Klonowski, M., Herms, I., Goetzl, G., Borović, S., Garcia-Gil, A., Ditlefsen, C., Boon, D., Veloso, F., Petitclerc, E., Janža, M., Erlström, M., Holeček, J., Hunter Williams, N.H., Vandeweijer, V.P., Černak, R. & Malyuk, B. 2020: Managing urban shallow geothermal energy (Preliminary results of the MUSE project). Proceedings, World Geothermal Congress 2020+1, Reykjavik, Iceland, IGA: 8 p.
- Lund, J.W. & Toth, A.N. 2021: Direct utilization of geothermal energy 2020 worldwide review. Geothermics, 90. <https://doi.org/10.1016/j.geothermics.2020.101915>
- Ragnarsson, A., Steingrimsson, B. & Thorhallsson, S. 2020: Geothermal development in Iceland 2015–2019, Proceedings, World Geothermal Congress 2020+1, Reykjavik, Iceland: 14 p.
- Rajver, D. 2015: 5. Svetovni geotermalni kongres v Melbournu (Avstralija). Geologija, 58/2: 263–264.
- Rajver, D., Rman, N., Lapanje, A. & Prestor, J. 2020a: Geothermal country update report for Slovenia, 2015–2019. Proceedings, World Geothermal Congress 2020+1, Reykjavik, Iceland, IGA: 16 p.
- Rajver, D., Casasso, A., Capodaglio, P., Cartannaz, C., Maragna, C., Prestor, J. & Jež, J. 2020b: Shallow geothermal potential with borehole heat exchangers (BHEs): three case studies in the Alps. Proceedings, World Geothermal Congress 2020+1, Reykjavik, Iceland, IGA: 13 p.
- Rajver, D., Pestotnik, S., Prestor, J., Svetina, J., Janža, M., Rman, N. & Lapanje, A. 2021: Uveljavljanje plitve geotermalne energije med drugimi obnovljivimi viri energije za ogrevanje in hlajenje. V: Senegačnik, A. (ur.): Mineralne surovine v letu 2020 (bilten), GeoZS, Ljubljana: 143–156.
- Turnšek, M., Thorarinsdottir, R., Boedijn, A., Baeza, E., Espinal, C., Van Den Ven, R. & Pavlakovič, B. 2020: Adding value to geothermal food production through experience design. Proceedings, World Geothermal Congress 2020+1, Reykjavik, Iceland, IGA: 9 p.

## Poročilo o aktivnostih Slovenskega geološkega društva v letu 2020

Branka BRAČIČ ŽELEZNICKA

JP VOKA SNAGA d.o.o., Vodovodna cesta 90, SI-1000 Ljubljana, Slovenija;  
e-mail: branka.bracic.zeleznik@vokasnaga.si

Leto 2020 je nedvomno izstopalo v 69 letnem delovanju Slovenskega geološkega društva. Bilo je leto omejitev in prepovedi zaradi epidemije koronavirusa, zato skoraj ni bilo organiziranih dogodkov v živo in ni bilo druženja članov.

V letu 2020 smo v živo izvedli le eno strokovno predavanje in sicer je predaval Jernej Krčmar, univ. dipl. inž. geol. (Petrol Geo d.o.o. z naslovom »Visokotemperaturni geotermalni viri v Sloveniji z možnostjo proizvodnjo električne energije« je bilo 5. februarja 2020 ob 17.00 uri v Ljubljani na

Oddelku za geologijo NTF, Aškerčeva 12, v predavalnici 210.

Klub zelo omejenim pogojem dela, je bilo v letu 2020 v sklopu Aktivnosti za promocijo geologije izvedenih nekaj naravoslovnih dni:

Pazi, geolog na delu je bil naslov naravoslovnega dne za otroke 9. razreda iz OŠ Železniki, ki je potekal 5. marca 2020. Na delavnici so sodelovali Petra Žvab Rožič, Rožič Boštjan, Primož Miklavc, Ema Hrovatin, Kaja Šušmelj, Kristina Šavli, Miha Štruc in Blaž Pucihar.

Niz delavnic se je nadaljeval v septembru in oktobru 2020. V okviru projekta Noč raziskovalcev - Humanistika, to si ti! je bila delavnica za učence petih razredov OŠ Stična in njenih podružnic na lokaciji Terme Čatež, 9. in 15. septembra 2020. Delavnico so vodili Nina Rman, Petra Žvab Rožič, Katja Koren, Simona Adrinek, Rok Brajković in Nina Valand.

V okviru Mura festivala je bila 9. septembra delavnica Geo dogodivščine za učence 3. in 4. razreda OŠ Apače, ki sta jo vodili Mojca Bedjanič in Sandra Zvonar. V sklopu Mura festivala je bila 25. septembra izvedena delavnica Geo dogodivščine za otroke vrtca Veržej, 2020.

S povodnim možem Vodovnikom spoznavam naravo Bistriškega vintgarja je bil naslov naravoslovnega dne v okviru DEKD za učence 6. razredov OŠ Pohorskega odreda Slovenska Bistrica, ki je potekal 28. in 29. september 2020. Naravoslovni dan so vodile Andreja Senegačnik, Mojca Bedjanič in Lenka Stermecki.

V okviru DEKD je bil 2. oktobra 2020 organiziran naravoslovni dan Sprehod skozi geološki čas za učence 6. razredov OŠ Mežica, kjer so sodelovale Mojca Bedjanič, Lenka Stermecki, Aljoša Šafran, Danijela Modrej, Suzana Fajmut Štrucl, Metka Tajzel, Metka Rožen in Janja Gril.

Člani sekcije za promocijo geologije so bili zelo aktivni tudi na področju sodelovanja na mednarodnih konferencah, ki pa so žal potekale le preko spleta. Pripravili so sledeče prispevke in predavanja:

RockCheck the rocks – innovative pedagogical approaches for active learning about rock, EGU General Assembly 2020, online, 4-8 May 2020 (Petra Žvab Rožič, Nina Valand, Helena Gabrijelčič Tomc, Jože Guna, Žiga Fon, Rok Brajković);

Stories of Montanistica – experience through comics, AR and VR, EGU General assembly 2020, online, 4-8 May 2020 (Petra Žvab Rožič, Matevž Novak, Boštjan Rožič, Nace Pušnik, Helena Gabrijelčič Tomc in ostali);

RockCheck application rocks the world: blog 18. maj 2020 (Nina Valand, Rok Brajković, Petra Žvab Rožič);

24 hours with the Mura river: Conservation of natural and cultural heritage in the UNESCO MAB Mura River Biosphere Reserve. V: Fostering heritage communities, 8-11 may 2020, web conference 2020. 2nd ed. Wutzenhausen, SALM, 2020 (Mojca Bedjanič, Andreja Senegačnik, Simona Kaligarič, Lenha Stermecki);

Geo-interpretation as support for increasing the recognition of the Karavanke-Karawanken UNESCO Global Geopark, Fostering heritage communities, 8-11 may 2020, conference proceedings, web conference 2020, 2nd ed Witzenhausen, SALM, 2020 (Mojca Bedjanič, Darja Komar, Gerald Hartmann, Simona Kaligarič, Andreja Senegačnik, Milan Piko, Lenka Stermecki, AntoniaWeissenbacher);

Petega septembra 2020 je bila v sodelovanju treh društev, Geomorfološkega društva, Slovenskega geološkega društva in Kranjskega



Sl. 1. Predstavitev geologije Dolžanove soteske (foto: M. Prelovšek).

gozdarskega društva, organizirana strokovna ekskurzija v porečje Tržiške Bistrice. Vremenska ujma, ki se je oktobra 2018 zgodila v porečju Tržiške Bistrice, je med Tržičem in Jelendolom povzročila velike spremembe površja, še posebej strug vodotokov ter veliko gmotno škodo. Ujma je odprla tudi nekaj družbenih vidikov človekovega dojemanja in zgodovinskega spomina o naravnih nesrečah, pogostosti vremenskih ekstremlnih dogodkov in njihovih posledicah. Ekskurzija je odprla tudi dileme varstva narave, še posebej geoloških in geomorfoloških naravnih vrednot, naravnega spomenika ter območij Nature 2000.

SGD kot član Evropskega združenja geologov (EFG) je bilo v letu 2020 vključeno v pet evropskih projektih Obzorje 2020 (Horizon 2020).

V letu 2020 se je nadaljevalo delo na projektu INFACT – Inovativna, neinvanzivna in polnoma sprejemljiva tehnologija raziskovanja (Innovative, Non-Invasive and Fully Acceptable Exploration Technologies).

V letu 2020 smo v projektu opravljali naloge povezane s WP 7 Impact creation, ki ima za cilj promocijo projekta ter diseminacijo projektnih rezultatov in aktivnosti.

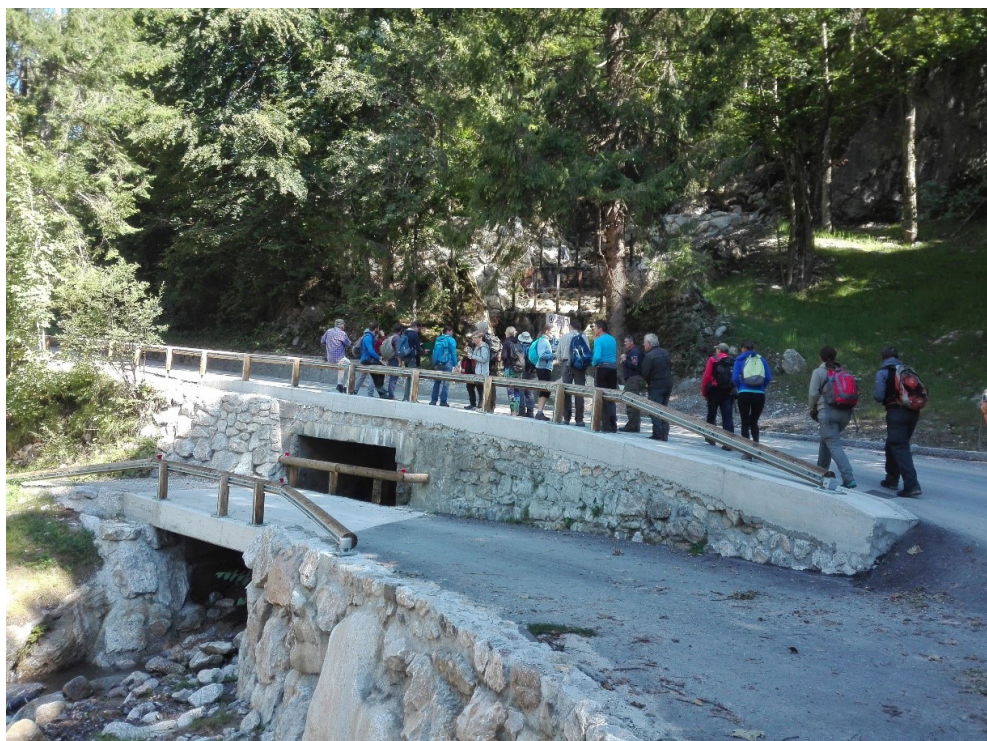
V sklopu diseminacije smo spremljali projektno družbene medije in delili njihova obvestila.

Udeležili smo se virtualnih projektnih dogodkov, ki so bili pripravljeni v sodelovanju z drugimi projekti in inštitucijami. 3. in 4. decembra 2020 je bil organiziran forum »Can mining make

the world a greener place« s serijo predavanj in razprav na temo trajnostnega rudarjenja. V slovenščino smo prevedli dve obvestili za javnost in ju delili na SGD spletni strani, (Sodelovanje v mednarodnih projektih ([slovenskogeoloskodrustvo.si](http://slovenskogeoloskodrustvo.si))) kjer je tudi promocijski in diseminacijski material projekta. Pripravili smo prispevek o projektu in projektnih rezultatih za strokovno revijo Mineral, ki je objavljen v februarju 2021 (Miletić & Novak, 2021: Projekt INFACT - Prihodnost raziskovanja mineralnih surovin v Evropi. Mineral št. 72 2021/1.).

V letu 2020 so se pričele aktivnosti na projektu ENGIE – Vzpodbujanje deklet za izbiro poklica geoznanstvenice (*Empowering Girls to become the geoscientists of tomorrow*). V okviru projekta ENGIE smo strokovno sodelovali v okviru treh delovnih paketov. Na začetku leta smo izvedli obširno raziskavo o zanimanju dijakinj in diakov srednjih šol za področja geoznanosti. Izdelana sta bila vprašalnika za dijake(inje) in učitelje, prevedena v vse jezike sodelujočih v projektu (tudi v slovenski jezik) in po posamezni državi poslana na osnovne in srednje šole. V Sloveniji je v raziskavi sodelovalo okoli 150 učencev in diakov ter 10 učiteljev.

V okviru projekta se izvaja tudi raziskava med že uveljavljenimi znanstvenicami z namenom razumeti, kako spol vpliva na uspešnost kariere v geoznanosti in geoinženirstvu. Zanima nas tudi, kako ženske aktivnosti svojega dela usklajujejo s privatnim življenjem in ali se na posameznih



Sl. 2. Ogled ureditve hudo-urnika (foto: M. Prelovšek).

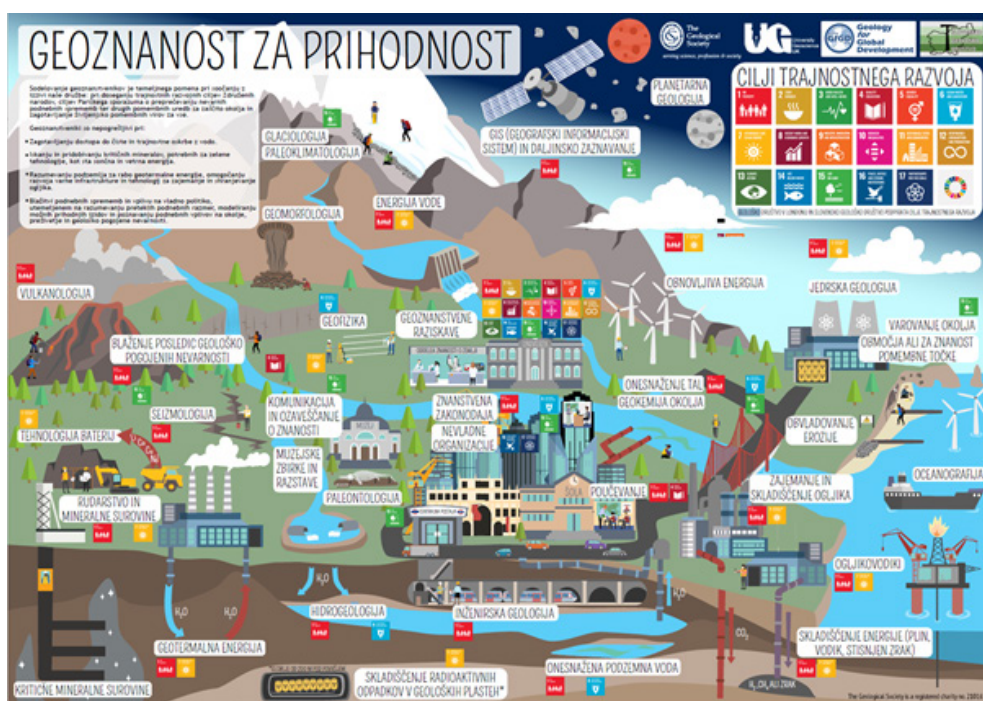
področjih dela znotraj geoznanosti in geoinženirstvu poznajo razlike v spolu. Slovenski partner je organiziral delavnico, ki se je udeležilo 8 strokovnjakinj s področja geoznanosti in geoinženirstva. Cilj projekta je tudi sodelovanje na Evropski noči raziskovalcev. V okviru projekta ENGIE in v sodelovanju s projektom Humanities rocks! smo v tednu Evropske noči raziskovalcev (27.11.2020) predstavili »Zgodbe Montanistike v svetu navidezne resničnosti«, kjer smo v tridimensionalnem prostoru na interaktivnem način prikazali geološke zanimivosti zgradbe Naravoslovnotehniške fakultete UL, v kateri danes deluje Oddelek za geologijo (<http://www.360montanistica.ntf.uni-lj.si/>). Dopolnjene in v angleški jezik prevedene so bile tudi brošure, kjer je stavba Montanistika predstavljena v tiskani obliki. V slovenski jezik sta bila za potrebe diseminacije projekta prevedena in tiskana brošura in plakat projekta. Predstaviti material bo uporabljen v okviru dejavnosti, ki so na tem področju planirane v letu 2021. Poleg tega smo v slovenski jezik dodatno prevedli tudi plakat »Geoscience for future«, ki je bil izdelan s strani Geološkega društva v Londonu. Plakat je prosto dostopen na spletni povezavi društva <https://www.geolsoc.org.uk/Posters>. Projekt ENGIE je bil v letu 2020 predstavljen ciljni publiku v okviru treh delavnic, ki jih je obiskalo 229 učencev v starosti od 11 do 14 let, dejavnosti na projektu pa so bile tudi predstavljene na različnih družbenih omrežjih.

CROWD THERMAL – Sodelovanje družbe pri razvoju geotermalnih projektov z uporabo alter-

nativnih virov financiranja (Community-based development schemes for geothermal energy) Leto 2020 je bilo drugo leto projekta CROWD THERMAL - Razvojne sheme za geotermalno energijo, ki temeljijo na skupnosti. Projekt je namenjen krepitvi družbe pri njenemu sodelovanju v razvoju geotermalnih projektov z uporabo alternativnih virov financiranja. V prvem letu sodelovanja smo se udeležili webinarja za TLPje, postavili spletno stran v slovenskem jeziku, izpolnili vprašalnik WP2 - Community-based geothermal energy financing principles, promovirali projekt preko Geonovic GeoZS in prevoda e-obvestil projekta, ki je bil objavljen na fb GeoZS in SGD. V letu 2021 je načrtovano nadaljnje sodelovanje v spletnih aktivnostih projekta, udeležba na skupnih e-dogodkih CROWD THERMAL - Geothermal-DHC, predstavitev projekta na geološkem posvetovanju ter zagotavljanje potrebnih podatkov za partnerje po njihovih navodilih.

ROBOMINERS – Razvoj bio-navdihnenega robotskega rudarja (*Resilient Bio-Inspired Modular Robotic Miner*).

V sklopu delovnega paketa WP5 je potekalo zbiranje podatkov o slovenskih rudnikih, ki so sestavni del projektne baze evropskih rudnikov. Zbranih je bilo 141 rudnikov, podatki so zajemali geografsko lokacijo, tip in velikost rudišča, obdobje obratovanja, kratek geološki opis, geotehnične lastnosti (tega podatka ni bilo mogoče pridobiti), izkoriščane surovine, geotermalni gradient, stanje nahajališča, vire in reference ter opombe.



Sl. 3. Geoznanost za prihodnost (<https://www.geolsoc.org.uk/Posters>)

Delovni paket WP10 je zajemal diseminacijske aktivnosti, v sklopu katerih sta bila prevedeni obvestili za javnost iz Madrixa (julij 2019) in iz Talina (januarja 2020), poslano je bilo tudi vabilo za sekcijsko tematiko uporabe robotike na več področjih geologije, predvsem na področju mineralnih surovin, v sklopu konference EGU 2021 (<https://www.egu.eu>). Prav tako smo vzpostavili spletno stran projekta Robominers znotraj strani SGD (<https://www.slovenskogeoloskodrustvo.si/index.php/mednarodno-sodelovanje/sodelovanje-v-mednarodnih-projektih>).

**REFLECT** - Redefiniranje lastnosti geotermalnih tekočin v ekstremnih pogojih (*Redefining geothermal fluid properties at extreme conditions to optimiza future geothermal energy extraction*)

Leto 2020 je bilo prvo leto projekta REFLECT, katerega cilj je preprečiti težave povezane s kemijsko geotermalnimi tekočinami še preden nastanejo. V letu 2020 smo postavili vsebine za projektno spletno stran v slovenskem jeziku in zbirali podatke o vrtinah, rezervoarjih, kemijski sestavi vode in geotermičnih lastnostih vzorcev kamnin, ki izhajajo iz globin nad 2,5 km oziroma kjer termalna voda dosega nad 50 stopinj Celzija. S tem smo zajeli vse srednje do visoko temperaturne javne podatke o objektih, ki podajo informacije, relevantne za geokemično modeliranje oz. napoved pogojev v večjih globinah v Sloveniji. Ugotovili smo, da kljub razmeroma velikem številu globljih vrtin, ki so večinoma v SV Sloveniji, podatkov o geokemijski sestavi kamnin sploh pa vode, niso pogosti, sploh količina javnih podatkov je zelo majhna.

Tudi v letu 2020 se je nadaljevalo članstvo SGD v domačih in tujih mednarodnih zvezah: European Federation of Geologists (EFG), International Union for Quaternary Research (INQUA), European Association for the Conservation of the Geological Heritage (ProGeo), European Mineralogical Union (EMU) in International Mineral Association (IMA). Včlanjeni smo tudi v Slovensko inženirska zvezo (SIZ), s čemer je izpolnjen pogoj za pridobitev naziva Evro inženir (EUR ING).

Največ aktivnosti je bilo v SINQUA, kje je predstavnik tudi v letu 2020 sodeloval na spletnih sestankih, volitvah in pri odločanju mednarodnega Sveta INQUA. Kot člani INQUA smo nadaljevali sodelovanje pri oblikovanju skupnih aktivnosti v okviru različnih komisij. Člani SINQUA smo vpeti v INQUA komisije CMP (Coastal and Marine Processes), PALCOM (Paleoclimates), SACCOM (Stratigraphy and Chronology) in TERPRO (Terrestrial Processes, Deposits and Histo-

ry). V okviru CMP komisije smo člani SINQUA sodelovali pri uspešni prijavi štiriletne projekta NEPTUNE - New Procedures and Technologies for Underwater Paleo-Landscape Reconstruction, ki je namenjen organizaciji letnih srečanj mlajših znanstvenikov, ki se ukvarjajo z raziskovanjem morskih in priobalnih območij, ki so bila potopljena po zadnji ledeni dobi. V septembru 2020 bomo organizirali prvo mednarodno srečanje v okviru projekta, ki pa bo zaradi pandemije potekalo preko spletja. V okviru TERPRO fokusne skupine Terrestrial Processes Perturbed by Tectonics je bil v letu 2020 uspešno pridobljen projekt EDITH - From Earthquake Deformation to Seismic Hazard Assessment, katerega cilj je organizacija letnih znanstvenih srečanj na temo študij potresnega cikla za namene ocene potresne nevarnosti. Člana SINQUA sta bila gostujoča urednika za Quaternary international, vol. 546 (Quaternary Stratigraphy and Karst & Cave Sediments: the INQUA-SEQS 2018 Meeting, uredniki: Guzel Danukalova, Markus Fiebig, Nadja Zupan Hajna, Pierluigi Pieruccini, Andrej Mihevc), ki je izšel aprila 2020. Sodelovali smo tudi pri pripravi vsebin za INQUA revijo Quaternary Perspectives št. 28, ki je izšla junija 2020.

Načrti za leto 2021? Zaradi izrednih razmer in ukrepov, ki so bili uvedeni zaradi epidemije koronavirusa, ne načrtujemo večjih dogodkov in predavanj. Vso energijo smo usmerili v aktivnosti v počastitev 70 let delovanja društva. V trenutku, ko pišem to poročilo imamo že nov logotip in novo grafično podobo društva. Pripravili in izdali smo osebne znamke z geološkimi motivi. Znamke si lahko ogledate na spletni strani društva in jih naročite.

Pripravljamo tudi monografijo Obrazi geologije, kjer so predstavljene besede, ki geologom doma in v tujini pomenijo delo, hobi in ljubezen do geologije. Izdaja knjige se načrtuje v septembru 2021.

Pričeli smo z aktivnostmi organizacije 6. slovenskega geološkega kongresa, ki se načrtuje v septembru 2022 v Rogaški Slatini.

Tudi v letu 2021 znaša članarina za člane 15 €, za študente pa 7,5 €. Vabljeni, da podaljšate članstvo oziroma postanete član.

Vabim vas, da obiščete spletno stran društva <https://www.slovenskogeoloskodrustvo.si/>, kjer lahko spremljate aktivnosti društva.

## V spomin akad. dr. Dragici Turnšek



V soboto 11. septembra 2021 se je poslovila akademikinja dr. Dragica Turnšek, svetovno priznana specialistka za fosilne grebenske organizme. Rodila se je 6. avgusta 1932 družini Kerčmar v Šalamencih. Po maturi na gimnaziji v Murski Soboti se je leta 1952 vpisala na študij geologije s paleontologijo na Prirodoslovno-matematični fakulteti Univerze v Ljubljani. Da bi lahko študirala, se je zaposlila. Najprej za eno leto na Republiškem zavodu za statistiko in evidenco in leta 1954 kot laborantka na takratnem Inštitutu za geologijo Slovenske akademije znanosti in umetnosti. Inštitutu, ki se je pozneje preimenoval v Paleontološki inštitut Ivana Rakovca ZRC SAZU, je ostala zvesta vse življenje. Po diplomi leta 1958 je bila najprej asistentka. Leta 1965 je doktorirala. V letih 1965 do 1973 je bila znanstvena sodelavka, v letih 1973 do 1976 višja znanstvena sodelavka in po letu 1976 znanstvena svetnica. V letih 1971–72 je bila Humboldtova štipendistka na univerzi v Stuttgartu. Krajši čas se je izpopolnjevala tudi v Angliji, na Irskem, v Švici, Avstriji in na Poljskem. Leta 1967 je prejela nagrado sklada Borisa Kidriča in leta 1987 Red dela z zlatim vencem. Leta 1985 je postala izredna in leta 1993 redna članica SAZU. Leta 1993 je postala članica Evropske akademije znanosti in umetnosti s sedežem v Salzburgu.

Njene prve paleontološke raziskave so obravnavale jurske alge in tintinine. Na začetku je več let veliko delala na terenu. V okviru projekta Osnovna geološka karta Jugoslavije, ki ga je v Sloveniji vodil Geološki zavod Ljubljana,

je kartirala, največ na Dolenjskem. Sodelovala je na listih Celje, Novo mesto, Ribnica in Postojna. Rada se je spominjala tega obdobja. Prilagodila se je programu inštituta in se pri terenskem delu osredotočila na zgornjejurske koralno-spongijске apnence, ki so bili takrat v Sloveniji še popolnoma neraziskani. Enako stare grebenske apnence je proučevala tudi na Trnovskem gozdu in ugotovila, da so skupaj tvorili obsežen greben, podoben današnjemu Velikemu bariernemu grebenu ob vzhodni obali Avstralije. V doktorski disertaciji je obravnavala stromatopore in hetetide. Obe skupini sta bili takrat uvrščeni med hidrozoje, po novem pa spadata k spongijam. Pozneje je z istih nahajališč raziskala še korale. Po njeni zaslugi je zgornjejurski greben osrednje Slovenije sedaj med najbolje proučenimi fosilnimi grebeni na svetu. Bila je med prvimi, ki je po strukturi skeletov in značilnih združbah fosilni greben razdelila na več vzporednih pasov od zunanjega grebena na robu odprtga morja do zagrebena na meji z laguno. Pozneje je raziskave razširila na spodnjejurske, triasne, kredne in v manjši meri tudi na paleozojske in terciarne grebene. Poleg sistematike in biostratigrafije so jo vedno privlačila vprašanja ekologije grebenskih organizmov. V sodelovanju s sedimentologi in regionalnimi geologi je proučevala manjše kopaste grebene različnih starosti, zgornjeteriasne grebene na robu izoliranih karbonatnih platform in kredne atole.

Že kmalu si je v svetu pridobila sloves odlične poznavalke svojega področja. Zaradi poglobljenega znanja in prijetnega samozavestnega značaja je bila med kolegi doma in v tujini zelo priljubljena. K njej na specializacijo so prihajali diplomanti in doktorandi iz Nemčije, Veliike Britanije, Švice in Hrvaške. V obdelavo je dobila material iz drugih jugoslovanskih republik, Francije, Švice, Nemčije, Avstrije, Madžarske, Romunije, Grčije, Španije, Italije, ZDA in Mehike. Vse, česar se je lotila, je tudi dokončala. Z več kot 200 nahajališč je opisala 450 vrst koral, stromatopor in hetetid. Sedemnajst rodov in 93 vrst je novih.

Pri delu je bila neverjetno organizirana – izjemno sistematična in nepopustljivo disciplinirana. Na to je bila ponosna. Ko je projektne naloge prijavila, je imela rezultate v resnici že v predalu. Njen opus obsega 60 znanstvenih člankov, med katerimi so obsežna temeljna dela o taksonomiji, ekologiji in biostratigrafiji grebenskih organizmov. Še posebej odmevna je leta 1997 objavljena monografska sinteza Mezozojske korale Slovenije.

Enako resno in zavzeto, kot se je lotevala raziskovalnega dela, je opravljala tudi administrativne funkcije. Od leta 1983 do upokojitve leta 1992 je bila upravnica Paleontološkega inštituta Ivana Rakovca. V letih 1980–86 je bila predsednica programskega sveta za geologijo pri Raziskovalni skupnosti Slovenije. V letih 1996–2000 je bila članica komisije Republike Slovenije za nagrade za znanstvenoraziskovalno delo. Kot predstavnica SAZU je bila vpeta v vodenje ZRC SAZU. V letih 2005–2019 je bila v Upravnem odboru ZRC SAZU in v znanstvenih svetih več inštitutov, v letih 2016–2020 je bila predsednica Znanstvenega sveta Paleontološkega inštituta Ivana Rakovca.

Dejavna je bila v strokovnih združenjih in uredniških odborih. V mednarodnem združenju International Fossil Cnidaria and Porifera Association (sedaj International Fossil Coral and Reef Society) je bila dopisnica za jugovzhodno Evropo. V letih 1988–1995 je bila članica odbora tega društva in v letih 1985–1992 članica mednarodne delovne skupine za revizijo koral. V dveh štiriletnih mandatih (1965–1969 in 1982–1986) je bila tajnica in od 1995 do 2014 članica častnega razsodišča Slovenskega geološkega društva. Od leta 1994 je bila članica uredniškega odbora revije Geologija. Ker je že od mladosti gojila prav posebno ljubezen do jezika, je na svojo željo slovenske povzetke v Geologiji tudi lektorirala.

Kot vodja inštituta nam je bila Dragica vedno v oporo. Z nami je debatirala o geologiji, nas potrpežljivo spodbujala pri raziskovalnem delu in kljub skromnim sredstvom poskrbela, da smo lahko odhajali na izobraževanja v tujino. Bila je modra, pravična, prijateljska, a vedno dosledna in odločna. Tudi po upokojitvi, ko formalno ni bila več upravnica, je ostala naša učiteljica, svetovalka in nesporna moralna avtoriteta.

Dokler ji je zdravje dopuščalo, je vsak dan prihajala na inštitut. Ker je imela rada svoje delo in ker je bila rada z nami. Še v zadnjih dneh, ko smo se pogovarjali samo še po telefonu, je ohranila vedrino in smisel za humor. Na ZRC in še posebej na inštitut, s katerim je bila povezana 67 let, je gledala kot na svoj dom. Bila nam je mama in bila nam je vzor. Spominjali se je bomo z veliko ljubeznijo in neizmernim spoštovanjem.

Špela Goričan

### Akad. dr. Dragica Turnšek: bibliografija 1962–2019

Seznam obsega objavljena znanstvena in strokovna dela. Povzetki predavanj, poljudni članki in prispevki v enciklopedijah v pregledu niso zajeti. Popoln seznam bibliografskih enot je dostopen na spletnih straneh v sistemu COBISS.

- Kerčmar, D. 1962: Prve najdbe zgornjejurskih apnenih alg v Sloveniji. *Geologija*, 7: 9–24.
- Turnšek, D. 1965: Velike tintinine v titonskih in valangijskih skladih severozahodne Dolenjske. *Geologija*, 8: 102–111.
- Turnšek, D. 1965: On the "Tithonian" in reef facies. *Bulletin scientifique. Section A, Sciences naturelles, techniques et medicales*, 10: 211.
- Turnšek, D. 1966: Zgornjejurska hidrozojska favna iz južne Slovenije. *Razprave IV. razreda SAZU*, 9: 335–428, 19 pls.
- Turnšek, D. & Buser, S. 1966: Razvoj spodnjekrednih skladov ter meja med juro in kredo v zahodnem delu Trnovskega gozda. *Geologija*, 9: 527–548.
- Turnšek, D. 1967: Sistematski položaj rodu *Burgundia* (Hydrozoa). *Razprave IV. razreda SAZU*, 10: 265–275.
- Turnšek, D. 1968: Hidrozoji in korale iz jurskih in krednih skladov v južnozahodni Jugoslaviji. *Razprave IV. razreda SAZU*, 11: 351–376, 9 pls.
- Turnšek, D. 1969: Prispevek k paleoekologiji jurških hidrozojev v Sloveniji. *Razprave IV. razreda SAZU*, 12/5: 209–237, 1 pl.
- Turnšek, D. & Barbulescu, A. 1969: Upper Jurassic Hydrozoa in Central Dobrogea (Romania). *Geologija*, 12: 73–84.
- Turnšek, D. 1970: Devonska stromatoporoidna favna s Karavank. *Razprave IV. razreda SAZU*, 13/5: 165–192, 14 pls.
- Turnšek, D. 1970: Kredni hidrozoji z Zlatibora v zahodni Srbiji. *Razprave IV. razreda SAZU*, 13/6: 193–208, 11 pls.
- Turnšek, D. & Mihajlović, M. 1971: Prikaz hidrozojske faune titonskih krečnjaka Srbije. *Glasnik Prirodnjačkog muzeja u Beogradu. Serija A: Mineralogija, geologija, paleontologija*, 25: 41–69.
- Turnšek, D. 1972: Zgornjejurske korale iz južne Slovenije. *Razprave IV. razreda SAZU*, 15/6: 145–265, 37 pls.
- Turnšek, D. & Masse, J.-P. 1973: The Lower Cretaceous Hydrozoa and Chaetetidae from Provence (South-eastern France). *Razprave IV. razreda SAZU*, 16/6: 217–244, 27 pls.
- Turnšek, D. & Mihajlović, M. 1973: Prikaz koral-ske faune titonskih krečnjaka Srbije. *Glasnik Prirodnjačkog muzeja u Beogradu. Serija A: Mineralogija, geologija, paleontologija*, 28: 93–129.
- Turnšek, D. & Buser, S. 1974: Spodnjekredne korale, hidrozoji in hetetide z Banjške planote in Trnovskega gozda. *Razprave IV. razreda SAZU*, 17/2: 81–124, 16 pls.
- Turnšek, D., Seyfried, H. & Geyer, O.F. 1975: Geologische und paläontologische Untersuchungen an einem Korallen-Vorkommen im subbetischen Unterjura von Murcia (Süd-Spanien). *Razprave IV. razreda SAZU*, 18: 117–151, 25 pls.
- Turnšek, D. 1975: Malmian corals from Zlobin, south-west Croatia. *Palaeontologia Jugoslavica*, 16: 1–23, 12 pls.
- Turnšek, D. & Buser, S. 1976: Knidarijska favna iz senonijske breče na Banjški planoti. *Razprave IV. razreda SAZU*, 19/3: 37–88, 25 pls.
- Turnšek, D. 1978: Solitarne senonijske korale iz Stranic in Medvednice. *Razprave IV. razreda SAZU*, 21/3: 61–128, 31 pls.
- Turnšek, D. & Polšak, A. 1978: Senonijske kolonjske korale iz biolititnega kompleksa v Orešju na Medvednici. *Razprave IV. razreda SAZU*, 21/4: 129–180, 16 pls.
- Polšak, A., Devidé-Nedela, Turnšek, D., D., Gušić, I. & Benić, J. 1978: Biostratigrafski odnosi grebenskih, prigrebenskih i bazenskih naslaga gornje krede u području Donjeg Orešja, SI Medvednica. *Geološki vjesnik*, 30: 189–197.
- Dieni, I. & Turnšek, D. 1979: *Parkeria sphaerica* Carter, 1877 (Hydrozoan) in the Vraconian (Lower Cretaceous) of Orosei (Sardinia). *Bollettino della Società Paleontologica Italiana*, 18/2: 200–206.
- Turnšek, D. & Herb, R. 1980: Eine neue Chaetetiden-Art aus den Drusberg-Schichten (Barrémien) des Kistenpass-Gebiets (Sedimentbedeckung des östlichen Aarmassivs, Schweizer Alpen). *Eclogae Geologicae Helvetiae*, 73: 1109–1121.
- Čar, J., Skaberne, D., Ogorelec, B., Turnšek, D. & Placer, L. 1981: Sedimentological characteristics of Upper Triassic (Cordevolian) circular quiet water coral bioherms in western Slovenia, northwestern Yugoslavia. In: Toomey, D.F. (Ed.). European fossil reef models. SEPM special publication, 30: 233–240.
- Turnšek, D., Buser, S. & Ogorelec, B. 1981: An Upper Jurassic reef complex from Slovenia, Yugoslavia. In: Toomey, D.F. (Ed.). European fossil reef models. SEPM special publication, 30: 361–369.
- Turnšek, D. & Mihajlović, M. 1981: Lower Cretaceous cnidarians from eastern Serbia. *Razprave IV. razreda SAZU*, 23/1: 1–54, 50 pls.
- Turnšek, D., Buser, S. & Ogorelec, B. 1982: Carnian coral-sponge reefs in the Amphiclina beds between Hudajužna and Zakriž (western Slovenia). *Razprave IV. razreda SAZU*, 24/2: 51–98, 12 pls.
- Buser, S., Ramovš, A. & Turnšek, D. 1982: Triassic reefs in Slovenia. *Facies*, 6: 15–24.
- Ramovš, A. & Turnšek, D. 1984: Lower Carnian reef buildups in the northern Julian Alps (Slovenia, NW Yugoslavia). *Razprave IV. razreda SAZU*, 25/4: 161–200, 15 pls.
- Turnšek, D., Buser, S. & Ogorelec, B. 1984: The role of corals in Ladinian reef communities of Slovenia, Yugoslavia. *Palaeontographica Americana*, 54: 201–209.
- Turnšek, D., LeMone, D.V. & Scott, R.W. 1984: Corals from Cerro de Cristo Rey, Doña Ana County, New Mexico and Chihuahua, Mexico. *Palaeontographica Americana*, 54: 475.
- Turnšek, D. 1985: Carnian coral *Thamnotropis rakoveci* n. sp. from Perbla near Tolmin (NW Yugoslavia). In: Grafenauer, S., Pleničar, M., Drobne, K. (Eds.). *Zbornik Ivana Rakovca*. *Razprave IV. razreda SAZU*, 26: 305–312, 3 pls.
- Turnšek, D., Buser, S. & Ogorelec, B. 1987: Upper Carnian reef limestone in clastic beds at Perbla near Tolmin (NW Yugoslavia). *Razprave IV. razreda SAZU*, 27: 37–64, 7 pls.
- Turnšek, D. & Ramovš, A. 1987: Upper Triassic (Norian-Rhaetian) reef buildups in the northern Julian Alps (NW Yugoslavia). *Razprave IV. razreda SAZU*, 28: 27–67, 16 pls.
- Drobne, K., Ogorelec, B., Pleničar, M., Zucchi-Stolfa, M.L. & Turnšek, D. 1988: Maastrichtian, Danian and Thanetian Beds in Dolenja vas (NW Dinarides, Yugoslavia) Mikrofacies, foraminifers, rudists and corals. *Razprave IV. razreda SAZU*, 29: 147–224, 35 pls.
- Turnšek, D. 1989: Diversification of corals and coral reef associations in Mesozoic palaeogeographic units of northwestern Yugoslavia. *Memoirs of the*

- Association of Australasian Palaeontologists, 8: 283–289.
- Rosen, B.R. & Turnšek, D. 1989: Extinction patterns and biogeography of scleractinian corals across the Cretaceous/Tertiary boundary. Memoirs of the Association of Australasian Palaeontologists, 8: 355–370.
- Turnšek, D. & Buser, S. 1989: The Carnian reef complex on the Pokljuka (NW Yugoslavia). Razprave IV. razreda SAZU, 30: 75–127.
- Drobne, K., Ogorelec, B., Pleničar, M., Barattolo, F., Turnšek, D. & Zucchi-Stolfa, M.L. 1989: The Dolenja vas section, a transition from Cretaceous to Paleocene in the NW Dinarides, Yugoslavia. Memorie della Società Geologica Italiana, 40 (1987): 73–84.
- Jamnik, A., Ramovš, A. & Turnšek, D. 1990: *Heterastridium conglobatum* Reuss, 1865 (?hidrozoj) v norijskem apnencu Kamniških Alp. Geologija, 31/32: 199–207.
- Ramovš, A. & Turnšek, D. 1991: The Lower Norian (Latian) Development with Coral Fauna on Razor and Planja in the Northern Julian Alps (Slovenia). Razprave IV. razreda SAZU, 32: 175–213.
- Turnšek, D. & Buser, S. 1991: Norian-Rhaetian coral reef buildups in Bohinj and Rdeči rob in Southern Julian Alps (Slovenia). Razprave IV. razreda SAZU, 32: 215–257.
- Turnšek, D. 1992: Tethyan Cretaceous corals in Yugoslavia. In: Kollmann, H.A. & Zapfe, H. (Eds.), New Aspects on Tethyan Cretaceous Fossil Assemblages. Österreichische Akademie der Wissenschaften, Schriftenreihe der Erdwissenschaftlichen Kommissionen, 9: 155–170.
- Turnšek, D., Pleničar, M. & Šribar, L. 1992: Lower Cretaceous Fauna from Slovenski vrh near Kočevje (South Slovenia). Razprave IV. razreda SAZU, 33: 205–257.
- Dozeti, S. & Turnšek, D. 1993: Litostratigrafske enote in biostratigrafska razčlenitev jurskih plasti na Logaški planoti. Rudarsko-metalurški zbornik, 40/1–2: 59–78.
- Turnšek, D. & Löser, H. 1993: The history of Mesozoic coral research after 1940. Courier Forschungsinstitut Senckenberg, 164: 37–46.
- Turnšek, D. 1994: Upper Cretaceous reef building colonial corals of Gosau facies from Stranice near Slovenske Konjice (NE Slovenia). Razprave IV. razreda SAZU, 35: 3–41.
- Turnšek, D. & Senowbari-Daryan, B. 1994: Upper Triassic (Carnian–Lowermost Norian) Corals from the Pantokrator Limestone of Hydra (Greece). Abhandlungen der Geologischen Bundesanstalt, 50: 477–507.
- Drobne, K., Ogorelec, B., Barattolo, F., Dolenc, T., Pleničar, M., Turnšek, D., Zucchi-Stolfa, M.L. & Marton, E. 1995: Stop 1: The Dolenja vas section (Upper Maastrichtian, Lower and Upper Danian, Thanetian. Atti del Museo Geologico-Paleontologico di Monfalcone, Quaderno Speciale, 3: 99–115.
- Vecsei, A., Moussavian, E. & Turnšek, D. 1996: Paleocene Reef Evolution on the Maiella Carbonate Platform (Italy). In: Reitner, J., Neuweiler, F. & Gunkel, F. (Eds.), Global and Regional Controls on Biogenic Sedimentation. I. Reef Evolution. Research Reports. Göttinger Arbeiten zur Geologie und Paläontologie, Sb 2: 175–178.
- Császár, G. & Turnšek, D. 1996: Vestiges of atoll-like formations in the Lower Cretaceous of the Mecsek Mountains, Hungary. Cretaceous Research, 17: 419–442.
- Turnšek, D. 1997: Mesozoic corals of Slovenia. Zbirka ZRC, 16. Založba ZRC, ZRC SAZU, Ljubljana: 512 p.
- Turnšek, D. & Drobne, K. 1998: Paleocene corals from the northern Adriatic Platform. In: Hottinger, L. & Drobne, K. (Eds.) Paleogene Shallow Benthos of the Tethys. 2. Dela – Opera SAZU, IV. razred, 34/2: 129–154.
- Turnšek, D. & Buser, S. 1999: *Stylophyllopsis veneta* (Airaghi), a Liassic coral from the northern Dinaric Carbonate Platform (Slovenia). Profil, 16: 173–180.
- Turnšek, D., Dolenc, T., Siblík, M., Ogorelec, B., Ebli, O. & Lobitzer, H. 1999: Contributions to the Fauna (Corals, Brachiopods) and Stable Isotopes of the Late Triassic Steinplatte Reef/Basin-Complex, Northern Calcareous Alps, Austria. Abhandlungen der Geologischen Bundesanstalt, 56/2: 121–140.
- Košir, A., Goričan, Š., Debeljak, I., Otoničar, B., Turnšek, D. 1999: Vodnik po ekskurziji. Ob 50. obletnici ustanovitve Paleontološkega inštituta Ivana Rakovca ZRC SAZU. Založba ZRC, ZRC SAZU, Ljubljana: 20 p.
- Jelen, B., Šimunić, A., Drobne, K., Skaberne, D., Čosović, V., Avanić, R., Báldi-Beke, M., Cimerman, F., Čar, J., Fodor, L., Kedves, M., Márton, E., Monostori, M., Pavlovec, R., Placer, L., Šikić, L., Toumarkine, M., Turnšek, D. & Zagoršek, K. 2000: Eocene in NE Slovenia and NW Croatia: excursions 6 and 7. In: Bassi, D. (Ed.): Shallow water benthic communities at the Middle–Upper Eocene boundary: southern and north-eastern Italy, Slovenia, Croatia, Hungary: field trip guidebook. Annali dell'Università di Ferrara, Sezione Scienze della Terra, 8, supplement: 104–147.
- Turnšek, D. & Košir, A. 2000: Early Jurassic corals from Krim Mountain, Slovenia. Razprave IV. razreda SAZU, 41/1: 81–113.
- Turnšek, D., Buser, S. & Debeljak, I. 2003: Liassic coral patch reef above the "Lithiotid limestone" on Trnovski gozd plateau, west Slovenia. Razprave IV. razreda SAZU, 44/1: 285–331.
- Turnšek, D., LeMone, D.V. & Scott, R.W. 2003: Tethyan Albian corals, Cerro de Cristo Rey uplift, Chihuahua and New Mexico. In: Scott, R.W. (Ed.), Cretaceous Stratigraphy and Paleoecology, Texas and Mexico: Perkins Memorial Volume. Gulf Coast Section Society of Economic Paleontologists and Mineralogists Foundation, Special publications in Geology, 1: 147–185.
- Turnšek, D. & Klepač, K. 2003: Koralji – Anthozoa. In: Klepač, K. (Ed.). Fosilna fauna otoka Krka. Prirodoslovna biblioteka, 5. Prirodoslovni muzej Rijeka: 235–267.
- Turnšek, D. & Košir, A. 2004: *Bacarella vipavica* n. gen., n. sp. (Anthozoa, Scleractinia) from reefal blocks in Lower Eocene carbonate megabeds in the Vipava Valley (SW Slovenia). Razprave IV. razreda SAZU, 45/3: 145–169.
- Turnšek, D. 2006: Triasni koralno-spongijski greben v Hudajužni. In: Torkar, S. & Kofol, K. (Eds.), Baški zbornik. Tolminski muzej, Tolmin: 7–12.
- Rožič, B., Gerčar, D., Oprčkal, P., Švara, A., Turnšek, D., Kolar-Jurkovšek, T., Udovč, J., Kunst, L., Fabjan, T., Popit, T. & Gale, L. 2019: Middle Jurassic limestone megabreccia from the southern margin of the Slovenian Basin. Swiss Journal of Geosciences, 112/1: 163–180.

## V spomin prof. dr. Valeriji Osterc



V letosnjem poletju nas je v 97-letu starosti zapustila prof. dr. Valerija Osterc, priznana mineraloginja in do upokojitve redna profesorica na Oddelku za geologijo, Naravoslovnotehniške fakultete, Univerze v Ljubljani.

Valerija Žerjav se je rodila leta 1924 v Žlebiču pri Ribnici, od koder jo je želja po znanju vodila v Ljubljano. Po zaključeni nižji gimnaziji se je vpisala na državno učiteljišče, kar je pustilo pečat tudi v njeni nadaljnji poklicni poti. Pri izbiri študija je prevladala ljubezen do naravoslovja. Leta 1947 se je vpisala na mineraloško-petrografska smer geološkega oddelka Filozofske fakultete. Izstopala je po znanju in razumevanju snovi in že kot študentka pomagala pri izvedbi vaj. Po diplomi, leta 1954, se je zaposnila kot asistentka, a morala kasneje mesto zaradi družbeno-političnih razmer zapustiti. Poklicno pot je 1958 nadaljevala na Geološkem zavodu in 1960 na Zavodu za avtomatizacijo.

Začela se je ukvarjati z raziskavami elektrotehnične keramike, ker je njen nadaljnji strokovni razvoj vodilo v smer tehnične mineralogije in nekovinskih materialov. Leta 1963 je odšla na študij v Nemčijo, na aachensko Rensko-westfalsko tehnično visoko šolo. Raziskave je posvetila reakcijam med cirkonom in aluminotermičnimi žlindrami. Doktorat je zaključila 1967 z najvišjo možno oceno ter zanj prejela tudi Borchersovo plaketo. Znanje s področja keramike je prenesla v Slovenijo najprej na Zavod za avtomatizacijo in potem na Zavod za raziskavo materiala in konstrukcij.

Na Odseku za geologijo so prepoznali njen potencial in 1970 se je kot docentka vrnila na ljubljansko univerzo. Njen prispevek k posodobitvi študija je bil izjemen z uvedbo predmetov Tehnična mineralogija, Preiskovalne metode v mineralogiji in Preiskava nekovinskih mineralov. Prva na Oddelku za geologijo je aktivno pristopila k ureditvi laboratorija in uvedbi novih analitskih tehnik, ki so zahtevale dražjo opremo. Uspela je z nabavo rentgenskega difraktometra in njegovo uporabo predstavila preko 30 podiplomskim študentom, ko je leta 1977 samostojno izvedla seminar o rentgenskem preiskovanju kristalnih snovi. Istega leta je postala izredna in 1984 redna profesorica. Pod njenim mentorstvom je študij zaključil en doktorand, štirje magistranti in 21 diplomantov. Aktivno se je vključevala tudi v delovanje takratnega Odseka za geologijo, kjer je bila en mandat predstojnica. Med leti 1982 in 1986 je bila delegatka v skupščini SR Slovenije.

Bibliografija prof. dr. Valerije Osterc zajema tako številna poročila kot tudi prispevke na kongresih in znanstvene članke. Posvečala se je predvsem raziskavam gline, boksita, manganovih mineralov, nekovinskih izdelkov, sekundarnih surovin, mikrostruktur in arheološke keramike. Poljudno-strokovni del obsega preko 80 ocen novih knjig, članke v Proteusu in prispevke o geoloških zanimivostih na Radiu Ljubljana.

Po upokojitvi leta 1988 se na fakulteto ni več vračala. Kljub temu so predavanja in študenti ostali del njenega sveta. Ob obisku ob njeni 90-letnici je osupnila s svojim neverjetnim spominom na imena študentov in njihove diplomske naloge. Njeno sistematično in razumljivo podano znanje se je ohranilo v številnih generacijah študentov. Prof. dr. Valerija Osterc se uvršča med tiste, ki so vidno prispevali tako k razvoju geološke stroke kot tudi k ljubljanski geološki šoli.

Nina Zupančič

## V spomin dr. Bogomirju Celarcu



Jeseni, tridesetega oktobra 2021 nas je nenadoma zapustil dr. Bogomir Celarc, univerzitetni diplomirani inženir geologije. Umrl je star petdeset let. Bil je izjemen.

Bogomir, Mirko, Mire, za geologe največkrat Bogo, je odraščal in živel v okolici Borovnice, a so mu bile kot strastnemu gorniku, jamarju in plezalcu domače tudi slovenske gore, s katerimi je bilo tesno povezano njegovo znanstveno delovanje. Pred vpisom na fakulteto je Bogomir na takratni Srednji naravoslovni šoli Ljubljana končal program Geološki tehnik. Na univerzitetnem dodiplomskem študiju geologije na Naravoslovnotehniški fakulteti se je izkazal kot odličen študent. Zaključil ga je leta 1998 z diplomskim delom Geološka zgradba ozemlja okolice Borovnice. Isto leto se je zaposlil kot mladi raziskovalec na Geološkem zavodu Slovenije (GeoZS).

Doktorsko disertacijo z naslovom Geologija severovzhodnega dela Kamniško-Savinjskih Alp je zagovarjal leta 2004. Od samega začetka svoje poklicne poti je prevzemal najzahtevnejše geološke projekte in sodeloval pri ključnih odločitvah na GeoZS. Od leta 2007 je bil v sedmih mandatnih ob-

dobjih član Znanstvenega sveta GeoZS. Od leta 2014 je zelo uspešno vodil oddelek Regionalna geologija, ob tem pa je bil en mandat kot predstavnik zaposlenih tudi član Upravnega odbora GeoZS.

Kot klasičnega regionalnega geologa so ga odlikovale terenske izkušnje, odlična prostorska predstava, smisel za razumevanje strukture ter dobro poznavanje strukturne geologije in stratigrafije. Njegova strokovna zapuščina obsega 130 poročil, elaboratov in strokovnih mnenj, ki med drugim obsegajo geološke prognoze in poročila o spremljavi največjih infrastrukturnih projektov, kot sta v zadnjih letih tudi gradnja drugega tira železniške proge Divača–Koper in nove cevi predora Karavanke, seizmotektonске modele in poročila o geološko pogojenih nevarnostih ter ekspertize v podporo različnim hidrogeološkim raziskavam. Bil je eden od najbolj izkušenih kartirajočih geologov v Sloveniji.

Svoje znanje na teh področjih je kot mentor prenašal tudi na mlajše geologe. Sodeloval je pri več diplomskih, magistrskih in doktorskih delih mlajših kolegov. Kot gostujoči predavatelj in soorganizator vaj iz terenskega kartiranja je sodeloval z Oddelkom za geologijo Naravoslovnotehniške fakultete Univerze v Ljubljani. S predavanji, snovanji učnih poti in geoloških stolpcev je geologijo približeval tudi laični javnosti.

Kljub močni vpetosti v operativno strokovno delo je ostajal vrhunski raziskovalec. Kot avtor ali soavtor je objavil 24 znanstvenih člankov, večino s področja stratigrafije triasa, strukturne geologije in tektonike. Njegova prva raziskovalna ljubezen so bile temeljne raziskave v slovenskih gorah. V sodelovanju z uglednimi domačimi in tujimi raziskovalci je opustil nekatere stare koncepte razumevanja triasne stratigrafije in postavil temelje za poznejše raziskave. Zapomnili si ga bomo po reviziji stratigrafskega zaporedja v Kamniško-Savinjskih Alpah, po objavah o Podolševskem prelomu, reševanju problematike starosti in poimenovanja »cordevolskega« apnena in dolomita, progradacije platforme Dachsteinskega apnena, srednjetriasnih polgrabnov in opisu Trbiškega bazena. Na podlagi njegovega dela je bilo najdenih več nahajališč triasnih vretenčarjev v Kamniško-Savinjskih Alpah. Žal se je tudi njegova znanstvena pot končala pred izidom članka o sedimentarnem razvoju člena Velike planine in o zapolnitvi srednjetriasnega polgrabna pod Vernarjem. Več let se je ukvarjal z razrešitvijo stratigrafskega zaporedja na severni strani Mangarta, razmišljal je o opustitvi nekaterih, pri nas dolgo zakoreninjenih izrazov, kot sta Dinarska in Julij-ska karbonatna platforma. Delo je ostalo nedokončano.

Bogomirja si bomo zapomnili po tehtnih besedah, milem, nevsiljivem značaju, po njegovi preprostosti in skromnosti. Vedno je bil odkrit, pošten in konstruktiven, zato je bilo z njim lahko in prijetno sodelovati. Kljub vsemu znanju je skromno in brez sramu priznal, da številnih stvari ne razume. Nekoč je dejal: »Več kot študiram, manj mi je jasno.« Tudi v tem se kaže njegova skromnost in veličina. Pogrešali ga bomo kot človeka, sodelavca in predvsem prijatelja.

Miloš Bavec

Luka Gale

Matevž Novak

## dr. Bogomir Celarc: izbrana bibliografija (2002–2021)

- Celarc, B. 2002: Tektonski stik med paleozojskimi in triasnimi kamninami pod Podolševe = Tectonic contact between Paleozoic and Triassic rocks south of Podolševa (Slovenia). *Geologija*, 45/2: 341-346. <https://doi.org/10.5474/geologija.2002.030>
- Kralj, P. & Celarc, B. 2002: Shallow intrusive volcanic rocks on Mt. Raduha, Savinja-Kamnik Alps, Northern Slovenia = Plitve intruzivne vulkanske kamnine na Raduhi, Savinjsko-Kamniške Alpe. *Geologija*, 45/1: 247-253. <https://doi.org/10.5474/geologija.2002.018>
- Celarc, B. 2002: Triglav thrust has been (unconsciously)discovered by Ivan Gams in 1961 = Triglavski nariiv je (nevede) odkril že Ivan Gams 1961 leta. *RMZ - Materials and geoenvironment*, 49/2: 281-283.
- Celarc, B. 2004: Problematika cordevolskih apnenecov in dolomitov v slovenskih Južnih Alpah = Problems of the Cordevolian limestone and dolomite in the Slovenian part of the Southern Alps. *Geologija*, 47/2: 139-149. <https://doi.org/10.5474/geologija.2004.011>
- Celarc, B. 2008: Karnijski boksitni horizont na Kopitovem griču pri Borovnici - ali je v njegovi talnini "pozabljenja" stratigrafska vrzel? = Carnian bauxite horizon on the Kopitov grič near Borovnica (Slovenia) - is there a "forgotten" stratigraphic gap in its footwall? *Geologija*, 51/2:147-152. <https://doi.org/10.5474/geologija.2008.015>
- Celarc, B., Kolar-Jurkovšek, T. 2008: The Carnian-Norian basin-platform system of the Martuljek mauntain group (Julian Alps, Slovenia): progradation of the Dachstein carbonate platform. *Geologica Carpathica*, 59/3: 211-224.
- Placer, L., Vrabec, M. & Celarc, B. 2010: The bases for understanding of the NW Dinarides and Istria peninsula tectonics = Osnove razumevanja tektonske zgradbe NW Dinaridov in polotoka Istre. *Geologija*, 53/1: 55-86. <https://doi.org/10.5474/geologija.2010.005>
- Žalohar, J. & Celarc, B. 2010: Zgornjetriiasne plasti slovenskih Alp. *Scopolia*, suppl. 5: 180-187.
- Žalohar, J. & Celarc, B. 2010: Geološka zgradba Kamniško-Savinjskih Alp. *Scopolia*, suppl. 5: 43-51.
- Goričan, Š., Košir, A., Rožič, B., Šmuc, A., Gale, L., Kukoč, D., Celarc, B., Črne, A. E., Kolar-Jurkovšek, T., Placer, L. & Skaberne, D. 2012: Mesozoic deep-water basins of the eastern Southern Alps (NW Slovenia). In 29th IAS Meeting of Sedimentology (10-13 September 2012, Schladming): field trip guides. *Journal of Alpine geology*, 54: 101-143.
- Celarc, B., Goričan, Š. & Kolar-Jurkovšek, T. 2013: Middle Triassic carbonate-platform break-up and formation of small-scale half-grabens (Julian and Kamnik-Savinja Alps, Slovenia). *Facies*, 59/3: 583-610. <https://doi.org/10.1007/s10347-012-0326-0>
- Celarc, B., Gale, L. & Kolar-Jurkovšek, T. 2014: New data on the progradation of the dachstein carbonate platform (Kamnik-Savinja Alps, Slovenia) = Novi podatki o progradaciji dachsteinske karbonatne platforme (Kamniško-Savinjske Alpe, Slovenija). *Geologija*, 57/2: 95-104. <https://doi.org/10.5474/geologija.2014.009>
- Marinšek, A., Celarc, B., Grah, A., Kokalj, Ž., Nagel, T.A., Ogris, N., Oštir, K., Planinšek, Š., Roženberger, D., Veljanovski, T., Vochl, S., Železnik, P. & Kobler, A. 2015: Žledolom in njegove posledice na razvoj gozdov - pregled dosedanjih znanj = Impacts of ice storms on forest development - a review. *Gozdarski vestnik*, 73/9: 392-405.
- Gale, L., Celarc, B., Caggiati, M., Kolar-Jurkovšek, T., Jurkovšek, B. & Gianolla, P. 2015: Paleogeographic significance of Upper Triassic basinal succession of the Tamar Valley, northern Julian Alps (Slovenia). *Geologica Carpathica*, 66/4: 269-283. <https://doi.org/10.1515/geoca-2015-0025>
- Zajc, M., Celarc, B. & Gosar, A. 2015: Structural-geological and karst feature investigations of the limestone-flysch thrust-fault contact using low-frequency ground penetrating radar (Adria-Dinarides thrust zone, SW Slovenia). *Environmental earth sciences*, 73/12: 8237-8249. <https://doi.org/10.1007/s12665-014-3987-x>
- Mohorič, N., Grigillo, D., Jemec Aušlič, M., Mikloš, M. & Celarc, B. 2016: Longitudinal profiles of torrential channels in the Western Karavanke mountains = Vzdolžni profili hudourniških strug v Zahodnih Karavankah. *Geologija*, 59/2: 273-286. <https://doi.org/10.5474/geologija.2016.017>
- Miklavc, P., Celarc, B. & Šmuc, A. 2016: Anisian Strelovec formation in the Robanov kot, Savinja Alps (Northern Slovenia) = Anizijska Strelovska formacija v Robanovem kotu, Savinjske Alpe (Severna Slovenija). *Geologija*, 59/1: 23-34. <https://doi.org/10.5474/geologija.2016.002>
- Caggiati, M., Gianolla, P., Breda, A., Celarc, B. & Preto, N. 2017: The start-up of the Dolomia Principale / Hauptdolomit carbonate platform (Upper Triassic) in the eastern Southern Alps. *Sedimentology: the journal of the International Association of Sedimentologists*, 35 p. <https://doi.org/10.1111/sed.12416>
- Zajc, M., Gosar, A. & Celarc, B. 2018: GPR Study of a Thrust-fault in an Active Limestone Quarry (SW Slovenia). *Journal of environmental & engineering geophysics*, 23/4: 457-468. <https://doi.org/10.2113/JEEG23.4.457>
- Gale, L., Peybernes, C., Celarc, B., Hočevar, M., Šelih, V.S. & Martini, R. 2018: Biotic composition and microfacies distribution of Upper Triassic build-ups: new insights from the Lower Carnian limestone of Lesno Brdo, central Slovenia. *Facies*, 64/3:1-24. <https://doi.org/10.1007/s10347-018-0531-6>
- Gale, L., Kolar-Jurkovšek, T., Karničnik, B., Celarc, B., Goričan, Š. & Rožič, B. 2019: Triassic deep-water sedimentation in the Bled Basin, eastern Julian Alps, Slovenia = Triasna globljevodna sedimentacija v Blejskem bazenu, vzhodne Julijske Alpe, Slovenija. *Geologija*, 62/2: 153-173. <https://doi.org/10.5474/geologija.2019.007>
- Bicknell, R.D.C., Žalohar, J., Miklavc, P., Celarc, B., Križnar, M. & Hitij, T. 2019: A new limulid genus from the Strelovec Formation (Middle Triassic,

- Anisian) of northern Slovenia. Geological Magazine, 156/12: 2017-2030. <https://doi.org/10.1017/S0016756819000323>
- Novak, A., Šmuc, A., Poglajen, S., Celarc, B. & Vrabec, M.: 2020: Sound velocity in a thin shallowly submerged terrestrial-marine Quaternary succession (Northern Adriatic Sea). Water, 12/2: 1-19. <https://doi.org/10.3390/w12020560>
- Atanackov, J., Jamšek Rupnik, P., Jež, J., Celarc, B., Novak, M., Milanič, B., Markelj, A., Bavec, M. & Kastelic, V. 2021: Database of active faults in Slovenia: compiling a new active fault database at the junction between the Alps, the Dinarides and the Pannonian Basin tectonic domains. Frontiers in earth science, 9: 21 p. <https://doi.org/10.3389/feart.2021.604388>
- Placer, L. Jamšek Rupnik, P. & Celarc B. 2021: The Sistiana Fault and the Sistiana Bending Zone (SW Slovenia) = Sesljanski prelom in sesljanska upogibna cona. Geologija, 64/2: <https://doi.org/10.10.5474/geologija.2021.013>

## Navodila avtorjem

**GEOLOGIJA** objavlja znanstvene in strokovne članke s področja geologije in sorodnih ved. Revija izhaja dvakrat letno. Članek recenzirajo domači in tudi strokovnjaki z obravnavanega področja. Ob oddaji člankov avtorji lahko predlagajo **tri recenzente**, uredništvo pa si pridržuje pravico do izbiре recenzentov po lastni presoji. Avtorji morajo članek popraviti v skladu z recenzentskimi pripombami ali utemeljiti zakaj se z njimi ne strinjajo.

**Avtorstvo:** Za izvirnost podatkov, predvsem pa mnenj, idej, sklepov in citirano literaturo so odgovorni avtorji. Z objavo v GEOLOGIJI se tudi obvežejo, da ne bodo drugje objavili prispevka z isto vsebino.

Avtorji z objavo prispevka v GEOLOGIJI potrjujejo, da se strinjajo, da je njihov prispevek odprto dostopen z izbrano licenco **CC-BY**.

**Jezik:** Članki naj bodo napisani v angleškem, izjemoma v slovenskem jeziku, vsi pa morajo imeti slovenski in angleški izvleček. Za prevod poskrbijo avtorji prispevkov sami.

### Vrste prispevkov:

#### Izvirni znanstveni članek

Izvirni znanstveni članek je prva objava originalnih raziskovalnih rezultatov v takšni obliki, da se raziskava lahko ponovi, ugotovitve pa preverijo. Praviloma je organiziran po shemi IMRAD (Introduction, Methods, Results, And Discussion).

#### Pregledni znanstveni članek

Pregledni znanstveni članek je pregled najnovejših del o določenem predmetnem področju, del posameznega raziskovalca ali skupine raziskovalcev z namenom povzemati, analizirati, evalvirati ali sintetizirati informacije, ki so že bile publicirane. Prinaša nove sinteze, ki vključujejo tudi rezultate lastnega raziskovanja avtorja.

#### Strokovni članek

Strokovni članek je predstavitev že znanega, s poudarkom na uporabnosti rezultatov izvirnih raziskav in širjenju znanja.

#### Diskusija in polemika

Prispevek, v katerem avtor ocenjuje ali komentira neko delo, objavljeno v GEOLOGIJI, ali z avtorjem strokovno polemizira.

#### Recenzija, prikaz knjige

Prispevek, v katerem avtor predstavlja vsebino nove knjige.

**Oblika prispevka:** Besedilo pripravitev v urejevalniku Microsoft Word. Prispevki naj praviloma ne bodo daljši od 20 strani formata A4, v kar so vštete tudi slike, tabele in table. Le v izjemnih primerih je možno, ob predhodnem dogovoru z uredništvom, tiskati tudi daljše prispevke.

Članek oddajte uredništvu vključno z vsemi slikami, tabelami in tablami v elektronski obliki po naslednjem sistemu:

- Naslov članka (do 12 besed)
- Avtorji (ime in priimek, poštni in elektronski naslov)
- Ključne besede (do 7 besed)
- Izvleček (do 300 besed)
- Besedilo
- Literatura
- Podnaslovi slik in tabel
- Tabele, Slike, Table

**Citiranje:** V literaturi naj avtorji prispevkov praviloma upoštevajo le objavljene vire. Poročila in rokopise naj navajajo le v izjemnih primerih, z navedbo kje so shranjeni. V seznamu literature naj bodo navedena samo v članku omenjena dela. Citirana dela, ki imajo DOI identifikator (angl. Digital Object Identifier), morajo imeti ta identifikator izpisani na koncu citata. Za citiranje revije uporabljamo standardno okrajšavo naslova revije. Med besedilom prispevka citirajte samo avtorjev priimek, v oklepaju pa navajajte letnico izida navedenega dela in po potrebi tudi stran. Če navajate delo dveh avtorjev, izpišite med tekstom prispevka obo priimka (npr. Pleničar & Buser, 1967), pri treh ali več avtorjih pa napišite samo prvo ime in dodajte et al. z letnico (npr. Mlakar et al., 1992). Citiranje virov z medmrežja v primeru, kjer avtor ni poznan, zapišemo (Internet 1). V seznamu literaturo navajajte po abecednem redu avtorjev.

Imena fosilov (rod in vrsta) naj bodo napisana poševno, imena višjih taksonomskih enot (družina, razred, itn.) pa normalno. Imena avtorjev taksonov naj bodo prav tako napisana normalno, npr. *Clypeaster pyramidalis* Michelin, *Galeanella tollmanni* (Kristan), Echinoidea.

### Primeri citiranja članka:

Mali, N., Urbanc, J. & Leis, A. 2007: Tracing of water movement through the unsaturated zone of a coarse gravel aquifer by means of dye and deuterated water. Environ. geol., 51/8: 1401–1412. <https://doi.org/10.1007/s00254-006-0437-4>

Pleničar, M. 1993: *Apricardia pachiniana* Sirna from lower part of Liburnian beds at Divača (Triest-Komen Plateau). Geologija, 35: 65–68

### Primer citirane knjige:

Flügel, E. 2004: Mikrofacies of Carbonate Rocks. Springer Verlag, Berlin: 976 p.

Jurkovšek, B., Toman, M., Ogorelec, B., Šribar, L., Drobne, K., Poljak, M. & Šribar, Lj. 1996: Formacijska geološka karta južnega dela Tržaško-komenske planote – Kredne in paleogenske kamnine 1: 50 000 = Geological map of the southern part of the Trieste-Komen plateau – Cretaceous and Paleogene carbonate rocks. Geološki zavod Slovenije, Ljubljana: 143 p., incl. Pls. 23, 1 geol. map.

### Primer citiranja poglavja iz knjige:

Turnšek, D. & Drobne, K. 1998: Paleocene corals from the northern Adriatic platform. In: Hottinger, L. & Drobne, K. (eds.): Paleogene Shallow Benthos of the Tethys. Dela SAZU, IV. Razreda, 34/2: 129–154, incl. 10 Pls.

### Primer citiranja virov z medmrežja:

Če sta znana avtor in naslov citirane enote zapišemo:

Čarman, M. 2009: Priporočila lastnikom objektov, zgrajenih na nestabilnih območjih. Internet: [http://www.geo-zs.si/UserFiles/1/File/Nasveti\\_lastnikom\\_objektov\\_na\\_nestabilnih\\_tleh.pdf](http://www.geo-zs.si/UserFiles/1/File/Nasveti_lastnikom_objektov_na_nestabilnih_tleh.pdf) (17. 1. 2010)

Če avtor ni poznan zapišemo tako:

Internet: <http://www.geo-zs.si/> (22. 10. 2009)

Če se navaja več enot z medmrežja, jim dodamo še številko:

Internet 1: <http://www.geo-zs.si/> (15. 11. 2000)

Internet 2: <http://www.geo-zs.si/> (10. 12. 2009)

**Slike, tabele in table:** Slike (ilustracije in fotografije), tabele in table morajo biti zaporedno oštreljene in označene kot sl. 1, sl. 2 itn., oddane v formatu TIFF, JPG, EPS ali PDF z ločljivostjo 300 dpi. Le izjemoma je možno objaviti tudi barvne slike, vendar samo po predhodnem dogovoru z uredništvom. Če avtorji oddajo barvne slike bodo te v barvah objavljene samo v spletni različici članka. Pazite, da bo tudi slika tiskana v sivi tehniki berljiva. Grafični materiali naj bodo usklajeni z zrcalom revije, kar pomeni, da so široki največ 172 mm (ena stran) ali 83 mm (pol strani, en stolpec) in visoki največ 235 mm. Večji formatov od omenjenega zrcala GEOLOGIJE ne tiskamo na zgib, je pa možno, da večje oziroma daljše slike natisnemo na dveh straneh (skupaj na lev in desni strani) z vmesnim "rezom". V besedilu prispevka morate omeniti vsako sliko po številčnem vrstnem redu. Dovoljenja za objavo slikovnega gradiva iz drugih revij, publikacij in knjig, si pridobijo avtorji sami.

Če je članek napisan v slovenskem jeziku, mora imeti celotno besedilo, ki je na slikah in tabelah tudi v angleškem jeziku. Podnaslovi naj bodo čim krajsi.

**Korektura:** Avtorji prejmejo po elektronski pošti članek v avtorski pregled. Popravijo lahko samo tiskarske napake. Krajsi dodatki ali spremembe pri korekturah so možne samo na avtorjeve stroške.

Prispevki so prosti dostopni na spletnem mestu: <http://www.geologija-revija.si/>

### Oddaja prispevkov:

Avtorje prosimo, da prispevke oddajo v elektronski obliki na naslov uredništva:

## GEOLOGIJA

Geološki zavod Slovenije

Dimičeva ulica 14, SI-1000 Ljubljana

bernarda.bole@geo-zs.si ali urednik@geologija-revija.si

## Instructions for authors

**Scope of the journal:** GEOLOGIJA publishes scientific papers which contribute to understanding of the geology of Slovenia or to general understanding of all fields of geology. Some shorter contributions on technical or conceptual issues are also welcome. Occasionally, a collection of symposia papers is also published.

All submitted manuscripts are peer-reviewed. When submitting paper, authors can suggest **three reviewers**. Note that the editorial office retains the sole right to decide whether or not the suggested reviewers are used. Authors should correct their papers according to the instructions given by the reviewers. Should you disagree with any part of the reviews, please explain why. Revised manuscript will be reconsidered for publication.

**Author's declaration:** Submission of a paper for publication in GEOLOGIJA implies that the work described has not been published previously, that it is not under consideration for publication elsewhere and that, if accepted, it will not be published elsewhere.

Authors agree that their contributions published in GEOLOGIJA are open access under the licence CC-BY.

**Language:** Papers should be written in English or Slovene, and should have both English and Slovene abstracts.

### Types of papers:

#### Original scientific paper

In an original scientific paper, original research results are published for the first time and in such a form that the research can be repeated and the results checked. It should be organised according to the IMRAD scheme (Introduction, Methods, Results, And Discussion).

#### Review scientific paper

In a review scientific paper the newest published works on specific research field or works of a single researcher or a group of researchers are presented in order to summarise, analyse, evaluate or synthesise previously published information. However, it should contain new information and/or new interpretations.

#### Professional paper

Technical papers give information on research results that have already been published and emphasise their applicability.

#### Discussion paper

A discussion gives an evaluation of another paper, or parts of it, published in GEOLOGIJA or discusses its ideas.

#### Book review

This is a contribution that presents a content of a new book in the field of geology.

#### Style guide:

Submitted manuscripts should not exceed 20 pages of A4 format including figures, tables and plates. Only exceptionally and in agreement with the editorial board longer contributions can also be accepted.

Manuscripts submitted to the editorial office should include figures, tables and plates in electronic format organized according to the following scheme:

- Title (maximum 12 words)
- Authors (full name and family name, postal address and e-mail address)
- Key words (maximum 7 words)
- Abstract (maximum 300 words)
- Text
- References
- Figure and Table Captions
- Tables, Figures, Plates

**References:** References should be cited in the text as follows: (Flügel, 2004) for a single author, (Pleničar & Buser, 1967) for two authors and (Mlakar et al., 1992) for multiple authors. Pages and figures should be cited as follows: (Pleničar, 1993, p. 67) and (Pleničar, 1993, fig. 1). Anonymous internet resources should be cited as (Internet 1). Only published references should be cited. Manuscripts should be cited only in some special cases in which it also has to be stated where they are kept. Cited reference list should include only publications that are mentioned in the paper. Authors should be listed alphabetically. Journal titles should be given in a standard abbreviated form. A DOI identifier, if there is any, should be placed at the end as shown in the first case below.

Taxonomic names should be in italics, while names of the authors of taxonomic names should be in normal, such as *Clypeaster pyramidalis* Michelin, *Galeanella tollmanni* (Kristan), Echinoidea.

### Articles should be listed as follows:

Mali, N., Urbanc, J. & Leis, A. 2007: Tracing of water movement through the unsaturated zone of a coarse gravel aquifer by means of dye and deuterated water. Environ. geol., 51/8: 1401–1412. <https://doi.org/10.1007/s00254-006-0437-4>

Pleničar, M. 1993: *Apicardia pachiniana* Sirna from lower part of Liburnian beds at Divača (Triest-Komen Plateau). Geologija, 35: 65–68.

### Books should be listed as follows:

Flügel, E. 2004: Mikrofacies of Carbonate Rocks. Springer Verlag, Berlin: 976 p.

Jurkovšek, B., Toman, M., Ogorelec, B., Šribar, L., Drobne, K., Poljak, M. & Šribar, Lj. 1996: Formacijska geološka karta južnega dela Tržaško-komenske planote – Kredne in paleogenske kamnine 1: 50.000 = Geological map of the southern part of the Trieste-Komen plateau – Cretaceous and Paleogene carbonate rocks. Geološki zavod Slovenije, Ljubljana: 143 p., incl. Pls. 23, 1 geol. map.

### Book chapters should be listed as follows:

Turnšek, D. & Drobne, K. 1998: Paleocene corals from the northern Adriatic platform. In: Hottinger, L. & Drobne, K. (eds.): Paleogene Shallow Benthos of the Tethys. Dela SAZU, IV. Razreda, 34/2: 129–154, incl. 10 Pls.

### Internet sources should be listed as follows:

Known author and title:

Čarman, M. 2009: Priporočila lastnikom objektov, zgrajenih na nestabilnih območjih. Internet: [http://www.geo-zs.si/UserFiles/1/File/Nasveti\\_lastnikom\\_objektov\\_na\\_nestabilnih\\_tleh.pdf](http://www.geo-zs.si/UserFiles/1/File/Nasveti_lastnikom_objektov_na_nestabilnih_tleh.pdf) (17. 1. 2010)

Unknown authors and title:

Internet: <http://www.geo-zs.si> (22.10.2009)

When more than one unit from the internet are cited they should be numbered:

Internet 1: <http://www.geo-zs.si> (15.11. 2000)

Internet 2: <http://www.geo-zs.si> (10.12. 2009)

**Figures, tables and plates:** Figures (illustrations and photographs), tables and plates should be numbered consecutively and marked as Fig. 1, Fig. 2 etc., and saved as TIFF, JPG, EPS or PDF files and submitted at 300 dpi. Colour pictures will be published only on the basis of previous agreement with the editorial office. If, together with the article, you submit colour figures then these figures will appear in colour only in the Website version of the article. Be careful that the grey scale printed version is also readable. Graphic materials should be adapted to the journal's format. They should be up to 172 mm (one page) or 83 mm wide (half page, one column), and up to 235 mm high. Larger formats can only be printed as a double-sided illustration (left and right) with a cut in the middle. All graphic materials should be referred to in the text and numbered in the sequence in which they are cited. The approval for using illustrations previously published in other journals or books should be obtained by each author.

When a paper is written in Slovene it has to have the entire text which accompanies illustrations and tables written both in Slovene and English. Figure and table captions should be kept as short as possible.

**Proofs:** Proofs (in pdf format) will be sent by e-mail to the corresponding author. Corrections are made by the authors. They should correct only typographical errors. Short additions and changes are possible, but they will be charged to the authors.

GEOLOGIJA is an open access journal; all pdfs can be downloaded from the website: <http://www.geologija-revija.si/en/>

**Submission:** Authors should submit their papers in electronic form to the address of the GEOLOGIJA editorial office:

### GEOLOGIJA

Geological Survey of Slovenia

Dimičeva ulica 14, SI-1000 Ljubljana, Slovenia

bernarda.bole@geo-zs.si or urednik@geologija-revija.si

# GEOLOGIJA

št.: 64/2, 2021

[www.geologija-revija.si](http://www.geologija-revija.si)

- 143 Spahić, D. & Gaudenyo, T.  
The role of the pre-Alpine polycrystalline basement in the paleogeographic configuration of multiple Neotethyan oceanic basins
- 159 Jemec Auflič, M., Bokal, G., Kumelj, Š., Medved, A., Dolinar, M. & Jež, J.  
Impact of climate change on landslides in Slovenia in the mid-21st century
- 173 Gale, L., Kukoč, D., Rožič, B. & Vidervol, A.  
Sedimentological and paleontological analysis of the Lower Jurassic part of the Zatrnik Formation on the Pokljuka plateau, Slovenia
- 189 Čar, J., Jež, J. & Milanič, B.  
Strukturne razmere na stiku Južnih Alp in Dinaridov na zahodnem Cerkljanskem
- 205 Serianz, L., Cerar, S. & Vreča, P.  
Using stable isotopes and major ions to identify recharge characteristics of the Alpine groundwater-flow dominated Triglavská Bistrica River
- 221 Placer, L., Rupnik Jamšek, P. & †Celarc, B.  
The Sistiana Fault and the Sistiana Bending Zone (SW Slovenia)
- 253 Torkar, A., Zajc, M., Atanackov, J., Gosar, A. & Brenčič, M.  
Geophysical investigations in the Radovna River Spring area (Julian Alps, NW Slovenia)
- 267 Mali, N., Koroša, A. & Urbanc, J.  
Pesticidi v vodonosniku Krško-Brežiškega polja

ISSN 0016-7789